INVESTIGATING THE EFFECTS OF COMMON DIETARY ISOFLAVONES ON BREAST CANCER CELL PROLIFERATION, APOPTOSIS, AND POTASSIUM CHANNEL ACTIVITY

JOANNE WALLACE

A thesis submitted in partial fulfillment of the requirements for the degree of

Doctor of Philosophy

QUEEN MARGARET UNIVERSITY

2013

Table of Contents

Abstract

Epidemiological evidence suggests that due to its high isoflavone (genistein and daidzein) content a diet rich in soy could protect against breast cancer, particularly tumours expressing oestrogen receptor alpha (ERα+). Isoflavones are weakly oestrogenic, and have other wide ranging cellular activities. Contradictory *in vitro* evidence means that isoflavones' mechanism(s) of action remain to be elucidated.

ERα+ MCF7 and ERα-/ERβ+ MDA-MB-231 cell proliferation and apoptosis were quantified at a range of achievable serum concentrations of genistein or daidzein (0.01nM to 31.6μM) with or without pre-/post-menopausal 17β-oestradiol (E2) levels (1nM and 1pM). Additionally, cell volume regulation and macroscopic K+ current modulation by isoflavones and E2 in MCF7 cells were investigated.

In MCF7 cells isoflavones (≥1μM) induce apoptosis, even in the presence of E2, but this did not reverse the synergistic effect of postmenopausal E2 and isoflavones on proliferation. Isoflavones slightly reduced MDA-MB-231 proliferation at all concentrations, dropping dramatically at 31.6μM. This response was partially maintained in the presence of postmenopausal E2. Isoflavones also induced markers of apoptosis. Treating MCF7 with 1nM E2 or 1μM genistein resulted in cell swelling, and a significant increase in whole cell current (E2 only), indicating a proliferative response. Conversely, treatment with 31.6μM genistein resulted in shrinkage, and inhibition of outward K+ current (not statistically significant). Daidzein treatment inhibited current to a lesser extent. Co-treatment with K+ channel blockers indicated the hEAG channel as a potential molecular target of genistein in MCF7.

These results suggest that in ERα+ breast cancers, isoflavones may act by inducing apoptosis, shrinkage, and inhibition of hEAG current. There was no evidence suggesting that isoflavones reduce E2-promoted ERα+ cancer cell proliferation. Importantly, the inhibition of K+ channel activity by isoflavones represents a novel target for anti-cancer therapies. However, even low levels of isoflavones may be beneficial chemotherapeutic agents against ERα-/ERβ+ breast cancer, indicating an urgent requirement for further characterization of the effects of isoflavones in these breast cancers.

Key words: breast cancer, soy, isoflavones, proliferation, apoptosis, potassium channel

Dedication

This work is dedicated to my grandfather, Professor John D. Nisbet, O.B.E. (17th October 1922 to 5th October 2012).

You have been an amazing source of inspiration, a generous provider of financial support when it has been most needed, and you helped to shape this thesis.

Acknowledgements

First and foremost, this thesis would not have been possible without the seemingly endless support, advice, scrounged funding and late nights put in by my supervisors, Drs Iain Gow and Mary Warnock. I promise there will be no more drafts for you to read!

In addition, I am sincerely grateful for the technical advice and time generously provided by Dr. Forbes Howie (Edinburgh University; QMRI), Mark Anderson (Charles River Laboratories, Tranent), Dr. Martyn Reynolds (Cairn Research, Glasgow) and Dr. Elizabeth Ellis (Strathclyde University).

I am eternally grateful to my husband, Rob Vinall, and my mother, Liz Wallace, for their *pro bono* proof reading services, encouragement, and patient endurance of all my rants.

Finally, the past three years would have been much harder without the friendship, tea breaks, advice and moral support of my fellow PhD colleagues at our desk at the end of the level 2 leg 2 office. Likewise, the advice and support of the School of Health Sciences technicians, particularly Jo Petit and Shirley Coyle, have been invaluable.

List of Figures

List of tables

List of abbreviations and definitions of terms

4-AP	4-Aminopyridine
6-CFDA	6-Carboxyfluorescein Diacetate
α-DTx	alpha-Dendrotoxin
αERKO	Oestrogen Receptor α Knock-Out
βERKO	Oestrogen Receptor β Knock-Out
Δf	Rate of change of fluorescence intensity per second
ADP	Adenosine Diphosphate
AIF	Apoptosis Inducing Factor
AM	Acetomethoxy (ester)
ANOVA	Analysis Of Variance
APAF-1	Apoptotic Protease Activating Factor-1
AST	Astemizole
ATP	Adenosine Triphosphate
AVD	Apoptotic Volume Decrease
aΔf	Adjusted rate of change of fluorescence intensity per second
BK	Large conductance K+ channel
BMI	Body Mass Index
BrdU	Bromodeoxyuridine
BSA	Bovine Serum Albumin
BSA-E2	Bovine Serum Albumin conjugated 17β-oestradiol
CaM	Calmodulin
CI	Confidence Interval
CTx	Charybdotoxin
CVD	Cardiovascular Disease
DAPI	4',6-diamidino-2-phenylindole
DBD	DNA Binding Domain
DC-FBS	Dextran/Charcoal-stripped Fetal Bovine Serum
df_M	Degrees of freedom of the model
df_R	Residual degrees of freedom
DMBA	Dimethylbenzanthracene
DMEM	Dublecco's Modified Eagle's Medium
DMSO	Dimethyl Sulfoxide
DOF	Dofetilide
E2	17β-oestradiol
EC_{50}	Concentration required for a half-maximal effect
EGF	Epidermal Growth Factor
EGFR	Epidermal Growth Factor Receptor
ELISA	Enzyme Linked Immunosorbent Assay
E_m	Membrane Potential
ER (+/-)	Oestrogen Receptor (positive/negative)
ERE	Oestrogen Responsive Element
ERα	Oestrogen Receptor alpha
ERβ	Oestrogen Receptor beta

FBS	Fetal Bovine Serum
FFQ	Food Frequency Questionnaire
FRET	Fluorescence Resonance Energy Transfer
GC-MS	Gas Chromatography-Mass Spectrometry
GIRK	G-protein coupled Inwardly Rectifying K+ channel
GLM	General Linear Model
HDL	High Density Lipoprotein
hEAG	human ether-a-go-go K^+ channel
HER1 / HER2	Human Epidermal Growth Factor Receptor 1 / 2
hERG	human ether-a-go-go Related Gene
HPLC	High Pressure Liquid Chromatography
HR	Hazard Ratio
HRT	Hormone Replacement Therapy
HUGO	Human Genome Organisation
I	Current (Amps)
I/V	Current/Voltage
IbTx	Iberiotoxin
IC_{50}	Concentration required to inhibit an action by 50%
ICD10	International Classification of Diseases 2010
IGF1/2	Insulin-like Growth Factor 1/2
IGFBP3	Insulin-like Growth Factor Binding Protein 3
IGFR	Insulin-like Growth Factor Receptor
IK	Intermediate conductance K^+ channel
I_{KS}	Delayed rectifier K^+ current
IUPHAR	International Union of Pharmacology
K_{2P}	2-pore domain K^+ channel
K_{ir}	Inwardly rectifying K^+ channel
K_v	Voltage Gated K^+ channel
LBD	Ligand Binding Domain
LDL	Low density Lipoprotein
M	Molar, mol/l
MANOVA	Multivariate Analysis of Variance
MAPK	Mitogen Activated Protein Kinase
MNU	1-methyl-1-nitrosourea
MOMP	Mitochondrial Outer Membrane Permeability
MTT	3-(4, 5-dimethylthiazol-2-yl)2, 5-diphenyl tetrazolium bromide
Na^+K^+-ATPase	Sodium Potassium exchanger
NAF	Nuclear Area Factor
NCCD	Nomenclature Committee on Cell Death
NF-κB	Necrosis Factor Kappa B
NICE	National Institute for health and Clinical Excellence
NS	Not Significant
NT	Normal Tyrode
OD	Optical Density
OR	Odds Ratio
p.p.m.	parts per million
PBFI	Potassium Binding Benzofuran Isophthalate

PBS	Phosphate Buffered Saline
PCR	Polymerase Chain Reaction
PI	Propidium Iodide
PI-3-K	Phosphatidylinositol 3-Kinase
PKA (-B, -C)	Protein Kinase A (-B, -C)
PR	Progesterone Receptor
PS	Phosphatidylserine
PTFE	Polytetrafluoroethylene
PTK	Protein Tyrosine Kinase
PTP	Protein Tyrosine Phosphatase
R	Resistance (Ohms)
RBA	Relative Binding Affinity
rERG	rat homologue of hERG
ROI	Region of Interest
RT-PCR	Real Time PCR
RVD	Regulatory Volume Decrease
RVI	Regulatory Volume Increase
SD	Standard Deviation
SERD	Selective Oestrogen Receptor Down-regulator
SERM	Selective Oestrogen Receptor Modulator
SHBG	Sex Hormone Binding Globulin
siRNA	small interfering RNA
SK	Small conductance K+ channel
SMAC	Second Mitochondrial Activator of Caspases
ssDNA	single stranded DNA
TASK	TWIK-related Acid Sensitive K+ channel
TEA	Tetraethyl Ammonium
TNFR1/2	Tumour Necrosis Factor Receptor 1/2
TNFα	Tumour Necrosis Factor alpha
TUNEL	Terminal deoxynucleotidyl-transferase mediated d-UTP Nick End Labelling
UV	Ultraviolet
V	Voltage / potential difference (Volts)
v/v	volume/volume
VGKC	Votlage Gated K+ Channel
WHO	World Health Organisation
XIAP	X chromosome-linked Inhibitor of Apoptosis

Publications

Wallace, J.L., Gow, I.F., Warnock, M. 2011. *The life and death of breast cancer cells: proposing a role for the effects of phytoestrogens on potassium channels*. Journal of Membrane Biology. 242 (2) pp 53-67.

Wallace, J.L., Warnock, M. and Gow, I.F. 2012. *Physiological levels of soy isoflavones inhibit the growth of oestrogen receptor β-positive but not α-positive breast cancer cells*. Endocrine Abstracts, Vol 28, pp 146.

Wallace, J.L., Warnock, M. and Gow, I.F. 2012. *Physiological levels of soy isoflavones reduce proliferation and promote apoptosis in the ERβ-positive breast cancer cell line MDA-MB-231*. Proceedings of the Nutrition Society. 71 (OCE1) E9.

Wallace, J.L., Foy, D., Yousuf, H., Warnock, M. and Gow, I.F. 2012. *The Effect of 17-β Oestradiol, Resveratrol, and Genistein on Na+/H+ Exchange in Breast Cancer Cells Lines*. Proceedings of the Nutrition Society. 71 (OCE1) E10.

CHAPTER 1. Introduction

1.1 Overview of breast cancer

Breast cancer is defined as a malignant tumour of the breast, and is classified by the International Classification of Diseases (ICD10) code C50 (WHO 2012). It is typically a painless lump in the breast or under the armpit. Bleeding or discharge from the nipple can occur, but are not diagnostic. Fibrosis around the tumour can lead to pitting or discoloration of the skin. The tumour can metastasize further to the other breast, bones, lungs or liver. Diagnosis is typically by mammography and physical examination, and confirmed by biopsy (Baum and Schipper 2000). Breast cancers can be classified according to their invasiveness, and site, but also by the presence or absence of various hormone receptors, including oestrogen receptors (positive or negative; ER+/-) progesterone receptors (PR+/-) and human epidermal growth factor receptor 1 or 2 (HER1/HER2+/-). A tumour is classed as receptor positive if over 5% of the cells express that receptor. The receptor status of the disease affects rate of invasion and has implications for treatment choices (Smith and Chua 2006a; Smith and Chua 2006b; Suzuki et al. 2008).

1.1.1 Incidence and mortality

In the United Kingdom, breast cancer is the most common female cancer, accounting for 37% of all female cancer incidence between 2007 and 2009, at a rate of 124.2 incident cases per 100 000 adults in the age adjusted female population (Office for National Statistics 2012). Rates in males are very low and will not be discussed. Female breast cancer mortality rates are relatively low, at 21% of the incidence rate, or 26.1 deaths per 100 000 adults, with female mortality from lung cancer occurring at a higher rate. Since 1993 the incidence rate of breast cancer in the UK has been steadily increasing. During the same period mortality rates have fallen by 22% (Westlake and Cooper 2008). Data from developed countries worldwide is similar (Jemal et al. 2011). The introduction of breast screening, which reached full UK coverage in the mid-1990s has made a significant contribution to both trends, allowing earlier diagnosis and treatment, resulting in an improved prognosis for affected women (Reddy and Given-Wilson 2006). Developments in treatment have also contributed the downward trend in mortality (Westlake and Cooper 2008).

Most breast cancers are ER+, with one cohort reporting over 70% (Balfe et al. 2004; Suzuki et al. 2008; Ziv et al. 2004). However, in human tissue two ERs are expressed. The classical ER is known as ERα. In the mid-1990s a second ER, referred to as ERβ was identified. Their expression levels vary throughout the body, but they are both expressed in breast and most female reproductive tissues (Taylor and Al-Azzawi 2000). Traditionally, the ER status of a patient is determined based on their ERα expression level. This ER is the dominant form in human breast cancer (Balfe et al. 2004). However, both ER+ and ER- tumours have been found to express ERβ, complicating classification (Skliris et al. 2008).

1.1.2 Breast cancer treatment

Effective treatment for breast cancer depends on the size, stage and characteristics of the tumour. Frequently, treatment is surgery to remove the tumour (lumpectomy) or the entire affected breast (mastectomy), with or without radiotherapy, followed by a course of adjuvant chemotherapy. For large inoperable tumours, adjuvant therapy is used first, to attempt to slow growth or even promote regression (NICE 2009a; NICE 2009b; Pollak 2001; Smith and Chua 2006a). However each causes additional physiological and psychological challenges for the patient, including the physical risks associated with any surgery, and the side effects of chemotherapy which may include alopecia, nausea, fatigue, weight gain and early menopause (Miller et al. 2007; Smith and Chua 2006a).

Endocrine chemotherapy regimes, designed to block either the production or actions of oestrogens, are well established treatments for postmenopausal women with ERα+ breast cancer (NICE 2009b)[1]. Modern endocrine breast cancer treatments are diverse (Miller et al. 2007; NICE 2009b). Selective oestrogen receptor modulators (SERMs), such as tamoxifen, reduce breast cancer proliferation by competitively binding to the ER and partially inhibiting its signaling, although they act as agonists in some other tissues. Selective oestrogen receptor down-regulators (SERDs) act similarly but more completely inhibit the ER-signal. Aromatase inhibitors selectively bind to and inhibit aromatase, a key enzyme in the synthesis of oestrogens, thereby reducing oestrogen levels.

However, around a third of breast cancers are ERα-, which are frequently more aggressive but fail to respond to endocrine therapies (Balfe et al. 2004; Suzuki et al. 2008; Ziv et al. 2004). Alternative chemotherapies exist, such as the HER2-receptor antibody trastuzumab (Herceptin). This treatment is advised for women with early stage ER-/HER2+ breast cancer, but it is associated with cardiotoxicity, and is unsafe for women with cardiac disease (NICE 2006). Furthermore, a major obstacle to the treatment of breast cancer is the development of resistance to therapies over long term treatment regimes, resulting in relapse, and requiring a switch to another

[1] The pioneer of these treatments was the physician George Beatson, who discusses in his 1896 letter to *The Lancet* how the removal of the ovaries reversed the progression of three cases of breast cancer (Beatson 1896).

therapy (Miller et al. 2007). There is a great need to develop more effective preventative strategies and therapeutic treatments for breast cancer.

1.1.3 Unmodifiable risk factors

Being female is the major risk factor for breast cancer, closely followed by increasing age, with relative risk doubling every 10 years (Information Services Division Scotland 2012; Kurian et al. 2010; McPherson et al. 2000). In addition, genetic predisposition for the condition is implicated in around 10% of cases in Western countries, with mutations in the genes BRCA1 and BRCA2 accounting for much of this (McPherson et al. 2000). Many of the remaining risk factors relate to a woman's reproductive history. Risk is reduced by late onset of menstruation, early menopause (natural or induced), pregnancy (reducing further with each subsequent pregnancy after the first), being younger at first pregnancy, and breast feeding (Chlebowski et al. 2009; Clavel-Chapelon and the E3N-EPIC group 2002). Extended use of Hormone Replacement Therapy (HRT) or oral contraceptives can lead to an increase in risk, although this decreases upon cessation of use (Beral 2003; Collaborative Group on Hormonal Factors in Breast Cancer 1997). Many of these risk factors are inter-related, and have a complex relationship with risk, depending on receptor status of the cancer, and whether pre- or post-menopausal breast cancer risk is being assessed. Importantly, they are all unmodifiable, or difficult/unethical to modify. Each of these factors affects a woman's levels of serum sex hormones.

In postmenopausal women not taking HRT, serum total concentrations of 17β-oestradiol (E2), the main circulating human oestrogen, are typically between 40 and 100 pM (Braunstein et al. 2008; Kaaks et al. 2005a; Rock et al. 2008). Premenopausal women (not taking oral contraceptives) have higher levels, ranging between 0.1 to 1 nM depending on the point in their menstrual cycle (Eliassen et al. 2006; Gruber et al. 2002; Kaaks et al. 2005b; Rubin et al. 2005). However, a proportion of this E2 is bound in the serum by sex hormone binding globulin (SHBG) preventing its biological activity, or albumin (Fortunati et al. 2010; Gruber et al. 2002). Accordingly, the levels of unbound, or free, bioavailable E2 are lower. In premenopausal women, the level of serum SHBG was found to be between 50 and 60nM, and does not vary with the menstrual cycle (Eliassen et al. 2006; Kaaks et al. 2005b). Levels were slightly lower in postmenopausal women: closer to 35nM (Kaaks et al. 2005a). Consequently, in postmenopausal women free E2 has been determined to be between 1 and 30 pM (Braunstein et al. 2008; Kaaks et al. 2005a;

Rock et al. 2008). In premenopausal women free E2 varied between around 200pM during the follicular phase, and 500pM during the luteal phase (Eliassen et al. 2006).

In a nested case-control group comprising nearly 2000 postmenopausal women taking part in the European Prospective Investigation into Cancer and Nutrition (EPIC) cohort study, elevated levels of both E2 and free E2 were positively associated with breast cancer risk ($p < 0.0001$) while SHBG levels were inversely related to risk ($p = 0.04$) (Kaaks et al. 2005a). Likewise, elevated levels of oestrogens and testosterone (a precursor of oestrogen) have been linked to risk of breast cancer independent of other risk factors (Cummings et al. 2005; Dorgan et al. 2010; Eliassen et al. 2006; Mady 2000; Platet et al. 2004).

There are two mechanisms through which E2 exposure may cause breast cancer. Firstly, oestrogens promote mitotic cell growth in the breast epithelium, directly promoting the growth of the cancerous tissue (Matsumura et al. 2005; Schmidt et al. 2005), and by increasing the number of cell divisions also result in a proportionately larger number of possibilities for DNA mutation (Yager 2000). Secondly, oestrogens may be metabolized into genotoxic products, resulting again in DNA damage (Jefcoate et al. 2000). These two mechanisms are likely to be synergistic, with mutations caused by carcinogenic oestrogens propagated rapidly by oestrogen enhanced growth, with insufficient time for repair.

Genetic predisposition accounts for approximately 10% of breast cancer cases in western countries. Additionally, a history of previous benign breast disease, such as cysts, can increase breast cancer risk. Previous breast cancer greatly increases a woman's chances of developing a tumour in the other breast (contralateral) (McPherson et al. 2000). There is growing evidence to suggest that exposure to xenoestrogens (chemicals which mimic oestrogens), found in some plastics, packaging and pesticides, can increase risk of breast cancer also (Mitra et al. 2004).

1.1.4 Modifiable risk factors

The modifiable risk factors for breast cancer are few, and often have little influence on final risk compared to the factors discussed above. Smoking divides opinion regarding breast cancer. Iwasaki and Tsugane (2011) argue that it is a risk factor, although others suggest that it is not (McPherson et al. 2000). Among postmenopausal women who are not using HRT, adult weight gain or high Body Mass Index (BMI) contributes to increased risk (Feigelson et al. 2004). For most dietary factors, such as dietary fat, fruit, vegetables, antioxidant vitamins or whole grains, there is no, or very limited evidence for an affect on breast cancer risk (World Cancer Research Fund / American Institute for Cancer 2007). However, high levels of alcohol consumption may increase risk by as much as 10% per 10 g/day ethanol (Iwasaki and Tsugane 2011; World Cancer Research Fund / American Institute for Cancer 2007).

However, there is a considerable field of research demonstrating an inverse relationship between breast cancer risk and the consumption of high levels of plant-derived oestrogens known as phytoestrogens, and in particular the isoflavones found in soy. There are countless proposed mechanisms through which isoflavones might mediate these effects. These include but are not limited to modulating oestrogen responsive gene expression, oestrogen synthesis, cell cycle control, induction of apoptosis, breast tissue development, antioxidant actions, angiogenesis and protein tyrosine kinase inhibition (Steiner et al. 2008). However the precise mechanisms of isoflavone action in breast cancer remain to be elucidated.

1.2 Soy isoflavone phytoestrogens

Isoflavones are natural, plant metabolites with weak oestrogenic activity (Hwang et al. 2006; Kuiper et al. 1998). For this reason they are often referred to as phytoestrogens. Many plants produce oestrogenic compounds (Table 1.1), but, of the types consumed by humans, the isoflavones and lignans are most relevant for health. Phytoestrogens have a structure similar to mammalian oestrogens like E2 (Figure 1.1). The main groups of plant derived phytoestrogens are the isoflavones, flavonoids, lignans and coumestans (Dixon 2004). They each arise naturally in a range of grains, legumes and fruits.

Of these phytoestrogens, the isoflavones have received the most scientific attention. They are a distinctive class of flavonoids, almost entirely limited to the subfamily Papilionoideae of the Leguminosae family, and all sharing the same diphenolic skeleton. There are many hundreds of isoflavone chemical structures discovered to date, differentiated by their substituent groups, oxidation levels and the presence of extra heterocyclic rings (Dewick 1994). Most significant to human health are the soy isoflavones genistein and daidzein, the chickpea isoflavone biochanin A, and equol, a metabolite of daidzein which around half of the population can synthesize. Genistein differs from daidzein only by the presence of an additional hydroxyl group on the 5 position.

Table 1.1: Classification of the main types of plant-derived phytoestrogens

Class of phytoestrogen	Main types	Main sources
Isoflavone	Genistein, daidzein, glycitein	Soybean, clover
	Biochanin A	Chickpea
Flavonoid	Resveratrol	Grapes (and wine), peanuts
	Quercetin	Tea, onions, fruits
Lignan	Enterodiol, enterolactone	Whole cereals and grains (especially rye and flaxseed), berries, garlic
Coumestans	Coumestrol	Alfalfa sprouts, clover, soybean

(Adlercreutz 1995; Dixon 2004)

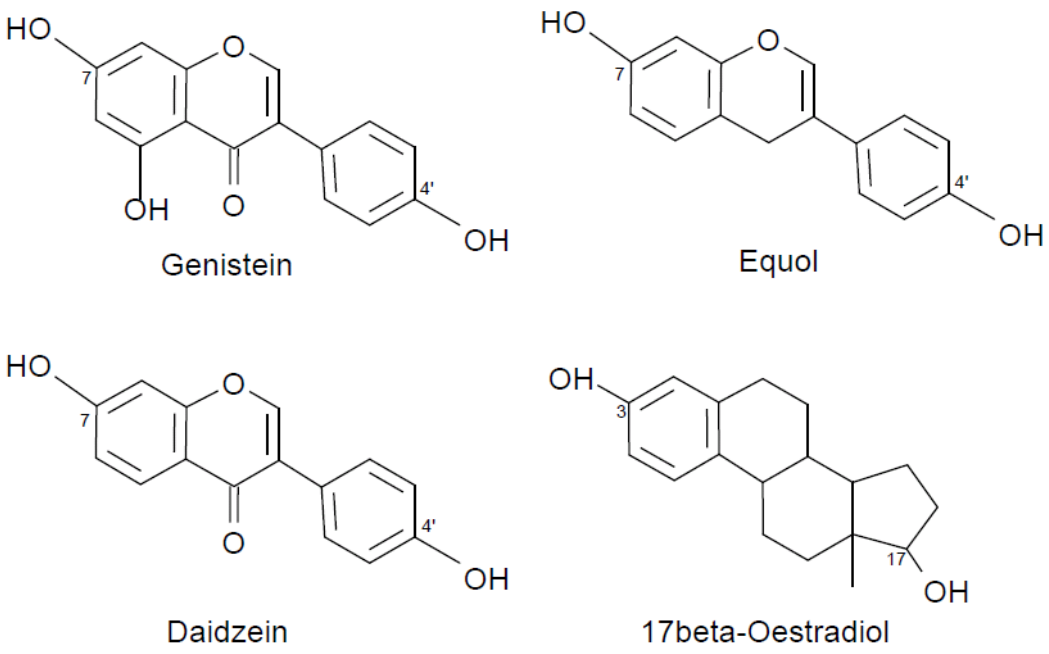

Figure 1.1: Structure of the main isoflavones and 17β-oestradiol

1.2.1 Food sources of isoflavones

The main dietary sources of isoflavones are soy foods. Miso, tofu, natto and soy beans are particularly rich sources, as is texturized vegetable protein (Bhagwat et al. 2008). These soy foods contain between 100 and 200 mg/100g total genistein and daidzein. In addition, products such as doughnuts made with soy flour contain isoflavones, although to a lesser extent, as does red clover extract. Finally, other legumes such as mung beans, and kidney beans contain low levels, as do some nuts, and fruits (Bhagwat et al. 2008; Kuhnle et al. 2008; Liggins et al. 2000). There is likely to be variation in preparation techniques and brands used, which will affect the ultimate isoflavone content (Fletcher 2003). Furthermore, within a product, the isoflavone content varies over time, possibly due to changes in the cultivar and growing conditions of the soy plants (Setchell and Cole 2003). Despite this, it is clear that soy products contain more isoflavones than other sources, by several orders of magnitude, and that the method of processing can influence the isoflavone content. Soy based infant formulas are also rich sources of isoflavones, although the precise content can vary greatly by brand (Setchell et al. 1997). Some infant formulae can contain up to 30 mg/100g dry (powder) weight (Bhagwat et al. 2008). Isoflavones can also pass from a soy-consuming mother to her infant, through breast milk (Franke et al. 2006).

1.2.2 Intakes of isoflavones

Soy foods, including tofu and miso, are associated with a “traditional” Eastern-Asian diet, such as Japanese, North Korean and some parts of China, and so isoflavone intakes are much higher in these populations than in Western countries. Average Eastern Asian intakes have been shown to range between 25 and 50 mg/day isoflavones (Arai et al. 2000; Iwasaki et al. 2008; Lee et al. 2009; Shu et al. 2009). In these populations intake increases with age and rural location (Messina et al. 2006). Consumption of two cups of soy milk, 20g roasted soy beans or 120g tofu will provide around 40mg of isoflavones (Zhan and Ho 2005).

Western countries have lower isoflavone intakes, typically between 0 and 3 mg/day, and often highly skewed towards the lower end of this scale (dos Santos Silva et al. 2004; Grace et al. 2004; Hedelin et al. 2008; Horn-Ross et al. 2002; Linseisen et al. 2004; Travis et al. 2008; Ward et al. 2010). This is due, for the most part, to lack of familiarity with soy foods and the feeling that they are bland compared to the animal products they substitute (Schyver and Smith 2005). Asian migrants to Western countries maintain relatively high isoflavone intakes, although these are higher in direct migrants than their descendants, and decrease with increasing length of time since migration (Wu et al. 2002). Vegetarian women (Travis et al. 2008), and postmenopausal breast cancer patients (Lammersfeld et al. 2009) are also more likely to consume isoflavones than the general population. In the latter group, use of isoflavone supplements can lead to intakes of over 100 mg/d isoflavones. Only a very few in Asian countries achieve this level through diet alone.

In Western countries soy foods such as tofu and miso are available, but they are not consumed widely beyond small sub-groups of the population. For most European and American consumers the soy in their diet comes from other sources. Small quantities of isoflavones are consumed in other (non-soy) legumes and vegetables. However, the bulk of isoflavone consumption for these populations can be split into two categories: ‘second-generation soy foods’, and ‘hidden’ soy ingredients (Fletcher 2003). The first category largely comprises soy analogues of familiar Western foods, particularly dairy and meat products, such as milk, yogurt, cheese, sausages and bacon. These are sold as lactose-free, healthier, or vegetarian alternatives, again to small, defined groups within the population. The second category is where soy derivatives are used in manufactured foods often for

economic or technological reasons, such as soy flour in bread to improve the quality of the loaf, and texturised soy protein (texturised vegetable protein) as a meat extender. In particular this latter group of foods makes dietary analysis of isoflavone intake in the West difficult due to the unavailability of sufficient data (Fletcher 2003; Horn-Ross et al. 2000).

1.2.3 Bioavailability and metabolism

Dietary assessment may not provide an accurate picture of physiological isoflavone levels due to differences in bioavailability between individuals. In the plant, the isoflavones exist mostly in a glycoside form (genistin, daidzin). These have relatively low oestrogenic activity, but are hydrolyzed by food processing, or gut wall enzymes and gut bacteria into their aglycone forms (genistein, daidzein), with greater activity (Kano et al. 2006; Peterson et al. 1998). The bioavailability (based on plasma levels of genistein and daidzein up to 48 hours after ingestion) is comparable regardless of whether the aglycone or glycoside forms are consumed (Zubik and Meydani 2003). In general, studies have shown that daidzein is more bioavailable that genistein, but that between individuals absorption can vary greatly depending on the gut bacteria present (Xu et al. 1995; Xu et al. 1994).

In the human liver and intestine a large proportion (as high as 99%) of these aglycones are further conjugated to glucuronic or sulphate (Bloedon et al. 2002; Gu et al. 2006; Peterson et al. 1998; Setchell 1998; Setchell et al. 2011). In addition to modification by gut enzymes and microflora, the ratio of glycosides, aglycones and conjugates can be altered by cooking and processing method (Coward et al. 1998). This is of particular significance for equol, a metabolite of daidzein. Its formation is entirely dependent on gut microflora (germ-free animals and human infants do not produce it), and 30-50% of human adults do not excrete it (Setchell et al. 2002). The precise bacteria and reasons behind this are unclear. There is evidence of further metabolism of these metabolites into other forms, and deconjugation back into the aglycones (Yuan et al. 2012).

Many of these have been found to have biological effects of their own. Equol acts in a similar, although more oestrogenic, manner to genistein and daidzein (Setchell et al. 2002). The glucuronides of genistein and daidzein are less oestrogenic than their aglycone counterparts, but can activate human natural killer cells (Zhang et al. 1999). Sulfate 4'- and 7-conjugation of genistein and daidzein also reduced the oestrogenic capacity of the parent compounds (Pugazhendhi et al. 2008).

A supplementation trial in healthy postmenopausal women (n=24) found that the plasma half-life of free (unconjugated) genistein and daidzein to be relatively short, averaging at 3.8 and 7.7 hours respectively (Bloedon et al. 2002). The half-life for

total genistein and daidzein (including metabolites) was found to be slightly longer (10.1 and 10.8 hours respectively for genistein and daidzein). However, in each case the range of values measured was large, varying from 1.7 to 21 hours between individuals. A parallel intervention in a group of 30 men of comparable age produced similar results (Busby et al. 2002). This argues against progressive accumulation of these isoflavones upon repeated consumption.

1.2.4 Biomarkers of intake

Due to the difficulties associated with measuring intake, urine or plasma isoflavone levels are frequently used as biomarkers of intake. They are relatively non-invasive, and a variety of assessment methods have been used, including gas chromatography-mass spectrometry (GC-MS) and High Pressure Liquid Chromatography (HPLC). Unlike the dietary assessment methods, serum and urine measurements are found to be consistent and reproducible (Zeleniuch-Jacquotte et al. 1998). In addition, they correlate well with the results of dietary assessment (Grace et al. 2004; Lampe 2003; Verkasalo et al. 2001; Wu et al. 2004). Furthermore, 24 hour urinary isoflavone levels correlate strongly with plasma values (Arai et al. 2000; Grace et al. 2004), and with dose in supplementation interventions (Perez-Jimenez et al. 2010). Age and gender had no significant effect (Kunisue et al. 2010).

Mean plasma levels of genistein and daidzein from Western populations consuming low levels of isoflavones are typically beneath 10nM (Adlercreutz et al. 1993; Grace et al. 2004; Piller et al. 2006; Verheus et al. 2007; Verkasalo et al. 2001; Wu et al. 2004). As with the dietary intakes, this remains highly skewed towards the lower end of the scale. Plasma levels measured in Eastern-Asian, high soy consuming populations were several orders of magnitude higher, with the mean level typically between 0.1 and 1μM for both genistein and daidzein (Adlercreutz et al. 1993; Arai et al. 2000a; Iwasaki et al. 2008). UK women consuming a high soy diet achieved comparable mean levels to these Eastern Asian individuals (Verkasalo et al. 2001). Concerningly, American (caucasian) infants four months old fed exclusively on soy-based infant formulae had particularly high mean plasma isoflavone levels of over 1μM (Setchell et al. 1997). As the safe high doses have been determined historically, based on traditional eastern-Asian diets in adults, this could have implications for the reproductive development of these infants (see section 1.2.6).

While blood or urine samples are relatively non-invasive to collect, it may be the case that the effects of isoflavones in breast cancer are related specifically to their levels in the breast. Nipple Aspirate Fluid is secreted into the breast ducts continuously in non-pregnant and non-lactating women. It can be collected, and may better reflect hormone and isoflavone levels within the breast than serum concentrations. However, to date there has been very little research in this field,

participant numbers were small, drop-out rates were high, and the results are contradictory (Hargreaves et al. 1999; Maskarinec et al. 2008). Additionally these results still do not inform directly about the distribution of isoflavones within breast epithelial tissue.

Among two groups of women taking soy or isoflavone supplements (between 50 and 70mg isoflavones per day) or a placebo for five days prior to undergoing elective breast reduction surgery, no significant relationships were seen between the serum/urine levels of isoflavones, and the levels detected in the breast tissue (homogenised), breast adipocytes, or mammary gland epithelial cells (Bolca et al. 2010; Maubach et al. 2004). However as before, numbers were small, and there were problems with compliance.

Overall, the only conclusion that can be drawn from these studies is that further investigation is required to establish whether serum and urine concentrations of isoflavones correlate with tissue levels, and if tissue levels reflect dietary exposure at all. Studies suffer from low numbers, large inter-individual variation in bioavailability, differences in the length of time from supplementation to sampling, varied dosing regimens, and differing formulation of the supplement given (i.e. ratio of glycoside:aglycone, or genistein:daidzein). In addition, due to the invasive nature of the investigations, these studies suffer from a high level of recruitment bias. Considerably more research is required to determine whether isoflavones accumulate in the breast tissue, and if so, whether this is limited to discrete regions.

1.2.5 Health benefits of isoflavones

Evidence exists suggesting that isoflavones could provide benefits for numerous health conditions. Most of the protective effects of isoflavones against cardiovascular disease (CVD) are related to their ability to improve lipid profiles. There is considerable evidence, including a number of recent meta-analyses, suggesting that intake of soy or isoflavones lowers serum total and low density lipoprotein (LDL) cholesterol, may reduce serum triglycerides, and can increase high density lipoprotein (HDL) cholesterol (Taku et al. 2007; Zhan and Ho 2005). Together these changes lower both the total:HDL and LDL:HDL cholesterol ratios, reducing CVD risk. Additionally, these effects are much greater in hypercholesterolemic individuals than in healthy adults. Animal studies, including those using primates, have yielded similar results (Anthony et al. 1998). Based on data such as these, the US Food and Drugs Administration made the health claim that foods containing at least 6.25g of soy protein per serving could be of benefit to heart health (Food and Drug Administration 1999). The cardio-protective role of isoflavones may be supported by their antioxidant effects, reducing oxidative DNA damage and lipid oxidation (Djuric et al. 2001; Wiseman et al. 2000) although results of other groups are contradictory (Heneman et al. 2007; Vega-Lopez et al. 2005).

The evidence that isoflavones could protect against osteoporosis is inconclusive. A number of studies have demonstrated that isoflavones, either habitual dietary or supplemental, can attenuate femoral and spinal bone loss in peri- and post-menopausal women (Alekel et al. 2000; Mei et al. 2001; Ye et al. 2006). However, a recent meta-analysis shows little overall effect after several months of supplementation with an average of 56mg isoflavones on markers of bone turnover in this population (Taku et al. 2010). Likewise, evidence for similar effects in premenopausal women is contradictory (Ho et al. 2001; Mei et al. 2001).

There is a suggestion that isoflavones may be protective against other endocrine cancers such as prostate cancer in men. Urinary excretion of isoflavones, in particular daidzein, was significantly lower in prostate cancer cases than controls (Park et al. 2009). In prostate cancer cell lines genistein down-regulates growth and survival genes such as survivin, DNA topoisomerase II and cell cycle progression genes (Suzuki et al. 2002). In addition, isoflavone supplementation reduced Prostate Specific Antigen (PSA) levels in prostate cancer patients (Hussain et al.

2003). However, many human dietary studies have failed to show a link between dietary isoflavones and prostate cancer (Park et al. 2008; Ward et al. 2010).

In the last decade there have been a number of large and well designed studies looking into the effects of HRT on breast cancer risk (Beral 2003; Chlebowski et al. 2003). These showed conclusively that current and recent use of HRT, regardless of the specific oestrogens and progestins prescribed, increased risk of breast cancer and delayed diagnosis. The latter trial was very publicly halted before completion due to safety concerns. This had a dramatic and immediate effect on HRT use, with current users discontinuing, and less new users (Kim et al. 2005). Upon breast cancer diagnosis, HRT use is now contraindicated (NICE 2009b). This is of particular significance, since breast cancer chemotherapy can often induce menopause (Smith and Chua 2006a).

In light of this, many studies have been conducted looking into the effectiveness of plant extracts as 'safe' and 'natural' ways to treat menopausal symptoms, including soya isoflavone extracts. One small study found that soy isoflavone supplementation (60 mg/day for 3 months, n = 51) reduced hot flushes and night sweats (Cheng et al. 2007). However, on the whole there is little evidence with regard to isoflavone remedies, with comparison between studies difficult due to trials providing limited data, and suffering from methodological shortcomings such as being underpowered or lacking control groups. It is generally agreed that there are few side effects to isoflavone supplementation, unless a very large dose is taken long-term (150 mg a day for five years). However, the effects of isoflavones on menopausal symptoms appear minimal or non-existent (Low Dog 2005; Tice et al. 2003; Van Patten et al. 2002). Due to their possible oestrogenic effects, and little or no evidence supporting their efficacy, soy or isoflavones are currently not recommended for treatment of menopausal symptoms in women with, or survivors of, breast cancer (NICE 2009b).

1.2.6 Isoflavone toxicity

Epidemiological evidence suggests that dietary levels of isoflavones are safe for humans. In addition, a supplementation intervention where women consumed a single genistein dose of 2, 4, 8 or 16 mg/kg body weight (approximate total genistein intakes of from 100 to 1000mg), resulting in plasma levels peaking at approximately 10µM and 0.1µM total and free (unconjugated) genistein respectively, found that there was no change in lymphocyte apoptosis 24 hours after supplementation, and a slight (non-significant) drop in blood pressure observed in one group (Bloedon et al. 2002). Despite observing several isolated cases of pedal oedema and breast tenderness, they concluded that there was very minimal clinical toxicity as a result of this treatment. The long term toxicity of these doses in women is not known.

The feeding of soy formulas to infants is a relatively new practice, and little is known about its long term safety. However, preliminary data from an American longitudinal prospective study of around 300 children suggests that all formula fed infants, regardless of whether it is soy or milk-based, grow and develop normally (Badger et al. 2009). Similarly, Gilchrist et al. (2010) found no evidence that soy formula feeding produces any oestrogenic effects on the reproductive organs of four month old infants.

Toxicity studies in rats suggest that pharmacological doses of 1000x higher than a typical Japanese isoflavone intake (calculated as mg per kg body weight) reduced adult body weight and slightly altered reproductive development, although did not affect fertility (Guan et al. 2008; Lamartiniere et al. 2002). This raises some concerns about the safety of high dose isoflavone supplementation, especially in women of child bearing age, as a safe upper dose is yet to be established.

1.3 Isoflavones and breast cancer risk *in vivo*

1.3.1 Human epidemiological evidence

The possible protective effect of soy and isoflavones originated from epidemiological studies which consistently showed lower rates of breast cancer among women in Eastern Asian countries than in the West (Parkin et al. 2002; Parkin et al. 2005). The most recent data available estimates that in Western Europe in 2008 the rate of breast cancer incidence (age standardized per 100 000 population) was 89.9 while in Eastern Asia the rate was 25.3 (Jemal et al. 2011). Evidence that this might be related to lifestyle rather than genes comes from numerous sources. Migration studies demonstrated that when Asian women moved to the West, their breast cancer rates increased quickly with each successive generation born in the new home country (Ziegler et al. 1993). This suggests that exposure to a Western lifestyle and environment, including reduced consumption of soy, is responsible. Additionally, since the 1970s many Eastern Asian countries such as South Korea, and more recently China, have rapidly become 'Westernised' in terms of their economies, lifestyle and diets. This has brought with it an increase in saturated fat intake, and a fall in use of cereals, with animal products replacing soy as the main dietary protein. In parallel, their breast cancer rates have quickly risen to near-Western levels (Kim et al. 2000; Popkin and Du 2003). It is important to note that in a Western lifestyle, soy is a marker for a healthier lifestyle, with lower energy intake, less saturated fat, and more fruit and vegetables, not smoking (Nechuta et al. 2012).

There have been many studies looking for an association between isoflavone intake and breast cancer. However, comparison is difficult, and should be interpreted with caution, since they are often highly variable in the population studied, exposure measures and the level of controlling for confounders. Study design varied, with some being prospective cohorts, some nested case-controls, and some population- or hospital-based case-controls. A number of the studies have stratified their results according to menopausal status or the oestrogen receptor status of the tumour, but this has been carried out inconsistently. In addition, in many of the studies the subgroups had relatively small numbers of breast cancer cases, meaning that the results may have occurred by chance.

These studies have been collated in a meta-analysis carried out by Trock et al. (2006). This review of 23 studies reported an overall significant, although slight, inverse association between soy intake and breast cancer risk (odds ratio, OR = 0.86, 95% confidence interval (CI) = 0.75 to 0.99). They found that this inverse association was stronger for breast cancers diagnosed premenopausally (OR = 0.70, 95% CI = 0.58 to 0.85) than post menopausal women (OR = 0.77, 95% CI = 0.60 to 0.98), and similarly was stronger among women from Western countries (including two studies of Asian Americans; OR = 0.84, 95% CI = 0.70 to 1.00) than in Asian women (OR = 0.89, 95% CI = 0.71 to 1.12). However, the latter two odds ratios did not differ significantly. It is possible that the slightly greater inverse association between soy intake and breast cancer risk in Western women may be because soy intake in Asian countries is fairly universal, and that even low intake (which is similar to high Western intakes) may be enough to reduce risk. Alternately, in Western countries soy intake may act as a marker for other risk reducing behaviour.

A more recent publication described a separate meta-analysis for the Asian (n = 8) and Western (n = 11) studies (Wu et al. 2008), as each set of populations possess distinct lifestyle characteristics relating to breast cancer, and consume very different amounts and sources of soy, which may reduce the value of any direct comparison. Their findings contradicted those of Trock et al. by proposing a significant protective effect of consuming high levels of soy in Asian but not Western populations. Among Asian consumers, compared to the lowest level of soy food intake (≤ 5 mg/day isoflavones), breast cancer risk was intermediate (OR = 0.88, 95% CI = 0.78 – 0.98) for those with modest isoflavone intake (around 10 mg/day) and lowest (OR = 0.71, 95% CI = 0.60–0.85) among those with high isoflavone intake (≥20 mg/day). In contrast, the 11 Western populations (with average highest and lowest soy isoflavone intakes of 0.8 and 0.15 mg/day) included in the analysis demonstrated no relationship between isoflavone intake and breast cancer. However, it must be noted that this meta-analysis excluded much of the prospective cohort data available, on the grounds that they contained an insufficient level of detail about the soy foods consumed. Much of the remaining evidence came from case-control studies. Additionally, and perhaps significantly, Wu et al. included Asian American women in the Asian group, and not the Western group. The result is that while a relationship between soy intake and breast cancer risk can be proposed, inferences regarding the mechanism must be interpreted with caution.

Although data is limited, where the results have been stratified according to the oestrogen receptor status of the tumour, protective effects of isoflavones have been limited to the ERα+ subgroup, having no effect on ERα- tumours, although individuals in this group may have tumours expressing ERβ (Linseisen et al. 2004; Suzuki et al. 2008).

Interestingly, these groups and a third meta-analysis reporting similar findings (Dong and Qin 2011) did not observe any dose-response relationship associated with soy intake and breast cancer risk, other than that reported as the difference between high and low intakes. This may relate to the study designs used, and a limited number of eligible studies for each meta-analysis, or it could imply a threshold isoflavone level is required for protective effects to be seen.

High intake of soy isoflavones has been associated not only with reduced risk of breast cancer, but also reduced breast cancer mortality (Zhang et al. 2012). Although they did not find a linear relationship between soy intake and mortality, they suggested that intakes above 17.3mg isoflavones per day might reduce mortality by 36% (n = 616 breast cancer cases), after adjusting for other factors which may have an influence such as age, smoking, alcohol consumption, physical activity and treatment regime.

In humans, there has only been one occasion where a significant relationship between high urinary and serum isoflavones (equol and daidzein) and increased breast cancer risk has been observed in a prospective (UK) cohort (Grace et al. 2004). They determined the $\log_2$ odds ratios (where the risk estimates represent a doubling in phytoestrogen exposure) to be 1.220 (1.005–1.481; p = 0.044) and 1.455 (1.051–2.017; p = 0.024) for serum daidzein and equol respectively. The effect of genistein did not achieve statistical significance. However, this study included a small number of breast cancer cases (n = 114 out of 333 women) increasing the chance that the results were coincidental.

1.3.2 Adolescent isoflavone intake

Several studies have looked retrospectively at adolescent soy intake in women of different backgrounds (Shu et al. 2001; Thanos et al. 2006; Wu et al. 2002). In a case-control study of Chinese (Shanghai) women with 1459 cases of breast cancer and 1556 controls, adolescent soy intake was found to be inversely associated with breast cancer risk, with ORs for the second to the highest quintiles of soy intake compared to the lowest reported as 0.75 (95% CI, 0.57– 0.93), 0.69 (95% CI, 0.55–0.87), 0.69 (95% CI, 0.55– 0.86), and 0.51 (95% CI, 0.40–0.65) respectively (p for trend < 0.001; Shu et al. 2001). Similar ORs were reported for breast cancer diagnosed both pre- and postmenopausally. Adolescent soy intake was assessed by FFQ, with measures for portion size as well as frequency, of intake of 17 soy food ingredients or food groups. This group attempted to control for confounding issues arising from recall of historical diet by assessing not only self reported adolescent intake, but also using the same FFQ with mothers of study participants (where possible) regarding their daughter's adolescent intake. Significant correlations were reported between maternal and self reported adolescent soy intakes among both cases and controls.

Similar ORs were reported for Asian American women (Los Angeles; Wu et al. 2002) and white Canadian women (Thanos et al. 2006). This reduction in risk is independent of adult isoflavone intake, and the effects combine additively, leading to the greatest reduction in risk among women with high adult and adolescent intakes (Wu et al. 2002).

It is thought, through work in rats and mice, that in prepubertal mammary tissue, genistein upregulates the epidermal growth factor (EGF) signaling pathway, promoting differentiation and proliferation. The resulting adult mammary cells experience reduced proliferation and less EGF signaling, and the adult tissue has more lobules and branching, and fewer terminal end buds, rendering it less sensitive to carcinogens (Brown et al. 2010; Lamartiniere et al. 1998; Rowell et al. 2005). In humans, self reported high soya or isoflavone intake, over the long term, is associated with reduced mammographic parenchymal patterning (a function of the breast density and structure) and consequently, reduced breast cancer risk (Jakes et al. 2002; Maskarinec et al. 2004; Ziv et al. 2004).

There have been no studies to date considering the impact of maternal soy consumption during pregnancy, and subsequent breast cancer risk in the female offspring. However, due to the ability of isoflavones to modify the hormone environment (see Section 1.3.4) it is possible that they can alter the oestrogen environment in utero. Furthermore, a study of maternal and neonatal isoflavone levels during birth found comparable total and individual isoflavone levels in the plasma of the mother (Japanese women aged 20 to 30 years, n = 7), umbilical cord, and amniotic fluid, suggesting that isoflavones can freely pass the placental barrier and may influence development of the foetus (Adlercreutz et al. 1999).

1.3.3 Contradictory results from animal studies

There are numerous studies showing the protective effects of isoflavone feeding (between 50 and 250 mg/kg diet) or treatment (intraperitoneal injection) on both chemically induced and spontaneous mammary tumours in rats, and xenografts in mice. In each of these studies isoflavones have reduced tumour size, latency, or aggressiveness, although they have had little or no effect on tumour incidence rate (Gallo et al. 2001; Garvin et al. 2006; Hewitt and Singletary 2003; Jin and MacDonald 2002; Kang et al. 2009; Moon et al. 2008).

Interestingly, dietary genistein or daidzein (200 mg/kg diet) alone or combined (100 mg/kg each) had very little in the way of chemoprotective effects on dimethylbenzanthracene (DMBA)-induced mammary tumours in female Sprague-Dawley rats (Constantinou et al. 2001). However, in the same study, a soy protein-containing diet reduced tumour number, weight, incidence and latency. This diet had similar isoflavone content to the above diets, each resulting in serum genistein and daidzein levels of around 1µM. This suggests that it was some other unforeseen component of soy that was responsible for the protective effect in this case. It is important to note, that in this, and many of the previously mentioned studies, soy/isoflavone feeding and tumour induction began when the mammary tissue of the rats was fully developed, so any protective effects seen were on mature breast tissue, and not in the tissue differentiation and development stage. Furthermore, the mouse models used implanted tumours, such as MCF7, so do not provide any information regarding the transformation of normal breast tissue into tumours.

A recent study suggested that feeding a regimen to neonatal and prepubertal female Sprague-Dawley rats (*via* lactating dam) of equol or genistein (250 mg/kg diet) resulted in significantly altered regulation of 23 proteins involved in a range of pathways including metabolism, structure, motility, cell cycle control and transport at either (or both) 21 (prepubertal) and 50 days (young adult) post partum, again for female Sprague-Dawley rats (Wang et al. 2011). This group found that prepubertal genistein significantly reduced proliferation (determined by K_i67 antigen staining) in the 50 day old rat mammary gland, although not at 21 days.

In addition, a study by Brown et al. (2010) suggests that neonatal or prepubertal exposure of rats to equol (250mg/kg diet) resulted in a significant increase in the differentiation of mammary tissue (i.e. a greater number of mature lobules and significantly reduced numbers of immature terminal end buds) which should confer protection against carcinogens.

However, numerous groups failed to demonstrate any long term protective effect of isoflavones in female rats against chemically induced breast tumour development (Brown et al. 2010; Cohen et al. 2000; Ueda et al. 2003). In addition, under certain experimental conditions soy isoflavones stimulated the growth of oestrogen-sensitive breast tumours in rodents due to their oestrogen-like effects. Ju et al. (2001) found that the growth of implanted ERα+ MCF7 breast cancer cells in mice was promoted in an oestrogenic manner by dietary genistein between 125 and 1000 mg/kg diet (resulting in serum levels between 0.39 and 3.36 µM). Similar results were also seen in mice with dietary isoflavones (Allred et al. 2001) and E2 or chemically induced (MNU: 1-methyl-1-nitrosourea) mammary tumours in rats (Allred et al. 2004; Ju et al. 2001; Singh et al. 2010).

Concerningly, the inhibitory effect of tamoxifen on E2-induced implanted MCF7 tumours in ovariectomised athymic mice was abrogated by genistein feeding (250 or 500 p.p.m. in their standard diet) (Du et al. 2012). The serum levels of genistein and its metabolites that this regimen led to was not determined, but the higher dose used (1000 p.p.m.) did not interfere with the inhibitory tamoxifen effect. This echoes the biphasic effect of isoflavones on breast cancer cell proliferation often seen *in vitro* (see Section 1.4). Similar results were seen in earlier studies, also using this model (Ju et al. 2002; Liu et al. 2005). In this case they determined the total (conjugated and aglycone) plasma genistein after four weeks of feeding to be between 4 and 5 µM (Ju et al. 2002), and again, the treatments began when the mice were adult.

On the contrary, a study looking DMBA induced mammary tumours in rats (female Sprague-Dawley) found daidzein to improve the tumour-preventing capacity of tamoxifen (Constantinou et al. 2005). Again, the study began once the rats were 50 days old, so only looked at the effects of isoflavones on adult breast tissue. Daidzein or genistein were provided in the diet (140 and 105 mg/kg diet) as was tamoxifen (0.125 mg/kg diet), and serum levels of total genistein, and total daidzein and equol, were determined to be approximately 0.5µM after prolonged feeding.

Tamoxifen was found to reduce tumor multiplicity, latency and weight, and as before, genistein slightly reduced the efficacy of tamoxifen. However, daidzein alone was slightly beneficial, and the combination of daidzein and tamoxifen resulted in the greatest protection against mammary DMBA-induced carcinogenesis in each case. The relevance of DMBA-induced mammary tumours in rats to women is not apparent. However this result suggests that in terms of their interaction with tamoxifen, genistein and daidzein may not act in the same manner.

Overall, the impact of genistein and daidzein on the development of mammary tumours in rat or mouse models of the disease is inconclusive. In some cases a protective effect is seen, but this could depend upon the dose, age upon commencement of treatment, and route of tumor induction. Furthermore, genistein and daidzein appear to interact in opposite manners with tamoxifen, and there could be other as yet undiscovered elements of a high soy diet that provide protection against mammary carcinogenesis to rodents.

It must be noted that in many cases the doses described which induce the proliferation of mammary tumours in rodents are comparable to the protective doses used in other rodent studies. In particular, one study found that while 10 mg/kg body weight dietary daidzein increased mammary tumour growth and the level of metastasis to other organs of green fluorescent protein tagged MDA-MB-435 tumours implanted into mice, the same dose of genistein reduced both tumour growth and metastasis compared to a vehicle only control (Martinez-Montemayor et al. 2010).

There are a number of major criticisms of rodent models of breast cancer, which must be borne in mind when considering these results. Firstly, murine models of breast cancer are rarely hormone responsive, unlike the majority of human cases, due to low expression of ERα and PR (Cardiff 2001). In addition, spontaneous murine breast tumours tend to develop while the mouse is fertile, which again differs from human breast cancer. Finally, the mouse tumours are known to develop and metastasise differently than the human variants. With regard to NMU induced tumours, their validity compared to human breast tumours has been assessed by comparative gene expression profiling (Chan et al. 2005). Of the 25 NMU-induced tumours assessed, they were found to be largely ERα+, and not invasive or metastatic. They were most similar to non-invasive human ERα+ breast tumours of

a low or intermediate grade. This suggests that this model may be of some value when considering the impacts of isoflavones upon this type of breast cancer, but the results should not be generalized.

A number of other criticisms can be leveled at these rodent isoflavone studies which may be the cause of this inconsistency. These are described in detail by Messina and Wood (2008) but will be summarized here. Firstly, numerous rodent studies used doses of isoflavones of over 50 times higher than is found in traditional Asian diets, and many injected purified isoflavones directly into the animals. Both result in comparatively higher serum levels that are found in humans.

In addition, while the levels used in animals are based on doses known to induce oestrogenic effects in these animals, the corresponding level in humans is unknown despite years of investigation. In order to investigate oestrogenic effects of isoflavones ovariectomised animals are frequently utilized, to minimize the impact endogenous oestrogens. Consequently, these animals have considerably lower circulating levels of oestrogens than postmenopausal women, meaning that the effect seen is of isoflavones in an oestrogen-depleted environment, of questionable physiological relevance. Primate or human models would generate more representative results, but both bring ethical concerns and complications.

Finally, the rate of isoflavone absorption and metabolic profile of soy isoflavones is strikingly different between species (Gu et al. 2006; Setchell et al. 2011). Both the extent of isoflavone metabolism, and the range of metabolites detected after a comparable soy meal fed to human women, and female Sprague-Dawley rats, Hampshire/Duroc Cross pigs and cynomolgus monkeys differed (Gu et al. 2006). Presumably mice would metabolise isoflavones differently to humans also. Of the species tested, pigs provided the closest metabolite profile to humans, although even then there were considerable differences noted. This implies that soy feeding of rodents would not generate a human-like profile of isoflavone metabolites, and consequently the implications for breast cancer incidence, proliferation and protective mechanisms may not be the same, and the relevance of inter-species comparison of specific dose-effects is limited.

1.3.4 Human isoflavone supplementation trials and breast cancer risk factors

Increased mammographic density is a risk factor for breast cancer (Ziv et al. 2004). It has been shown that self reported high levels of soy intake, determined by FFQ, is associated with higher breast density in a study of over 500 pre- and post-menopausal women (Maskarinec and Meng 2001). The same effect was found with recalled lifetime soy intake (Maskarinec et al. 2004). However, in three separate interventions this group found no significant effect of a range of daily isoflavone supplement doses from 50 to 100 mg/day over one or two years in pre- or post-menopausal women (Maskarinec et al. 2003; Maskarinec et al. 2004; Maskarinec et al. 2009). These results offer some reassurance that isoflavone supplements may not increase breast density. On the other hand, it is possible that the adult and lifetime intakes of soy described by Maskarinec et al. (2001; 2004) are markers for adolescent intakes, which could modify breast development and consequently increase risk.

Another three interventions are described where women of varying age, menopausal status, and breast cancer status, underwent an exploratory breast biopsy before and after a period of isoflavone supplementation with doses ranging from 36 to 200 mg/day, and durations between two weeks and three months (Cheng et al. 2007; Hargreaves et al. 1999; Sartippour et al. 2004). None of these groups reported any change in breast epithelial cell proliferation as a result of the supplementation intervention. A study of premenopausal women suggested that isoflavone supplementation (n = 14, 45mg isoflavones daily for 14 days) enhanced proliferation of non-malignant breast cells, and increased expression of progesterone receptors and the number of cells in S-phase (McMichael-Phillips et al. 1998). However, once again numbers were small, and the invasive nature of each of these procedures is likely to introduce considerable selection bias.

Supplementation studies in women have highlighted several other physiological mechanisms through which isoflavones may reduce breast cancer risk. A recent meta-analysis has shown that isoflavone supplementation reduces circulating levels of luteinizing hormone and SHBG in premenopausal women, although it has no significant effects in postmenopausal women (Hooper et al. 2009). Moreover, isoflavone supplementation increased menstrual cycle length by one day due to

lengthening of the follicular phase, which reduces overall exposure to the luteal phase, where breast tissue proliferation is more rapid due to higher progesterone levels (Kumar et al. 2002). Finally, while no significant effects on overall circulating oestrogen levels were seen, isoflavones have been demonstrated to alter the ratios of various oestrogen metabolites, increasing the benign 2(OH) forms, while reducing the levels of the more carcinogenic 16α (OH)-oestrone and 4(OH)-oestrogens (Xu et al. 2000).

The insulin-like growth factors IGF1 and IGF2 are important regulators of mammary gland proliferation at key developmental stages including pregnancy, lactation and involution (Hadsell 2003). Furthermore they are potent mitogens, and both IGF1 and its associated receptor tyrosine kinase (IGF1-R) play key roles in breast cancer cell proliferation, survival, and metastasis (Jin and Esteva 2008). High levels of IGF1 and its main binding protein IGFBP-3 are associated with an increased risk of premenopausal breast cancer incidence and mortality (Burgers et al. 2011; Renehan et al. 2004). A two year soy isoflavone supplementation reported no significant impact of isoflavone supplementation on IGF1, IGFBP-3, or their molar ratio at any point during the intervention (Maskarinec et al. 2005). In this study 196 premenopausal Hawaiian women consumed two servings of soy foods daily (equivalent to approximately 100mg isoflavones daily) for two years, as a replacement for a meat, dairy, or snack food. Likewise, there was no correlation between habitual soy intake and serum IGF1 and IGFBP-3 in a group of 261 premenopausal Japanese women (Nagata et al. 2003).

However, one smaller intervention (55 American postmenopausal women) found that 10 week supplementation with a powdered soy product (approximately 75g soy protein per day; isoflavone content unknown) resulted in a slight, although significant increase in serum IGF1 and IGFBP-3 (increased by 21.6 and 154.7 µM respectively, $p = 0.001$ for both), and a reduction in SHBG by 5.4µM ($p < 0.001$; McLaughlin et al. 2011). The implications of this result are unclear, as elevated IGF1 levels do not appear to be a risk factor for postmenopausal breast cancer (Renehan et al. 2004).

Overall, isoflavone supplementation appears safe, and interventions show no increased risk of breast cancer. None-the-less, concerns remain regarding the safety of supplements, as isoflavones are known to act oestrogenically, and could increase risk of recurrence.

1.3.5 Isoflavones and recurrence in breast cancer survivors

Little is known about the effects of isoflavones on cancer recurrence in breast cancer survivors, or regarding how they interact or interfere with the oestrogen antagonists used to treat breast cancer, such as tamoxifen. Animal research gives contradictory results (Constantinou et al. 2005; Ju et al. 2002) and human evidence is scant.

However, there exist a number of prospective cohorts where isoflavone intake and breast cancer recurrence have been examined. A pooled analysis of these cohorts, where n = 4856 (China) and 4658 (United States) breast cancer cases found a net reduction in risk of breast cancer specific mortality (HR: 0.83; 95% CI: 0.64, 1.07) and a statistically significant reduction in risk of recurrence (HR: 0.75; 95% CI: 0.61, 0.92) associated with isoflavone intakes of ≥ 10mg/day (Nechuta et al. 2012). By country, a slight reduction in risk associated with consumption of ≥10mg/day isoflavones remained for the Chinese women, although non-significant, but in the United States the effect of consumption of this level of isoflavones maintained its statistical significance.

The results of individual cohorts tend to agree (Kang et al. 2012), and furthermore, suggest that the reduction in mortality and recurrence seen occurs irrespective of anastrozole, an inhibitor of aromatase, a key enzyme in E2 biosynthesis (Kang et al. 2010) or tamoxifen use (Shu et al. 2009). Where a protective effect was seen, it was stronger among women with ERα+ or PR+ breast cancers, and postmenopausal women (Guha et al. 2009; Kang et al. 2010).

One prospective study (n = 339 breast cancer cases in South Korean women) found that high soy of isoflavone intakes increased risk of cancer recurrence in women with HER2+ cancer (Woo et al. 2012). However these increases in risk failed to achieve statistical significance, and the numbers with recurring HER2+ cancer were very low (n = 8 out of 25 recurrent cases).

Overall, this data implies that dietary soy may reduce risk of breast cancer recurrence, particularly among postmenopausal women diagnosed with ERα+ cancers, although its effects in cancers of differing receptor statuses may vary. More importantly, these studies suggest no increased risk associated with dietary soy intake in breast cancer survivors regardless of endocrine therapy use, and that

soy does not appear to abrogate the effects of these therapies. The use of isoflavone supplements in post menopausal breast cancer survivors is currently contraindicated in the UK (NICE 2009b) and accordingly, reported supplement usage amongst this group is low. Likewise, the level reported in an American cohort (n = 1954) was 2.7% (Guha et al. 2009), and 4% reported isoflavone supplement use (soy and/or red clover) in a Canadian (n = 417) group of breast cancer patients (Boucher et al 2012). However, this remains an area where further study is required, as very little is known about the effects or safety of isoflavone supplements (pharmacological doses) in breast cancer survivors.

1.4 Proliferative effects of oestrogen and isoflavones *in vitro*

1.4.1 Expression levels of the oestrogen receptors in breast cancer cell lines

In an attempt to understand the mechanisms behind the effects of isoflavones on breast cancer risk, there have been many investigations *in vitro*, typically using the human breast cancer cell lines MCF7, T47-D, MDA-MB-231, and several others with varying genetic make-up (Table 1.2). The use of cultured breast cancer cell lines as a model for breast cancer will be discussed in section 6.5.2. It is apparent that many of the effects of isoflavones on the growth of cultured cell lines are mediated through the ERs. Where present, oestrogens and isoflavones bind to ERs and initiate transcription of oestrogen responsive genes. Typically, genistein and daidzein bind to the ERs dose responsively, with around 100- to 1000-fold lower affinity than E2 (Hwang et al. 2006; Sotoca et al. 2008).

Table 1.2: Expression levels of ERα and ERβ in the breast cancer cell lines discussed in this review (Tong et al. 2002)

Cell line	Source[1]	ERα[2]	ERβ[2, 3]
BT20	Breast carcinoma	-	+
BT474	Ductal carcinoma	+	+
MCF7	Breast adenocarcinoma, pleural effusion	+	+
MDA-MB-231	Breast adenocarcinoma, pleural effusion	**-**	+
MDA-MB-361	Breast adenocarcinoma derived from brain metastatic site	+	+
MDA-MB-435(s)	Melanocyte – previously described as pleural effusion, ductal carcinoma	**-**	+
MDA-MB-468	Breast adenocarcinoma, pleural effusion	**-**	?
SK-BR-3	Breast adenocarcinoma, pleural effusion	**-**	**-**
T47D	Ductal carcinoma, pleural effusion	+	+
ZR75-1	Ductal carcinoma, malignant ascitic effusion	+	+

[1] *References (Health Protection Agency 2012; LGC-ATCC 2012)*

[2] *(Tong et al. 2002)*

[3] *Refers to ERβ1 expression, the full length isoform (Moore et al. 1998)*

In human breast tissue, normal, non-malignant breast epithelial cells are significantly more likely to be ER-, or solely express ERβ, than cells from malignant breast tissue which frequently express ERα (Speirs et al. 1999). The levels of the two ERs differ between cultured breast cancer cell lines (Table 1.2). Along with the majority of breast cancers, MCF7 cells express both ERs, although with much lower levels of ERβ mRNA (Kurebayashi et al. 2000; Le Corre et al. 2004; Tong et al. 2002; Yuan et al. 2012). Similarly, ER+ T47D and BT474 cells express both receptors (Lattrich et al. 2011; Strom et al. 2004; Yuan et al. 2012). In MDA-MB-231 breast cancer cells, traditionally thought to be ER-, expression of ERα is absent but low level ERβ expression occurs (Kurebayashi et al. 2000; Lattrich et al. 2011; Rajah et al. 2009; Tong et al. 2002). In breast tumour biopsy samples ERβ protein was also present, although at a lower level in most cases than ERα protein (Saunders et al. 2002).

It is important to note that although the full length ERβ isoform (ERβ1) is the dominant form, there exist 4 truncated isoforms, ERβ2, -3, -4 and -5 (Skliris et al. 2008). They have varying transcriptional activating ability, and are expressed at a range of levels in cancerous tissue and cell lines (Lattrich et al. 2011; Tong et al. 2002; Wong et al. 2005; Zhao et al. 2007). Representations of the five isoforms are provided in Figure 1.2. Their expression levels, on the whole, display no clear relationship to tumor invasiveness or ERα expression level. The cell lines MCF7 and MDA-MB-231 each express the ERβ1, 2, 4 and 5 isoforms (Tong et al. 2002). Little is known about the function of the truncated ERβ isoforms. The full length isoform, ERβ1, will be referred to as ERβ throughout this document.

As with E2, isoflavone treatment can moderate the expression level of numerous proteins, including the ERs. Treatment of MCF7 cells for 48 hours with 25 μM genistein reduced the expression level of ERα mRNA (Lavigne et al. 2008). Similarly, 24 hour treatment with 1μM genistein or apigenin reduced the mRNA and protein levels of ERα in MCF7 (Seo et al. 2006). However, 48 hour treatment with the phytoestrogen resveratrol (30 μM) increased mRNA levels of ERβ in MCF7, MDA-MB-231 and a fibrocystic mammary cell line MCF10A (50 μM), although the reported increase in MCF7 was non-significant (Le Corre et al. 2006; Le Corre et al. 2004). This group found that resveratrol treatment had no impact upon ERα mRNA levels in MCF7.

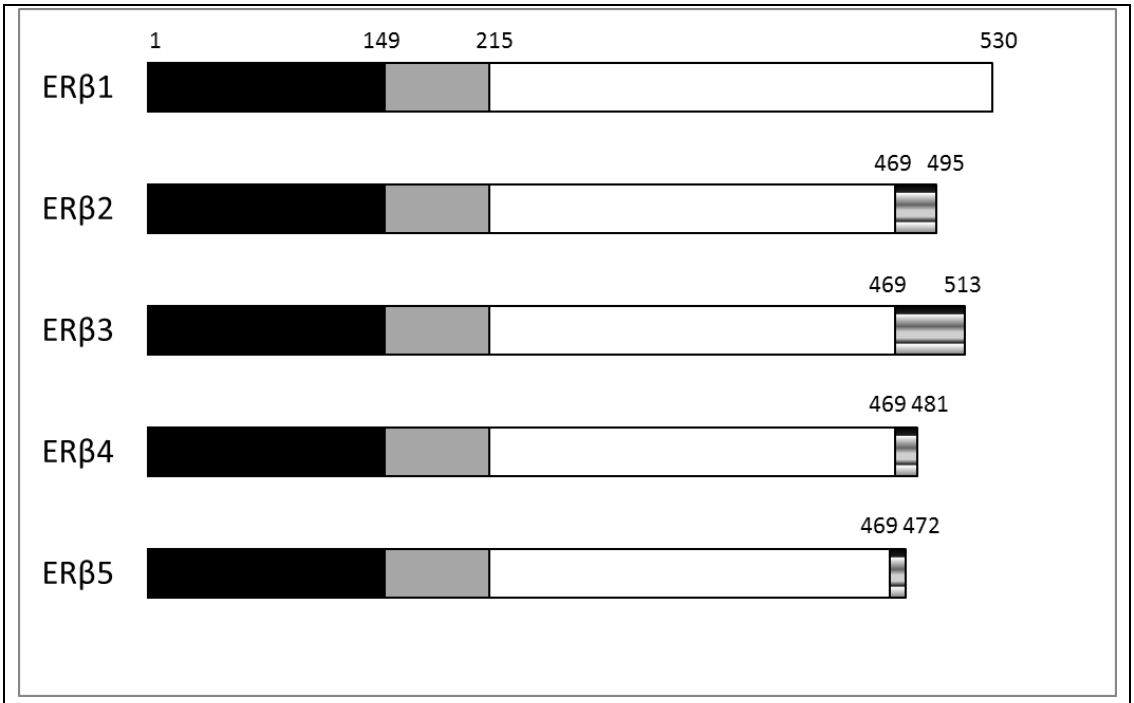

Figure 1.2: Known isoforms of human ERβ

Based on the description by Moore et al. (1998). The main, wild type, human ERβ (ERβ1, 530 amino acids long), and its four isoforms (ERβ2-5), generated by alternate exon splicing. N-D (black bar) represents the N-terminal domain, DBD (grey bar) is the DNA binding domain, and LBD represents the ligand binding domain. Of the latter, the white bar represents the conserved LBD sequence, and the striped bars show where sequences diverge between the isoforms.

However, an *in vivo* study investigating the effect of a soy phytochemical-rich diet on MCF7 tumour xenografts in mice showed that the isoflavone diet reduced levels of ERα protein (by Western blot), but had no effect on transfected wild-type ERβ protein levels (Zhou et al. 2004). Genistein (up to 30 µM), or E2 (0.01 to 1 µM) treatment both increased the levels of the full length and β2 isoforms of ERβ in T47D cells, whilst reducing the levels of β5 (Cappelletti et al. 2006). At the same time, quercetin had slight but not significant effects, and only E2 treatment increased the levels of ERα present. Three or six months tamoxifen treatment reduced the level of ERα antibody staining observed in tumour biopsy samples from women with ERα+ breast cancer (n = 33). However, at the same time, this treatment had no impact upon the level of ERβ, or ERβ2 antibody staining (Miller et al. 2006). Furthermore, this group found no correlation between ERα, ERβ, and ERβ2 levels.

This suggests isoflavones, and other SERMS such as tamoxifen regulate the levels of ERα and ERβ differently in these breast cancer models. There may be an additional effect of the type of isoflavones used, or differences post-transcription in the transfected mouse model compared to the human colorectal and bovine models described previously. This would require further study to confirm.

In humans, the presence of ERα remains an important biomarker in breast cancer as it indicates a possible beneficial effect to the patient of endocrine treatment, although much remains to be determined regarding its precise role in mammary development and carcinogenesis (for review see Palmieri et al. 2002). Studies using individual or combined knock-outs of ERα and ERβ in mice have demonstrated that the two receptors have different roles in mouse fertility. These two knockout mouse lines, known as αERKO and βERKO respectively, are widely used, and their reproductive phenotype is well established. They both display differing sexual behaviour, and both αERKO males and females are infertile, but βERKO males have normal fertility, and βERKO females are subfertile to varying degrees (Dupont et al. 2000; Hewitt and Korach 2003; Kudwa and Rissman 2012).

Although the role of ERα and ERβ in mammary development is difficult to measure due to the presence of ERβ splice variants, and also the likelihood of ovarian disruption which is common in ERKO mice, prepubertally, βERKO female mice develop mammary glands which appear normal (Hewitt and Korach 2003). However, sexually mature βERKO female mammary glands are less developed with less branching than wild type, although often able to function and lactate near-normally, and have a normal proliferation response upon E2 treatment (Hewitt and Korach 2003; Palmieri et al. 2002). By contrast, αERKO females do not develop mammary glands (Hewitt and Korach 2003). This implies that ERβ has a role in the differentiation of the mammary gland during puberty, but is not required for E2-induced mammary proliferation or pre-pubertal mammary gland formation, while ERα has an indispensable role early on in mammary gland development.

The two receptor subtypes have overlapping and yet unique sets of downstream oestrogen responsive target genes, as shown by gene expression profiling microarrays (Zhao et al. 2008). Similarly, gene expression profiling of aortas isolated from mice with either ERα or ERβ knockout have shown that while ERα is essential for the majority of E2-mediated increases in gene expression, ERβ

mediates nearly 90% of E2-induced decreases in gene expression (O'Lone et al. 2007).

In human breast cancer cells it is generally agreed that ERα mediates the proliferative effects of E2 and isoflavones (Maggiolini et al. 2001), and transfection with an antisense ERα gene to silence ERα expression inhibited E2 induced proliferation in human BG-1 and 2008 ovarian cancer cells (Albanito et al. 2007). Regrettably there have been few quality studies examining the role of ERβ in breast cancer, and its role is not fully understood. Expression of full length ERβ (wild type; ERβ1) appears to relate to more aggressive tumor types, such as HER2+ or triple negative (ERα-, PR-, HER2-) cancers, and acts as an independent predictor of recurrence, but also indicates promising response to endocrine therapy and overall survival (Skliris et al. 2008; Speirs 2008). This positive association with good response to endocrine therapy and promising prognosis may relate to the fact that in approximately 58% of breast tumours ERβ1 is co-expressed with ERα, or 60% in the case of total ERβ (Skliris et al. 2008). However, a further 18% of all breast tumours can be classified as ERα-/ERβ+ (Skliris et al. 2008). Evidence also exists to suggest that ERβ is a tumor suppressor gene: compared to normal or benign breast tissue, expression of ERβ is lost or reduced in the majority of malignant breast tumours (Rody et al. 2005; Zhao et al. 2003).

1.4.2 Techniques for assessing the impact of isoflavones on breast cancer cell proliferation *in vitro*

Numerous techniques have been used to assess the effect of isoflavones on the proliferation of breast cancer cell lines (Table 1.3). Traditionally, cell counting using a haemocytometer with or without Trypan Blue dye has been widely used in this field (Maggiolini et al. 2001; Ying et al. 2002). This method is discussed in detail in (Sections 2.2 and 2.3). However, it is relatively insensitive and open to error (Burton 2005). This can be overcome by use of an automated cell counter (Matsumura et al. 2005).

Frequently, labeled thymidine (^{3}H-thymidine) is incorporated into cell growth medium, allowing proliferation to be quantified by the degree of incorporation of the radioactive label into newly synthesized DNA during cell division (Hwang et al. 2006; Kang et al. 2009). While this method considered valid for this use by some (Burton 2005), considerable evidence exists suggesting that the presence of the low energy β-irradiation emitting tracer can inhibit proliferation, induce apoptosis, and reduce DNA synthesis (Hu et al. 2002).

However, the most widely used method in this subject area is the MTT assay (Cherdshewasart and Sriwatcharakul 2008; Liu et al. 2010; Rajah et al. 2009; Theil et al. 2011; Umehara et al. 2009; Yang et al. 2010; Ying et al. 2002; Yuan et al. 2012). This technique is discussed further in sections 2.4 and 6.11). Briefly, it utilizes a yellow, water soluble dye, 3-(4, 5-dimethylthiazol-2-yl)2, 5-diphenyl tetrazolium bromide (MTT), which is metabolized by viable, actively metabolizing cells into a purple product. The intensity of the purple colour can be quantified using a spectrophotometer, and directly reflects the number of actively metabolizing cells present. Other groups have used the WST-1 assay (Ying et al. 2002), or the MTS assay (Seo et al. 2006), which are related techniques, with slight variations to the tetrazolium-type dye used. The AlmarBlue dye used by Umehara et al. (2009) works by a similar mechanism, whereby the stain is metabolized by viable cells into a fluorescent product.

Table 1.3: Summary of methods used to investigate the effects of isoflavones on breast cancer cell proliferation

Study	Cell line	Vehicle (dose used for control)	Proliferation assay	Isoflavone treatment (days)
Cherdshewasart and Sriwatcharakul (2008)	MCF7	DMSO (2%)	MTT	3
Choi et al. (2009)	MCF7	DMSO (x)	MTT	1
Constantinou et al. (1998)	MCF7, MDA-MB-468	DMSO (x)	Haemocytometer / Trypan Blue dye exclusion	3
Davis et al. (2008)	MCF7, MDA-MB-231	DMSO (x)	CellTiter 96® aqueous non-radioactive cell proliferation assay (MTS)	6
Ferenc et al. (2010)	MCF7, MDA-MB-231	Vehicle unknown - Untreated control	MTT / automated cell counter	1, 2
Hwang et al. (2006)	MCF7	Vehicle unknown (x)	Labelled thymidine incorporation	2
Jacobs et al. (2000)	MCF7, T-47D, MDA-MB-231	DMSO (0.2%)	MTT	5-14 *
Jin et al. (2010)	MCF7	DMSO (0.1%)	MTT	1, 2, 3
Kang et al. (2009)	MCF7, MDA-MB-231	Vehicle unknown (x)	Labelled thymidine	3

Study	Cell line	Vehicle (dose used for control)	Proliferation assay	Isoflavone treatment (days)
Li et al. (2008)	MDA-MB-231	Ethanol (0.1%)	MTT	2
Liu et al. (2010)	MCF7, MDA-MB-231	Ethanol (0.1%)	MTT	3
Maggiolini et al. (2001)	MCF7	Vehicle unknown (x)	Haemocytometer, MTT	6
Matsumura et al. (2005)	MCF7	Ethanol (0.1%)	Automated cell counter	7, 14
Peterson and Barnes (1996)	MCF7, T47D, BT20, ZR75-1	DMSO (1%)	MTT, labelled thymidine incorporation	4
Rajah et al. (2009)	MDA-MB-231, T-47D	DMSO (0.1%)	MTT	3
Sakamoto et al. (2010)	MCF7	DMSO (x)	Colony formation assay	14
Schmidt, Michna and Diel (2005)	MCF7	DMSO - untreated control	Flow cytometry - % cells in S phase of cell cycle	5
Seo et al. (2006)	MCF7	Ethanol (0.1%)	CellTiter 96® aqueous non-radioactive cell proliferation assay (MTS)	2, 3, 6, 8
Seo et al. (2011)	MDA-MB-231	DMSO (0.2%)	Haemocytometer	3

Study	Cell line	Vehicle (dose used for control)	Proliferation assay	Isoflavone treatment (days)
Shim et al. (2007)	MCF7	DMSO/Ethanol, 1:1 (0.05%)	MTT	1
Shon et al. (2006)	MCF7, MDA-MB-231	Vehicle unknown (x)	MTT	2, 4, 6
So et al. (1997)	MCF7	DMSO (0.6%)	MTT, labelled thymidine incorporation	3
Song et al. (2007)	MCF7	Ethanol (x)	Automated cell counter	4
Theil et al. (2011)	MCF7, BT20	Ethanol (1%)	MTT, BrdU	1
Umehara et al. (2009)	MCF7, T47D	DMSO (1%)	AlmarBlue fluorescence	4
Yang et al. (2010)	MCF7, ZR75-1, MDA-MB-435,	Vehicle unknown (x)	MTT	6
Ying et al. (2002)	T47D	DMSO (0.1%)	WST1, Trypan Blue dye exclusion	1, 2
Yuan et al. (2012)	MCF7, T47D	DMSO/Ethanol, 1:4 (0.1%)	MTT	3
Zava and Duwe (1997)	MCF7, T47D, MDA-MB-468	Ethanol (0.1%)	Total DNA content (by propidium iodide fluorescence assay)	10

** Not isoflavones, E2 only; (x) dose for control not given*

1.4.3 Oestrogen and isoflavones at physiological concentrations enhance the proliferation of ERα+ breast cancer cells similarly

Numerous animal and *in vitro* studies suggest that E2 induces proliferation in a range of mammalian cell types (Dos Santos et al. 2010; Kumar et al. 2010; Miki et al. 2009; Ren et al. 2010). Likewise, in ERα+ breast cancer models such as MCF7, ZR75-1 or T47D cells, at its range of physiological concentrations (between 1 pM and 10 nM) E2 stimulates proliferation (Davis et al. 2008; Jacobs et al. 2000; Lau et al. 2009; Matsumura et al. 2005; Rajah et al. 2009; Schmidt et al. 2005; Song et al. 2007; Sotoca et al. 2008; Zava and Duwe 1997). However, E2 (1nM) had no significant effect on the proliferation of ERα-/ERβ+ MDA-MB-231 cells (Jacobs et al. 2000; Rajah et al. 2009).

Similarly, low doses of isoflavones (ranging from 1 nM to 10 µM, reflecting serum levels seen with low to high consumers of soy) induce the proliferation of ERα+ breast cancer cells including MCF7 and T-47D dose dependently. This effect occurs with genistein, daidzein, equol, and other isoflavones, although daidzein frequently results in a lower magnitude effect than genistein. This effect of the isoflavones is similar to that of E2, although at least 1000-fold higher concentrations of isoflavones are required to achieve comparable proliferation (Cherdshewasart and Sriwatcharakul 2008; Hendrix et al. 2006; Hwang et al. 2006; Kang et al. 2009; Liu et al. 2010; Maggiolini et al. 2001; Matsumura et al. 2005; Rajah et al. 2009; Seo et al. 2006; Umehara et al. 2009; Yang et al. 2010; Ying et al. 2002; Yuan et al. 2012; Zava and Duwe 1997). Microarray gene expression analysis confirms that 48 hour treatment of MCF7 cells with 1 or 5 µM genistein elicits gene expression patterns indicative of increased mitotic growth (Lavigne et al. 2008).

A wide range of techniques have been used to generate this information, summarized in Table 1.3. On the whole, broadly similar growth conditions have been used in each instance. These comprise a period of 1 to 3 days oestrogen washout prior to treatment, in phenol red free[2] growth medium supplemented with dextran/charcoal stripped fetal bovine serum (DC-FBS), to eliminate the possibility of the oestrogenic content of these components confounding the oestrogenic effects

[2] Phenol red, a pH indicator commonly added to tissue culture medium has a weak oestrogenic effect (Katzenellenbogen et al. 1987).

seen. This is followed by isoflavone treatment for between one and 14 days, then measurement. On the one hand the range of methods and time scales used argues that the effects of isoflavones on the proliferation of breast cancer cells is reproducible regardless of method used, and stands up to scrutiny. However, as different methods have been used, care must be taken when comparing their results.

Notable exceptions are Ying et al. (2002), who conducted their experiments with standard media containing phenol red, and Kang et al. (2009) used FBS that was not stripped of hormones. While their results do not appear to differ from those of the other groups, the presence of phenol red and standard serum in the media can increase the growth rate of MCF7 cells in a weakly oestrogenic manner, and this could influence their results (Katzenellenbogen et al. 1987).

Most groups have compared their treatments to a control treated with the ligand vehicle alone: dimethyl sulfoxide (DMSO), ethanol, or a mixture of both. The majority of these groups used these solvents at a dose of 0.1% in the final solution, which is unlikely to cause any significant effects. However, in some cases, discussed in further detail in section 6.1.2, the choice and dose of solvent may have an impact on cell proliferation. Furthermore, in several cases it is not apparent which solvents and doses were used.

It is interesting to note that the phase II metabolites of genistein (genistein-7-glucuronide, genistein-7-sulfate and genistein-4'-sulfate) had very little impact upon the proliferation of MCF7 or T47D cells after 72 hour treatment with 5.1nM to 80µM doses (Yuan et al. 2012). However, the overall impact of these metabolites can only be guessed at, as the preparations used in this study were not pure. In addition, this group demonstrated that even in the cell lines, genistein was quickly and extensively metabolized to these products, and others, which also demonstrated metabolism back into the aglycone form. Based on this, and the low oestrogenic activity of numerous of the metabolites compared to the parent aglycones (Pugazhendhi et al. 2008; Zhang et al. 1999), Yuan et al. concluded that the metabolism of genistein had no discernible impact upon its effects on the proliferation of the cell lines tested.

Concerningly, these proliferation-enhancing concentrations of isoflavones echo the circulating levels seen in most European and American women. However, this

growth-enhancing effect is limited to ERα+ cells. Addition of oestrogen receptor blockers such as tamoxifen or ICI 182780, also known as fulvestrant or Faslodex, prevents isoflavones from inducing proliferation (Hwang et al. 2006; Liu et al. 2010; Maggiolini et al. 2001). This suggests that isoflavones may act on proliferation through the ERs, and are acting as oestrogen agonists.

Interestingly, tamoxifen (10 nM) also promotes the proliferation of MCF7 breast cancer cells (Coiret et al. 2007). This effect has been shown in a number of ERα+ breast cancer cell models, and is associated with the development of tamoxifen resistance (Clarke et al. 2001; Keeton and Brown 2005). Higher concentrations of tamoxifen, from 1μM upwards, inhibit the growth of both MCF7 and MDA-MB-231 breast cancer cells, in addition to a number of human prostate and colon cancer cell lines (Abdul et al. 2003; Tanos et al. 2002). On the contrary, the full oestrogen antagonist ICI 182 780 inhibits proliferation and induces apoptosis in MCF7 cells at all doses tested between 10 nM and 10 μM (Schmidt et al. 2005).

1.4.4 Physiological doses of isoflavones and ERα-/β+ cell proliferation

As ERα-/β+ cell lines such as MDA-MB-231 have traditionally been regarded as ER-negative, there has been very little research into the effects of the doses of isoflavones known to promote proliferation in an oestrogenic manner (≤ 1 μM). However, the few studies identified yield some very interesting results. Rajah et al. (2009) showed that while 1 nM to 1 μM genistein treatment for 72 hours resulted in a dose-dependent increase in the proliferation of T47D cells, compared to the vehicle (0.1% DMSO) alone, the same regime with MDA-MB-231 cells resulted in approximately 20% inhibition of proliferation. Similar results have been generated by Kang et al. (2009) using MCF7 and MDA-MB-231 cells, although with the higher dose of 18 μM genistein.

A different approach was taken by Sotoca et al. (2008). This group used T47D cells, with or without a tetracycline-inducible ERβ gene. This cell line normally expresses ERβ at a relatively low level compared to ERα (Tong et al. 2002). With this low level of ERβ expression, 48 hours of genistein or quercetin treatment (0.001 to 5 μM) increased proliferation compared to a DMSO only control. However, increasing the expression of ERβ reduced the isoflavone induced enhancement of proliferation previously seen. Similarly, it was found that by artificially increasing ERβ levels in a number of ERα-dominant breast cancer models (including MCF7 and T47D cell culture, and MCF7 tumours implanted into mice) E2 treatment began to exert a negative effect on cell proliferation as ERβ expression levels increased to match ERα (Chang et al. 2006; Paruthiyil et al. 2004; Sotoca et al. 2008; Strom et al. 2004). A variety of different methods were used in these studies to quantify ERβ expression and protein levels, including use of FLAG antibodies, polymerase chain reaction (PCR), and quantification of the levels of fluorescence from a luciferase reporter gene product stably transfected along with the ERβ gene. It has been hypothesised that ERα mediates the growth promoting effects of physiological levels of isoflavones, while through ERβ they act in a growth inhibitory manner, with the outcome depending upon the ratio of ERα:ERβ This will be further discussed in section 6.1.5.

In the apparently ERα-/ERβ- cell line MDA-MB-435, genistein treatment at levels between 0.1 and 10 μM had no significant effect on cellular proliferation (Seo et al. 2006; Yang et al. 2010). Similar results were also demonstrated with the

phytoestrogen apigenin (Seo et al. 2006). Interestingly, genistein up to 10μM had no effect on the proliferation of MDA-MB-435 cells transfected with ERβ (Yang et al. 2010). However, the relevance of these results are debatable. Firstly, a variant of this cell line known as MDA-MB-435s is known to express ERβ, calling into question its ERβ- status. Secondly, evidence exists suggesting that this cell line is in fact of melanoma origin, not breast (Rae et al. 2007).

Likewise, genistein treatment at levels up to 10μM had no impact upon the proliferation of the breast cancer cell line BT20 (Theil et al. 2011). They proposed this cell line to be ERα-/β-, as it showed no reaction with an ERβ antibody. However, ERβ mRNA for a number of the known ERβ isoforms (β1, β2 and β4) is present in BT20 cells (Tong et al. 2002). This discrepancy may relate to post-transcriptional events, or may be an artefact introduced by the choice of antibody used by Thiel et al., and as a result the ERβ status of BT20 remains unclear.

Similarly, genistein treatment up to and including 1μM had no significant impact upon the proliferation of MDA-MB-468 cells (Zava and Duwe 1997). This cell line is known to be ERα-, but its levels of ERβ are not known (Table 1.2).

1.4.5 Inhibition of proliferation by isoflavones in breast cancer cells

The effect of isoflavones on the growth of ERα+ breast cancer cells is biphasic. At higher concentrations (10 µM upwards), similar to the circulating levels in the very highest soy consuming Eastern-Asians (Arai et al. 2000), isoflavones are cytotoxic, reducing proliferation in MCF7 (Table 1.4), ZR75-1 and T47D breast cancer cell lines in a dose responsive manner (Choi et al. 2009; Constantinou et al. 1998; Davis et al. 2008; Ferenc et al. 2010; Jin et al. 2010; Kang et al. 2009; Liu et al. 2010; Maggiolini et al. 2001; Peterson and Barnes 1996; Sakamoto et al. 2010; Shim et al. 2007; Shon et al. 2006; Theil et al. 2011; Yang et al. 2010; Ying et al. 2002).

As with the lower isoflavone concentrations, a wide range of techniques and time scales have been used to investigate the impact of this higher concentration range of isoflavones on breast cancer cell proliferation (Table 1.4). Most studies have used phenol red free medium supplemented with 10% DC-FBS for the duration of their experiments. Exceptions to this are Liu et al. (2010), who used 5% FBS, and a number of groups used standard phenol-red containing medium and 10% FBS for experimental treatments (Choi et al. 2009; Ferenc et al. 2010; Seo et al. 2011; Shon et al. 2006).

These differences in protocol make direct comparisons between these studies difficult. Accordingly, the groups propose a wide range of concentrations at which genistein ceases to promote MCF7 proliferation, and begins to inhibit it. In MCF7 the IC_{50} (dose required for inhibition of the maximal response by 50%) for the inhibition of proliferation by 24 hour genistein treatment has been proposed to be 27.5µM (Shim et al. 2007). This figure seems broadly representative of the studies described, with the exceptions of Liu et al. (2010) and Yuan et al. (2012) which suggest that genistein concentrations vastly in excess of this would be needed to see an inhibitory effect on proliferation. The treatment duration does not appear to have an impact upon the concentration of genistein required to inhibit proliferation in MCF7.

Table 1.4: Inhibition of MCF7 proliferation by genistein, summary of previous results

Study	Lowest genistein conc. at which growth inhibition occurs	Time (days)
Choi et al. (2009)	3.5μM	1
Constantinou et al. (1998)	10μM	3
Davis et al. (2008)	10μM	6
Shim et al. (2007)	15μM	1
Yang et al. (2010)	17μM	6
Kang et al. (2009)	37μM	3
Ferenc et al. (2010)	50μM	1, 2
Shon et al. (2006)	50μM	2, 4, 6
Maggiolini et al. (2001)	>10μM*	6
Sakamoto et al. (2010)	>10μM*	14
Liu et al. (2010)	>50μM*	3
Yuan et al. (2012)	>80μM*	3

** Proliferation at these concentrations was still greater than with the control treatment, although it had peaked at a lower concentration and was dropping.*

Microarray gene expression analysis has shown that 48 hour treatment of MCF7 cells with 25 µM genistein results in a reduced proliferative gene expression profile (Lavigne et al. 2008). However, often the isoflavone doses used are very high, up to 150 µM. These doses are not achievable in the blood through diet alone, making their physiological relevance questionable.

Where daidzein has been used the effect is comparable (Jin et al. 2010; Ying et al. 2002), although possibly slightly higher concentrations may be required to have the same effect (Constantinou et al. 1998). This again is dose dependent.

A similar effect is seen in the ERα-/ERβ+ breast cancer cell lines MDA-MB-231 (Table 1.5), and BT20 and MDA-MB-468 (ERβ-status not known), with treatment with isoflavones above 10 µM reducing proliferation in a dose responsive manner (Constantinou et al. 1998; Ferenc et al. 2010; Kang et al. 2009; Li et al. 2008; Peterson and Barnes 1996; Rajah et al. 2009; Seo et al. 2011; Shon et al. 2006; Theil et al. 2011; Zava and Duwe 1997). Most studies have used genistein for this, although resveratrol, daidzein, equol and biochanin A act similarly. As discussed, lower concentrations of genistein (down to 1nM) have only been used with MDA-MB-231 cells on one occasion, and were also found to inhibit proliferation (Rajah et al. 2009).

Interestingly, 2' hydroxylation of genistein by the enzyme isoflavone 2'-hydroxylase made it approximately twice as effective at decreasing MCF7 viability at the same dose of unhydroxylated genistein (Choi et al. 2009). This genistein metabolite also has greater antioxidant capacity than its parent molecule, and may more closely reflect the impact of partial metabolism of genistein by gut microflora.

Concentrations of genistein above 10µM have not been widely used to assess their impact on proliferation of breast cancer cell lines with other hormone receptor status. However, 17 and 50µM genistein reduced the proliferation (MTT assay) of MDA-MB-435, ZR75-1 and SK-BR-3 breast cancer cells (Tong et al. 2002; Yang et al. 2010). This suggests that the inhibition of proliferation by high (upwards of 10 or 50µM) concentrations of isoflavones may be a universal phenomenon in breast cancer cell lines, regardless of ER status. Furthermore, inhibition of MCF7 proliferation by the pharmacological dose of 100µM genistein was not abrogated by

the ER-antagonist ICI 182780 (Maggiolini et al. 2001). However, the significance of the use of this very high dose is limited, as it was likely to be acting in a non-specific cytotoxic manner.

Table 1.5: Inhibition of MDA-MB-231 proliferation by genistein, summary of previous studies

Study	Lowest genistein conc. at which growth inhibition occurs	Time (days)
Rajah et al. 2(009)	1nM	3
Li et al. (2008)	5µM	2
Kang et al. (2009)	18.5µM	3
Ferenc et al. (2010)	50µM	1, 2
Seo et al. (2011)	100µM	3

1.4.6 Combinatory effects of isoflavones and oestrogen on breast cancer cell proliferation

These studies do not explain why in epidemiological studies isoflavones appear to be more protective against premenopausal, and ERα+ breast cancers, or why dietary isoflavones do not significantly increase breast cancer risk when in low doses. The interactions between isoflavones and endogenous oestrogens have been investigated to attempt to answer some of these questions.

At high isoflavone concentrations previously shown to reduce proliferation (5μM and above) several laboratories have shown that in ERα+ MCF7 and T47D cells, genistein partially or fully reversed the growth stimulatory effect of premenopausal and postmenopausal E2 levels (Maggiolini et al. 2001; Matsumura et al. 2005; Miodini et al. 1999; Peterson and Barnes 1996; So et al. 1997; Wang and Kurzer 1998; Zava and Duwe 1997). This ability of the isoflavones is unrelated to their oestrogenic activity, as an identical response was seen in a hormone insensitive strain of MCF7 (Maggiolini et al. 2001), and in ERα- MDA-MB-231 cells (Rajah et al. 2009). In a more recent study, 10 nM E2 and 10 μM glycitein (and genistein and daidzein to a lesser extent) resulted in significantly less MCF7 proliferation than the control (vehicle only) or E2 alone (Sakamoto et al. 2010). These results correspond with data from epidemiological studies showing a reduction in breast cancer risk (premenopausally) associated with high isoflavone intake (Section 1.3.1), although the isoflavone concentrations used *in vitro* are frequently higher than those observed *in vivo*.

However, the results of studies looking at the effects of lower (more relevant to Western populations) concentrations of isoflavones at physiological E2 levels are less conclusive. At postmenopausal E2 concentrations (10pM), one study suggested that expression of a reporter gene tagged to an oestrogen responsive (ERα or ERβ) promoter in human embryonic kidney 239 cells was increased by treatment of 1 nM to 1 μM daidzein or several of its metabolites (tetrahydrodaidzein, equol and O-desmethylangolensin), making them oestrogen agonists in these conditions, and acting in an additive manner with E2 (Hwang et al. 2006). With premenopausal E2 (1 nM) equol and tetrahydrodaidzein tended to inhibit oestrogen induced reporter transcription *via* ERα, and to a greater extent *via* ERβ (Hwang et al. 2006). The same group reported a similar pattern of results for proliferation in

MCF7 cells, although did not show the results. Likewise, activity of rat ERα and ERβ-mediated luciferase reporter gene (where the ERs and reporter were transfected into human hepatoma HepG2 cells) was enhanced in an additive manner by genistein (0.1μM to 1nM) at low concentrations of E2 (10pM and 100pM), but at E2 concentrations above this (1nM to 100nM) there was maximal reporter activity which was not affected by the presence of genistein (Casanova et al. 2012).

In MCF7 cells, 24 hour treatment with genistein up to 1μM and low levels (10pM or 100pM) of E2 had a synergistic effect on DNA synthesis (labeled thymidine incorporation), which was not apparent at higher E2 concentrations (Wang and Kurzer 1998). Similarly, others present data demonstrating that the ability of these lower concentrations of genistein to induce MCF7 proliferation or expression of ERE-reporter gene constructs in MCF7 was lost when they were treated with genistein or daidzein in combination with physiological levels of E2 between 0.1 and 1nM (Matsumura et al. 2005; Schmidt et al. Diel 2005).

Overall, these studies imply that *in vitro*, post-menopausally, low (1nM to 1μM) levels of isoflavones may function as oestrogen agonists, promoting ERα-induced transcription and the growth of ERα+ breast cancer cells, while pre-menopausally they are masked by the stronger oestrogenic effect, or may have some slight inhibitory effect.

On the other hand, Rajah et al. (2009) present evidence for a synergistic inhibitory effect of genistein (1nM to 100μM) and 1nM E2 on MDA-MB-231 proliferation. In this case they report approximately 40% reduction in proliferation with the combined treatments, compared to around 17% with genistein alone.

These studies provide some evidence for the mechanism through which high levels of isoflavones, similar to those achieved in the diet of Eastern-Asians consuming 'traditional' high-soy diets, could protect against breast cancer. Additionally, lower levels of genistein may be of benefit against ERα- tumours, and ERα+ breast cancer in a premenopausal E2-environment, but could increase risk postmenopausally. However, many of the conclusions regarding the effects of lower levels of isoflavones at physiological E2 levels are based on ER-induced transcription (including that mediated by the rat homologues of ERα and ERβ) rather than cell proliferation, and what remains regarding MCF7 proliferation, particularly at

postmenopausal E2 levels, is less convinving. Many of the studies have replicated either pre- or postmenopausal E2 concentrations (not the full set) and there is no data available regarding the effect of daidzein at postmenopausal E2 levels on proliferative outcomes. Additionally, in epidemiological studies, the protective effect of isoflavones appears stronger for ERα+ breast cancers, but *in vitro* the anti-proliferative and cytotoxic properties of isoflavones are independent of the ER status of the cells. Furthermore, the majority of studies described are limited by only using ERα+ cell lines.

1.4.7 Summary of the effects of isoflavones on breast cancer cell proliferation

Overall, the impact of isoflavones on breast cancer cell proliferation relates to the oestrogen environment and relative levels of the receptors ERα and ERβ. E2 alone at its physiological range of concentrations promotes the proliferation of ERα+ cell lines such as MCF7, but not ERα-/ERβ+ MDA-MB-231 cells.

Likewise, in the absence of E2, isoflavones promote the proliferation of ERα+ breast cancer cell lines in a dose responsive manner up to concentrations of around 10μM. This occurs oestrogenically, *via* ERα, and is inhibited by the addition of ER antagonists. Proliferation is biphasic in these cell lines, and peaks at around 10μM then begins to drop. The inhibition of proliferation in MCF7 is not mediated by the ERs.

In MDA-MB-231 and other ERα-/ERβ+ cell lines however, even relatively low concentrations of genistein (1nM to 1μM) result in a slight inhibition of proliferation, although more dramatic inhibitory effects are seen at higher concentrations (>10μM). The inhibitory effect appears to be related to the ratio of ERα:ERβ, with increasing expression of ERβ resulting in a more pronounced inhibitory effect on proliferation.

As many of the effects of isoflavones are oestrogen-agonistic, and are mediated by the ERs, it follows that the presence of endogenous oestrogens will impact upon their effectiveness. However, there is little data regarding their impact upon proliferation in the presence of E2, and what exists to date is of questionable value. In MCF7 high (>10μM) concentrations of genistein antagonize the proliferative effect of physiological E2 levels, in an ER-independent manner. However, depending on the concentration of E2 present, lower (more physiologically relevant) genistein concentrations have been shown variously to act synergistically with E2 (postmenopausally), have no net effect, or act as E2 antagonists (premenopausally). As discussed, much of this is based on data regarding ER-mediated transcription of reporter genes rather than proliferation. This requires clarification.

Many questions remain regarding the effects of isoflavones at endogenous E2 levels, particularly postmenopausally, and in ERα-/ERβ+ cell lines. In addition to this, caution must be exercised when directly translating *in vitro* results to *in vivo*

effects, as many factors may affect the physiological response in the different systems. It is vital that evidence regarding the mechanisms through which isoflavones act *in vitro* is confirmed *in vivo* before recommendations are made. However, it remains possible that much of the proposed anti-proliferative activity of isoflavones lies in their ability to compete with endogenous oestrogens for oestrogen receptor binding sites.

However, it is apparent that they may also moderate breast cancer risk through their pro-apoptotic, anti-angiogenic, antioxidant and numerous other non-genomic mechanisms.

1.5 Induction of apoptosis in breast cancer cells

The mechanisms through which isoflavones have been proposed to mediate their anti-proliferative effects are many, and cannot all be discussed in this review. Some of these effects include acting as antioxidants (Choi et al. 2009), modifying the activity of growth factor signaling including the Mitogen Activated Protein Kinase (MAPK) and IGF1 pathways (Chen et al. 2007; Liu et al. 2010; Lucki and Sewer 2011), antagonizing oestrogen and androgen mediated signaling (Banerjee et al. 2008), inhibition of angiogenesis (Garvin et al. 2006; Yu et al. 2012) and inhibition of oestrogen biosynthesis (Brooks and Thompson 2005). Furthermore, E2 and isoflavones have been shown to regulate a number of the intracellular processes required for apoptosis in breast cancer cells. These include modifying intracellular calcium levels and caspase activation, both of which may be central to their effects on the induction of apoptosis.

1.5.1 Morphological definition of apoptosis

The term 'apoptosis'[3] was first coined in 1972 to describe a distinct series of well defined morphological events known as programmed cell death (Kerr et al. 1972). Apoptosis is a highly regulated process, which is essential to growth and development. It is triggered extrinsically by membrane bound 'death' receptors or ligand deprivation-induced dependence receptor, or intrinsically by intracellular stress conditions, leading to the permeablization of the mitochondrial outer membrane which triggers mitochondria mediated signaling pathways (Galluzzi et al. 2011; Roy and Hajnoczky 2008).

Following this are the morphological events which give apoptosis its name. This begins with the severing of attachments to other cells and extracellular matrix and the cell becoming more round. In parallel, the cell shrinks. This is followed by the plasma membrane forming protrusions known as "blebs" whilst retaining its integrity. Meanwhile chromatin condenses (pyknosis) then DNA and the nucleus fragments (karyorrhexis). Vacuoles have been observed in the cytoplasm of dying cells. Finally the cell disintegrates into membrane bound apoptotic bodies which are taken up by phagocytes (Hacker 2000; Kroemer et al. 2009; Krysko et al. 2008; Maeno et al. 2000; Orrenius et al. 2003).

These morphological changes, along with changes to mitochondrial outer membrane permeability (MOMP), externalization of phosphatidyl serine on the outer leaflet of the plasma membrane, and activation of caspases make apoptosis readily distinguishable from other forms of cell death (Galluzzi et al. 2011; Krysko et al. 2008). Most notably this differs from necrosis, which is characterized by the unregulated swelling and bursting of cells, release of their contents, and resulting inflammation in neighbouring tissue.

[3] word "apoptosis" is derived from the Greek word "απόπτώσις" describing the "dropping off" of petals from flowers or leaves from trees.

1.5.2 Biochemical events leading to intrinsic apoptosis

Intracellular stress such as DNA damage, oxidative stress and cytosolic Ca^{2+} overloading can result in the triggering of intrinsic apoptosis. Intracellular Ca^{2+} concentrations are a particularly versatile signaling mechanism in cells. Ca^{2+} levels can be controlled locally and at a cellular or tissue level by plasma membrane Ca^{2+} channels and the release of intracellular stores in the endoplasmic reticulum. Extracellular [Ca^{2+}] is usually over 1 mM, and under normal growth conditions cytoplasmic [Ca^{2+}] is around 100 nM (Roy and Hajnoczky 2008). Nuclear and mitochondrial matrix concentrations are typically similar, and concentrations inside the endoplasmic reticulum between 100 and 500 μM. Low amplitude transient fluctuations in concentrations activate processes such as secretion into vesicles and muscle contraction, and longer term oscillations in Ca^{2+} levels control many processes including proliferation and smooth muscle contraction. However, prolonged high levels of cytoplasmic Ca^{2+} result in apoptosis (Berridge et al. 1998; Roy and Hajnoczky 2008).

Sustained high concentrations of free intracellular Ca^{2+} induce Ca^{2+} uptake into the mitochondria, triggering the intrinsic apoptotic pathway (Figure 1.3). This is characterised by an increase in MOMP, as the Bcl2 family proteins, Bax and Bak, activated by Bid, form mitochondrial pores. This allows the release of the pro-apoptotic molecules cytochrome C, apoptosis inducing factor (AIF), apoptotic protease activating factor (APAF-1) and second mitochondrial activator of caspases (SMAC). Cytochrome C triggers the formation of the apoptosome, which recruits and mediates auto-activation of caspase 9 (Galluzzi et al. 2011; Orrenius et al. 2003; Roy and Hajnoczky 2008; Yigong 2009). Caspase 9 belongs to the cysteine-aspartic protease (caspase) family. Caspase 9, along with the extrinsically activated caspases 8 and 10 are known as initiator caspases. They exist as monomers in their inactive forms, and in response to various signals oligomerise into proteolytic caspases. They in turn cleave and activate a cascade of inactive effector caspase zymogens (Figure 1.4) into active proteins (Boatright and Salvesen 2003; Kauffmann et al. 2008; Riedle and Scott 2009). The effector caspases have over 400 substrates within the cell, and result in the morphological changes discussed, including DNA fragmentation and chromatin condensation. Inhibitors of apoptosis such as survivin and X chromosome-linked inhibitor of apoptosis (XIAP) bind to

caspases and deactivate them (Boatright and Salvesen 2003; Kauffmann et al. 2008; Yigong 2009).

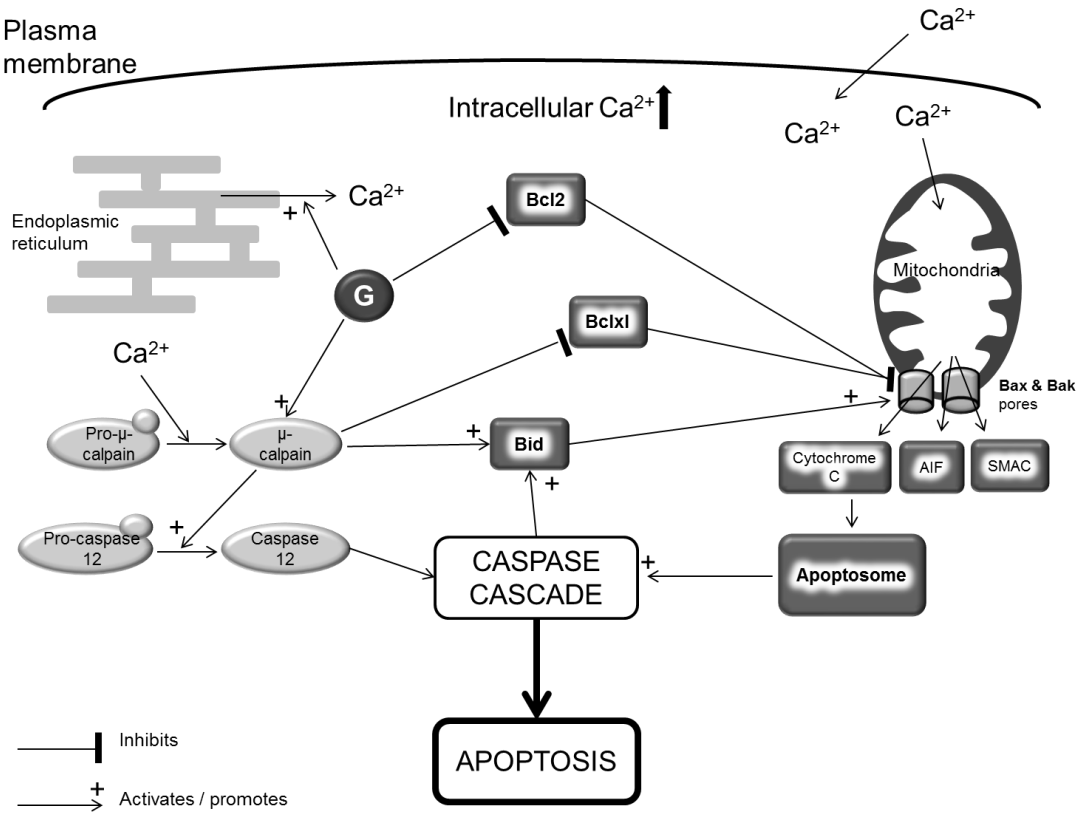

Figure 1.3: Genistein activates the intrinsic apoptotic pathway in MCF7 cells

AIF: Apoptosis inducing factor, G: genistein, SMAC: second mitochondrial activator of caspases

The triggering of the proteolytic caspase cascade results in activation of the pro-apoptotic proteins. Also among their many target proteins are the usually anti-apoptotic Bcl2 and Bcl-xl, which are converted to pro-apoptotic forms by proteolysis, and are then known to deactivate cyclin D1, DNA polymerase and several other growth and survival proteins (Orrenius et al. 2003).

In their anti-apoptotic forms, Bcl2 and Bcl-xl bind to Bax and Bak, preventing formation of the mitochondrial pore to release cytochrome C. Bcl2 can also block the release of Ca^{2+} from the endoplasmic reticulum. Both are oncogenes which are frequently overexpressed in tumours (Wen-Xing and Xiao-Ming 2009). E2 treatment of MCF7 cells has been shown to down-regulate expression of Bcl2 antagonists and

caspase 9, preventing induction of apoptosis by the intrinsic pathway in these cells (Frasor et al. 2003).

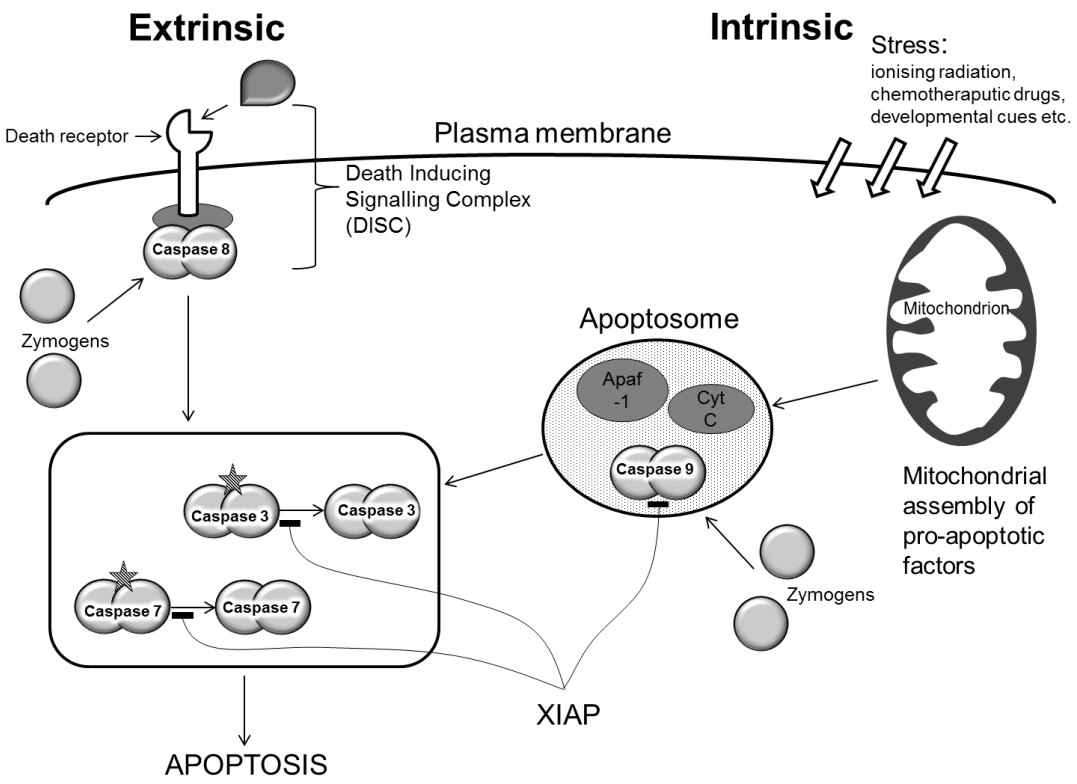

Figure 1.4: Role of the caspase activation cascade in apoptosis

During extrinsically induced apoptosis, the ligand activated death receptor (such as Fas receptor bound to Fas ligand) triggers the dimerization of caspase 8 (or caspase 10) from inactive zymogen monomers, forming a Death Inducing Signaling Complex (DISC). Intrinsic apoptosis is triggered by extracellular cues such as radiation and chemotherapeutic drugs, developmental cues, or mitochondrial stress. The mitochondrion triggers the formation of the apoptosome, including cytochrome C (Cyt C), apoptotic protease activating factor (Apaf-1), and dimerized, active caspase 9. Both caspase 8 and caspase 9 trigger proteolytic cleavage and hence exposure of the active sites of caspases 3 and 7. Activation of caspases 3, 7 and 9 can be inhibited by X-chromosome-linked inhibitor of apoptosis (XIAP). Active caspases 3 and 7 have many downstream targets, leading to the regulated death of the cell.

1.5.3 Techniques to assess apoptosis in breast cancer cells

The previously discussed morphological changes undergone by most apoptotic cells are very similar, and well defined. The key events of shrinkage of the cell, plasma membrane "blebbing", chromatin and nuclear condensation, nuclear fragmentation, and then disintegration of the cell into membrane bound 'apoptotic bodies' can be identified by microscopy (light or fluorescent), and are cheap and widely used methods for measurement of apoptosis (Hacker 2000; Krysko et al. 2008). However they are subjective and laborious to assess and fail to detect the early stages of lethal cascades which often do not result in gross morphological changes (Doonan and Cotter 2008; Galluzzi et al. 2009; Martin 2008). At the magnification levels used for light microscopy healthy cells containing large granules, and some cells which have recently undergone mitosis can appear apoptotic (Doonan and Cotter 2008). This can be avoided by using electron microscopy (Krysko et al. 2008), but many laboratories lack the facilities for this. So while light microscopy remains the simplest and most cost effective method to detect apoptosis, it must be used in combination with biochemical methods to generate reliable data.

Furthermore, many microscopy techniques (light, fluorescent and electron) require a fixation step prior to visualization. However, all fixatives modify cell structure to a greater or lesser extent (Bacallo et al. 2006). In particular, ethanol, methanol and acetone fixation result in cell shrinkage in the "z" dimension, and glutaraldehyde renders tissue auto-fluorescent so is of no use for fluorescence techniques. Formaldehyde/formalin fixation avoids these issues and it crosslinks nucleic acids, recommending it for the study of nuclear changes. However it can lead to extensive vesiculation of the plasma membrane.

Gross morphological changes in apoptotic cells can also be detected by flow cytometry. This is a laser based technique routinely used for cell sorting and biomarker detection. Cells are suspended in a stream of liquid and passed through a detection apparatus. This technique allows simultaneous detection of multiple parameters in 1000's of cells per minute. It can be used to assess the size of cells, presence of blebs, and granularity (Krysko et al. 2008). However, it requires the cells to be in suspension. Treatment of adherent cell lines such as MCF7 with trypsin can result in damage or permeablisation of the plasma membrane,

influencing the result, and their ability to grow in suspension may be limited so should be tested in advance.

Changes in nuclear morphology unique to apoptosis are widely used in its assessment, due to the ease with which they are detected with light, or fluorescence microscopy using DNA intercalating dyes such as Hoescht (Akter et al. 2012) or 4',6-diamidino-2-phenylindole (DAPI; Lai et al. 2003; Miglietta et al. 2006). Initially this comprises chromatin condensation around the nuclear membrane, which then spreads to encompass the whole nucleus (Hacker 2000). The condensation appears firstly as a brighter ring of fluorescence around the outside of the nucleus, then the whole nucleus becomes smaller, more circular and more brightly stained. The condensed nucleus then fragments within the cell. In MCF7 cells DAPI is known to bind to DNA with greater affinity than Hoechst, and is less toxic (Bielawski et al. 2001). The use of DAPI to assess apoptosis is described further in section 2.6. Apoptotic nuclei can appear smaller than normal nuclei, and this can be assessed by calculating the Nuclear Area Factor (NAF), which is a ratio of the size of the nucleus and its circularity (Daniel and DeCoster 2004; DeCoster 2007). However, this method is only effective in the very early stages of apoptosis (a matter of hours after the inducing treatment), before the nucleus fragments (Daniel and DeCoster 2004).

Nuclear morphological changes occur in parallel to caspase dependent fragmentation of chromosomal DNA. One widely used and sensitive method to assess this is the identification of the extensive fragmentation of nuclear DNA by Terminal deoxynucleotidyl transferase-mediated d-UTP Nick End Labeling (TUNEL) staining (Darzynkiewicz et al. 2008). An alternate way to identify this was to look for “DNA laddering” when DNA is extracted and separated by agarose gel electrophoresis. However, both methods are labour intensive, with the risk of disrupting or losing much of the signal. Furthermore, while DNA breaks are common in apoptosis, they are not a universal event, and the degree to which they occur can vary (Hacker 2000; Martin 2008). Searching for DNA ladders is now considered obsolete in this field (Kroemer et al. 2005).

Fragmentation and loss of nuclear DNA can also be assessed by flow cytometry using fluorescent DNA binding agents such as DAPI. Propidium iodide (PI), while frequently used as a counterstain to determine cell viability as it is excluded from

viable cells, is also widely used to assess cellular DNA content (Krysko et al. 2008). In this instance it allows classification of cells according to the quantity, and degree of fragmentation of DNA that they possess. Cells in the G1 stage of the cell cycle are diploid, and contain a uniform quantity of DNA. Cells in G2/M phase contain twice as much DNA as G1 cells (tetraploid). Apoptotic cells are hypodiploid, containing less DNA, which is fragmented. These cells are described as sub-G1 or sub-G0, and can be readily identified by this method. It is rapid and reproducible, and allows simultaneous use of other flurochromes such as Annexin V. However, as with the above techniques, there are a number of criticisms to consider. The non-universal nature of DNA fragmentation is a concern, and with this method the group of sub-G1 cells can also represent nuclear fragments and cells with abnormal chromatin structure (Riccardi and Nicoletti 2006). Additionally, the process recognizes apoptosis based on a reduced amount of DNA, but if the cell enters apoptosis from the tetraploid G2 or M stage then it is likely to have a greater DNA content than the diploid G1 population (aneuploiud) and so will not appear in the sub-G1 peak.

For these reasons a growing number of biochemical methods have been developed to measure features of apoptotic cells. The activation of caspases is commonly considered to be an unambiguous sign of apoptosis, detected either immunologically or fluorochrometrically, by cleavage of specific substrates or of the caspases themselves (Krysko et al. 2008). The initiator pro-caspases 8 or 9 are widely activated during apoptosis, but this feature is not universal (Galluzzi et al. 2011; Shim et al. 2007). Likewise, different downstream effector caspases can be activated in different caspase cascades depending upon the cell line and method of induction of apoptosis (Galluzzi et al. 2011). Effector caspase 3 is very widely involved in apoptosis in many cell lines (Jakob et al. 2008) but is absent in MCF7 (Janicke et al. 1998). Similarly, caspases 2, -6 and -7 are not universal (Galluzzi et al. 2011; Kauffmann et al. 2008). Care must be taken to make an appropriate choice of marker caspase.

Additionally, caspases are known to participate in non-death related scenarios meaning that specific substrates must be examined which are only cleaved by caspases in death scenarios (Galluzzi et al. 2009; Martin 2008). However, even the use of specific caspase substrates is limited, due to variable background caspase activity, and considerable overlap in the substrates available to each caspase

(Kauffmann et al. 2008). Immunoblotting to detect cleaved (active) forms of the effector caspases is an important approach to assess their activity. But this does not take into account the variable stability of the active form, or the presence of inhibitors such as XIAP inside the cell, meaning that the amount of cleaved caspase present may not reflect the amount that has been activated, or indeed whether they retain their activity (Kauffmann et al. 2008). Additionally, as discussed, some caspases acquire at least some of their activity without proteolytic cleavage. Taken together, complementary caspase assays should be used to demonstrate caspase activation.

Where caspase inhibitors have been used to disrupt apoptosis, caution is also required. The "universal" caspase inhibitor Z-VAD-fmk does not in fact inhibit all caspases to the same extent. In addition, while caspase inhibition does prevent some caspase-dependent signs of apoptosis such as chromatin condensation of DNA fragmentation, it has been shown to only retard, and not prevent death (Kroemer et al. 2005).

Fluorescent or immunofluorescent microscopy is more sensitive than light microscopy and can allow simultaneous or independent analysis of multiple apoptotic parameters as long as care is taken to ensure that emission spectra of dyes do not overlap (Galluzzi et al. 2009). Likewise, numerous fluorescent techniques have been modified for use with flow cytometry. Annexin V coupled fluorochromes are frequently used to detect phosphatidyl serine (PS) externalisation on the plasma membrane, and use of counterstains such as DAPI, PI or hoescht are common to detect nuclear changes. However, while fluorescence techniques are popular, they have several limitations which must be considered (Cannel and Thomas 1994). Firstly, the photons supplied to the cells will interact with any molecule which absorbs in the range of that photon, which can lead to false positives or autofluorescence. This energy supplied to the cell generates heat which can lead to cell damage, and bleaching of the fluorescent probe. Finally, frequently, the fluorescent molecule is required to be inside the cell. This can disturb the system, influencing the cells viability or other parameters. There may also be the issue of getting the probe to the correct compartment within the cell. These limitations must be addressed in any technique utilizing fluorescent probes.

Quenching of fluorescent probes can lead to the reduction or loss of signal. Quenching refers to any process which reduces the intensity of fluorescence, such as energy transfer or complex formation. Oxygen, iodide or acrylamide ions are common quenchers. However, quenching does not appear to be a concern for the commonly used fluorescent dyes such as PI, DAPI, Annexin V-conjugates, or Hoescht under the experimental conditions commonly used (Galluzzi et al. 2009). However, leakage and bleaching of the fluorescent molecule may occur. To reduce the impact of these, rapid capture of images and minimal exposure to ultraviolet light sources are necessary.

PS is normally almost completely confined to the inner leaflet of the plasma membrane (Martin et al. 1995). During apoptosis it is actively and rapidly transported to the outer leaflet. This is a widespread apoptotic event, occurring regardless of the route of induction of apoptosis, and it occurs early in the process, preceding nuclear changes and loss of membrane integrity by several hours. Externalised PS acts as a "flag" to attract macrophages, facilitating the engulfment of the cell preventing membrane rupture and release of cytoplasmic contents.

Annexins, of which there are 12 known, are human proteins which are membrane impermeable, and have a high affinity for aminophospholipids in the presence of calcium. Annexin V (Annexin A5) is a 36 kDa member of this family which preferentially binds to PS. It can be conjugated with fluorescent or radio-labelled moieties and used to specifically label externalised PS. The results of this can be quantified using microscopy or flow cytometric techniques (Krysko et al. 2008; Martin et al. 1995; Martin 2008). Use of Annexin V to quantify apoptosis is a rapid, reliable, and widely used tool, and will be discussed in greater detail in sections 2.5 and 6.2.1.

This list is by no means exhaustive, and new techniques and fluorescent dyes or antibodies allowing the detection of numerous apoptotic events are continuously being developed. However, there are a number of major limitations which can be leveled at any apoptosis assay. Firstly, each method discussed is hampered by the fact that in the absence of phagocytes (i.e. pure cultured cell lines) apoptotic cells eventually proceed to secondary necrosis, which shares many features with primary necrosis, including cell swelling and membrane rupture (Krysko et al. 2008). Secondly, the term "apoptosis" covers a range of morphologically similar apoptotic

subtypes which are distinct in their triggering and biochemistry, and differences in phenotype occur between *in vitro* and *in vivo* apoptosis, and with different cell lines and stimuli (Hacker 2000; Kroemer et al. 2009). Finally, discussed are some of the drawbacks associated with each specific technique. Taken together, along with the lack of any absolute "gold standard" assay for apoptosis, the Nomenclature Committee on Cell Death (NCCD) emphasises the importance of combining at least two distinct methods to quantify apoptosis *in vitro*, which are complementary but unrelated (Galluzzi et al. 2009; Galluzzi et al. 2011). Likewise they advise against use of terms like "percentage apoptosis" instead opting for specific definitions such as "percentage Annexin V-binding" or "percentage cells with condensed chromatin" (Kroemer et al. 2005).

1.5.4 Isoflavones regulate apoptosis, intracellular calcium, and the activity of caspases and calpain in breast cancer cell lines

Isoflavones, in particular genistein, are thought to trigger a novel alternative to the intrinsic apoptotic pathway (Figure 1.3). Treatment of MCF7 cells with 50 or 25μM genistein or daidzein up to 100μM caused an increase in the prevalence of numerous apoptotic markers including fragmented DNA, accumulation of subG0/G1 cells in the cell cycle, apoptotic nuclear morphology and PS externalization (Davis et al. 2008; Ferenc et al. 2010; Jin et al. 2010; Sergeev 2004; Shim et al. 2007). This occurred at a range of treatment durations from 24 to 72 hours. There is littIe information available regarding the effect of lower, more physiologically relevant isoflavone concentrations on the induction of MCF7 apoptosis. However, under these conditions, 5 day treatment with genistein or daidzein between 0.1 and 10μM resulted in a slight inhibition of apoptosis compared to an untreated control (Schmidt et al. 2005). These studies are summarized in Table 1.6.

Under low serum conditions (0.5% FBS, 24 hours) 10μM genistein was also found to induce apoptosis (Sakamoto et al. 2010). Silencing of the ERα gene in MCF7 cells had no effect on this (Sakamoto et al. 2010). Similar apoptotic events were seen in response to genistein in ERα- MDA-MB-231 cells (Davis et al. 2008; Li et al. 2008; Seo et al. 2011), although in this case concentrations of as low as 5μM were effective. Furthermore, addition of the ER-blocker ICI 182780 caused an additional increase in the number of apoptotic cells (Sakamoto et al. 2010). These factors suggest that ER-independent mechanisms may be involved in the induction of apoptosis by isoflavones.

Genistein also induced apoptosis in fibrocystic mammary MCF10A cells (Seo et al. 2011) and neuroblastoma cells (Mohan et al. 2009). Additionally, the phytoestrogens resveratrol and glycitein induced apoptosis in MCF7 and MDA-MB-231 cells (Garvin et al. 2006; Sakamoto et al. 2010), and daidzein in MDA-MB-453 cells (Choi and Kim 2008).

Table 1.6: Summary of the methods used to investigate the induction of apoptosis by isoflavones in breast cancer cell lines

Reference	Cell line	Vehicle (control dose used)	Apoptosis assay	Isoflavone treatment
Davis et al. (2008)	MDA-MB-231, MCF7	Vehicle? (Control untreated)	- ELISA: ssDNA	48h
Ferenc et al. (2010)	MCF7, MDA-MB-231	Vehicle? (Control untreated)	- Flow cytometry: cell cycle analysis - Caspase 7 activity (cleaved fluorescent substrate MCA-VDQVDGWK(dnp)-NH_2) - DAPI nuclear morphology - Relative expression and protein levels of Bcl2/Bax	6h to 48h
Garvin et al. (2006)	MDA-MB-231	Ethanol (0.46%)	- Caspase 3 activity (substrate Ac-DEVD-AMC) - Nuclear morphology (Giesma staining and electron microscopy) - Flow cytometry of PI stained cells - TUNEL staining of implanted tumour sections from mice	48h
Jin et al. (2010)	MCF7	DMSO (0.1%)	- Nuclear morphology (Hoechst and PI) - Flow cytometry: Annexin V-FITC, PI - Measurement of MOMP with DiOC6 - Western blot: cleaved caspases 7 and 9, Bcl2, Bax, subcellular location of cytochrome C	24h

Study	Cell line	Vehicle (control dose used)	Apoptosis assay	Isoflavone treatment
Li et al. (2008)	MDA-MB-231	Ethanol (x)	- Flow cytometry: Annexin V-FITC, PI - Caspase 3 activity (substrate DEVD-pNA) - Western blot: Bcl2, Bax, cleaved caspases 3 and 8	48h
Sakamoto et al. (2010)	MCF7	DMSO (x)	- Flow cytometry (PI) cell cycle analysis - PCR: Bcl2/Bax transcription level - p53 dependent transcription: luciferase reporter plasmid	24h
Schmidt et al. (2005)	MCF7	DMSO (untreated control)	- Flow cytometry: cell cycle analysis	120h
Seo et al. (2011)	MDA-MB-231 MCF10A	DMSO (0.2%)	- Flow cytometry (PI) cell cycle analysis - PCR: p53 and Bcl-xL transcription	24h, 72h
Sergeev (2004)	MCF7	DMSO (0.1%)	- Brd-U TUNEL assay kit - Plasma membrane changes: Annexin V staining for PS externalisation, YOPRO-1 and PI for membrane disruption - Nuclear fragmentation: Hoechst 33258 - Calpain/caspase12 activity: substrates BOC-LM-CMAC and ATAA-AFC respectively	72h
Shim et al. (2007)	MCF7	Ethanol and DMSO 1:1 v/v (0.05%)	- DNA laddering - Calpain activity (substrate DABCYL-TPLKSPPPSPR-EDANS) - Western blot: pro- and cleaved caspase 7 and poly(ADP ribose) polymerase (PARP)	24h (up to 48h for DNA laddering)

(x) vehicle dose for control unknown

The apoptosis assays have been carried out at a range of different time-points, between six hours and three days depending on the method used, and the results are similar. This allows both early and late apoptotic events to be characterized. However, a wide range of methods has been used to quantify apoptosis. This can make cross-study comparison difficult, but it shows that numerous apoptotic markers are induced by isoflavone treatment, and avoids the individual drawbacks associated with each specific technique. Notably, numerous groups used multiple assays to quantify apoptosis, in accordance with the advice of the NCCD.

Treatment of MCF7 cells with 50 µM genistein for up to 6 days showed that genistein-induced apoptosis was associated with a sustained increase in intracellular [Ca^{2+}], and co-treatment with thapsigargin (prevents Ca^{2+} re-entry into the endoplasmic reticulum) or ionomycin (a Ca^{2+} ionophore) suggested that this may be the result of the release of intracellular Ca^{2+} from the endoplasmic reticulum (Sergeev 2004). Treating MCF7 cells with dantrolene, an inhibitor of Ca^{2+} release from the endoplasmic reticulum, or the cytosolic Ca^{2+} buffer BAPTA prevented genistein induced apoptosis (Sergeev 2004; Shim et al. 2007). A number of other studies have also implicated Ca^{2+} deregulation and a rise in intracellular Ca^{2+} levels in apoptosis in MCF7 cells and lung carcinoma cell lines (Gil-Parrado et al. 2002; Mathiasen et al. 2002). One study determined that the antioestrogen tamoxifen (2 to 10µM) induced an increase in intracellular Ca^{2+} in the breast cancer cell line ZR75-1, which was suggested to be due not only to Ca^{2+} release from the endoplasmic reticulum, but also to increased influx from the extracellular medium (Chang et al. 2002). It is not known whether isoflavones act similarly.

In MCF7 cells 50 µM genistein treatment activated the protease µ-calpain (Sergeev 2004; Shim et al. 2007). The calpains, like the caspases, are cysteine proteases, although they differ in their target sequence specificity. There are two isoforms, µ-calpain and m-calpain, which are both Ca^{2+} activated, but require relatively high (µM and mM respectively) Ca^{2+} concentrations for their activity, hence their names (Orrenius et al. 2003). Treatment of MCF7 cells with dantrolene reduced genistein-enhanced calpain and caspase 7 activity (Shim et al. 2007). Additionally, treatment of MCF7 cells with a calpain inhibitor (PD 151746) reduced apoptosis in genistein treated cells (Sergeev 2004). *In vitro*, both µ- and m-calpain cleaved Bid, Bcl2 and Bcl-xl into their pro-apoptotic forms, resulting in the release of cytochrome C from

the mitochondria (Gil-Parrado et al. 2002; Nakagawa and Yuan 2000; Orrenius et al. 2003).

Interestingly, initial studies into the role of calpains in apoptosis indicated a possible role for them as negative regulators, as they also cleaved pro-caspases 3, 7, 8 and 9 into inactive fragments (Chua et al. 2000). Further investigation suggested a complex pattern of cross-talk between the caspase and calpain apoptotic pathways. An endogenous calpain inhibitor exists, calpastain, which is cleaved by caspase 3, activating the calpains (Orrenius et al. 2003). Overexpression of calpastain reduced calpain activity, increased caspase 3 activity, and accelerated apoptosis (Neumar et al. 2003). In wild type human neuroblastoma cells (SH-SY5Y), calpain initially slowed the execution phase of apoptosis, but was necessary in the later stages, adding to the effects of the caspases (Neumar et al. 2003).

In MCF7 cells this is possibly the case, as inhibition of either the calpains or caspases reduced apoptosis (Sergeev 2004), and treatment with 100 µM genistein resulted in the activation and cleavage of both µ-calpain and caspase 7 (Shim et al. 2007), and cleavage of a caspase 7 substrate (Ferenc et al. 2010). However Shim et al. (2007) found no activation of caspases 8 or 9 by genistein treatment up to 200 µM (results were not shown)[4]. On the contrary, both caspase 7 and 9 were cleaved into active forms in MCF7 and MDA-MB-453 (ERα-) cell lines upon 24 hour treatment with daidzein between 10 and 100µM compared to untreated controls (Choi and Kim 2008; Jin et al. 2010). As caspase 9 is known to activate caspase 7 in the intrinsic apoptotic pathway (see Figure 1.4) it is probable that it plays a role in isoflavone-induced apoptosis in MCF7. Genistein treatment (50 µM) of MCF7 cells also resulted in an increase in the cleavage of a specific caspase 12 substrate (Sergeev 2004). Finally, treatment of MCF7 with the pan-caspase inhibitor Z-VAD-FMK prevented or reduced genistein induction of apoptosis (Jin et al. 2010; Sergeev 2004).

Downstream of these events, 24 hour treatment with pro-apoptotic concentrations of daidzein in MCF7 has been observed to result in an increase in the ratio of Bax:Bcl2 proteins (Jin et al. 2010), and genistein (10µM for 24 hours) resulted in a corresponding increase in Bax:Bcl2 mRNA levels, which occurred irrespective of the

[4] MCF7 does not express caspase 3 (Janicke et al. 1998; Janicke 2009). This may partly explain its carcinogenicity (i.e. the cells are resistant to some apoptosis inducing factors), although to a certain extent other caspases compensate.

presence or absence of 10 nM E2, and was unaffected by ERα silencing (Sakamoto et al. 2010). This was associated with a dose-responsive increase in cytochrome C relocation to the cytoplasm, and a reduction in mitochondrial transmembrane potential (Jin et al. 2010). However, no change was reported in Bcl2 mRNA levels after 24 hour 50μM genistein treatment (Ferenc et al. 2010).

In MDA-MB-231 breast cancer cells a very similar series of apoptotic events occurs. Treatment with 50μM genistein for 24 hours resulted in an increase in cleavage of a caspase-7-specific substrate and an increase in the ratio of Bax:Bcl2 protein and mRNA (Ferenc et al. 2010). The higher dose of 100μM also reduced protein levels of anti-apoptotic Bcl-xL (Seo et al. 2011). Longer treatment with a lower dose (48 hours of 5 to 20μM genistein) also increased the Bax:Bcl2 protein ratio, and increased the levels of active caspase 3 and cleavage of a specific caspase 3 substrate (Li et al. 2008). As in MCF7, no effect on caspase 8 activity was observed by this group.

In MDA-MB-231 cells 100 μM genistein treatment induced phosphorylation of p53 tumour suppressor protein (Seo et al. 2011). This increases the stability and transcriptional activating ability of the protein, and accordingly, pro-apoptotic concentrations of genistein (and other isoflavones) result in an increase in the amount of p53 protein and p53-induced transcriptional activity in MDA-MB-231 and MCF7 cells respectively (Ferenc et al. 2010; Sakamoto et al. 2010). Studies have shown that in MCF7 cells, Bcl2 promoter activity is downregualted by the p53 transcription factor, while it enhances Bax promoter activity (Kim et al. 2008). This suggests that the impact of genistein on Bax:Bcl2 may be mediated by p53 activity. Additionally, Bcl2 promoter activity is negatively regulated by the nuclear transcription factor κB (NF-κB), and 5 to 20 μM genistein treatment dose dependently reduces NF-κB levels in MDA-MB-231 cells suggesting another mechanism of action (Kim et al. 2008; Li et al. 2008).

Finally, genistein resulted in the activation of apoptosis signaling kinase 1 (ASK1) and p38 MAPK (Shim et al. 2007), the latter leading to phosphorylation of various downstream apoptotic activators. Simultaneous treatment with dantrolene diminished these latter responses. Additionally, expression levels of the MAPK family growth genes were reduced by treatment of MDA-MB-231 cells with 5 to 20 μM genistein (Li et al. 2008). The involvement of numerous genes such as these

has been confirmed by microarray gene expression analysis, showing that overall 48 hour treatment of MCF7 cells with 25 µM genistein results in a pro-apoptotic, reduced proliferation gene expression profile (Lavigne et al. 2008).

Overall, in MCF7 cells genistein in µM concentrations appear to increase intracellular Ca^{2+} levels, associated with depletion of the endoplasmic reticulum stores. The result is calcium-dependent µ-calpain activation, which then cleaves and activates caspases 7 and 12. These feed into the intrinsic pathway, increasing Bax:Bcl2, inducing MOMP and the subsequent release of cytochrome C from the mitochondria. Daidzein treatment had similar results, and activated initiator caspase 9. The inclusion of this step in genistein-induced MCF7 apoptosis should not be ruled out. Caspase 8 is not involved. The latter mitochondrial events may be mediated by the activity of the transcription factors p53 and NF-κB, which also are modulated by genistein treatment. There is no apparent involvement of the ERs during any stage of this, and events unfold in the ERα-/ERβ+ MDA-MB-231 cell line similarly.

1.5.5 17β-oestradiol, and isoflavone/17β-oestradiol combinations regulate the induction of apoptosis in MCF7 breast cancer cells

In MCF7 cells, physiological concentrations of E2 (10 and 100pM) have been demonstrated to inhibit the induction of apoptosis (Schmidt et al. 2005; Song et al. 2007). This is in line with the protective / growth promoting effect that E2 is known to have on this cell line (section 1.4.4). These studies are summarized in Table 1.6.

Information regarding the impact of isoflavone/E2 combinations of the induction of MCF7 apoptosis is scant. Schmidt et al. (2005) present evidence suggesting that 1μM genistein or daidzein in a physiological E2 environment (1 to 100pM E2) inhibit apoptosis to a greater extent than the untreated control. However they present no comparison of these results to those of any treatment individually, so although it appears that the isoflavone/E2 combinations act in a similar manner to the isoflavones alone, this should only be concluded with caution.

Sakamoto et al. (2010) demonstrated that alone, a premenopausal E2 concentration (10 nM) prevented apoptosis during serum starvation (0.5% FBS, 24 hours), and treatment with genistein (10 μM) caused more apoptosis than the control cells (serum starvation, no treatment). Combinations of E2 and genistein, or E2 and daidzein, at these concentrations induced apoptosis to a similar extent to the isoflavone treatment alone.

Although these results suggest that isoflavone/E2 combinations induce apoptosis in MCF7 to a similar extent to the isoflavones alone, it is important to note that one investigates basal (no stress) induction of apoptosis, while the latter has used serum starvation induced apoptosis, and each has focused on a single isoflavone concentration. In particular, there is very little information available regarding the impact of daidzein on MCF7 apoptosis in the presence of physiological E2 levels, or lower (Western) levels of isoflavones. A comprehensive study in this field is urgently required, as the induction of apoptosis by dietary levels of isoflavones represents a potential route through which their protective effects in vivo may be mediated.

1.5.6 Summary of the apoptotic effects of isoflavones

Overall, what is known regarding the induction of apoptosis in breast cancer cell lines by isoflavones appears to feed into their net effect on proliferation. In MCF7, concentrations of genistein and daidzein previously shown to reduce proliferation (>25µM) induce many markers of apoptosis. They trigger the intrinsic apoptosis pathway, including activation of µ-calpain and caspase 7, an increase in the ratio of Bax:Bcl2 and cytochrome C release. Similar events occur in MDA-MB-231, although lower concentrations of isoflavones (>5µM) are equally effective. There does not appear to be any involvement of the ERs in these processes, although E2 does inhibit apoptosis in MCF7 cells.

However, common experimental practice is to use pharmacological concentrations of isoflavones (>50µM), and the physiological relevance of this is not known. Nothing is known regarding the impact of isoflavones on the induction of apoptosis at physiological concentrations more relevant to Western women (<1µM), or how the presence of E2 may interact with these responses.

1.6 Potassium channels and breast cancer

1.6.1 The role of potassium channels in cell physiology

The membrane potential (E_m) of a cell is the difference in voltage between the interior and exterior of the plasma membrane. As the membrane itself is impermeable to ions, the membrane potential arises from the actions of various ion channels and pumps embedded in the lipid bilayer. The majority of these channels regulate the flow of K^+, Na^+, Cl^- and Ca^{2+} ions. Ion channels are classified according to how they are regulated. The main groups consist of: ligand gated channels, voltage gated channels, channels which respond to sensory stimuli such as stretching or temperature, and finally leakage, or rectifier channels. The latter group are the simplest, with very little in the way of regulation, although they frequently operate better in one direction (rectification) than the other, and may be closed by some ligands. In addition to being gated in these manners, the majority of voltage and ligand gated channels are susceptible to regulation by tyrosine phosphorylation. This allows intracellular signaling pathways and growth factors to acutely regulate the electrophysiological properties of both excitable and non-excitable cells (Davis et al. 2001 and references therein). Further information regarding the activities of ion channels can be found in the comprehensive handbook by Hille (2001).

In excitable cells such as neurons or muscle cells (resting E_m = -70mV; Schwarz and Bauer 2004), ion channels (voltage gated Na^+ and Ca^{2+} channels) are used to generate action potentials, where an electric current transmits signals through the cell. Non-excitable cells on the other hand, are characterized by their inability to generate action potentials due to a lack of voltage gated Na^+ or Ca^{2+} channels (Mahaut-Smith et al. 1999). Resting E_m in these cells varies widely with cell type, from -20 to -40mV (human and murine neuroblastoma cells; Arcangeli et al. 1995), and -33mV in cells from mouse mammary epithelial tissue (Enomoto et al. 1986), to -85mV (MCF7; Klimatcheva and Wonderlin 1999; Wonderlin and Strobl 1996), and generally corresonds to the ability of the cell to proliferate (Sundelacruz et al. 2009). In numerous non-excitable cell types, including breast cancer cells, regulation of E_m is key to many processes including osmolarity, proliferation and apoptosis (Davis et al. 2001; Felipe et al. 2006; Ouadid-Ahidouch and Ahidouch 2008). The interactions

between membrane potential regulation and various physiological cellular processes are summarized in the review by Sundelacruz et al. (2009).

In addition, through their ability to regulate the osmolarity of cells, and consequently the inward and outward flow of water and osmolytes, ion channels play an important role in cell volume regulation. It is widely accepted that swelling is necessary for S phase progression during proliferation (Dubois and Rouzaire-Dubois 2004; Hoffmann 2011), and that shrinkage inhibits proliferation and is an essential early step in apoptosis (Vu et al. 2001). There is a role in cell volume regulation for the aquaporins, a family of membrane proteins which facilitate transport of water across the plasma membrane, and these proteins have been linked to proliferation and migration (Chen et al. 2011; Ishibashi et al. 2011). However, more relevant to this work is the fact that a number of ion channel types are implicated in volume regulation, including the potassium channels (Bortner and Cidlowski 1999; Gow et al. 2005; Hughes, Jr. et al. 1997; Storey et al. 2003; Wang 2004).

Potassium is maintained in the cytosol at a considerably greater concentration than in the extracellular fluid. Typical mammalian cells have an intracellular K^+ level of 139mM, compared to extracellular (blood) concentrations of 4mM (Lodish et al. 2008). Inward movement of K^+ into the cell to maintain this high intracellular concentration is mediated by the Na^+ K^+-ATPase pump. This ubiquitous protein uses the energy from the hydrolysis of ATP to move K^+ ions into the cell against their concentration gradient, in exchange for Na^+ ions. This channel has been identified as a potential target for breast cancer drugs, due to its roles in signal transduction and cancer progression (for a review see Chen et al. 2006). However, far more versatile regulation of K^+ currents and intracellular K^+ concentrations lies with the role of the K^+ channels themselves.

Potassium channels are the largest and most diverse family of ion channels. They play well established roles in many diseases such as congenital deafness, arrhythmias, and multiple sclerosis, and show cell and tissue-specific regulation of expression levels (Felipe et al. 2006). In addition, the deregulation of potassium channels is implicated in breast cancer development and progression (Ouadid-Ahidouch and Ahidouch 2008; Wang 2004; Wonderlin and Strobl 1996). Table 1.7 lists all the K^+ channels referred to within this text.

Table 1.7: Potassium channel nomenclature and gene names

IUPHAR[1]	HUGO[2]	Other names
K_v1.1	*KCNA1*	Shaker-related
K_v1.2	*KCNA2*	
K_v1.3	*KCNA3*	
K_v1.5	*KCNA5*	
K_v1.6	*KCNA6*	
K_v7.1	*KCNQ1*	KVLQT
K_v10.1	*KCNH1*	Human *ether-a-go-go* K^+ channel, hEAG, eag1
K_v11.1	*KCNH2*	Human *ether-a-go-go* related gene, hERG, erg1
K_{Ca}1.1	*KCNMA1*	Large conductance calcium-activated K^+ channel, BK, BK_{Ca}
K_{Ca}2.1	*KCNN1*	Small conductance calcium-activated K^+ channel, SK, SK_{Ca}
K_{Ca}2.2	*KCNN2*	
K_{Ca}2.3	*KCNN3*	
K_{Ca}3.1	*KCNN4*	Intermediate conductance calcium-activated K^+ channel, IK, IK_{Ca}
K_{2P}5.1	*KCNK5*	Two-pore domain K+ channel subunit, TWIK-related acid sensitive channel 2, TASK2
K_{2P}9.1	*KCNK9*	Two-pore domain K^+ channel subunit, TWIK-related acid sensitive channel 3, TASK3
K_{ir}3.1	KCNJ3	G-protein coupled inwardly rectifying K+ channel, GIRK1
K_{ir}3.2	*KCNJ6*	G-protein coupled inwardly rectifying K^+ channel, GIRK2
K_{ir}3.3	*KCNJ9*	G-protein coupled inwardly rectifying K^+ channel, GIRK3
K_{ir}6.1	*KCNJ8*	ATP-sensitive K^+ channel
K_{ir}6.2	*KCNJ11*	ATP-sensitive K^+ channel
----	*KCNE1*	mink/ IsK, voltage gated potassium channel auxiliary subunit associated with K_v7.1 and K_v11.1

[1] Protein names assigned by the International Union of Pharmacology (IUPHAR) (International Union of Pharmacology 2010)

[2]HUGO Gene Nomenclature Committee (HGNC) approved gene name (HUGO Gene Nomenclature Committee 2011)

Potassium channels can be broadly grouped into four families (Felipe et al. 2006). These are the voltage gated, calcium-activated, inward rectifier (K_{ir}), and two pore domain K^+ channels (K_{2P}). The voltage gated potassium channels (VGKCs) form the largest group, comprising the peptides K_v1 to K_v12 (Gutman et al. 2005). Each K_v peptide forms a channel subunit, of which four are required to act as a functional K^+ channel. These can be as homo- or hetero-tetramers. Their structure is summarized in Figure 1.5. The activity of these channels is voltage dependent. They tend to be closed at resting potential and open upon membrane depolarization to mediate an outward K^+ current, resulting in hyperpolarization. The current that this family of channels mediates is a well defined delayed rectifier K^+ current (I_k) (Wang 2004).

There are two groups of calcium-activated K^+ (K_{Ca}) channels. The small conductance (SK) and intermediate conductance (IK) calcium activated channels are voltage insensitive and are activated by low concentrations of internal calcium (<1 μM). These channels do not directly bind Ca^{2+}, but instead detect it using a calmodulin-dependent mechanism. On the contrary, the large conductance (BK) calcium activated K^+ channel is activated by voltage and internal Ca^{2+}. The latter it detects not *via* calmodulin, but probably utilizing several cation binding sites on the C terminal domain of each channel subunit (Wei et al. 2005).

The K_{2P} group can be regulated by a range of chemical and physical stimuli including pH, mechanical stretch, lipids, and various ligands. They are active at resting potentials, and mediate background, or “leak” outwardly rectifying K^+ currents that stabilize membrane potential and allow repolarisation (Enyedi and Czirjak 2010; Goldstein et al. 2005). Finally, the K_{ir} channels mediate an inward K^+ current activated upon hyperpolarization (Kubo et al. 2005). Significant amongst this group of channels are the ATP-sensitive inwardly rectifying channels ($K_{ir}6.1$ and $K_{ir}6.2$) which perform the important role of linking ion channel physiology to the metabolic state of the cell, as they are closed by the presence of ATP and opened by ADP (Seino and Miki 2003).

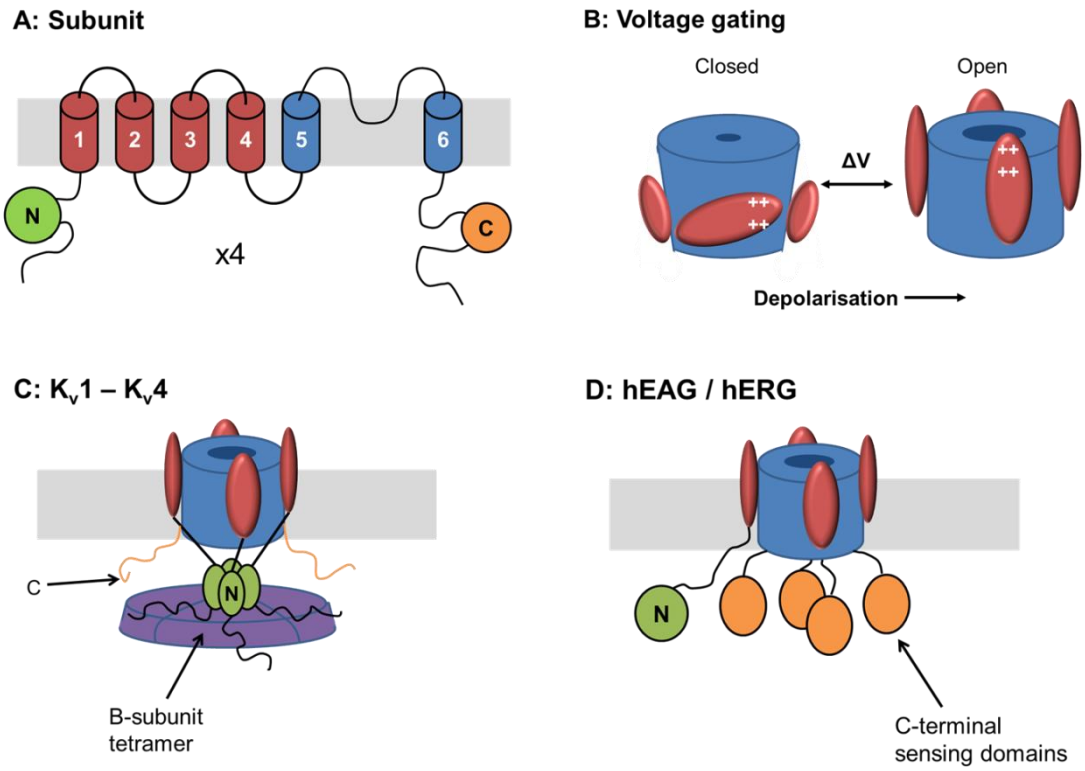

Figure 1.5: Voltage gated potassium channel structure

This diagram is based on work by Jiang et al. (2003), Sanguinetti et al. (2006) and Yellen (2002), characterising the relatively conserved structure of the VGKCs. The same colour scheme for subunits is used throughout the image. Each channel is a homotetramer or heterotetramer of 4 subunits (A), each with 6 transmembrane α-helices, and C and N terminal domains for protein-protein interactions or other regulatory functions. Helices 1 to 4 form the voltage sensing mechanism, and helices 5 and 6 make up the channel pore. The "Shaker" channels ($K_v1.$ to $K_v4.$) share a similar structure (C), with the N-terminal domains combining to form a "tetramerisation domain" which determines the specific subunits which bind, and acts as an anchor for additional β-subunits. The hEAG and hERG channels have a related structure (D), although their N and C terminal domains have differing regulatory functions. These frequently are the sites for binding other regulatory subunits, and in hERG, the C-terminal domain binds cAMP. The voltage gating mechanism of these channels is thought to be similar (B), whereby upon membrane depolarization the gating charges (+ signs) are carried across the membrane from bottom to top by voltage sensing "paddles", which as they turn, open the pore.

1.6.2 Techniques to investigate potassium channel physiology in breast cancer cells

1.6.2..1 Whole cell patch clamping

Patch clamping is considered to be the gold standard method with which to measure ion currents as it allows the channels to be gated by physiologically relevant membrane potentials (Birch et al. 2004). This technique and its limitations are discussed further in sections 4.3 and 6.4.2. It is based on the principle that variations in channel activity (i.e. opening or closing of channel proteins) results in changes in membrane resistance, which can be studied by measuring the resulting current at a constant (clamped) membrane voltage (Sontheimer and Olsen 2007). Modifications have been made to the patch clamping procedure to allow analysis of the activity of channels in excised patches, or single channels. The latter facilitates the investigation of particular parameters of individual channel proteins, such as the durations of opening and shutting, or the rate of flow of ions.

However, whole cell patch clamping assesses the net activity of thousands of channels present in the whole cell membrane, generally of multiple types (the macroscopic current). A critical step in the analysis of macroscopic currents is their separation into component parts. Numerous methods exist to facilitate this, however five are commonly used (Sontheimer and Olsen 2007; Standen et al. 1994).

1.6.2..1.1 Kinetic

The speed of activation or inactivation of a channel can vary substantially, so assessing macroscopic currents at different time points following stimulation can facilitate isolation of different current types. For instance, Na^+ currents activate and inactivate more rapidly than other channel types, typically becoming activated within 300µs, and inactivating completely by 5ms. On the other hand, K^+ currents are slower, taking several milliseconds to activate, and inactivating very slowly or not at all. Measuring current 500µs after activation will determine Na^+ current activity, and tens or hundreds of milliseconds later K^+ current amplitude can be assessed.

1.6.2..1.2 Stimulus protocols

The voltage dependence of activation or inactivation of certain ion channels can allow separation of the activities of some subpopulations using voltage stepping protocols. Large or small amplitude Ca^{2+} currents can be separated depending upon the holding potential used for the voltage stepping. Similarly, voltage steps applied from particularly negative potentials (-110mV) activates the transient and delayed rectifying K^+ currents. However stepping from a more positive holding potential (-50mV) inactivates the transient K^+ currents whilst not affecting activation of the delayed rectifying K^+ channels. The latter group includes numerous VGKCs.

1.6.2..1.3 Ion dependence

The compositions of bath and pipette solutions are commonly manipulated to favour movement of the ions of interest, and inhibit others. Replacement of K^+ ions in the pipette solution with impermeable N-methyl-D-glucamine prevents the majority of K^+ channel activity allowing isolation of the Na^+ currents. Similarly, tetramethyl-ammonium chloride can replace Na^+, allowing isolation of the K^+ currents.

1.6.2..1.4 Pharmacology

Numerous toxins and synthetic agents are utilized to inhibit specific or broad groups of ion channels. The best practice is to record the current trace in the presence and absence of the pharmacological agent, and the difference in current represents the effect of the drug. An advantage of this technique is the elimination of capacitance and leak currents. However, in numerous instances, doses of pharmacological agents used have been in vast excess of their IC_{50} to guarantee an effect. They may be cytotoxic or generate non-specific effects at these high doses. Validation of the relevance of the doses used is required, possibly by comparison of the patch clamp results with results of other methods of assessing K^+ movement, such as use of radiolabelled rubidium or fluorescent probes, such as potassium-binding benzofuran isophthalate (PBFI), although these methods too are not without their limitations.

1.6.2..1.5 I-V curves

Current-voltage relationships are an effective way to summarize the activity of ion channels. These allow dissemination of a number of key parameters which are not apparent from the raw data, such as reversal potential (the potential at which the current reverses direction: goes from negative to positive), voltage dependence (rectification), activation threshold, and quality of the clamp.

1.6.2..2 Fluorescent methods to assess potassium movement

The most widely used potassium sensing fluorescent probe is PBFI, used in several of the studies previously described (Bortner and Cidlowski 1999; Hughes, Jr. et al. 1997; Vu et al. 2001) either by conventional fluorescent microscopy or flow cytometric analysis. Dyes such as this are theoretically useful tools due to the complex and time consuming nature of patch clamping. They are considerably easier to use than patch clamping, and allow simultaneous measurement of numerous cells (Sundelacruz et al. 2009). However PBFI is limited in its biological applications due to a relatively low fluorescence level and low selectivity for K^+ over other actions such as Na^+ (Hirata et al. 2011). Novel fluorescent potassium probes such as B3TAC which overcome some of these problems are available, but are not widely used. This may relate to the fact that even a very sensitive fluorescent probe will only detect net changes in intracellular K^+, compared to the wealth of kinetic, voltage-sensitive, and single channel data that is it possible to extract from a patch clamped cell. In addition, a major disadvantage to using fluorescent dyes to assess membrane potential is that they are difficult to calibrate, and so most data is reported as percentage changes in fluorescence, rather than absolute potential values (Sundelacruz et al. 2009).

A different approach is to use fluorescent probes to detect changes in plasma membrane potential directly such as the bis-barbituric acid oxonol, $DiBAC_4$, with or without flow cytometric analysis. This is relatively widely used, and robust to changes in cell volume influencing intracellular dye concentration. However, as with the potassium sensing dyes it is limited in the sense that it can only detect overall changes in potential. Furthermore, dyes such as $DiBAC_4$ are relatively slow to respond to changes in potential, so they are only of value to study steady state membrane potential, or slow- and non-inactivating ion channels (Wolff et al. 2003).

A number of novel dye systems based on fluorescence resonance energy transfer (FRET) have been developed which are sensitive to rapid changes in membrane potential. However, none are ideal, and the choice of which should depend on the target channel and equipment available (Wolff et al. 2003).

The intensity of fluorescence can be influenced by changes in protein content, which will modify the levels of bound to free dye. Fixation of the cells will increase the number of dye binding sites and consequently fluorescence. The results of this method can also be influenced by depolarization of organelle membranes such as the mitochondria. However, as Klapperstruck et al. (2009) suggest, with careful calibration, this method is capable of generating results that are comparable with patch clamping. Each of these fluorescent methods is further constrained by the general limitations of use of fluorescent molecules, discussed previously (section 1.5.3).

1.6.2..3 Modification of expression levels of ion channels

Effective isolation of an ionic current through a given channel is frequently possible by expressing artificially that channel in a cell type which contains few or no intrinsic ion channels, so that measured currents represent the pure current through the channel of interest. The most commonly used system is *Xenopus* oocytes, which have very little in the way of endogenous ion channel activity. However, a limitation of this is that the cloned channel activity may not always reflect the behaviour of the native channel due to alterations in subunit structure or lack of certain regulatory proteins (Standen et al. 1994). This is particularly relevant for the VGKCs which exist as functional hetero-tetramers (Gutman et al. 2005).

1.6.2..4 Radiolabelled rubidium as a potassium tracer

Use of radiolabelled rubidium ($^{86}Rb^{+}$) as a tracer is a relatively common method to assess K^{+} flux, and has been used several times in the studies described, both with MCF7 and MDA-MB-231 breast cancer cell lines, and other cell types (Caplanusi et al. 2006; Gow et al. 2005; Huang et al. 2011; Kirkegaard et al. 2010). This method allows real time measurements of net K^{+} movements to be made, by loading the cells with $^{86}Rb^{+}$, washing them, then scintillation counting of the extracellular supernatant can be carried out at various time-points to determine its $^{86}Rb^{+}$ content.

It is based on the assumption that $^{86}Rb^{+}$ will behave in the same manner as K^{+}, and is not toxic at the doses used. Again, as with the use of fluorescent dyes, this method cannot extract data on the kinetic, voltage activated and single channel scale. However, in addition to the inherent safety concerns when working with radioisotopes, numerous laboratories do not have the facilities to safely store and dispose of these materials.

1.6.2..5 Changes in cell volume

Due to the regulatory role of K^{+} channels in cell volume regulation, measurement of volume changes is frequently carried out alongside K^{+} channel activity assessment. However, this must not be used as a direct measure of K^{+} channel activity, as other ions including Na^{+} and Cl^{-} are also involved in volume regulation.

The most widely used method of assessing changes in cell volume is electronic sizing using a Coulter-type multisizer (Feranchak et al. 2003; Hoffmann 2011; Huang et al. 2011; Kirkegaard et al. 2010; Kossler et al. 2012). This technique is based on the principle that when particles flow through a small aperture over which an electric current is passed, they will displace their own volume of liquid, increasing the resistance to the current flow by a tiny, but proportional and measurable amount. This is a reproducible and automatable method which is sensitive enough to detect very small changes in cell size. However, due to the nature of the technique it is only possible to measure populations of cells in suspension before or after a treatment, and changes to individual cells cannot be followed over time. Care must be taken regarding the choice of time-points measured to ensure that compensatory mechanisms such as regulatory volume decrease (RVD) do not obscure results.

Another frequently used and reproducible method is the assessment of light scattering by flow cytometry (Bortner and Cidlowski 1999; Storey et al. 2003; Vu et al. 2001). However a criticism of this technique is that it is limited by variations in cell surface geometry and intracellular refractive indices (Farinas and Verkman 1996). As with the coulter method, changes in cells cannot be followed over time, and only inferred to by measurements taken in populations treated for different timescales.

There exist techniques to assess changes in size over time, using microscopy, with or without fluorescent dyes. A number of groups have used light microscopy together with image analysis software to measure the cross sectional area of cells (Okumura et al. 2009; Roy et al. 2008; vanTol et al. 2007). However, with numerous software types this is limited to the analysis of spherical objects, which may not represent the entire population, and the method is relatively labour-intensive. Another group used height (z axis dimension of a composite image) as an index for volume (Caplanusi et al. 2006), however this too assumes a uniformity of shape across the population.

To avoid these limitations several groups have utilized fluorescent intracellular dyes, frequently calcein-AM (-acetomethoxy derivative). Dyes such as this will be taken up into the cell in ester form. The ester group is then cleaved making them plasma membrane impermeable, so the content inside the cell is relatively constant. In this manner, changes in cell volume will be expressed by changes in fluorescence intensity, i.e. shrinkage will make the intracellular dye more concentrated and so fluoresce brighter, with the opposite occurring upon swelling. This technique was first described in 1995 (Crowe et al. 1995), and is considered to be a sensitive technique for the measurement of volume changes in single cells. This is discussed further in sections 4.1 and 6.3.1. Changes in the intensity of fluorescence can be assessed by image analysis software (Chen et al. 2011), or using the higher throughput microplate method (Pan et al. 2007). Either method is reproducible and accurate. However, as previously, there are a number of general limitations of fluorescent techniques which apply to these methods also (section 1.5.3).

1.6.3 Expression levels of potassium channels in MCF7 breast cancer cells and cancerous mammary tissue

In MCF7 breast cancer cells many plasma membrane K^+ channels have been identified (Table 1.8). A number of these channels have been found to have roles in the proliferation of breast cancer cells, and their overexpression is associated with the promotion of tumour formation and resistance to apoptotic stimuli (Abdul et al. 2003; Brevet et al. 2008; Mu et al. 2003).

Of particular note is the human *ether-a-go-go*[5] (hEAG) K^+ channel, also known as *KCNH1* or $K_v10.1$. This was found, by use of both reverse transcription real time PCR (RT-PCR) and immunostaining, to be overexpressed in over 80% of breast carcinoma biopsies. In normal tissue its distribution was restricted to areas of the brain and several other tissues (Hemmerlein et al. 2006).

A related channel is human *ether-a-go-go* related gene (hERG), also known as *KCNH2* or $K_v11.1$. This channel carries a rapidly activated delayed rectifier K^+ current. Like hEAG, hERG is expressed in numerous human cancer cell lines and tissues but not in corresponding healthy cells (Bianchi et al. 1998; Cherubini et al. 2000; Lastraioli et al. 2004; Pillozzi et al. 2002), suggesting that it may also confer some selective advantage to the tumour cells. In cancer cell lines hERG expression varies greatly, but appears to relate to chemosensitivity, with the highest expression levels corresponding with the greatest sensitivity to anticancer drugs (Chen et al. 2005). In colonic cancerous tissue hERG expression level and activity appears to correlate with the invasiveness of the cancer (Lastraioli et al. 2004).

[5] The gene was named in the 1960s by William Kaplan and William Trout of the City of Hope Medical Centre, Duarte, California. From their work in the Drosophila fly they discovered a mutation which resulted in convulsions in the legs when the flies were anaesthetized with ether, which reminded them of the style of dancing at the Whisky A-Go-Go nightclub in West Hollywood (Kaplan and Trout, III 1969)

Table 1.8: Potassium channels found in MCF7 breast cancer cells

Channel Family	K^+ Channel	References
Voltage gated	hEAG (Human *ether-a-go-go*; K_v10.1)	Borowiec et al. 2007; Hemmerlein et al. 2006; Roy et al. 2008
	hERG (Human *ether-a-go-go* related gene; K_v11.1)	Bianchi et al. 1998; Chen et al. 2005; Roy et al. 2008; Wang et al. 2002
	K_v1.1	Ouadid-Ahidouch et al. 2000
	K_v7.1	vanTol et al. 2007
Ca^{2+} activated	IK (Intermediate Ca^{2+} activated channel)	Ouadid-Ahidouch et al. 2004b
	BK (Large Ca^{2+} activated channel)	Khaitan et al. 2009; Lee et al. 2012; Ouadid-Ahidouch et al. 2004a; Roger et al. 2004
	SK (Small conductance Ca^{2+} activated K^+ channel)	Abdul et al. 2003
Inwardly rectifying	K_{ir}3.1 (GIRK1; G-protein inwardly rectifying)	Dhar and Plummer, III 2006
	K_{ir}3.2 (GIRK2)	Dhar and Plummer, III 2006
	K_{ir}3.3 (GIRK3)	Dhar and Plummer, III 2006
Two pore domain	K_{2P}9.1 (TASK3)	Lee et al. 2012

Similarly, the Shaker family potassium channel subunit K_v1.3 was detected by immunostaining in high or moderate levels in nearly 90% (53 out of 60) of breast cancer biopsy epithelial samples, while none was detected in four corresponding non-cancerous samples (Abdul et al. 2003). However, Brevet et al. (2008) found the opposite, suggesting that both K_v1.3 and related K_v1.1 proteins were present at lower levels in cancerous tissue than normal tissue. For this study immunostaining methods were used on 33 primary invasive breast carcinomas of varying stages and invasiveness, and 31 normal breast specimens. They related the reduction in K_v1.1

and $K_v1.3$ to their role in apoptosis in breast epithelial cells. $K_v1.3$ channel protein was not detected in MCF7 cells by immunohistochemical analysis (Ouadid-Ahidouch et al. 2000), indicating its absence from this cell line.

Jang et al. (2009) proposed that this discrepancy in results may be because expression of the $K_v1.3$ gene depends upon the invasiveness and stage of the cancer. This group found that weakly invasive M13SV1R2 cells showed considerable and significantly greater $K_v1.3$ mRNA expression levels than in normal, untransformed M13SV1 cells, but that in the highly invasive line M13SV1R2-N1, $K_v1.3$ gene expression was half of that seen in the normal line. They also discovered that compared to normal breast tissue, the expression of $K_v1.3$ was only higher during early (I, IIA, and IIB), late (IIIC), and metastatic (IV) stage breast cancer tissue. Expression during the mid-stages IIIA and IIIB, was not significantly different from normal tissue. However, Jang et al. (2009) also analyzed protein levels of $K_v1.3$ using Western blot analysis, and found that this was significantly higher in both the weakly and highly invasive cell lines compared to the untransformed cells, and that protein levels were related to the tumourigenicity of the cell line. $K_v1.3$ protein levels did not correlate with mRNA levels. This is not an uncommon occurrence, and suggests differences in translation regulation, post-translational events, or protein half-life.

This data suggests a possible explanation for the discrepancies in results between Abdul et al. (2003) and Brevet et al. (2008). However, it must be noted that the latter group did not find any significant relationships between the levels of $K_v1.1$ or $K_v1.3$ and markers of tumour grade or invasiveness, such as ER status or K_i67 levels. Clearly further research into the regulation of $K_v1.3$ is required. Whether the regulation of $K_v1.3$ levels according to tumour stage and invasiveness can account for the apparent absence of $K_v1.3$ in MCF7 cells reported by Ouadid-Ahidouch et al. (2000) is not known.

Similarly, the K^+ channel $K_{2P}9.1$ (TASK3), encoded by the gene *KCNK9*, was found to be overexpressed at least 5-fold and up to over 100-fold in 44% (28 out of 64) human breast cancer biopsy samples (Mu et al. 2003). It was also overexpressed in 35% of lung cancer samples analyzed (Mu et al. 2003). In the breast cancer samples, the *KCNK9* locus was amplified between 3- and 10-fold in 10% of the samples. Immunohistochemical analysis of the same samples confirmed the

presence of high levels of $K_{2P}9.1$ protein in the samples where the gene was overexpressed, and Mu et al. (2003) also found overexpression of *KCNK9* to be associated with tumour formation, increased viability in low-serum conditions, and resistance to hypoxia. Conversely, reduced cellular levels of both gene expression and protein for this channel have been linked with increased cell migration (Lee et al. 2012). In this study, relatively high levels of $K_{2P}9.1$ were found in MCF7 (non-invasive), while considerable lower levels of both its mRNA and protein were present in MDA-MB-231 (invasive). Modifying $K_{2P}9.1$ levels by either overexpression or knock-out (siRNA) generated corresponding results. This suggests that $K_{2P}9.1$ can act either oncogenically or to reduce tumour invasiveness depending on the cancer model used, and could potentially be more oncogenic *in vivo* than in cell culture. Alternately, its levels may change depending on tumor stage, with high protein levels present during the tumor formation and initial non-invasive stages, but dropping as the tumor becomes metastatic.

$K_{ir}3.1$ has been found to be overexpressed in cancerous breast tissue compared to normal tissue, using immunostaining methods (Brevet et al. 2008). Unlike the other K^+ channels differentially expressed in cancerous compared to normal breast tissue, which mediate outward K^+ currents, $K_{ir}3.1$ facilitates an inwardly rectifying K^+ current. $K_{ir}3.1$ levels related to tumour grade, with significantly higher expression seen in grade II than grade III tumours (Brevet et al. 2008). These results agree with those of Stringer et al. (2001), who used a gene expression profiling technique with a paired sample of breast carcinoma and adjacent normal breast tissue from the same patient, followed by RT-PCR with 56 separate benign and invasive breast carcinomas and 6 normal, non-malignant breast tissue samples. In the latter investigation, $K_{ir}3.1$ overexpression was found to correlate significantly with the presence of lymph node metastasis. $K_{ir}3.1$ has also been identified by both immunostaining and RT-PCR in a number of breast cancer cell lines including MCF7, MDA-MB-453, and ZR75-1 (Dhar and Plummer, III 2006).

Of the SK channels, the expression of SK1 (*KCNN1*) is restricted to neuronal tissues (Chen et al. 2004). While SK2 (*KCNN2*) is more widespread, there remains very little or no expression in the mammary epithelium. On the contrary, SK3 (*KCNN3*) was detected in almost every tissue tested, including the mammary gland. However this study was limited to healthy, not cancerous tissue samples. At the time of

writing, the protein or expression levels of the SK channels have not been compared between healthy and cancerous breast epithelial cells.

Similarly, the IK channel (*KCNN4*) mRNA is expressed in the normal mammary gland (Chen et al. 2004), but no comparison to cancerous breast tissue has been made by this group. IK channel mRNA, protein, and functional channel activity have been detected in human breast cancer epithelial primary cell cultures and breast cancer tissue samples (Haren et al. 2010). However, again no non-cancerous controls were used for comparison so how the levels of IK compare between cancerous and non-cancerous breast tissue is not known. However, Haren et al. (2010) also demonstrated that IK expression level correlates significantly with tumour grade, indicating that this channel may contribute to tumour formation or progression.

Khaitan et al. (2009) documented very low levels of both expression and protein levels for the BK channel in normal mammary tissue and untransformed mammary cell line MCF10A. They found slightly higher expression levels in primary breast cancer tissue samples (n = 6). On the contrary, Brevet et al. (2008) found lower levels of BK protein among 33 primary invasive ductal breast carcinomas compared to normal breast tissue from the same individuals. Regrettably, the low numbers of specimens used by both groups makes it impossible to reach a definitive conclusion regarding the relative levels of BK in cancerous and normal breast tissue at this stage. However, BK expression appears to be considerably higher among tissue samples of breast cancer metastasised to other organs, particularly the brain (n=4), suggesting a role for the BK channel in brain metastasis (Khaitan et al. 2009). BK channel mRNA is present in MDA-MB-231 cells at a similar level as was seen in MCF7 (Lee et al. 2012).

1.6.4 The involvement of potassium channels in the proliferation of MCF7 breast cancer cells

K^+ currents are frequently studied in the MCF7 breast cancer cell model. Treatment of MCF7 cells with the ATP-sensitive K^+ channel opener minoxidil resulted in an increase in cell proliferation (Abdul et al. 2003). Similarly, treatment of other cell lines with agents known to increase proliferation, such as 5nM prolactin added to the LNCaP prostate cancer cell line, increased the macroscopic K^+ current and open probability of individual K^+ channels in a tyrosine kinase dependent manner (Van Coppenolle et al. 2004). This has not been repeated with MCF7 cells.

In addition, treatment of MCF7 cells with a number of specific and non-specific K^+ channel blockers results in inhibition of proliferation, as summarized in Table 1.9. This data implicates the SK channels, ATP sensitive channels ($K_{ir}6.1$ and $K_{ir}6.2$) and the voltage-gated channels (Pardo 2004; Wonderlin and Strobl 1996) in the proliferation of MCF7 cells. Interestingly, the role of K^+ channels in proliferation appears to be cell line-specific, as in colorectal adenocarcinoma cells, blocking VGKC activity, but not calcium activated- or ATP sensitive K^+ channel activity, significantly inhibited proliferation (Yao and Kwan 1999). This means that results from one cell line should not be generalized to other cell types.

Incubation with iberiotoxin or charybdotoxin (both Ca^{2+} activated K^+ channel blockers) had no effect on MCF7 proliferation, even at doses far in excess of their IC_{50} for the reduction of K^+ channel activity (Abdul et al. 2003; Ouadid-Ahidouch et al. 2000; Ouadid-Ahidouch et al. 2004a). Neither did E-4031, a specific hERG blocker, have any effect, even though the drug was shown to be stable in the cells over the duration of proliferation assessment, and this channel is known to be present in MCF7 and is functional in the regulation of cell volume in this cell line (Roy et al. 2008). Given that astemizole (AST) treatment reduces MCF7 proliferation, and is known to block both hERG and hEAG, this connects hEAG, but not hERG, with the proliferation of these cells.

Another VGKC with a potential role in the proliferation and cell cycle progression of MCF7 cells is $K_v1.1$. This channel is expressed in these cells, while a number of other VGKCs, including $K_v1.2$ and $K_{v1}.3$, have not yet been identified, or are absent (Ouadid-Ahidouch et al. 2000; Ouadid-Ahidouch and Ahidouch 2008).

Table 1.9: The effects of K^+ channel blockers on MCF7 proliferation and channel activity

Channel Blocker	Channel	Inhibition of MCF7 proliferation	K^+ channel activity IC_{50} (cell line[1])	References
4-amino-pyridine (4-AP)	VGKCs	IC_{50} 1.6 mM[2]	Between 0.1 and 4 mM (range of cell types including 3T3, human T lymphocytes and human melanoma cells)	Grissmer et al. 1994; Wonderlin and Strobl 1996; Yao and Kwan 1999
α-Dendrotoxin (α-DTx)	$K_v1.1$	30% inhibition: 10 nM	0.6 nM	Ouadid-Ahidouch et al. 2000
Amiodarone	Non-specific ion channel blocker	IC_{50} 1 μM (approx)		Abdul et al. 2003
Astemizole (AST)	hEAG and hERG	IC_{50} between 5 and 30 μM	hEAG: 196nM (HEK-293), 5μM effective in MCF7 hERG: 0.9nM (HEK-293)	Borowiec et al. 2007; Garcia-Ferreiro et al. 2004; Ouadid-Ahidouch et al. 2004b; Roy et al. 2008; Salata et al. 1995; Zhou et al. 1999
Charybdotoxin (CTx)	BK and IK	No effect up to 100 nM	50 nM	Coiret et al. 2005; Ouadid-Ahidouch et al. 2000; Ouadid-Ahidouch et al. 2004a; Ouadid-Ahidouch et al. 2004b
Clotrimazole	IK	25% inhibition: 5μM	2 μM (approx.)	Ouadid-Ahidouch et al. 2004b

Channel Blocker	Channels affected	Inhibition of MCF7 proliferation	K+ channel activity IC50 (cell line1)	References
Dequalinium	SK	IC_{50} 1 μM (approx.)		Abdul et al. 2003
E-4031	hERG	No effect < 300 nM	7.7 nM (HEK-293)	Roy et al. 2008; Zhou et al. 1998
Glibenclamide	ATP-sensitive K^+ channels	IC_{50} 50 μM	<0.05nM (pancreatic type in HEK-293) 51 nM (cardiac type in HEK-293)	Abdul et al. 2003; Stephan et al. 2006; Wonderlin and Strobl 1996
Iberiotoxin (IbTx)	BK	No effect up to 500 nM	100 nM approx.	Ouadid-Ahidouch et al. 2000; Coiret et al. 2005; Ouadid-Ahidouch et al. 2004a
Tetraethyl-ammonium (TEA)	VGKCs, ATP-sensitive K^+ channels, BK	IC_{50} 5.8 mM	2 mM 500 μM blocks BK channel	Coiret et al. 2007; Coiret et al. 2005; Grissmer et al. 1994; Ouadid-Ahidouch et al. 2000; Ouadid-Ahidouch et al. 2004a; Wonderlin and Strobl 1996; Yao and Kwan 1999

[1] *if no data available for MCF7*

[2] *Doses ≤1mM were not found to inhibit MCF7 proliferation (Abdul et al. 2003)*

Care must be taken when extrapolating the IC_{50} data summarized in Table 1.9, as in several cases (indicated) no data exists for MCF7 cells. However, in general, the data for MCF7 cells corresponds with other cell lines (Wonderlin and Strobl 1996). This highlights areas where the effects of these compounds in MCF7 require further characterization.

Where dose-response relationships have been studied, the IC_{50} for inhibition of proliferation is frequently higher than the IC_{50} for inhibition of K^+ current activity. This suggests that inhibition of proliferation may be through non-specific, or cytotoxic actions of the channel blocker, rather than through inhibition of K^+ channel activity, or that the effects on channel activity contribute a proportion of the response only. However, serum is added to the proliferation media but not the solutions used to record K^+ movement, and it is thought that components of the serum (e.g. albumin, the major FBS protein; Zheng et al. 2006) may either bind the channel blocker, reducing its effectiveness, or further promote proliferation (Wonderlin and Strobl 1996). In addition, where these channels have been ablated by silencing the gene (Koeberle et al. 2010; Weber et al. 2006), or transfected into cells known to not normally express them, similar results have been achieved (Cayabyab and Schlichter 2002; Dong et al. 2010; Gierten et al. 2008; Grissmer et al. 1994; Szabo et al. 2008; Zhang and Wang 2000) . These studies add strength to the argument that the channel blockers inhibit proliferation through blockade of K^+ channels, rather than through non-specific mechanisms.

Work is ongoing to understand the mechanisms through which these channels and channel blockers affect proliferation in breast cancer cells. As discussed, IGF1 is an important regulator of mammary gland development, and plays a key role in the initiation and progression of breast cancer (Hadsell 2003; Jin and Esteva 2008; Weinstein et al. 2009). Treatment of MCF7 with the growth factor IGF1 (0.1 to 20ng/ml for 48 hours) results in an increase in proliferation (Allan et al. 2006; Borowiec et al. 2007). This increase in proliferation was associated with a rapid (within 1 to 2 minutes) increase in K^+ current, membrane hyperpolarisation, and an increase in levels of the K^+ channel hEAG mRNA (Borowiec et al. 2007). IGF1 stimulated increase in proliferation was prevented by AST treatment, showing that hEAG is not only regulated by IGF1, but also plays a vital role in IGF1 mitogenic signaling in breast cancer cells. However, as discussed, AST is a relatively non-specific channel blocker, and has been shown to block hERG also (Pardo et al.

2005; Roy et al. 2008). It is possible that the results of these studies may reflect the combined activities of the two channels, although the lack of any effect of the hERG antagonist E4031 may suggest that hEAG is physiologically more important in this instance.

Activation of hEAG in MCF7 cells, by membrane depolarization to potentials higher than -20 mV, results in membrane hyperpolarisation. This is associated with cell cycle progression from G1 to S phase (Borowiec et al. 2007; Ouadid-Ahidouch and Ahidouch 2008; Ouadid-Ahidouch et al. 2004b; Strobl et al. 1995). Membrane hyperpolarisation is generally accepted to be involved in cell cycle progression, in what is known as the "membrane potential model" of proliferation (Ouadid-Ahidouch and Ahidouch 2008; Pardo 2004). Blocking hEAG or IK by silencing with small interfering RNA (siRNA) or use of inhibitors AST (blocks hEAG and hERG) and clotrimazole (IK blocker), leads to membrane depolarization, reduced intracellular Ca^{2+} $[Ca^{2+}]_i$ and accumulation of the cell cycle progression inhibitor p21 (Ouadid-Ahidouch and Ahidouch 2008; Ouadid-Ahidouch et al. 2004b). Their inhibitory effect was additive, but blocking hEAG resulted in greater proliferation inhibition and G1 phase arrest, than did blocking IK, leading to the suggestion that progression through G1 towards S phase is dependent on hEAG activity, while IK regulates membrane potential at the G1/S transition.

The relationship between calcium and potassium channels in breast cancer cells is complex, at times paradoxical, and poorly understood. Both hEAG and IK are regulated by an increase in $[Ca^{2+}]_i$ and calmodulin (CaM), a Ca^{2+} binding protein. However, while hEAG activity is inhibited by Ca^{2+}/CaM binding to its N-terminal domain (Ziechner et al. 2006), IK is activated by Ca^{2+}/CaM (Fanger et al. 1999). These effects can occur simultaneously in MCF7 cells (Ouadid-Ahidouch and Ahidouch 2008).

Calmodulin is required for the proliferation of numerous breast cancer cell lines including MCF7, T47D and MDA-MB-231, regardless of E2 treatment or ER status. This is demonstrated by incubation with CaM antagonists (Jacobs et al. 2000). In addition, inhibition of the calcium-calmodulin-dependent kinases (CaM-Ks) by siRNA or antagonists also reduced proliferation and caused G1 phase arrest in MCF7 cells (Rodriguez-Mora et al. 2005), possibly by inhibiting cyclin D1 synthesis and retinoblastoma protein phosphorylation. Interestingly, CaM also binds to the ERs,

increasing their stability and cellular levels, in a Ca^{2+}-dependent, E2-independent manner (Li et al. 2001), and calcium-calmodulin-dependent kinase IV was determined to be activated by ERα/E2 in MCF7 cells, although not by ERα in combination with resveratrol or a number of xenoestrogens (Li et al.2006).

Ouadid-Ahidouch et al. (2008) propose the following basic model for the regulation of hEAG and IK by Ca^{2+}/CaM, and their role in proliferation, which is summarized in Figure 1.6. In early G1 phase membrane potential is depolarized (around -20mV) and $[Ca^{2+}]_i$ is low, resulting in the activity of hEAG but not IK. The Ca^{2+} channels are inactive at this point. Mitogenic stimuli result in an increase in hEAG expression, and activity (hEAG is depolarization activated, so operational at this potential). The result is that the membrane becomes hyperpolarized (more negative) as G1 phase progresses. This deactivates hEAG, but causes an influx of Ca^{2+} into the cell cytoplasm from internal stores, and from the external environment by way of the increased electrochemical driving force for Ca^{2+} promoting its movement through inwardly rectifying (voltage-insensitive) plasma membrane channels (depolarisation induced an increase in $[Ca^{2+}]_i$ in rat megakaryocytes even in Ca^{2+} free medium; Mahaut-Smith et al. 1999). Increasing levels of $[Ca^{2+}]_i$ and Ca^{2+}/CaM activate IK, resulting in stronger membrane hyperpolarization. As G1 progresses to S phase, CaM and the CaM-Ks are also involved in the regulation of levels of cell cycle proteins such as cyclin D1 and p21. The end result is progression to s phase, and enhanced proliferation of the breast cancer cells.

In MCF7 cells, a non-inactivating outward K^+ current was found which was inhibited dose- and voltage-dependently by α-dendrotoxin (α-DTx), with maximal inhibition being obtained at 10nM α-DTx after 7 minutes of treatment, and an IC_{50} of 0.6 ± 0.3 nM (Ouadid-Ahidouch et al. 2000). Alpha-DTx is a toxin from the Black Mamba (*Dendroaspis augusticeps)*, and blocks the channels $K_v1.1$, $K_v1.2$ and $K_v1.6$ (Harvey and Robertson 2004). RT-PCR and immunocytochemical methods have shown that $K_v1.1$ is present in MCF7 cells, but anti-$K_v1.2$ antibodies did not label these cells (Ouadid-Ahidouch et al. 2000), indicating that $K_v1.1$ may be the pharmacological target of α-DTx in this case. $K_v1.6$ was not included in this examination, and it is not known whether this channel is present in MCF7. [^{3}H]-Thymidine labeling of DNA was used to determine that α-DTx inhibited MCF7 proliferation in a dose-dependent manner, at the same doses which inhibited K^+ current. Ouadid-Ahidouch et al. (2000) suggest that this implicates $K_v1.1$ in the proliferation of MCF7 breast cancer

cells, however, the involvement of $K_v1.6$ cannot be ruled out. Down-regulation of $K_v1.1$ expression by siRNA significantly reduced the proliferation of rat gastric mucosal epithelial cells, also measured by [^{3}H]-Thymidine incorporation (Wu et al. 2006).

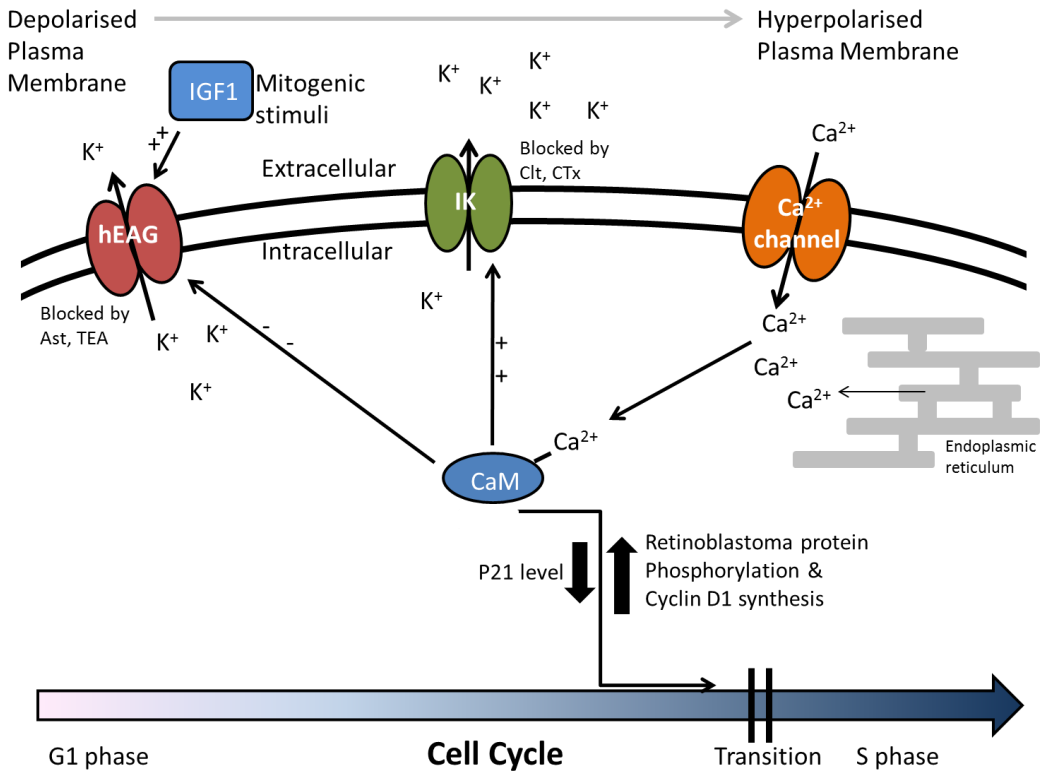

Figure 1.6: Membrane potential model of breast cancer cell proliferation

Ast, Astemizole; CaM, Calmodulin; Clt, Clotrimazole; CTx, Charybdotoxin; hEAG, Human ether-a-go-go K^+ channel; IGF1, Insulin-like growth factor 1; IK, Intermediate conductance K^+ channel; TEA, Tetraethyl Ammonium

Membrane depolarization and mitogenic stimuli in early G1 resuslts in the activation of hEAG. The resulting K^+ efflux causes membrane hyperpolarization, and an increase in $[Ca^2]_i$ due to an influx along its the electrochemical gradient (through voltage-insensitive inwardly rectifying Ca^{2+} channels, and the release of internal stores. This activates the IK channel, resulting in further hyperpolarization and the cell progresses to S phase.

The BK channels appear to have only a minor role in the normal proliferation of MCF7 cells, and their blockade induces only weak depolarization. However, their expression level and activity is cell cycle dependent, both peaking at the end of G1 phase (Ouadid-Ahidouch et al. 2004a). The relevance of this linkage to the cell cycle is unknown, but may signify that they have small a regulatory role. However, BK expression may relate to the invasiveness of breast cancer cell lines. MDA-MB-361 cells, with high levels of both *KCNMA1* mRNA and BK protein, were considerably more invasive on a matrigel coated membrane than either MDA-MB-231 or MCF7 cells, which both display much lower levels of the protein and mRNA. Un-transformed mammary epithelial cell line MCF10A was not invasive and had very low levels of BK protein present (Khaitan et al. 2009).

1.6.5 Potassium channels mediate an essential early stage of apoptosis

Interestingly, the K^+ channels have also been implicated as key regulators of apoptosis in many cell types (Wang 2004). Cell shrinkage under isotonic conditions is known to be an essential early stage in apoptosis in a wide range of mammalian cell types including MDA-MB-231 breast cancer cells, Jurkat T lymphocytes and human renal HEK239 cells, epithelial HeLa cells, lymphoid U937 cells and the neuronal cell lines NG-108-15 and PC12 (Gow et al. 2005; Kossler et al. 2012; Maeno et al. 2000; Vu et al. 2001). It is also referred to as apoptotic volume decrease (AVD). AVD occurs prior to other hallmarks of apoptosis such as cytochrome C release, caspase activation and DNA degradation (Maeno et al. 2000). A number of studies have shown that AVD is attributable largely to K^+ efflux, on the basis that net changes in cell osmolarity regulates the flow of water (Bortner and Cidlowski 1999; Bortner and Cidlowski 2004; Gow et al. 2005; Hughes, Jr. et al. 1997; Storey et al. 2003). However, Cl^- efflux, and the activity of the sodium-potassium exchanger (Na^+/K^+-ATPase) also play a role in this process (Bortner and Cidlowski 2004; Maeno et al. 2000).

In vitro studies have shown that K^+, at normal, non-apoptotic intracellular levels, directly inhibits apoptotic DNA fragmentation and caspase 3 activation in rat thymocytes (Hughes, Jr. et al. 1997). In the same study, disrupting K^+ efflux in these cells by incubating them in high K^+ medium inhibited apoptosis and caspase 3 activation in response to apoptotic agents, suggesting that K^+ efflux is a necessary event in apoptosis.

The interaction between caspase activation, shrinkage and K^+ efflux is complex. Caspase activation correlates with K^+ efflux in lymphocytes treated with Fas apoptosis inducer or UV exposure (Vu et al. 2001). This laboratory found that caspase 3 and 8 inhibitors blocked DNA degradation in lymphocytes treated with Fas, but failed to prevent AVD and K^+ efflux, suggesting that K^+ efflux is an early cellular response which occurs prior to caspase activation (Bortner and Cidlowski 1999). Refer to Figure 1.4 for a summary of Fas (extrinsic) and UV (intrinsic) apoptotic pathways. In apparent contradiction to this, the same group later demonstrated that the polycaspase inhibitor z-VAD-fmk abrogated AVD and K^+ efflux, in addition to preventing DNA damage and caspase activation in Fas-treated

lymphocytes (Vu et al. 2001). However, it was less effective at preventing UV-induced apoptosis. They went on to show, using specific caspase inhibitors and mutants lacking individual caspase genes, that caspase 8 is required for Fas-induced AVD, K^+ efflux, and programmed cell death. This confirms the role of caspase 8 described in the literature (Medema et al. 1997). Correspondingly, caspase 9 has similar indispensable roles in UV induced apoptosis (Vu et al. 2001). In EATC cells, AVD mediated by the loss of K^+, Na^+, Cl^- and amino acids is essential for caspase 3 activation in response to 5μM cisplatin (Hoffmann 2011). Together, these findings suggest that apoptotic K^+ efflux and caspase activation are tightly coupled but differentially regulated depending on the route of apoptosis induction, and are possibly also cell line specific.

In a number of human tumour cell lines functional hERG K^+ channels are required for effective induction of apoptosis in response to H_2O_2, and H_2O_2 treatment increased the outward flow of K^+ (Wang et al. 2002). In this study, cells lacking functional hERG required much higher concentrations of H_2O_2 to induce apoptosis, and in cells with functional hERG, co-treatment with the hERG blocker dofetilide (1μM) caused a dramatic reduction in the number of apoptotic cells after H_2O_2 treatment. It is possible that this function of hERG relates to the relationship between the expression levels of this channel and the increasing sensitivity to anticancer drugs described by Chen et al. (2005). However, while the hERG channel protein is present in MCF7, this effect has not been investigated in these cells.

Expression of hERG is similarly required for tumour necrosis factor α (TNFα; 1 and 10 ng/ml) induced apoptosis (Wang et al. 2002). Interestingly, lower doses of TNFα (1 and 0.1 ng/ml), which were less effective at inducing apoptosis, also enhanced proliferation. Again, this effect was more pronounced in cells expressing hERG, but was not affected by dofetilide treatment. Fluorescent antibodies were then used to suggest that hERG recruits the TNF-receptor (TNFR1) to the plasma membrane. The TNFRs (TNFR1 and TNFR2) have complex roles in the regulation of both apoptosis and proliferation, which are incompletely understood (Baxter et al. 1999; Haider and Knofler 2009). In apoptosis TNFR1 activates caspase 3, triggering the caspase cascade in this manner. The TNFRs induce proliferation through the transcription factor NF-κB (Haider and Knofler 2009). In accordance with this, cells expressing hERG showed higher levels of NF-κB activity than cells lacking hERG

expression, and that TNFα treatment induced a further increase in NF-κB activity (Wang et al. 2002). Interestingly, hERG has also been implicated in tumour proliferation (Pardo et al. 2005).

In T lymphocytes activity of the IK channel appears to be an essential early stage in calcimycin induced apoptosis and AVD (Elliott and Higgins 2003). This apoptosis inducer acts by increasing the inward flow of Ca^{2+} into the cell, initiating the Ca^{2+} dependent intrinsic apoptotic pathway. In this cell line at least, an increase in $[Ca^{2+}]_i$ triggered AVD *via* IK-mediated K^+ current, which was essential for the induction of apoptotic PS externalization, and later, increased membrane permeability.

In addition to their roles in the proliferation of breast cancer, there is also evidence to suggest that the channels $K_v1.1$ and $K_v1.3$ are involved in apoptosis in some cell lines. One group used the lymphocyte cell line CTTL-2, which is known to be deficient in K_v channels, and transfected them with a $K_v1.3$ expression vector or control expression vector. It was found that the presence of $K_v1.3$ specifically on the mitochondrial membrane both amplified and accelerated the ability of the lymphocytes to induce apoptosis in response to a number of stimuli, including TNFα, actinomycin-D and staurosporine (Bock et al. 2002; Szabo et al. 2008). They also demonstrated that overexpression of Bax triggered massive apoptosis in the $K_v1.3$-positive cells, but had no effect in cells lacking $K_v1.3$. Similarly, in rat retinal ganglions which constitutively express $K_v1.3$, blocking this channel with the relatively specific channel blockers agitoxin-2 or margatoxin greatly inhibited the ability of these cells to undergo apoptosis, and reduced the expression of the pro-apoptotic genes encoding caspase 3, caspase 9 and Bad, as determined by RT-PCR. Silencing the gene with siRNA had the same effect (Koeberle et al. 2010).

Likewise, in Jurkat T lymphocytes K^+ efflux through $K_v1.3$ was stimulated by Fas ligand (inducer of extrinsic, death receptor-stimulated apoptosis), accompanied by cell shrinkage and DNA degradation (Storey et al. 2003). This increase in current was prevented by $K_v1.3$-specific margatoxin or Shk-Dap^{22} (a mono-substituted analogue of a sea anemone toxin). Activity of caspase 8, but not caspase 3, was required for Fas-activated $K_v1.3$ channel activity, as demonstrated by use of broad and caspase 8 specific pharmacological inhibitors, and a line of lymphocytes which did not express caspase 8.

$K_v1.1$ has also been identified on the mitochondrial membrane in addition to the cytoplasmic membrane and, like $K_v1.3$, appears to have a role in the induction of apoptosis in lymphocytes (Szabo et al. 2008) and retinal ganglions (Koeberle et al. 2010). However, the mechanisms through which the two channels induce apoptosis may be different, as siRNA silencing of the $K_v1.1$ gene in rat retinal ganglions had no significant effect on the expression levels of caspase 3, caspase 9 and Bad (pro-apoptotic member of the Bcl2 family), but increased the levels of the anti-apoptotic gene Bcl-xl (Koeberle et al. 2010). Neither $K_v1.1$ nor $K_v1.3$ knockdown was found to affect the levels of Bcl2 mRNA.

Silencing of the gene encoding $K_v1.2$ in rat retinal ganglions caused some reduction in their ability to undergo apoptosis, although this was to a much lesser extent than $K_v1.1$ or $K_v1.3$ silencing, and ablation of $K_v1.5$ was found to have no effect (Koeberle et al. 2010). The VGKCs are also involved in induction of apoptosis in pulmonary artery smooth muscle cells, where incubation with 4-AP prior to an apoptotic stimuli reduces apoptosis significantly, increases intracellular K^+ concentration, inhibits caspase activity and prevents mitochondrial cytochrome c release (Park et al. 2010). Breast cancer cells have been demonstrated to express a number of VGKCs at different levels to untransformed cells or normal tissue. While the involvement of $K_v1.3$ in breast cancer cells is controversial, it has been reported in lower levels in cancerous breast tissue compared to normal breast tissue by one group (Brevet et al. 2008). In addition, Ouadid-Ahidouch et al. (2000) confirmed that the protein is not present in MCF7 cells. Absence or low levels of this K^+ channel may be related to the low levels of apoptosis seen in cancerous cells. However, surprisingly, the involvement of the VGKCs in the induction of apoptosis in breast cancer cells has not been investigated.

1.6.6 Effect of oestrogen and anti-oestrogens on MCF7 potassium channel activity

In MCF7 cells 10 nM E2 rapidly and irreversibly induced the BK channels (Coiret et al. 2005). This induction was not prevented by co-treatment with the ER antagonist ICI 182780 (1 µM). The rapid induction of BK channel activity by E2 treatment was considered likely to occur extra-cellularly since membrane impermeable BSA-conjugated E2 (10 nM) also caused the same effect. This study argues that E2 and BSA-E2 non-genomically and dose dependently stimulate proliferation of MCF7 cells. They also found that BSA-E2 stimulated proliferation was reduced by non-toxic doses of the BK channel blockers iberiotoxin (100 nM), charybdotoxin (50 nM) and TEA (500 µM), implicating this channel in E2-induced proliferation.

Interestingly, the same channels in MCF7 breast cancer cells were also induced by 10 nM treatment with the partial oestrogen antagonist tamoxifen (Coiret et al. 2007). This effect was not additive to the effects of E2 or BSA-E2, and it was unaffected by the presence of ICI 182780. Together, these results suggest that tamoxifen also acts independently of the ERs, possibly through the same extra-cellular mechanism as E2 in this case. Both 10nM E2 and 10nM tamoxifen induced proliferation of MCF7 cells, but similarly this effect was not additive. In addition, the BK channel blockers significantly reduced the 10nM tamoxifen effect on proliferation, suggesting, as with E2-induced proliferation, this channel may play a role in (low dose) tamoxifen-induced growth of MCF7 cells. It is important to note that this study was carried out using a low dose of tamoxifen, which was known to induce proliferation in MCF7 cells. In patients receiving tamoxifen as chemotherapy, there is considerable inter-individual variance in serum levels, but generally it is in the range of 0.1 to 5µM (Fahey et al. 1994).

The effects of higher, growth-inhibitory concentrations of tamoxifen, from 1µM upwards, on K^+ channel activity in breast cancer cells have not been investigated. However, the growth inhibitory effects of tamoxifen, and amiodarone (1µM) or dequalinium (1µM) strengthened each other, suggesting that tamoxifen may inhibit growth of MCF7 cells in a manner unrelated to ion channel activity (Abdul et al. 2003).

The effects of tamoxifen and ICI 182780 on the BK channels in other cell lines vary. They have both been shown to activate this channel in canine colonic smooth muscle cells (1 μM tamoxifen and 10 μM ICI 182780) (Dick et al. 2001; Dick 2002), but 10μM tamoxifen treatment had no effect on BK activity in vascular endothelial (HUVEK) cells (Li et al. 2000). ICI 182780 had an inhibitory effect on BK channel activity in human coronary artery epithelial cells, with all doses between 1 and 30 μM rapidly reducing channel activity in a dose dependent manner, with an IC_{50} of 3 μM (Liu et al. 2003). However, in human coronary artery smooth muscle cells, ICI 182780 caused a bell shaped dose-response for BK channel activity, with doses below 3 μM increasing the number of open channels, while higher doses reduced channel activity (Dick 2002; Liu et al. 2003).

Evidently, the effects of oestrogen and antioestrogens on BK channel activity are complex and differ depending on cell type, but are unlikely to relate to their ability (or otherwise) to activate transcription through the ERs. In MCF7 cells, the ability of E2 and low dose-tamoxifen to induce proliferation is associated with their ability to activate BK channel activity, but the effect of ICI 182780, which does not induce proliferation, or growth-inhibitory doses of tamoxifen, on BK in MCF7 cells is unknown.

1.6.7 Effects of isoflavones on the activity of potassium channels: a possible breast cancer protective mechanism

Due to its non-specific protein tyrosine kinase (PTK) inhibitory actions, genistein is frequently utilized in studies investigating the regulation of K^+ channel activity. In this manner it has been determined that genistein and other isoflavones, at concentrations ranging from 10 to 100 µM inhibit K^+ current through many channels in a number of expression models or excitable cardiac cells and lymphocytes, with resting membrane potentials of around -70 mV. In the majority of these cases the response to genistein, or other protein tyrosine kinase inhibitors has been very rapid (within seconds or minutes of treatment) arguing for a direct influence on signaling pathways or the channel proteins themselves, rather than changes in gene expression.

Since many of these channels have roles in proliferation and apoptosis, the impact of K^+ channel inhibition by isoflavones may be relevant to the pro-proliferative or pro-apoptotic actions of these compounds. However, as far as can be ascertained, no studies to date investigating the effects of isoflavones on K^+ channels in breast cancer cells (resting membrane potential of around -50 mV) have been conducted, so their impact on breast cancer proliferation or apoptosis is unknown. The next section addresses current knowledge regarding the impact of soy isoflavones on the potassium channels known to be associated with breast cancer proliferation, apoptosis, or the MCF7 cell line.

1.6.7..1 hERG and the rat homologue rERG

Using human embryonic kidney (HEK293) cells stably transfected with hERG, it was found that the K^+ current through this channel was inhibited by 30 µM genistein (Zhang et al. 2008). Co-treatment with 1 mM orthovanadate, a protein tyrosine phosphatase (PTP) inhibitor, countered the suppression of current, signifying that hERG K^+ current inhibition by genistein is dependent upon its ability to inhibit protein tyrosine kinase activity. Orthovanadate alone failed to have the opposite, current promoting effect suggesting that basal levels of TK-substrate phosphorylation may be saturated. Daidzein (a PTK inactive analogue of genistein) treatment resulted in some current inhibition at higher doses, although this was much less pronounced,

making it impossible to rule out the possibility that higher doses of genistein may have some direct channel blocking properties also.

Additionally, Zhang et al. (2008) demonstrated that the hERG current was inhibited by the selective PTK inhibitors AG556 and PP2 (both at 10 μM). These compounds inhibit epidermal growth factor receptor (EGFR) and Src-family tyrosine kinase activity respectively, and consequently implicate both kinases in the regulation of hERG. Whether genistein, AG556 and PP2 inhibit current through hERG in the same manner was not investigated. However, Western blots demonstrate that genistein, AG556 and PP2, at the doses described, each reduce phosphorylation of the channel protein in a manner antagonized by orthovanadate (Zhang et al. 2008). Again the PTP inhibitor alone had no effect on channel phosphorylation suggesting that under control conditions hERG phosphorylation is saturated.

Whole cell patch clamp recordings taken from MSL-9 cells derived from rat microglia identified a depolarization activated inwardly rectifying current that was fully and specifically blocked by 1 μM E-4031 treatment, suggesting that it was mediated by the rat homologue of hERG (rERG; 99% homology) (Cayabyab and Schlichter 2002). Following 15 to 20 minutes of treatment with the broad spectrum PTK inhibitors lavendustin A or genistein (each at 50 μM) current amplitude was reduced to a significantly greater extent than the spontaneous rundown effect (35% and 60% respectively). Daidzein (50 μM) had no significant effect. The same group demonstrated that treatment with the Src-selective PTK inhibitor herbimycin A for over 12 hours, reduced current amplitude by around 70%. This data indicates that rERG K^+ current is inhibited by broad and Src-specific PTK inhibitors. Using Western blots with anti-rERG and anti-phosphotyrosine antibodies, Cayabyab and Schlichter (2002) proceeded to show that rERG was constitutively tyrosine phosphorylated in these circumstances, and that 12 hours of pre-treatment with genistein (50 μM) or herbimycin A (3 μM) significantly reduced tyrosine phosphorylation of rERG, by 40% or 25% respectively.

These studies together suggest that hERG, and the rat homologue rERG, are regulated by PTK activity, including by the EGFR and Src-related kinases, and that genistein treatment inhibits h/rERG K^+ current through its ability to inhibit a broad spectrum of PTK activity. No attempt has been made to distinguish between direct inhibition of PTK phosphorylation of the channel or upstream interactions with other

signaling molecules. The precise mechanism of inhibition is not known in either case. The close homology between rERG and hERG makes it likely that the two channels are regulated in a similar manner, although caution must be used when making direct comparisons.

The hERG channel does not appear to have a role in the proliferation of breast cancer cells (Roy et al. 2008), so its inhibition by genistein is unlikely to directly relate to the growth inhibitory effects of this isoflavone. Instead, the inhibition of hERG by genistein may dampen the pro-apoptotic effects of this channel, and so in this manner relate to the growth-promoting properties of isoflavones. Although the doses of genistein used to inhibit hERG K^+ current are comparable to the range of doses used to inhibit proliferation and induce apoptosis in both ERα+ and ER- breast cancer cell lines, as discussed it may be of little value to directly compare effective concentrations between patch clamping and proliferation experiments. Regrettably, neither of the above groups has provided data for a dose-response or IC_{50} for genistein and hERG activity. It would be of considerable interest to investigate the effect of genistein on the activity of hERG in breast cancer tissue or cell lines.

1.6.7..2 $K_v1.3$

Whole cell voltage-sensitive K^+ current amplitude was reduced to below 50% by 40μM genistein in circulating human T lymphocytes by the whole cell patch clamp method (Teisseyre and Michalak 2005). Current blockade by genistein was dose-dependent, with half-maximal blockage occurring in the concentration range between 10 and 40 μM. Current activation was also slower after genistein treatment. In these cells the VGKC current is carried predominantly by the $K_v1.3$ channel (Cahalan et al. 2001), and the current was completely blocked by addition of 5 mM 4-AP, suggesting that these channels may be the target of genistein inhibition in lymphocytes.

Teisseyere and Michalak (2005) also found that the current measured, after co-treatment with 10 μM genistein and 1 mM orthovanadate, was not significantly different to that after genistein treatment alone. This suggests that in the case of $K_v1.3$ channels in human T lymphocytes, current inhibition by genistein occurs in a predominantly PTK-independent manner. $K_v1.3$ current was unaffected by

treatment with 40 μM daidzein. In both T lymphocytes and breast cancer cells expressing $K_v1.3$, treatment with the VGKC blocker tetraethyl ammonium (TEA) inhibited proliferation, as measured by the MTT assay and [^{3}H]-thymidine incorporation into DNA respectively (Cahalan et al.2001; Jang et al. 2009). In both cases the doses of TEA used were non toxic.

The doses of genistein used in to inhibit current through $K_v1.3$ (10 to 40 μM) correspond with the range of doses known to inhibit proliferation and induce apoptosis in breast cancer cell lines. These doses are slightly higher than the physiologically relevant high serum levels (1 to 10μM), however, as discussed, differences in experimental conditions and media may account for incongruities between the IC_{50}s for genistein on K^+ channel activity and proliferation. Bearing this in mind it is possible that genistein may inhibit breast cancer proliferation *via* inhibition of the $K_v1.3$ channel. $K_v1.3$ is also involved in the induction of apoptosis in a number of cell lines, but there is no evidence to suggest that genistein treatment inhibits the induction of apoptosis. However, while this channel is expressed in many breast cancer tissues, it has not been detected in MCF7 cells (Ouadid-Ahidouch et al. 2000). It is interesting to note that $K_v1.3$ in human T lymphocytes was also inhibited in a similar manner by resveratrol, a phytoestrogen found in grapes and wine, with an IC_{50} value calculated to be 40.9 ± 5.0 μM (Teisseyre and Michalak 2006).

1.6.7..3 BK channel

Resveratrol has been demonstrated to dose dependently stimulate outward BK and IK channel activity in vascular endothelial HUVEC cells, with an EC_{50} (concentration required for a half-maximal effect) of 20 μM, using the whole cell patch clamp technique. This same group found that quercetin (30 μM) had no effect (Li et al. 2000). Resveratrol appeared to enhance channel activity by increasing the length of time that each channel was open for, rather than raising the conductance of individual channels.

Puerarin, the main isoflavone found in the root of the leguminous creeper Kudzu (*Pueraria lobata)*, also potently and rapidly activated the BK channel in *Xenopus* oocytes, when applied to the cytoplasmic side of an excised cell membrane patch at negative potentials in a Ca^{2+} dependent manner, with EC_{50}s of 12.6nM and 0.8nM

with and without 10 μM Ca^{2+} respectively (Sun et al. 2007). This indicates either that calcium may facilitate BK activation by puerarin, or that puerarin increases the Ca^{2+} sensitivity of the channel. Daidzein, a hydrolysate of puerarin, lacking a glycosyl residue at the 8-position, also increased the BK current, but to a lesser extent than puerarin, suggesting that the 8-glucosyl residue has a role in the activation of the channel.

To the author's knowledge, the effect of genistein on the activity of the BK channel is not known. While BK channel activity appears to be unrelated to the regulation of proliferation in breast cancer, there is evidence suggesting that it plays a role in invasiveness or metastasis (Khaitan et al. 2009). This may be a mechanism through which isoflavones exert some of their protective effects against breast cancer.

1.6.7..4 The delayed rectifier K^+ current (I_{KS})

The slowly activated delayed rectifier current I_{KS} in Guinea pig ventricular myocytes is an outward K^+ current carried by a channel formed from *KCNQ1* (K_v7.1) and *KCNE1* subunits (Chen et al. 2009; Vanoye et al. 2010). Mutations in these proteins are implicated in severe hereditary cardiac arrhythmias such as long QT syndrome.

K_v7.1 was dose-dependently inhibited by treatment with genistein at concentrations between 3 and 100μM (Dong et al. 2010). This team used the perforated patch clamp technique[6] with HEK293 cells stably expressing recombinant K_v7.1. Daidzein (100μM; PTK inactive analogue of genistein) treatment resulted in some current inhibition, although it was much less pronounced than lower doses of genistein, making it impossible to rule out the possibility that higher doses of genistein may have some direct channel blocking properties also. Co-treatment with 1mM orthovanadate (PTP inhibitor) countered the suppression of current by 30 μM genistein, suggesting that K_v7.1 current inhibition by genistein is dependent upon its ability to inhibit PTK activity. Orthovanadate alone failed to have the opposite, current promoting effect suggesting that basal levels of TK-substrate phosphorylation may be saturated.

[6] Perforated patch: whereby the pipette pulls back once the gigaseal is formed, rupturing the membrane and leaving a membrane-vesicle over the end of the pipette tip. As the membrane is now inside out, this allows changes to the bath solution composition to reflect changes in the cytosol.

By using the selective PTK inhibitors PP2 (Src-related kinase inhibitor; 1 μM) and tyrphostin AG556 (EGFR kinase inhibitor; 20 μM) at doses vastly in excess of their IC_{50} for PTK inhibition, it was determined that $K_v7.1$ was regulated by EGFR kinase but not the Src kinases. Similarly, immunoprecipitation and Western blotting revealed that both genistein (30 μM) and AG556 (30 μM) significantly reduced phosphorylation of $K_v7.1$ in a manner reversible by addition of 1 mM orthovanadate, while PP2 had no effect. Interestingly, Dong et al. (2010) demonstrated that the higher dose of 20 μM PP2 substantially inhibited the current, but this effect was not countered by addition of orthovanadate, implying that it acts through PTK-independent mechanisms at these doses, or again masks the weaker opposing effect of orthovanadate.

Overall, it appears that genistein reduces I_{KS} by inhibiting the tyrosine phosphorylation of $K_v7.1$, either directly or by inhibiting EGFR kinase, while daidzein, with far lower PTK-inhibitory action, had a significantly reduced effect. However, no significant alterations in EGFR phosphorylation were seen after treatment with genistein concentrations up to twice the IC_{50} for growth inhibition (Peterson and Barnes 1996). This points to direct inhibition of PTK phosphorylation of the channel by genistein, possibly in a similar manner to AG556. However in this case the hypothesis was not investigated further.

Similarly I_{KS} in guinea pig ventricular myoctyes was dose-dependently and reversibly inhibited by genistein, with an IC_{50} of 64 ± 4 μM (Missan et al. 2006). The Hill coefficient of this response was significantly different from one, indicating that other molecules may be involved in regulation of I_{KS}. On this occasion the current was measured by voltage clamping using the whole cell method. They found that treatment of myocytes with the non-specific PTK inhibitors tyrphostin A25 and A23 also suppressed I_{KS} (IC_{50} 12.1 ± 2.1 and 4.1 ± 0.6 μM respectively). Current inhibition was likely to be caused by the PTK–inhibitory actions of each of these compounds, as the PTK-inactive analogues genistin, tyrphostin A1 and tyrphostin A63 had no effect on current amplitude up to doses of 200 μM. Daidzein inhibited current dose-dependently but to a substantially lesser extent, again suggesting that genistein may also have some direct channel-blocking activity.

In agreement with Dong et al. (2010), Missan et al. (2006) demonstrated that current inhibition by 50 μM genistein was significantly reduced by co-treatment with

orthovanadate (1 mM), while the PTP inhibitor alone had no effect. This confirms that genistein regulates I_{KS} through its PTK inhibitory properties. They present data which appears to rule out the possibility of orthovanadate acting through parallel mechanisms, by regulating the activity of serine/threonine kinases such as PKA. This tends to suggest simply that a stronger inhibition of PTK activity by higher doses weakens the ability of orthovanadate to restore I_{KS}. Inhibition of the serine/threonine kinases PKA, PKB, PKC, ERK1/2 and the stress-activated protein kinase p38 had no effect on the inhibition of I_{KS} by PTK inhibitors, although these experiments used tyrphostin A25 in the place of genistein, suggesting that I_{KS} is not regulated by any of these signaling kinases.

Missan et al. (2006) demonstrate that treatment with the Src-related kinase inhibitor PP2 (10 μM) reduced the amplitude of I_{KS} while AG1478, another EGFR PTK inhibitor (10 μM) had little effect, suggesting that Src-PTK activity is involved in regulating I_{KS} activity, but EGFR-PTK is not. This directly contradicts the results of Dong et al. (2010) who proposed that EGFR but not Src played a role in the regulation of this current. The discrepancies between these results may relate to the different cell line used by each group. However, it is possible that it reflects different regulatory mechanisms of the two channel subunits, KCNQ1/K_v7.1 and KCNE1. While Missan et al. (2006) studied “wild type” currents in cardiac cells, Dong et al. (2010) transfected the K_v7.1 subunit into another cell line to study it in isolation.

Overall, these two groups have generated clear evidence for the tyrosine kinase regulation of I_{KS}, and each concludes that genistein inhibits K^+ flux through this channel *via* its ability to inhibit PTK activity. In each case daidzein, with weaker PTK activity than genistein, resulted in weaker inhibition of current, and inactive genistin (precursor molecule) had no effect at the doses used. Their conclusions regarding the mechanisms of inhibition are inconclusive. However, while K_v7.1 is known to be present in MCF7 cells, any involvement it may have in the regulation of proliferation or apoptosis is yet to be documented.

1.6.8 Osmotic volume regulation

It is apparent that an element of the involvement of K^+ channels in proliferation, and more so in apoptosis, is related to their effects on osmolarity and volume regulation. Alterations in the osmolarity of the extracellular medium result in rapid movements of water in or out of the cell, driven by the osmotic gradient, and resulting in volume change. Swelling is induced by a change into a hypotonic solution, and shrinkage by a hypertonic solution. Following this, in numerous cell types plasma membrane ion pumps or channels are activated, resulting in a loss or gain (as appropriate) of intracellular ions, and corresponding osmotic movement of water returning cell volume to its former level (Dubois and Rouzaire-Dubois 2004). Regulatory Volume Increase (RVI) refers to the process of the cell swelling after shrinkage in a hypertonic solution, and is largely related to the activity of Na^+-K^+-Cl^- cotransporters and/or the Cl^--H^+ and Cl^- HCO_3^- exchangers. The corresponding pathway Regulatory Volume Decrease (RVD) occurs after hypotonic-induced swelling, and is mediated by the Cl^- and K^+ channels (Caplanusi et al. 2006; Dubois and Rouzaire-Dubois 2004).

RVD occurs in numerous cell types, including MCF7 and MDA-MB-231 breast cancer cells (Gow et al. 2005; Roy et al. 2008; vanTol et al. 2007), and can reduce cell volume back to near isotonic levels within 30 minutes (Huang et al. 2011; Pan et al. 2007). It is regulated by the MAPKs, although in a tissue specific manner, and can be prevented by agents which block these pathways. Little is known about the regulation of RVI. Although RVD is a response to a non-physiological stimulus, very similar regulatory mechanisms are proposed to play a role in volume regulation during proliferation and apoptosis (Wonderlin and Strobl 1996). Likewise, RVD is coupled to AVD, and both are regulated by similar mechanisms in numerous cancerous cell lines (Hoffmann 2011; Maeno et al. 2000).

1.6.8..1 Regulatory volume decrease in MCF7

Upon treatment of MCF7 with relatively non-specific K^+ channel blockers such as BaCl (5mM), quinine (0.5mM), TEA (10mM), and imipramine (100µM) in a hypotonic solution, the cells underwent swelling as expected, but RVD was reduced or prevented (Roy et al. 2008; vanTol et al. 2007). This helps to confirm the role of K^+ channels in RVD in MCF7. Charybdotoxin (100nM) and clotrimazole (30µM) had no

effect, ruling out the BK and IK channels in this response. However treatment with a hypotonic solution and 300nM E4031 or 30µM AST both prevented RVD, suggesting that the hERG, and perhaps hEAG channels are involved in this response (Roy et al. 2008). This supports the role of hERG in AVD and apoptosis.

Similarly, the $K_v7.1$ channel blockers 293B and XE991 were also found to prevent MCF7 RVD (vanTol et al. 2007). To confirm the role of this channel in volume regulation, this group transfected MCF7 with a dominant-negative *KCNQ1* ($K_v7.1$ gene), which also prevented RVD. In MCF7 (wild type) they were able to record a small 293B-sensitive current using whole cell patch clamping under hypotonic but not isotonic conditions, and overexpression of KCNQ1 increased this current component. The apparent parallels between RVD and AVD indicate that $K_v7.1$ may have a role in the induction of apoptosis in MCF7, although this is circumstantial, and yet to be proven.

1.6.8..2 Isoflavones and regulatory volume decrease

Treatment with upwards of 100µM genistein has been shown to attenuate RVD and swelling induced K^+ efflux in a wide range of cell types, including human bronchial epithelial 16HBE14o$^-$ cells (Caplanusi et al. 2006), Ehrlich ascites tumour cells (EATC; Kirkegaard et al. 2010) and the human erythroleukemic cell line K562 (Huang et al. 2011). Other K^+ channel inhibitors such as gadolinium and quinine (both 0.5mM), the PTK inhibitor tyrphostin (100µM) and other Src and EGFR-kinase specific inhibitors acted similarly (Caplanusi et al. 2006; Huang et al. 2011). In addition, the PTK inhibitor monoperoxo(picolinato)-oxo-vanadate (mpVpic; 10µM) prevented genistein-inhibition of K^+ efflux and RVD in EATC cells (Kirkegaard et al. 2010). The latter group also present evidence to suggest that RVD in this cell line is mediated by the TASK2 channel, and does not involve the K^+-Cl^- cotransporter as K^+ efflux continued to occur when all extracellular Cl^- was replaced with NO_3^-. It is possible based on this that PTK regulation of RVD is cell line specific. Regardless, in each of these studies discussed a large, non-physiological genistein dose has been used, which may have non-specific or cytotoxic effects. In the case of Kirkegaard et al. (2010) this went as high as 371µM (at least 10-fold greater than a physiological dose).

There was only one instance of use of a lower, genistein dose to study cell volume regulation. Treatment with 30µM genistein inhibited the swelling activated chloride current in isolated rabbit articular chondrocytes (Okumura et al. 2009). The same concentration of daidzein had a related, although lower magnitude effect. Treatment of rat hepatoma HTC cells with 10µM genistein prevented RVI (Feranchak et al. 2003). However this was related to an effect on Na^+ channels rather than K^+. The impact of these concentrations of isoflavones on K^+- related volume regulation is not known.

1.6.9 Summary of the impact of isoflavones on K^+ current and volume regulation

This section has discussed the growing body of evidence supporting the theory that K^+ channels, through their ability to regulate E_m and cell volume regulation, have roles in the proliferation of breast cancer cell lines, and progression of the disease in patients. Of the numerous K^+ channels discovered, some of those to show altered expression in cancerous breast tissue biopsies include hEAG, hERG and $K_v1.3$. While the latter channel is not present in MCF7 cells, hEAG and hERG are, along with $K_v1.1$, and a number of Ca^{2+} activated and inwardly rectifying K^+ channels.

Through altering their expression levels, and pharmacological blockade or activation, hEAG, $K_v1.1$, and several of the Ca^{2+} activated K^+ channels have been demonstrated to play important roles in MCF7 proliferation. This is conjectured to be through the mitogen-stimulated "membrane potential model of breast cancer proliferation", whereby altered patterns of K^+ channel activity result in changes in membrane potential on a large scale, stimulating cell cycle progression.

However, paradoxically, a number of the K^+ channels (often the same ones that are involved in proliferation) have indispensable roles in the induction of apoptosis in a range of cell types including some tumour cell lines. The major players in this process appear to be hERG, the IK channel, and some VGKCs. Their involvement in apoptosis seems to relate not to their impact on membrane potential, but their ability to regulate osmolarity, and consequently cell volume (shrinkage is widely accepted to be an essential early stage in apoptosis).

In its capacity as a tyrosine kinase inhibitor, genistein is frequently called upon to block the activity of numerous K^+ channels in a wide range of cell types, although never in cultured breast cancer cell lines. A number of these channels have significance to breast cancer, in the context discussed. Genistein blocks the activity of the hERG channel, and in this manner may lessen the role of hERG in the induction of apoptosis. Likewise, genistein inhibits the activity of several of the other VGKCs ($K_v1.3$ and $K_v7.1$), which may relate to inhibition of breast cancer cell proliferation seen with higher concentrations of isoflavones. On the whole, pharmacological concentrations of genistein have been used (typically in excess of 50µM). The effect of physiological concentrations is not known. The impact of

daidzein on K^+ channel activity is not widely known, but where it has been investigated it tends to be less active than genistein. Interestingly, E2 and the selective antioestrogen tamoxifen have been found to activate the BK channel in MCF7. In each case, genistein, daidzein and E2 have acted upon the K^+ channels quickly (within minutes of treatment) arguing a direct interaction with the channel protein or activation of a rapid signaling cascade rather than a genomic response.

An element of the role of K^+ channels is linked to their impact on cell volume. This is of particular significance for shrinkage and the induction of apoptosis. AVD is coupled in its regulatory mechanisms to the non-physiological process of RVD, which is widely studied in MCF7 and other cell lines. There is evidence supporting the role of hERG in apoptosis, and also $K_v7.1$, through their implication in RVD.

Genistein attenuates RVD in many cell types, although once again often very high concentrations are used. The prevention of RVD by genistein, and accordingly prevention of AVD, may contribute to a pro-proliferative mechanism of isoflavones. However considerable further testing of these hypotheses is required, importantly, at physiologically relevant isoflavone concentrations.

1.7 Proposed investigations

1.7.1 Study design and aims

The aim of this project was to further investigate the effects of common dietary soy isoflavones on breast cancer cell proliferation, apoptosis, and potassium channel activity.

To achieve this there were two main objectives:

1. To determine the effect of achievable levels of specific isoflavones, at pre- and post- menopausal oestrogen concentrations, on breast cancer cell apoptosis and proliferation

2. To characterize the effect of isoflavones on volume regulation and K^+ channel activity in breast cancer cells, and to investigate whether this contributed to their pro-apoptotic or pro-proliferative properties

This was a two phase project. Both stages were conducted *in vitro*. Firstly apoptosis and proliferation were measured in ERα+ and ERα-/ERβ+ breast cancer cell lines after treatment with a range of concentrations of genistein and daidzein, the main isoflavone phytoestrogens in soy, and either pre- or post-menopausal E2. These were as single treatments or in combination with each other. Secondly, the impact of several concentrations of genistein, daidzein and 17β-oestradiol identified in the first stage was investigated on cell volume (mediated by ion movement, including K^+) and the activity of the VGKCs, specifically hEAG and hERG. How these factors related to the proliferative effects of these isoflavones was explored.

1.7.2 Rationale and study design for the investigation of the proliferative and apoptotic effects of isoflavones and oestrogen, alone and in combination

The proliferative effects of the soy isoflavones genistein and daidzein at a wide range of physiologically relevant concentrations (<10μM) are well defined in ERα+ and ERα-/ERβ+ breast cancer cell lines. Furthermore, there is a considerable body of evidence suggesting that the induction of apoptosis may be a mechanism through which the soy isoflavones mediate their putative breast cancer protective effects. However, the induction of apoptosis by isoflavones in these cell lines has not been reported on at physiologically relevant concentrations of the isoflavones below 5μM. Likewise, their effects on proliferation and apoptosis in combination with pre-and post-menopausal oestrogen levels are relatively unclear. It has been suggested that at premenopausal E2 levels high concentrations of isoflavones, comparable to those seen in the blood of individuals consuming a very high soy diet, reduce proliferation and induce apoptosis in breast cancer cells. However the effects of soy isoflavones on ERα-/ERβ+ breast cancer cells and at post-menopausal E2 levels is less clear. Research in these areas is a priority as this population of women are at greater risk of the disease, and frequently consume isoflavone supplements for relief of menopausal symptoms.

The neoplastic human breast epithelial cell lines MCF7 and MDA-MB-231 were used as models of ERα+ and ERα-/ERβ+ breast cancer, respectively. While this environment may not be identical to that of an *in vivo* model of the disease, they are regarded as valid for this use, are well characterized, and behave reproducibly. The cell lines were treated with physiologically relevant levels (serum levels achievable through the diet) of two soy isoflavones at pre- and post-menopausal 17β-oestradiol levels, to determine the effects of these combinations of treatments on the ability of the cells to proliferate and/or induce apoptosis.

Proliferation was assessed in both cell lines using the MTT assay. This is a very widely used method, which is sensitive, reproducible, and relatively high throughput. This method, and the rationale behind its choice is discussed fully in sections 2.4 and 6.1.1. The method was also validated against the Trypan blue dye exclusion assay in both cell lines for a range of the treatments used. The impact of the vehicle solvent, genistein and daidzein at a range of physiological concentrations, and pre-

and post-menopausal E2 concentrations on proliferation were investigated. Following this, the effect of combined treatments of genistein or daidzein at pre- and post-menopausal E2 levels was assessed.

In accordance with the advice of the NCCD, two methods to assess the impact of the isoflavones on the induction of apoptosis in MCF7 and MDA-MB-231 cells were used. The first was the Annexin V-Cy3™ Apoptosis Detection Kit (Sigma), which identified apoptotic cells externalizing phosphatidyl serine on their plasma membrane (sections 2.5 and 6.2.1). Following this the DAPI fluorescent nuclear stain was used to characterize nuclear morphology and identify apoptotic changes (sections 2.6 and 6.2.1). Hydrogen peroxide was used as a positive control for the induction of apoptosis. Following this, the effect of the solvent, and a range of physiological concentrations of genistein, daidzein, and E2 (alone and in combination with each other) was assessed on the induction of apoptosis in both cell lines using the two techniques.

1.7.3 Rationale and study design for the investigation into the effects of isoflavones on K^+ channel activity and volume regulation in breast cancer cells

Potassium channels appear to have a central role in the regulation of proliferation and apoptosis in breast cancer, in both breast tissue and breast cancer cell lines such as MCF7. Their role in apoptosis appears to relate particularly to their involvement in cell volume regulation. To date, much remains to be determined regarding their mechanisms of action.

An enhancing effect of 17β-oestradiol has been demonstrated on K^+ channel activity in MCF7 cells, and this appears to relate directly to its proliferation promoting properties. Genistein, through its ability to inhibit protein tyrosine kinase activity and other mechanisms, has been shown inhibit K^+ channel activity in a number of cell lines, but surprisingly never in neoplastic breast epithelial cells. Likewise, isoflavones may induce apoptotic volume changes, which, as discussed, are largely mediated by the osmoregulatory effects of the K^+ channels (including hERG). Evidence suggests that an early event in the mechanism through which soy isoflavones reduce proliferation may involve their ability to inhibit key membrane potassium channels. Similarly, their impact on other K^+ channels and cell volume regulation may relate to their pro- or anti-apoptotic properties. However, this is a new field and currently only based on conjecture.

Pilot data regarding the impact of isoflavones on potassium channels in breast cancer cells, and how this relates to their regulation of proliferation or apoptosis could open up a new avenue of investigation in the field of isoflavone therapy in the prevention and treatment of breast cancer. K^+ channels show some promise as a pharmacological target against breast cancer, and may represent a mechanism through which isoflavones act on these cells. Since a major characteristic of many tumours is the development of resistance to therapies, the discovery of treatments targeting alternative key processes such as this in breast cancer cells is much needed.

Only the MCF7 cell line was used for this part of the investigation, as the K^+ channels it expresses are relatively well characterized. The intention was to focus on the activity of the VGKCs, in particular hEAG and hERG, as these channels are

known to be expressed in MCF7 cells, and they have demonstrated an involvement in the processes of proliferation and apoptosis. Additionally, several VGKCs, including hERG have previously been shown to be inhibited by genistein in other cell lines, suggesting that this channel may be a target of genistein in MCF7 breast cancer cells also.

Firstly, the impact of key concentrations of soy isoflavones and E2, identified in the previous stage of the project, on MCF7 volume regulation was ascertained. Due to the known roles of swelling and AVD in cell proliferation and apoptosis, and the potential involvement of K^+ ion flux in these processes, it was hypothesized that genistein and E2 treatment could regulate MCF7 volume accordingly. Changes in MCF7 volume were assessed using the Calcein fluorescence volume change assay (sections 4.1 and 6.3.1). This technique was chosen based on its reproducibility and its ability to assess volume changes in cells regardless of their shape.

In parallel, the effect of a number of specific and broad range K^+ channel blockers was tested with regard to their influence on the proliferation in MCF7 cells (section 6.4.1). The MTT assay was again used for this purpose. This was to confirm their presence and proliferative role in MCF7.

Finally, the impact of the soy isoflavones and E2 on K^+ channel activity was investigated. If the isoflavones were found to influence K^+ channel activity then the intention was to explore whether the VGKCs, specifically hEAG and hERG, are their targets. This was conducted using the whole cell patch clamping technique (sections 4.3 and 6.4.2), which is the gold standard technique for measuring the characteristics of ion channels, as it allows the channels to be gated by physiologically relevant membrane potentials.

CHAPTER 2. Methods: proliferation and apoptosis

Apoptosis and proliferation were assessed in MCF7 and MDA-MB-231 breast cancer cell lines at a range of physiological isoflavone concentrations in the presence and absence of E2. The MTT assay was used to measure proliferation (section 2.4). This is a standard and widely used procedure. Two methods of apoptosis quantification were utilised: the Annexin V-Cy3™ apoptosis kit (Sigma: APOAC) and staining with DAPI to assess nuclear morphological changes (sections 2.5 and 2.6). There exist numerous techniques to measure apoptosis in cultured cells, and regrettably no "gold standard" method. However, the use of two complementary but unrelated techniques to quantify apoptosis is in accordance with the advice of the NCCD (Galluzzi et al. 2009; Galluzzi et al. 2011). The protocol for each assay was optimised prior to use with positive and negative controls.

2.1 Culture techniques for MCF7 and MDA-MB-231 cell lines

To investigate the effects of isoflavones on breast cancer, MCF7 and MDA-MB-231 cell culture models of the disease were used. Both cell lines were held in storage at -70^{o}C, and were a gift from Strathclyde University (Prof. D. Flint, Hannah Research Institute, Ayr).

All work with cell lines, or medium and solutions required for the growth of the cell lines, was conducted in a class two biological safety hood (Microflow MS1310/1). All surfaces and containers upon entering and leaving the hood were sterilised with 70% ethanol and allowed to dry. When changing from one cell line to the other, all equipment and surfaces were sterilised, and left for a minimum of ten minutes to prevent cross-contamination. All waste was decontaminated by autoclave (121^{o}C for 15 minutes) or soaking overnight in a hypochlorite solution (1 x 2.5g Presept tablet in a maximum of 500ml water, 2500ppm).

2.1.1 Preparation of growth and experimental medium

Growth medium

Growth medium for the MDA-MB-231 cell line was prepared in sterile conditions. To a 500ml bottle of Dublecco's Modified Eagle's Medium (DMEM, Sigma) with phenol red, 1000 mg/L glucose, and sodium bicarbonate, without L-glutamine: Foetal Bovine serum (FBS; Biosera), L-Glutamine (Sigma) and penicillin/streptomycin (BioWhittaker) were added to final concentrations of 10%, 2mM, 100 units/ml (penicillin) and 100µg/ml (streptomysin) respectively.

Growth medium for the MCF7 cell line was identical to this other than the addition of 1 mM non-essential amino acids (NEAA; Sigma).

Experimental medium

All experimental treatments were conducted in medium made with phenol red free DMEM and dextran/charcoal-stripped FBS (DC-FBS; Biosera) to minimise the possibility of weak oestrogenic effects of endogenous serum oestrogens and phenol red in the medium confounding results. Both cell lines used the same experimental medium, which was prepared as follows. In sterile conditions, to a 500ml bottle of phenol red free DMEM with 1000 mg/L glucose, and sodium bicarbonate, without L-glutamine (Sigma), 10% DC-FBS, 2 mM L-Glutamine and 0.1% penicillin/streptomycin were added. Extended periods of growth in phenol red free medium with DC-FBS can result in MCF7 cells adapting to the low oestrogen environment and losing their ability to exhibit stimulated growth in response to added oestrogen (Katzenellenbogen et al. 1987), so this medium was used for experimental treatments only.

2.1.2 Resuscitation of frozen cell samples

Polypropylene cryogenic vials (0.5ml; Wheaton Science Products) of MCF7 and MDA-MB-231 cells were stored at -70^{o}C in a freezing medium comprising 10% DMSO (Fisher Scientific) in FBS until needed. To reanimate, vials were thawed in a waterbath set at 37^{o}C for around 1 minute, whereupon the contents of the vial were pipetted into a 75cm^{2} culture flask with a filtered cap (Greiner) containing 20ml of the appropriate pre-warmed growth medium. These were placed in a humidified incubator (Sanyo MCO-17AIC) at 37^{o}C with a 5% CO_2/95% air atmosphere. After 24 hours, any dead cells and debris were removed by careful extraction of the growth medium, and replaced with 20ml pre-warmed, fresh medium.

2.1.3 Maintenance of cell lines – normal growth and experimental

Cells were maintained at 37^{o}C in an incubator (as above) in 75cm^{2} culture flasks (Greiner) with 20ml of growth medium. All cells, whether in growth medium or experimental medium were maintained under these conditions, and only removed from the incubator environment for the minimum required time. To ensure sufficient nutrients, medium was changed every three to four days. Cells were maintained in exponential growth phase and passaged as they approached 90% confluence, assessed visually using a Nikon Phase Contrast microscope at a total magnification of x100. This also verified the absence of contamination.

All medium, solutions and reagents used were warmed to 37^{o}C in a waterbath prior to use. As both cell lines were adherent, to subculture they were rinsed gently with 10ml PBS (Sigma) and then treated with 3ml of 0.25% trypsin-EDTA (Sigma) at 37^{o}C for 5 minutes to detach. Once all cells were dislodged, the trypsin was deactivated by addition of 10 ml of culture medium (as above). The cell suspension was decanted into a centrifuge tube and centrifuged (Biofuge Primo, Heraeus) at 161xG for 5 minutes at room temperature. The spent medium was then removed.

The cells were then subcultured or prepared for freezing as appropriate. To subculture, the cells were resuspended in 3 ml of fresh medium and divided equally into three flasks containing pre-warmed medium, and placed in an incubator. To freeze, the cells were resuspended in 3ml chilled freezing medium (4^{o}C; 10% DMSO in FBS). Aliquots of this suspension were pipetted quickly into each of three cooled cryo-vials. These were immediately placed on ice then removed to a -70^{o}C freezer.

2.2 Enumeration of cells using the haemocytometer

To ensure accurate and reproducible seeding, cells were counted using a haemocytometer (Neubauer Improved, Hawksley, Sussex). The flask of cells was trypsinized as above, and resuspended in 5ml of medium. The haemocytometer and cover slip were wiped clean using a lens wipe, and the cover slip was then placed tightly over the counting squares. Appearance of *Newton's rainbow rings* indicates that this was achieved satisfactorily. A small pipette was used to place a drop of cell suspension next to the cover slip, which then filled the counting chamber by capillary action. The haemocytometer was viewed with a standard microscope (Nikon Phase Contrast) at a total magnification of x100 so that a single square filled the viewing field (see Figure 2.1: where the single squares are numbered 1 to 5). The number of cells was counted in 5 of the 9 large squares, including cells on the top and right boundary lines (represented by the labels A and B in Figure 2.1), and excluding those on the bottom or left boundary lines (labels C and D in Figure 2.1). Care was taken to ensure the same five squares were always counted. This was repeated for the other counting chamber. If the results for each chamber differed by over 20%, a third counting chamber was prepared to validate.

The number of cells per ml of sample was calculated with the following formula:

Cell number = mean number of cells per square x 10^4 x dilution factor (if appropriate)

(10^4 corrects for the size of the counting square)

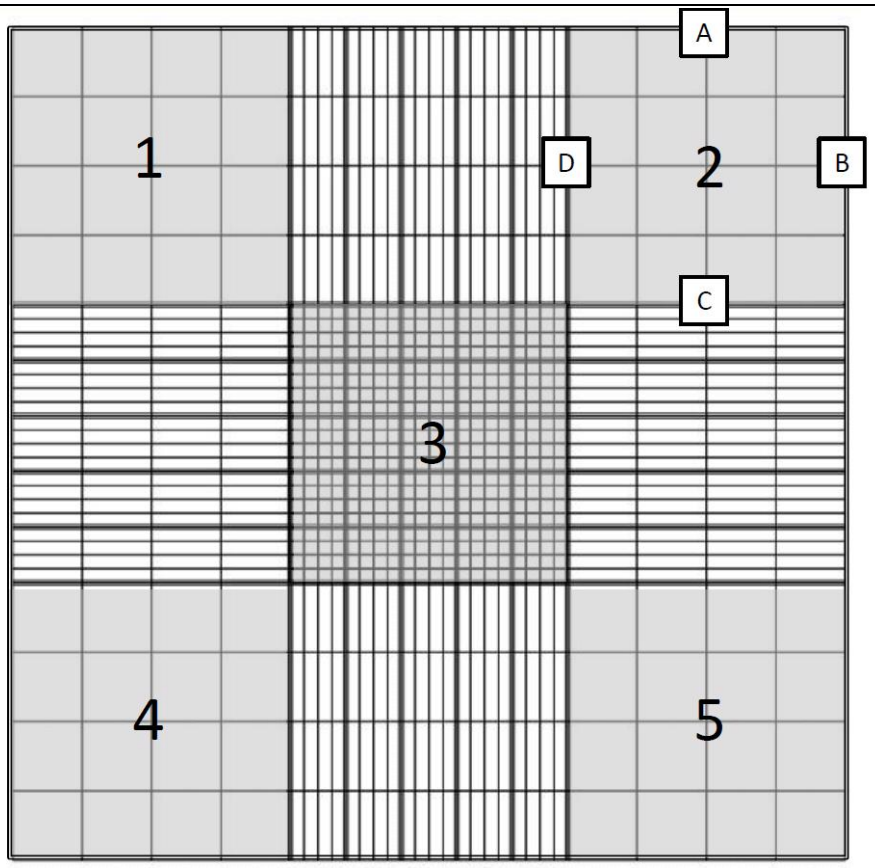

Figure 2.1: Diagrammatic representation of the Neubauer Improved haemocytometer counting chamber

Large squares to be counted are numbered 1 to 5. Cells of the top and right-hand boundary lines of any square (labelled A and B) are included in the count.

2.3 Viability assay: Trypan Blue dye exclusion method

2.3.1 Background to method

This is a routinely used technique to count the number of viable and non-viable cells, based on their membrane integrity. It is considered to be valid in the cell lines to be investigated here (Cherdshewasart and Sriwatcharakul 2008; Maggiolini et al. 2001; Shim et al. 2007). In order to determine the number of viable cells present, the cells were treated with Trypan Blue dye. This is membrane-impermeable for healthy viable cells, so these do not take up the dye, and remain opalescent. However, non-viable, or dead cells, can take up the dye and appear dark blue. Visualisation of the cells using a standard microscope and haemocytometer allows the number of viable cells in a given volume of medium to be counted.

As this method it based on the loss of membrane integrity as the cell becomes non-viable, it has a number of limitations. Firstly, damage to the membrane may allow the dye to enter the cell, making it appear non-viable in the short term, however the cell may be able to repair itself and restore viability. More likely, the cell may be non-viable without yet losing membrane integrity, making it impermeable to they dye and appear viable for a short time. Finally, as the determination of viability is subjective, by visualisation, small amounts of damage, leading to small amounts of dye entering the cell, may go unnoticed. For these reasons, this method is considered too insensitive to accurately determine proliferation. However, for the purposes of cell counting, when they have been used together, the results of the Trypan Blue dye exclusion assay and the MTT assay to assess proliferation in MCF7 and MDA-MB-231 cells correlate well (Simoes-Wust et al. 2002).

2.3.2 Procedure for Trypan Blue viability assay

The procedure was as for standard haemocytometer counting, however, once the cell suspension was prepared, 50µl was placed in a microfuge tube, with 75µl PBS and 125µl (0.4%) Trypan blue solution (Sigma) and vortexed briefly to mix. The total dilution factor was 5. This was left at room temperature for 5 minutes, vortexed again to resuspend the cells, then counted using the haemocytometer method as described.

Viable cells (those which have excluded the blue stain) and total cells were counted, and percentage viability calculated as:

% viability = (number viable cells / total number of cells counted) x 100

2.4 MTT proliferation assay

2.4.1 Background to MTT assay method

The MTT assay is a widely used, robust, reproducible, and high throughput method to determine the degree of cellular proliferation (Twentyman and Luscombe 1987). It utilizes a tetrazolium-type dye (MTT) which is yellow, water soluble, and can cross both the plasma and mitochondrial membranes of cells. In the mitochondria of viable, actively metabolising cells, MTT is reduced into an insoluble purple formazan product by mitochondrial dehydrogenase enzymes. The amount of purple formazan produced depends on the number of cells present and their viability. As the reaction progresses, the cells die, and the formazan can be dissolved by addition of a solvent. The intensity of the purple colour in solution is measured as optical density (OD), using a multiwell plate reader, and reflects the number of viable cells present after the given period of proliferation (Burton 2005). The absorption maximum for formazan solubilised in DMSO is in the range of 560 to 570 nm (Plumb et al. 1989). The same 96 well plate is used for both cell growth and measurement, reducing the number of steps needed.

This assay was first developed by Mosmann (1983), with later modifications to include use of DMSO as the solvent (Carmichael et al. 1987; Twentyman and Luscombe 1987). The method here has also been used by others (Cherdshewasart and Sriwatcharakul 2008; Jin et al. 2010; Li et al. 2008) in both MCF7 and MDA-MB-231 cells for similar isoflavone screening assays.

While the MTT assay is frequently used to assess proliferation in MCF7 and MDA-MB-231 cells, there is a question as to whether the isoflavones themselves cause an overestimation of the MTT assay results (see section 6.1.1). For this reason, the assay was validated for use here by comparison to the Trypan Blue cell counting method, with isoflavones present (see section 2.4.6). It was also optimised during the pilot phase for cell seeding density and treatment duration (see section 2.4.3). Additionally, an aliquot of the purple formazan DMSO solution was analysed with a scanning spectrophotometer (Thermo Helios α) to determine that maximal absorption was achieved between around 550 and 570 nm, confirming that 550nm was an appropriate wavelength with which to analyse the plates.

2.4.2 Preparation of solutions

Stock solutions

A stock solution of $1x10^{-2}$M (10mM) E2 (Sigma) was prepared in DMSO. Stock solutions of $5x10^{-2}$ M (0.0316M) genistein and daidzein (both Sigma) were also prepared in DMSO. Each was filtered using sterile 22µm polytetrafluoroethylene (PTFE; Whatman) syringe filters and stored in sterile glass universals at -20^{o}C until use and thawed at room temperature. Serial dilutions were prepared in filtered DMSO down to concentrations of $1x10^{-8}$M (10nM) for the phytoestrogens and $1x10^{-9}$M (1nM) for E2. A 5µl of the relevant stock dilution was added to 5ml of experimental medium to give the relevant ligand dose in a final DMSO concentration of 0.1% (i.e. to prepare medium with a genistein concentration of 1nM, 5µl of the 1µM stock was added to 5ml medium) . In the case of the combined treatments the final DMSO concentration was 0.2%. This was impossible to avoid because the E2 and isoflavones were dissolved to their maximum concentrations. These stock solutions were stored at -20^{o}C and used for all experiments to follow.

MTT working solution

MTT working solution (100µl of 0.5 mg/ml MTT in DMEM without FBS) was prepared fresh on the day of use, from a stock solution of 5 mg/ml MTT (Sigma) in PBS. The stock solution was filtered using a 0.22µm mixed cellulose ester (MCE) syringe filter (Millex Millipore) and stored in the dark at 4-8^{o}C. The working solution was prepared fresh on a weekly basis, although this preparation may be stable for up to six weeks (Twentyman and Luscombe 1987).

2.4.3 Optimisation of the MTT proliferation assay

To generate the protocol described, the MTT proliferation assay required optimisation prior to use. In order to do this, the MCF7 cell line was seeded in 96 well tissue culture plates (Nunc) at a range of densities from 1000 to 9000 cells per well, and treated for a range of durations (from 24 to 96 hours) with experimental medium or medium containing 1nM E2. The latter acted as a positive control for the induction of proliferation in this cell line. The MTT assay was then conducted as described in the next section. Optimisation of this protocol was carried out with MCF7 cells only.

Sample results are described in Figure 2.2. Based on this, the experimental conditions of a 72 hour treatment and seeding density of 6000 cells per well were selected. These conditions allowed for maximum effect of the E2 treatment without being negatively impacted by overcrowding and lack of nutrients or being overly sparse preventing accurate measurement.

Additionally prior to data collection, the effect of various doses of solvents on the proliferation of MCF7 cells was examined (Figure 2.3). This was to confirm that the chosen dose of vehicle had no effect on proliferation by itself. Both ethanol and DMSO were examined, at doses ranging from 0.1 to 5%, and compared to untreated cells. DMSO was toxic in a dose-responsive manner, with percentage proliferation compared to untreated cells dropping at concentrations above 1%.

This suggests that 0.1 and 0.2% DMSO were appropriate under these circumstances, as no effect on proliferation was observed up to 0.5%. However, ethanol at concentrations of 0.5% and above promoted the proliferation of the cells. This is an interesting result which could have implications for the results of many studies, as ethanol is a frequently used solvent. This data is in agreement with that of Singletary et al. (2001). For this research, use of ethanol as a solvent was discontinued.

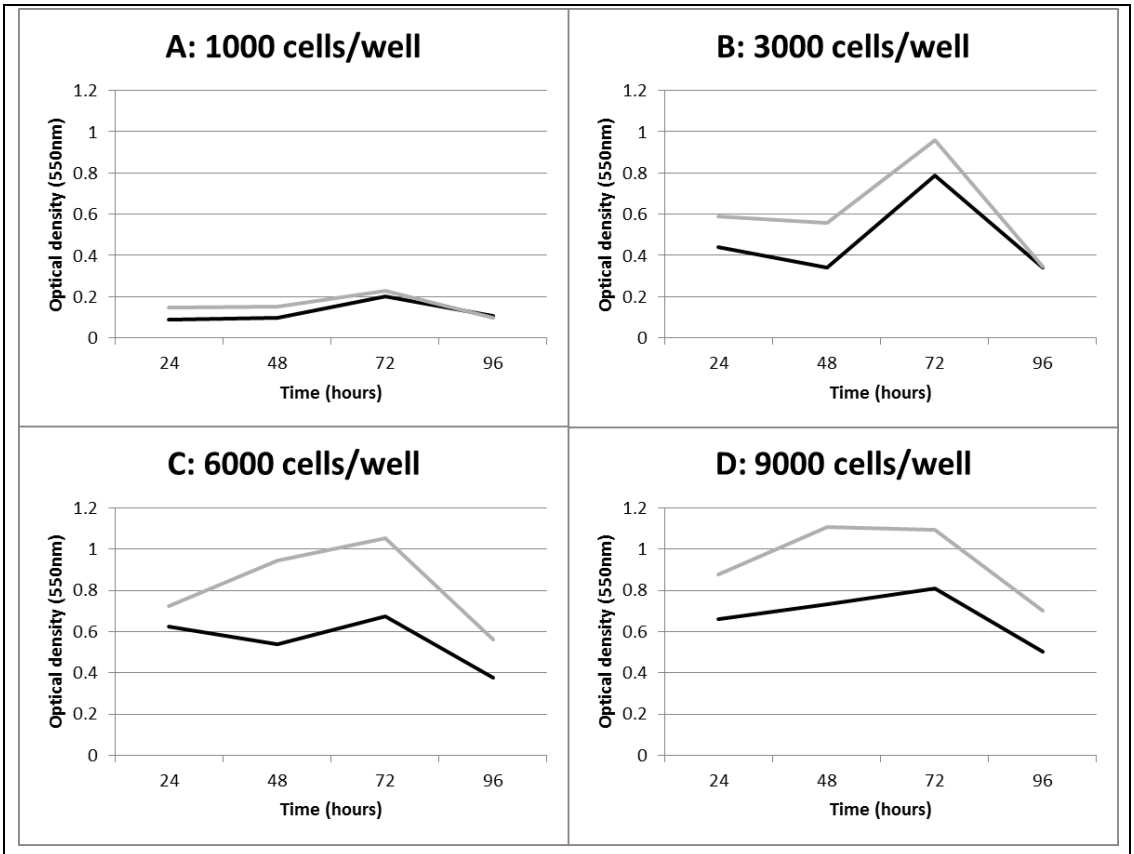

Figure 2.2: Impact of seeding density and treatment duration on MCF7 proliferation

Mean optical density (measured at 550nm) after MTT assay of MCF7 cells incubated with or without 1nM E2 over a period of time up to 96 hours. Cells were initially seeded in 96 well plates in oestrogen free media at a range of cell densities per well (A: 1000, B: 3000, C: 6000 and D: 9000 cells per well) and incubated for 24 hours to allow washout of oestrogenic effects. Following this, medium was replaced with fresh media in the presence (grey line) or absence (black line) of 1nM E2, and incubated for up to 96 hours. Data shown is the mean optical density (read at 550nm) of at least three wells prepared on three separate occasions (n=3).

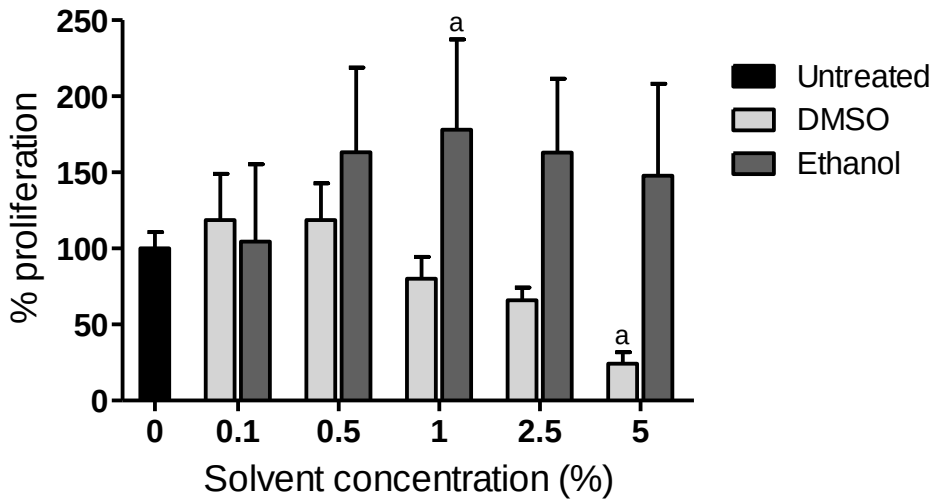

Figure 2.3: Effect of various solvents on the proliferation of MCF7

MCF7 cells were prepared as described, before the addition of fresh medium containing the stated concentrations of ethanol or DMSO, and incubated for 72 hours. Data presented is the mean + standard deviation of the value from 8 wells prepared on the same day. a*: significant difference from the untreated control ($p < 0.05$).*

2.4.4 MTT proliferation assay protocol

Upon reaching 80 to 90% confluence, the cells were rinsed with PBS, trypsinised, and counted using a haemocytometer. They were then seeded in 96 well tissue culture plates at a density of 6000 cells per well, in 0.2 ml experimental media. The cells were returned to the incubator and allowed to adhere for a period of 24 hours. This also served to wash out oestrogenic compounds in the growth media. At this time, the medium was removed by inverting and gentle tapping, and 0.2ml fresh experimental medium added to each well, with the inclusion of the compounds to be tested. Once prepared, the plates were returned to the incubator. On each plate at least 3 "blank" wells were included, containing medium but no cells, which were treated in the same manner as the cell-containing wells throughout.

Following treatment for 72 hours, the medium was removed by inverting and gentle tapping, and replaced with 100µl of MTT working solution. The cells were incubated at 37^{o}C in the dark for a further 4 hours to allow reduction of the MTT. From this point sterile conditions were no longer required. The MTT solution was removed by inversion and gentle tapping. Formazan crystals were solublised by addition of 100µl DMSO to each well, and after 5 to 10 minutes and gentle tapping, the density of the purple colour determined in a multiwell-plate spectrophotometer (Dynex MRX) at a wavelength of 550nm.

Each treatment was replicated in at least 3 wells on the plate, and in at least 3 plates prepared on different occasions. No treatments contained more than 0.2% DMSO. Results were presented as the percentage of the appropriate vehicle-only control.

% change in proliferation for each well was calculated as:

(OD* reading – blank) ÷ (mean control OD – blank) x 100

*OD: Optical Density

2.4.5 Test conditions for the MTT assay

Controls

The single treatments of isoflavone and E2 were compared with their vehicle-only control (0.1% DMSO). The combined E2 and isoflavone treatments contained 0.2% DMSO, so this slightly higher concentration of the vehicle was used as the control treatment in these instances. To determine the appropriateness of these solvent levels as controls, proliferation was assessed in both MCF7 and MDA-MB-231 cells grown with no additions, or the vehicle only (0.1% and 0.2% DMSO) for 72 hours.

Oestrogen Treatment

Proliferation was assayed in both cell lines after treatment with 1 pM ($1x10^{-12}$M; postmenopausal) and 1 nM ($1x10^{-9}$M; premenopausal) E2. These values were chosen based on published serum levels of total E2 (Gruber et al. 2002). In premenopausal women E2 levels vary with the menstrual cycle, with 1nM representing the mid-point of this range. This was intended to confirm past results and act as a positive control for the induction of proliferation in ERα+ (MCF7) cells.

Isoflavone Treatment

Following this, both cell lines were treated with genistein and daidzein between 0.01nM ($1x10^{-11}$M) and 31.6µM ($1x10^{-4.5}$M) to allow confirmation of their effects on proliferation as single treatments. This concentration range is physiologically achievable in serum through diet alone, and represents both very high and low/never consumers of soy products, and women taking isoflavone supplements (Arai et al. 2000; Verkasalo et al. 2001). It was hoped that this would allow the full range of stimulatory and inhibitory dose-dependent effects of these isoflavones on proliferation to be seen (Maggiolini et al. 2001; Matsumura et al. 2005).

Combined Treatment

Finally, the proliferative and apoptotic effects of genistein and daidzein were measured again, at the concentration ranges described, in combination with 1nM or 1pM E2. The results of these combined treatments were compared to the effect of the relevant E2 treatment alone, to characterise whether the isoflavone is capable of modifying proliferation in a physiologically relevant E2 environment.

2.4.6 Validation of the MTT assay

To validate the results of the MTT assay, key treatments in both MCF7 and MDA-MB-231 cells were compared with the results of the Trypan Blue dye exclusion viability assay.

Both cell lines were seeded in 12 well plates (Greiner) in 1ml experimental medium per well, at a density of 5 x 10^4 cells/ml. As with the MTT assay, the cells underwent a 24 hour oestrogen washout period, then the medium was replaced with 1ml fresh medium containing the experimental treatments.

These comprised:

- Untreated medium
- 0.1% DMSO
- 1nM E2
- 0.1nM genistein
- 1µM genistein
- 31.6µM genistein

After three days of incubation, the medium was removed, and the cells were trypsinised by addition of 300µl trypsin per well. Once all cells were in suspension, the trypsin was deactivated by addition of 300µl medium per well, and each cell suspension was transferred to a 1.5ml polypropylene microcentrifuge tube (Fisher). These were centrifuged (Eppendorf 5415 R) for 5 minutes at 150xG (room temperature). Following this, the supernatant was removed, and the pellet was resuspended in 75µl PBS and 125µl Trypan Blue, as described in Section 2.3. The total volume in each tube, including the pellet was around 250µl.

The number of viable cells (per ml) in each sample was calculated as described (section 2.3.2). This value was divided by four to determine the total number of viable cells per well (i.e. each 250µl sample contained all the detached cells from a 1ml well).

This procedure was carried out on two separate occasions. The results for the MCF7 Trypan Blue viability assay are provided in Figure 2.4 , and for the MDA-MB-231 in Figure 2.5. In each case the data is compared with the results of the same experimental treatments in the MTT assay.

A: Cell numbers and optical densities after various treatments

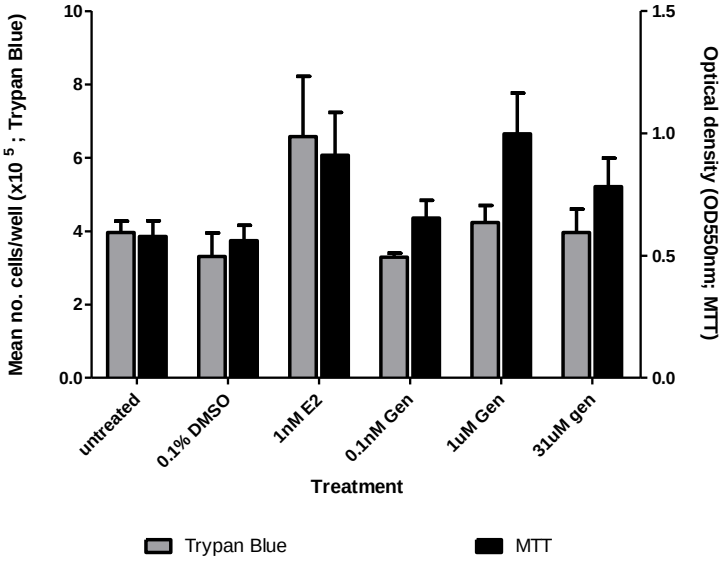

B: Scatterplot of mean values (cell number and optical density)

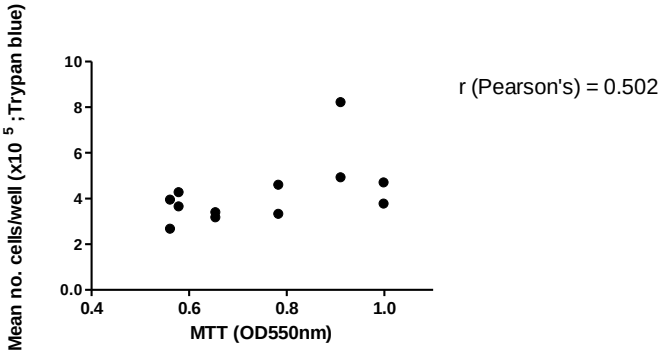

Figure 2.4: Comparison of MTT and Trypan blue validity assay results in MCF7 cells

MCF7 cells were assayed using the MTT assay and Trypan Blue dye exclusion assay as described, after 72 hour incubation in medium with no additions, vehicle-only, 1nM E2, or genistein (0.1nM, 1µM and 31.6µM). A: Numbers of cells per well (left hand side; mean ± range) and optical density at 550nm (right hand side; mean ± SD for each). For the MTT assay n = 3, and for the Trypan Blue assay n = 2. B: Mean cell numbers and optical densities for each treatment, and the Pearson's correlation coefficient (r, n = 12) describing the relationship between the two datasets.

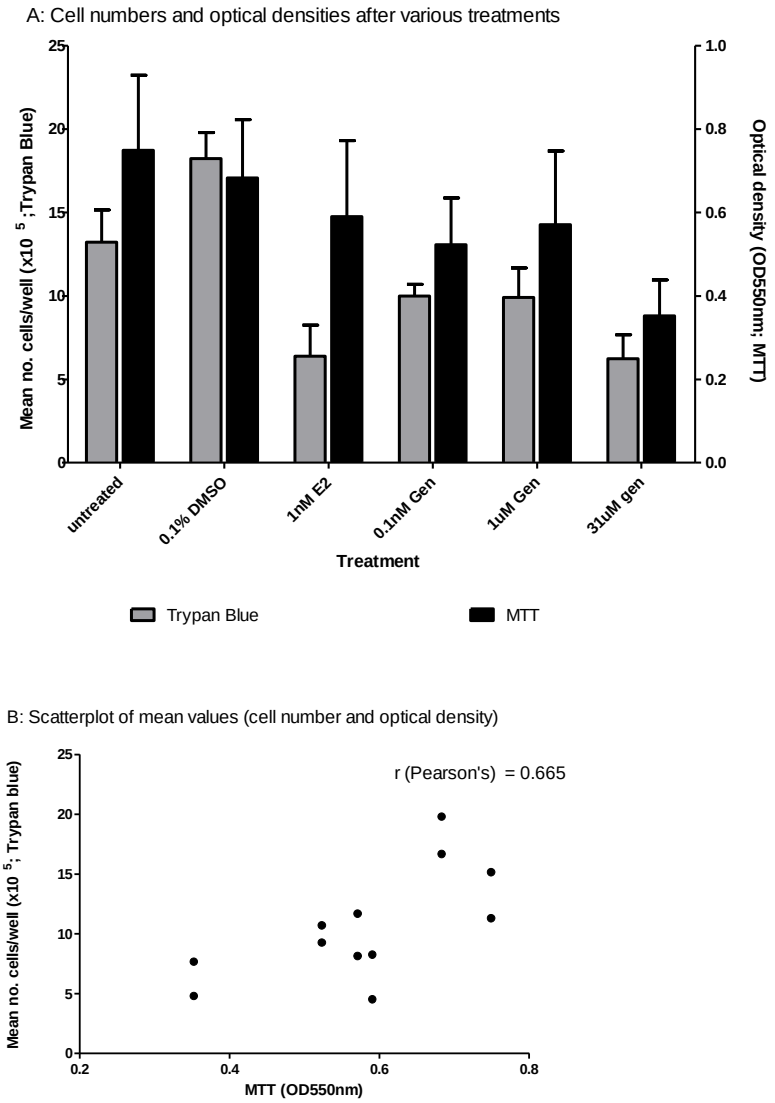

Figure 2.5: Comparison of the MTT and Trypan blue validity assay results in MDA-MB-231 cells

MDA-MB-231 cells were assayed using the MTT assay and Trypan Blue dye exclusion assay as described, after 72 hour incubation in medium with no additions, vehicle-only, 1nM E2, or genistein (0.1nM, 1μM and 31.6μM). A: Numbers of cells per well (left hand side; mean ± range) and optical density at 550nm (right hand side; mean ± SD for each). For the MTT assay n = 3, and for the Trypan Blue assay n = 2. B: Mean cell numbers and optical densities for each treatment, and the Pearson's correlation coefficient (r, n = 12) describing the relationship between the two datasets.

Pearson's correlation coefficients (r) were calculated (SPSS version 19, IBM Statistics, 2010) to determine the relationship between the mean OD values and cell counts for each cell line and treatment (see Figure 2.4B and Figure 2.5B), along with the significance of this relationship (p, n = 12).

For both cell lines the results of the two assays followed similar patterns. In MCF7 the Pearson's correlation coefficient was 0.502 (p one tailed <0.05, n = 12) indicating a fairly strong positive correlation between the MTT and Trypan Blue assay results, although this just failed to achieve significance at the two tailed level (p = 0.096). A stronger correlation was achieved with the MDA-MB-231 results (r = 0.665, p two tailed <0.05, n = 12). This suggests that the MTT assay is valid for use in determining the effects of isoflavone treatments on the proliferation of MCF7 and MDA-MB-231 breast cancer cells.

2.4.7 Statistical analysis

All values are the mean result of at least nine wells. Data is assumed to be normally distributed. Data is represented as the mean percentage change in proliferation compared to the control (0.1% DMSO unless otherwise stated) and standard deviation. Significant variation from the control results was determined using one way ANOVAs, with *post hoc* Bonferroni correction for multiple comparisons (SPSS version 19, IBM Statistics, 2010), and a value of $p < 0.05$ (two-tailed) was considered to be significant. The EC_{50} (concentration required for a half-maximal effect) for each isoflavone on proliferation was determined by nonlinear regression using Graphpad Prism software (Graphpad Software Inc, Version 5.01, 2007).

2.5 Annexin V-Cy3 Apoptosis Assay

2.5.1 Background to the Annexin V-Cy3 Apoptosis Assay method

The Annexin V-Cy3™ Apoptosis Detection Kit (Sigma, APOAC) is quick to use, and detects apoptosis earlier in the apoptotic pathway than DNA-based methods such as TUNEL staining. The assay is based on a 15 minute incubation with a solution containing Ca^{2+}, labelled Annexin V, and a counter-probe. It allows differentiation, using fluorescence microscopy, between early apoptotic, necrotic and viable cells. The Annexin V-Cy3.18 conjugate fluoresces more brilliantly for fluorescent microscopy that its Annexin-FITC counterpart used for flow cytometric methods.

The kit contains two fluorescent dyes. The first, Cy3.18 conjugated to Annexin V, binds to PS on the surface of apoptotic and necrotic cells. The second dye is the non-fluorescent compound 6-carboxyfluorescein diacetate (6-CFDA), which enters the cell and is hydrolyzed by the esterases present in living cells into the fluorescent compound 6-carboxyfluorescein, indicating that the cells are viable. The combinations of these dyes allow the state of the cells to be determined by fluorescence microscopy, as summarised in Table 2.1. Annexin V positive, 6-CFDA positive cells are still actively engaged in metabolism but also externalising PS so are in the early stages of apoptosis. Necrotic cells stain as Annexin V positive 6-CFDA negative. Finally viable cells are Annexin V negative, 6-CFDA positive. The results of random microscopic fields were photographed and quantified.

Table 2.1: Summary of Annexin V-Cy3 dye combination results

Cell type	Dye result		Cell colour (composite image)
	Annexin V-Cy3 (red)	6-CFDA (green)	
Viable	-	+	**Green**
PS externalising (apoptotic)	+	+	**Yellow (Green + Red)**
Necrotic	+	-	**Red**

The Annexin V-Cy3 kit been used successfully to determine apoptosis in both MCF7 and MDA-MB-231 cell lines by other laboratories (Perillo et al. 2000; Wiebe et al. 2010), and a related adherent breast cancer cell line MD- MB-435 (Castillo-Pichardo et al. 2009). A similar kit designed for flow cytometric analysis, Annexin V-FITC, has also been used with both cell lines in studies similar to this, investigating the role of isoflavones in apoptosis (Li et al. 2008; Sergeev 2004). There was no evidence that the isoflavones interfered with the activity of the fluorescent stains. This suggests that this kit is an appropriate method of quantification for apoptosis in the present investigation.

The binding buffer should contain Ca^{2+} between 1 and 3mM (1.8mM is optimal for many cell lines, higher concentrations will promote non-specific binding of Annexin V to other aminophospholipids), and simple salts. Phosphate buffers should be avoided (Krysko et al. 2008). For this reason RPMI growth medium is not advised due to its low Ca^{2+} high phosphate content. DMEM medium satisfies the PS-binding properties of Annexin V (Krysko et al. 2008).

2.5.2 Preparation of Solutions

The Annexin V-Cy3 kit contained the following:

- Annexin V-Cy3.18 conjugate (10 µg protein, 100 µg/ml) dissolved in 50mM Tris HCl, pH 7.5,
- 6-Carboxyfluorescein diacetate (6-CFDA) 10 mg
- 10x binding buffer 20ml containing 100mM HEPES/NaOH, pH 7.5 with 1.4M NaCl and 25mM $CaCl_2$

In advance, the following solutions were prepared from the kit, according to manufacturer's instructions:

1x binding buffer

10 fold dilution of 10x binding buffer with deionised water

50mM 6-CFDA in acetone solution

Dissolve 2.32mg 6-CFDA in 0.1ml acetone, store in amber vial at -20^{o}C, protected from light

Double label staining solution (1 µg/ml Annexin V-Cy3 and 500 µM 6-CFDA in 1x binding buffer)

Mix 20µl of the Annexin V-Cy3 100µg/ml solution, 20 µl of 50 mM 6-CFDA acetone solution, 200µl 10x binding buffer, and 1.76ml deionised water. Store in amber vial and protect from light

2.5.3 Optimisation and positive control

Exposure levels for capturing red and green fluorescence were optimised with the positive and negative control cells and then used throughout. In addition, at an early stage, cells treated with genistein or E2 (but not stained) were exposed to the excitation light source. There was no auto-fluorescence detected (results not shown).

Seeding conditions were optimised by testing a number of seeding densities (1×10^4 to 1×10^6 cells per well) and durations (24 to 72 hours) to determine the conditions which would yield approximately 100 cells per microscopic field. This was assessed visually using the Nikon Eclipse TS100 microscope (data not shown). Optimum conditions required to give the appropriate final cell numbers were determined to be a 48 hour washout and seeding density of 5×10^4 cells per well. This is similar to conditions used in several related studies (Jin et al. 2010; Schmidt et al. 2005).

Treatment with hydrogen peroxide is known to induce apoptosis in a number of cell lines, including human leukaemia HL-60 cells (Wagner et al. 2002), human histiocytic lymphoma U937 cells (Perez et al. 2004) and various tumour cell lines (Wang et al. 2002). In MCF7 cells treatment with 5mM H_2O_2 for 90 minutes resulted in approximately 50% of cells to become apoptotic (Perillo et al. 2000). Likewise, in murine lymphocyte FL5.12 cells lower doses of 0.25 to 1mM H_2O_2 also induced apoptosis although over a longer timeframe (Hockenbery et al. 1993). Based on these studies a one hour incubation in medium containing either 1mM or 5mM H_2O_2 treatment was used as a positive control for the induction of apoptosis in this project.

Plates (12 well) were prepared as described with both MCF7 and MDA-MB-231 cells, in 1ml experimental medium, and incubated at 37^{o}C in a humidified 5% CO_2 incubator for 72 hours. H_2O_2 was added to the medium from a stock of 0.09M, to achieve a final concentration of 1mM or 5mM. These doses were tested for durations ranging from one to four hours. These were initially assessed visually, and then several treatments were stained and examined as described (see section 2.5.4).

Sample images are provided in Figure 2.6 and results are displayed in Figure 2.7. Significant increases were seen in the percentage of apoptotic MCF7 cells after treatment with both 1 and 5mM H_2O_2 compared with no treatment. The impact H_2O_2

treatment on MDA-MB-231 cells was lower in magnitude, but a significant increase in PS-externalising apoptosis was still observed in the MDA-MB-231 cells after 5mM H_2O_2 treatment for an hour. This suggests that the test is capable of generating comparable results to those seen in other published studies for the induction of apoptosis in these cell lines (Perillo et al. 2000).

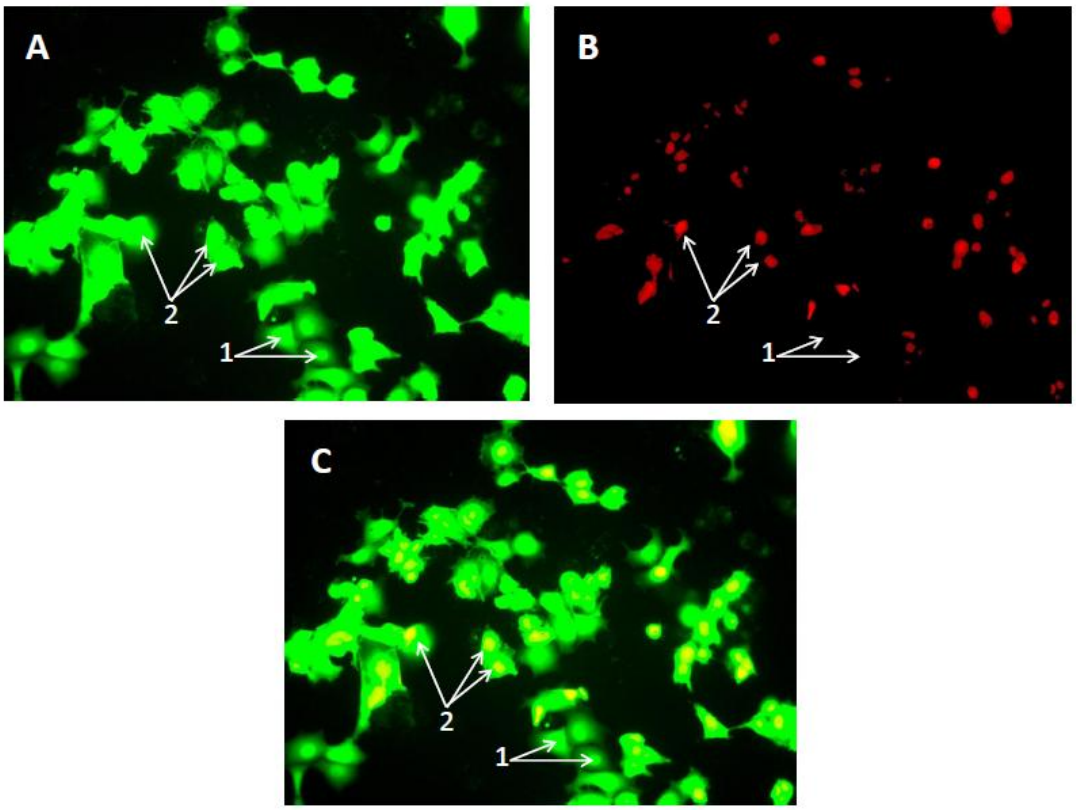

Figure 2.6: Representative images showing the results of the Annexin V-Cy3 apoptosis assay on hydrogen peroxide treated MCF7 cells

MCF7 cells prepared as described then treated with 1mM H_2O_2 for 1 hour, stained with the Annexin V-Cy3 apoptosis detection kit, and fluorescent images captured. A: green fluorescence from 6-CFDA dye. B: red fluorescence from Annexin V conjugate dye. C: Composite image. In each image 1 indicates a number of viable cells, stained by 6-CFDA only, and 2 indicates apoptotic cells stained with both. In this region of the slide apoptosis was calculated to be 68.54%.

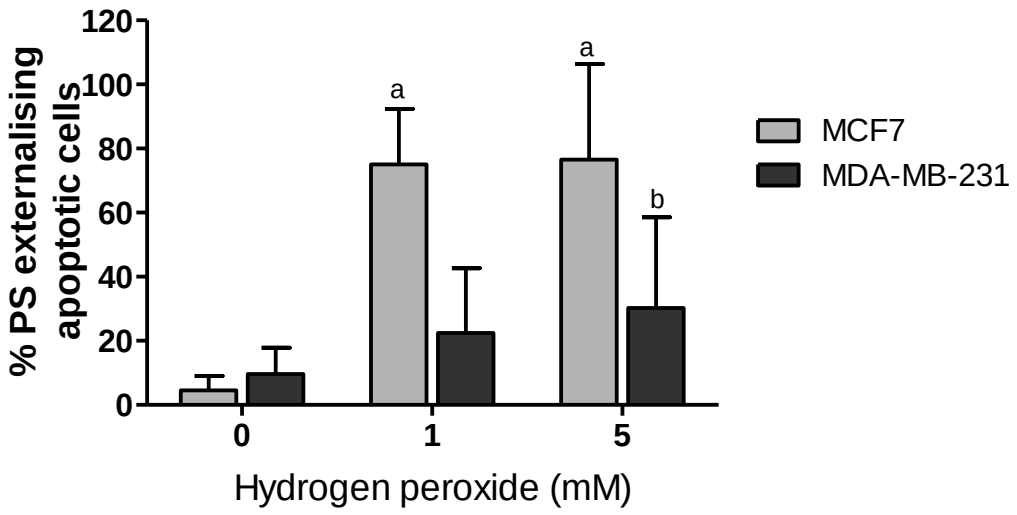

Figure 2.7: Induction of apoptosis by hydrogen peroxide treatment (1 hour)

Cells were seeded in oestrogen free medium and incubated for 48 hours to allow oestrogens to wash out. Following this, medium was replaced with fresh oestrogen free medium. After a further 24 hour incubation, hydrogen peroxide was added at 1 and 5 mM, for 1 hour, to induce apoptosis. Results presented as mean % PS externalising apoptotic cells per treatment and SD (n=3). Significant variation from the relevant untreated controls are indicated by a ($p < 0.001$) or b ($p < 0.05$).

Subsequently, treatment with various test ligands was piloted using the described protocol for both 24 hours and 48 hours (results determined visually, data not shown). Both time periods are frequently used to generate significant results in MCF7 and MDA-MB-231 cell lines for the induction of apoptosis by isoflavone treatment, although to date this has not been assessed by the Annexin V-Cy3 method (Garvin et al. 2006; Jin et al. 2010; Li et al. 2008; Sergeev 2004; Shim et al. 2007). Based on this pilot testing, 24 hour treatment was chosen.

2.5.4 Annexin V-Cy3 apoptosis assay protocol

This procedure for MCF7 and MDA-MB-231 cells is based on the manufacturer's instructions and the method used by Castillo-Pichardo et al. (2009) for adherent MDA-MB-435 breast cancer cells. Optimisation of conditions were described previously in section 2.5.3.

Upon reaching 80 to 90% confluence, the cells were rinsed with PBS, trypsinised, and counted using a haemocytometer. They were then seeded in 12 well plates (Greiner) at a density of 5 x 10^4 cells per well in 1 ml experimental medium, on 10 mm glass cover slips (Agar Scientific). Prior to placing in the wells, the cover slips were sterilised by autoclaving.

The plates were returned to the incubator and the cells allowed to adhere and grow for a period of 48 hours. This also served to wash out oestrogenic compounds in the growth media. Following this, the medium was gently removed by pipette, and replaced with 1 ml of experimental, oestrogen free medium containing appropriate doses of the ligands under scrutiny. The plates were then returned to the incubator for another 24 hours.

The following stages did not require sterile conditions. To stain, each cover slip was extracted gently from the well with watchmaker's forceps, and washed twice gently with 100µl PBS. Excess liquid was blotted off with a tissue gently at the side of the cover slip, not directly on top, as this would damage or dislodge the cells. Subsequently, the surface of the cover slip with the adherent cells was washed gently three times with 50µl 1x binding buffer, blotted each time as before, and placed cell side up on a slide or Petri dish. 50µl double staining solution was dropped onto the cover slip, which was then covered with foil and incubated for 15 minutes at room temperature. After staining, each cover slip was washed five times with 50µl 1x binding buffer as before, to remove excess label. Following this, 35µl of 1x binding buffer was dropped onto the cover slip, which was then inverted over a glass slide.

The results were observed and rapidly photographed using a fluorescence microscope (Nikon Eclipse TS100) with a 20x/0.50 Nikon Plan Fluor objective. 6-CFDA is excited by light at 485nm, and emitted light is transmitted through a 505 nm dichroic mirror and long-pass 520 nm emission filter (B-2A filter, Nikon) to be

observed as green fluorescence. Annexin V-Cy3.18 is excited by light at 530 nm, and emitted light is transmitted through a 575 nm dichroic mirror and 580 nm emission filter (G-2A filter, Nikon) appearing as red fluorescence. Images were captured using a Diagnostic Spot RT Colour 2.2.1 camera, and thresholded and analysed with Image J software (NIH: Version 1.44). This stage was completed rapidly, with minimum exposure of the cells to the light source, to reduce the potential for leakage and bleaching of the dye. The analyst was blinded to the treatment as far as possible, by assigning all images a numerical name unrelated to the experimental conditions. A sample set of images is provided in Figure 2.8.

Three random areas from each cover slip were analysed, and at least three separate cover slips were prepared on different occasions for each treatment. At x200 magnification approximately 100 cells were visible per field, resulting in approximately 900 to 1000 cells being assessed for each treatment.

Percentage induction of PS externalising apoptotic cells for each cover slip field was determined as follows:

% apoptotic cells = (no. apoptotic cells) ÷ (total no. cells*) x 100

* Total no. cells = viable + apoptotic + necrotic

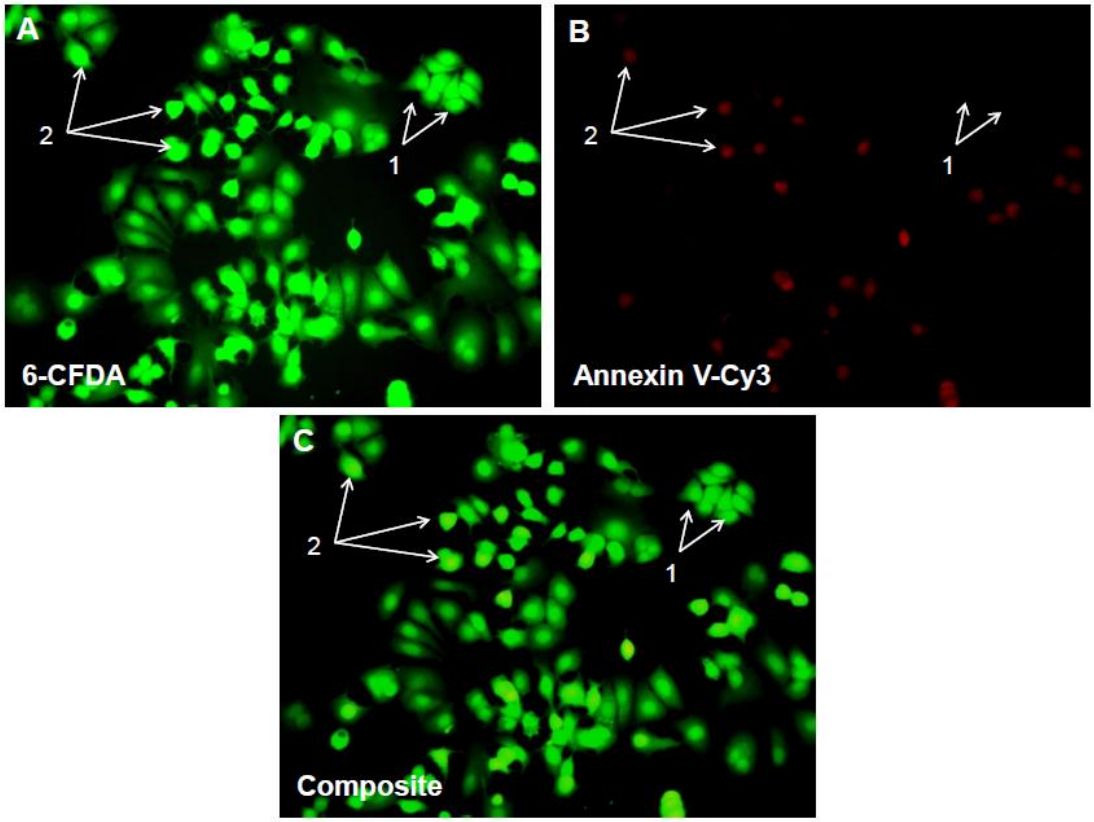

Figure 2.8: Sample images of Annexin V-Cy3 kit results

MCF7 cells seeded as described then treated with 1µM genistein for 24 hours. Following this, the Annexin V-Cy3 apoptosis assay was carried out and digital images acquired. 6-CFDA fluoresces green (A) and Annexin V-Cy3 fluoresces red (B). A composite image (C) has been generated for illustrative purposes. Cells which fluoresce green only (1) are viable and cells which fluoresce in both colours (2; appear yellow in composite image) are apoptotic.

2.5.5 Test conditions

Positive and negative controls

Untreated cells, and cells grown for 24 hours in medium containing the vehicle only treatments of 0.1% DMSO were tested for induction of apoptosis in MCF7 and MDA-MB-231 cell lines. In addition, the impact of 0.2% DMSO was assessed in MCF7 cells. The DMSO-only controls were compared to the untreated cells to verify that they did not significantly modify levels of apoptosis in either cell line. This confirmed their appropriateness to act as controls for the other test conditions.

Oestrogen and isoflavone single treatments

Apoptosis and was quantified in both cell lines after 24 hour treatment with 1 pM and 1 nM E2. Similarly, both cell lines were treated with physiological levels of genistein and daidzein (0.1, 1, 10 and 31.6 µM). These treatments were intended to confirm the results in the scientific literature.

Combined Treatment

Finally, the apoptotic effects of genistein and daidzein were assayed again, at the concentration ranges described, in combination with 1nM and 1pM E2. This was conducted in the MCF7 cells only due to financial constraints. As the combination of E2 and isoflavones had little further effect on proliferation of MDA-MB-231 cells over that of the isoflavones alone, this treatment was not expected to modify the levels of apoptosis in these cells. The results of the combined MCF7 treatments were compared to the effect of the relevant E2 treatment alone and isoflavone concentration alone, to characterise whether the isoflavone was capable of inducing apoptosis in a physiologically relevant E2-containing environment.

2.5.6 Statistical analysis

For all conditions the mean and standard deviation of the percentage induction of apoptosis data was determined. Data is assumed to be normally distributed. The single treatments of isoflavone and E2 were compared to their vehicle only control (0.1% DMSO). Combined E2 and isoflavone treatments were compared to the relevant E2 only treatment as a control. Significant variation from the control results was determined using one way ANOVAs with Bonferroni *post hoc* corrections (SPSS version 19, IBM Statistics, 2010), and a value of $p < 0.05$ (two-tailed) was considered to be significant.

2.6 DAPI staining and determination of apoptotic nuclear morphology

2.6.1 Background to method

The second measure of apoptosis used was DAPI staining and subsequent determination of changes to nuclear morphology: namely the appearance of a bright fluorescent ring of condensed DNA around the outside of the nucleus, subsequent spreading of this to encompass the whole nucleus, which becomes smaller and more brightly stained, before fragmenting (Hacker 2000).

DAPI is a blue fluorescent dye that fluoresces brightly when bound to the minor groove of double-stranded DNA. In this state its fluorescence is approximately 20-fold greater than when unbound. This selectivity for DNA, along with cell permeability, allows the staining of nuclei with little background interference, making DAPI a classic nuclear dye for assessing apoptosis. Use of DAPI staining followed by assessment of the percentage of cells displaying apoptotic nuclear morphology has been used in a number of cell lines, including MDA-MB-231 (Miglietta et al. 2006), the human gastric cancer cell line SGC7901 (Wang et al. 2010) and several human ovarian cancer cell lines (Lai et al. 2003) to quantify apoptosis. On several of these occasions apoptosis was also assessed by other methods, and the results were comparable (Miglietta et al. 2006; Wang et al. 2010).

Briefly, the MCF7 and MDA-MB-231 cells were treated with vehicle only, genistein, daidzein and 17β-oestradiol both alone and in combination, and then stained with DAPI after 3 hours to assess any early apoptotic nuclear changes. Following this, digital images of the fluorescent cells were collected and analysed, and the percentage of cells displaying nuclear apoptotic morphology was calculated.

2.6.2 Preparation of Solutions

10% Formalin (Formaldehyde) solution

Formalin (37%; Sigma) diluted with deionised H_2O.

60% Isopropanol (2-propanol / isopropyl alcohol)

Isopropanol (≥ 99.7%; Sigma) diluted with deionised H_2O.

DAPI stock solution

DAPI was dissolved in deionised H_2O (1mg/ml), then stored at -20^{o}C in the dark.

DAPI working solution

Add 100µl DAPI stock to 9.9ml PBS (10µg/ml final concentration) and filter using a 0.22µm MCE syringe filter (Millex Millipore). Store at -20^{o}c in the dark

2.6.3 Optimisation of the DAPI apoptosis assay

As with the Annexin V assay (optimisation section 2.5.3), auto-fluorescence was assessed and determined to be of no concern.

Initial observations (not shown) indicated the necessity of the formalin fixation step, and allowed optimisation of the DAPI concentration used and cell seeding density. The latter was of particular importance as sufficient cell numbers were needed to ensure generation of reproducible results, while attempting to avoid large numbers of overlapping cells. Overlapping was of particular concern for the MCF7 cell line as they had a tendency to clump.

The positive control for induction of apoptosis (H_2O_2) and untreated MCF7 cells were used to optimise the DAPI assay (Figure 2.9). Treatment with 1mM H_2O_2 resulted in a significant increase in the percentage of apoptotic cells after 120 mins, although not 60 minutes. All the durations tested with 5mM H_2O_2 resulted in an increased percentage of apoptotic cells, and this was statistically significant at 120 minutes. This suggests that apoptotic changes in nuclear morphology (nuclear condensation and fragmentation) were taking place, and that this method was valid for their quantification.

Following this stage, genistein (1 and 31.6μM), 0.1% DMSO, and 1nM E2 were assayed after two, three and four hours of treatment in MCF7 and MDA-MB-231 cells to determine the timescale which would allow any changes in nuclear morphology to be reproducibly measured (assessed visually, data not shown). Based on this, three hour incubation was deemed to be optimum.

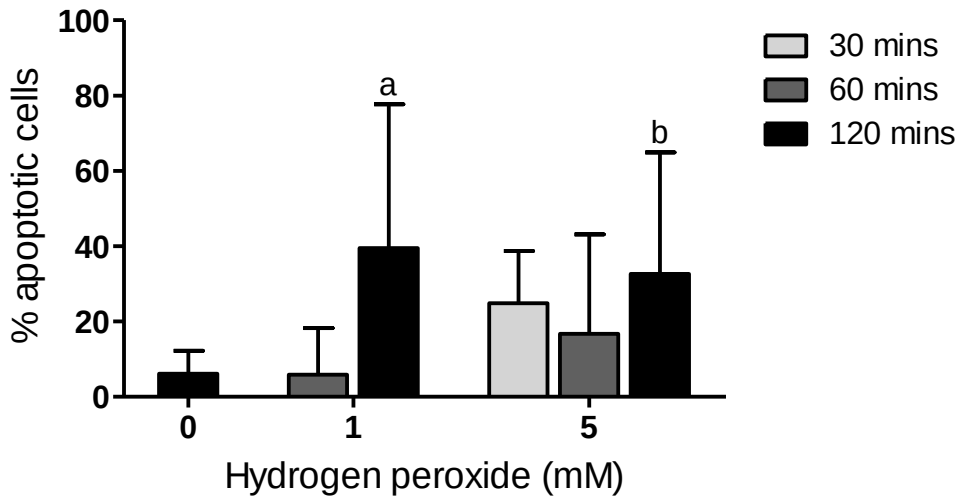

Figure 2.9: Induction of apoptotic nuclear morphology in MCF7 by hydrogen peroxide treatment

MCF7 cells were seeded as described and incubated for 48 hours to allow oestrogens to wash out. Following this, medium was replaced with fresh oestrogen free medium. This was either left with no additions for 120 mins, or H_2O_2 (1 and 5mM) for between 30 and 120 mins, to induce apoptosis. The percentage of apoptotic cells was determined after DAPI staining. Results are presented as mean and SD (n=3) for each treatment. Significant variation from the untreated control is indicated by a *($p < 0.01$) and b ($p < 0.05$).*

2.6.4 DAPI apoptosis assay protocol

This procedure is based on that described by Doonan and Cotter (2008). Similar techniques have been used in other human cancerous cell lines (Lai et al. 2003; Wang et al. 2010).

MCF7 and MDA-MB-231 cells were seeded in 24 well plates (Greiner) at a density of 1 x 10^4 cells per well in 0.5ml experimental (oestrogen free) medium. They were incubated for 48 hours at 37^{o}C in a humidified 5% CO_2 environment to allow for oestrogen washout. The medium was removed and each well was washed once with 1ml PBS (37^{o}C).

Positive control for apoptosis (MCF7 only):

Each well was filled with 0.5 ml experimental medium and H_2O_2 (1 and 5mM) and incubated at 37^{o}C in a humidified 5% CO_2 environment for up to two hours.

For test compounds (MCF7 and MDA-MB-231):

To each well 0.5ml of experimental medium was added with appropriate concentrations of the test compounds or vehicle only to get a final DMSO concentration of 0.1 or 0.2%. Plates were incubated for 3 hours at 37^{o}C in a humidified 5% CO_2 environment.

For all plates:

Formalin fixation

After 3 hours (or the stated duration), the medium was removed from the wells, and 0.3ml of 10% formalin was added to each well. This was incubated for 10 minutes at room temperature, then the formalin was discarded and the same volume of fresh formalin was added. This was incubated for at least an hour, although at this stage the plates could be left for a couple of days, wrapped in Parafilm to prevent evaporation. The formalin was then removed, wells were washed with 60% isopropanol (0.3ml per well) and allowed to air dry completely.

DAPI staining

Following fixation, each well was washed twice gently with warmed PBS, this was removed, and 200µl DAPI working solution was added to each well. This was incubated at room temperature in the dark for 20 minutes, agitating gently occasionally to ensure complete coverage. Each well was washed five times gently with warmed PBS to remove any unbound DAPI.

The results were observed and photographed using a fluorescence microscope (Nikon Eclipse TS100) with a 20x/0.50 Nikon Plan Fluor objective. The excitation wavelength for DAPI was 345nm, and the emission wavelength was 455nm, observed as blue fluorescence using UV-2A filter (Nikon) with 400nm dichroic mirror and barrier filter of 420nm. Images were captured using a Diagnostic Spot RT Colour 2.2.1 camera, and analysed with Image J software (NIH, Version 1.44). Six images from each well were captured, each containing approximately 50 cells. This stage was completed rapidly, with minimum exposure of the cells to the light source, to reduce the potential for leakage and bleaching of the dye. Each treatment was repeated on three separate occasions, meaning that for each experimental treatment approx. 1000 cells were analysed.

2.6.5 Calculation of the percentage of cells displaying apoptotic morphology

Images were analysed using ImageJ software. As far as possible, the analyst was blinded to the experimental treatment, by assigning each digital image a numerical identifier independent of the treatment. For each image, the total number of cells, and the number displaying apoptotic nuclear condensation, punctuated nuclei or fragmentation (Figure 2.10) as defined by Hacker (2000) was determined.

The percentage of cells displaying apoptotic morphology for each image was calculated as follows:

% apoptotic cells = (no. apoptotic cells) ÷ (total no. cells*) x 100

* Total no. cells = apoptotic + non-apoptotic

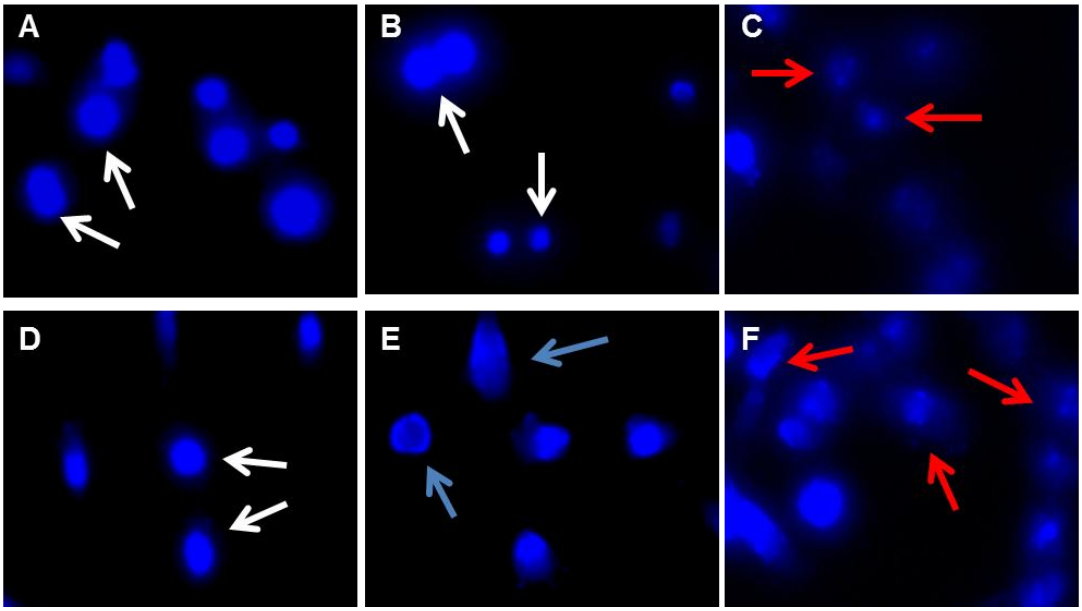

Figure 2.10: Breast cancer cells displaying normal or apoptotic nuclear morphology

Following treatment, MCF7 (A, B, C) and MDA-MB-231 (D, E, F) cells were stained with DAPI and nuclear morphology was assessed by fluorescence microscopy. A, D: 0.1% DMSO. B: 31.6µM daidzein. C: 1mM H_2O_2. E: 31.6µM genistein. F: 31.6µM daidzein + 1pM E2. Cells with evenly stained, rounded nuclei (white arrows) were counted as non-apoptotic. Cells displaying condensed chromatin (blue arrows) or punctuated nuclei (red arrows) were considered to be apoptotic.

2.6.6 Test conditions

Positive and negative controls

Positive controls for MCF7 apoptosis of 1 and 5mM H_2O_2 were used based on the results of the Annexin V-Cy3 apoptosis assay. These were tested at half, one and two hours, to ensure the capture of early apoptotic nuclear morphological changes. Following this, untreated cells, and cells treated with 0.1 and 0.2% DMSO were used to quantify the level of apoptosis measured by this method under control conditions in both MCF7 and MDA-MB-231 cells.

Oestrogen and isoflavone single treatments

As with the Annexin V-Cy3 apoptosis assay, nuclear morphology was assessed in MCF7 and MDA-MB-231 cells after a three hour treatment with 1pM and 1nM E2. Both cell lines were then treated with a physiological range of concentrations of genistein and daidzein (0.01, 1, 10 and 31.6 μM).

Combined Treatments

Changes to nuclear morphology were assessed in both MCF7 and MDA-MB-231 at the concentrations of genistein and daidzein described, in combination with premenopausal and postmenopausal E2 levels. The decision to extend this assay to the MDA-MB-231 cell line was based on the results of the Annexin V-Cy3 apoptosis assay suggesting a slight increase in the levels of PS externalising apoptosis in these cells by both isoflavones and E2 as single treatments.

2.6.7 Statistical analysis

For all conditions the mean and standard deviation of the percentage of apoptotic cells were determined. Normal distribution of the data was assumed. The single treatments of phytoestrogen and E2 were compared with their vehicle-only control (0.1% DMSO). Combined E2 and phytoestrogen treatments were compared with the 0.2% DMSO vehicle only control, and the relevant E2 only and single isoflavone treatments. Significant variation was determined using one way ANOVAs with Bonferroni *post hoc* corrections (SPSS version 19, IBM Statistics, 2010), and a value of $p<0.05$ (two-tailed) was considered to be significant.

CHAPTER 3. Results: proliferation and apoptosis

3.1 MTT proliferation assay

3.1.1 MCF7 proliferation results

3.1.1..1 Impact of control treatments and oestradiol on MCF7 proliferation

72 hour treatment with 0.1% DMSO had no significant affect on proliferation compared to an untreated control (Figure 3.1). Treatment with 0.2% DMSO caused a slight reduction in proliferation compared to the untreated cells, but this did not achieve statistical significance. The relative values for proliferation were 100 ±10.34%, 96.96 ± 10.35% and 74.03 ± 12.18%, for untreated, 0.1% DMSO and 0.2% DMSO respectively.

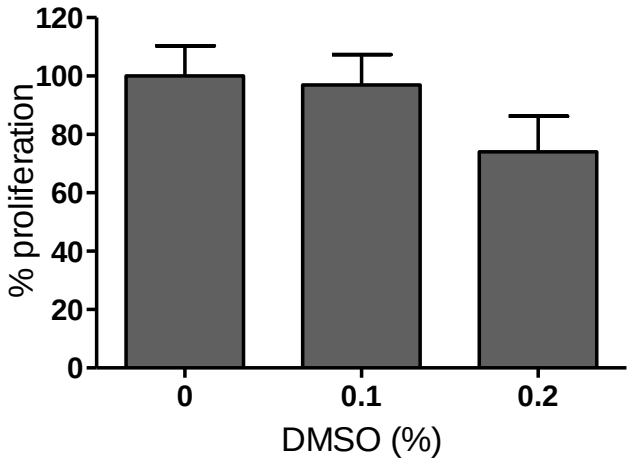

Figure 3.1 Impact of DMSO treatment on MCF7 proliferation

MCF7 cells were prepared as described. After a 24 hour oestrogen washout, their medium was replaced with medium containing no additions, or DMSO at 0.1 and 0.2%. They were incubated in this for 72 hours. Results were expressed as percentage of the untreated value (mean + standard deviation, n=3).

The single treatments of E2 and isoflavone used the DMSO vehicle at 0.1%, and consequently this treatment is considered appropriate as a control for these

conditions. The combined E2/isoflavone treatments described to follow contained DMSO at 0.2%. As this dose of the solvent did not have a significant impact upon MCF7 proliferation it was also considered to be an appropriate vehicle and control treatment for these experiments.

Treatment for 72 hours with 1pM E2 promoted the proliferation of MCF7 significantly ($p < 0.05$; Figure 3.2 and Table 3.1). The higher dose of 1nM E2 had an even greater effect ($p < 0.001$).

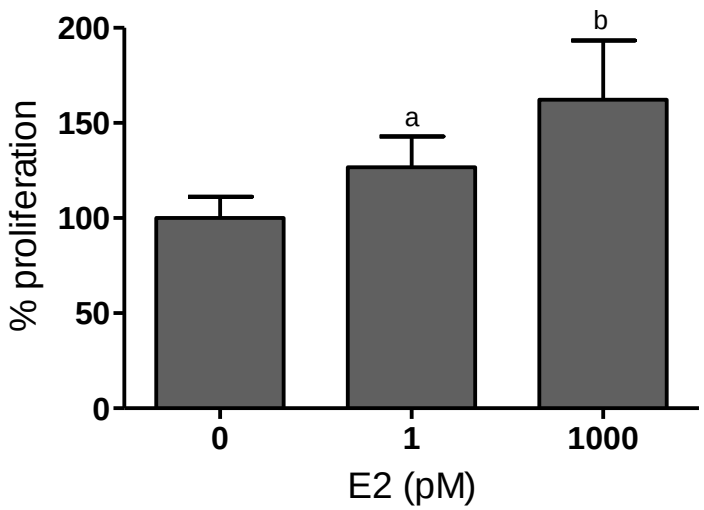

Figure 3.2: Impact of 17β-oestradiol on MCF7 proliferation

MCF7 cells were prepared as described. After a 24 hour oestrogen washout, their medium was replaced with medium containing vehicle-only, or E2 at 1pM or 1nM. They were incubated in this for 72 hours. Results were expressed as a percentage of the control treatment (mean + standard deviation, n=3). a*: significance of difference from vehicle-only control (p) < 0.05, b: significant difference from vehicle-only control (p) <0.001.*

3.1.1..2 Biphasic effect of isoflavones on MCF7 proliferation

The results of the experiments looking at the effects of isoflavones on MCF7 proliferation are shown in Figure 3.3, and Table 3.1.

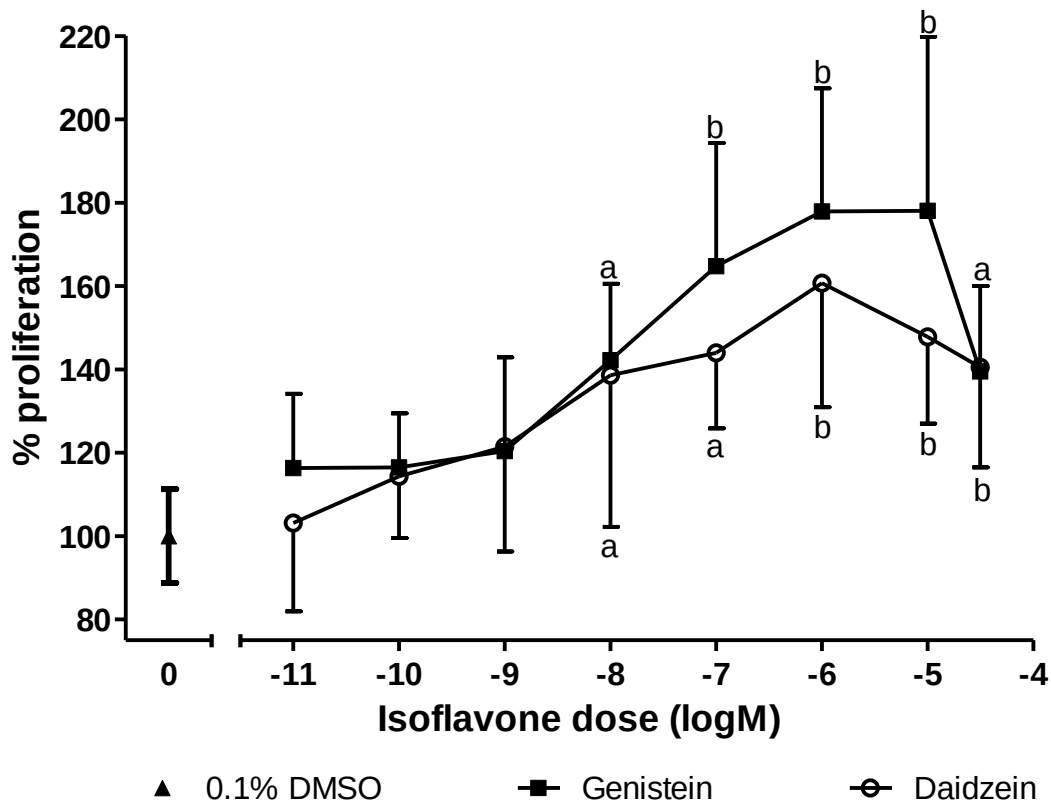

Figure 3.3: Effect of genistein and daidzein on MCF7 proliferation

MCF7 cells were prepared as described. After a 24 hour oestrogen washout, their medium was replaced with medium containing the vehicle only, or genistein or daidzein between $1x10^{-11}$ M (0.01nM) and $5x10^{-4}$M (31.6μM) and incubated in this for 72 hours. Proliferation was assessed by MTT assay and expressed as a percentage of the control treatment (mean + SD). a: significance of difference from vehicle-only control (p) < 0.01, b: significant difference from vehicle-only control (p) <0.001.

Genistein between 0.01 and 1nM had no significant effect on MCF7 proliferation compared to the 0.1% DMSO control. However, from 10nM up to the highest concentration tested of 31.6μM, proliferation was significantly increased, peaking at 10μM ($p < 0.001$). Up to and including 10μM a clear dose response can be seen,

with an EC_{50} of 12.88nM. The biphasic effect seen by some groups was not completely apparent here, as the highest concentration of genistein used (31.6µM) still resulted in some increase in proliferation compared to the control, but the trend is heading in a downward direction, and it is very likely that if higher doses were used then a toxic effect would become apparent.

Very similar effects, although slightly lower in magnitude (this difference never achieved statistical significance), were seen with 72 hour daidzein treatments for MCF7. Doses up to and including 1nM had no significant effect on proliferation. Higher doses significantly promoted proliferation in a dose-responsive manner, peaking at 1µM ($p < 0.001$). The EC_{50} for the effect of daidzein on MCF7 proliferation was calculated to be 72.1nM, suggesting that genistein was five times more effective at promoting MCF7 proliferation than daidzein. As with genistein, higher doses of daidzein continued to have a significant positive effect on proliferation compared to the control although again the trend was heading in a downward direction. As above, if higher doses were used then it is likely that a toxic effect would become apparent.

Table 3.1: Results of single treatments on MCF7 proliferation

Treatment	% Proliferation[1]	SD	P[2]
No treatment	103.14	11.29	NS
0.1% DMSO	100.00	11.25	-
0.2% DMSO	76.35	13.24	NS
G 0.01nM	116.37	17.79	NS
G 0.1nM	116.52	12.94	NS
G 1nM	120.42	22.51	NS
G 10nM	142.21	18.31	<0.01
G 100nM	164.74	29.60	<0.001
G 1μM	177.90	29.54	<0.001
G 10μM	178.04	41.76	<0.001
G 31.6μM	139.49	20.55	<0.01
D 0.01nM	103.14	21.20	NS
D 0.1nM	114.33	14.84	NS
D 1nM	121.44	25.12	NS
D 10nM	138.62	36.41	<0.01
D 100nM	143.99	18.12	<0.01
D 1μM	160.73	29.80	<0.001
D 10μM	147.83	20.80	<0.001
D 31.6μM	140.53	24.05	<0.001
E2 1pM	126.80	16.19	<0.05
E2 1nM	162.24	31.19	<0.001

G: Genistein, D: Daidzein, E2: 17β-oestradiol, SD: standard deviation, NS: not significant ($p \geq 0.05$)

[1] % proliferation compared to control cells treated with vehicle only (0.1% DMSO)

[2] significance of difference compared to cells treated with vehicle only (0.1% DMSO)

3.1.1..3 Synergistic effect of isoflavones and oestradiol on MCF7 proliferation

The effects of the combined isoflavone/E2 treatments on MCF7 are displayed in Figure 3.4 and Table 3.2. Compared with the 0.2% DMSO control, all of the combined E2/isoflavone treatments resulted in a significant increase in MCF7 proliferation.

The combinations of postmenopausal E2 (1pM) and genistein appear to affect proliferation in additive manner (Figure 3.4A), with most of the genistein treatments increasing proliferation significantly on top of the effect of the oestrogenic effect. Percentage proliferation peaked at 10µM genistein, mirroring the effects seen with the single treatments. The impacts of these combined treatments on proliferation are very similar numerically to the sum of the relevant single treatments.

The impact of daidzein and 1pM E2 on proliferation was comparable to that seen with genistein (Figure 3.4B), again peaking at the same concentration as the single daidzein treatment (1µM). Genistein and daidzein in combination with premenopausal E2 (1nM) levels was less dramatic. There is a trend towards an additional effect but in many cases the isoflavone fails to induce any statistically significant increases in proliferation on top of the effect of 1nM E2.

Furthermore, virtually all of the E2-isoflavone combinations resulted in significantly greater induction of MCF7 proliferation that the relevant isoflavone alone treatment. For p values see Table 3.2.

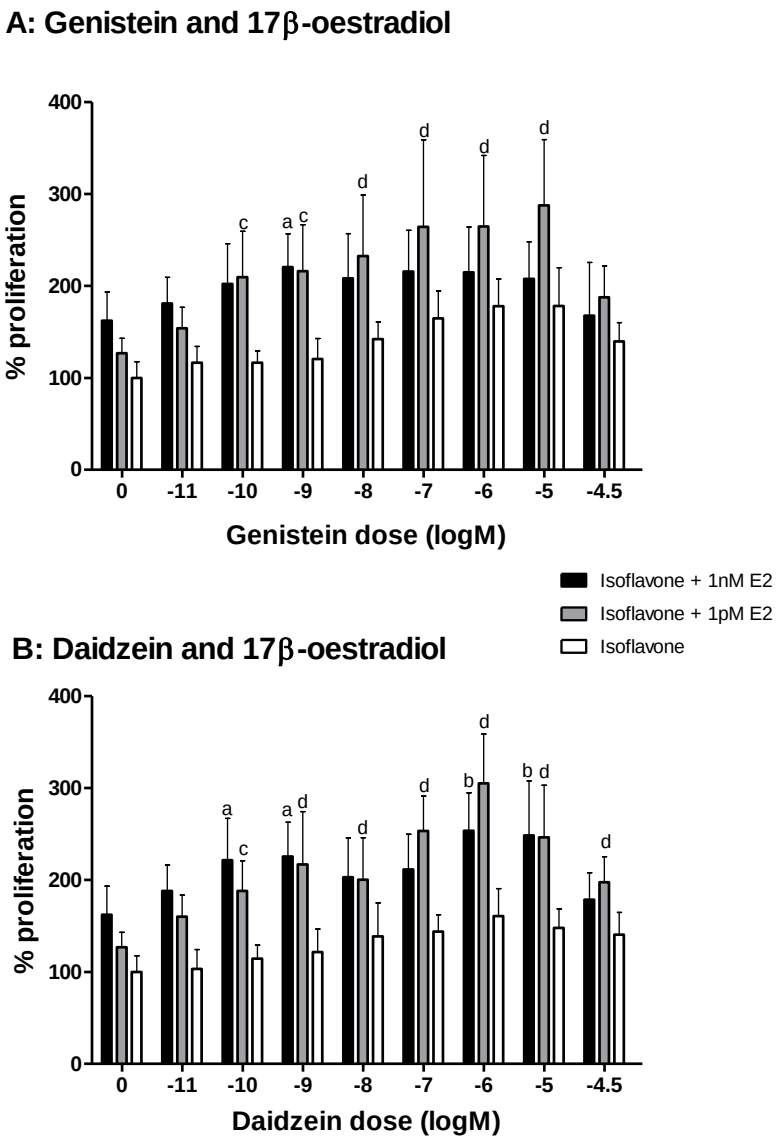

Figure 3.4: Effect of isoflavones at physiological E2 levels on MCF7 proliferation

MCF7 cells were prepared as described. After a 24 hour oestrogen washout, their medium was replaced with medium containing genistein (A) or daidzein (B) between $1x10^{-11}$M (0.01nM) and $5x10^{-4}$M (31.6µM) with pre- or post-menopausal E2 concentrations (1nM and 1pM respectively) and incubated for 72 hours. Proliferation was assessed by MTT assay and results were expressed as a percentage of the control treatment (mean ± SD, n = 3). Significant differences indicated from 1nM E2 (a: p <0.05, b: p <0.001) or from 1pM (d: p <0.05, e: p <0.001).

Table 3.2: Results for combined treatments on MCF7 proliferation

Treatment	Mean % change compared to 0.2% DMSO	Standard Deviation	Significance (p) compared to:			
			0.2% DMSO	1nM E2	1pM E2	corresponding ISF alone
0.2% DMSO	100	13.24	-	-	-	-
G 0.01nM + 1nME2	180.94	28.49	<0.001	NS	-	<0.01
G 0.1nM + 1nME2	202.19	43.70	<0.001	NS	-	<0.001
G 1nM + 1nME2	220.55	36.17	<0.001	<0.05	-	<0.001
G 10nM + 1nME2	208.44	48.37	<0.001	NS	-	<0.01
G 100nM + 1nME2	215.79	44.65	<0.001	0.086	-	<0.05
G 1µM + 1nME2	214.85	49.16	<0.001	NS	-	NS
G 10µM + 1nME2	207.66	40.31	<0.001	NS	-	NS
G 31.6µM + 1nME2	167.63	57.94	<0.001	NS	-	NS
G 0.01nM + 1pME2	154.08	22.64	0.014	-	NS	NS
G 0.1nM + 1pME2	209.60	49.86	<0.001	-	<0.01	<0.001
G 1nM + 1pME2	215.92	50.68	<0.001	-	<0.01	<0.001
G 10nM + 1pME2	232.42	66.51	<0.001	-	<0.001	<0.001
G 100nM + 1pME2	264.31	94.75	<0.001	-	<0.001	<0.001
G 1µM + 1pME2	264.76	77.33	<0.001	-	<0.001	<0.01
G 10µM + 1pME2	287.63	71.61	<0.001	-	<0.001	<0.001
G 31.6µM + 1pME2	187.53	34.30	<0.001	-	NS	NS

Treatment	Mean % change compared to 0.2% DMSO	Standard Deviation	Significance (p) compared to:			
			0.2% DMSO	1nM E2	1pM E2	corresponding ISF alone
D 0.01nM + 1nME2	188.08	28.48	<0.001	NS	-	<0.01
D 0.1nM + 1nME2	221.51	45.58	<0.001	<0.05	-	<0.001
D 1nM + 1nME2	225.63	37.10	<0.001	<0.01	-	<0.001
D 10nM + 1nME2	203.08	42.54	<0.001	NS	-	<0.01
D 100nM + 1nME2	211.50	38.17	<0.001	NS	-	<0.01
D 1μM + 1nME2	253.63	41.15	<0.001	<0.001	-	<0.001
D 10μM + 1nME2	248.52	59.46	<0.001	<0.001	-	<0.001
D 31.6μM + 1nME2	178.61	29.18	<0.001	NS	-	NS
D 0.01nM + 1pME2	160.21	23.36	<0.001	-	NS	<0.05
D 0.1nM + 1pME2	188.01	32.69	<0.001	-	<0.05	<0.001
D 1nM + 1pME2	216.91	57.61	<0.001	-	<0.001	<0.001
D 10nM + 1pME2	200.34	45.51	<0.001	-	<0.001	<0.01
D 100nM + 1pME2	253.38	37.82	<0.001	-	<0.001	<0.001
D 1μM + 1pME2	305.02	53.79	<0.001	-	<0.001	<0.001
D 10μM + 1pME2	246.40	56.70	<0.001	-	<0.001	<0.001
D 31.6μM + 1pME2	197.37	28.01	<0.001	-	<0.01	<0.01

G: genistein, D: daidzein, E2: 17β-oestradiol, ISF: isoflavone, NS: not significant ($p \geq 0.05$)

3.1.2 MDA-MB-231 proliferation results

3.1.2..1 Impact of control treatments and oestradiol on MDA-MB-231 proliferation

The result of 72 hour treatment with 0.1% DMSO on MDA-MB-231 proliferation was not significantly different from the untreated control (Figure 3.5). 0.1% DMSO is considered as an appropriate control for the rest of the data. However, 0.2% DMSO treatment for 72 hours resulted in a significant reduction in proliferation compared to the untreated control. This must be borne in mind while considering the results of the combined treatments, which use this DMSO level as a vehicle and control. The relative values for proliferation were 100 ± 25.35%, 90.15 ± 19.31% and 75.93 ± 13.48%, for untreated, 0.1% DMSO and 0.2% DMSO respectively.

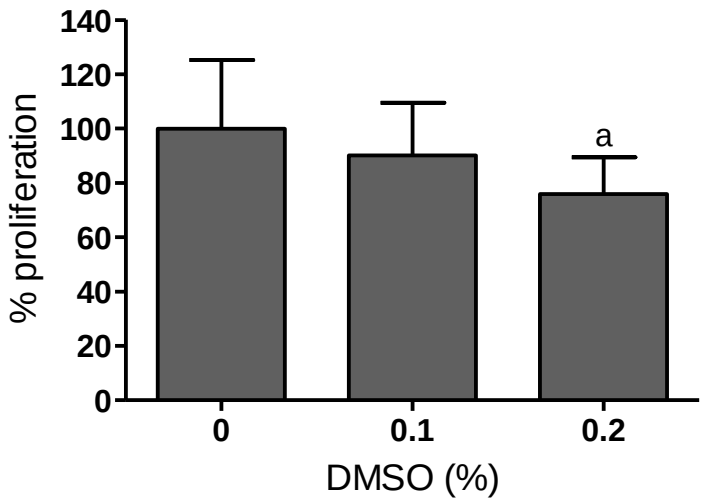

Figure 3.5: Impact of DMSO on MDA-MB-231 proliferation

MDA-MB-231 cells were prepared as described. After a 24 hour oestrogen washout, their medium was replaced with medium containing no additions, or DMSO at 0.1 and 0.2%. They were incubated in this for 72 hours. Proliferation was assessed by MTT assay and results expressed as a percentage of the untreated control (mean + standard deviation, n=3). a*: significance of difference from untreated control (p) < 0.05.*

72 hour treatment of MDA-MB-231 with pre- and post-menopausal concentrations of 17β-oestradiol inhibited the proliferation of MDA-MB-231 cells compared to the 0.1% DMSO control (Figure 3.6). With postmenopausal E2 (1 pM) this difference achieved statistical significance.

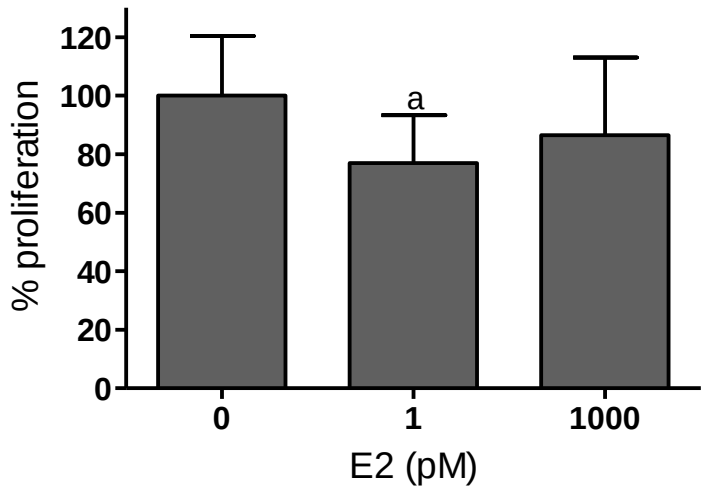

Figure 3.6: 17β-oestradiol reduces MDA-MB-231 proliferation

MDA-MB-231 cells were prepared as described. After a 24 hour oestrogen washout, their medium was replaced with medium containing vehicle-only, or E2 at 1pM or 1nM (1000pM). They were incubated in this for 72 hours. Proliferation was assessed by MTT assay and results expressed as a percentage of the control treatment (mean + standard deviation, n=3). a*: significance of difference from vehicle-only control (p) < 0.05.*

3.1.2..2 Isoflavones inhibit proliferation of MDA-MB-231

The results for the experiments looking at the impact of single treatments on the proliferation of MDA-MB-231 are shown in Table 3.3 and Figure 3.7. All 72 hour genistein treatments between 0.01 nM and 10μM slightly inhibited proliferation, although did not reach statistical significance. The highest dose (31.6μM) caused a dramatic and significant ($p<0.01$) decrease in proliferation. Daidzein treatment resulted in a broadly similar pattern, with the exception that 0.01nM significantly inhibited proliferation also ($p<0.001$).

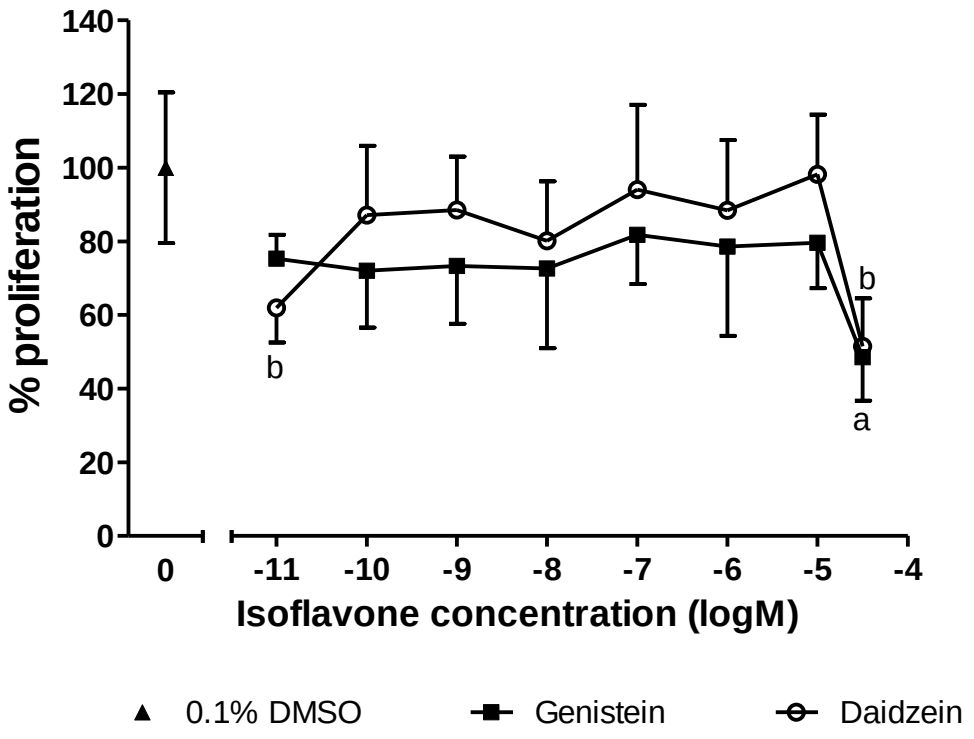

Figure 3.7: Effect of genistein and daidzein on MDA-MB-231 proliferation

MDA-MB-231 cells were prepared as described. After a 24 hour oestrogen washout, their medium was replaced with medium containing the vehicle only or genistein or daidzein between $1x10^{-11}$ M (0.01nM) and $5x10^{-4}$M (31.6μM) and incubated in this for 72 hours. Proliferation was assessed by MTT assay and expressed as a percentage of the control treatment (mean + standard deviation, n=3). a*: significance of difference from vehicle-only control (p) < 0.01, b: significance of difference (p) from vehicle-only control <0.001.*

Table 3.3: Impact of single treatments on MDA-MB-231 proliferation

Treatment	% proliferation[1]	SD	P[2]
No treatment	109.05	26.38	NS
0.1% DMSO	100	20.43	-
0.2% DMSO	84.97	15.25	NS
G 0.01nM	75.34	6.83	NS
G 0.1nM	76.59	16.39	NS
G 1nM	77.97	16.68	NS
G 10nM	77.19	22.96	NS
G 100nM	86.92	14.21	NS
G 1µM	83.59	25.85	NS
G 10µM	84.68	13.19	NS
G 31.6µM	48.53	12.57	<0.01
D 0.01nM	58.26	9.40	<0.001
D 0.1nM	87.09	18.82	NS
D 1nM	88.52	14.53	NS
D 10nM	80.11	16.18	NS
D 100nM	94.00	23.08	NS
D 1µM	88.45	19.04	NS
D 10µM	98.21	16.16	NS
D 31.6µM	48.40	13.06	<0.001
E2 1pM	76.95	16.34	<0.05
E2 1nM	86.46	26.62	NS

G: Genistein, D: Daidzein, E2: 17β-oestradiol, SD: standard deviation, NS: not significant ($p \geq 0.05$)

[1] % proliferation compared to control cells treated with vehicle only (0.1% DMSO)

[2] significance of difference compared to cells treated with vehicle only (0.1% DMSO)

3.1.2..3 Absence of synergy between isoflavones and oestradiol with MDA-MB-231 proliferation

The results for the MTT assays undertaken with combined treatments of genistein (A) and daidzein (B) with pre- and post-menopausal E2 concentrations are shown in Figure 3.8, with the p values for all comparisons in Table 3.4.

Although the majority continue to demonstrate a trend towards inhibition of proliferation compared with the 0.2% DMSO control, no value was significantly different from the control, or from the E2-alone treatment. Likewise, only three of the combinations tested differed significantly from the relevant isoflavone single treatment, and there was no pattern to them. These were 10nM genistein / 1nM E2 ($p < 0.05$), 1nM daidzein / 1nM E2 ($p < 0.01$) and 10µM daidzein / 1pM E2 ($p< 0.05$).

The combinations of 1pM E2 and daidzein were more effective at reducing proliferation in MDA-MB-231 cells than any other combined or single treatment, resulting in values of around 70% of the control level of proliferation, although the only significant difference achieved was between 10µM daidzein and the combined 10µM daidzein/1pM E2 treatment ($p < 0.05$; Figure 3.8B). This set of combined treatments showed a trend towards a synergistic inhibitory effect, with the majority of the sets of conditions resulting in slightly lower proliferation than either daidzein or 1pM E2 alone. The other E2/isoflavone combinations were less effective at reducing proliferation than the isoflavones alone, although in several cases there was still a slight effect.

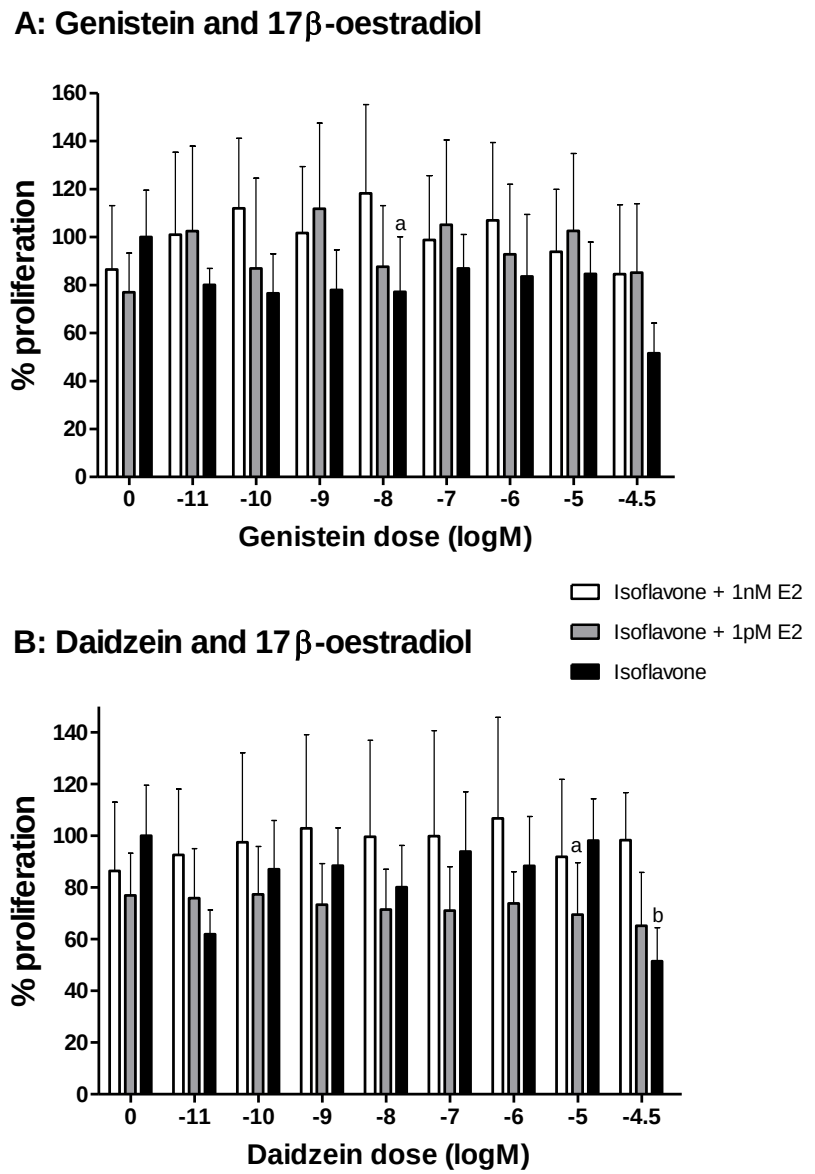

Figure 3.8: The effects of isoflavones at physiological E2 levels on MDA-MB-231 proliferation

MDA-MB-231 cells were prepared as described. After a 24 hour oestrogen washout, medium was replaced with medium containing the vehicle only (0.2% DMSO) or genistein (A) or daidzein (B) between $1x10^{-11}$ M and $5x10^{-4}$M with pre- or post-menopausal E2 concentrations (1nM and 1pM respectively) and incubated in this for 72 hours. Proliferation was assessed by MTT assay and expressed as the percentage of the control treatment (mean + SD, n=3). Significant difference from the relevant isoflavone-only treatment is indicated by a *($p < 0.05$) or b ($p < 0.01$).*

Table 3.4 Results for the combined treatments on MDA-MB-231 proliferation

Treatment	Mean % change compared to 0.2% DMSO	Standard Deviation	Significance (p) compared to:			
			0.2% DMSO	1nM E2	1pM E2	corresponding ISF alone
0.2% DMSO	100.00	17.95	-	-	-	-
G 0.01nM + 1nME2	101.01	34.38	NS	NS	-	NS
G 0.1nM + 1nME2	111.99	29.16	NS	NS	-	NS
G 1nM + 1nME2	101.71	27.61	NS	NS	-	NS
G 10nM + 1nME2	118.20	37.05	NS	NS	-	<0.05
G 100nM + 1nME2	98.78	26.86	NS	NS	-	NS
G 1µM + 1nME2	107.05	32.33	NS	NS	-	NS
G 10µM + 1nME2	93.96	25.98	NS	NS	-	NS
G 31.6µM + 1nME2	84.62	28.95	NS	NS	-	NS
G 0.01nM + 1pME2	102.48	35.39	NS	-	NS	NS
G 0.1nM + 1pME2	86.91	37.65	NS	-	NS	NS
G 1nM + 1pME2	111.82	35.77	NS	-	NS	NS
G 10nM + 1pME2	87.62	25.52	NS	-	NS	NS
G 100nM + 1pME2	105.12	35.28	NS	-	NS	NS
G 1µM + 1pME2	92.77	29.33	NS	-	NS	NS
G 10µM + 1pME2	102.52	32.35	NS	-	NS	NS
G 31.6µM + 1pME2	85.18	28.73	NS	-	NS	NS

Treatment	Mean % change compared to 0.2% DMSO	Standard Deviation	Significance (p) compared to:			
			0.2% DMSO	1nM E2	1pM E2	corresponding ISF alone
D 0.01nM + 1nME2	92.60	25.57	NS	NS	-	NS
D 0.1nM + 1nME2	97.62	34.56	NS	NS	-	NS
D 1nM + 1nME2	102.86	36.37	NS	NS	-	NS
D 10 nM + 1nME2	99.65	37.32	NS	NS	-	NS
D 100nM + 1nME2	99.99	40.75	NS	NS	-	NS
D 1µM + 1nME2	106.84	38.98	NS	NS	-	NS
D 10µM + 1nME2	91.97	29.86	NS	NS	-	NS
D 31.6µM + 1nME2	98.36	18.33	NS	NS	-	<0.01
D 0.01nM + 1pME2	75.98	19.07	NS	-	NS	NS
D 0.1nM + 1pME2	77.40	18.52	NS	-	NS	NS
D 1nM + 1pME2	73.40	15.87	NS	-	NS	NS
D 10 nM + 1pME2	71.47	15.66	NS	-	NS	NS
D 100nM + 1pME2	71.11	16.98	NS	-	NS	NS
D 1µM + 1pME2	73.90	12.26	NS	-	NS	NS
D 10µM + 1pME2	69.59	20.05	NS	-	NS	<0.05
D 31.6µM + 1pME2	65.20	20.62	NS	-	NS	NS

G: genistein, D: daidzein, E2: 17β-oestradiol, ISF: Isoflavone, NS: not significant (p ≥ 0.05)

3.2 Annexin V-Cy3™ Apoptosis Assay Results

3.2.1 MCF7 Annexin V-Cy3 apoptosis results

3.2.1..1 Impact of control treatments on PS externalisation in MCF7

Neither 0.1% or 0.2% DMSO had any significant effect on the percentage of PS externalising apoptotic cells compared to no treatment in MCF7 (Figure 3.9). A representative set of images is provided in Figure 3.10, suggesting that at these levels DMSO is an appropriate vehicle for the ligands and does not impact upon the induction of MCF7 PS-externalising apoptosis.

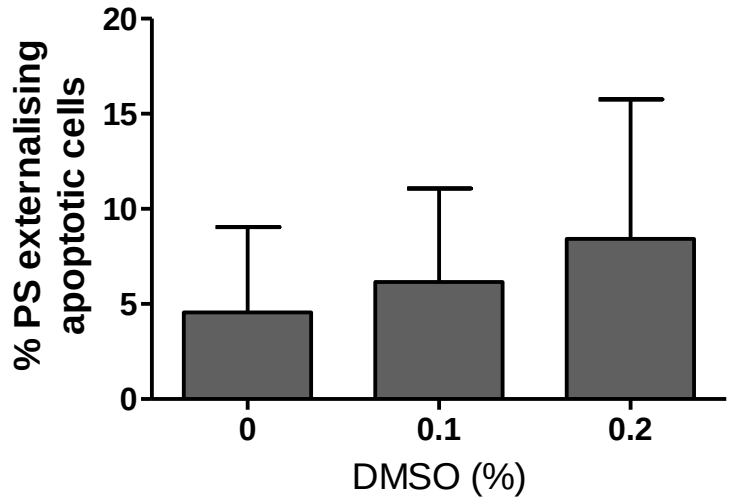

Figure 3.9: Induction of PS-externalising apoptosis in MCF7 by control treatments

MCF7 cells were prepared as described. Following 48 hours of oestrogen washout, medium was replaced with fresh oestrogen free medium with no addition, or 0.1 or 0.2% DMSO, and incubated for a further 24 hours. Results presented as mean % PS externalising apoptotic cells per treatment + SD (n=3). There were no significant differences between these results.

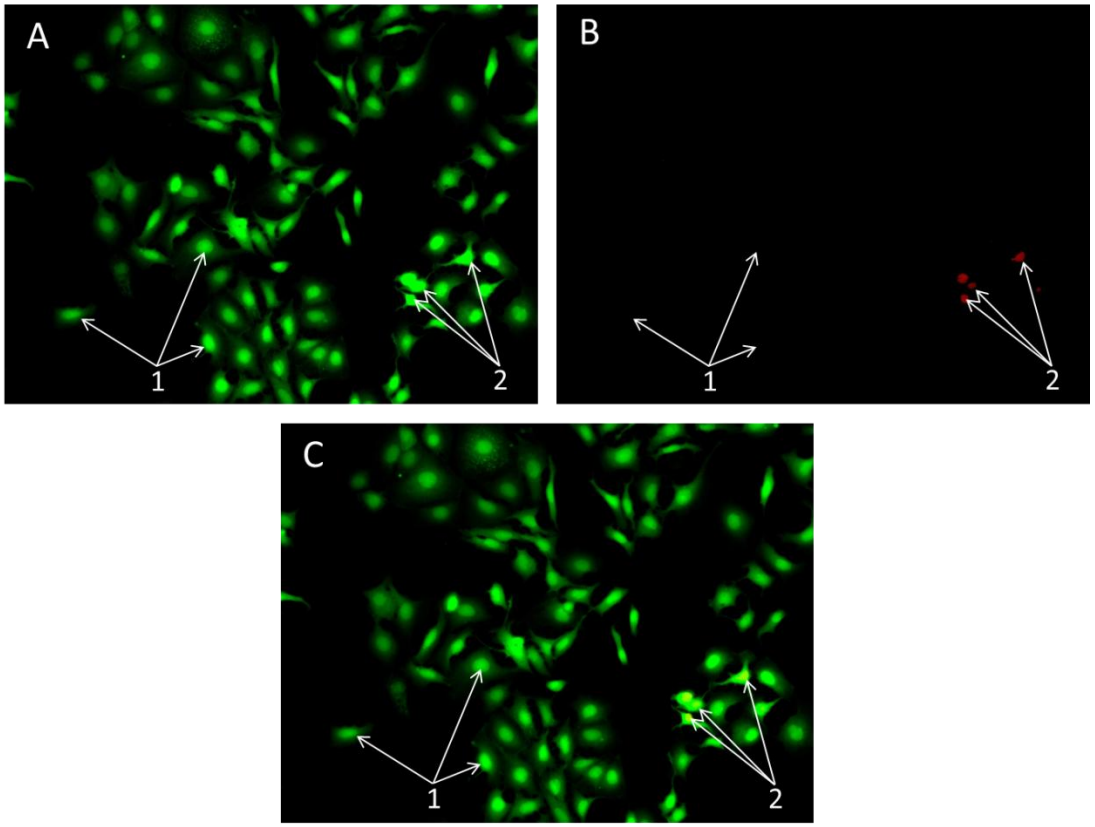

Figure 3.10: Captured images of MCF7 cells treated with 0.1% DMSO

MCF7 cells were prepared as described then incubated for 24 hours with medium containing 0.1% DMSO, stained with the Annexin V-Cy3 apoptosis detection kit, and fluorescent images captured. A: green fluorescence from 6CFDA dye. B: red fluorescence from Annexin V-conjugate dye. C: Composite image where yellow indicates overlap of the two colours. In each image 1 indicates a number of viable cells, stained by 6-CFDA only, and 2 indicates PS externalising apoptotic cells stained with both. In this region of the slide apoptosis was calculated to be 5.21%.

3.2.1..2 Effect of 17β-oestradiol treatments on PS externalisation in MCF7

24 hour treatment with pre- or post-menopausal concentrations of 17β-oestradiol (1nM and 1pM respectively) had no significant impact on the percentage of PS externalising apoptotic cells calculated for MCF7 (Figure 3.11).

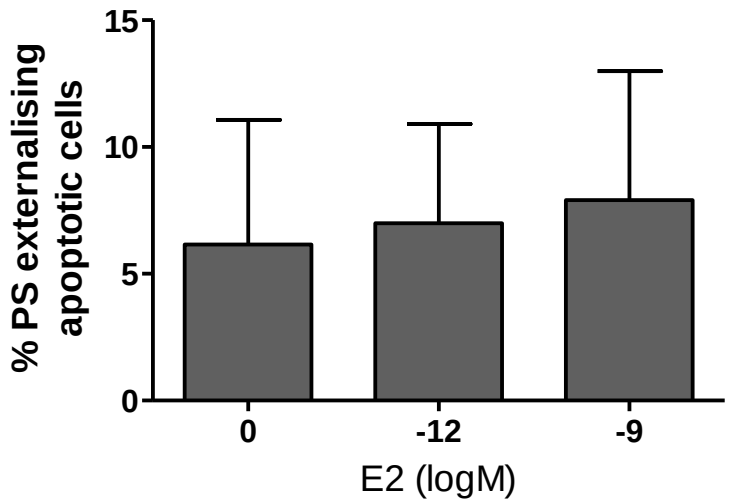

Figure 3.11: Induction of MCF7 PS-externalising apoptosis by 17β-oestradiol

MCF7 cells were prepared as described. Following 48 hour oestrogen washout, medium was replaced with fresh oestrogen free medium containing vehicle only, or 1pM ($1x10^{-12}$) or 1nM ($1x10^{-9}$) E2, and incubated for a further 24 hours. Results represented as mean % PS externalising apoptotic cells per treatment + SD (n=3). There were no significant differences between these results.

3.2.1..3 Isoflavones increase PS externalising apoptosis in MCF7

A sample set of images from the Annexin V-Cy3 assay in MCF7 with single isoflavone treatments are displayed in Figure 3.12. The results of these assays and the p values for comparisons to 0.1% DMSO are given in Figure 3.13 and Table 3.5. There is a trend towards a greater rate of apoptosis with PS externalisation in MCF7 cells after 24 hour genistein or daidzein treatment, between 0.1 and 31.6µM compared to the vehicle only. With 1 and 10µM daidzein and 1µM genistein this increase in the percentage of apoptotic cells became statistically significant ($p < 0.05$). The highest rate measured was with 1µM genistein. However, there is no dose effect or appreciable difference between the two isoflavones. Each data point has a wide SD, reflecting great variation in the levels of apoptosis seen in the cells on the separate occasions that the tests were repeated.

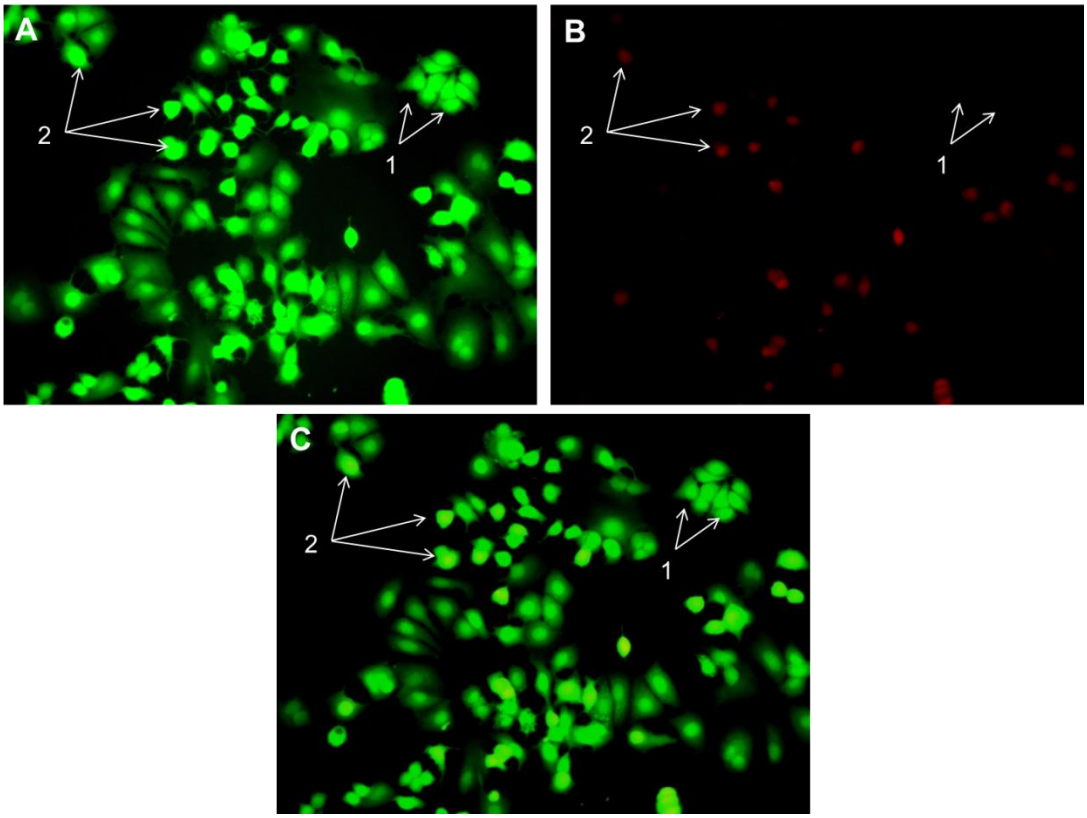

Figure 3.12: Captured images of MCF7 cells treated with 1µM genistein

MCF7 cells were prepared as described then incubated for 24 hours with medium containing 1µM genistein, stained with the Annexin V-Cy3 apoptosis detection kit, and fluorescent images captured. A: green fluorescence from 6CFDA dye. B: red fluorescence from Annexin V conjugate dye. C: Composite image where yellow indicates overlap of the two colours. In each image 1 indicates a number of viable cells stained by 6CFDA only, and 2 indicates apoptotic PS externalising cells stained with both. In this region of the slide apoptosis was calculated to be 21.3%.

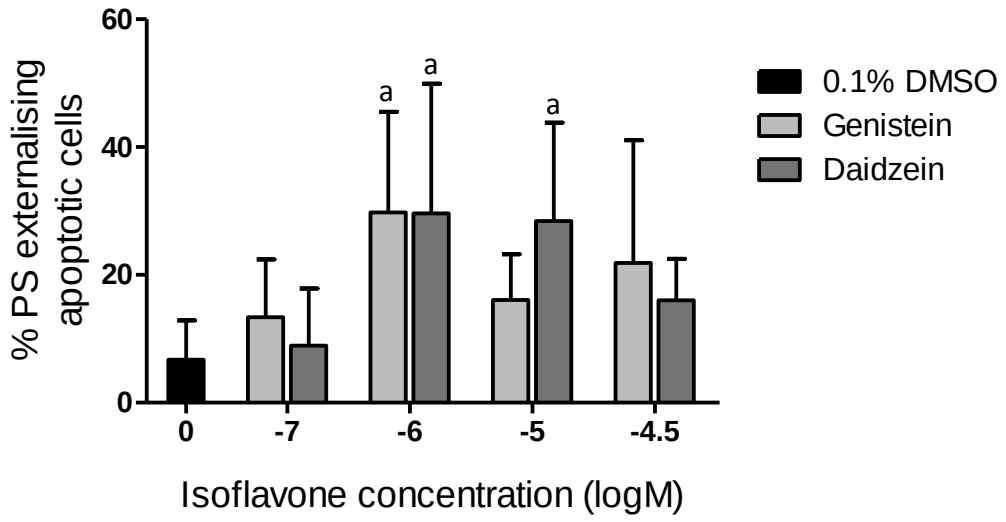

Figure 3.13: Induction of PS-externalising apoptosis in MCF7 by isoflavones

MCF7 cells were prepared as described. Following 48 hour oestrogen washout, medium was replaced with fresh oestrogen free medium with vehicle only (0.1% DMSO), genistein or daidzein, between 0.1µM and 31.6µM, and incubated for a further 24 hours. Results presented as mean % PS externalising apoptotic cells per treatment + SD (n=3). Significant variation from the vehicle-only control ($p < 0.05$) indicated by a.

Table 3.5: Results for induction of PS-externalising apoptosis by single treatments in MCF7

Treatment	MCF7		
	% apoptosis[1]	SD	P[2]
No treatment	4.56	4.48	NS
0.1% DMSO	6.16	4.91	-
0.2% DMSO	8.43	7.32	NS
G 0.1μM	13.37	9.06	NS
G 1μM	29.77	15.74	<0.05
G 10μM	16.09	7.12	NS
G 31.6μM	21.89	19.17	NS
D 0.1μM	8.91	8.99	NS
D 1μM	29.62	20.28	<0.05
D 10μM	28.41	15.42	<0.05
D 31.6μM	16.04	6.50	NS
E2 1pM	6.99	3.92	NS
E2 1nM	7.90	5.09	NS

G: Genistein, D: Daidzein, E2: 17β-oestradiol, SD: Standard Deviation, NS: not significant (p ≥ 0.05)

[1] mean percentage apoptotic PS externalising cells per treatment

[2] significant differences compared to cells treated with vehicle only (0.1% DMSO)

3.2.1..4 Combinations of isoflavones and 17β-oestradiol induce PS externalising apoptosis in MCF7

The impact of combinations of isoflavones and E2 on PS-externalising apoptosis in MCF7 is shown in Figure 3.14A (genistein) and B (daidzein) and Table 3.6. Each of the combination treatments resulted in a greater percentage of PS-externalising apoptosis than the 0.2% DMSO control. This achieved statistical significance on a number of occasions (highlighted in Table 3.6).

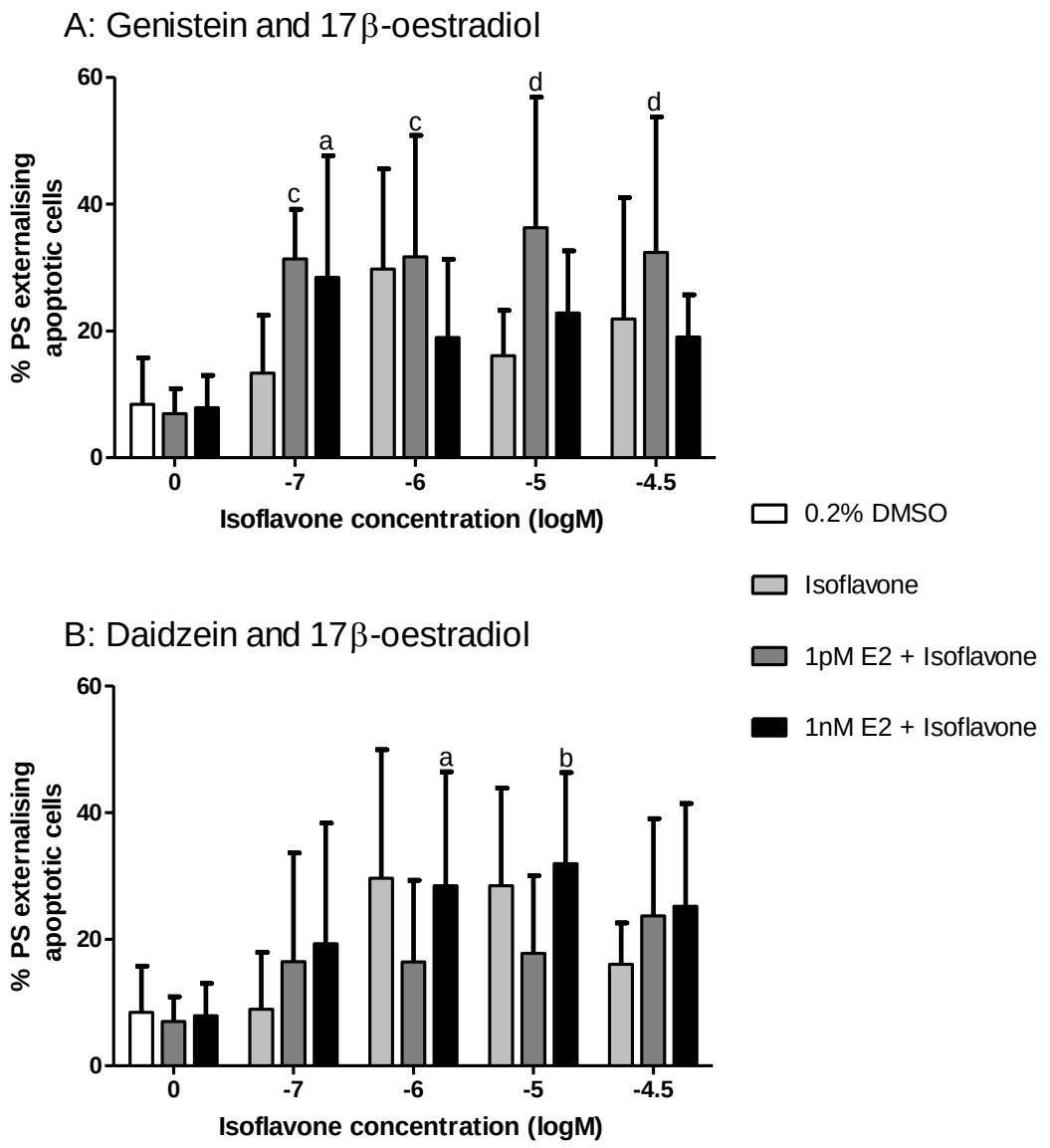

Figure 3.14: Induction of PS-externalising apoptosis in MCF7 by isoflavones combined with 17β-oestradiol

Cells were prepared as described. Following 48 hour oestrogen washout, medium was replaced with fresh oestrogen free medium with vehicle only, genistein (A) or daidzein (B) between 0.1µM and 31.6µM, with or without E2 at pre- and post-menopausal concentrations, and incubated for a further 24 hours. Results presented as mean % apoptotic PS externalising cells per treatment and SD (n=3). Significant difference from 1nM E2 is indicated by a *($p < 0.05$) and b ($p < 0.01$). Significant difference from 1pM E2 is indicated by c ($p < 0.05$) and d ($p < 0.01$).*

Table 3.6: Induction of PS externalising apoptosis in MCF7 by combinations of isoflavones and E2

Treatment	% apoptosis[1]	SD	Significance (p) compared to:			
			0.2% DMSO	1nM E2	1pM E2	corresponding isoflavone alone
0.2% DMSO	8.43	19.19	-	-	-	-
G 0.1μM + 1nME2	28.45	12.31	NS	<0.05	-	NS
G 1μM + 1nME2	18.98	9.83	NS	NS	-	NS
G 10μM + 1nME2	22.81	6.68	NS	NS	-	NS
G 31.6μM + 1nME2	19.03	7.86	NS	NS	-	NS
G 0.1μM + 1pME2	31.33	19.14	0.061	-	<0.05	NS
G 1μM + 1pME2	31.68	20.52	<0.05	-	<0.05	NS
G 10μM + 1pME2	36.29	21.35	<0.01	-	<0.01	NS
G 31.6μM + 1pME2	32.39	19.02	<0.05	-	<0.01	NS
D 0.1μM + 1nME2	19.29	18.01	NS	NS	-	NS
D 1μM + 1nME2	28.41	14.37	0.099	<0.05	-	NS
D 10μM + 1nME2	31.96	16.22	<0.05	<0.01	-	NS
D 31.6μM + 1nME2	25.21	17.14	NS	NS	-	NS

Treatment	% apoptosis[1]	SD	Significance (p) compared to:			
			0.2% DMSO	1nM E2	1pM E2	corresponding isoflavone alone
D 0.1μM + 1pME2	16.46	12.90	NS	-	NS	NS
D 1μM + 1pME2	16.42	12.31	NS	-	NS	NS
D 10μM + 1pME2	17.73	15.36	NS	-	NS	NS
D 31.6μM + 1pME2	23.66	19.19	NS	-	NS	NS

[1] *mean percentage of apoptotic PS externalising cells per treatment*

G: genistein, D: daidzein, E2: 17β-oestradiol, SD: Standard Deviation, NS: not significant (p ≥ 0.05)

Likewise, the combined treatments each resulted in a greater level of PS externalisation that the relevant E2-alone treatment, reaching statistical significance on the occasions indicated. The combination of genistein and 1pM E2 (postmenopausal) appeared to be particularly effective at inducing PS externalising apoptosis in MCF7 compared to 1pM E2 alone (Figure 3.14A). Furthermore, each genistein and 1pM E2 combination also resulted in a higher percentage of PS externalising apoptotic cells than genistein alone at the same concentrations, although none of these comparisons achieved significance.

The lack of statistical significance for many of the combined treatments compared to either the 0.2% DMSO or appropriate E2-alone treatment reflects the variability in the data (see the SDs, in Table 3.6). Despite this, virtually all the individual values were numerically higher.

None of the isoflavone/E2 combination results differed significantly in their effect on PS-externalising apoptosis compared to the relevant isoflavone alone. However, there is variability in the results, with no consistent pattern. A number of the isoflavone/E2 combinations induce a lower level of apoptosis than the isoflavone alone (not significant), and some had no clear impact upon the induction of PS externalising apoptosis in either direction. The results for genistein and daidzein at both E2 concentrations are largely comparable, and no clear dose-related patterns emerge.

3.2.2 MDA-MB-231 Annexin V-Cy3 apoptosis results

3.2.2..1 The impact of DMSO on PS-externalising apoptosis in MDA-MB-231 cells

After 24 hours treatment, 0.1% DMSO had no significant impact upon PS-externalisation compared to medium with no additions. The respective values (mean ± standard deviation, n = 3) for untreated and 0.1% DMSO treated cells were 9.66 ± 8.22% and 6.74 ± 6.15% PS externalising apoptosis. All Annexin V-Cy3 assays in this cell line were conducted at the 0.1% solvent dose. As this had no significant impact upon PS-externalising apoptosis, it is considered to be an appropriate control. These results are summarised in Table 3.7.

3.2.2..2 Effect of 17β-oestradiol on PS-externalising apoptosis in MDA-MB-231 cells

The impact of physiological concentrations of E2 on the induction of PS-externalising apoptosis in this cell line is shown in Figure 3.15 and Table 3.7. These treatments had no impact on the percentage of PS externalising apoptotic cells after 24 hours.

3.2.2..3 Isoflavones increase PS externalising apoptosis in MDA-MB-231

In MDA-MB-231, 24 hour treatment with genistein or daidzein led to a slight increase in the rate of PS externalising apoptotic cells compared to vehicle only controls, however this effect is not statistically significant (Figure 3.17; representative images in Figure 3.16). The full dataset is provided in Table 3.7. Daidzein was slightly more effecting at inducing apoptotic PS externalisation than genistein at each concentration used, with the highest rate recorded after 10μM daidzein treatment, although the difference between the isoflavones is non-significant. The very wide range of actual results on the different occasions that the tests were repeated, reflected by the wide standard deviations seen, may underpin the lack of statistical significance to the results. As with the MCF7 cells, there is no clear dose-effect.

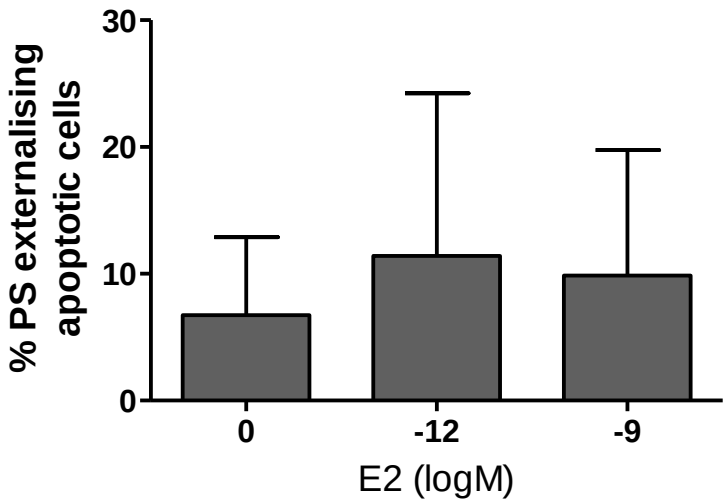

Figure 3.15: The effect of 17β-oestradiol on PS-externalising apoptosis in MDA-MB-231 cells

MDA-MB-231 cells were prepared as described. Following 48 hour oestrogen washout, medium was replaced with fresh oestrogen free medium with vehicle only (0.1% DMSO), or 1pM or 1nM E2, and incubated for a further 24 hours. Results represented as mean % PS externalising apoptotic cells per treatment and SD (n=3). There were no significant differences between these results.

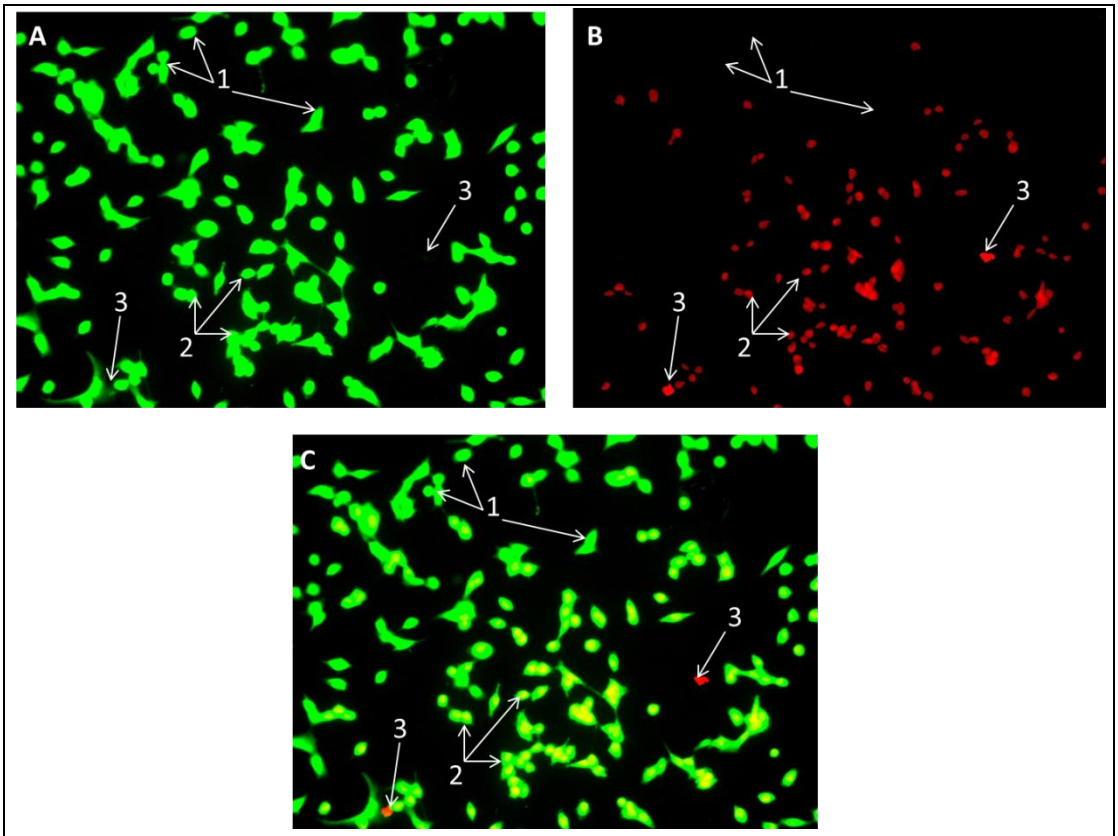

Figure 3.16: Captured images of MDA-MB-231 cells treated with 1µM daidzein

MDA-MB-231 cells were prepared as described then incubated for 24 hours with medium containing 1µM daidzein, stained with the Annexin V-Cy3 apoptosis detection kit, and fluorescent images captured. A: green fluorescence from 6CFDA dye. B: red fluorescence from Annexin V conjugate dye. C: Composite image where yellow indicated overlap of the two colours. In each image 1 indicates a number of viable cells, stained by 6CFDA only, 2 indicates apoptotic cells stained with both, and 3 indicates necrotic cells stained with the Annexin V conjugate only. In this region of the slide apoptotic PS-externalisation was calculated to be 65.56%.

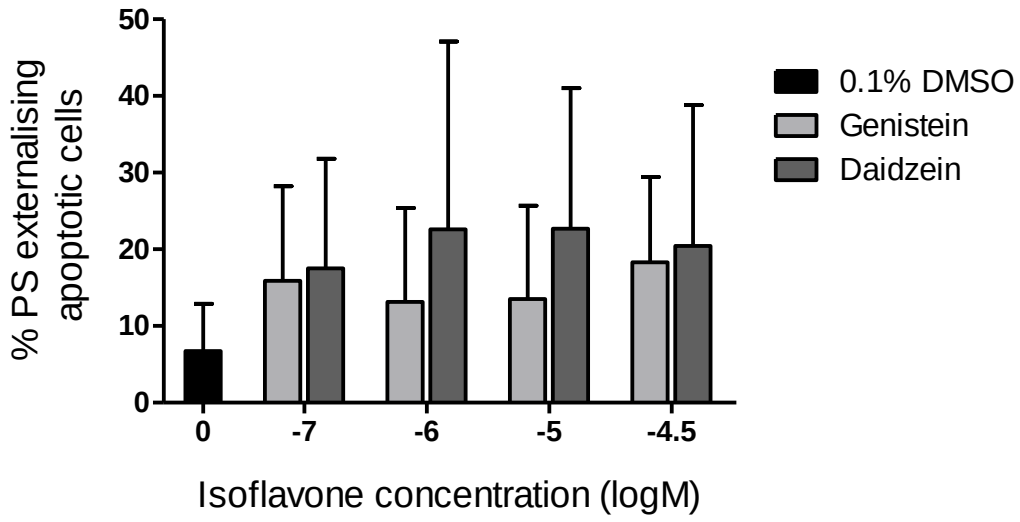

Figure 3.17: Induction of PS-externalising apoptosis in MDA-MB-231 by isoflavones

Cells were prepared as described, then the medium was replaced with fresh oestrogen free medium with vehicle only (0.1% DMSO), or genistein or daidzein between 0.1µM and 31.6µM, and incubated for a further 24 hours. Results presented as mean percentage PS externalising apoptotic cells per treatment and SD (n=3). There were no significant differences between treatments and control.

Table 3.2: Results for the induction of PS-externalising apoptosis in MDA-MB-231 cells by single isoflavone and oestradiol treatments

Treatment	% apoptosis[1]	SD	P[2]
No treatment	9.66	8.22	NS
0.1% DMSO	6.74	6.15	-
G 0.1μM	15.90	12.32	NS
G 1μM	13.15	12.23	NS
G 10μM	13.52	12.18	NS
G 31.6μM	18.30	11.14	NS
D 0.1μM	17.52	14.31	NS
D 1μM	22.60	24.52	NS
D 10μM	22.67	18.35	NS
D 31.6μM	20.43	18.38	NS
E2 1pM	11.41	12.84	NS
E2 1nM	9.86	9.89	NS

G: Genistein, D: Daidzein, E2: 17β-oestradiol, SD: Standard Deviation, NS: not significant ($p \geq 0.05$)

[1] mean percentage apoptotic PS externalising cells per treatment

[2] significant differences compared to cells treated with vehicle only (0.1% DMSO)

3.3 Results of DAPI Staining and Determination of Nuclear Changes

3.3.1 MCF7 DAPI results

3.3.1..1 Effect of control treatments on MCF7 nuclear morphology

Results for the control experiments on the percentage of MCF7 cells displaying apoptotic nuclear morphology are depicted in Figure 3.18. DMSO up to 0.2% had no significant effect on the percentage of apoptotic cells compared to untreated cells after three hours. Representative sets of fluorescent, bright field and composite images showing no evidence of apoptotic nuclear changes are provided for 0.1% DMSO treatment (Figure 3.19).

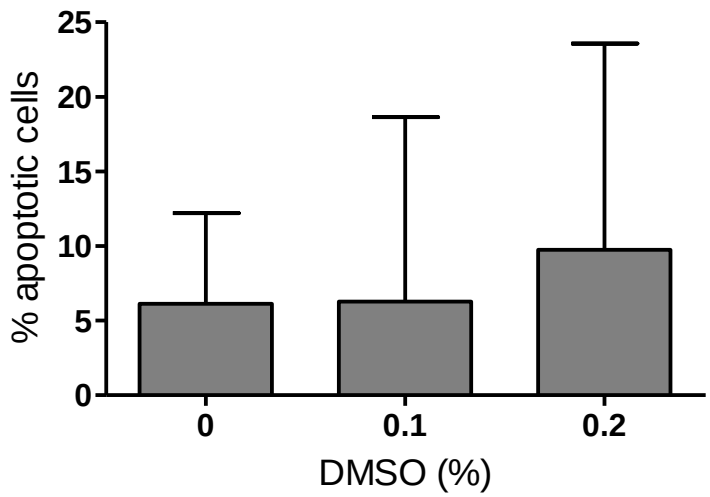

Figure 3.18: The impact of various concentrations of DMSO on the percentage of MCF7 cells displaying apoptotic nuclear morphology

MCF7 cells were prepared as described, and incubated for 48 hours to allow oestrogens to wash out. Following this, medium was replaced with fresh oestrogen free medium with no additions, 0.1 or 0.2% DMSO. The percentage of apoptotic cells after DAPI staining was determined. Results are presented as mean + SD for each treatment (n=3). There were no significant variations ($p < 0.05$) in results.

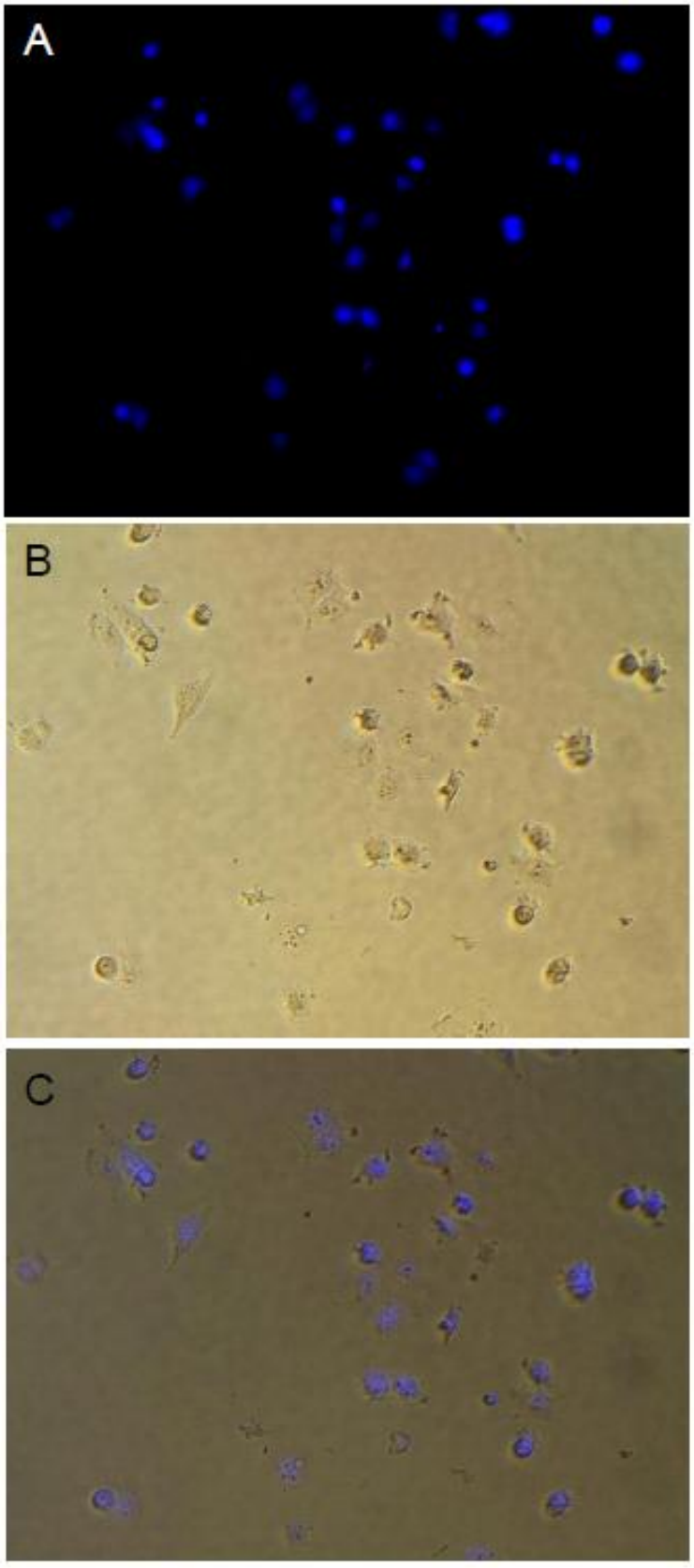

Figure 3.19: MCF7 breast cancer cells treated with 0.1% DMSO

Representative images of MCF7 cells treated as described with 0.1% DMSO. A: DAPI fluorescent image, B: bright field, C: composite. No evidence of apoptotic nuclear changes.

3.3.1..2 17β-Oestradiol does not induce apoptotic nuclear morphology in MCF7

The results of the experiments looking at the effects of physiological concentrations of E2 on the induction of apoptotic nuclear morphology are shown in Figure 3.20 and Table 3.8. There was no effect apparent after three hour treatment with either concentration compared to the vehicle only control.

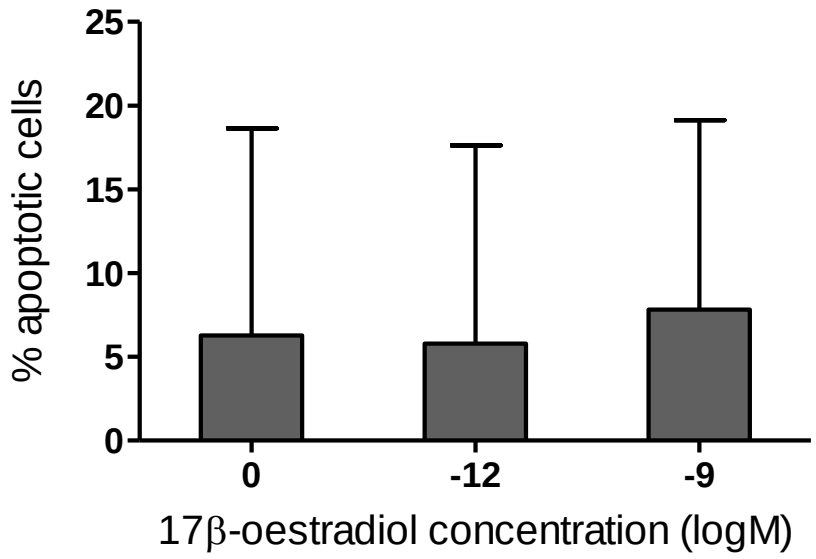

Figure 3.20: Induction of apoptotic nuclear morphology by 17β-oestradiol in MCF7

MCF7 cells were prepared as described. Following this, medium was replaced with fresh oestrogen free medium with 0.1% DMSO or 17β-oestradiol at pre- and post-menopausal concentrations (1 x 10^{-9}M and 1 x 10^{-12}M respectively). Levels of apoptosis were quantified after DAPI staining, by calculation percentage of cells displaying apoptotic nuclear morphology and results presented as mean and SD for each treatment (n=3). There were no significant variations from the vehicle-only control ($p < 0.05$).

3.3.1..3 The effect of isoflavones on nuclear morphology in MCF7

The impact of isoflavones on apoptotic nuclear morphology in MCF7 is shown in Figure 3.21 and Table 3.8. Three hour treatment of MCF7 with genistein between 10nM and 10µM had no significant effect on apoptotic nuclear morphology. However, the highest concentration of genistein used (31.6µM) resulted in a significant increase in the percentage of apoptotic cells ($p < 0.01$). Daidzein had no significant effect at any concentration.

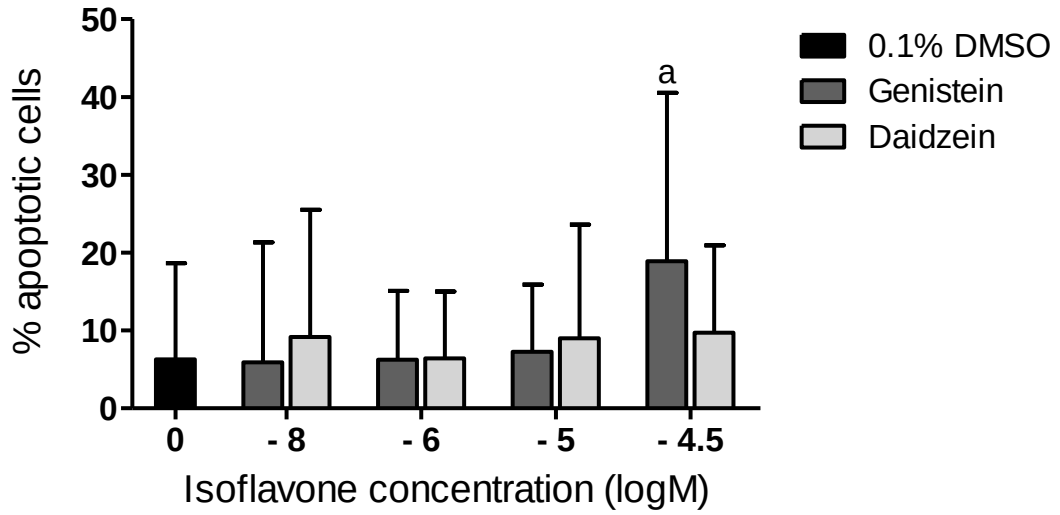

Figure 3.21: The effect of isoflavones on apoptosis in MCF7 breast cancer cells

MCF7 cells were prepared as described, and incubated for 48 hours to allow oestrogens to wash out. Following this, medium was replaced with fresh oestrogen free medium with 0.1% DMSO, or genistein or daidzein at 0.01, 1, 10 and 31.6µM. Induction of apoptosis was quantified by calculation of the percentage of cells displaying apoptotic nuclear morphology after DAPI staining, and results presented as mean + SD for each treatment (n=3). a *indicates significant variation from the vehicle-only control ($p < 0.01$).*

Table 3.8: Effect of single isoflavone and 17β-oestradiol treatments on apoptotic nuclear morphology in MCF7 cells

Treatment	% apoptosis[1]	SD	P[2]
untreated	6.12	6.08	NS
0.1% DMSO	6.28	12.36	-
0.2% DMSO	9.75	13.82	NS
1pM E2	5.78	11.84	NS
1nM E2	7.82	11.30	NS
10nM G	5.92	15.39	NS
1µM G	6.24	8.85	NS
10µM G	7.24	8.66	NS
31.6µM G	18.90	21.63	<0.01
10nM D	9.18	16.32	NS
1µM D	6.40	8.59	NS
10µM D	9.01	14.58	NS
31.6µM D	9.71	11.22	NS

G: Genistein, D: Daidzein, E2: 17β-oestradiol, SD: Standard Deviation, NS: not significant (p ≥ 0.05)

[1] mean percentage of cells displaying apoptotic nuclear morphology per treatment

[2] significant differences compared to cells treated with vehicle only (0.1% DMSO)

3.3.1..4 The effect of combined isoflavones and E2 on MCF7 apoptotic nuclear morphology

The results for the effect of combinations of isoflavones at physiological concentrations with pre- or postmenopausal E2 levels on apoptotic nuclear morphology in MCF7 breast cancer cells are described in Figure 3.22 and Table 3.9.

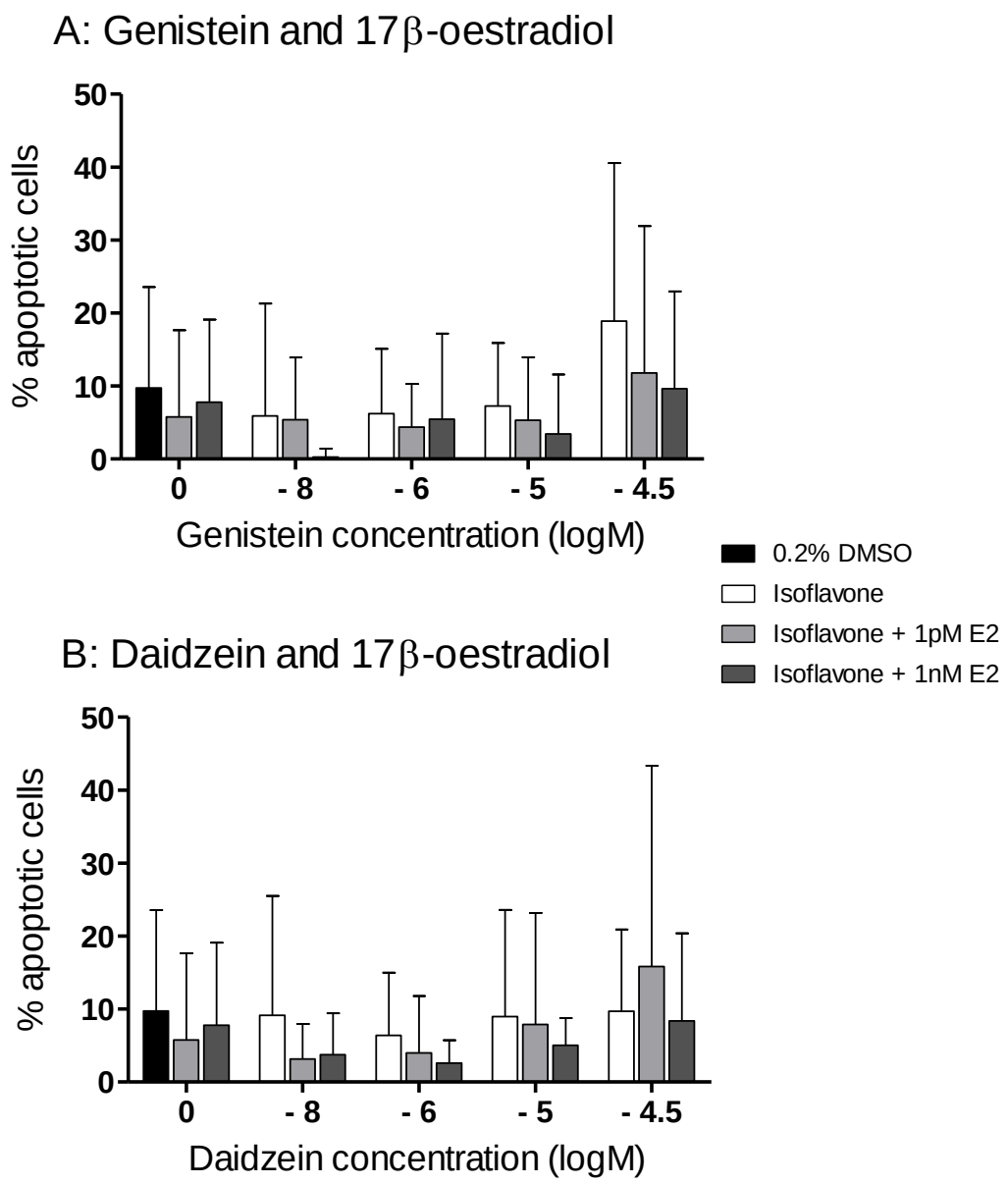

Figure 3.22: The effect of combinations of isoflavones and 17β-oestradiol on apoptotic nuclear morphology in MCF7

MCF7 cells were prepared as described. After 48 hours the medium was replaced with fresh oestrogen free medium with 0.2% DMSO, 1nM or 1pM E2 with or without genistein (A) or daidzein (B) at (0.01, 1, 10 and 31.6μM). Induction of apoptosis was quantified by percentage of apoptotic cells after DAPI staining, and results presented as mean + SD for each treatment (n=3). There were no significant variations ($p < 0.05$) between any results.

Table 3.9: Results for the percentage of MCF7 cells displaying apoptotic nuclear morphology after treatment with combinations of isoflavones and 17β-oestradiol

Treatment	mean %	SD	Significance (p) compared to:			
			0.2% DMSO	1nM E2	1pM E2	corresponding ISF alone
1pM E2 10nM D	3.17	4.82	NS	-	NS	NS
1pM E2 1μM D	3.98	7.80	NS	-	NS	NS
1pM E2 10μM D	7.88	15.29	NS	-	NS	NS
1pM E2 31.6μM D	15.87	27.48	NS	-	0.075	NS
1nM E2 10nM D	3.73	5.68	NS	NS	-	NS
1nM E2 1μM D	2.62	3.11	NS	NS	-	NS
1nM E2 10μM D	5.05	3.74	NS	NS	-	NS
1nM E2 31.6μM D	8.40	12.00	NS	NS	-	NS
1pM E2 10nM G	5.38	8.54	NS	-	NS	NS
1pM E2 1μM G	4.37	5.92	NS	-	NS	NS
1pM E2 10μM G	5.29	8.66	NS	-	NS	NS
1pM E2 31.6μM G	11.80	20.10	NS	-	NS	NS
1nM E2 10nM G	0.28	1.14	NS	NS	-	NS
1nM E2 1μM G	5.50	11.71	NS	NS	-	NS
1nM E2 10μM G	3.43	8.14	NS	NS	-	NS
1nM E2 31.6μM G	9.61	13.37	NS	NS	-	NS

G: Genistein, D: Daidzein, E2: 17β-oestradiol, SD: Standard Deviation, ISF: Isoflavone, NS: not significant (p ≥ 0.05)

None of the combination isoflavone/E2 treatments differed significantly from the 0.2% DMSO control, or the relevant single concentrations of isoflavone or E2 with regard to the percentage of cells displaying apoptotic nuclear morphologies. As with the single isoflavone treatments, the combinations of the highest concentration of genistein and daidzein used (31.6μM) with 1pM or 1nM E2 tended to induce a slightly greater percentage of apoptotic cells compared to the control, and the combination of 1pM E2 / 31.6μM daidzein approached a significant difference from the E2 alone treatment (p = 0.075).

3.3.2 MDA-MB-231 DAPI apoptosis results

3.3.2..1 Effect of control treatments on MDA-MB-231 nuclear morphology

DMSO up to 0.2% had no significant effect on the percentage of MDA-MB-231 cells displaying apoptotic nuclear morphology after DAPI staining (Figure 3.23). Representative images of this treatment are shown in Figure 3.24.

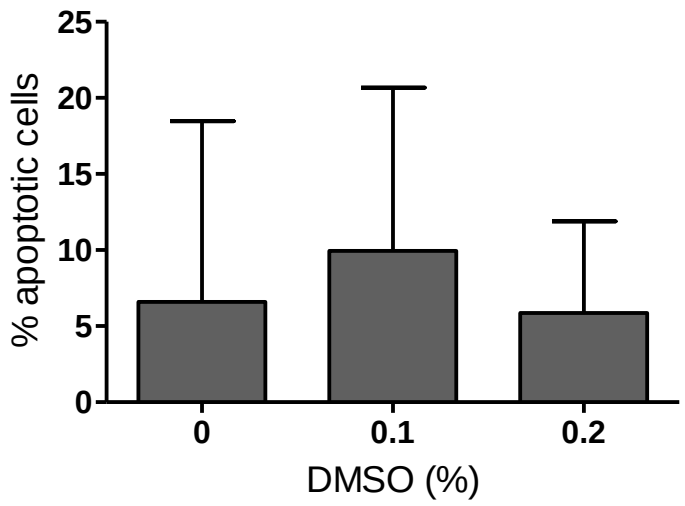

Figure 3.23: Effect of DMSO on the percentage of MDA-MB-231 cells displaying apoptotic nuclear morphology

MDA-MB-231 cells were prepared as described. Following this, medium was replaced with fresh oestrogen-free medium with no additions, 0.1 or 0.2% DMSO. Induction of apoptosis was quantified by calculating the % of apoptotic cells after DAPI staining. Results are presented as mean and SD for each treatment (n=3). There were no significant variations ($p < 0.05$) in results.

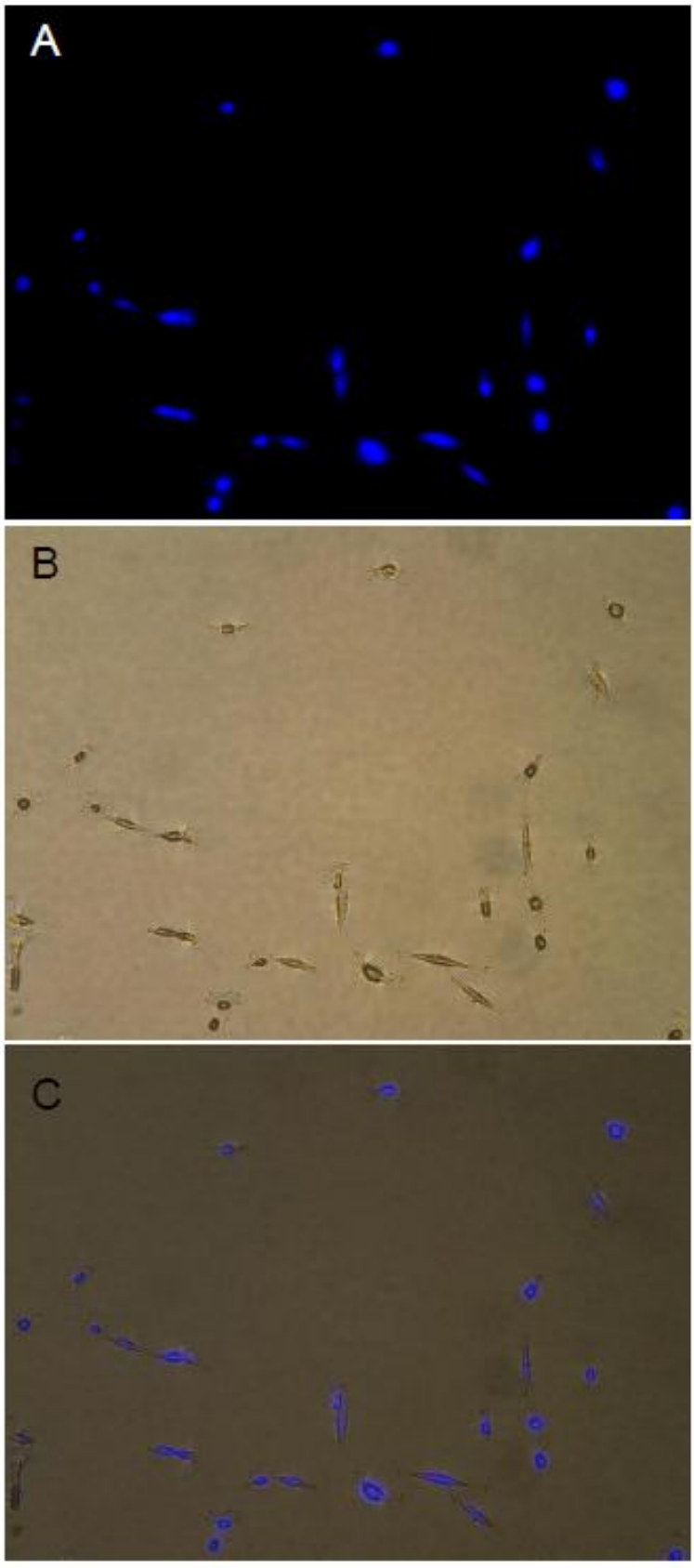

Figure 3.24: MDA-MB-231 treated with 0.1% DMSO

Representative images of MDA-MB-231 cells treated as described with 0.1% DMSO. A: DAPI fluorescent image, B: bright field, C: composite. No evidence of apoptotic nuclear changes and cells maintain elongated shapes indicative of normal growth.

3.3.2..2 The effect of 17β-oestradiol on nuclear apoptotic morphology in MDA-MB-231 cells

The results for the impact of E2 at physiological concentrations on the percentage of MDA-MB-231 cells displaying apoptotic nuclear morphology are displayed in Figure 3.25 and in Table 3.10. Although these treatments had very little impact, there was a slight trend towards increasing induction of apoptosis with increasing E2 concentration.

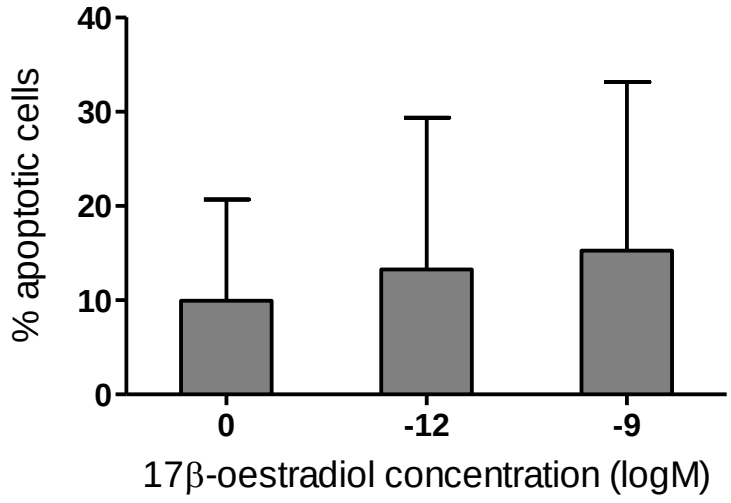

Figure 3.25: The impact of E2 on apoptotic nuclear morphology in MDA-MB-231 cells

MDA-MB-231 cells were prepared as described. Following this, medium was replaced with fresh oestrogen-free medium with vehicle only or 17β-oestradiol at pre- and post-menopausal concentrations (1 x 10^{-9}M and 1 x 10^{-12}M respectively). Levels of apoptosis were quantified after DAPI staining, by calculation percentage of cells displaying apoptotic nuclear morphology and results presented as mean and SD for each treatment (n=3). There were no significant variations from the vehicle-only control ($p < 0.05$).

3.3.2..3 Isoflavones induce apoptotic nuclear morphology in MDA-MB-231

Sample images of this cell line after treatment with 1nM and 31.6μM genistein are provided (Figure 3.26 and Figure 3.27). The results showing the percentage of

MDA-MB-231 cells displaying apoptotic nuclear morphology after three hour treatment with isoflavones are displayed in Table 3.10 and Figure 3.28. Treatment for three hours with isoflavones resulted in a trend towards increasing levels of apoptotic nuclear morphology in this cell type, at all concentrations tested. This achieves statistical significance with 31.6µM genistein ($p < 0.01$) and 10nM daidzein ($p < 0.001$). In addition, the increase seen after 31.6µM daidzein treatment approached significance ($p = 0.09$). With genistein treatment, there is a slight dose effect.

Table 3.10: Full results showing the effect of single isoflavone and 17β-oestradiol treatments on the induction of apoptotic nuclear morphology in MDA-MB-231 cells

Treatment	% apoptosis	SD	P[1]
Untreated	6.59	11.87	NS
0.1% DMSO	9.94	10.74	-
0.2% DMSO	5.87	6.02	NS
1pM E2	13.25	16.11	NS
1nM E2	15.25	17.88	NS
10nM G	15.68	18.88	NS
1µM G	12.17	12.88	NS
10µM G	17.78	16.21	NS
31µM G	23.46	23.05	<0.01
10nM D	28.61	24.89	<0.001
1µM D	18.43	17.86	NS
10µM D	18.53	19.52	NS
31.6µM D	21.44	21.04	0.09

G: Genistein, D: Daidzein, E2: 17β-oestradiol, SD: Standard Deviation, NS: not significant ($p \geq 0.05$)

[1] *Significance of difference compared to 0.1% DMSO*

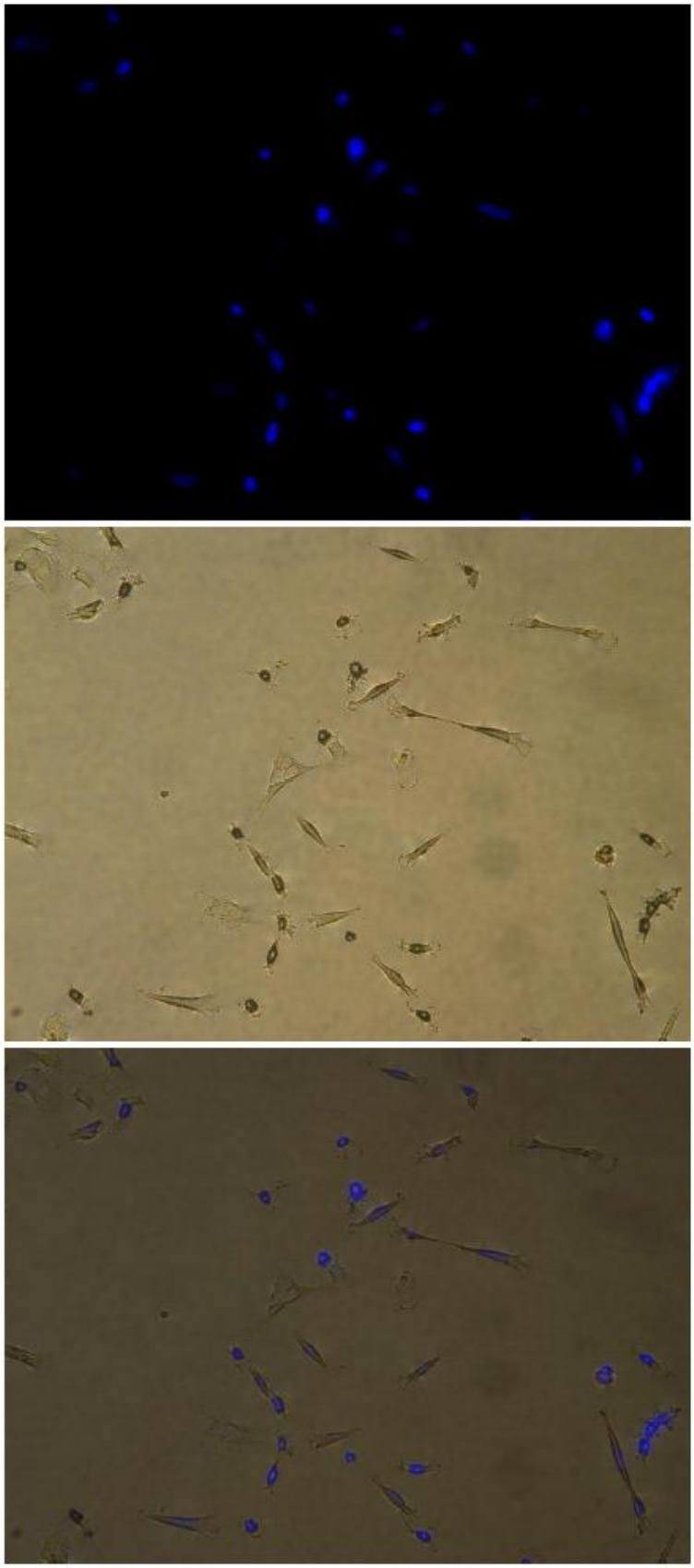

Figure 3.26: MDA-MB-231 cells treated with 10nM genistein

Representative images of MDA-MB-231 cells treated as described with 10nM genistein. A: DAPI fluorescent image, B: bright field, C: composite. No evidence of apoptotic nuclear morphology, and cells show characteristic elongated shape indicative of normal growth.

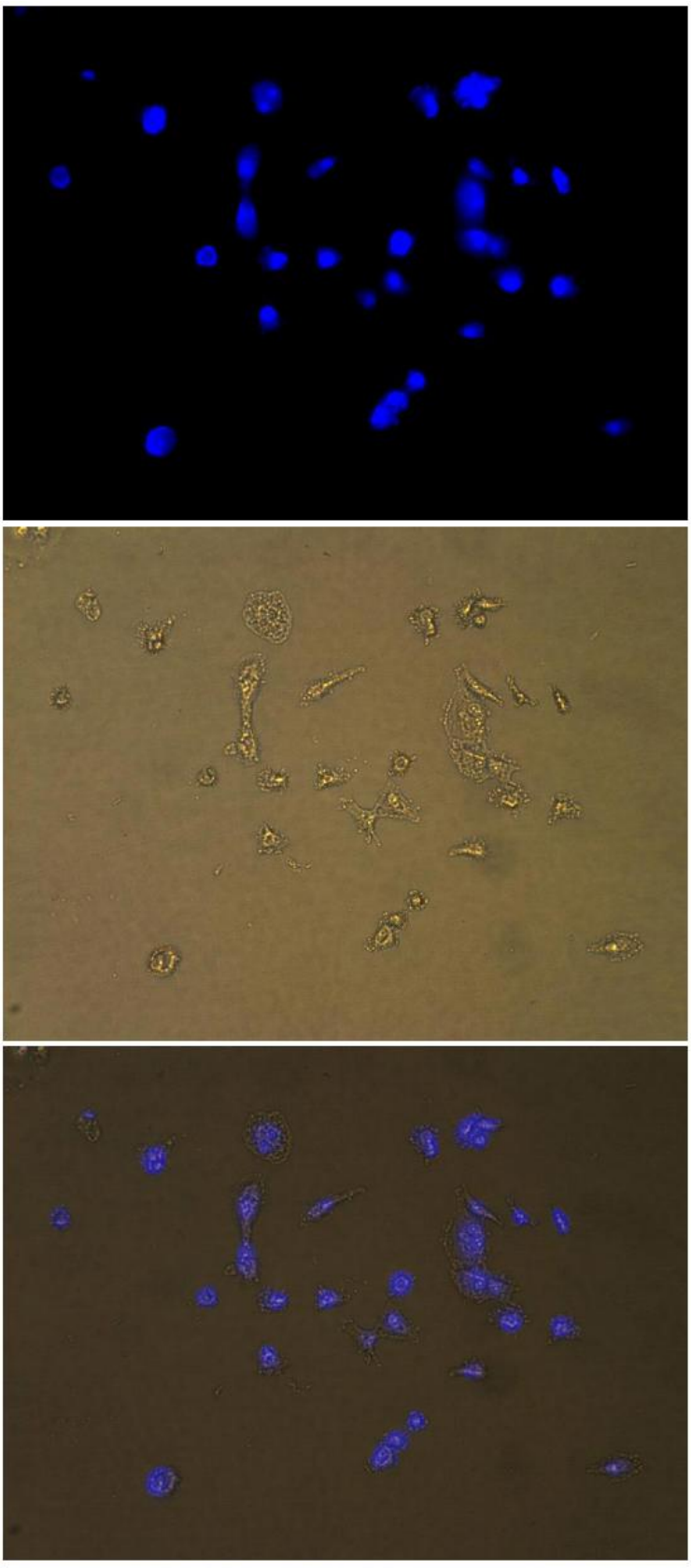

Figure 3.27: MDA-MB-231 cells treated with 31.6μM genistein

Representative images of MDA-MB-231 cells treated as described with 31.6μM genistein. A: DAPI fluorescent image, B: bright field, C: composite. There is evidence of apoptotic nuclear fragmentation, resulting in irregular nuclear forms, and nuclear condensation. Blebbing of the plasma membrane is also apparent.

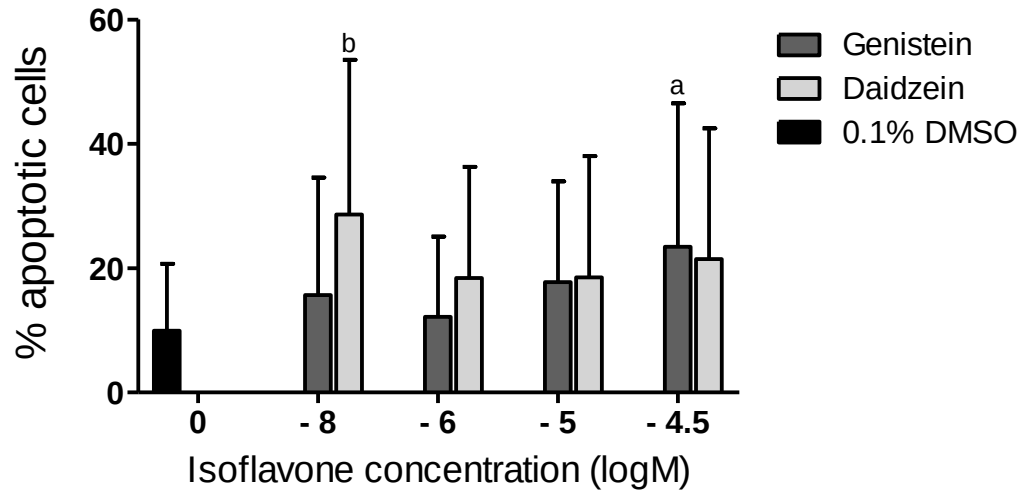

Figure 3.28: The effect of isoflavones on apoptosis in MDA-MB-231 cells

MDA-MB-231 cells were prepared as described. Medium was replaced with fresh oestrogen free medium with 0.1% DMSO, or genistein or daidzein at 0.01, 1, 10 and 31.6μM. Induction of apoptosis was quantified by calculating the percentage of cells displaying apoptotic morphology after DAPI staining, and results presented as mean and SD for each treatment (n=3). Where results differed significantly from the vehicle-only control this is indicated by a *(p < 0.01) or b (p < 0.001).*

3.3.2..4 The combination of isoflavones and 17β-oestradiol induces apoptotic nuclear morphology in MDA-MB-231

A representative image of these cells treated with 1nM E2 and 31.6μM genistein is provided in Figure 3.29. The results for the effect of combinations of isoflavones at physiological concentrations with pre- or postmenopausal E2 on the percentage of cells displaying apoptotic nuclear morphology in MDA-MB-231 breast cancer cells are described in Figure 3.30 and Table 3.11. As with the single isoflavone treatments in this cell line, the combined E2/isoflavone treatments show a trend towards an increase in the level of apoptotic nuclear morphology apparent after three hours, with a number of these being significantly higher than the control value (see Table 3.11).

Several of the combined treatments also induced significantly greater levels of apoptosis than the relevant single E2 treatments. These were daidzein at 31.6μM with both E2 concentrations, and 31.6μM genistein with 1pM E2 ($p < 0.001$ for each), and the combination of 10μM genistein with 1pM E2 ($p < 0.05$). In addition, a number of the combined treatments also induced a greater level of apoptosis than the relevant isoflavone alone (largely the same combinations as above; see table 3.11).

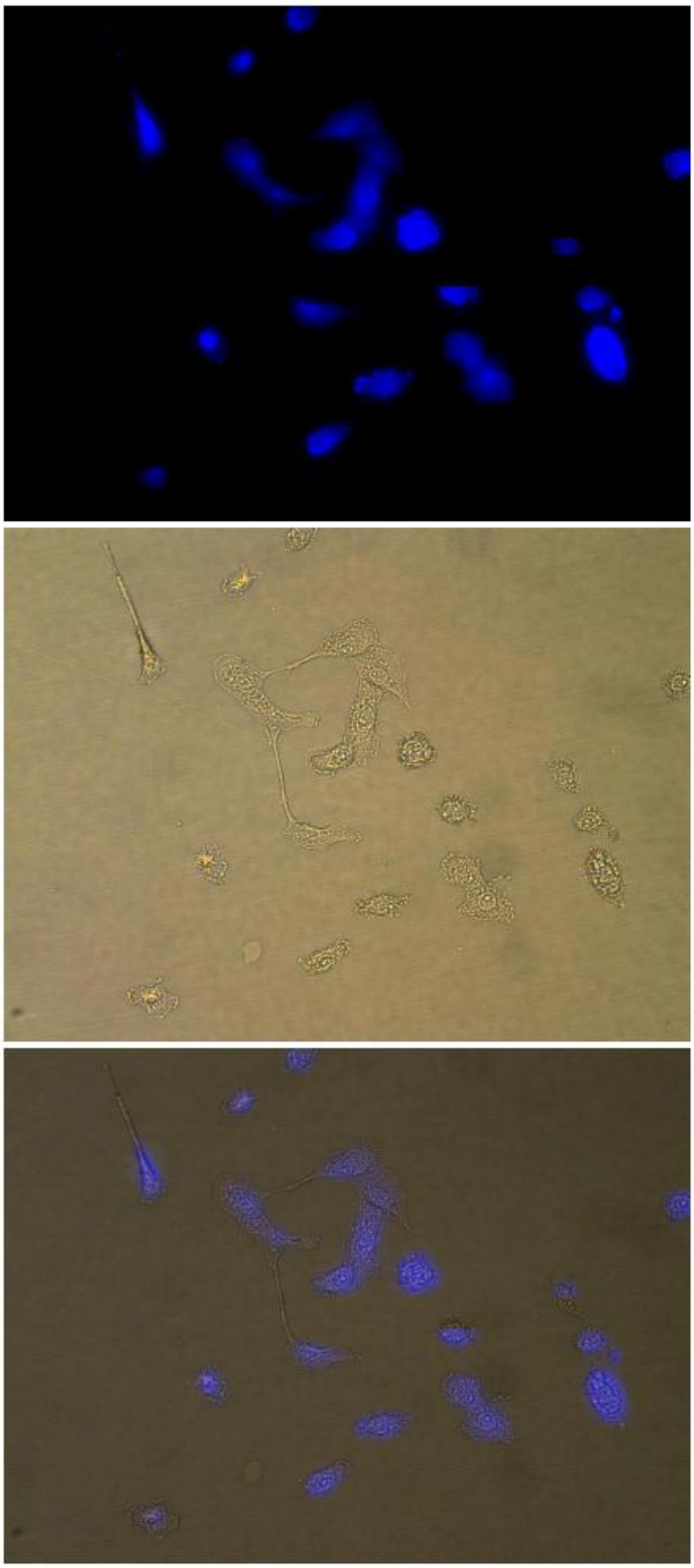

Figure 3.29: MDA-MB-231 treated with 1nM E2 and 31.6μM genistein

Representative images of MDA-MB-231 cells treated as described with a combination of 31.6μM genistein and 1nM E2. A: DAPI fluorescent image, B: bright field, C: composite. Apoptotic nuclear condensation and fragmentation are apparent, resulting in irregular nuclear forms. Plasma membrane blebs are evident on some cells, indicating apoptosis.

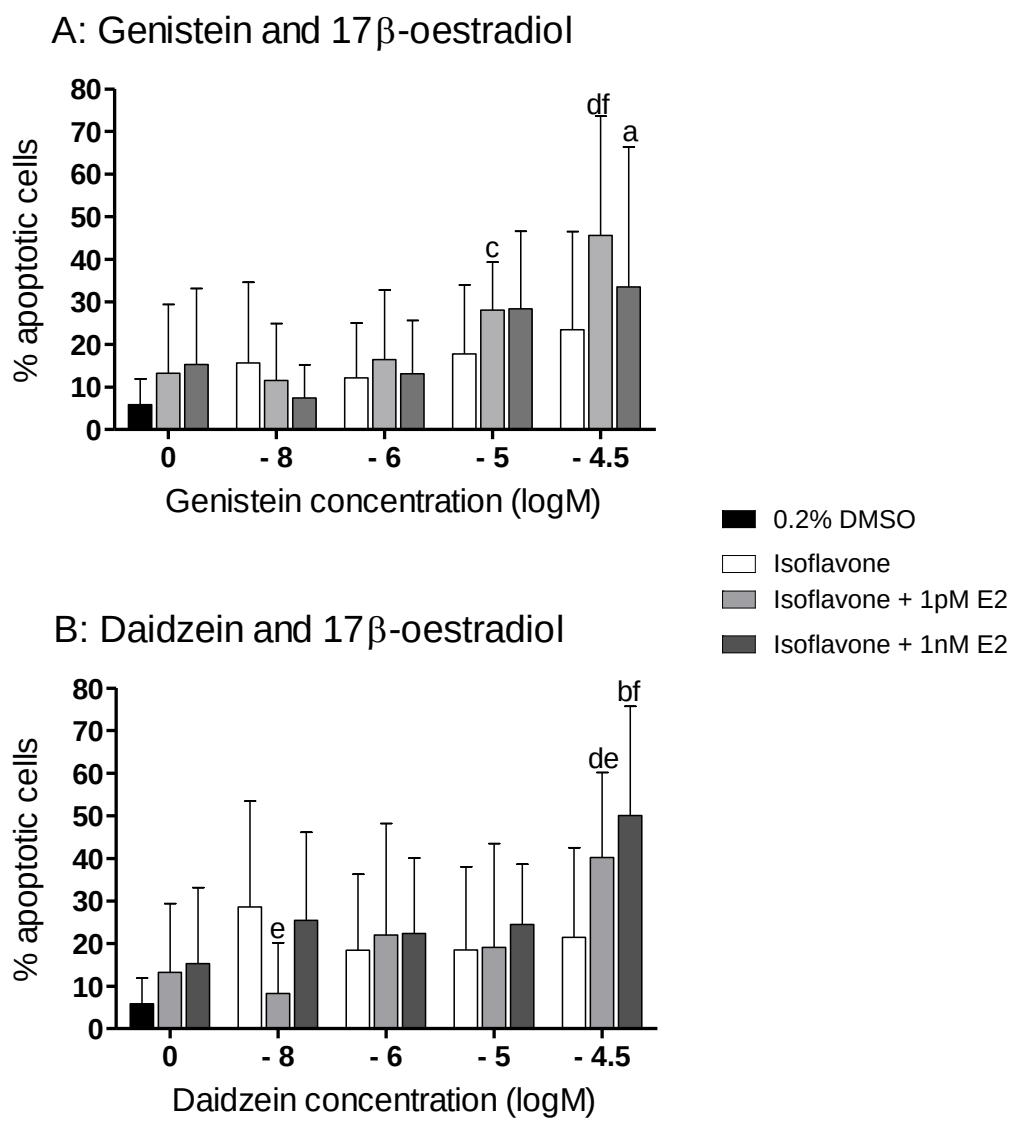

Figure 3.30: The effect of combinations of isoflavones and 17β-oestradiol on apoptosis in MDA-MB-231 cells

MDA-MB-231 cells were seeded as described. After 48 hours, the medium was replaced with fresh oestrogen free medium with 0.2% DMSO, 1nM or 1pM E2 with or without genistein (A) or daidzein (B) at (0.01, 1, 10 and 31.6μM). Induction of apoptosis was quantified by calculation of the percentage of cells displaying visible signs of apoptotic nuclear morphology after DAPI staining, and results presented as mean and SD for each treatment (n=3). Significant variation from the 1nM E2-alone treatment is indicated by a *($p < 0.05$) and b ($p < 0.001$), and from the 1pM E2-alone treatment by c ($p < 0.05$) and d ($p < 0.001$). Significant variation from the relevant isoflavone-alone treatment is indicated by e ($p < 0.05$) and f ($p < 0.001$).*

Table 3.11: Full results for isoflavone/17β-oestradiol combinations on the induction of apoptotic nuclear morphology in MDA-MB-231 breast cancer cells

Treatment	mean % apoptosis	SD	Significance (p) compared to:			
			0.2% DMSO	1nM E2	1pM E2	corresponding isoflavone alone
1pM E2 10nM D	8.30	11.90	NS		NS	<0.05
1pM E2 1μM D	22.01	26.16	NS		NS	NS
1pM E2 10μM D	19.14	24.34	NS		NS	NS
1pM E2 31.6μM D	40.21	19.96	<0.001		<0.001	<0.05
1nM E2 10nM D	25.46	20.72	<0.05	NS		NS
1nM E2 1μM D	22.40	17.64	NS	NS		NS
1nM E2 10μM D	24.49	14.17	<0.05	NS		NS
1nM E2 31.6μM D	50.10	25.59	<0.001	<0.001		<0.001
1pM E2 10nM G	11.54	13.36	NS		NS	NS
1pM E2 1μM G	16.43	16.35	NS		NS	NS
1pM E2 10μM G	28.08	11.21	<0.001		<0.05	NS
1pM E2 31.6μM G	45.61	27.99	<0.001		<0.001	<0.001
1nM E2 10nM G	7.41	7.80	NS	NS		NS
1nM E2 1μM G	13.13	12.49	NS	NS		NS
1nM E2 10μM G	28.32	18.28	<0.01	NS		NS
1nM E2 31.6μM G	33.51	32.93	<0.001	NS		NS

G: Genistein, D: Daidzein, E2: 17β-oestradiol, SD: Standard Deviation, NS: not significant ($p \geq 0.05$)

3.4 Summary of the effects of soy isoflavones on proliferation and apoptosis in MCF7 and MDA-MB-231 cells

This section briefly summarises the impact of genistein and daidzein, in the presence and absence or premenopausal and postmenopausal E2 levels, on the proliferation and apoptosis outcomes measured here in MCF7 and MDA-MB-231 breast cancer cells. For a full discussion of these results see sections 6.1 and 6.2.

3.4.1 MCF7

The MTT proliferation results confirm the biphasic effect of isoflavones on this cell line that was expected. Maximal proliferation was achieved between 1 and 10μM for both isoflavones, and was similar in magnitude to that observed after E2 treatment, although approximately 1000-fold greater isoflavone concentrations were required for a comparable effect. Genistein was slightly more effective at promoting proliferation than daidzein, as evidenced by their EC_{50} concentrations. This confirms the validity of the growth conditions used and suggests that the cell line is behaving as expected, and has not experienced genetic drift or contamination. In each case, a higher concentration of isoflavone would be required (outwith the physiological range) to inhibit proliferation.

The combined isoflavone/E2 treatments at both premenopausal (1nM) and postmenopausal (1pM) levels resulted in very high rates of proliferation in MCF7. Numerically, the evidence for an additive effect for isoflavones and the postmenopausal E2 dose is strong. This suggests a synergistic effect on proliferation rather that the protective mechanism hypothesised. Some synergy remains between the isoflavones and the higher premenopausal E2 dose, although the effect is less striking.

Both measures of apoptosis used suggested that premenopausal and postmenopausal E2 levels had no effect on the induction of apoptosis in MCF7. However, physiological levels of genistein and daidzein, particularly at the higher concentrations tested, did result in an increase in the percentage of apoptotic cells both externalising PS and displaying distinctive apoptotic nuclear morphology. The characteristics of this response differ according to the analysis method used. Either

way, this increase in the induction of apoptosis seen especially with the higher concentrations may relate to the decrease in proliferation observed with the highest isoflavone concentrations.

The impacts of the combined isoflavone/E2 treatments on the induction of apoptosis were largely similar to that seen with the single isoflavone treatments, regardless of assay method. This is perhaps unsurprising since in both cases E2 was found to have little effect on apoptosis.

3.4.2 MDA-MB-231

As expected, premenopausal and postmenopausal E2, and the single isoflavone treatments up to and including 10μM all resulted in a trend towards inhibition of MDA-MB-231 proliferation compared to the control treatment. There was no dose effect apparent. As with the MCF7 cells, this confirms that the conditions used are valid for the experiments to follow, and suggests that the cell line has not experienced genetic drift or contamination with other cells. The highest concentrations of genistein and daidzein used resulted in a sharp drop in proliferation to around 50% of control levels.

The addition of E2 to the isoflavones seemed to largely abrogate the inhibitory effect of the lower concentrations, although the drop seen at the highest isoflavone concentration was still apparent. The exception to this was the combination of daidzein and postmenopausal E2, which was particularly effective at inhibiting proliferation. As the level of solvent used in these latter experiments (0.2% DMSO) was found to have a slight inhibitory effect on MDA–MB-231 proliferation itself, it is possible that this confounds or masks the results slightly, and must be considered in this context.

Both methods of assessing the induction of apoptosis agree that E2 had very little impact upon the induction of apoptosis in MDA-MB-231 cells. However, the isoflavones at all single concentrations tested result in a slight increase in the percentage of apoptotic cells, which achieved significance on several occasions. No dose effects were observed. This corresponds with the inhibition of proliferation seen and may suggest a mechanism.

The combinations of E2 and isoflavones were not assessed by the Annexin V-Cy3 method. However, the DAPI assay suggests that the addition of E2 does not prevent the isoflavone-induced induction of apoptosis observed, and indeed hints at a possible synergistic effect with the higher isoflavone concentrations.

CHAPTER 4. Methods: volume regulation and potassium channel activity

The impact of physiological levels of isoflavones and E2 on MCF7 volume regulation and macroscopic voltage gated K^+ channel activity was assessed. Volume changes were measured using the calcein volume change assay (section 1.6.2..5), and the whole cell patch clamping technique was used to identify and analyse macroscopic K^+ currents (section 1.6.2..1). Measuring changes in fluorescence intensity is one of several standard and sensitive techniques used to infer volume change in cultured cells. Whole cell patch clamping is the "gold standard" technique with which to assess the characteristics of ion channels under physiological membrane potential conditions. In addition, the MTT assay (described previously; section 2.4) was used to assess the role of these K^+ channels in general, and several specific channels, on the proliferation of MCF7 breast cancer cells.

These experiments were conducted with MCF7 cells only, and not the MDA-MB-231 cell line. This was partly due to time constraints, but also because very little is known regarding the types and activities of K^+ channels in the MDA-MB-231 cell line (consequently no data exists to compare any results with).

4.1 Calcein cell volume assay

4.1.1 Background to method

Isoflavones are known to inhibit RVD in numerous cell types (Section 1.6.8..2), but this is a response to non-physiological environmental changes. Whether they directly modulate cell volume over the short term in MCF7 is not known. This may relate to their ability to regulate proliferation or apoptosis (see Chapter 3), either as a regulatory mechanism or as a downstream effect. Here, acute changes in MCF7 volume were assessed over 30 minutes (the maximum time period during which the cells remained viable) during treatment with genistein or E2 by measuring the changes in intensity of intracellular calcein fluorescence, in a method initially described by Crowe et al. (1995), and used recently by Chen et al. (2011) to assess volume changes in lung adenocarcinoma cells (SPC-A1). Volume changes have been measured in MCF7 previously (Roy et al. 2008; vanTol et al. 2007), although not by this method. Both groups used a similar process of light microscopy, digital photography, and analysis of the area of the cell based on the radius measured. However, this method is based on the assumption that the cells are spherical, which is rarely the case.

After a two day oestrogen washout, the cells were loaded with the dye in its membrane permeable ester (AM) form. Once internalized, intracellular esterases remove the acetomethoxy group, and the molecule becomes trapped within the cell. Upon hydrolysis, calcein fluoresces green. Prior to experimentation, the absorption wavelength of 480nm was determined to be optimal, and was used throughout. Emission peaked at 515nm. Once the remaining extracellular dye was washed away, the quantity of calcein within the cells remained relatively constant over the short term (up to approximately 45 minutes; data not shown). Fluorescence intensity varied directly with dye concentration (and cell volume), and so acted as a marker for cell size.

In accordance with standard procedures, these experiments were conducted at 37^{o}C. Volume regulation is known to occur at measurable levels in MCF7 at both this and room temperature, but the magnitude of the response is greater at the higher temperature (vanTol et al. 2007).

4.1.2 Preparation of solutions

Normal Tyrode (NT)

The following were dissolved in 1l deionised water: NaCl (Fisher Scientific; 7.831g, 134mM), KCl (Sigma; 0.447g, 6mM), $MgCl_2.6H_2O$ (Sigma; 1mM), $CaCl_2.6H_2O$ (Sigma; 1mM) and HEPES (Sigma; 2.383g, 10mM). This was titrated to pH 7.4 at 37^oC with 4M NaOH (Fisher Scientific; approximately 1.29ml was required for 1l buffer), and stored at 4^oC. Glucose (Sigma; 10mM, 180mg per 100ml) was added immediately prior to use.

Zero Sodium Tyrode

The following were dissolved in 1l deionized water: $MgCl_2.6H_2O$ (1mM), $CaCl_2.6H_2O$ (1mM) and HEPES (2.383g, 10mM). This was titrated to pH 7.4 at 37^oC with 4M KOH (BDH Prolabo; approximately 1.29ml was required for 1l buffer). This was stored at 4^oC.

Hyposmotic buffer (50% Na Tyrode)

This was prepared by mixing 50% each of the NT and zero sodium Tyrodes, and was also stored at 4^oC. Again, glucose (10mM, 180mg per 100ml) was added immediately prior to use.

Test Tyrodes

To 100ml NT, glucose (180mg) and 100µl of DMSO (0.1%) or the appropriate stock concentration of genistein or E2 (also in DMSO) were added (i.e. to prepare 100ml of 1nM E2 Tyrode, 100µl of $1x10^{-6}$M E2 was added to 100ml NT). In each case 0.1% DMSO was present. This was stored for a maximum of 4 days at 4^oC.

Calcein-AM stock

A 1mM stock of calcein-AM (Molecular Probes) was prepared in DMSO, and stored in the dark at -20^oC.

4.1.3 Calcein volume change protocol

MCF7 cells were seeded in six well plates (Greiner) on 10mm sterile glass cover slips (Agar Scientific). Prior to placing in the wells, the cover slips were sterilised by autoclaving (121^{o}C for 15 minutes). The cells were seeded at an initial density of 1x10^{5} cells per well, in 3ml of experimental medium. This was returned to the incubator for 48 hours to allow the cells to grow and adhere, and for the washout of any oestrogenic compounds.

Following this, sterile conditions were no longer required, and all reagents were warmed to 37^{o}C prior to use.

4.1.3..1 Calcein loading

After incubation, the medium was removed, and cells were washed twice gently with 1ml NT. Fresh NT was added (1ml) along with 5µl of 1mM calcein-AM stock (final calcein concentration 5µM). This is well below the concentrations which would trigger calcein self-quenching (section 1.6.2..5). The dye was allowed to load for 1 hour, incubated in the dark at 37^{o}C. Following this, any dye not taken up by the cells was removed by washing three times each with 1ml NT, and 1ml fresh NT was added to the well. Intracellular calcein-AM was allowed to esterify to calcein during a further 30 minute incubation period (37^{o}C in the dark) as per standard proceedures (Pan et al. 2007).

4.1.3..2 Perfusion and measurement of fluorescence

The perfusion and assessment of fluorescence intensity was carried out using a Cairn Optoscan Monochromator (Cairn Research Ltd., Kent) mounted to an inverted microscope (Olympus, OM-2; Japan). Perfusion of the cells with various Tyrodes was carried out by a peristaltic pump (Gilson Minipuls 3) and in-line thermostatically controlled stage heating system (Warner Instrument Corporation, TC-324B). This was calibrated prior to use to maintain a constant flow rate and temperature of 1ml/min and 37^{o}C. Images were captured at a rate of two per second using a digital camera (Hamamatsu C4742-95), which was controlled, along with the excitation wavelength (480nm) and bandwidth (10nm), by WinFluor software (V.3.0.8, John Dempster, University of Strathclyde Electrophysiology Software).

Prior to the addition of cells, the microscope chamber was flushed with pre-warmed NT for at least five minutes, to allow the temperature of the NT in the dish to reach 37^{o}C. Once this was achieved, a coverslip of loaded cells was removed gently from its well with watchmaker's forceps, and placed (cell side up) on the bottom of the microscope chamber. Using the forceps, the plate was carefully pressed to the bottom of the dish, so that capillary suction would hold it in place. Cells were visualized by light microscopy (magnification x100) to find an appropriate region of the coverslip to assess, with sufficient cells which were not densely packed and so able to change in volume freely. The microscope light was then switched off and the equipment curtained off with black curtains to prevent extraneous light "noise" affecting the image.

The cells were illuminated with the excitation light (480nm) and light emitted at >515nm was collected by the microscope dichroic and filter system (Omega XF2058) and transmitted to the camera. Regions of interest (ROIs) in the live image were monitored using the software to show gross changes and confirm that the intensity of fluorescence was stable prior to analysis, but this data was discarded, and not used for the later analysis.

Once fluorescence with NT perfusion had stabilized, recording was initiated. Solutions were perfused over the cells as described below. The system has an approximate lag time of two minutes due to the physical dead volume of the tubing, from changing a solution to it reaching the cells. This was considered when analyzing the results. Once the end of a protocol was reached, the coverslip was discarded and the perfusion system flushed before re-use.

At an early stage, as with pervious fluorescence protocols (Annexin optimisation Section 2.5.3), cell auto-fluorescence was assessed and determined to have negligible effect (i.e. was the same as the background of a cell-free area of the coverslip).

4.1.3..3 Image analysis

Images were analysed using ImageJ software (NIH: Version 1.44). Files containing every third frame or more were too large for ImageJ to process. Mean fluorescence intensity from a three minute interval of an image set of MCF7 cells (n = 3 cells: the

same ones were selected on each occasion) was compared following the export and analysis of every 4th, 6th, 8th and 10th frame (Figure 4.1).

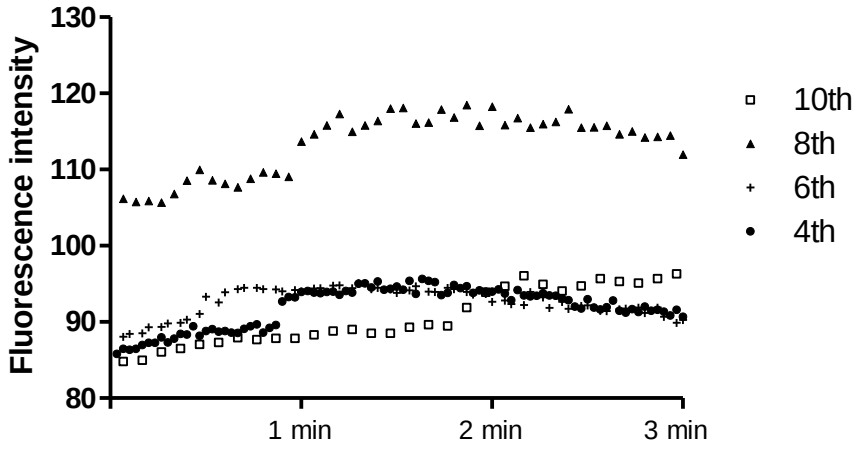

Figure 4.1: Comparison of results after exporting every 'n'th frame

MCF7 cells were prepared and assessed for calcein fluorescence as described. The mean fluorescence intensity of the same three cells over a three minute interval (minus background) was determined using ImageJ after the export and analysis of every 10th, 8th, 6th and 4th frame, as indicated.

The results from every 4th, 6th and 8th frame followed a similar pattern, which was not apparent after the export of every 10th frame. Why the results obtained after the export of every 8th frame were higher than the other sets of data is not known, although it is possible that slightly different regions of the cells were selected for analysis, resulting in greater mean fluorescence intensity. Based on this the export and analysis of every 8th frame into ImageJ was deemed appropriate.

Each file was assessed as an 8 bit greyscale image. Circular ROIs were chosen in the centre of at least ten cells, and a further one in an area of cell-free background (Figure 4.2). Cells were excluded from the analysis on the basis of being cropped by the edge of the image, death or dislodgement from the cover slip prior to the end of the recording, or excessive movement excluding the possibility of finding a constant region within the cell.

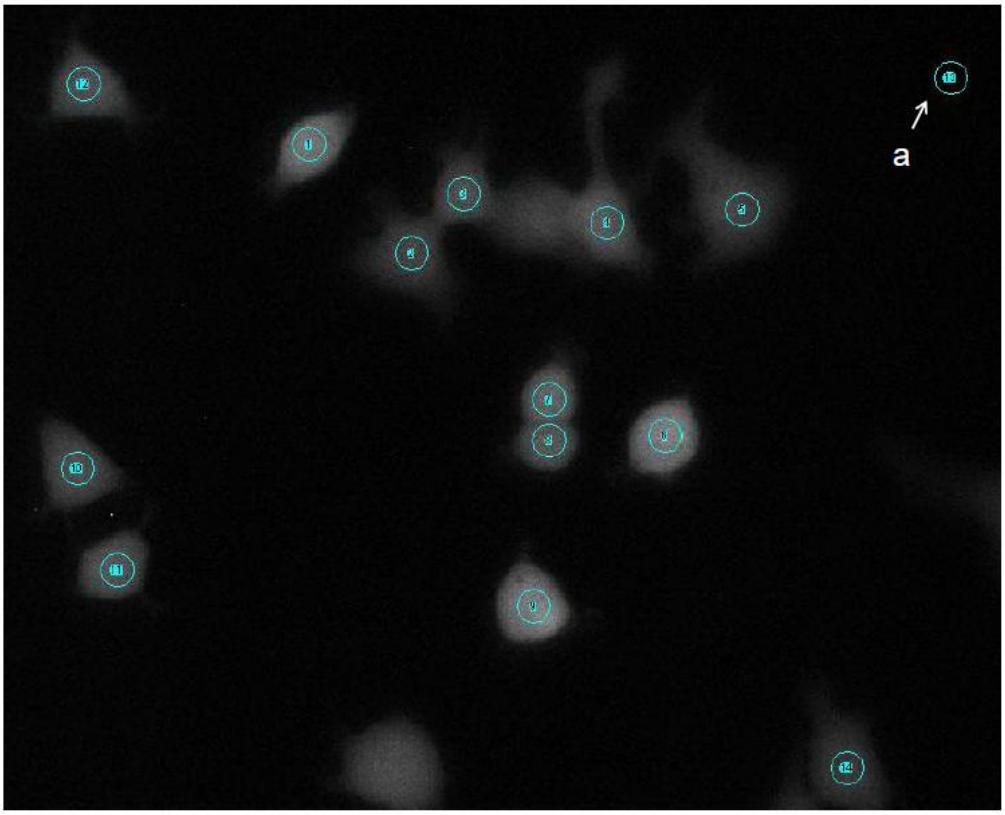

Figure 4.2: Representative image of calcein-loaded MCF7 cells

ImageJ analysis of MCF7 cells. ROIs (indicated) are selected inside cells which meet the criteria, ensuring that they remain within the cell as the image series progresses. A cell-free background ROI (a) is also selected.

The background value was subtracted from the cell values at each time point. Following this, ImageJ was used to calculate the fluorescence intensity (mean grey value; arbitrary units from 0 to 255) in each selected cell region, every four seconds (from every 8th frame) for the duration of the experiment. For each treatment, this procedure was repeated on three independent occasions, on different days and with different cell preparations, so that n = 3, and includes data from at least 30 cells. Data is presented as a graph of the mean fluorescence intensity over time.

To determine the rate of change of fluorescence intensity (Δf per second), and thus the rate of cell swelling or shrinkage, for each cell the slope of the line between two points (indicated) was determined by linear regression using Graphpad Prism software (Graphpad Software Inc, Version 5.01, 2007). Mean slope (ratio between the change in time and the change in fluorescence) and SD were calculated, and

expressed as the rate of fluorescence intensity change per second (Δf). For the test conditions, the slope was calculated in the final two minutes of DMSO treatment (8 to 10 minutes DMSO), then at 10 to 12 minutes, and 15 to 17 minutes into the experimental treatment. These are referred to as Δf_0, Δf_{10}, and Δf_{15} respectively.

The adjusted rates of change ($a\Delta f_{10}$ and $a\Delta f_{15}$) were determined for each treatment at 10-12 and 15-17 minutes respectively to show the impact of that treatment alone, without any background or DMSO effects. This was calculated as follows:

$a\Delta f = \Delta f$(treatment) – Δf_0(same treatment)

4.1.4 Test conditions

Hyposmotic shock

MCF7 cells are known to undergo RVD rapidly after an initial swelling phase during hyposmotic shock (Roy et al. 2008; vanTol et al. 2007). This was used as a positive control to determine that the above protocol was appropriate for assessing volume changes in this cell line.

Images were captured during perfusion for 10 minutes with NT, then perfusion was switched to the hyposmotic buffer for 30 minutes, then returned to NT for 20 minutes. These time points were chosen to ensure that the full hypotonic swelling and ensuing RVD response were captured (Roy et al. 2008; vanTol et al. 2007).

17β-oestradiol and genistein

To determine the effect of E2 and genistein on MCF7 volume, the cells were perfused with these compounds following Calcein loading. Images were recorded for 5 minutes in NT, then 10 mins 0.1% DMSO so each cell acted as its own control. Following this the cells were perfused for 30 minutes with the test Tyrode (either 1nM E2, or 1 or 31.6μM genistein). If the cells remained viable following this treatment, then they were followed for a further 10 minutes in normal Tyrode to determine if the effects were reversible, but cell damage due to the UV light prevented this from occurring frequently enough to generate usable data.

4.1.5 Statistical analysis

For the hyposmotic shock data, the fluorescence values from 1 minute regions in the centre of the sections of the trace of interest were collated, and the mean and SD calculated. These were compared with each other by paired Student's t test (SPSS version 19, IBM Statistics, 2010), and significant variations (p, two tailed < 0.05) were indicated.

In addition, the Δf values were compared by paired t tests as above, and significant variations (p, two tailed < 0.05) indicated.

4.2 MTT assay: assessing the role of potassium channels in MCF7 proliferation

The activities of the VGKCs on proliferation were pharmacologically identified using broad and specific channel blockers (see Table 1.9 for more information). These comprised Tetraethyl ammonium (TEA; a non-specific K^+ channel blocker), 4-amino pyridine (4-AP; VGKC blocker), astemizole (AST; blocks hEAG and hERG channels) and dofetilide (DOF; blocks hERG).

MCF7 proliferation was assessed using the previously optimized MTT assay, as described in Section 2.4, after treating the cells with a range of concentrations of the channel blocking compounds.

4.2.1 Preparation of solutions

TEA

A stock solution of 1M TEA (Sigma) was prepared in deionised water (d.H_2O), and filtered using a 0.22 µm mixed cellulose ester (MCE) syringe filter (Millex Millipore).

4-AP

The lower concentration of 0.5M was used for the stock solution of 4-AP (Tocris Bioscience). Again this was prepared in d.H_2O and filtered as above.

AST

AST (Sigma) was dissolved to the maximum stock concentration of 50mM in sterile DMSO. This was filtered using a 0.22µm Polytetrafluoroethylene (PTFE) syringe filter (Whatman).

DOF

DOF (Sigma) would only dissolve in DMSO to the stock levels of 10mM. This was filtered using a 0.22µM PTFE syringe filter.

Serial dilutions of each compound were prepared in sterile DMSO or sterile water as appropriate. These were stored at -20^{o}C until use, and thawed at room temperature. For experimental use, 5µl of the appropriate AST or DOF stock dilution was added to 5ml of experimental medium to give the relevant channel blocker, with DMSO concentration never exceeding 0.1%. As higher final concentrations of 4-AP and TEA were required, but their solubility in water was a limiting factor, a maximum final solvent concentration of 4% was unavoidable. The impact of this change in osmolarity upon the growth of the cells was inescapable but minimal.

4.2.2 MTT assay protocol

As previously, MCF7 cells were seeded into 96 well plates at a density of 6000 cells per well in 0.2ml experimental medium, and incubated at 37^{o}C in a humidified 5% CO_2 environment. After a 24 hour period of oestrogen washout, the medium was replaced with fresh experimental medium containing a range of concentrations of the K^+ channel blockers. Care was taken to ensure that DMSO never exceeded 0.1% in any preparation. After incubation for 72 hours, the MTT assay was carried out using the protocol described (Section 2.4). Again, proliferation was expressed as the percentage of proliferation compared to the appropriate control treatment.

4.2.3 Test conditions

Controls

DMSO (0.1%) was used as the control for the AST and DOF experiments. The impact of this on the proliferation of MCF7 had been assessed previously, and was not found to affect growth.

TEA and 4-AP were dissolved in d.H_2O, containing up to a maximum of 4% of the solvent. Accordingly, a series of treatments containing from 0.1% to 4% d.H_2O were prepared, to determine the effect of this on MCF7 proliferation.

K^+ channel blockers

Cells were incubated with the following:

- TEA between 1μM and 20mM
- 4-AP between 1μM and 20mM (adjusted where necessary to contain 4% filtered d.H_2O)
- AST between 1nM and 50μM
- DOF between 1nM and 10μM

As no specific blockers of the hEAG channel were available, the combination of AST and DOF was used to pharmacologically identify the activity of this channel. That is, it was hypothesized that if an activity is prevented by AST treatment but not DOF, then it is likely to be the hEAG-blocking component of AST that is responsible in that instance.

4.2.4 Statistical analysis

AST and DOF results were compared to the 0.1% DMSO control. The TEA treatments were compared to the 2% H_2O control. To determine the effects of the 4-AP treatments the 4% H_2O control was used for comparison. The treatments containing 0.1 to 4% d.H_2O were compared to the untreated control from Section 3.1.1..1. The impact of 0.1% DMSO on MCF7 proliferation had been determined previously (Section 3.1.1..1). The significance of variation from the appropriate control treatment was determined by ANOVA (SPSS version 19, IBM Statistics, 2010) with Bonferroni *post hoc* corrections for multiple comparisons, and significant values (p, two tailed, <0.05) are indicated.

Where a compound was found to inhibit proliferation sufficiently, the IC_{50} was determined by non-linear regression using Graphpad Prism software (Graphpad Software Inc., Version 5.01, 2007).

4.3 Whole cell patch clamping to assess potassium channel physiology

4.3.1 Background to method

In parallel to this, the impact of genistein and E2 on MCF7 K^+ current was identified, by whole cell patch clamping, and preliminary attempts were made to pharmacologically identify the specific channels through which they might be acting.

Electrophysiological measurement using the patch clamping technique is the gold standard technique for measuring the characteristics of ion channels, as it allows the channels to be gated by physiologically relevant membrane potentials (Birch et al. 2004). This is particularly important as the gating (opening and closing) of numerous channels is affected by voltage. This technique is used to measure ionic currents in whole cells under a voltage clamp, in which near-perfect control of membrane potential is possible. It is routinely used to measure ion channels in virtually any cell type, including MCF7 breast cancer cells (Ouadid-Ahidouch et al. 2000; Roy et al. 2008; Sontheimer and Olsen 2007). It operates along the principle that channel activity results in changes in membrane resistance, which can be studied by measuring current at a constant (clamped) membrane voltage. In these conditions, membrane resistance is directly proportional to the current under scrutiny (Sontheimer and Olsen 2007). This is the fundamental principle of Ohm's law, dictating that the current between two points is directly proportional to the potential difference between those points, and indirectly proportional to the degree of resistance (opposition to current flow). A comprehensive discussion of this technique can be found in the Plymouth Workshop Handbook (Ogden 1994).

Ohm's law: $I = V \div R$

I = current (Amps), V = voltage / potential difference (Volts),
R = resistance (Ohms)

With cells bathed in the appropriate media and test compounds, a glass micro-pipette electrode is used to form a seal with the surface of one cell, and electrical continuity is achieved. From this point, voltage is manipulated and current continuously recorded and analysed. The whole cell patch clamp technique is most

widely used to measure macroscopic currents. It is common practice to design the composition of the bathing solution to resemble the extracellular environment that the cell would be exposed to *in vivo*, whilst reducing all ionic currents with the exception of the current of interest. Many natural toxins and pharmacological agents can be used to reduce or eliminate the activity of specific channels or a broader range of channels. This allows the isolation and assessment of specific currents (Sontheimer and Olsen 2007). It is a limitation of this technique that this treatment of the cell will result in its death, so recordings must be made quickly, within 20 minutes, before the results are affected (Coiret et al. 2007).

Firstly the K^+ channel signature of untreated MCF7 cells was measured at a range of voltages. This allowed confirmation that the system was functional and that the currents present were mostly due to K^+ flux and not other ions (Ouadid-Ahidouch et al. 2000). Following this, the effect of the non-specific K^+ channel blocker, TEA, and the VGKC blocker 4-AP on the patch clamp signature for MCF7 cells was assessed at a range of voltages, confirming the role of the VGKCs on K^+ current in these cells. Finally, the effect of the specific channel blockers for the hEAG and hERG K^+ channels on the patch clamp signature was assessed at a range of voltages. This was intended to confirm the presence of these channels in the cells studied, and also that their activity was as expected (Ouadid-Ahidouch and Ahidouch 2008). The specific activity of each channel was measured by blocking it and subtracting the resulting trace from an untreated K^+ channel signature (Cayabyab and Schlichter 2002; Ouadid-Ahidouch et al. 2000).

The next step was to investigate whether E2, genistein and daidzein influenced K^+ flux and the activities of the VGKCs, including hEAG and hERG in MCF7. As far as possible following this, the intention was to begin to elucidate which of the channels they affect. This was done by whole cell patch clamping before and after co-incubation with both the specific channel blocker and the isoflavone. If the isoflavone and the channel blocker inhibit the activity of different K^+ channels, their effects on the K^+ signature would be expected to be additive. There would be no further inhibitory effect if they both act on the same channel (Coiret et al. 2007).

The following experiments were carried out at room temperature (21 to 23^{o}C), although this is non-physiological. As discussed (section 1.6.2) the impact of this reduced temperature compared to 37^{o}C is likely to be minimal. Additionally, the use

of room temperature made these results comparable with other groups looking at K^+ current in MCF7 (Coiret et al. 2007; Ouadid-Ahidouch et al. 2000; Ouadid-Ahidouch et al. 2004b), and it reduces the potential for electrical interference from the heating equipment.

This was a complex, multistage procedure, with a number of steps built in to ensure the standardization of the settings used and measurements taken throughout. The stages were carried out in the order described in Sections 4.3.3 and 4.3.4.

4.3.2 Preparation of solutions

Normal Tyrode buffer

Extracellular solution, described in section 4.1.2.

Intracellular / pipette solution

This was intended to match the intracellular environment as closely as possible in terms of the concentration of the main ions present. The following were dissolved in d.H_2O: KCl (150mM), HEPES (10mM), EGTA (Sigma; 0.1mM), $MgCl_2$ (2mM). It was the titrated to pH7.2 with 4M KOH at room temperature.

Test Tyrodes

As required, appropriate quantities of K^+ channel blocker solutions, genistein, E2 or DMSO were added to the perfusing NT buffer. DMSO concentration never exceeded 0.1%.

4.3.3 Whole cell patch clamp protocol

4.3.3..1 Optimisation of seeding conditions

Seeding density and duration of incubation were optimized prior to experimentation to allow sufficient cells in each dish whilst avoiding the cells reaching confluence, or becoming too densely packed to select individual target cells. Densities between $1x10^4$ and $1x10^6$ cells per dish were assessed visually after 24 and 48 hours growth (data not shown). An optimal density of $1x10^5$ cells per dish was selected.

4.3.3..2 Preparation of cells

For whole cell patch clamping, MCF7 cells were seeded at a density of $1x10^5$ cells per dish in experimental media in individual glass bottomed ethanol sterilised 35mm dishes. Each dish contained 2ml media. The cells were then incubated at 37^oC in a humidified 5% CO_2 environment for 48 hours.

The remaining steps were conducted at room temperature, and did not require sterile conditions. All removal and addition of solutions was conducted with care to avoid dislodging cells. When required, medium was removed from the dish by pipette. The cells were washed once with 1ml NT buffer, this was removed, and replaced with 2ml fresh NT.

4.3.3..3 Pulling pipette electrodes

Micropipettes for the intracellular electrode were prepared from 1.5mm diameter filamented borosilicate glass thin walled capillaries 100mm long (GF150, Harvard Apparatus UK). Each capillary made two pipettes. A Narashige PB-7 two stage vertical pipette puller was used for this. The first pull and heating stage extends the tube by 5 to 8mm, thinning the middle section to around 0.1mm diameter, but not allowing this to shear. During the second heating and pull stage the tube is pulled apart by gravity. A tip of around 1µM with electrical resistance of between 3 and 10MΩ is optimal for whole cell patch clamping (Ogden and Stanfield 1994). Reducing the weight applied and increasing the temperature of the second pull made a thinner electrode with higher tip resistance.

The settings for the first and second pull, and applied weight, were optimised for the capillaries used, with the procedure described to measure tip resistance in Section 4.3.3..5. To compensate for drift, tip resistance was checked each time, and the settings adjusted if necessary.

Following the manufacturer's instructions, the capillary was inserted so that 1.5cm (approximately) appeared above the top of the apparatus. No weights were used. The first pull was set to have a drop of 6mm, with the temperature set to 88. Following this the capillary was adjusted to be 3mm lower, so that the filament was in the centre of the thinned region. For the second pull the temperature was set to 93. With these settings the tip resistance was consistently between 3 and 7MΩ. With careful storage the pipettes can be prepared several hours or a day in advance of use.

4.3.3..4 Preparing the platform

MCF7 cells were patch clamped using a Cairn Optopatch amplifier rig (Cairn Research Ltd., Kent) with a microscope (Olympus OM-2, Japan; Figure 4.3), inside a Faraday cage to reduce airborne electromagnetic radiation, and on an antivibration table (TMC Vibration Control, Massachusetts). The latter uses a cushion of air to prevent vibrations from the surroundings being transferred to the cell and electrode, as this would be fatal to the stability of the seal. Cells were visualised at x200 using light microscopy.

A fresh dish of MCF7 cells in NT buffer was inserted into the stage of the microscope. This was perfused with NT using a peristaltic pump (Gilson Minipuls 3) at a rate of 1ml/min to wash away debris or non-adherent cells. The AgCl bath electrode was submerged in the NT solution in the dish. During current recordings the pump was required to be switched off as it introduced electrical interference (noise) into the circuitry.

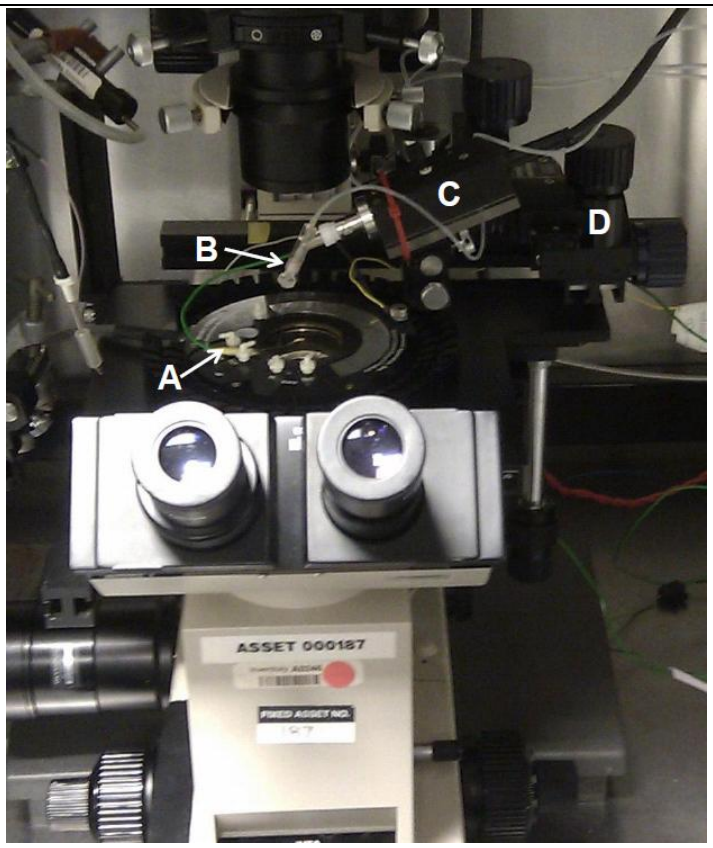

Figure 4.3: Olympus microscope and headstage inside the Faraday cage

Bath electrode (A), pipette holder / internal electrode (B), headstage (C) and coarse manipulator (D) are indicated.

When handling and using the micropipettes, great care was required at all times to avoid damaging the tips. A pre-prepared micropipette was filled to about 2/3 full with intracellular solution using a syringe needle fitted with a 0.22µm PTFE filter. The internal filament allows a continuous liquid circuit through the pipette, uninterrupted by bubbles due to capillary action. However large bubbles in the tip were dislodged by tapping. Once filled, the pipette was attached to the electrode holder on the headstage, ensuring that the silver electrode wire was in contact with the solution inside the pipette. The pipette was then lowered into the bath using the course manipulator. This completes the electrical circuit (Figure 4.4). Slight pressure (0.5ml of displaced air) was applied and locked in place using a syringe attached to the air line to prevent debris contacting the electrode tip. The amplifier, camera and antivibration table were switched on at this stage.

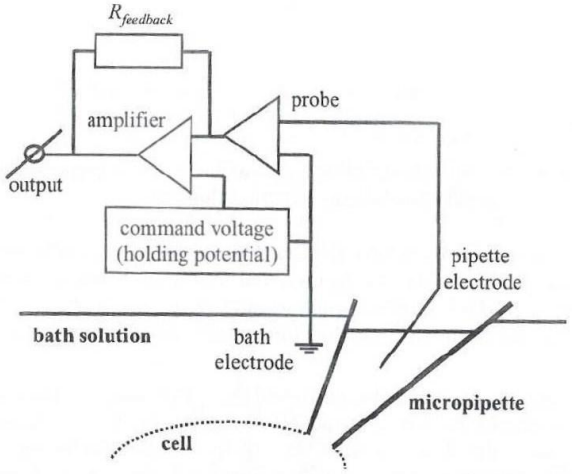

Figure 4.4: Basic schematic of whole cell patch clamp circuitry

Image from Molleman (2002). The voltage is "clamped" by the experimenter, and the current between the bath and pipette electrodes is continuously measured. Any change in plasma membrane resistance (i.e. channel activity) is immediately compensated for by a change in current, which is then recorded.

4.3.3..5 Checking pipette resistance

Pipette resistance was checked regularly to determine consistency. With the electrode in the bath, whether using the Cairn amplifier or the seal test window in the associated computer software (WinWCP: V.4.4.1, John Dempster, University of Strathclyde Electrophysiology Software, 2011) a 10mV pulse was applied from a holding potential of 0mV, for 35ms. This will be referred to as pulse 1. The junction potential was adjusted to compensate for the difference in ionic compositions between the bath and electrode solutions (this generates an ion bridge potential) using the amplifier until there was no current at zero applied voltage (junction potential will be approximately 160mV using the solutions described). The electrode resistance was noted. The ideal range was between 3 and 10MΩ, corresponding with the appropriate tip diameter for whole cell patching large cells such as MCF7. Pipettes with tip resistances outwith this range were discarded. The junction potential settings were then switched off, as when the pipette is in contact with the cell there should be no junction potential.

The system was initially calibrated with a “dummy cell” (Cairn) of known resistance and capacitance, so the readings generated were considered accurate.

4.3.3..6 Generating the Giga-ohm seal on the cell

A cell was selected visually which sat isolated from other cells, as immediate neighbours could interfere with the signal measured. Care was taken to select cells of similar sizes on each instance. Using the coarse manipulators, then the fine micromanipulator (Narashige MWH-3 water hydraulic 3 way) the cell was approached with the tip of the pipette, until the tip sat just above the centre of the cell, as viewed on the monitor. Another 0.5ml of pressure was gently applied using the syringe and air line, to slightly depress the surface of the cell. Using only the micromanipulator, the tip was lowered incrementally towards the plasma membrane.

Contact with the membrane is determined by watching the current signal and resistance generated by pulse 1. This is indicated by a sudden (although slight) increase in resistance at the tip of the pipette electrode and a drop in current by around 10%. Quickly, the plasma membrane was pulled onto the pipette by releasing the pressure on the air line.

If the membrane seals around the tip (if both the tip and membrane are un-occluded) the resistance will rise to above 3GΩ (the gigaseal, or giga-ohm seal), reflecting the very close association between the pipette and the membrane. Seals of less than 3GΩ were insufficient for the integrity of the circuit, and would result in overwhelming leakage of electrolytes from the cell. Seals of 10GΩ or more were optimal. Once the gigaseal had formed, the current recorded from pulse 1 was virtually zero (Figure 4.5 and Figure 4.6A). Where the cell failed to form a seal around the pipette tip (or at later stages the seal ruptured), the pipette was discarded, a new cell selected, and the process repeated.

Once a stable 10GΩ seal was generated, the software was used to change the holding potential to -50mV (closely matching the membrane potential of the cell). The 10mV 35ms pulse was maintained. These settings will be referred to as pulse 2. The seal was allowed to stabilise at the new settings.

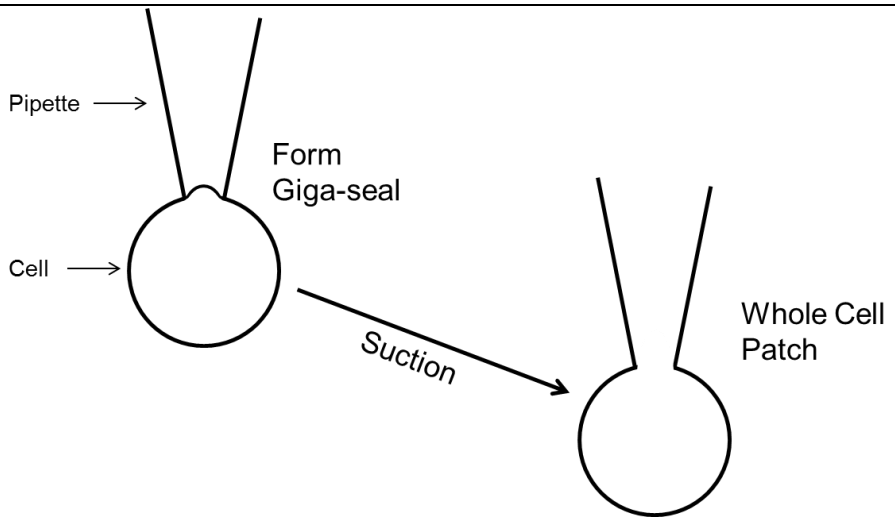

Figure 4.5: Schematic representation of a whole cell patch clamp

4.3.3..7 Creating the whole cell patch

With a tight and stable seal formed around the pipette, the next stage was to rupture the plasma membrane inside the tip. This was achieved by applying sharp suction to the air line. Successful formation of the whole cell patch was indicated by a sudden increase in current, a drop in resistance, and the formation of fast transient spikes of current at either side of the trace generated by pulse 2 (Figure 4.6B).

The trace generated by pulse 2 was then adjusted electrically to get a square current pulse and compensate for the capacitance currents and series resistance. This was carried out by switching the amplifier to resistance capacitance compensation mode, and adjusting the series resistance and capacitance. The fast and slow mag and tau settings were used to eliminate transient elements of the current. The series resistance and capacitance were noted, since these were characteristic to MCF7.

The membrane capacitance of biological membranes is relatively predictable, and is determined roughly by cell size (approximately 1pF per 100µm^2 of membrane). The average surface area of MCF7 is around 800µm^2 (Nassarre et al. 2003) so the capacitance was predicted to be approximately 8pF. Cells were discarded if uncompensated series resistance exceeded 25mV.

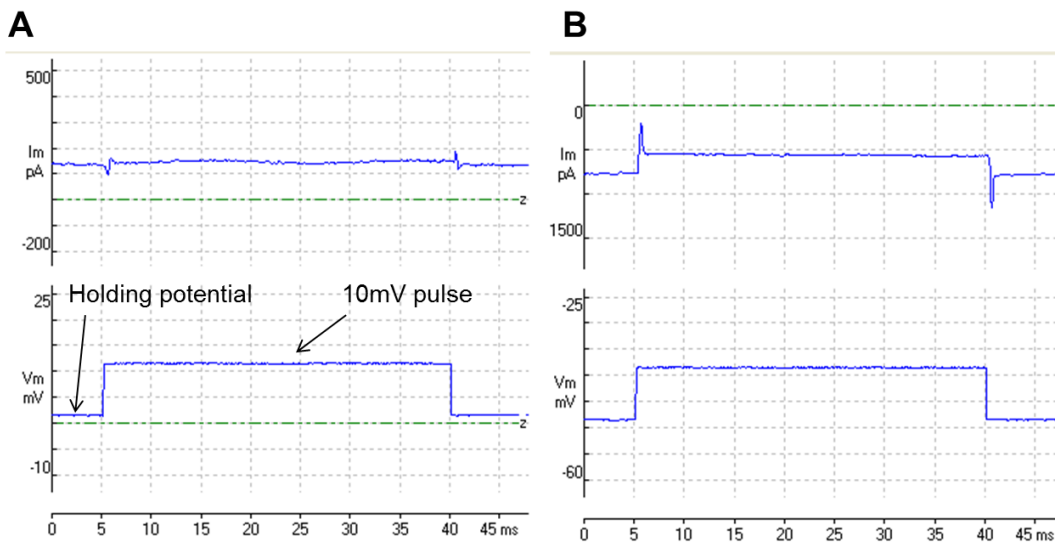

Figure 4.6: Example traces generated during whole cell patch clamping

The very high resistances generated when the giga-seal forms result in virtually no current during the 10mV pulse for 35ms from a holding potential of 0mV (A; pulse 1). When the membrane within the pipette is ruptured and a successful whole cell patch is achieved, resistance drops and a current is generated with fast transient capacitance spikes when pulse 2 is applied (B; 10mV pulse for 35ms from a holding potential of -50mV).

4.3.3..8 VGKC activating voltage stepping protocol

Whole cell currents were allowed to stabilize for up to five minutes after patching, due to gradual equilibration of pipette contents and cell cytoplasm. Following this, a voltage stepping protocol was then applied to the cell to determine the activity of the VGKCs. The same protocol was used throughout. From the holding potential of -50mV, voltage was sequentially stepped up from -70mV to 120mV in 10mV increments for 250ms, with 250ms between each step at the holding potential (Figure 4.7A). Similar protocols are widely used in MCF7 to assess VGKCs (Coiret et al. 2007; Ouadid-Ahidouch et al. 2000).

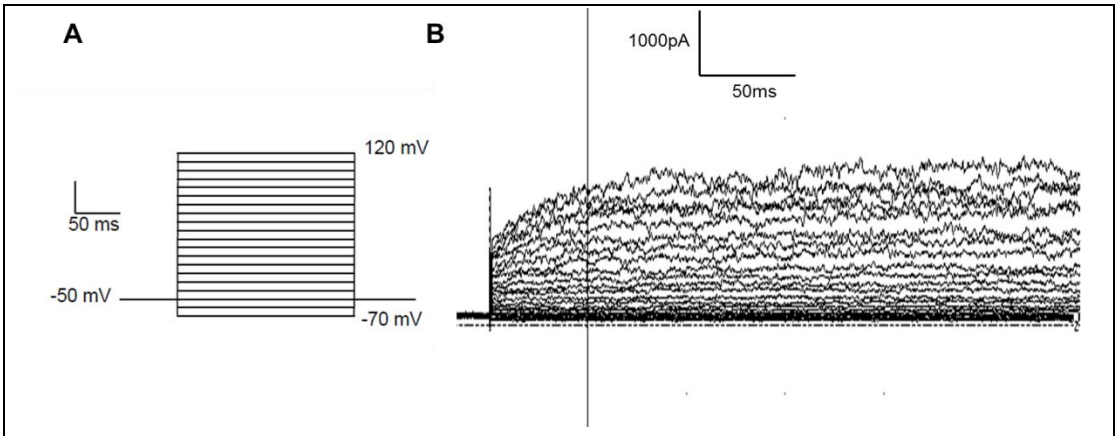

Figure 4.7: Voltage stepping protocol and resulting voltage sensitive current recording from MCF7

Schematic representation of the voltage stepping protocol (A) from a holding potential of -50mV voltage was sequentially stepped from -70mV to 120mV in 10mV increments held for 250ms. The resulting current from a whole cell patch clamped MCF7 cell (B) showing very little current response at and around the holding potential, but increasingly activating as the cell becomes more depolarized.

4.3.4 Test conditions

For each successfully patched cell the above voltage stepping protocol was applied prior to treatment. If this confirmed the activity of VGKCs (Figure 4.7B), then the cell was perfused for up to 20 minutes with NT containing test compounds in the appropriate concentrations. Table 4.1 describes the concentrations of the various channel blockers, control and test agents chosen, in relation to their IC_{50} concentration for proliferation (determined in Section 5.2.2) where appropriate and any previously published information regarding an impact on K^+ channel activity.

The concentrations of the K^+ channel blockers used were based on similar studies, as they were sufficient to block the channels in question to a greater or lesser extent without showing significant cytotoxicity (under the IC_{50}, or resulted in no significant inhibition of proliferation) over the time-scales used (Coiret et al. 2007; Coiret et al. 2005; Roy et al. 2008; Yao and Kwan 1999).

Table 4.1: Concentrations of test agents used for patch clamping

Treatment	IC_{50} for MCF7 proliferation	IC_{50} for K^+ channel activity[1]	Dose used
TEA	18.8mM	5mM	10mM
4-AP	2.69mM	Between 0.1 and 4 mM	1mM
AST	4.91µM	200nM	1µM
DOF		1µM (effective concentration)[2]	1µM
Genistein		30 to 100µM (effective concentration)[3]	31.6µM
Daidzein			31.6µM
E2			1nM
DMSO			0.1%
Untreated (NT)			N/A
Genistein + 4-AP			31.6µM + 1mM
Genistein + AST			31.6µM + 1µM

[1] *See Table 1.9*

[2] *(Wang et al. 2002)*

[3] *See Section 1.6.7*

The voltage stepping protocol was applied again at 1, 3, 5, 7, 9, 12, 15, 17, and 20 minutes into the treatment, or as long as the seal integrity remained. Note that at each time point the perfusion pump was required to be briefly switched off to prevent interference, and that the pump had a two minute lag time due to the volume of the tubes. In the instances where normal Tyrode was in the tubing, 2 minutes was subtracted from all the measurement time points post-treatment to compensate.

4.3.5 Analysis of results

WinWCP software (John Dempster, University of Strathclyde Electrophysiology Software, 2011) was used to determine the current at each voltage step. At each voltage level the mean current was calculated for a section of the trace in the second half of the 250ms step, as the current was generally more stable than early in the step, and this avoids the effects of the Na^+ channels.

The effect of each treatment on the macroscopic MCF7 current was initially assessed at each time point, and 5 minutes treatment (not including the 2 minute lag time) was chosen for the comparison of treatments. This allowed for maximum effect of the treatment (when evident) and avoided the subsequent degradation of the seal interfering with results.

Each treatment was repeated on at least three independent occasions on different days. Current/voltage (I/V) curves showing the mean I/V relationship before and 5 minutes into the treatment were plotted.

There was an unavoidable element of current leakage in many of the cells. Whether this was due to the cells and the presence of secreted matrix proteins, their treatment, or the equipment was not known. It is standard practice to assume that leakage is relatively constant over time as long as the seal retains integrity, so to determine the net effect of the treatment on the outward curent, the recorded current after treatment was subtracted from the initial (untreated) current at each voltage step, in the manner of Ouadid-Ahidouch et al. (2000). With some equipment, leak subtraction can be carried out automatically (Grissmer et al. 1994; Ouadid-Ahidouch et al. 2000). This I/V response generated is referred to as the “treatment” sensitive current. In this manner, when the treatment inhibited current, the element sensitive to it was positive, and when the treatment increased current the sensitive element appeared negative. The effect of current over the course of the protocol was illustrated for each treatment, at the voltage which induced the greatest magnitude of treatment-sensitive effect (i.e. the greatest difference before and 5 minutes after treatment).

4.3.6 Statistical analysis

For each treatment, the results for each cell before and 5 minutes into the protocol were compared using the General Linear Model (GLM; SPSS version 19, IBM Statistics, 2010) for repeated measures, using the within subject (cell) variables of treatment (before and after) and voltage (20 levels). Since there were only two levels in the treatment variable, sphericity was assumed. Results are quoted as the F value, degrees of freedom of the model (df_M) and residual degrees of freedom of the model (df_R) and the significance (p) of F. Where $p<0.05$ F was assumed to be significant. Where a significant effect of 5 mins treatment on response to voltage was found, further analysis was conducted by MANOVA (Simple Effects Analysis) to determine the effect of treatment at each level of voltage within a cell (F and p).

The treatment-sensitive elements of the combined treatments (genistein and 4-AP or AST) were compared to the relevant single treatments using ANOVA (SPSS version 19, IBM Statistics, 2010) with Bonferroni *post hoc* corrections for multiple comparisons, and significant values (p, two tailed, < 0.05) are indicated.

CHAPTER 5. Results: volume regulation and potassium channel activity

5.1 Results of the calcein cell volume assay in MCF7

5.1.1 Hyposmotic shock

The response of MCF7 cells (n=3) to a hyposmotic shock is shown in in Table 5.1 and Figure 5.1, highlighting four specific regions of interest (1, 2, 3, 4).

Table 5.1: MCF7 fluorescence levels during hyposmotic shock

Region of trace	Time (secs)	Mean fluorescence	SD	p(2)*	p(4)*
1	240-300	91.00	5.31	<0.001	
2	566-626	94.60	6.62	-	NS
3	962-1022	92.05	8.99	<0.001	
4	1426-1480	94.83	10.76	NS	-

** Significance of difference compared with region 2 or 4 as indicated*

The increase in fluorescence (1 to 2) was significant ($p < 0.001$), and occurred approximately 2.5 minutes into the hyposmotic treatment, taking into account the 2 minute lag. This may be an early effect of the treatment. An increase in fluorescence can suggest cell shrinkage, however cell size appeared unaffected (visual observation; Figure 5.1B).

Approximately seven minutes after the change to hypotonic solution, fluorescence intensity dropped as the cells underwent hypotonically induced swelling (2 to 3). This continued for around five minutes, and the difference between the mean values at 2 and 3 was significant ($p < 0.001$). The mean rate of fluorescence intensity change per second (Δf) during this time (700 to 1000 seconds) was -0.008 ± 0.021.

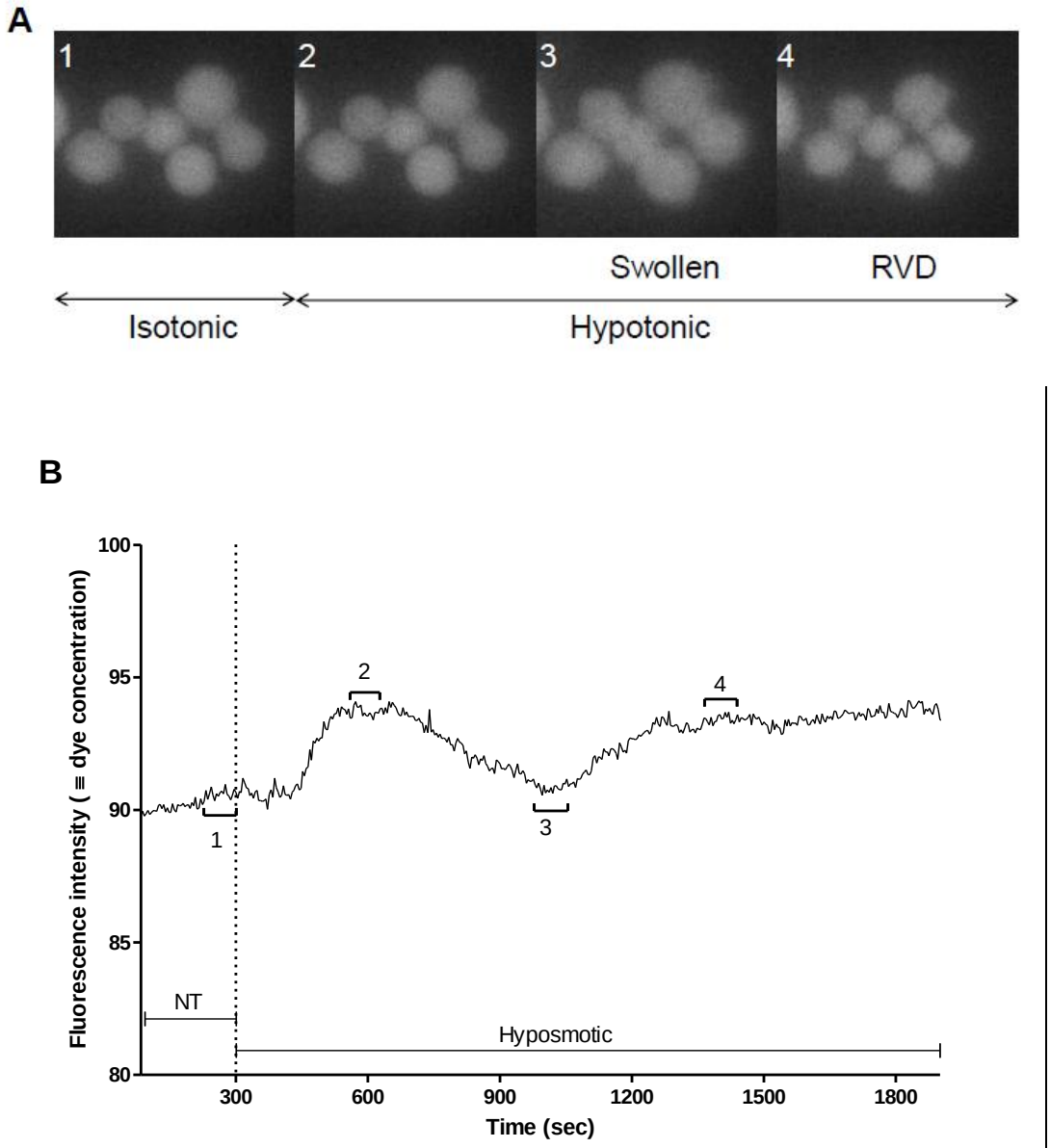

Figure 5.1: MCF7 calcein fluorescence during hyposmotic shock

MCF7 cells were prepared as described. Fluorescent images (excitation at 480nm) taken at four second intervals were analysed, following initial perfusion with NT, then 30 minutes in a 50% Na (hyposmotic) Tyrode. Sample images are provided in A, and the results of the analysis are shown in B (mean of three independent experiments, following 54 cells). Indicated are 60 second regions representing the cells prior to hyposmotic shock (1), after an initial increase in fluorescence (2), following swelling and resulting fluorescence drop (3) and after RVD (4). The numbered images in A correspond with these regions in B.

Immediately after this, the cells underwent a period of RVD (3 to 4), as the fluorescence, and their volume, returned to the levels seen in 2, by approximately 16 minutes after the change to hypotonic solution. This increase in fluorescence was again significant ($p < 0.001$), and Δf for this (1004 to 1300 seconds) was 0.010 ±0.020. Comparison between the two slopes (2-3 and 3-4) by paired t test indicated that they were significantly different ($p < 0.001$).

5.1.2 17β-oestradiol and genistein induce opposing changes in MCF7 cell volume

The mean results of the experiments looking at calcein fluorescence intensity in MCF7 after treatment with 1nM E2, 1µM genistein and 31.6µM genistein are shown in Figure 5.2, Figure 5.3 and Figure 5.4 respectively (n = 3 for each). For each treatment Δf for region 1 (Δf_0; after 8 minutes treatment with 0.1% DMSO), region 2 (Δf_{10}; after 10 minutes treatment with the test agent) and region 3 (Δf_{15}; 15 minutes into treatment) are provided in Figure 5.5.

The background change in fluorescence or the impact of 0.1% DMSO varied greatly between treatments. Prior to 1nM E2 treatment (Figure 5.2) mean fluorescence was relatively stable, and did not appear to be impacted upon by the vehicle-only treatment. Prior to the 1µM genistein treatment (Figure 5.3), mean fluorescence intensity was increasing. Again this was not affected by the presence of the control treatment. However, prior to the 31.6µM genistein treatment (Figure 5.4) there was a decrease in mean fluorescence associated with the addition of 0.1% DMSO. Whether these changes were in response to the solvent or the treatment protocol was unknown. Overall the mean fluorescence change during 0.1% DMSO treatment was slight ($\Delta f_0 = 0.003 \pm 0.017$; Figure 5.5).

To eliminate the variable background or vehicle-effects on fluorescence seen, Δf for each treatment/time was compared to its own pre-treatment 0.1% DMSO value in a paired fashion, rather than the mean Δf_0. Likewise, adjusted Δf values ($a\Delta f_{10}$ and $a\Delta f_{15}$) for each treatment/time point were calculated as the difference between the slopes in regions 1 and 2, or 1 and 3 (Figure 5.6).

Overall, 1nM E2 treatment resulted in a drop in fluorescence intensity (Figure 5.2) associated with a significant reduction from a positive Δf_0 to negative values at both 10 and 15 minutes into treatment ($p < 0.001$ and < 0.01 respectively), and consequently negative values for aΔf (Figure 5.5 and Figure 5.6). Together this suggests that by 10 minutes into this treatment, an increase in cell volume has resulted.

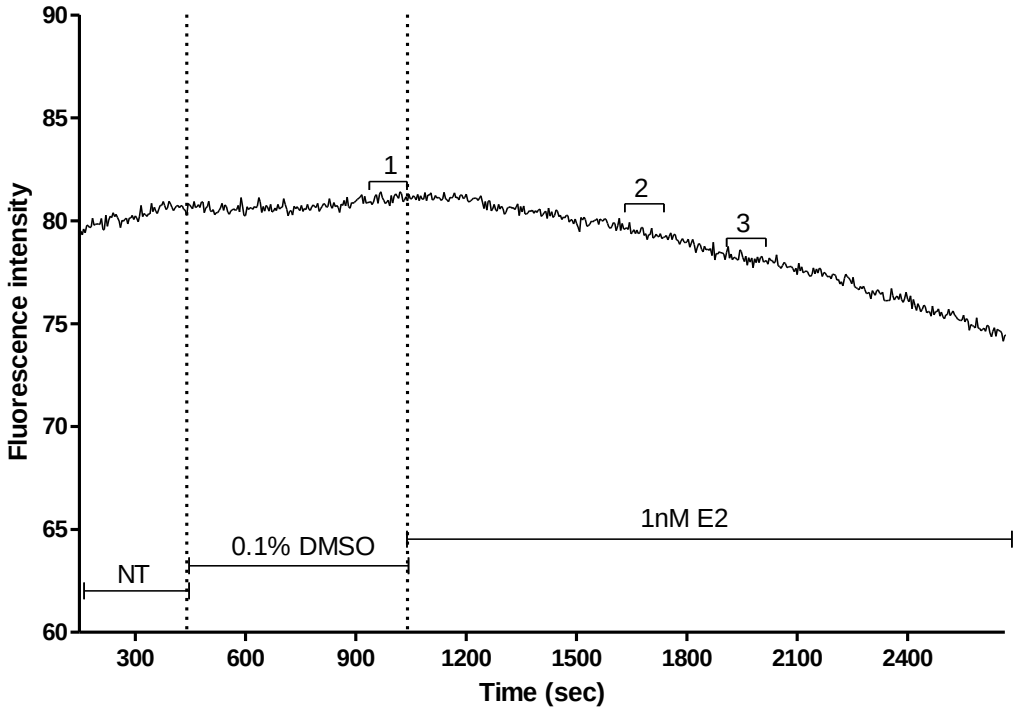

Figure 5.2: MCF7 calcein fluorescence during treatment with 1nM E2

MCF7 cells were prepared as described. Fluorescent images (excitation at 480nm) taken at four second intervals were analysed, following initial perfusion with NT, then 10 minutes in a 0.1% DMSO Tyrode, and 30 minutes in Tyrode containing 1nM E2. Results shown are the mean of three independent experiments, following 39 cells. Indicated are 2 minute regions representing the cells after 8 minute perfusion with 0.1% DMSO (1; 920 to 1040 seconds) and 10 (2; 1640 to 1760 seconds) and 15 (3; 1940 to 2060 seconds) minutes perfusion with 1nM E2.

There was no evidence of E2 auto-fluorescence, determined by assessing the background fluorescence in a cell-free area before and during perfusion with 1nM E2 Tyrode, mean and SD fluorescence were 14.08 ± 3.22 and 14.01 ± 3.31 respectively, p (Student's t test, two tailed) ≥ 0.05.

The strong background upward trend in mean fluorescence intensity seen in the 1µM genistein-treated cells continued after treatment, although to a lesser extent (Figure 5.3). This is reflected by a drop in Δf from Δf_0, which achieved statistical significance ($p < 0.001$) by 15 minutes into the treatment regime (Δf_{15}), although not at 10 minutes (Δf_{10}; Figure 5.5). Likewise, aΔf has a small negative value after 10

minutes treatment, but this has become more negative by 15 minutes (Figure 5.6). This indicates that despite the background upward trend in fluorescence, 1µM genistein treatment results in an increase in MCF7 cell volume, although this is slightly slower to take effect than that seen with 1nM E2.

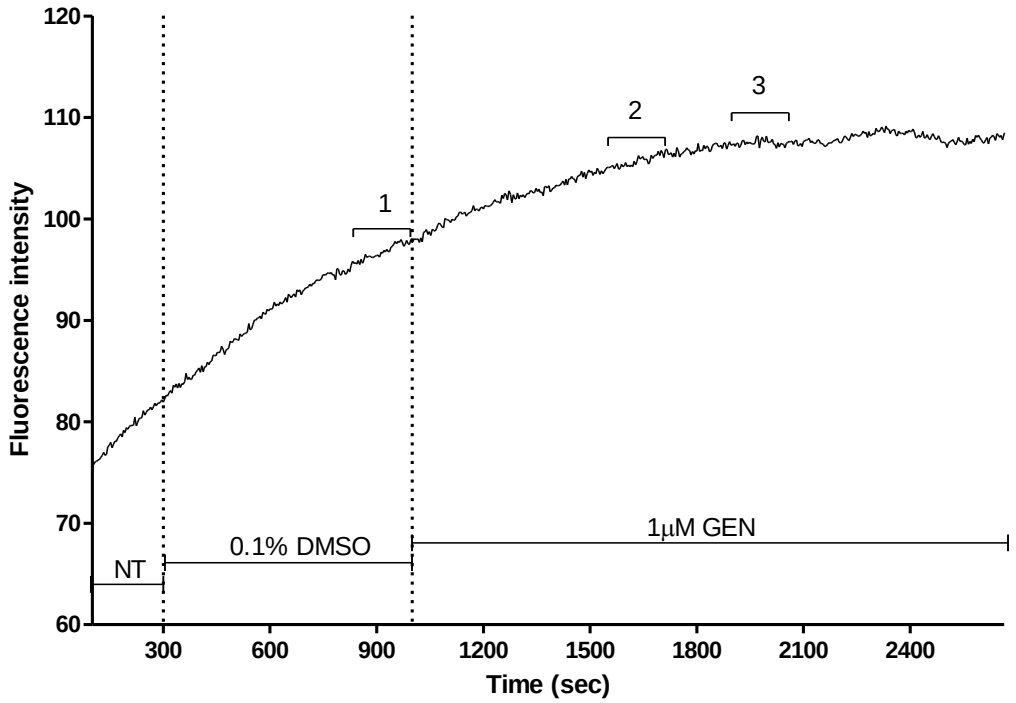

Figure 5.3: MCF7 calcein fluorescence during 1µM genistein treatment

MCF7 cells were prepared as described. Fluorescent images (excitation at 480nm) taken at four second intervals were analysed, following initial perfusion with NT, then 10 minutes in a 0.1% DMSO Tyrode, and 30 minutes in Tyrode containing 1µM genistein. Results shown are the mean of three independent experiments, following 34 cells. Indicated are 2 minute regions representing the cells after 8 minute perfusion with 0.1% DMSO (1; 880 to 1000 seconds) and 10 (2; 1600 to 1720 seconds) and 15 (3; 1900 to 2020 seconds) minutes perfusion with 1µM genistein.

In the 31.6µM genistein treated cells there was an initial (pre-treatment) trend towards decreasing fluorescence intensity (Figure 5.4). The genistein treatment rapidly reversed this, initially resulting in the fluorescence stabilising, and then after 10 minutes intensity began to increase, suggesting shrinkage. This is confirmed by

a significant increase from negative to positive values for Δf_{10} ($p < 0.001$), and a subsequently large positive $a\Delta f$ at this time point (Figures 5.5, and 5.6).

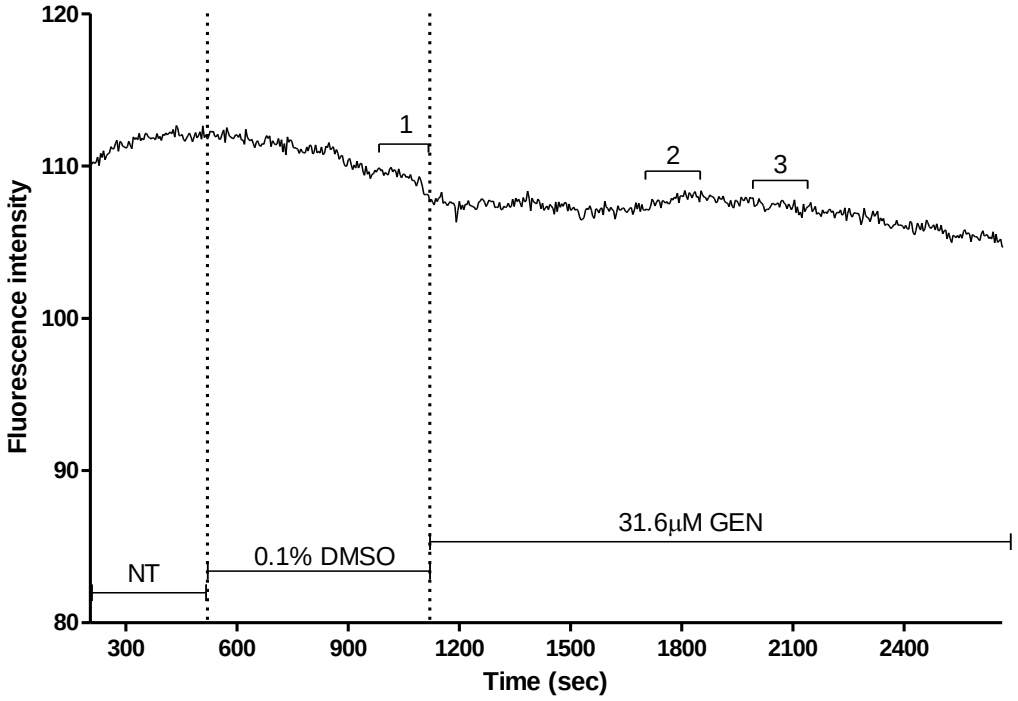

Figure 5.4: MCF7 calcein fluorescence during 31.6µM genistein treatment

MCF7 cells were prepared as described. Fluorescent images (excitation at 480nm) taken at four second intervals were analysed, following initial perfusion with NT, then 10 minutes in a 0.1% DMSO Tyrode, and 30 minutes in Tyrode containing 31.6µM genistein. Results shown are the mean of three independent experiments, following 22 cells. Indicated are 2 minute regions representing the cells after 8 minute perfusion with 0.1% DMSO (1; 1000 to 1120 seconds) and 10 (2; 1720 to 1840 seconds) and 15 (3; 2020 to 2140 seconds) minutes perfusion with 31.6µM genistein.

However, by 15 minutes into the 31.6µM genistein treatment, fluorescence intensity had returned to its downward trend. Accordingly Δf_{15} has a small negative value. However, this is still significantly lower in magnitude to the downward rate of change seen in Δf_0 ($p < 0.01$), and accordingly $a\Delta f_{15}$ still has a positive value, although lower than that seen at $a\Delta f_{10}$. This suggests that although the MCF7 cells continued to

shrink after 15 minutes, it was not rapid enough to counter the background loss in fluorescence seen in these cells.

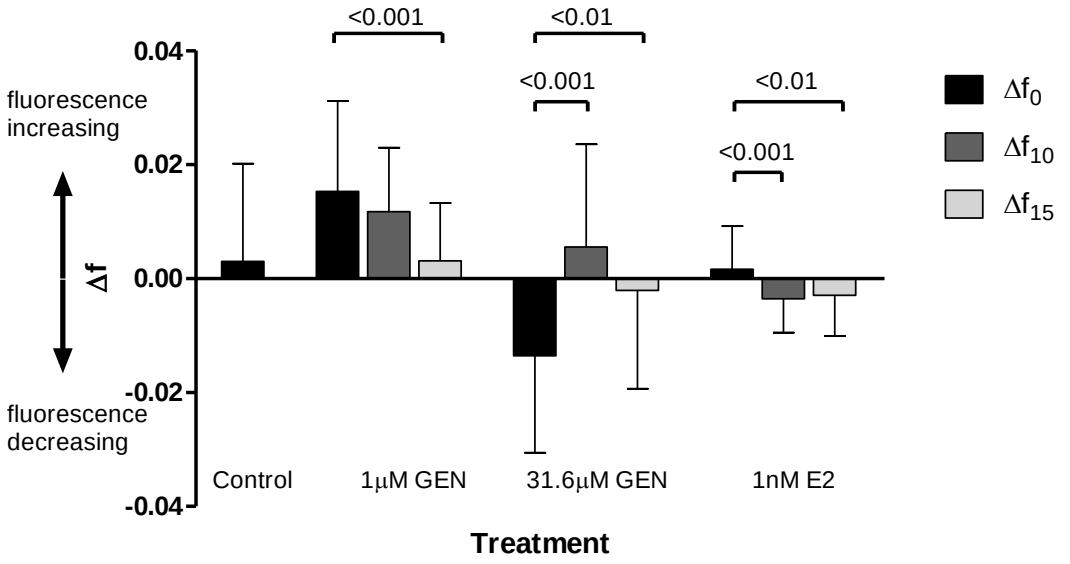

Figure 5.5: Rate of MCF7 calcein fluorescence change per second, prior to, and 10 and 15 minutes into treatment

Values were calculated as described for the mean and standard deviation of Δf after 8 to 10 minutes of 0.1% DMSO treatment (Δf_0), 10 to 12 minutes (Δf_{10}) and 15 to 17 minutes (Δf_{15}) treatment with 1nM E2, 1μM genistein, and 31.6μM genistein. Significant differences from the indicated Δf_0 value ($p < 0.05$) are provided. The control value is the mean of the 0.1% DMSO Δf_0 results. Positive Δf indicates increasing fluorescence, and negative Δf indicates reducing fluorescence.

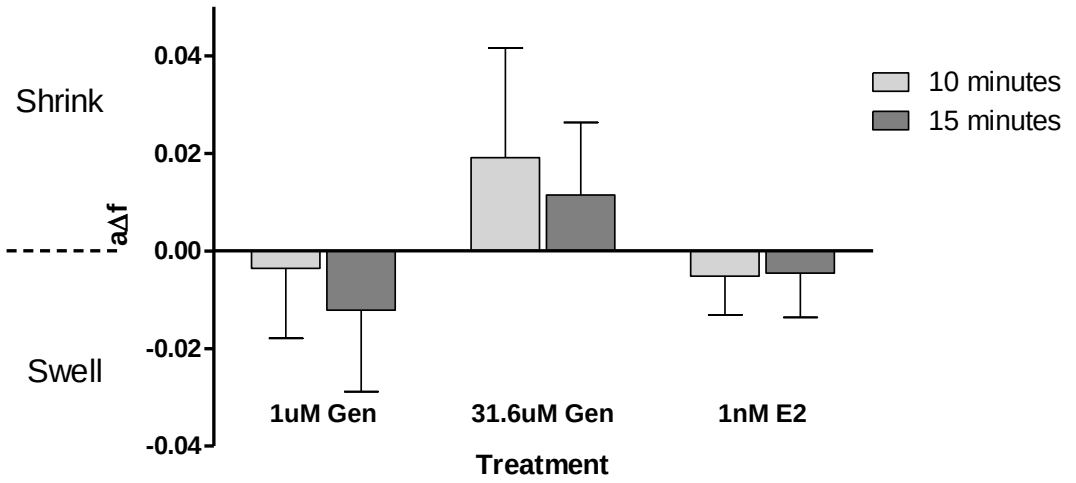

Figure 5.6: Adjusted rate of MCF7 calcein fluorescence change after treatment

Adjusted Δf (aΔf) was calculated as described at 10 and 15 minutes into treatment of MCF7 with 1μM genistein, 31.6μM genistein, and 1nM E2 (mean and standard deviation). Positive aΔf indicates shrinkage, and negative aΔf indicates swelling.

5.2 Results of the MTT assays assessing the role of K^+ channels in MCF7 proliferation

5.2.1 Control treatments

TEA and 4-AP used water as a solvent, so for reference it was determined whether this had an effect on proliferation. The addition of water up to and including 2% did not affect proliferation, but 4% water resulted in a slight reduction in proliferation compared to the untreated control (Figure 5.7). This may have been due to dilution of nutrients.

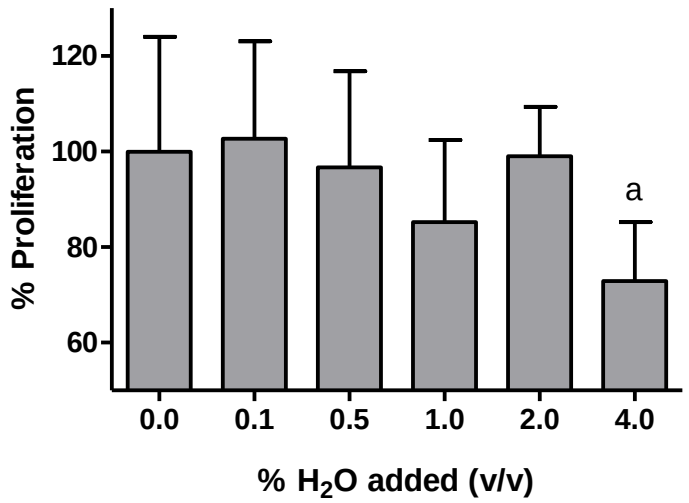

Figure 5.7: The impact of increasing quantities of added water on MCF7 proliferation

MCF7 cells were prepared as described, and incubated for 72 hours in experimental medium containing d.H_2O added at levels between 0 and 4%, then cell proliferation was assessed by the MTT assay. The impact of these treatments on percentage proliferation, compared to the untreated (0%) control are shown (mean ± SD, n=3). Significant variation from the untreated control ($p< 0.01$) is indicated (a).

The TEA experiments used a maximum of 2% water. As this level had no impact on MCF7 proliferation, it was considered appropriate as a control treatment, and the effect of each concentration of TEA on proliferation was compared to this. However, a higher level of 4% water was unavoidable for the highest of the 4-AP

concentrations, due to limitations of its solubility. To factor in the impact of this level of water on MCF7 proliferation, all remaining 4-AP treatments were adjusted to contain 4% H_2O, then this level of water was used for control comparison with these treatments. The channel blockers DOF and AST used DMSO as a solvent. This did not exceed 0.1% in any instance, and had already been shown to have no effect on MCF7 proliferation at this dose (Section 3.1.1..1).

5.2.2 The impact of various K^+ channel blockers on MCF7 proliferation

Treatment with increasing concentrations of TEA reduced the proliferation of MCF7 in a dose-responsive manner, compared to the control (Figure 5.8). This achieved statistical significance at 10 and 20mM ($p < 0.01$ and < 0.001 respectively). The IC_{50} for the effect of TEA on MCF7 proliferation was determined to be 18.84mM.

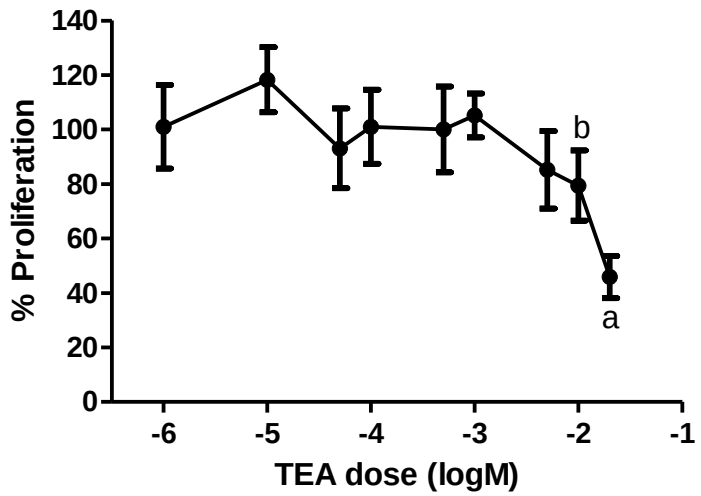

Figure 5.8: The impact of TEA on MCF7 proliferation

MCF7 cells were prepared as described, and incubated for 72 hours in experimental medium containing TEA between 1µM and 20mM, then proliferation was assessed by the MTT assay. The impact of these treatments on percentage proliferation, compared to the 2% d.H_2O control are shown (mean ± SD, n=3). Significant variation from the control is indicated (a; $p < 0.001$, b; $p < 0.01$).

Treatment with 4-AP reduced MCF7 proliferation to a comparable extent (Figure 5.9), with significantly lower percentage proliferation values calculated at all concentrations above and including 1mM ($p < 0.001$). The IC_{50} for this channel blocker on MCF7 was the slightly lower value of 2.7mM. This implies that of the K^+ channels involved in MCF7 proliferation, the VGKCs undoubtedly play an important role.

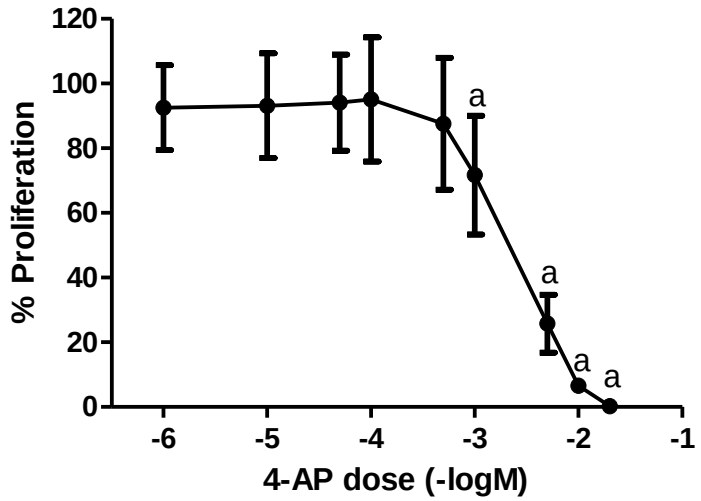

Figure 5.9: The impact of 4-AP on MCF7 proliferation

MCF7 cells were prepared as described, and incubated for 72 hours in experimental medium containing 4-AP between 1µM and 20mM, then proliferation was assessed by the MTT assay. The impact of these treatments on percentage proliferation, compared to the 4% d.H_2O control are shown (mean ± SD, n=3). Significant variation from the control (p< 0.001) is indicated (a).

To narrow down some of the individual K^+ channels implicated in MCF7 proliferation, the specific channel blockers AST and DOF were also tested. AST, a blocker of the hEAG and hERG channels, resulted in a dose responsive inhibition of MCF7 proliferation (Figure 5.10), which achieved statistical significance at all concentrations tested above 1µM ($p < 0.001$). The IC_{50} for this treatment on MCF7 proliferation was calculated to be 4.9µM.

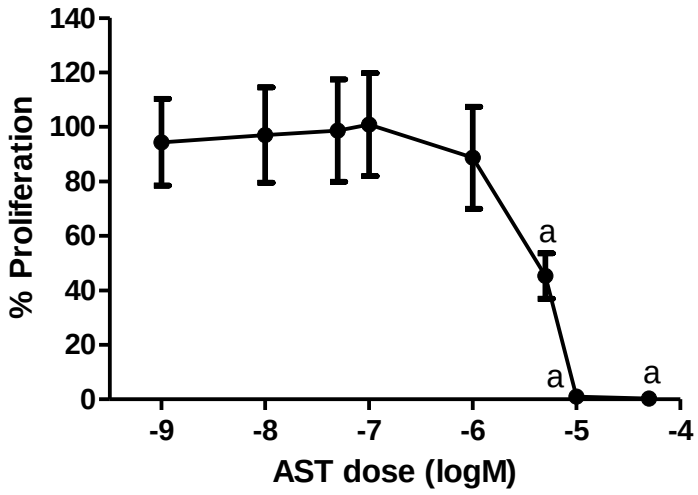

Figure 5.10: The impact of AST on MCF7 proliferation

MCF7 cells were prepared as described, and incubated for 72 hours in experimental medium containing AST between 1nM and 50µM, then proliferation was assessed by the MTT assay. The impact of these treatments on percentage proliferation, compared to the 0.1% DMSO control are shown (mean ± SD, n=3). Significant variation from the control (p< 0.001) is indicated (a).

However, there was no significant effect of DOF on the percentage of MCF7 proliferation measured at any of the concentrations tested up to and including 10µM (Figure 5.11). Together these last two experiments illustrate that AST but not DOF inhibit the proliferation of MCF7 cells, and so accordingly suggest that the hEAG channel, but not hERG, are involved in this response. Alternatively, higher concentrations of DOF may be required to have an impact on proliferation, but due to limitations in its solubility, this would have required unacceptable quantities of solvent present.

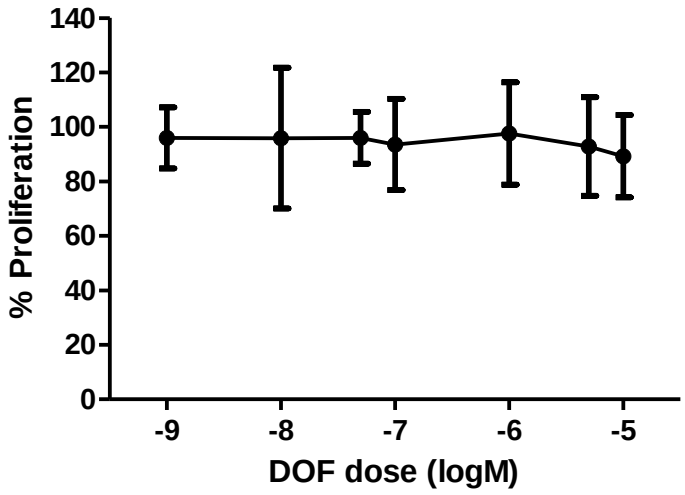

Figure 5.11: The impact of DOF on MCF7 proliferation

MCF7 cells were prepared as described, and incubated for 72 hours in experimental medium containing DOF between 1nM and 10µM, then proliferation was assessed by the MTT assay. The impact of these treatments on percentage proliferation, compared to the 0.1% DMSO control are shown (mean ± SD, n=3). There was no significant variation from the control.

5.3 Results of the whole cell patch clamping experiments assessing the impact of isoflavones on K^+ channel activity in MCF7 cells

5.3.1 Cell characteristics

The characteristics of the patched cells and electrodes used in the following experiments are provided in Table 5.2.

Table 5.2: Characteristics of cells and electrodes used in MCF7 patch clamp experiments

	Mean	SD
Electrode resistance (MΩ)	3.56	0.34
Uncompensated series resistance (MΩ)	9.16	5.34
Uncompensated capacitance (pF)	25.74	14.99

The electrode resistances measured were well within the tolerable range of 3 to 10MΩ, and as such were appropriate for whole cell patch clamping.

The series resistance value confirms that cells were excluded if the uncompensated series resistance exceeded 25MΩ. Series resistance relates to the degree of clogging that occurs inside the pipette tip, and is further discussed in section 6.4.2. Although it was compensated for electronically, it cannot be completely eliminated, and is consequently a source of error. The values here indicate that this was reduced as far as possible.

Finally, the capacitance figures give an indication of the size of cells used. The average surface area of MCF7 is 800μm^2, providing an approximate capacitance reading of 8pF (section 4.3.3..7). The readings generated here suggest that the cells being used were larger than average, although they were roughly representative of the individual cells observed which were not constrained by the proximity of their neighbours.

5.3.2 The impact of control treatments on macroscopic current in MCF7

The voltage sensitivity of the macroscopic current was assessed in MCF7 cells under untreated control conditions (Figure 5.12).

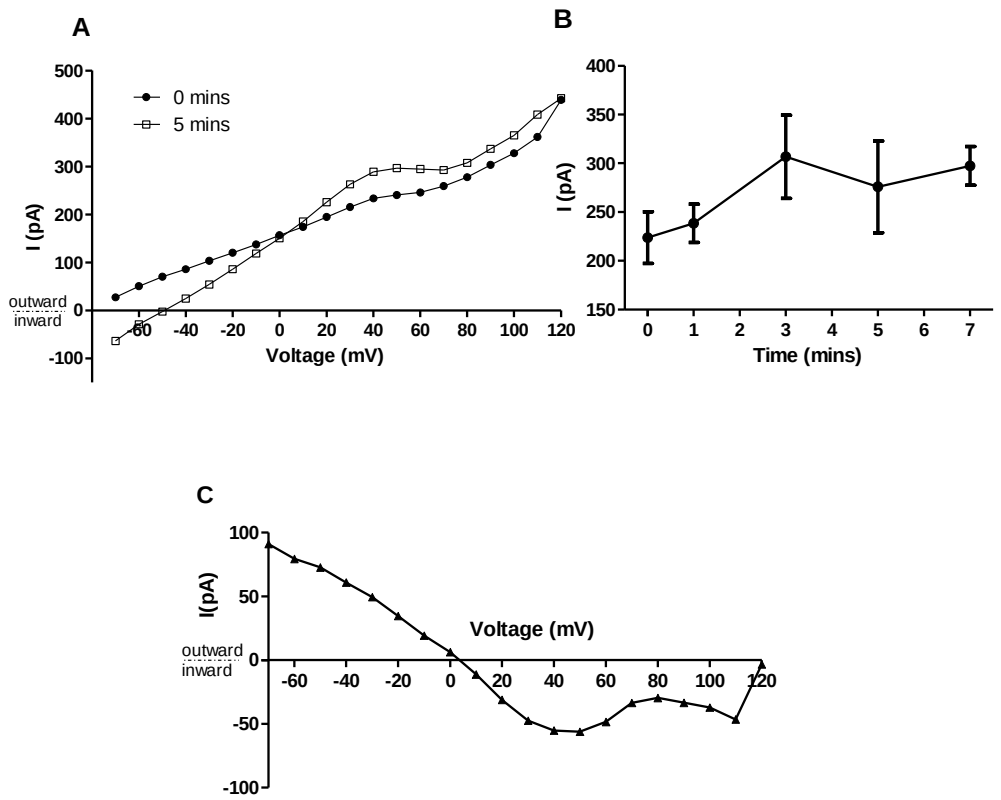

Figure 5.12: Current/voltage relationship in untreated MCF7 cells

The voltage dependent current in MCF7 was elicited by whole cell patch clamping and a series of depolarizing voltage steps from a holding potential of -50mV, ramping from -70mV to 120mV in 10mV steps. After recording the initial (time = 0 minutes) current with no additional treatment, the cells were perfused with normal Tyrode. The voltage sensitivity of the current was recorded again at various time points into the treatment. The effect of voltage on current is shown after 0 and 5 minutes treatment (A), and the time-course of the current at 50mV (mean and SD) is provided (B). The net effect of 5 minutes treatment with normal Tyrode is shown in C. All graphs are the mean result of three MCF7 cells assessed on different days.

In normal Tyrode with no additions, depolarization from -50mV to 110mV resulted in an increase in outward current at 0 and 5 minutes (Figure 5.12A). The magnitude of this current increased over time slightly, with the greatest increase occurring between 1 and 3 minutes into the protocol (Figure 5.12B). The resulting impact of 5 minutes perfusion with NT on the current/voltage (I/V) relationship is shown in Figure 5.12C. Analysis of variance for repeated measures (GLM) indicated that the effect of 5 minutes further treatment on the response to voltage within cells was significant, $F(19, 38) = 2.782$, $p < 0.01$. Further scrutiny by Simple Effects Analysis showed that this achieved significance within cells at voltages equaling and above -20mV (Table 5.3).

Table 5.3: Simple Effects Analysis of the impact of the protocol on voltage sensitivity

Voltage	F	p	Voltage	F	p
-70	0.21	NS	**30**	486.23	<0.01
-60	0.09	NS	**40**	345.52	<0.01
-50	1.16	NS	**50**	404.00	<0.01
-40	3.82	NS	**60**	524.60	<0.01
-30	11.04	NS	**70**	133.37	<0.01
-20	29.94	<0.05	**80**	96.59	<0.05
-10	93.53	<0.05	**90**	61.05	<0.05
0	338.43	<0.01	**100**	50.55	<0.05
10	4336.39	<0.001	**110**	42.77	<0.05
20	2368.33	<0.001	**120**	27.36	<0.05

Extrapolation of the initial untreated I/V curve predicts that the reversal potential (point at which there is no current before it reverses direction) would be approximately -80mV. The reversal potential is close to the resting membrane potential of the cell. In MCF7 this is largely dictated by the K^+ equilibrium potential, and is known to be around -85mV (Klimatcheva and Wonderlin 1999; Ouadid-Ahidouch et al. 2000; Wonderlin and Strobl 1996). This suggests that while other ions are likely to play a role in the current recorded here, it is largely due to movement of K^+ ions.

The impact of 5 minutes treatment with 0.1% DMSO on the macroscopic current in MCF7 was similar to that of normal Tyrode (Figure 5.13).

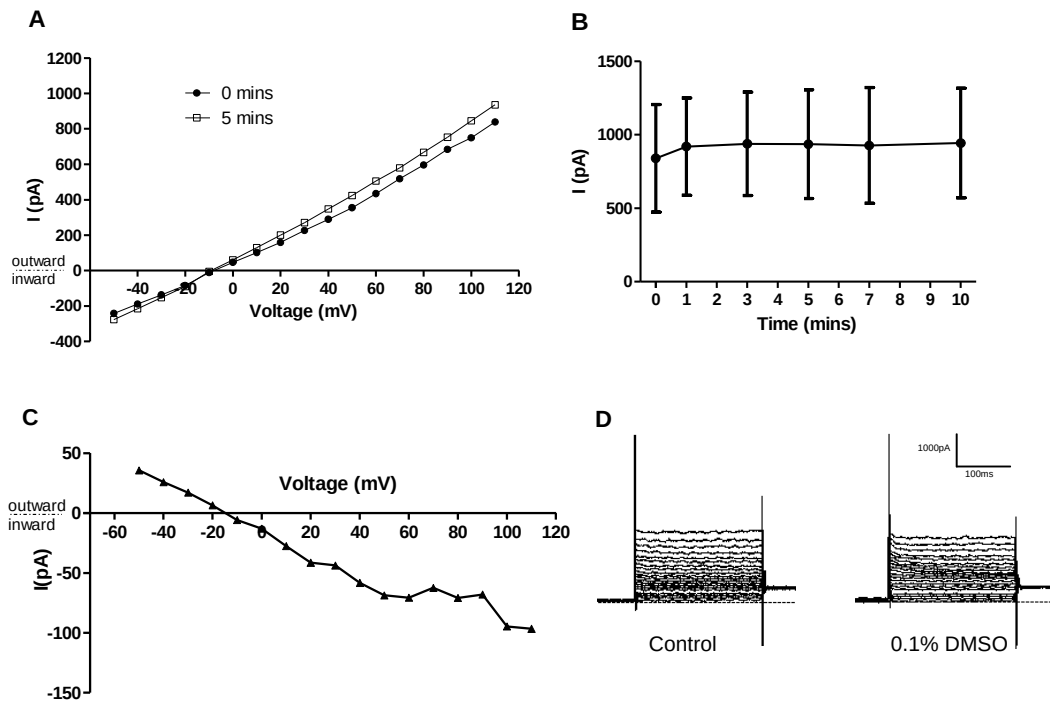

Figure 5.13: Current/voltage relationship in 0.1% DMSO treated MCF7 cells

The voltage dependent current in MCF7 was elicited by whole cell patch clamping and a series of depolarizing voltage steps from a holding potential of -50mV, ramping from -50mV to 110mV in 10mV steps. After recording the initial (time = 0 minutes) current with no additional treatment, the cell was perfused with Tyrode containing 0.1% DMSO. The voltage sensitivity of the current was recorded again at various time points into the treatment. The effect of voltage on current is shown after 0 and 5 minutes treatment (A), and the time-course of the current at 110mV (mean and SD) is provided (B). The net effect of 5 minutes treatment is shown in C. All graphs are the mean result of three MCF7 cells assessed on different days. Example traces before and after 5 minutes 0.1% DMSO treatment are provided in D.

This treatment resulted in a slight increase in the depolarization-activated element of the current, however, within cells the effect of five minutes treatment with 0.1% DMSO on the current response to voltage was not significant, $F(16, 32) = 1.187$. The reversal potential of the current here (approximately -10mV) is more positive

than previously recorded, but it remains negative. This suggests that while movement of K^+ ions contributes to the current, it has other elements also. Figure 5.13B shows the time-course for current at 110mV during perfusion with 0.1% DMSO. This indicates that current was relatively stable over time with this treatment.

5.3.3 The effect of K^+ channel blockers on the MCF7 macroscopic current

Having identified the impact of the solvent, and the treatment protocol on the voltage sensitivity of the macroscopic MCF7 current, the next step was to determine to what extent it was mediated by the potassium channels. Accordingly, following initial perfusion with normal Tyrode, the cells were perfused with a range of general and specific K^+ channel blockers.

Perfusion with 10mM TEA (non-specific K^+ channel blocker) resulted in a sudden (within 1 minute) drop in depolarization activated current (Figure 5.14). This suggests that the K^+ channels mediate an element of this current, shown in Figure 5.18. The reversal potentials of these currents were negative (between -20 and -30mV) suggesting again that K^+ ion movement played a role. The inhibition of current then remained stable. This treatment also reduced the leakage seen at negative potentials. The effect of 5 minutes treatment with TEA on the voltage response of MCF7 was significant, $F(14, 42) = 4.396$, $p < 0.001$. Further analysis (Table 5.4) indicated that this became significant within cells for all potentials above 20mV.

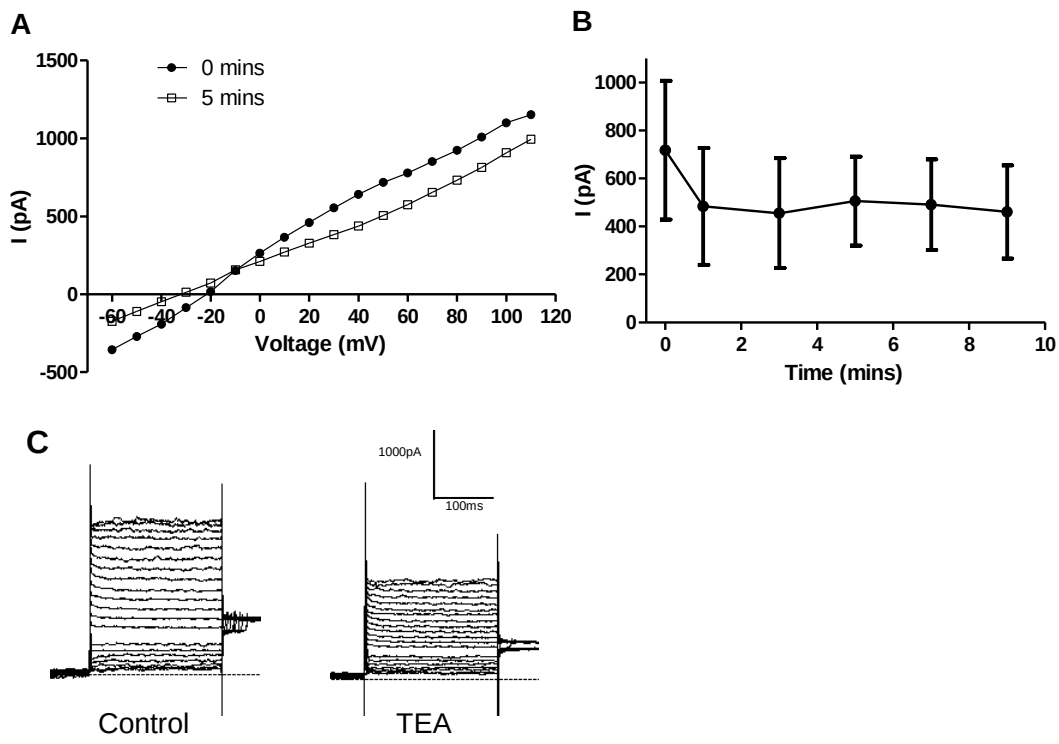

Figure 5.14: Current/voltage relationship in MCF7 treated with TEA 50mV

The voltage dependent current in MCF7 was elicited by whole cell patch clamping and a series of depolarizing voltage steps from a holding potential of -50mV, ramping from -60mV to 110mV in 10mV steps. After recording the initial (time = 0 minutes) current with no additional treatment, the cell was perfused with Tyrode containing 10mM TEA, and the voltage sensitivity of the current was recorded again. The effect of voltage on current is shown after 0 and 5 minutes treatment (A), and the time-course of the current at the potential which showed the greatest impact of treatment (50mV; mean and SD) is provided (B). Both graphs are the mean result of four MCF7 cells assessed on different days. Example traces before and after 5 minutes TEA perfusion are shown in C.

Table 5.4: Simple Effects Analysis of the impact of TEA on voltage sensitivity

Voltage	F	p
-60	1.77	NS
-50	0.97	NS
-40	0.41	NS
-30	0.04	NS
-20	0.07	NS
-10	1.11	NS
0	3.25	NS
10	7.06	NS

Voltage	F	p
20	14.11	<0.05
30	23.27	<0.05
40	29.88	<0.05
50	29.99	<0.05
60	27.41	<0.05
70	24.11	<0.05
80	21.32	<0.05

Treatment of MCF7 for 5 minutes with the VGKC specific blocker 4-AP (1mM) resulted in a similar, if lower in magnitude inhibition of voltage activated current (Figure 5.15), suggesting that the VGKCs were responsible for an element of this (the 4-AP sensitive current; Figure 5.18). Again, extrapolation of the I/V curves suggests that the reversal potential would be approximately -90mV, confirming that K^+ is responsible for the majority of the current in this case. The inhibition of current attributed to 4-AP treatment acted within the first minute of treatment then remained relatively stable. The effect of 5 minutes treatment with 4-AP on the voltage response of MCF7 was significant, $F(19, 38) = 2.747$, $p < 0.01$. Further analysis indicated that there was a significant within-cell effect of treatment at each voltage tested (Table 5.5).

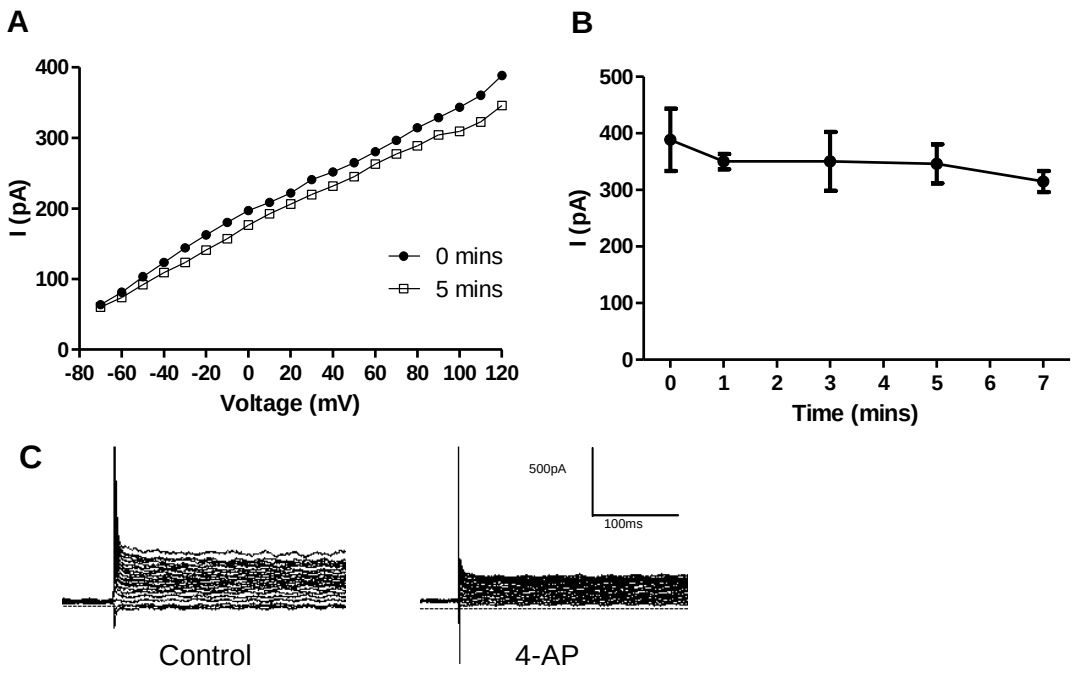

Figure 5.15: Current/voltage relationship in MCF7 cells treated with 4-AP

The voltage dependent current in MCF7 was elicited by whole cell patch clamping and a series of depolarizing voltage steps from a holding potential of -50mV, ramping from -70mV to 120mV in 10mV steps. After recording the initial (time = 0 minutes) current with no additional treatment, the cell was perfused with Tyrode containing 1mM 4-AP. The voltage sensitivity of the current was recorded again at various time points into the treatment. The effect of voltage on current is shown after 0 and 5 minutes treatment (A), and the time-course of the current at the potential which showed the greatest impact of treatment (120mV; mean and SD) is provided (B). Both graphs show the mean result of three MCF7 cells assessed on different days. Example traces before and after 5 minutes 4-AP perfusion are shown in C.

Table 5.5: Simple Effects Analysis of the impact of 4-AP on voltage sensitivity

Voltage	F	p	Voltage	F	p
-70	28.77	<0.05	**30**	144.73	<0.01
-60	47.85	<0.05	**40**	182.82	<0.01
-50	70.96	<0.05	**50**	218.48	<0.01
-40	77.98	<0.05	**60**	182.29	<0.01
-30	83.47	<0.05	**70**	199.31	<0.01
-20	84.48	<0.05	**80**	204.84	<0.01
-10	86.66	<0.05	**90**	202.49	<0.01
0	93.65	<0.05	**100**	365.74	<0.01
10	109.73	<0.01	**110**	405.73	<0.01
20	135.66	<0.01	**120**	203.16	<0.01

Treatment of MCF7 with 1µM AST for 5 minutes also resulted in a reduction of the voltage activated outward current (Figure 5.16). The reversal potential of these currents was approximately -30mV, suggesting that K^+ movement was responsible for a large part of it. The AST-sensitive current observed is shown in Figure 5.18. This confirms that hEAG and hERG are responsible for some of the K^+ current observed. Again this effect was rapid, acting within a minute of treatment, and the reduction in current was stable following this. However, analysis with GLM for repeated measures found that within individual cells the effect of AST treatment on the voltage sensitivity of the MCF7 macroscopic current failed to achieve significance, $F(17, 34) = 0.096$, $p \geq 0.05$.

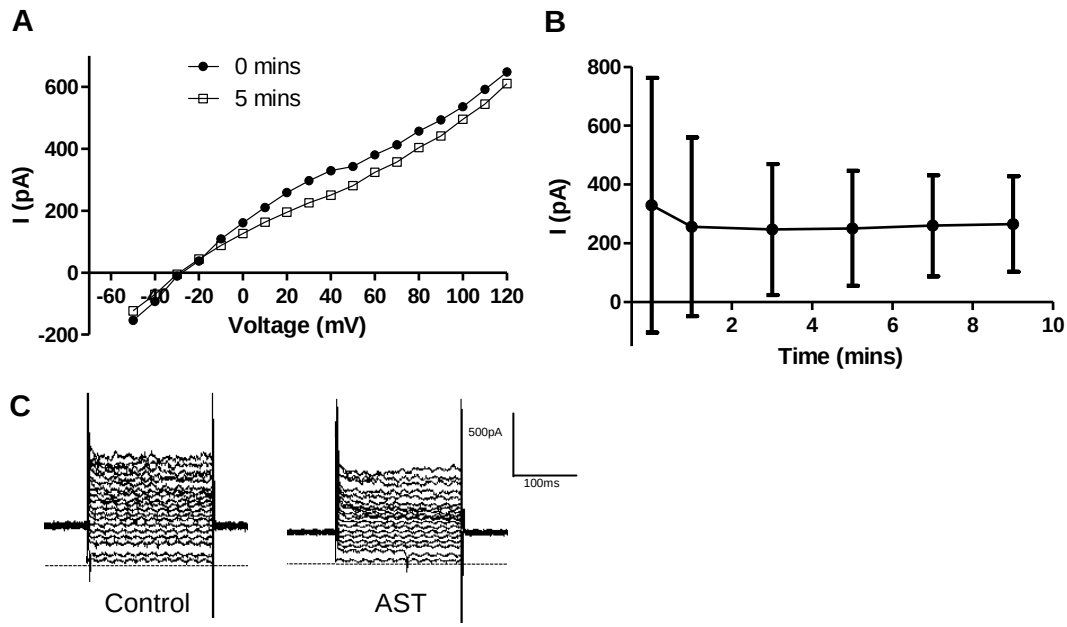

Figure 5.16: Current/voltage relationship in MCF7 cells treated with AST

The voltage dependent current in MCF7 was elicited by whole cell patch clamping and a series of depolarizing voltage steps from a holding potential of -50mV, ramping from -50mV to 120mV in 10mV steps. After recording the initial (time = 0 minutes) current with no additional treatment, the cell was perfused with Tyrode containing 1µM AST. The voltage sensitivity of the current was recorded again at various time points into the treatment. The effect of voltage on current is shown after 0 and 5 minutes treatment (A), and the time-course of the current at the potential which showed the greatest impact of treatment (40mV; mean and SD) is provided (B). Both graphs show the mean result of three MCF7 cells assessed on separate occasions. Example traces before and after 5 minutes perfusion with AST are provided in C.

There was no observable effect of 1µM DOF on the macroscopic current recorded in MCF7 at any voltage over the entire treatment period (Figure 5.17). The reversal potential of these currents were between -70 and -80mV, indicating that it was largely due to K^+ flux. GLM repeated measures analysis confirmed this, $F(19, 38) = 0.351$, $p \geq 0.05$. This indicates that the current AST-sensitive current observed above was mediated by the hEAG channel, and hERG had no measurable impact.

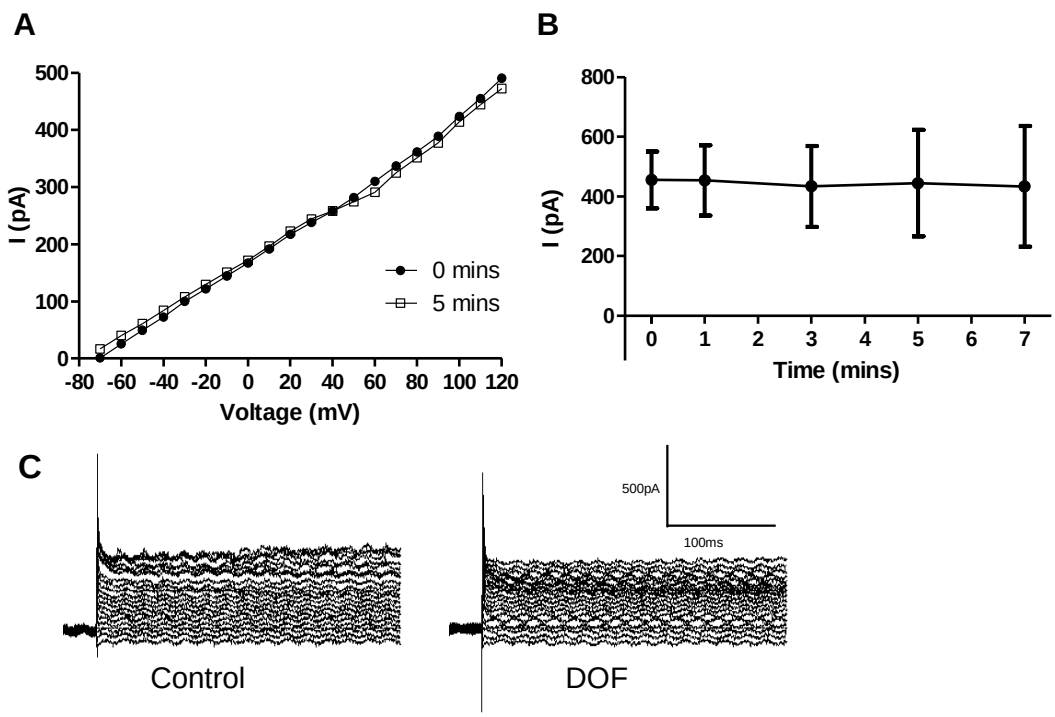

Figure 5.17: Current/voltage relationship in MCF7 cells treated with DOF

The voltage dependent current in MCF7 was elicited by whole cell patch clamping and a series of depolarizing voltage steps from a holding potential of -50mV, ramping from -70mV to 120mV in 10mV steps. After recording the initial (time = 0 minutes) current with no additional treatment, the cell was perfused with Tyrode containing 1µM DOF. The voltage sensitivity of the current was recorded again at various time points into the treatment. The effect of voltage on current is shown after 0 and 5 minutes treatment (A), and the time-course of the current at the potential which showed the greatest impact of treatment (110mV; mean and SD) is provided (B). Both graphs show the mean result of three MCF7 cells assessed on separate occasions. Example traces before and after 5 minutes perfusion with DOF are provided in C.

When the currents sensitive to the various channel blockers are compared (Figure 5.18), it is apparent that 10mM TEA has the greatest impact on macroscopic K^+ current in MCF7, inhibiting current at positive potentials and enhancing it at negative potentials.

Treatment with 1mM 4-AP has resulted in slight inhibition of an outward K^+ current, which becomes more active at more depolarized potentials. A similar profile to TEA treatment was achieved with 1µM AST, although smaller in magnitude. This suggests inhibition of a current which becomes active at depolarization to potentials of around -10mV or more positive. Finally, treatment with 1µM DOF did not inhibit macroscopic current in MCF7, having even less impact than the DMSO-only control.

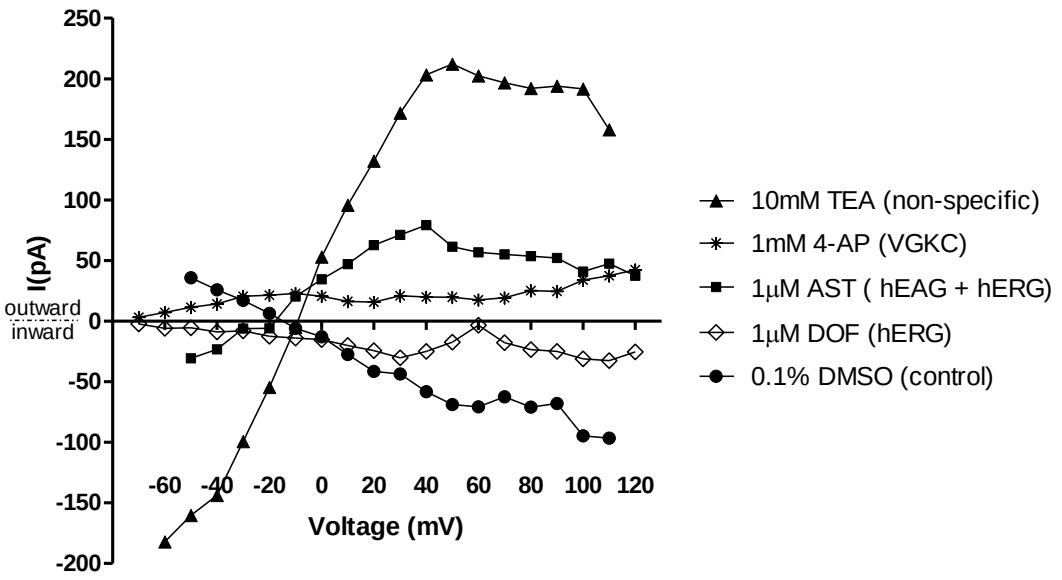

Figure 5.18: I/V relationships of potassium channel blocker sensitive currents

The voltage dependent current in MCF7 was assessed using a voltage stepping protocol as described. The I/V curve after 5 minutes treatment with various K^+ channel blockers (and 0.1% DMSO for reference) was subtracted from the current/voltage curve recorded prior to commencing treatment (time = 0 minutes) to show the element of the current that was sensitive to each channel blocker. The I/V curves shown are the mean of at least 3 cells.

5.3.4 Treatment with 17β-oestradiol enhances the MCF7 macroscopic current

Treatment of MCF7 cells with 1nM E2 for 5 minutes resulted in a significant increase in the voltage activated current (Figure 5.19A), $F(17, 34) = 7.927$, $p < 0.001$.

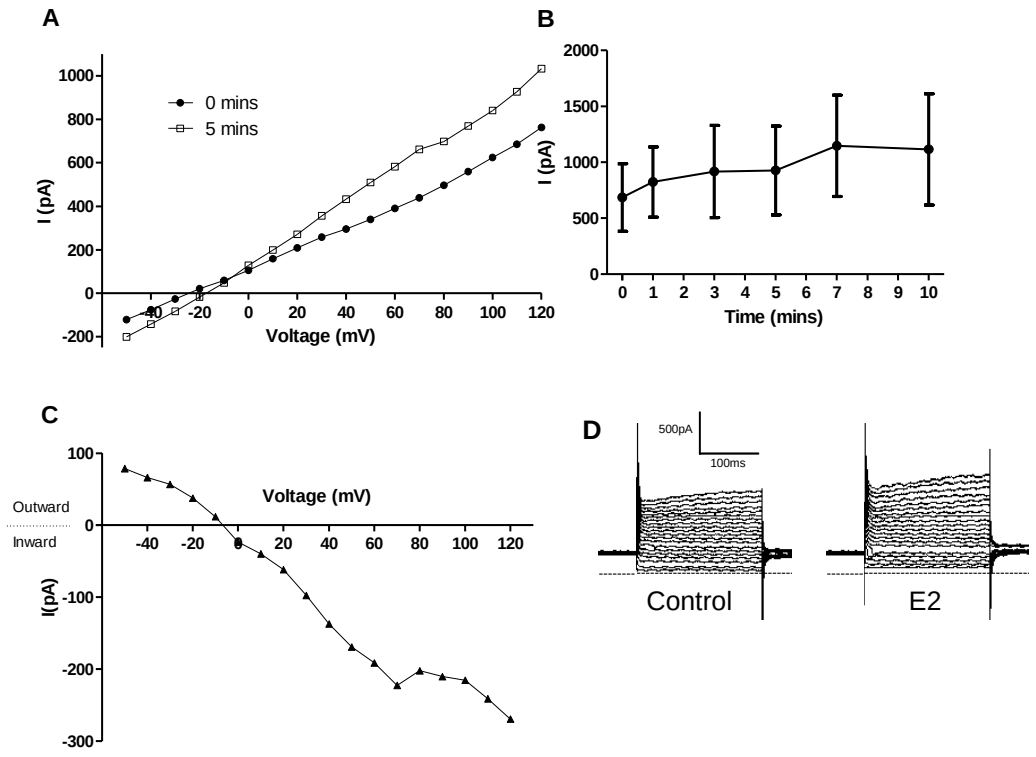

Figure 5.19: Current/voltage relationship of MCF7 cells treated with E2

The voltage dependent current in MCF7 was elicited by whole cell patch clamping and a series of depolarizing voltage steps from a holding potential of -50mV, ramping from -70mV to 120mV in 10mV steps. After recording the initial (time = 0 minutes) current with no additional treatment, the cell was perfused with Tyrode containing 1nM E2. The voltage sensitivity of the current was recorded again at various time points into the treatment. The effect of voltage on current is shown after 0 and 5 minutes treatment (A), and the time-course of the current at the potential which showed the greatest impact of treatment (50mV; mean and SD) is provided (B). The net effect of 5 minutes E2 treatment on the I/V response is shown in C. All graphs show the mean result of three MCF7 cells assessed on different days. Example traces before and after 5 mins perfusion with E2 are provided in D.

Further analysis found that the effect of treatment was significant at the within-cell level ($p < 0.05$) at depolarization to levels between 40 and 90mV (Table 5.6). The 5 minute E2-induced element of the current is shown in Figure 5.19C. The increase seen occurred rapidly (within 1 minute of treatment at 110mV) and continued rise beyond 5 minutes treatment (Figure 5.19B). Again, the reversal potential of the recorded currents was approximately -20mV, suggesting that K^+ was responsible for an element of this.

Table 5.6: Simple Effects analysis of the impact of E2 treatment on voltage sensitivity in MCF7

Voltage	F	p	Voltage	F	p
-50	2.21	NS	**40**	34.76	<0.05
-40	1.01	NS	**50**	74.6	<0.05
-30	0.27	NS	**60**	117.73	<0.01
-20	0	NS	**70**	101.51	<0.05
-10	0.26	NS	**80**	44.65	<0.05
0	1.43	NS	**90**	26.85	<0.05
10	3.55	NS	**100**	18.29	NS
20	8.11	NS	**110**	15.97	NS
30	15.47	NS	**120**	14.49	NS

5.3.5 Soy isoflavones inhibit the macroscopic MCF7 current

Treatment of MCF7 cells with 31.6µM genistein for 5 minutes resulted in a significant reduction in the voltage activated current (Figure 5.20), F (149, 38) =2.431, $p < 0.05$.

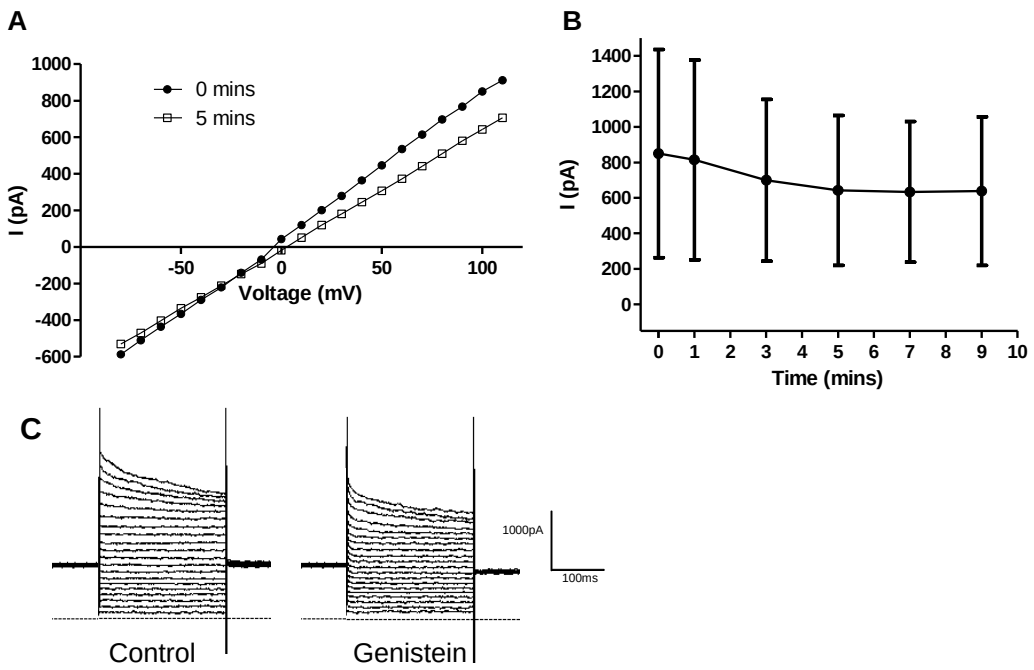

Figure 5.20: Current/voltage relationship in MCF7 cells treated with genistein

The voltage dependent current in MCF7 was elicited by whole cell patch clamping and a series of depolarizing voltage steps from a holding potential of -50mV, ramping from -70mV to 120mV in 10mV steps. After recording the initial (time = 0 minutes) current with no additional treatment, the cell was perfused with Tyrode containing 31.6µM genistein. The voltage sensitivity of the current was recorded again at various time points into the treatment. The effect of voltage on current is shown after 0 and 5 minutes treatment (A), and the time-course of the current at the potential which showed the greatest impact of treatment (100mV; mean and SD) is provided (B). Both graphs show the mean result of three MCF7 cells assessed on different days. Example traces from before and after 5 minutes genistein perfusion are provided in C.

However, further analysis of each individual depolarization level found that the effect of treatment failed to achieve statistical significance at any individual voltage point. The genistein sensitive current after 5 minutes is shown in Figure 5.22. The time-course of inhibition of macroscopic current at 100mV suggests that the inhibitory effect of genistein was slow to develop; taking 5 minutes to reach its maximum level (Figure 5.20B). The reversal potential of the currents recorded in these experiments averaged at around 0mV. These were the greatest (most positive) reversal potentials identified. This implies that while genistein treatment appears to inhibit K^+ current, it is likely that it inhibits the movement of other ions also.

Treatment of MCF7 with 31.6µM daidzein for 5 minutes resulted only in a very slight inhibition of voltage activated current (Figure 5.21A) which was not significant, $F(18, 36) = 1.295$. There was no clear effect over time (Figure 5.21B). The daidzein sensitive element of the voltage sensitive macroscopic current is shown in Figure 5.22. The reversal potentials of these currents were more negative, averaging around -20mV. This indicates that while K^+ flow was a factor in the current, it may also have other elements.

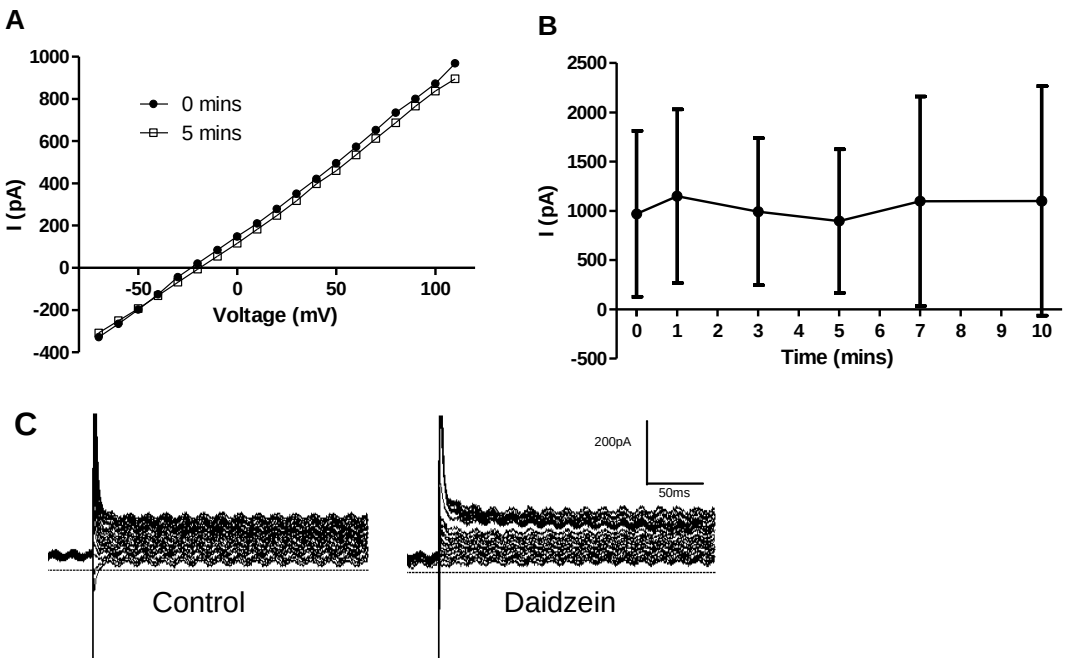

Figure 5.21: Current/voltage relationship in MCF7 cells treated with daidzein

The voltage dependent current in MCF7 was elicited by whole cell patch clamping and a series of depolarizing voltage steps from a holding potential of -50mV, ramping from -70mV to 120mV in 10mV steps. After recording the initial (time = 0 minutes) current with no additional treatment, the cell was perfused with Tyrode containing 31.6µM daidzein. The voltage sensitivity of the current was recorded again at various time points into the treatment. The effect of voltage on current is shown after 0 and 5 minutes treatment (A), and the time-course of the current at the potential which showed the greatest impact of treatment (110mV; mean and SD) is provided (B). Both graphs show the mean result of three MCF7 cells assessed on different days. Example traces from before and after 5 minutes perfusion with daidzein are provided in C.

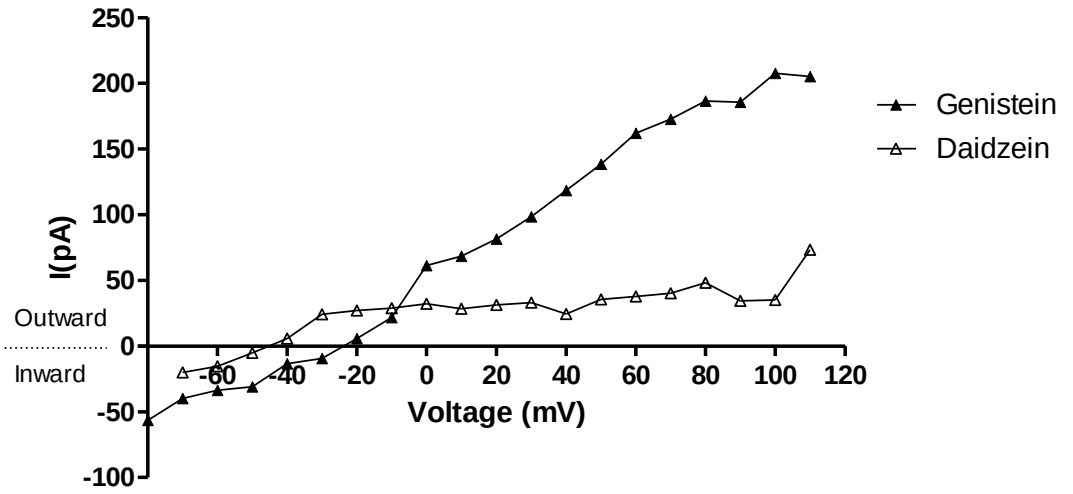

Figure 5.22: I/V relationships of isoflavone sensitive currents in MCF7

The voltage dependent current in MCF7 was assessed using a voltage stepping protocol as described. The I/V curve after 5 minutes treatment with genistein or daidzein (31.6µM) was subtracted from the current/voltage curve recorded prior to commencing treatment (time = 0 minutes) to show the element of the current that was sensitive to each isoflavone. The I/V curves shown are the mean result from 3 cells.

5.3.6 The impact of combinations of genistein and K^+ channel blockers on the macroscopic MCF7 current

To begin to elucidate which channels were the molecular targets of genistein in MCF7, the cells were treated with combinations of genistein and 4-AP or genistein and AST. TEA was considered too non-specific to provide any information regarding target specificity, and DOF had no measurable effect on K^+ current in this cell line.

Treatment of MCF7 cells for 5 minutes with the combination of 31.6µM genistein and 1mM 4-AP resulted in a slight increase in current at the more depolarized voltages tested (Figure 5.23A), although this effect did not achieve statistical significance, $F(19, 38) = 0.671$, $p \geq 0.05$.

The reversal potential of the current was between -50 and -60mV, indicating that it was largely due to movement of K^+ ions. Up to and including 5 minutes into the treatment regime, the current measured at 40mV was relatively stable, however after this point the seal began to lose integrity in two of the three cases (Figure 5.23B), suggesting that this combined treatment may have been toxic to the cells.

Overall the I/V curve for the element of the current sensitive to the combination of 4-AP and genistein was lower than that calculated for either genistein or 4-AP alone (Figure 5.23C), suggesting that rather than acting synergistically, the two treatments interfered with each others activity. However, the net impact of the combined treatment was not significantly different from either of the corresponding single treatments at any voltage ($p \geq 0.05$, ANOVA).

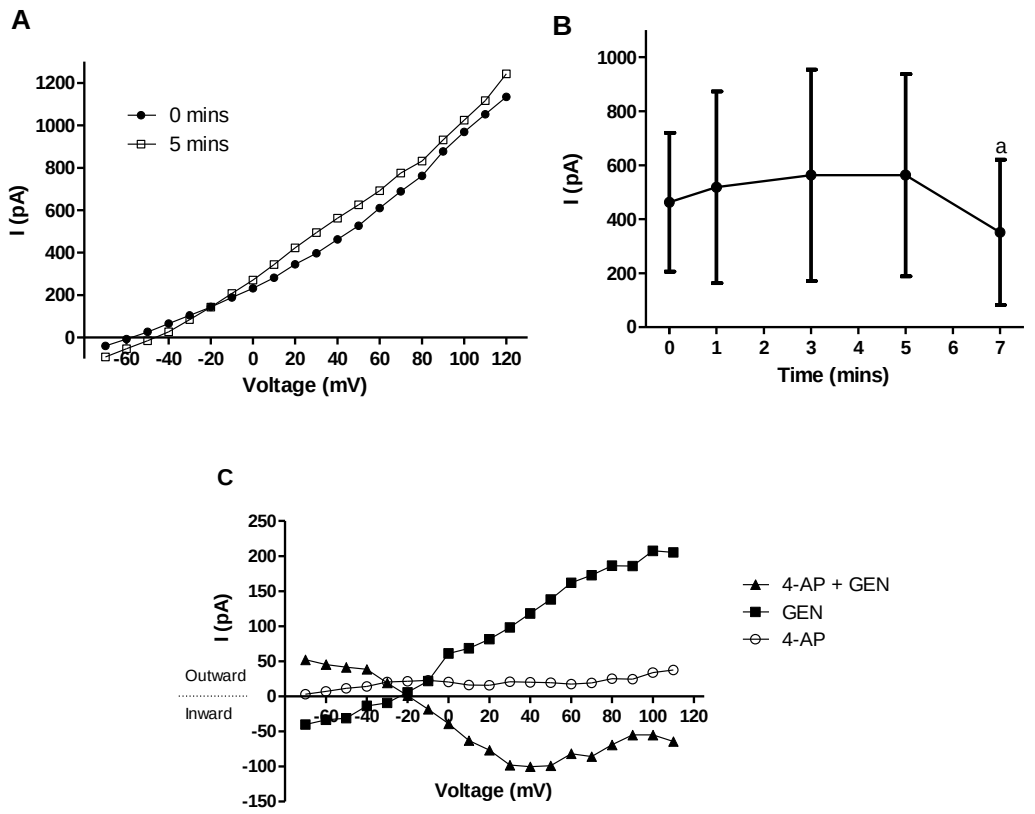

Figure 5.23: Current/voltage relationship in MCF7 cells treated with the combination of 4AP and genistein

The voltage dependent current in MCF7 was elicited by whole cell patch clamping and a series of depolarizing voltage steps from a holding potential of -50mV, ramping from -70mV to 120mV in 10mV steps. After recording the initial (time = 0 minutes) current with no additional treatment, the cell was perfused with Tyrode containing the combination of 31.6µM genistein (GEN) and 1mM 4-AP. The voltage sensitivity of the current was recorded again at various time points into the treatment. The effect of voltage on current is shown after 0 and 5 minutes treatment (A), and the time-course of the current at the potential which showed the greatest impact of treatment (40mV; mean and SD) is provided (B). C: the I/V responses of the elements of the current sensitive to the various treatments. Each graph shows the mean result of three MCF7 cells assessed on different days, with the exception of one point (a) for which n=2.

Treatment of MCF7 with the combination of 31.6µM genistein and 1µM AST led to a reduction in the depolarization-activated element of the macroscopic current after 3 minutes treatment (Figure 5.24A and B). However, the difference in the effect of voltage before and after the treatment failed to achieve significance, $F(18, 36) = 0.245$, $p \geq 0.05$. The reversal potential of this current was around -70mV suggesting that it was largely mediated by K^+ ion movement. After this time point the seal on the patched cells became unstable in two of the three cases. For this reason, the 3 minute time point was used for comparison in this case.

Recorded current was not significantly different after 3 minutes treatment with genistein compared to 5 minutes, with the sole exception of at 0mV (Table 5.7). The I/V curve for the genistein and AST-sensitive current at 3 minutes was similar to that obtained after 3 minutes treatment with 1µM AST alone or 31.6µM genistein (no significant differences, $p \geq 0.05$, ANOVA; Figure 5.24C). Since there was no additional effect of AST over that of genistein, this suggests that the hEAG channel is potentially a molecular target of genistein in MCF7. Furthermore, the combination of AST and genistein appeared to be particularly toxic to the cells in these experimental conditions.

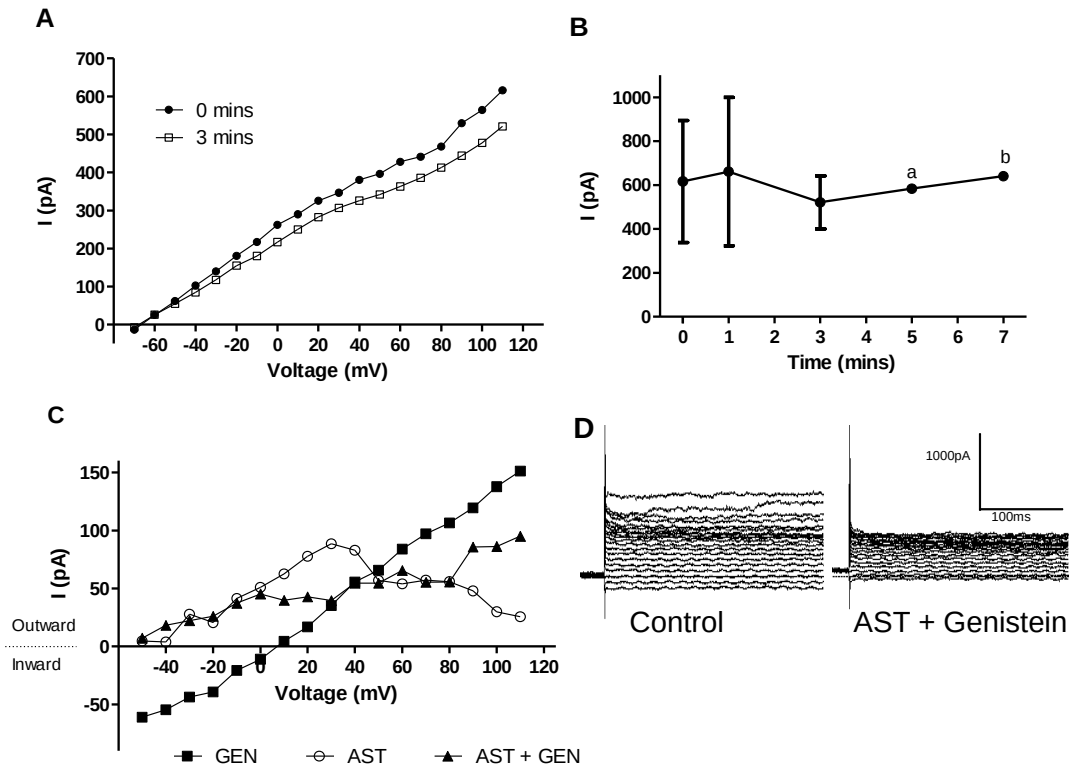

Figure 5.24: Current/voltage relationship in MCF7 cells treated with the combination of AST and genistein

The voltage dependent current in MCF7 was elicited by whole cell patch clamping and a series of depolarizing voltage steps from a holding potential of -50mV, ramping from -70mV to 120mV in 10mV steps. After recording the initial (time = 0 minutes) current with no additional treatment, the cell was perfused with Tyrode containing the combination of 31.6µM genistein (GEN) and 1µM AST. The voltage sensitivity of the current was recorded again at various time points into the treatment. The effect of voltage on current is shown after 0 and 3 minutes treatment (A), and the time-course of the current at the potential which showed the greatest impact of treatment (110mV; mean and SD) is provided (B). C: the I/V responses of the elements of the current sensitive to the various treatments. Each graph shows the mean result of three MCF7 cells assessed on different days, with the exception of the points indicated with a (n=2) and b (n=1). Example traces from before and after 3 minutes perfusion with AST + genistein are provided in C.

Table 5.7: Current recorded after 3 and 5 minutes of treatment with 31.6μM genistein

Voltage	3 minutes		5 minutes		p [1]
	Mean	SD	Mean	SD	
-80	-506.04	260.46	-530.33	204.89	NS
-70	-434.32	240.86	-470.85	185.38	NS
-60	-375.17	214.02	-402.62	156.03	NS
-50	-311.35	174.72	-335.03	128.94	NS
-40	-245.56	147.35	-275.93	101.07	NS
-30	-181.65	117.89	-211.44	83.21	NS
-20	-120.76	93.93	-147.22	66.92	NS
-10	-57.67	68.50	-90.42	46.32	NS
0	38.44	22.43	-18.36	26.01	< 0.05
10	102.65	34.21	51.00	37.32	NS
20	165.83	65.78	119.47	71.55	NS
30	223.30	94.81	180.41	103.02	NS
40	297.96	140.91	245.19	137.12	NS
50	361.78	181.91	307.18	171.06	NS
60	437.84	230.96	372.95	210.78	NS
70	508.50	279.66	442.19	258.28	NS
80	577.01	334.02	509.91	308.45	NS
90	628.92	390.13	580.90	376.05	NS
100	698.91	456.06	642.46	422.33	NS
110	769.94	525.52	705.97	480.32	NS

[1] *significance of difference between current recorded after 3 and 5 minutes (ANOVA)*

SD: standard deviation

5.4 Summary of the changes in MCF7 cell volume and K^+ channel activity observed

This section briefly summarizes the changes in MCF7 cell volume and K^+ channel activity recorded upon treatment with soy isoflavones or E2. For a full discussion of the results see sections 6.3 and 6.4.

Treatment of MCF7 for 10 minutes with 1nM E2 resulted in swelling of the cells. In parallel to this, a significant increase in voltage sensitive whole cell current was observed. Treatment of MCF7 with 1µM genistein (proliferative concentration) also increased cell volume. These treatments and responses are in line with the expected proliferative response.

On the contrary, short term treatment with the higher concentration of 31.6µM genistein resulted in a brief period of cell shrinkage, and inhibition of outward macroscopic MCF7 current. Daidzein treatment inhibited current also, although to a considerably lesser extent.

DOF treatment had no effect on MCF7 proliferation or whole cell current. However, the K^+ channel blockers TEA, 4-AP and AST each resulted in dose-responsive inhibition of MCF7 proliferation. This implicated the VGKCs, and in particular the hEAG channel in the proliferation of this cell line. To begin to determine if the inhibition of specific K^+ channels by soy isoflavones could be a mechanism through which they may be protective against breast cancer proliferation, preliminary attempts were made to characterize which K^+ channels were the specific targets of genistein. To this end, several combined treatments of K^+ channel blockers and genistein were used. The combination of 4-AP and genistein appeared to have a negative effect on the stability of the cells, and as a result lead to extraneous results that little can be concluded from. However, the combination of AST and genistein lead to comparable current inhibition to each individual treatment. This suggests that the hEAG channel (a target of AST) is likely to be a key molecular target of genistein in MCF7, and accordingly a potential mechanism through which genistein could reduce the proliferation of this cell line.

CHAPTER 6. Discussion

6.1 Isoflavones and breast cancer cell line proliferation

6.1.1 Technique: the MTT assay

A major criticism of the MTT assay (described in sections 1.4.2 and 2.4) and related techniques such as the MTS or WST-1 assays, is that they measure proliferation indirectly, by assessing the rate of metabolism (or viability) of the cells. While cell number will have a great impact on the quantity of MTT (or other dye) that is metabolised, other factors will also have an effect, such as the size and age of the cells, and the number of mitochondria. None-the-less, the above methods are less labour intensive, and higher throughput than the traditional alternative method of counting viable cells using the Trypan Blue dye exclusion assay.

A number of groups report that the MTT assay routinely overestimates viability or cell numbers when compared to other methods, in a number of cell types including human lung cancer cells (Carmichael et al. 1987; Ulukaya et al. 2008), Chinese hamster lung fibroblast V79 cells, and Manin–Darby canine kidney cells (Vellonen et al. 2004). The reasons behind this discrepancy are unclear, although it has been suggested that compared to Trypan Blue cell counting the MTT assay is more sensitive, as is not open to subjective errors by the observer. However, the two methods correlate well where they are both used (Carmichael et al. 1987; Simoes-Wust et al. 2002).

Another proposed limitation of the MTT assay is that isoflavones themselves may lead to an overestimation of the amount of growth or viability of the cells. This effect has been demonstrated in a number of cell types including MCF7 breast cancer cells, Jurkat cells, L-929 transformed mouse fibroblasts (Pagliacci et al. 1993) and lymphocytic leukaemia cells (Bernhard et al. 2003) with genistein, resveratrol, and quercetin at concentrations above 20µM. Very high concentrations (100µM genistein) appear to be able to reduce MTT even in the absence of cells (Bernhard et al. 2003). This may relate to the antioxidant capacity of the isoflavones, as this group found that vitamin C acted similarly. Others suggest that genistein at these concentrations may influence mitochondrial number and function (Pagliacci et al.

1993) and induce swelling in isolated rat mitochondria (Salvi et al. 2002). In each case the net result has again been an overestimation of viability by the MTT method. However, it must be noted that the very high concentrations of isoflavones which have been associated with this effect (>100µM) are not associated with the present study. Importantly, in MCF7 cells, the presence of genistein between 3.7 and 74µM was shown to have no impact upon mitochondrial reduction of MTT (Peterson and Barnes 1996).

On the contrary, numerous groups demonstrate unequivocally that concentrations of isoflavone phytoestrogens above 10µM reduce the proliferation of a range of breast cancer cell lines, including the MCF7 and MDA-MB-231 lines used in this study (section 1.4.5). Likewise, the effects of lower concentrations appear to relate to the ER-status of the cell line (sections 1.4.3 and 1.4.4), and there is no evidence of an overestimation of growth when the MTT assay has been used. Indeed, in the present investigation MDA-MB-231 cells treated with 1nM to 10µM genistein resulted in around 80% of the control level of proliferation when measured by the MTT assay (section 3.1.2..2), confirming that there was no inherent overestimation of proliferation associated with the MTT assay in this case.

To further validate the use of the MTT assay to accurately determine the extent of cell proliferation in this investigation, it was compared to the results of the Trypan blue dye exclusion assay in both MCF7 and MDA-MB-231 cells (see section 2.4.6). In each cell line, the correlations between cell number and optical density were positive and significant. Furthermore, others have found the results of the MTT assay and the Trypan blue dye exclusion assay to correlate well in the above two cell lines (Simoes-Wust et al. 2002). Altogether, this suggests that the MTT assay is a valid method to assess proliferation under these circumstances, and that the concerns discussed regarding overestimation of proliferation appear to be unfounded.

6.1.2 The solvent and control treatments

Due consideration was given to the choice of solvent used for the isoflavones and E2, and the concentration of solvent to be present in the control (vehicle only) experiments. Ethanol was rejected as a solvent despite its wide use (Table 1.3) as preliminary investigations found it to promote MCF7 proliferation (Figure 2.3). These results agree with those of Singletary et al. (2001), who demonstrated that ethanol, at a range of physiologically relevant concentrations (10 to 100 mM) can induce the proliferation of MCF7 cells. This is likely to have implications for some of the other work discussed where groups have used ethanol as a solvent and control treatment.

Furthermore, it was apparent that DMSO inhibited MCF7 proliferation in a dose-responsive manner (Figure 2.3). However, compared to an untreated control, doses of DMSO up to and including 0.2% were found to have no significant impact on the proliferation of MCF7 (Figure 3.1). As 0.1% DMSO was the most widely used solvent and dose in previous studies (Table 1.3), it was felt that levels of 0.1% and 0.2% were appropriate for use in the current investigation, and that they would impart minimal impact on the proliferation of the cells. The related studies presented by Umehara et al. (2009) and Cherdshewasart et al. (2008) describe using DMSO in MCF7 cells at 1 and 2% respectively. These doses are likely to be toxic and may interfere with the results. Interestingly, Blom et al. (1998) found that 0.8 and 1% DMSO decreased MCF7 cell proliferation, but 0.1 to 0.6% DMSO had a growth promoting effect. They propose a reason for this: since proliferation was assessed after only 24 hours in the experimental medium, in some cases the cells may have still been in the initial “lag” phase of growth, while in others they may have passed more quickly into the “exponential” growth phase. The effect of various organic solvents on MCF7 proliferation does not appear to have been published on any other occasions.

Use of 0.1% DMSO in MDA-MB-231 cells had no significant impact upon proliferation, but 72 hour treatment with the 0.2% dose resulted in a significant, if slight, reduction in cell proliferation (Figure 3.5). There do not appear to be any instances where the impact of solvents on the proliferation of this cell line has been published. Use of the 0.2% DMSO dose was unavoidable in the combined treatments, due to limitations in the solubility of the isoflavones. The additional

impact upon the level of MDA-MB-231 cell proliferation of this level of solvent over and above that of any treatment, must be considered in the analysis of the results. Furthermore, in two of the MDA-MB-231 proliferation studies discussed, 0.2% DMSO was used for the vehicle-only control treatment (Jacobs et al. 2000; Seo et al. 2011), and may have had an unforeseen effect on their results. When considering the current results for this cell line, and indeed for the MCF7 cells, in the context of other published studies, it is essential to note the choice and dose of solvent used, the presence or absence of experimental controls, and the potential impact this may have on the results.

6.1.3 MCF7 proliferation – single isoflavone and 17β-oestradiol treatments

The results of the single treatments of genistein, daidzein and E2 on MCF7 (ERα+) proliferation were very much in line with previous findings. Both the pre- and post-menopausal E2 doses resulted in a significant increase in proliferation (Figure 3.2). This confirmed that the MCF7 cells obtained were capable of responding to E2 in the manner expected and described on numerous occasions (Davis et al. 2008; Jacobs et al. 2000; Lau et al. 2009; Matsumura et al. 2005; Rajah et al. 2009; Schmidt et al. 2005; Song et al. 2007). Furthermore, this acted as a positive control for the induction of MCF7 proliferation, allowing optimisation of the assay and confirming that the protocol used was appropriate for the measurement of changes in the proliferation of this cell line.

Likewise, the effects of the single isoflavone treatments on MCF7 proliferation (Figure 3.3) confirmed previous findings, whereby doses up to 10μM genistein and daidzein increased proliferation in a dose responsive manner (Hwang et al. 2006; Kang et al. 2009; Liu et al. 2010; Maggiolini et al. 2001; Matsumura et al. 2005; Seo et al. 2006; Yang et al. 2010; Yuan et al. 2012), and at concentrations above this point proliferation begins to drop (Table 1.4).

The proliferative effects of genistein and daidzein are mediated, at least in part, through their ability to bind with and induce E2-like transcription of genes through ERα (Hwang et al. 2006; Kuiper et al. 1998; Maggiolini et al. 2001), the dominant ER in MCF7 (Section 1.1.4). Typically, they bind to ERα with around a hundred to thousand-fold lower affinity than E2. The relative binding affinities (RBAs) compared to E2, and the ability of the soy isoflavones and E2 to induce the binding of the ERs to the oestrogen responsive element (ERE; a conserved region of oestrogen induced gene promoters), as a measure of the ability of the various ligands to induce ER-mediated transcription, are provided in Table 6.1.

The more strongly an isoflavone binds to an ER, the more effective it is at inducing E2-responsive transcription of reporter genes or proliferative genes (Hwang et al. 2006; Kuiper et al. 1998; Sotoca et al. 2008). This was reflected in the proliferation results, with approximately a thousand-fold more isoflavone required to induce a comparable proliferation response to E2 (1μM compared to 1nM). Furthermore, the

lower maximum impact of daidzein on MCF7 proliferation than genistein may reflect its lower ERα RBA.

Table 6.1: Ability of isoflavones and E2 to bind to the ERs and induce ER-ERE interaction

Ligand	ERα		ERβ	
	RBA[1]	ER-ERE EC_{50}[2]	RBA[1]	ER-ERE EC_{50}[2]
17β-oestradiol	100	0.03	100	0.01
Genistein	3.10	50	18.13	0.03
Daidzein	0.25	>300	0.79	0.35

[1] *RBA – relative binding affinities of isoflavones, calculated as a ratio of the concentration required to displace radiolabelled [^{3}H]-E2 by 50% from ERα in a liquid phase competition binding assay (Hwang et al. 2006)*

[2] *EC_{50} – in μM, the half maximal concentration of the ligand determined for promoting the interaction between the ER and the oestrogen response element (ERE), using Surface Plasmon Resonance (Kostelac et al. 2003). Note: this technique uses purified receptors and ligands, so concentrations may not be an exact reflection of the response in vivo or in cell culture.*

The magnitude of the peak effect of genistein was in the range expected. In the current study peak genistein-induced proliferation was at 178% of the control level after 3 days treatment with 10μM isoflavone. Similarly, previous studies using the MTT assay reported MCF7 proliferation of approximately 300% (after 6 days of 1μM genistein treatment) and 180% (after 3 days of 3.2μM genistein) of the control level (Maggiolini et al. 2001; Yuan et al. 2012).

As described in Table 1.4, the growth inhibitory effects of genistein in MCF7 cells were reported after a range of different treatment durations and isoflavone concentrations, between 1 and 14 days, and with 3.5μM up to 50μM genistein required to see an inhibitory effect. However, in two cases, although proliferation had peaked at a lower concentration and was dropping with increasing genistein dose, the proliferation recorded at the maximum dose was still greater than that of

the control treatment (50uM and 80uM respectively; Liu et al. 2010; Yuan et al. 2012). The results of the current investigation sit in approximately the middle of this range. While proliferation had peaked at 1µM (daidzein) and 10µM (genistein), and was dropping, no net inhibitory effect of either was recorded even at the highest concentration used of 31.6µM. Extrapolation of the graph suggests that an inhibitory effect would be seen with higher concentrations, but as the purpose of this project was to investigate the impact of physiological concentrations of isoflavones, and the stated issues regarding isoflavone solubility and vehicle doses, this was not pursued.

Overall, this implies that the results of 72 hour treatment with genistein and daidzein (single treatments) on MCF7 proliferation, assessed by the MTT assay, agree with the many other studies in this field. As was the intention, this confirms the ability of the cell line to respond to these treatments at their physiological (dietary) levels, and indicates that the assay and protocol described are appropriate for their intended use.

6.1.4 MCF7 proliferation after combined treatments

Genistein or daidzein at the range of physiological concentrations tested, in combination with E2 at the postmenopausal level, had a synergistic, additive effect on MCF7 proliferation, which achieved statistical significance in numerous cases (Figure 3.4). Where the isoflavones were added in combination with a premenopausal E2 level, the results were less dramatic. Although higher than either the isoflavone or E2 treatments alone, the magnitude of this effect was less than was observed with the lower, postmenopausal E2 concentration, and in many cases (genistein and premenopausal E2 particularly) failed to achieve statistical significance from the single treatments. This is summarized in Figure 6.1.

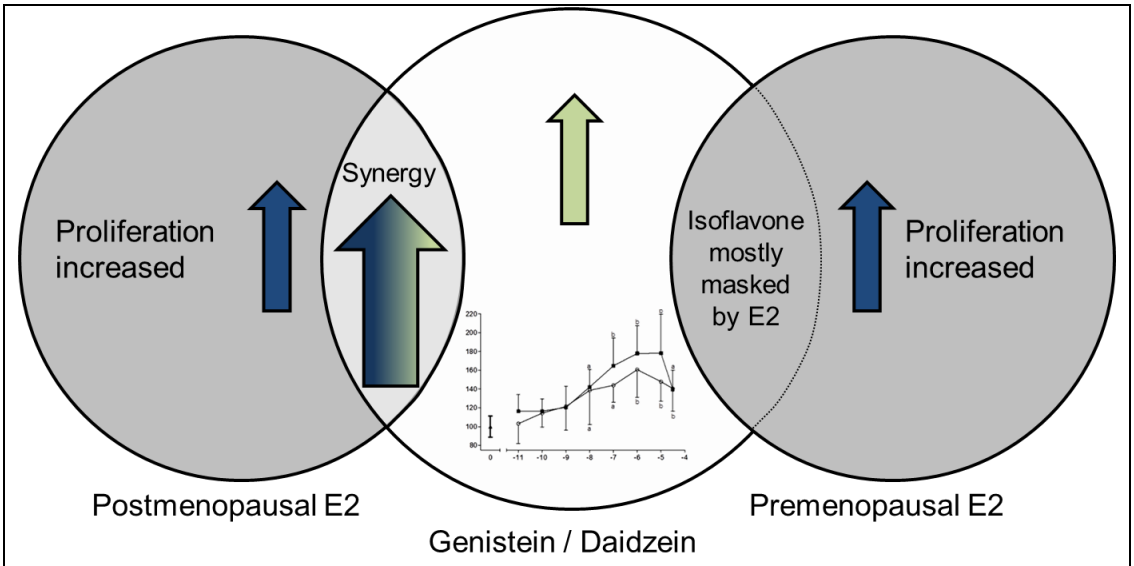

Figure 6.1: MCF7 proliferation after treatment with isoflavone/E2 combinations

The single treatments of genistein, daidzein or E2 (at pre- or postmenopausal levels) each induced MCF7 cell proliferation. In combination, the effect of the isoflavones was mostly masked by the stronger proliferation-enhancing effect of the premenopausal E2 level (1nM), although there was a slight additive effect. However the postmenopausal E2 level (1pM) and isoflavones showed a clear synergistic effect on MCF7 proliferation.

This is the first instance, according to the published literature, that the impact of genistein and daidzein on the proliferation of MCF7 cells has been determined in a full range physiologically relevant isoflavone and E2 concentrations. Much of the

previous research has used the higher E2 levels, better reflecting premenopausal women, genistein only, or selected isoflavone concentrations rather than a physiological range. The majority of the evidence supporting the role of isoflavones in postmenopausal E2 concentrations on cell proliferation is based on ER-mediated reporter gene transcription rather than proliferation itself. There are no previous studies available where the effect of low physiological concentrations of daidzein on the proliferation of any breast cancer cell line at postmenopausal E2 levels has been discussed.

The synergistic effect of genistein and daidzein with postmenopausal E2 levels on MCF7 proliferation is in agreement with the reported additive effect of 10pM E2 and daidzein (and several of its metabolites including equol and tetrahydrodaidzein) between 1nM and 1μM on the activity of an ERα promoter reporter gene construct in HEK239 cells (Hwang et al. 2006). Genistein was not tested on that occasion, and while this group claimed that similar results were seen for MCF7 cell proliferation, they did not publish their results. Likewise, these results are strengthened by the increase in DNA synthesis seen in MCF7 after treatment for 24 hours with genistein and postmenopausal E2 levels compared to E2 (10pM) alone (Wang and Kurzer 1998).

As previously discussed (Section 1.4.6), many of the other studies published in this field have used isoflavones with premenopausal E2 (10 to 0.1 nM) concentrations, and their results fail to reach a consensus. The confusing state of the literature appears to reflect the varying experimental conditions and outcome measures used. Low concentrations of isoflavones can act as ER antagonists in ERα+ cell lines such as MCF7, dampening its effect due to their high concentrations but lower oestrogenic activity (Casanova et al. 2012; Hwang et al. 2006). Alternately, in some experimental situations the effect of the isoflavones is masked by the stronger effect of E2 (Matsumura et al. 2005; Schmidt et al. 2005). Meanwhile, higher isoflavone concentrations (>10μM) inhibited proliferation in a manner which was not mediated by the ERs, and unaffected by the presence of E2 (section 1.4.6). It is important to note that several of the key studies described have used ER-mediated expression of a reporter gene as their outcome measure (Casanova et al. 1999; Hwang et al. 2006). This may not be the only mechanism through which isoflavones impact upon cell proliferation.

Accordingly, it has been reported that 10µM glycitein (and genistein and daidzein to a lesser extent) resulted in considerably reduced MCF7 proliferation compared to the vehicle-only control, even in the presence of 10nM or 0.3nM E2 (Sakamoto et al. 2010; Zava and Duwe 1997). Alternately, a number of groups suggest that treatment with 10µM genistein and other isoflavones can reverse the growth promoting effect of premenopausal E2 levels on MCF7 cells, resulting in no net change in proliferation compared to a control (Maggiolini et al. 2001; Matsumura et al. 2005; Miodini et al. 1999; Peterson and Barnes 1996; So et al. 1997; Wang and Kurzer 1998). Similarly, tetrahydrodaidzein (1nM to 1µM) inhibited 1nM E2-induced activation of the ERα promoter reporter gene construct described by Hwang et al. (2006). Finally, there exists a third body of evidence suggesting that any effect of isoflavones (0.1nM to 1µM) on MCF7 proliferation (and the activity of an E2-responsive reporter gene construct transfected into MCF7) is masked by the presence of 1nM E2 (Matsumura et al. 2005; Schmidt et al. 2005; Wang and Kurzer 1998).

With the current results, the trend towards a reduction in MCF7 proliferation by the highest concentrations of genistein and daidzein is still apparent in the presence of both 1pM and 1nM E2 levels, although as with the single isoflavone treatments, higher doses would be required to see inhibition of proliferation compared to the vehicle-only control. However, this agrees with the investigations described above, suggesting that higher concentrations of isoflavones could reverse E2-induced MCF7 proliferation, in this case at both pre- and post-menopausal E2 concentrations. However the isoflavone levels required for observation of these effects would be outwith the range of physiologically relevant concentrations which are the focus of this project.

The combinations of isoflavones with the premenopausal E2 level generated some interesting results with regard to MCF7 proliferation. No oestrogen-antagonistic activity was observed, unlike several of the studies described. However, the reduced synergy observed with the premenopausal E2 combinations, in comparison to the postmenopausal E2 combinations, particularly with genistein, bears a marked resemblance to several other studies which proposed that any effect of isoflavones on the proliferation of MCF7 was negated by the stronger E2 effect of this concentration (Matsumura et al. 2005; Schmidt et al. 2005; Wang and Kurzer 1998). Furthermore, it was reported that with postmenopausal E2, isoflavones acted

synergistically on E2-responsive promoter activity, but when premenopausal E2 was added the isoflavones inhibited the effect of E2 (Casanova et al. 2012; Hwang et al. 2006). A mechanism for the reduction in premenopausal breast cancer risk described in section 1.3.1 cannot be directly inferred from these results. However, they do imply that premenopausally, isoflavones may confer no additional breast cancer risk (or only a slight increase) over and above the carcinogenic effect of endogenous oestrogens.

A criticism of a number of the studies previously described is that either the final solvent content is not provided, or it greatly exceeds the 0.2% DMSO level used in this study (see Table 1.3; Hwang et al. 2006; Maggiolini et al. 2001; Peterson and Barnes 1996; Sakamoto et al. 2010; So et al. 1997). In two cases, an untreated control was used (Miodini et al. 1999; Schmidt et al. 2005), and others did not report the make-up of their control treatment (Wang and Kurzer 1998). As discussed in section 6.1.2, use of these levels of solvent may have unforeseen effects on proliferative outcome measured.

However, overall, this data suggests that genistein and daidzein, at a range of physiologically achievable concentrations between 0.01nM and 31.6µM, are capable of inducing the proliferation of MCF7 cells over and above that seen with postmenopausal E2, and to a lesser extent with premenopausal E2. There is no evidence from this current project to suggest that either isoflavone can reduce oestrogen-induced proliferation of the MCF7 cell line, although higher, non-physiological concentrations may have this effect. This appears to suggest that soy isoflavones could increase the proliferation of ERα+ (medically classified as ER+) breast tumours, particularly among postmenopausal women (the group most likely to consume isoflavone supplements for the relief of menopausal symptoms; see Section 1.2.5). This supports the advice provided by UK Health Boards contraindicating use of isoflavone supplements in post menopausal breast cancer survivors (NICE 2009b).

Based in the results of this one cell line, there is no explanation for the discrepancy between the epidemiological evidence, which suggests that consumption of soy isoflavones can reduce the risk of incidence, mortality, and recurrence, particularly for ERα+ tumours (see Sections 1.3.1 and 1.3.5), and the *in vitro* evidence from ERα+ cell lines discussed. However, the increased benefit of dietary soy seen for

premenopausal breast cancer, compared to postmenopausally, may be partly explained by the reduced additional proliferative capacity of the isoflavones in MCF7 over the effect of the higher dose of E2, in comparison to the clearly oestrogen agonistic synergistic behaviour seen at the lower postmenopausal E2 level. Furthermore, it is important to note that there is no epidemiological evidence for any health risks associated with dietary soy. However, the long term safety of the higher isoflavone intakes associated with supplement use has yet to be determined (Section 1.2.6).

6.1.5 MDA-MB-231 proliferation - single treatments of isoflavones and 17β-oestradiol

The effect of E2 on the proliferation of MDA-MB-231 cells has not been widely assessed, as they have traditionally been regarded as ER- and so not responsive to E2. However, as discussed, they do express ERβ (Section 1.4.1). The current finding, whereby 72 hour treatment with 1nM E2 had no significant impact on the proliferation of this cell line (Figure 3.6), is in agreement with previous research showing that 1 and 10nM E2 (72 hours; Rajah et al. 2009), and that 1nM treatment (5 to 14 days; Jacobs et al. 2000) did not affect MDA-MB-231 cell proliferation.

This was the first study to assess MDA-MB-231 cell proliferation after treatment with the lower (postmenopausal) level of 1pM E2. This treatment reduced proliferation to 77% of the control level. One explanation for the apparent disparity between the results of the two E2 levels is that 1nM E2 treatment did result in a reduced mean level of percentage proliferation (86%) compared to the control, but that the individual results were particularly variable for this treatment (see Table 3.3) and the net effect failed to achieve statistical significance.

This investigation showed a slight, if non-significant reduction in MDA-MB-231 cell proliferation after 72 hour genistein treatment at its range of physiological levels from 0.01nM up to 10μM (Figure 3.7). This agrees with the only other similar study in this field to use a wide range of physiologically achievable genistein levels (Rajah et al. 2009).

There exists a greater body of evidence to support the sharp drop in MDA-MB-231 cell proliferation observed after 72 hour treatment with 31.6μM genistein (Figure 3.7). Related studies have shown that genistein treatment, at a range of relatively high concentrations between 25 and 100μM (between 1 and 3 days) reduced the proliferation of this cell line to approximately 50% of the control level (Ferenc et al. 2010; Kang et al. 2009; Li et al. 2008; Rajah et al. 2009; Seo et al. 2011). Apigenin and quercetin were reported to have no impact upon MDA-MB-231 cell proliferation after 3 day treatment with 1 or 10μM, but again 100μM treatment of either caused a dramatic reduction in MDA-MB-231 proliferation (Seo et al. 2011).

The impact of daidzein on MDA-MB-231 proliferation was broadly similar to that of genistein, both in pattern and magnitude (Figure 3.7). This study represents the first

instance where the effect of daidzein on MDA-MB-231 proliferation has been reported.

As discussed in section 1.4.4, the relative levels of ERα and ERβ may explain the differences seen in proliferative differences between ERα+ MCF7 cells (expressing a small amount of ERβ) and ERα-/ERβ+ MDA-MB-231 cells: with ERα mediating many of the pro-proliferative effects of E2 and the isoflavones (up to 10μM), while through ERβ these treatments have a negative impact on proliferation. Meanwhile, the universal cytotoxic effects seen with higher isoflavone concentrations, above 10μM, are independent of the ERs (section 1.4.5).

Microarray analysis revealed that the two receptors regulated the expression of distinct sets of genes in response to E2 treatment, both positively and negatively, and that only half of the E2-regulated genes were common to both receptors (Chang et al. 2006). Among the genes known to be differentially regulated in this manner are a number with roles in cell cycle regulation. Cyclin D1 is a cell cycle progression gene. In the models described above (breast cancer cell lines with and without ERβ transfection), and in ER- HeLa cells transfected either ER, E2 enhanced cyclin D1 expression through ERα. However, through ERβ, E2 inhibited cyclin D1 expression, even in the presence of ERα (Liu et al. 2002; Paruthiyil et al. 2004; Strom et al. 2004). Associated with this was differential regulation of the cell cycle progression genes cyclin E, CDK25a and $p45^{skp2}$, and the cell cycle inhibitor p27 (Strom et al. 2004). Interestingly, ERβ potently activated the cyclin D1 promoter after treatment with the antioestrogens ICI 182780, tamoxifen or raloxifene, suggesting a regulatory role for ERβ on ERα induced activation of pro-proliferative gene targets (Liu et al. 2002; Paruthiyil et al. 2004).

These factors may be significant to the protective effects of isoflavones on breast cancer cells, as while ERα is the dominant receptor subtype in most tumours and the MCF7 cell line (Balfe et al. 2004; Kurebayashi et al. 2000; Ziv et al. 2004), ERβ is often present also, and isoflavones are known to bind to it with greater affinity than to ERα (Table 6.1). In addition, isoflavones may also have stronger transcriptional-inducing activity through the ERβ receptor. Specifically, genistein creates an Activation Function-2 (AF-2) surface on ERβ which recruits the GRIP1 co-activator (activating regulatory protein) more efficiently than on ERα, while 17β-oestradiol promotes GRIP1 recruitment non-selectively to both ERs (An et al. 2001).

However, while the negative regulatory effect of physiological levels (up to 10µM) of isoflavones and E2 on cell proliferation can be explained by the presence of ERβ in the MDA-MB-231 cell line, the absence of any dose-effect of the isoflavones up to 10µM, observed in the current study and by Rajah et al. (2009) is interesting. On several occasions, maximal activity of ERβ-luciferase induction by genistein was reported to be three times greater than was seen with E2 (Legler et al. 1999; Sotoca et al. 2008). This was due both to the relatively high affinity of the isoflavone for that particular receptor, and the higher ERβ receptor-mediated induction of gene expression by genistein described, and led to the term "superagonist" being coined for isoflavones such as genistein acting *via* ERβ (Legler et al. 1999). If, due to "superagonism", maximal isoflavone/ERβ mediated inhibition of MDA-MB-231 proliferation had been achieved at a lower concentration threshold that was not tested, then no dose effect would be observed. This corresponds with the epidemiological studies discussed earlier (section 1.3.1), which found no dose effect for breast cancer incidence other than the difference between the highest and lowest soy consumers. This again suggests a threshold isoflavone level is required to achieve a protective effect.

This phenomenon is of significance to the use of isoflavones in the treatment of ERα-/ERβ+ breast cancer, and warrants further study. In particular, it is necessary to determine the impact of ER antagonists on the inhibition of MDA-MB-231 proliferation by low dose isoflavones, to confirm the role of ERβ in this. Regrettably no specific ERβ antagonists have yet been developed, however several specific ERβ agonists exist which may be interesting to test, referred to as SERM-beta1 and SERM-beta2 (Clark et al. 2012). Furthermore, it would also be of value to investigate the effect on proliferation of transfecting the MDA-MB-231 cell line with ERα or silencing the ERβ gene in this cell line with siRNA. An alternate line of study would be to assess the impact of soy isoflavones on mammary tissue and mammary tumourigenesis in the βERKO (ERβ knockout) mouse line. This could be compared to wild-type mice, but regrettably the αERKO mouse line would not be appropriate for use, as these mice do not develop mammary glands beyond the rudimentary ductal structure which is present from birth (Hewitt and Korach 2003).

.

6.1.6 MDA-MB-231 proliferation after combined treatments

With the exception of the combination of premenopausal E2 concentration (1nM) and genistein at a range of physiological concentrations (Rajah et al. 2009), the impact of combinations of genistein or daidzein with pre- or post-menopausal E2 concentrations on MDA-MB-231 cell proliferation does not appear to have been previously investigated.

The synergy reported by Rajah et al. between genistein and 1nM E2 to inhibit MDA-MB-231 proliferation to a greater extent than either as single treatments, was not present in this investigation, and so consequently, their suggestion that genistein-ERβ / E2-ERβ heterodimers may be more effective at reducing proliferation than genistein-ERβ homodimers is unlikely to be the case. Indeed it is possible that the opposite occurs, and the heterodimer has less impact than the isoflavone-ERβ homodimers, although there is no evidence to support this.

The current results indicate that for the combinations of 1nM E2 with genistein or daidzein (≤ 10µM), and 1pM E2 with genistein, any inhibitory effect on MDA-MB-231 proliferation induced by the corresponding single treatments has been lost in combination (Figure 3.8). However, with the combinations of daidzein and 1pM E2 there was still a trend towards reduction in proliferation, to around 70% of the control value, although these comparisons were non-significant. Furthermore, these values were lower than either the daidzein (≤ 10µM) or 1pM E2 as single treatments (i.e. proliferation was reduced to approximately 90% and 77% with daidzein and E2 respectively; although again the comparisons failed to achieve statistical significance) suggesting possible synergy between the two compounds. This is summarized in Figure 6.2.

In all but one case (31.6µM daidzein and 1nM E2) the combined treatments including the highest isoflavone concentrations continued to demonstrate the drop in proliferation associated with 31.6µM isoflavone alone, although this drop was less dramatic than that seen with the single isoflavone treatments. As this effect occurs regardless of the ER status of the cell line, and does not appear to be mediated by the ERs (see Section 1.4.6), it is not surprising that it was still apparent here. Again, this effect was observed in the only comparable investigation, where genistein (≥25µM) in the presence of 1nM E2 resulted in a sharp decrease in MDA-MB-231 proliferation (Rajah et al. 2009). Why this effect would be apparent but muted in the current investigation is not known, however it may have been obscured by the

variability of the data generated, as evidenced by the large standard deviations calculated for the mean results.

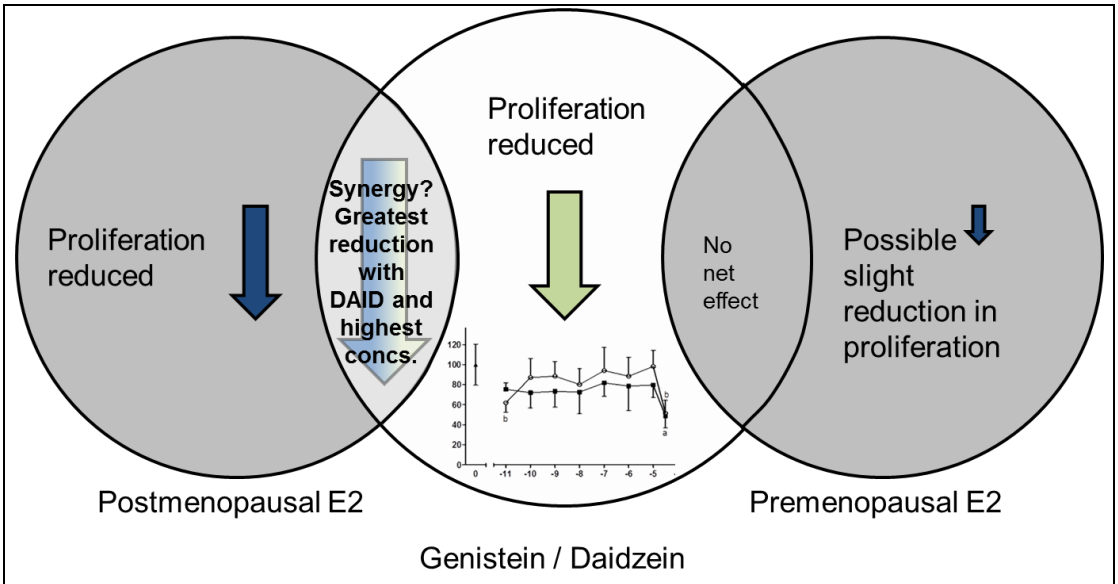

Figure 6.2: MDA-MB-231 proliferation after treatment with isoflavone/E2 combinations

The single treatments of genistein, daidzein or postmenopausal E2 each reduced MDA-MB-231 cell proliferation. In combination with premenopausal E2 (1nM) the inhibitory effect of the isoflavones was largely lost. However the postmenopausal E2 level (1pM) and some of the isoflavone treatments (in particular daidzein and the highest concentrations used) showed a slight synergistic effect on the inhibition of cell proliferation.

An explanation for the apparent interference between the isoflavones and E2 in MDA-MB-231 may be that the isoflavones (particularly daidzein) are acting as oestrogen agonists at low (1pM) doses of E2, further contributing to any ERβ-mediated proliferation inhibitory effect. However, at higher (1nM) E2 concentrations they become antagonistic, competing with E2 for ERβ binding sites, due to their high affinity for the receptor, and weakening the effect of E2. This suggestion is supported by the results of Hwang et al. (2006). Their paper describes a situation where human embryonic kidney (293) cells were transfected with either ERα or ERβ tagged with a luciferase reporter gene and treated with premenopausal (1nM) or postmenopausal (10pM) E2 concentrations, and daidzein or its metabolites, including equol and tetrahydrodaidzein. At postmenopausal levels, the isoflavones

acted as E2 agonists, and further increased the E2-induction of luciferase activity through either ER. However, premenopausally, particularly through ERβ, they inhibited E2 induced luciferase activity. This scenario can explain why daidzein and E2 are synergistic in a postmenopausal environment, but premenopausally they have no net effect. However, it does not explain the lack of effect of genistein and 1pM E2. Alternately, E2, genistein and daidzein may each be acting through different, as yet unresolved mechanisms to regulate the proliferation of MDA-MB-231 cells. The physiological or phenotypic effects of soy isoflavones and E2 together *in vivo* has not been investigated.

In addition, it is possible that the slight toxicity of the 0.2% DMSO level used throughout (Figure 3.5) may be masking any effects of the isoflavone-E2 combinations in this cell line, although to limit the impact of this, 0.2% DMSO was used as the control for comparisons for these treatments. As discussed, this was impossible to reduce due to limitations in the solubility of the isoflavones and the use of serial dilutions of stock solutions. A potential alternative to prevent this for future investigations would be to dissolve the E2 in ethanol, and compare the results of the combined treatments to a 0.1% DMSO / 0.1% ethanol control. However, for the present study it was felt that for the effects of soy isoflavones and E2 to be comparable, the same solvent should be used.

The results generated by this section of the investigation were fairly variable, and resulted in large SDs for the calculated means. It is likely that this contributed to the lack of statistical significance demonstrated for the comparisons. It is possible that the multiple variables including the isoflavones and E2 acting on the MDA-MB-231 cell line through different mechanisms, and also the slightly toxic effect of 0.2% DMSO have contributed to the variability seen. In future investigations, use of a different solvent, further optimisation of the protocol, or use of a different method to assess MDA-MB-231 proliferation may circumvent this.

The slight inhibitory effect of the single isoflavone treatments on ERα-/ERβ+ MDA-MB-231 cells, which was statistically significant in some cases even at relatively low physiologically achievable concentrations, suggests that soy isoflavones may be of potential chemotherapeutic benefit to the sizeable group of women with breast cancer of the same receptor status (18%; Skliris et al. 2008). However, there are a number of important issues which must first be addressed.

Firstly, their potentially reduced efficacy in a physiologically relevant premenopausal oestrogen environment must be considered. Other models for premenopausal ERα-/ERβ+ breast cancer must be found, to pursue the contradictory results generated by this and the only other study in this field. Due to the concerns discussed regarding the appropriateness of rodent models of breast cancer (Section 1.3.3), primary tissue samples may be a more beneficial route to follow. However, soy isoflavones may still be of benefit to postmenopausal women with ERα-/ERβ+ breast cancer due to their ability to work differentially as oestrogen agonists and antagonists depending on the level of oestrogen present. Furthermore, it is possible that higher, non-physiological doses of isoflavones may have a greater inhibitory effect. However this was outwith the mandate of this project to investigate, and as discussed, raises questions regarding the safety of such pharmacological doses.

One factor that is evident is from this and other studies, is that there is no evidence that soy isoflavones could increase the proliferation of ERα-/ERβ+ cell lines such as MDA-MB-231. This could cautiously be extrapolated to the population of women with ERα-/ERβ+ breast cancer, suggesting that even relatively high levels of dietary isoflavones may be safe for consumption.

However, as discussed (Section 1.1.1), the presence of ERβ is not routinely assessed in breast tumours, as it is has traditionally been regarded to be of little clinical relevance. For there to be any potential benefit of soy isoflavones to women with breast cancer, ERβ expression levels would have to be routinely assessed in the tumours, in parallel to ERα. Regrettably, no clinically significant downstream marker of ERβ expression has been identified (Skliris et al. 2008). Furthermore, although the full length ERβ isoform is the dominant form in breast tumours, the presence of its truncated isoforms (Section 1.1.4) can complicate its assessment. Depending on their target sequence, various ERβ antibodies vary in their isoform specificity (Skliris et al. 2008).

6.2 Isoflavones and the induction of apoptosis in breast cancer cell lines

6.2.1 Techniques: The Annexin V-Cy3 and DAPI nuclear morphology assays

As discussed (Section 1.5.3), due to the lack of any "gold standard" method with which to assess apoptosis, and the slight morphological and biochemical variations seen in apoptosis across different cell types and apoptotic induction methods, the best practice is to use two complementary techniques which assess different apoptotic markers. The Annexin V-Cy3 kit, assessing PS exposure on the outer plasma membrane, and DAPI fluorescent dye, to quantify apoptotic changes in nuclear morphology, were used in this project.

Use of Annexin V-based dyes to assess apoptosis is commonplace. As the dye is membrane impermeable, and only required to bind to externalised PS, no fixation or processing of the cells is required, resulting in minimal manipulation and loss of the sample (Brumatti et al. 2008; Galluzzi et al. 2009). The Annexin V-Cy3 dye emits light of a relatively long wavelength (red; >570nm) which permits the use of counterstains emitting in the blue or green spectral range. In this case the dye 6-CFDA was used. This is a membrane permeable fluorescein derivative, which permits cell viability to be assessed simultaneously, as described (section 2.5).

However, this method does have a number of limitations. Damage to the plasma membrane by intense scraping or trypsinisation (standard tissue culture techniques to remove adherent cells from a surface) can cause non-specific binding of Annexin V (Brumatti et al. 2008). This was minimised by growing the cells on a cover slip, which was then stained directly. PS externalisation can be a feature of some other forms of regulated cell death (Galluzzi et al. 2011) and can become accessible during certain stages of necrosis where the cell membrane becomes permeable, leading to false positive results (De Saint-Hubert et al. 2009). Counterstaining with 6-CFDA prevented this population of cells from confounding the results.

Finally, PS is not externalised when certain autophagy deficient cells undergo apoptosis (Qu et al. 2007). Autophagy is a pathway often accompanied by massive vacuolation of the cytoplasm. It has several physiological roles, including

cytoprotection in cells undergoing stress, and it can be responsible for cell death in some cancer cell lines deficient in certain apoptotic regulatory proteins like Bax, Bak and caspases (Galluzzi et al. 2011). However, both MCF7 and MDA-MB-231 cells are known to be able to undergo autophagy (Cui et al. 2007; Indelicato et al. 2010), so this was of no concern in this case.

Similarly, use of membrane permeable DNA-binding fluorescent dyes, such as DAPI or Hoechst, to assess changes in nuclear morphology is widely used in apoptosis detection (sections 1.5.3 and 2.6). In bacterial cells (*E. coli*) DAPI and Hoechst have been shown to give comparable quality results for the quantity of DNA present, as assessed by flow cytometry, over much of their concentration ranges (Bernander et al. 1998). However, in MCF7 DAPI demonstrates greater DNA binding activity than Hoechst, and is less cytotoxic (Bielawski et al. 2001).

In MCF7, apoptotic nuclear changes (Hoechst method) have been demonstrated to occur in parallel to numerous other apoptotic events including gross morphological changes such as membrane blebbing and changes in membrane permeability determined by Yo-PRO-1 and PI staining (Akter et al. 2012). Likewise, in primary neuronal cultures, nuclear changes (DAPI NAF method; see section 1.5.3) and double stranded DNA breaks (TUNEL staining) both occurred after treatment with phospholipase A2 (a potent apoptotic inducer), although each achieved significance at different time points after treatment (Daniel and DeCoster 2004). This emphasizes the importance of timing for the measurement of apoptosis, as many apoptotic events occur chronologically. A range of treatment time scales were assessed during the optimisation phase of this study, to determine a treatment duration which would allow reproducible induction of apoptosis to be measured (section 2.6.3).

Fixation prior to staining with DAPI is common practice with numerous cell types, including MCF7 and MDA-MB-231 (Daniel and DeCoster 2004; Koch and Stratling 2004; Miglietta et al. 2006; Wang et al. 2010). It is widely accepted that although DAPI is membrane permeable, and so can stain both live and fixed cells, the fixation process aids its passage through the plasma membrane and so improves the efficiency of staining. This was upheld during the optimisation of this protocol (section 2.6.3), and fixation was deemed to be necessary. Numerous techniques exist for fixation of cells prior to microscopy, discussed in section 1.5.3. Formalin

(formaldehyde) fixation was chosen, due to its nucleic acid crosslinking characteristics which commend it for the study of nuclear changes (Bacallo et al. 2006).

It has been suggested that one of the intracellular triggers for apoptotic nuclear condensation and fragmentation is caspase 3 (Hacker 2000). This caspase is known to be absent from MCF7 cells (see section 1.5.3). Furthermore, although widespread, apoptotic nuclear changes are not considered to be an essential apoptotic event (Hacker 2000). Based on this, it is possible that apoptotic nuclear changes do not occur in MCF7 cells. However, this was not the case, as they have been observed in this cell line (Akter et al. 2012), and also in MDA-MB-231 (Miglietta et al. 2006). Hacker et al. propose that caspase 6 or 2 may provide an alternate triggering method.

As with any technique assessing a morphological change, this method is operator dependent, and prone to underestimation of the degree of apoptosis, since cells in the early stages of apoptotic pathways may not yet display morphological changes (Galluzzi et al. 2009). In addition, there are a number of non-specific issues which relate to the use of fluorescence in both the Annexin V and DAPI assays. As discussed, quenching is a concern during any fluorescence technique (section 1.5.3). This was of particular relevance to the DAPI technique, as the fluorescence of this dye is known to be quenched by high concentrations of divalent cations (Mg^{2+}, Ca^{2+}) and heavy metals (Arbildua et al. 2006). However, DAPI fluorescence is largely stable between pH4 and 11, and in the current study pH was buffered at 7.4 by PBS. Under standard experimental conditions, quenching of Annexin V-Cy3 does not occur (Galluzzi et al. 2009).

Auto-fluorescence (section 1.5.3) was assessed in the case of each dye used and determined to be absent. However, the issues of bleaching by UV light, or leakage of the dye from the cell could not be so easily eliminated. To minimize their impact, images were collected rapidly, and UV exposure was reduced. When not required the UV light source was cut off.

As a further level of control for both apoptosis assays, H_2O_2 (at various concentrations and times) was used as a positive control for apoptosis. As discussed (section 2.5.3), this treatment is known to induce apoptosis in a range of cell types, presumably due to oxidative stress. Significant induction of apoptotic

nuclear morphology was identified in MCF7 cells (section 2.6.3), and PS-externalising apoptosis was recorded in both MCF7 and MDA-MB-231 after this treatment (section 2.5.3). This indicates that both techniques are capable of measuring changes in the level of apoptosis induced under the experimental conditions described.

6.2.2 Solvents

To allow comparison between the results of the proliferation and apoptosis assays, the same range of DMSO concentrations were used. Accordingly, the effect of 0.1% DMSO on the induction of both PS-externalising apoptosis and apoptotic nuclear morphology was assessed in both MCF7 and MDA-MB-231 cells, and the impact of 0.2% DMSO was assessed by both techniques in MCF7, and on DAPI nuclear morphology in MDA-MB-231 cells, as described (sections 3.2.1..1, 3.2.2..1, 3.3.1..1 and 3.3.2..1). Neither DMSO concentration had any impact on the induction of either apoptotic marker measured in either cell line. Accordingly, use of DMSO up to 0.2% as a solvent and control treatment was considered appropriate in MCF7 cells for both the Annexin V-Cy3 PS externalisation assay and DAPI nuclear morphology assay. Likewise, in the MDA-MB-231 cell line, 0.1% DMSO was valid for use with both apoptosis techniques, and the higher solvent level of 0.2% DMSO was appropriate for the nuclear morphology assay. The impact of 0.2% DMSO on the induction of PS-externalising apoptosis in MDA-MB-231 cells was not assessed as this solvent level and cell line combination was not used in any of the Annexin V-Cy3 assays.

However, higher solvent doses have been found previously to result in an increase in the level of apoptosis recorded by several groups. After 12 hour treatment with 2% (v/v) DMSO an increase in apoptosis (DNA laddering) was measured in mouse macrophages (Marthyn et al. 1998). A similar increase in DNA laddering was recorded in MCF7 cells after 48 hour treatment with 1% polyethylene glycol / ethanol mixture (55 and 45% respectively; Vandhana et al. 2010). Furthermore, many of the previous investigations looking at the induction of apoptosis in both MDA-MB-231 and MCF7 (Table 1.6) have not disclosed the maximum solvent level used. As DMSO may have either an influence on the induction of apoptosis at higher levels, this could have an impact, and should be considered in the analysis of these results.

6.2.3 MCF7 apoptosis - single treatments of isoflavones and 17β-oestradiol

The E2 treatments (both pre- and postmenopausal levels) had no significant impact on the induction of apoptosis in MCF7 cells, by either assay method (sections 3.2.1..2 and 3.3.1..2). The agreement between the two sets of results, and consequently, two different markers of apoptosis, adds strength to these results. Conversely, previous studies (section 1.5.5) suggested that E2 treatment, at physiological levels such as these would reduce the induction of both basal (Schmidt et al.2005; Song et al. 2007) and serum starvation induced apoptosis (Sakamoto et al. 2010). However, the two studies above looking at basal (without stress) induction of apoptosis used longer time scales (4 and 5 days E2 treatment) compared to the 3 and 24 hour treatments described for the current investigation. This implies that any inhibitory effects of E2 on apoptosis in MCF7 may take longer than 24 hours to manifest.

The single isoflavone treatments showed a tendency towards increasing the level of PS-externalising apoptosis at all concentrations tested (0.1µM upwards; Figure 3.13), and a significant increase in the presentation of apoptotic nuclear morphology was observed with the highest genistein concentration used. These results, and those of the other treatments in this cell line are summarized in Table 6.2. This contradicts the results of Schmidt et al. (2005) who found an inhibitory (oestrogen-like) effect of genistein and daidzein (0.1 to 10µM) on MCF7 apoptosis. However, they are more in line with the results of numerous other studies (although lower in the magnitude of the result) which indicate that soy isoflavones above 25µM can induce numerous apoptotic markers in this cell line (section 1.5.4). The lesser degree of apoptosis observed in the current study is not surprising given the dose-effect for apoptotic induction demonstrated with both genistein (Shim et al. 2007) and daidzein (Jin et al. 2010) in this cell line.

There are a number of factors which could potentially underpin the discrepancy in the results of lower isoflavone concentrations, casting doubt on the results of Schmidt et al. (2005). Firstly, they treated the MCF7 cells for five days in the test conditions, which may have resulted in the depletion of nutrients, or the cells approaching confluence, especially for the faster growing cultures. This could have influenced their results, but is not addressed in the publication. Secondly, their

results are compared to an untreated control, rather than vehicle-only. Although 0.1% DMSO was the maximum solvent level used in their study, and is unlikely to influence the results, it could still have had a slight impact. Furthermore, contrary to the advice of the NCCD, they only used one measure of apoptosis: flow cytometry to assess the proportion of cells in sub-G1 phase of the cell cycle. This technique is widely used, but it has some key limitations which are discussed in section 1.5.3. Use of multiple distinct measures of apoptosis (see section 1.5.3) would strengthen the evidence that they present.

Table 6.2: Summary of apoptosis results in MCF7 cells (both methods)

	Annexin V-Cy3: PS externalisation	**DAPI: apoptotic nuclear morphology**
E2	NE	NE
Genistein	**++**	**++** (31.6µM only)
E2 + genistein	**++** (as genistein)	+ (31.6µM only)
Daidzein	**++**	NE
E2 + daidzein	**++** (as daidzein)	+ (31.6µM only)

E2: 17β-oestradiol, NE: no effect, + non-significant increases in apoptosis, **++** *significant increases in apoptosis seen at some doses.*

On the whole, the data generated here regarding the generation of apoptotic nuclear morphology and externalization of PS provides an explanation for some of the proliferative properties of E2 and isoflavones. The lack of effect (or inhibitory effect) of E2 on the induction of MCF7 apoptosis corresponds with its strong positive impact on the proliferation of this cell line. Similarly, low doses of soy isoflavones (up to 10µM) which cause the dose-responsive increase in MCF7 proliferation, have very minimal (or indeed a slight inhibitory) impact upon apoptosis. However, higher levels, such as 31.6µM genistein (section 3.3.1..3) or 25µM daidzein (Jin et al. 2010) result in more pronounced induction of apoptosis. This will have a negative effect

on cell numbers, resulting in the biphasic effect of isoflavones seen on MCF7 proliferation.

This supports the theory proffered by Sakamoto et al. (2010), whereby in MCF7 ERα is heavily involved in the proliferative effects of soy isoflavones, but that their pro-apoptotic effects are mediated by other, ER-independent mechanisms. They support this with evidence showing that silencing of ERα (siRNA) had no impact on the apoptotic effects of isoflavones. The ER-blocker ICI 182780 alone (10nM to 10µ) resulted in a dramatic and significant dose-responsive increase in the rate of apoptosis, and co-incubation with ICI 182780 and genistein or daidzein resulted in a further increase in apoptosis over and above that caused either individually (Sakamoto et al. 2010; Schmidt et al. 2005). Much is already known regarding the mechanisms through which the soy isoflavones induce apoptosis in MCF7 cells. This has been discussed previously (section 1.5.4).

As the impact of soy isoflavones on MCF7 proliferation is known to be both dose- and time-dependent (Shim et al. 2007), it stands to reason that higher isoflavone concentrations or longer treatment times would result in the more pronounced induction of MCF7 apoptosis. However, higher concentrations would be of limited physiological relevance, and very long term isoflavone treatment in cell culture is both impractical and unrealistic. The longest treatment duration in the studies described was five days (Schmidt et al. 2005). A different approach was taken by Garvin et al. (2006), who implanted MDA-MB-231 cells into female athymic mice, and then treated them with daily injections of the isoflavone resveratrol (25mg/kg/day) for three weeks. This treatment resulted in a striking and significant increase in the level of apoptotic DNA fragmentation in the tumour (TUNEL staining). However, as discussed, it is difficult to compare the isoflavone doses provided *in vitro* and *in vivo* (section 1.3.3). Furthermore, it must be noted that this was a model of ERα-/ERβ+ breast cancer (see section 6.2.5), and used resveratrol, not the soy isoflavones. None of the other animal studies described (section 1.3.3) investigated the effect of soy isoflavones on markers of apoptosis in any ER-status model of the disease.

There is very little information regarding the effect of isoflavone intake on the rate of apoptosis in human breast cancer. However, one small pilot study of breast cancer patients undergoing a core needle breast biopsy (n=17), and then a two week soy

isoflavone supplementation (50mg/day) prior to surgery investigated the induction of apoptosis (Sartippour et al. 2004). Although no significant effects were seen compared to a historical control group (n=26), possibly due to the subjective apoptosis assessment method (microscopy), small numbers and short intervention duration, the intervention did result in a trend towards inhibition of proliferation associated with an increase in the ratio of apoptotic to mitotic cells. This data suggests that the induction of apoptosis *in vivo* (human) by soy isoflavones warrants further investigation, as this may be a mechanism through which their protective effects are mediated.

6.2.4 MCF7 apoptosis – the combination of isoflavones and 17β-oestradiol

The results described in sections 3.2.1..4 and 3.3.1..4 represent the first documented occasion where the induction of MCF7 apoptosis by genistein and daidzein in a physiologically relevant E2 environment has been reported, with the exception of a series of experiments by Schmidt et al. (2005). However, while this group used a range of E2 concentrations (1, 10 and 100pM) for their combined treatments, they only included one concentration of genistein and daidzein (10μM). Although this represents the high serum levels of isoflavones seen in very high soy consumers, it cannot be related to more moderate or low consumption of isoflavones, and imparts little about isoflavone/E2 interactions in most women.

In the current results for the MCF7 cell line, treatment with the combinations of isoflavones and E2 had largely the same impact as the single genistein and daidzein treatments on the induction of either apoptotic PS-externalisation (Figure 3.14) or apoptotic nuclear morphology (Figure 3.22). As with the single isoflavone treatments (discussed in section 6.2.3), time- and concentration-dependent were apparent. After 3 hours treatment (DAPI nuclear morphology assay) there was no impact on apoptosis until the highest isoflavone concentration (31.6μM) was reached. However, after 24 hour treatment (Annexin V-Cy3 PS externalization assay) each isoflavone/E2 combination resulted in some induction of apoptotic PS-externalisation compared to the control. In each combined treatment case, where an increase in the rate of apoptosis was observed compared to the control treatment, it was also higher than the rate documented after treatment with the relevant E2-only treatment. This is not surprising given that E2 alone had no impact on levels of MCF7 apoptosis in this investigation (Figures 3.11 and 3.20).

The lack of significant differences in the PS-externalising apoptosis data described for many of the combined treatments when compared to the control or E2 alone, despite considerably higher mean percentage values reported reflects the large range of actual values calculated (Table 3.6). Its roots may lie in error introduced by the apoptosis detection method. However, the optimisation proceedures and positive control treatments were designed to prevent this as far as possible. Consequently, this variability in the data probably reflects natural variation in the system.

These results are comparable to the only previous study, which suggested that 10µM genistein or daidzein in combination with E2 (1pM to 100pM) induced apoptosis in MCF7 to a similar extent than was seen with the isoflavones alone (Schmidt et al. 2005). However, in addition to the limitations of this study discussed in section 6.2.3, they have not directly compared the level of apoptosis calculated after the single isoflavone treatments and the isoflavone/E2 combinations. For one data set (single treatments) they reported the rate of apoptosis, and for the other (combined treatments) the results are in the form of the percentage of apoptotic cells out of the total population. It is apparent that each set of results follows a similar pattern, but the inconsistency in their outcome measures is not explained, and it rules out a direct comparison.

Further confirming the lack of any modulatory effect of E2 on the induction of MCF7 apoptosis by genistein or daidzein is work by Sakamoto et al. (2010). In their study of serum starvation-induced MCF7 apoptosis, they demonstrated that treatment with combinations of genistein or daidzein (10µM) with 1nM E2 induced apoptosis to a similar degree than with the isoflavone alone. However, their focus on apoptosis induced by serum starvation (5 days in 0.5% serum conditions) limits the physiological relevance of these results. As discussed (section 1.5.3), apoptosis induced by different stimuli can present many of the same morphological and biochemical characteristics, but the route of induction can lead to slight changes in the biochemistry and apoptotic phenotype observed (Hacker 2000; Kroemer et al. 2009). It is possible that this non-physiological apoptotic stimulus could result in a different role for isoflavones than with another stimulus in MCF7.

Overall, the data generated in this study builds on the previous studies, to further confirm that soy isoflavones are capable of inducing apoptosis in the MCF7 breast cancer cell line, despite the presence of E2 and even at relatively low, physiologically relevant concentrations. However, these pro-apoptotic effects occur in parallel (probably regulated by different mechanisms) to the massive synergistic, proliferation enhancing effect that both isoflavones and E2 have on MCF7 at these concentrations. At the isoflavone concentrations which represent the serum levels seen in low to even relatively high soy consumers (up to 10µM), the slight induction of apoptosis observed is insufficient to counter the strong, ERα-mediated impact of both the isoflavones and E2. However, there was a trend towards increasing induction of apoptosis with the highest isoflavone concentration used (31.6µM),

confirming the dose-effects documented previously. This may provide a mechanism for the growth inhibitory component of the biphasic effect of the isoflavones on MCF7 proliferation, which was apparent with both single and combined treatments.

While the ability of the isoflavone concentrations used in this study to induce apoptosis was limited, this data suggests that greater concentrations of genistein or daidzein (outwith the remit of this investigation) could induce apoptosis at a high enough rate to reverse these growth promoting properties. Furthermore, regulatory and mechanistic differences between *in vitro* models of breast cancer and the tumour environment in women mean that the ability of even relatively low levels of isoflavones to induce breast cancer cell apoptosis may contribute to their epidemiological protective effect. In addition, the cumulative effect of time on the apoptosis inducing effect of isoflavones argues for a greater benefit with longer term exposure in different models of breast cancer. However, as mentioned, evidence in this field from more complex models of breast cancer, such as humans or rodents, is scant. This argues that further research into the ability of soy isoflavones to induce apoptosis in ERα+ breast tumours is warranted.

6.2.5 MDA-MB-231 apoptosis - single treatments of 17β-oestradiol and isoflavones

Previous publications have described how genistein, at concentrations above 5μM, induces various apoptotic markers in MDA-MB-231 cells, including the proportion of cells in sub-G1/G0 phase of the cell cycle (Seo et al. 2011), the presence of single stranded DNA (Davis et al. 2008), PS externalisation and caspase 3 activity (Li et al. 2008). This was associated with a reduction in Bcl2 protein levels, and a corresponding increase in Bax (Li et al. 2008). These treatments ranged between 48 and 72 hours, and the response was dose-dependent. However, prior to the current study, nothing was known regarding the impact of lower levels of genistein on the induction of apoptosis in this cell line.

The current results show that even relatively low levels of genistein (10 and 100nM) are capable of inducing a trend towards increasing the level of apoptosis in MDA-MB-231 cells over 3 and 24 hours of treatment. These results were comparable for both the induction of nuclear morphology (Figure 3.28) and PS externalisation (Figure 3.17), and the effect on nuclear morphology became statistically significant at the highest genistein concentration used (31.6μM). The remainder of the results failed to achieve statistical significance. However, despite the variability in the generated data points, the majority were numerically higher than the control mean. All the apoptosis results in the MDA-MB-231 cell line are summarized in Table 6.3.

Very similar results were seen for daidzein treatment with this cell line. This too achieved statistical significance on one occasion (10nM) with regard to the impact on nuclear morphology (Figure 3.28). This represents the first occasion where daidzein at any concentration has been shown to induce apoptosis in an ERα-/ERβ+ cell line. This is an important result, as it shows that the induction of apoptosis by isoflavones in MDA-MB-231 cells is not limited to genistein.

Table 6.3: Summary of apoptosis results in MDA-MB-231 (both methods)

	Annexin V-Cy3: PS externalisation	DAPI: apoptotic nuclear morphology
E2	NE	NE
Genistein	+	**++**
E2 + genistein		**++** (31.6µM, synergy?)
Daidzein	+	**++**
E2 + daidzein		**++** (31.6µM, synergy?)

E2: 17β-oestradiol, NE: no effect, + non-significant increases in apoptosis, ***++*** *significant increases in apoptosis seen at some doses.*

These results correspond with the reduction in proliferation of MDA-MB-231 cells observed at the same concentrations (Figure 3.7). Although the inhibition of MDA-MB-231 proliferation by isoflavones is thought to relate to a genomic effect mediated by ERβ (see section 6.1.5), this data suggests that the induction of apoptosis may also play a part in the reduction in cell numbers observed.

It was shown that E2 at its pre- and post-menopausal concentrations had little or no impact on the level of either apoptotic marker tested in MDA-MB-231 cells (Figures 3.15 and 3.25). This represents the first occasion where this has been tested. The implication is that apoptosis has no role in E2-inhibiton of proliferation in this cell line (Figure 3.6), and that other mechanisms, such as an ERβ-mediated genomic effect are responsible.

The induction of apoptosis by high (≥10µM) soy isoflavone concentrations is widely agreed to occur to a similar extent in both ERα+ cell lines such as MCF7 and ERα-/ERβ+ MBA-MB-231 cells (section 1.5.4; current results). This study has generated novel data illustrating that the same occurs at lower isoflavone concentrations, of more physiological relevance to the serum levels observed in women. However, in keeping with the dose-responses observed, the magnitude of

the apoptotic effect of these lower concentrations was reduced compared to very high, non-physiological doses. This suggests that despite the strong proliferative effect of physiological levels of isoflavones seen *in vitro* with ERα+ cell lines, in parallel they also induce apoptosis, in a manner which is not mediated by ERα. Where ERα is absent, such as in MDA-MB-231 cells, there is nothing to mask the pro-apoptotic effect seen. The role of ERβ in breast cancer cell apoptosis is unknown and as yet un-tested.

Several possible alternate (non-ER) mechanisms for the induction of MDA-MB-231 apoptosis by isoflavones have been investigated. Genistein treatment at apoptosis-inducing levels between 5 and 20μM was associated with a reduction in the levels of NF-κB protein and activity, and protein levels of MEK5, ERK5 and phospho(active)-ERK5 (Li et al. 2008). Although many questions remain regarding the role of these signaling kinases in breast cancer, evidence exists supporting a role for them as anti-apoptotic in murine thymocytes and porcine aortic endothelial cells (Lennartsson et al. 2010; Sohn et al. 2008). Inhibition of the MEK5/ERK5/NF-κB signaling pathway may be a key mechanism through which isoflavones are acting to induce apoptosis in MDA-MB-231 cells. Genistein treatment has also been shown to increase the level of active p53 (a tumour suppressor) and p21 (a pro-apoptotic and cell cycle inhibiting regulatory protein) in MDA-MB-231 cells (Seo et al. 2011), although these may be downstream of MEK5/ERK5/NF-κB signaling.

Overall, this field of study appears promising with regard to understanding one of the mechanisms through which isoflavones may be protective against breast cancer. In particular, it is important to elucidate whether ERβ mediates the induction of apoptosis by isoflavones. This could be resolved by reassessing apoptosis with isoflavones in the presence of an ER antagonist, or silencing the ERβ gene. Furthermore, as with the anti-proliferative effects of isoflavones in MDA-MB-231 cells, it would be of value to identify whether their pro-apoptotic effects *in vitro* are mirrored in more comprehensive models of the disease, such as animals, primary tissue samples, or even in women. However, difficulties arise with the latter due to the large number of women that it would be necessary to recruit in order to have sufficient ERα-/ERβ+ cases for analysis after stratification by ER status.

6.2.6 MDA-MB-231 apoptosis – the combination of isoflavones and 17β-oestradiol

As seen in MCF7, the ability of soy isoflavones to induce apoptosis in MDA-MB-231 cells at concentrations ≤10μM was not affected by the presence of E2. However, with the highest concentrations of genistein and daidzein (31.6μM) there was clear evidence of synergy between the isoflavones and E2, with the combined treatments all inducing considerable levels of apoptosis, which was significantly higher than the isoflavone or E2 single treatments in virtually all of the comparisons. The conclusion to be drawn from this is that in a physiological E2 environment (either pre- or post-menopausal) levels of genistein and daidzein that can be achieved in the serum of high soy consumers or women consuming isoflavone supplements can induce a considerable level of MDA-MB-231 cell apoptosis.

In addition to the ERβ-mediated effects of isoflavones discussed previously, this increase in the rate of apoptosis could partly explain the anti-proliferative effect of isoflavone/E2 treatments on MDA-MB-231 cells. This provides evidence for a protective mechanism for isoflavones in ERα-/ERβ+ breast cancer. However, this study was the first of its kind to investigate the impact of isoflavones in physiologically relevant E2 conditions on the induction of apoptosis in an ERα-/ERβ+ breast cancer model. These promising results pave the way for further studies. Firstly this effect requires confirmation in MDA-MB-231 cells by assessing a second apoptotic marker (this set of conditions were only tested with the DAPI nuclear morphology assay, PS exposure was not assessed). Secondly, as discussed, little is known regarding the mechanism for the effect of isoflavones and E2 on apoptosis in this cell line, or indeed the reason for the synergistic effect at high isoflavone concentrations. As genistein and daidzein have potential as chemotherapeutic agents against ERα-/ERβ+ breast cancer, this area should be a priority.

6.3 Volume changes in MCF7

6.3.1 Technique: Calcein fluorescence

Although numerous techniques have been used to asses volume change in cultured cells (see section 1.6.2..5), the most reproducible and widely used is electronic sizing (Coulter Counter): measuring changes in the volume of liquid displaced as suspended cells pass an aperture of known size. However, this requires specialist equipment which was not available for the current research. Many alternate methods utilize light microscopy, and as cells are perfused with various test agents image analysis software is used to assess their area based on changes in radius or height. This technique has been used to assess volume regulation in MCF7 (Roy et al. 2008; vanTol et al. 2007). However, this assumes a degree of circularity, and uniformity of shape which is not representative of the majority of cultured cells. Assessment of changes in Calcein fluorescence intensity (sections 1.6.2..5 and 4.1) produced reproducible results which were not limited to the uniformly circular cells in the population. Where this method has been previously used in rabbit corneal epithelial cells (Pan et al. 2007) and human lung adenocarcinoma cells (Chen et al. 2011) it has generated comparable results to the other techniques.

However, there were several key limitations to the technique which required addressing. Firstly, unlike the fluorescent dyes discussed previously, Calcein is susceptible to self-quenching. This is a phenomenon whereby fluorescence intensity decreases with increasing dye concentration above a threshold of 3mM (Hamann et al. 2002). This is around 1000 times more concentrated than the typical levels used to load the cells in most experiments (5µM Calcein was used in the current investigation), and it is generally considered impossible for dyes such as Calcein to accumulate inside cells to concentrations >1mM, unless microinjection of the dye is undertaken (Hamann et al. 2002; Verkman 2000). Self-quenching was not observed on any occasion in this research.

Furthermore, despite the use of regulatory volume decrease during hyposmotic shock as a reference for measurable volume change in MCF7 to confirm the appropriateness of the test conditions, background changes in Calcein fluorescence intensity were found to be variable. In particular this was apparent with the 0.1% DMSO control treatment used prior to each test condition. This may have related to

slight changes in temperature, or incomplete esterification of Calcein. As discussed, WinFluor software was used to assess the stability of fluorescence prior to beginning the test protocol. This software was only capable of measuring changes in individual pixels rather than whole cell regions due to the ROI selection method, and as a result it failed to detect the background changes in fluorescence which were later detectable using ImageJ. This was accepted as an unavoidable limitation of the equipment used, but it is apparent from these results that WinFluor live image analysis was considerably less sensitive than ImageJ. Future investigation in this field will require further optimisation to determine the balance between time taken to allow dye esterification and avoiding fluctuations in the stability of cells brought on by extended periods of Tyrode perfusion. Alternately, more accurate software could be acquired to assess the stability of fluorescence prior to experimentation.

To reduce the impact of background changes in cell Calcein fluorescence on the treatment effect, the mean rate of fluorescence change per second was calculated during the control treatment and test treatment for each experiment (Δf_0, Δf_{10} etc.) and the net effect of the treatment over that of the background change was calculated ($a\Delta f$), as described in section 4.1.3..3. Similar calculations were used in related studies where Calcein fluorescence intensity was used to determine volume changes in SPC-A1 human lung adenocarcinoma cells (Chen et al. 2011) and rabbit corneal epithelial cells (Pan et al. 2007).

RVD in response to hyposmotic shock in MCF7 has been widely investigated, and is relatively well understood (section 1.6.8..1). The results described in section 5.1.1 show an initial phase of swelling in MCF7 cells from approximately 10 to 16 minutes into the hypotonic stress, illustrated by the reduction in Calcein fluorescence intensity observed. Following this, RVD occurred, restoring fluorescence intensity (and hence cell volume) to close to the pre-swelling values by around 23 minutes in the hyposmotic solution. These results are in agreement with those of other groups assessing RVD in MCF7 cells, and are over a similar time scale (Roy et al. 2008; vanTol et al. 2007). This suggests that the protocol described is appropriate for the measurement of volume changes in MCF7 cells over the time scales described.

However, each of the previous studies has focused on RVD after hyposmotic stress. As discussed previously (section 1.6.8) although the response is based on the mechanisms which regulate shrinkage during apoptosis, this stimulus is non-

physiological. In the current research the main focus was to identify acute changes in volume after isoflavone or E2 treatment. Despite the links between swelling and proliferation, and shrinkage and apoptosis being well established (section 1.6.5; Chen et al. 2011; Ishibashi et al. 2011) the impact of E2 and isoflavone treatments on these responses in cancer cell lines has not previously been studied.

6.3.2 The impact of 17β-oestradiol and genistein on MCF7 volume

6.3.2..1 Swelling

Treatment with both 1nM E2 and 1µM genistein resulted in a significant reduction in Δf compared to the pre-treatment value (Figure 5.5), and accordingly negative values for aΔf (Figure 5.6). This implies that these treatments have caused a reduction in fluorescence intensity over and above any background effects, and are causing Calcein concentration within the cell to drop due to an increase in size.

This result is not surprising in the face of data which suggests that swelling is a necessary step in S phase progression during proliferation (Dubois and Rouzaire-Dubois 2004; Hoffmann 2011), and both treatments have previously been shown to result in a dramatic increase in MCF7 proliferation (sections 3.1.1..1 and 3.1.1..2.). The specific ion channels thought to be involved in proliferative swelling of MCF7 cells are not known, although the Na^+-K^+-Cl^- co-transporters and the Cl^--H^+ and Cl^- HCO_3^- exchangers may play a role (Dubois and Rouzaire-Dubois 2004). It is not known whether E2 and isoflavones directly act upon the channels mediating the swelling of MCF7, and thus further promote proliferation in this manner over and above their other known mechanisms, or whether swelling is a down-stream effect.

It is relevant to note the speed with which E2 and genistein have begun to induce proliferation-like responses in MCF7 cells. In each case the difference achieved statistical significance after 10 or 15 minutes of treatment. This argues for a rapid induction of the proliferative signaling kinase pathways, or direct interaction with the membrane ion channel proteins which regulate cell volume. Slower induction of ERα-mediated transcription of pro-proliferative genes may occur in parallel to this, or downstream.

The suggestion that E2 treatment may induce very rapid signaling responses in MCF7 is not new. Treatment of MCF7 cells with 0.1nM E2 induces the activation (phosphorylation) of the signaling kinases IGF-1R and EGFR within 5 minutes (Song et al. 2007). By subsequent knockout (siRNA) of IGF-1R then EGFR, this group suggested that E2 sequentially induces the activation of IGF-1R, EGFR, then MAPK, in a cascade of activation.

MAPK signaling is also integral to the induction of MCF7 proliferation by genistein (Mawson et al. 2005; Yang et al. 2010), although the speed of the activation of these kinase signaling cascades by genistein treatment is not so clear. It has been suggested that up-regulation of ERα transcriptional activity by isoflavones requires MAPK / ERK1/2 signaling (Liu et al. 2010; Yang et al. 2010). Supporting this, Yang et al. (2010) present evidence suggesting that treatment with 10μM genistein induces phosphorylation of ERα in MCF7 cells.

This may relate to the hypothesis that even in the absence of ligands, phosphorylation of Ser^{118} of ERα by various signaling kinases increases its transcriptional efficiency (Deblois and Giguere 2003; Lucki and Sewer 2011; Yang et al. 2010). Phosphorylation of MCF7 Ser^{118} in ERα is induced rapidly (within 15 minutes) in response to 10 nM E2 treatment (Hamilton-Burke et al. 2010). The role of phosphorylation at this site in breast cancer is complex, with studies reporting paradoxical results with regard to its impact upon prognosis (Kok et al. 2009; Sarwar et al. 2006; Yamashita et al. 2008).

In addition to this, there is considerable evidence suggesting that both isoflavones and E2 can act on K^+ channel activity rapidly, within minutes or seconds (sections 1.6.6). As discussed, the activity of these channels can directly impact upon cell volume (see sections 1.6.1, 1.6.5 and 1.6.8). It has been suggested that E2 interacts directly with the plasma membrane BK channels of MCF7 (Coiret et al. 2005). To this end evidence was presented showing that 10nM membrane impermeable E2 (conjugated with BSA) had a comparable impact upon MCF7 proliferation to unconjugated E2 (10nM), and that both E2 and BSA-E2 induced BK channel activity to a similar extent. Furthermore, E2-induction of BK activity was rapid (within a minute) and not mediated by the ERs, as the addition of the ER antagonist ICI 182780 did not prevent E2-induction of BK activity. In addition, the BK channel blockers iberiotoxin, charybdotoxin and TEA prevented E2-induced MCF7 proliferation. However, although the expression levels of BK are cell cycle dependent (Ouadid-Ahidouch et al. 2004a), its role in basal (non-stimulated) MCF7 proliferation appears minimal. Blockade of BK by the same agents in the absence of E2 has no impact upon MCF7 proliferation (Coiret et al. 2005; Ouadid-Ahidouch et al. 2000; Ouadid-Ahidouch et al. 2004a; Ouadid-Ahidouch et al. 2004b).

Whether E2 works in the same extracellular manner on other ion channels is not known. Neither has the activity of a membrane impermeable form of genistein been investigated with regard to any aspect of MCF7 proliferation, apoptosis, or ion channel activity.

6.3.2..2 Shrinkage

In contrast to the other treatments, 31.6µM genistein treatment resulted in a significant shift in the rate of fluorescence change, from a negative to positive value, and a positive value for aΔf after 10 minutes treatment. This indicates that the dye is becoming more concentrated, and the MCF7 cells are shrinking. This corresponds with the previous results, showing that this treatment induced apoptosis in MCF7 (Figures 3.13 and 3.22). This may be evidence of apoptotic volume decrease (AVD), proposing a mechanism through which high concentrations of isoflavones could induce apoptosis in breast cancer cell lines such as MCF7. If so, then this could relate to the protective effect of dietary isoflavones against breast cancer discussed previously. Mechanisms such as this are potentially important to the anti-cancer properties of isoflavones, and provide information regarding novel pharmacological targets for future chemotherapeutic treatments.

As discussed (section 1.6.5), AVD is an essential early stage of apoptosis, it occurs prior to many of the other key apoptotic events, and requires K^+ efflux. In particular, the K^+ channels hERG, $K_v1.1$ and $K_v1.3$ appear to be involved in this process. In this manner, the apoptosis inducer would result in plasma membrane depolarization, activating the above K^+ channels. The resulting K^+ efflux hyperpolarizes the plasma membrane. As with the membrane potential model of proliferation (see section 1.6.4), this results in an increase in $[Ca^{2+}]_i$ following its electrochemical gradient into the cell. However, this increase is greater in magnitude than is seen during proliferation, sustained, and bolstered by the release of endoplasmic reticulum Ca^{2+} stores. The sudden and sustained increase in $[Ca^{2+}]_i$ that ensues activates the mitochondrial apoptotic pathway (Figure 1.3) and calpains (Ca^{2+} activated apoptotic proteases; see section 1.5.4). This activates the caspase cascade as described. However, there is cross-talk between the elements of this pathway, as caspase 8 or 9 activity is required for the induction of AVD, depending upon the route of apoptotic induction (Vu et al. 2001). For a summary of this potential pathway see Figure 6.3.

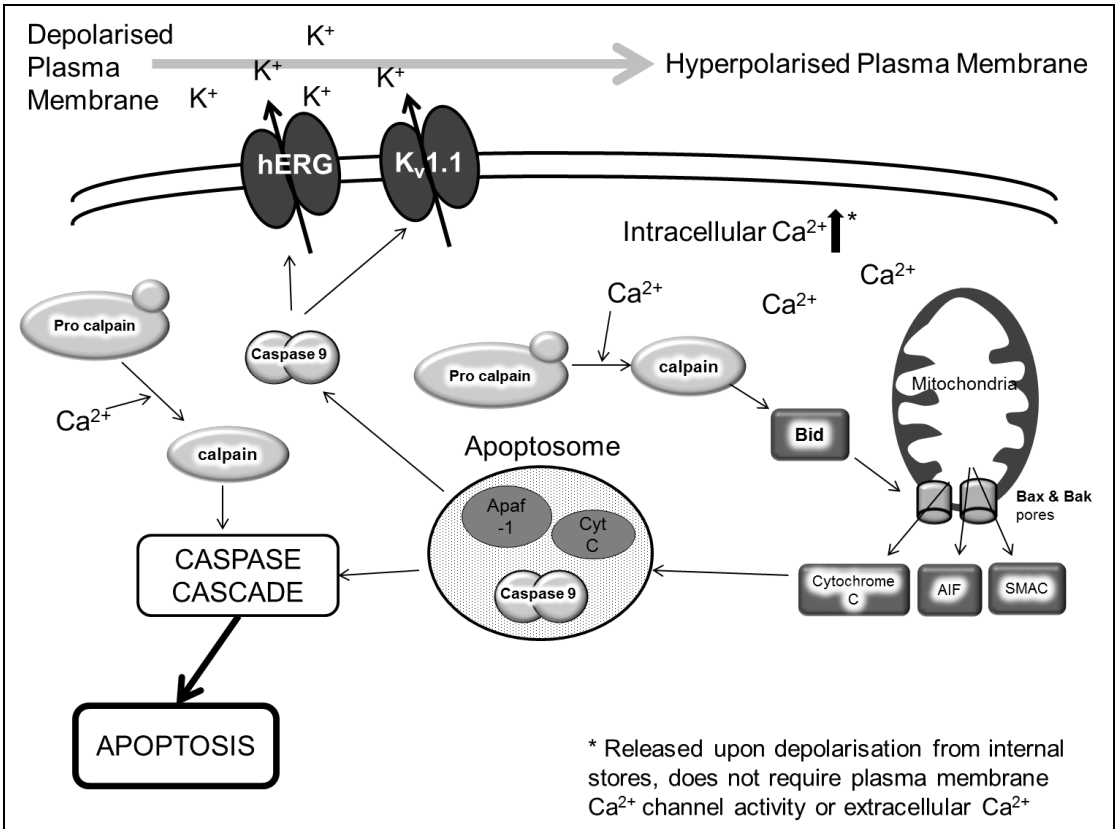

Figure 6.3: Revised model for the induction of intrinsic apoptosis, including the proposed role for K^+ channels

Apoptotic stimuli result in membrane depolarization, triggering the activity of hERG and $K_v1.1$ (and $K_v1.3$). The resulting plasma membrane hyperpolarisation causes an increase in $[Ca^{2+}]_i$ largely due to the release in intracellular stores. This triggers formation of the apoptosome by mitochondria, and the activation of calpains. The resulting caspase cascade results in apoptosis. There is an element of cross-talk, as caspase 9 activity is required for the initial efflux of K^+.

By 15 minutes into the treatment, the trend towards a reduction in fluorescence intensity has resumed, although to a lesser extent than prior to the treatment. However, aΔf still has a positive value, implying that the treatment still retains some of its net fluorescence-increasing capacity over and above the background changes. It is possible that the treatment has resulted in a loss of membrane integrity in these experimental conditions, resulting in loss of Calcein from the cell. Alternately, the shrinkage observed may be a temporary phenomenon, and the MCF7 cells recovered.

6.4 K^+ channel activity in MCF7 cells

6.4.1 The role of the VGKCs in MCF7 proliferation

The experiments looking at the impact of various VGKC blockers on the proliferation of MCF7 used the previously validated and optimised MTT assay, which is discussed in full in sections 1.4.2..1, 2.4 and 6.1.1.

By using pharmacological K^+ channel blocking agents of increasing specificity, it was possible to identify the impact of specific channels or groups of channels on the proliferation of this cell line. Firstly, TEA was calculated to have an IC_{50} for MCF7 proliferation of 18.84mM (Figure 5.8). TEA is a non-specific blocker of numerous K^+ channels. This indicates that K^+ channels are present in MCF7 and play a role in proliferation. Although slightly higher, this is generally comparable to the results of others showing that the IC_{50} for MCF7 proliferation with TEA is around 6mM (Ouadid-Ahidouch et al. 2004a; Wonderlin and Strobl 1996). In agreement with Coiret et al. (2007), lower concentrations below 1mM had little impact on the proliferation of this cell line.

Treatment with 4-AP confirmed that among the K^+ channels involved in MCF7 proliferation, the VGKCs played a role. The IC_{50} for MCF7 proliferation by 4-AP was calculated to be 2.7mM (Figure 5.9). This value is very similar to that previously published by Wonderlin and Strobl (1996) of 1.6mM. However, it must be noted that due to limitations in the solubility of 4-AP, a solvent (water) dose of 4% was required for the highest 4-AP concentration (20mM). The earlier finding that the addition of this level of water to the growth medium reduced MCF7 proliferation (Figure 5.7) was a concern. To minimize the impact of this, 4% $d.H_2O$ was added to each 4-AP treatment and the control used. Although this may have affected the result, any influence was universal to all 4-AP concentrations. At this level, it is probable that the reduction in MCF7 proliferation associated with the addition of water was related to the dilution of nutrients or an osmotic effect.

As the intention of this research was to study the K^+ currents mediated by the VGKCs hEAG and hERG, it was necessary to confirm the role of these channels on MCF7 proliferation also. The hERG blocker DOF was used for this purpose, along with AST, which blocks both hEAG and hERG. No specific hEAG blockers exist.

This technique is similar to that used by Roy et al. (2008), although in that case the hERG blocker E-4031 was used.

AST was found to inhibit MCF7 proliferation with an IC_{50} of 4.9µM (Figure 5.10). This is comparable with the finding of Ouadid-Ahidouch et al. (2004b) who observed approximately 50% reduction in MCF7 proliferation with 5µM AST. However, others have found 10µM AST to be ineffective at reducing MCF7 proliferation, or 30µM to be required to reduce it to 50% (Borowiec et al. 2007; Roy et al. 2008). The variation in results seen may reflect the different treatment durations and assays used. While Ouadid-Ahidouch et al. used an MTS assay kit after four days of treatment, Borowiec et al. used this assay after only 48 hours, and Roy et al. used the ^{3}H-thymidine incorporation proliferation assay after 72 hours of treatment.

Meanwhile DOF treatment up to 10µM had no impact on MCF7 proliferation after 72 hour treatment (Figure 5.11). While the effect of this K^+ channel blocker on MCF7 proliferation has not been assessed previously, the lower dose of 1µM DOF was sufficient to virtually completely prevent hERG current in the murine atrial tumor cell line HL-1 (Wang et al. 2002). Another specific hERG blocker E-4031 (300nM) had no effect on MCF7 proliferation (Roy et al. 2008) despite having an IC_{50} for hERG current of 7.7 nM (HEK-293 cells; Zhou et al. 1998).

Both the hEAG and hERG channels are known to be expressed in MCF7 (Table 1.8). As discussed previously, it was hypothesized that if an activity was blocked by AST (blocked hEAG and hERG) but not a specific hERG blocker, then it is likely to be the hEAG-specific component of AST's activity that is responsible. In this manner, the data suggests that the K^+ channel hEAG, but not hERG, has a role in MCF7 proliferation. This same conclusion was reached by Roy et al. (2008). In summary, this data confirms that the MCF7 cells in use respond to the K^+ channel blockers TEA, 4-AP, AST and DOF in the manner expected from previous publications.

6.4.2 Technique: whole cell patch clamping

Whole-cell patch clamping is a technique which can be applied to virtually any cell or tissue type, and has allowed great advances in the field of cell electrophysiology. As previously discussed in sections 1.6.2..1 and 4.3, it is the gold standard technique with which to assess the activity of ion channels, both in cultured cells and tissue, due to the ability to assess minute changes in the current across the plasma membrane in real time, under physiologically relevant membrane potentials. However, because of the nature of the technique, it is error-prone and may not always generate accurate recordings. There are a number of limitations which must be understood and corrected for in order to make accurate recordings.

Series resistance relates to the physical properties of the pipette tip, and clogging of the tip, introducing another source of resistance in series with the plasma membrane resistance under scrutiny. This is a major source of error in patch clamp recordings. To minimise this, voltage clamping is only considered to be successful when the membrane resistance greatly exceeds series resistance. As described by Sontheimer and Olsen (2007), uncompensated series resistance introduces error in the current recorded, which increases with the amplitude of the current. The patch clamp amplifier hardware can be used to compensate for series resistance to a certain extent, but not fully. Thus, to reduce this source of error several steps are essential. A maximum uncompensated series resistance (often 10MΩ) should be set as a cut off (Ouadid-Ahidouch et al. 2004a) and should be declared in the methodology. High concentrations of ethylene glycol tetracidic acid (EGTA) in the pipette solution can help to reduce “healing” of the plasma membrane inside the pipette, which can be a major source of clogging.

In addition, whole cell patch clamping requires several assumptions to be made regarding the plasma membrane. Firstly, it assumes that the membrane potential is equal at all points on the cell surface, and secondly, that current or voltage clamping (which affects the potential) is universally disseminated to all points on the plasma membrane. However, under most experimental (and naturally occurring) circumstances these are not necessarily appropriate (Sontheimer and Olsen 2007).

Furthermore, many experiments have looked in real time at the acute effects of compounds on channel activity, usually recording events occurring within 10 or 20 minutes of treatment. It is in the nature of the patch clamp methodology that

membrane integrity begins to deteriorate after this time, as the cell dies. Pre-treatment for longer periods would be required to occur in advance, and therefore longer term effects on K^+ currents cannot be measured in real time (Sundelacruz et al. 2009). The result is that only short term effects are seen, which are more likely to reflect post-translational regulation, direct channel gating, and activation cascades, rather than changes in gene expression, translational regulation, or protein half-life. In addition, as most systems, including the current one, are designed to study single cells, one at a time, the technique is laborious, low-throughput, and does not reflect cell-cell interactions. However, systems are being developed allowing electrophysiological recordings of many cells to be recorded in parallel, using microchips with numerous apertures serving as patch electrode tips (Sundelacruz et al. 2009).

Another potential limitation of patch clamping methodology is that typically, the experiments are carried out at room temperature rather than 37^{o}C. Reportedly, the lower temperature increases the stability of the patch. Where the effect of temperature on current under patch clamp has been assessed, large drops in temperature (29^{o}C to 9^{o}C) had a measurable impact on some elements of the macroscopic current particularly the transient components, but the change from 20^{o}C to 29^{o}C had little effect on the overall current recording (snail neurons; Lux and Brown 1984). This suggests that the difference in temperature between room temperature and 37^{o}C may not have a significant impact. However this has not been fully assessed in all cell types.

Finally, it is unrealistic to compare the concentrations of compounds used for K^+ channel experiments with the concentrations known to regulate other cellular processes *in vivo* or in cell culture conditions, such as a PTK inhibitory IC_{50} or doses which promote proliferation. This is due to the requirement for slightly different experimental conditions. While every attempt is made to make the media for a patch clamp experiment as physiologically relevant as possible, in order to accurately manipulate currents, the serum normally added to cell culture media is absent, and various ion concentrations and pharmacological agents are frequently used to allow the experimenter to isolate individual currents. It was suggested that serum may bind drugs such as 4-AP, and can reduce both their channel blocking and anti-proliferative properties (Wonderlin and Strobl 1996). Also, the pipette solution which bathes the intracellular space needs to mimic the normal intracellular

milieu as closely as possible, but it is at best a compromise. The result is that while comparable IC_{50} doses for reducing channel activity and proliferation might be used to argue for a common target, different values cannot be proposed as evidence to reject this hypothesis (Wonderlin and Strobl 1996). This makes it impossible to make direct links between K^+ flux effects and alterations in the proliferative or apoptotic activity of cells. However, as discussed, studies which have silenced specific channel genes, or transfected them into cells known to not normally express them, add strength to the arguments here.

Due to the diverse nature of plasma membrane ion channels, a number of standard measures were built into the patch clamp protocol used to optimise the recording of K^+ currents, and not those mediated by other ions. These have been discussed in greater detail in section 1.6.2..1, but are summarized briefly here. The speed of activation and inactivation of ion currents can vary greatly. In these experiments, each voltage step was relatively slow, lasting 250ms, and current was assessed in the second half of this. This minimised interference from the Na^+ currents, which typically activate and inactivate quickly, within 5ms (Sontheimer and Olsen 2007; Standen et al. 1994). Likewise, the choice of holding potential from which the voltage steps are applied from can separate different current types. Many K^+ currents will activate from a range of holding potentials, but the level of -50mV used here allows the activation of the delayed rectifier K^+ currents, including numerous VGKCs, whilst preventing many transient K^+ currents.

Pharmacological agents of varying specificity can be used to block undesirable currents, leaving the one under scrutiny. However, this can have unforeseen effects on the activity of the cell. Instead, the best practice is to assess the current in the presence and absence of the ligand under scrutiny, and subtract to observe the responsive element. This approach was adopted in this study, and was discussed in greater detail in section 4.3.5.

Finally, the use of current/voltage (I/V) curves to assess the data can generate information regarding the characteristics of the current which can aid in its identification. As discussed, these parameters include the reversal potential, voltage dependence, and quality of the patch clamp. Much of this information is difficult to infer from the raw patch clamp data.

The use of statistical analysis (General Linear Model for repeated measures; GLM) and discussion of the mean result of a number of repeated experiments ($n \geq 3$) to determine the significance of the effect of treatment on the voltage-response of the current (section 4.3.6) strengthens the results generated here in comparison to many related investigations. In contrast, numerous key studies in this field have elected simply to use descriptive statistics to describe the currents recorded, and discuss the results of individual, apparently representative, sets of results (Borowiec et al. 2007; Coiret et al. 2005; Garcia-Ferreiro et al. 2004; Ouadid-Ahidouch et al. 2004a). This is a key short-fall of these studies.

As discussed, in several cases an observed effect failed to achieve statistical significance despite showing a clear trend towards an increase or decrease in macroscopic current after treatment. This is likely to relate to the variability between cells in the recorded current. It is possible that a factor in this is differences in size of the cells used (section 5.3.1; a cell with greater surface area may have more ion channels present in the plasma membrane and hence, larger whole-cell current). Although measures were taken to reduce the impact of this, a degree of variability in cell size persisted due to visual observation of cell size. In future studies, this can be minimized further by reporting current density as a ratio of current and size/capacitance (i.e. pA/pF), in the manner of the Ouadid-Ahidouch group (Borowiec et al. 2007; Ouadid-Ahidouch et al. 2004a). Regrettably this was not possible for the current dataset. Alternately, this variation may reflect differences in the growth cycle stage of the selected cells. Many K^+ channels in MCF7 are known to be expressed differentially at various stages of the growth cycle, including hEAG (Ouadid-Ahidouch and Ahidouch 2008) and BK (Ouadid-Ahidouch et al. 2004a). Synchronization of the cell cycle prior to experimentation may reduce this. A final possible explanation for this variability is that MCF7 cells are known to secrete numerous proteins into the extracellular matrix, including metalloproteinases and the glycoprotein fibrinogen, each with roles in tumour invasiveness (Liu et al. 2002; Rybarczyk and Simpson-Haidaris 2000). Trypsinisation prior to patch clamping is a standard technique used by some groups to minimize interference from secreted protein (Ouadid-Ahidouch et al. 2000; Ouadid-Ahidouch et al. 2004a), however it provided no additional benefit in the current research, so was omitted from the protocol.

The reversal potential (i.e. potential where the net current flow was 0mV) of the recorded currents was often around -80mV, indicating that the current recorded was largely due to K^+ ions (see section 5.3.2; the equilibrium potential for K^+ is around -85mV, so at potentials more negative than this, K^+ ions will flow inward, and at more positive potentials K^+ will flow outward). However on several occasions the reversal potential was more positive. This may reflect the activation or inactivation of other ion channels by that treatment, in addition to the K^+ channels. Alternately, this variation may reflect slight methodological variations between the experiments, such as slight inconsistencies in the K^+ ion content of the extracellular and intracellular solutions used.

6.4.3 Control treatments

As shown in Figure 5.12, the patch clamping protocol with no additional treatment did impact upon the recorded MCF7 K^+ current significantly. Overall, the within cell effect of treatment became significant after depolarization from -50mV to -20mV, and all potentials greater than this. However, by higher potentials (≥80mV) the mean magnitude of this effect became minimal compared to that of the increasing applied voltage. By the highest membrane potential applied (120mV) the mean difference in current before and after treatment was negligible (although within individual cells is was still significant). This data implies that the protocol, and possibly handling of the cells, does have an impact upon the recorded K^+ current.

In the published literature (section 1.6) there was no occasion where the effect of the control treatment over time on the recorded current was discussed. It is not known how wide spread this phenomenon is.

Furthermore, even at very negative potentials there was a slight current recorded, which in some cases was negative. This suggests that despite achieving the prerequisite Giga-Ohm seal, the seal of the plasma membrane around the micropipette suffered from some leakage. In a hypothetically ideal voltage gated ion current (see Figure 4.7), there is virtually no current at very negative potentials, and as the potential steps up past the activation potential of the channels in question, positive current flows. However, this was not always the case. It was thought this may relate to the secretion of matrix proteins by MCF7 (observed visually). Attempts were made to minimize the impact of this, including trypsinisation of the cells prior to patch clamping (a standard technique to remove extracellular protein), and using newly passaged cells which had not had the opportunity to secrete fresh protein. Regrettably they provided no benefit. For future studies, further time taken during the optimisation stages should reduce the impact of this.

As the time-course shows (Figure 5.12B) after the initial increase in current between one and three minutes, there was minimal further degradation of the seal (which would be indicated by a further increase in current). To allow analysis of the remaining results, it was assumed that leakage occurred at a constant rate for each cell. This is an unavoidable limitation of the present study, and possibly the technique in general.

Both the pre-treatment I/V trace, and the 5 minute I/V trace show a response to the increasing voltage steps (voltage sensitivity). Furthermore, both have a reversal potential (the voltage at which the recorded current changes from negative, flowing into the cell, to positive, flowing out of the cell) of between approximately -50 and -80mV. As described in section 5.3.2, this indicates that the majority of the current is due to the flow of K^+ ions, as this value is close to the K^+ equilibrium potential.

As illustrated in Figure 5.13, 0.1% DMSO treatment for 5 minutes resulted in a slight increase in the depolarization activated current, as with the untreated cells. However this never achieved statistical significance, and after the initial increase (in the first minute) it too stabilised. This suggests that the presence of DMSO could act to stabilise the seal between the pipette and the MCF7 plasma membrane. However, it is more likely that at 0.1% in the perfusing Tyrode, DMSO has no significant impact upon K^+ current or seal integrity.

6.4.4 Pharmacological characterization of the whole cell MCF7 current using K^+ channel blockers

The impact of the K^+ channel blockers TEA, 4-AP, AST and DOF on macroscopic current in MCF7 was investigated. This was to confirm that the system and the cell line were capable of generating reproducible results that were in line with what was previously published.

TEA and 4-AP are both fairly broad spectrum channel blockers: TEA blocks the majority of the K^+ channels, while 4-AP prevents VGKC activity (Table 1.9). At the selected concentrations, both resulted in rapid (within 1 minute) and significant reduction in voltage activated current (Figures 5.14 and 5.15), which remained stable for several minutes following this. In both cases the difference within cells before and after treatment was statistically significant.

The concentration of TEA used (10mM) for this was below the IC_{50} for MCF7 proliferation calculated previously (18.8mM; section 5.2.2), so the impact on channel activity was unlikely to be due to a non-specific cytotoxic effect. The IC_{50} for current inhibition by TEA has been previously calculated as around 2mM (Ouadid-Ahidouch et al. 2004a), which is comparable to the 10mM dose used here. Previously, after 3 minutes perfusion with 5mM TEA, whole cell MCF7 current was reduced by approximately 88% (400ms depolarising step to +60mV from a holding potential of -60mV; Ouadid-Ahidouch et al. 2000). In the current study, on depolarization stepping to +60mV current was reduced by TEA by 26% (777.3 to 574.9 pA). A greater percentage reduction (32%) was seen on depolarization to +40mV. These results are more in line with those of Coiret et al. (2007), who describe a reduction in MCF7 current of around 40% after perfusion with 0.5mM TEA, upon stepping the potential from -100 to +100mV. In all cases, treatment with TEA inhibits current mediated by the movement of K^+ ions, confirming that this ion plays a significant role in whole cell MCF7 current.

As with TEA, the chosen 4-AP concentration of 1mM is below its IC_{50} for MCF7 proliferation (2.7mM; Figure 5.9). Again, this was selected to minimize the potentially cytotoxic effects of higher concentrations. The impact of 4-AP on K^+ current in MCF7 has not been determined prior to this. Accordingly, there is no calculated IC_{50} for the inhibition of MCF7 macroscopic current by 4-AP. In other cell types it has

been calculated as between 0.1 and 4mM (Table 1.9). After 5 minutes perfusion with 1mM 4-AP K^+ current was inhibited by approximately 11% (388.4 to 346.0pA), upon a voltage step from the holding potential of -50mV to 120mV. Although there are no other published results to compare this to, this suggests that the K^+ current measured in MCF7 is partly mediated by the VGKCs. It stands to reason that the 4-AP sensitive VGKC element of the current would be less than the TEA-sensitive current element, as it is one of many components to this current (the K^+ channel types inhibited by TEA are listed in Table 1.9.)

Perfusion of MCF7 with 1μM AST (blocker of hEAG and hERG currents) for 5 minutes inhibited a macroscopic current which became active upon depolarization to potentials of -10mV or more positive (Figures 5.16 and 5.18). The non-significance of this result may relate to variation in the size of cell selected for experimentation, as discussed in section 6.4.2. It is known that the hERG channel has a greater sensitivity to AST than the hEAG channel. The whole cell current in HEK293 cells with cloned hEAG was determined to have an AST IC_{50} of 196nM (Garcia-Ferreiro et al. 2004), while in HEK293 transfected with hERG the AST IC_{50} was 0.9nM (Zhou et al. 1999). This suggests that 1μM AST treatment should be able to inhibit both channels adequately. As discussed, treatment with 1μM DOF (blocks only hERG) had no impact upon MCF7 whole cell current (Figures 5.17 and 5.18). The conclusion is that the AST-sensitive current recorded is mediated by the hEAG channel, and not hERG.

The voltage sensitivity of the AST-sensitive hEAG current in MCF7 has not previously been demonstrated, despite 5μM AST being shown to inhibit whole cell MCF7 current on several occasions. The sensitivity of the current to AST was dependent on cell cycle stage, with the maximum effect being seen in G1 phase (Ouadid-Ahidouch et al. 2004b). This group later demonstrated that 5μM AST inhibited MCF7 current by 21% in cells arrested in G1 phase by 24 hour serum starvation (Borowiec et al. 2007). Although the conditions of this experiment were not analogous to the current study, the observed magnitude of the AST-sensitive current was similar. In this case, 5 minute perfusion with 1μM AST inhibited the MCF7 current recorded during a voltage step from -50mV to 40mV by 27.9% (note that these cells were not synchronized to any cell cycle stage).

Where the hEAG channel was cloned into HEK293 cells, depolarization steps between 0 and 120mV (from a holding potential of -70mV) showed that hEAG current was activated by depolarization but became insensitive to voltage at potentials above 60mV (Garcia-Ferreiro et al. 2004). This was consistent with the current results, which showed AST-sensitive current in MCF7 reaching a peak at 40mV, and reducing at membrane potentials ≥ 50mV.

Assuming that the activity of the hEAG channel is comparable between MCF7 cells and HEK293 model described above, the selected concentration of 1μM is above the IC_{50} for AST inhibition of hEAG current calculated by Garcia-Ferriero et al. (2004), but below its IC_{50} for MCF7 proliferation (4.9μM; Figure 5.10). As with 4-AP and TEA, this maximizes the effect of AST on the recorded current, whilst reducing the impact of non-specific cytotoxic effects of the agent.

Interestingly, no DOF-sensitive current was observed in MCF7, despite the presence of hERG channels being previously shown in these cells (Table 1.8). This suggests that either this channel is absent in this particular MCF7 strain, or it is not active under the basal conditions used. The latter corresponds with the known role of hERG in apoptosis in a number of cell types (section 1.6.5). This requires confirmation either by seeking hERG protein in the MCF7 cell line, or the assessment of hERG (DOF-sensitive) current under pro-apoptotic conditions. Furthermore, it would be of value to determine whether incubation with DOF impeded the ability of MCF7 cells to undergo apoptosis.

Current mediated by the hERG channel is known to be temperature sensitive, and increased in HEK293 cells transfected with hERG upon increasing temperature from 23 to 35^{o}C (Zhou et al. 1998). The DOF experiments were conducted at room temperature. Although a higher temperature may increase the DOF-sensitive current, the cost would be a reduction in the stability of the patch seal (section 6.4.2). Again this would be interesting to follow up.

Due to the lack of effect of the range of DOF concentrations used on MCF7 proliferation (1nM to 10μM; Figure 5.11), and corresponding inability of E-4031 (another hERG blocker; see Table 1.9) to impact upon the proliferation of this cell line, it was difficult to select an appropriate dose for the patch clamp experiments. Likewise, no published data regarding the inhibitory effect of this agent on MCF7 whole cell current was available. However, 1μM DOF was effective at inhibiting

hERG current in a number of cell types including HEK293 and HL-1 cells during 2.5 second depolarization steps from -60 to +40mV from the holding potential of -80mV (Wang et al. 2002). Based on this it is likely that this dose is appropriate for use in MCF7. In a more comprehensive study based on this initial data, higher concentrations of DOF could be tested for an effect on MCF7 hERG current.

Wang et al. (2002) reported that hERG current in SK-BR-3 breast cancer cells, HEK293 and HL-1 cells under control conditions was active at potentials more positive than -40mV. However, they found that the addition of H_2O_2 to the perfusing solution both increased the magnitude of the hERG current, and lowered its activation potential to -60mV. These experiments were conducted at 36^{o}C, in cell lines which do not express VGKCs, which were then stably transfected with vectors containing the hERG gene. The result is that all the observed current activity can be attributed to the hERG channel, but that the protein is in a non-physiological environment, and consequently, may not be regulated in a wild-type manner. In the MCF7 model used, numerous K^+ channels may be involved in any given current. While this makes analysis of the results more complex, it is more physiologically relevant, as no channel will act in isolation, and all are regulated by the correct mechanisms. It is possible that in the MCF7 model, the activity of other channels masks any effect of DOF on the hERG channel. Alternately, in MCF7 this channel may only become active upon pro-apoptotic stimulation.

Overall, this data from four K^+ channel blockers of varying target specificity confirms that the VGKCs, and in particular the hEAG channel are active in MCF7, and play a role in the proliferation of this cell line. It also confirms that the hERG channel is not involved in basal MCF7 proliferation. Furthermore, in non-stimulated and unstressed conditions this channel is not active in this cell line.

6.4.5 17β-oestradiol enhances MCF7 macroscopic current

Treatment of MCF7 cells with 1nM E2 resulted in a rapid (within 1 minute) and significant increase in outward K^+ current (Figure 5.19). This continued to increase for up to 10 minutes into the treatment. After 5 minutes treatment, upon voltage stepping from the holding potential of -50mV to +120mV, current was increased by approximately 35%, from 762.9 pA to 1032.3 pA.

E2 treatment is known to increase the activity of MCF7 BK channels (section 1.6.6). This effect of E2 was not mediated by the ERs, largely because it occurred very rapidly, but in addition, co-treatment with the ER-antagonist ICI 182780 had no effect (Coiret et al. 2007; Coiret et al. 2005). Furthermore, tamoxifen, in its growth promoting concentrations also increased BK current.

However, the role of the BK channels in MCF7 proliferation is not straightforward. The BK channel blockers IbTx (100nM) and CTx (50nM) have previously been shown to have no impact on basal MCF7 proliferation (Table 1.9). They also did not inhibit 10nM E2-stimulated MCF7 proliferation, but did reduce BSA-E2 (10nM; does not enter the cell) induced proliferation (Coiret et al. 2005). Interestingly, IbTx and CTx also inhibited 10nM tamoxifen-stimulated MCF7 proliferation (Coiret et al. 2007). This suggests that E2 acts to promote MCF7 proliferation by two parallel mechanisms: the classical genomic (ER driven) mechanism which is independent of the K^+ channels, and a non-genomic mechanism, which is driven by extracellular E2 and tamoxifen, comprising direct or indirect activation of the BK channels. The E2-mediated increase in macroscopic MCF7 current described above may to relate to E2-induced proliferation by the second pathway.

The K^+ current recorded here that was enhanced by E2 treatment is outwardly rectifying (passes current more readily in the outward direction). How it relates to the E2-induced inward flow of osmolytes, and hence the swelling observed is not apparent from this data, although it seems clear that the VGKCs (mediating outward flow of K^+ ions) do not play a role, at least in the first few minutes after treatment. It would be interesting to determine whether inhibition of the inwardly rectifying K^+ channels such as the GIRK channels is capable of preventing E2-induced swelling of MCF7.

It is possible that E2 treatment is enhancing the current mediated by other outward K^+ channels known to be involved in MCF7 proliferation, in addition to BK activity, such as the hEAG or $K_v1.1$ channels. However, the specific MCF7 K^+ channel targets of E2 continue to require elucidation. Knockout or silencing of the specific channels in MCF7, or treatment with specific channel inhibitors along with E2 would help to achieve this end in the future. However, even without that information, this study provides evidence for a rapid, non-genomic mechanism through which E2 could promote the proliferation of MCF7 cells.

6.4.6 Soy isoflavones inhibit MCF7 macroscopic current

As discussed in section 1.6.7, the impact of genistein and daidzein on K^+ channel activity, including many of the key channels involved in proliferation and apoptosis, is widely studied. However, this investigation represents the first instance where the impact of soy isoflavones on K^+ channel activity has been considered in a breast cancer cell line.

Treatment with 31.6µM genistein appeared to inhibit an outwardly rectifying voltage-sensitive K^+ current in MCF7 cells (Figures 5.20 and 5.22), although this failed to achieve statistical significance. The genistein-sensitive current was particularly apparent upon depolarization steps from the holding potential to 0mV or more positive potentials. After 5 minutes genistein treatment the current recorded at the 100mV voltage step was inhibited by 24.4%.

Daidzein treatment (31.6µM) had a similar impact upon outward whole cell MCF7 K^+ current; although the magnitude of the effect was considerably lower (Figures 5.21 and 5.22). In this case 5 minutes treatment resulted in only 7.6% inhibition of the current recorded upon voltage stepping from the holding potential to 110mV.

Previously, genistein has been shown to inhibit current carried by a number of the K^+ channels known to be expressed in breast cancer cell lines, including the hERG channel transfected into HEK293 cells (Zhang et al. 2008) and its rat homologue rERG in rat microglial cells (Cayabyab and Schlichter 2002), $K_v1.3$ in human T lymphocytes (Teisseyre and Michalak 2005), the delayed rectifier K^+ current carried by $K_v7.1$ and KCNE1 in HEK293 cells (Dong et al. 2010), and a similar current in guinea pig ventricular myocytes (Missan et al. 2006). In each case genistein was apparently acting as a PTK inhibitor, although whether it acts directly on the channel protein or on upstream signaling pathways is not known.

The genistein concentration used in many of these studies (10 to 40µM) was comparable with the dose used in this investigation, described in sections 4.3 and 5.3 of this thesis. However, in some cases up to 100µM genistein has been used (Dong et al. 2010; Missan et al. 2006). The physiological relevance of these very high doses is limited. The sensitivity of the current to genistein appears to be channel and cell type specific. $K_v1.3$ current in human T lymphocytes was approximately half blocked by genistein between 10 and 40µM (Teisseyre and

Michalak 2005). Likewise, in HEK293 cells stably expressing the K_v7.1/KCNE1 channel, the delayed rectifier K^+ current was inhibited by approximately 50% by 30µM genistein (Dong et al. 2010). However, a similar current in guinea pig ventricular myocytes (specific channels not identified) was less sensitive to genistein, as the IC_{50} was calculated to be around 64µM (Missan et al. 2006). It would be of value to determine the dose-response for genistein on the MCF7 macroscopic current recorded.

The studies described in section 1.6.7 use similar voltage stepping protocols to the protocol used here to analyse the impact of genistein on various VGKCs. These comprise a holding potential of -80mV, then voltage steps lasting up to two seconds from -60mV up to +60 or +70mV (Dong et al. 2010; Missan et al. 2006; Teisseyre and Michalak 2005; Zhang et al. 2008). In each case they found that genistein inhibited the voltage activated element of the whole cell current, the effect took 5 to 8 minutes to reach its full magnitude, and upon genistein washout the current inhibition reversed. The relatively long time taken for the inhibitory effect of genistein to develop was mirrored in the present study, during which the current reduced gradually over 5 minutes treatment before stabilising.

The minimal inhibitory effect of daidzein observed in MCF7 cells echoes previous studies in other cell types, where daidzein was found to have considerably less current inhibitory effect than genistein (Dong et al. 2010; Missan et al. 2006), or none at all (Cayabyab and Schlichter 2002; Teisseyre and Michalak 2005). In each case this was related to the lack of PTK-inhibitory properties of daidzein compared to genistein. Furthermore, genistin, the PTK-inactive precursor of genistein also had no impact upon K^+ current (Missan et al. 2006).

The mechanisms through which genistein, and to a lesser extent daidzein, may be working on MCF7 plasma membrane K^+ channels are not known. There is some evidence that both may have some direct K^+ channel blocking activity, although this is dependent on the channel type and cell line (section 1.6.7). Furthermore, a number of tyrosine kinases, including the Src-family kinases and/or EGFR have been implicated in the regulation of a number of K^+ channel types (section 1.6.7). However, despite the known PTK-inhibitory action of genistein (Peterson 1995), very high concentrations of 190µM were required to see significant inhibition of EGFR tyrosine phosphorylation in MCF7, and these concentrations also caused massive

and rapid cell death (Peterson and Barnes 1996). Furthermore, genistein up to this concentration had no effect on tyrosine phosphorylation of a number of other key signaling kinases in MCF7, including MAPK and phosphatidylinositol 3-kinase (PI-3-K; Peterson and Barnes 1996). Lower concentrations of genistein (≤10μM) actually increased the phosphorylation (activation) of a number of key signaling kinases including ERK1/2 and Src (Liu et al. 2010; Lucki and Sewer 2011; Maggiolini et al. 2004; Yang et al. 2010). This suggests that at the concentrations used in the present and previous studies, K^+ current inhibition by genistein is not mediated by PTK inhibition of these signaling kinases. However, there is considerable indirect evidence suggesting that numerous K^+ channels are directly or indirectly regulated by tyrosine phosphorylation, including studies involving a range of PTK inhibitors.

It is possible that genistein inhibits direct phosphorylation, and hence activation, of the channel proteins. These are described in section 1.6.7. Many of the K^+ channels do appear to be regulated by direct phosphorylation of the channel protein. The mammalian 2-pore domain K^+ channels, including several members of the TASK channel family, are inhibited by direct channel phosphorylation by protein kinase A (PKA) and PKC (Patel and Honore 2001). On the other hand, the K_v7.1/KCNE1 channel forms a macromolecular complex with a number of proteins including PKA, resulting in the serine phosphorylation of a residue on the amino terminus of the K_v7.1 protein, and activation of the channel (Chen and Kass 2011). Tyrosine phosphorylation of the amino terminal of a number of VGKCs increases channel activity, including the K_v1.2 and K_v1.3 channels (Davis et al. 2001 and references therein). Tyrosine phosphorylation is also implicated in the regulation of other K^+ channel groups, including BK, and the K_{ir} channels (Davis et al. 2001). However, to date, the effect of genistein on direct phosphorylation of the various K^+ channel proteins is as yet unknown. Whether phosphorylation has a positive or negative influence on channel activity appears to depend upon the channel type and site of phosphorylation.

Preliminary attempts were made to characterize some of the channels on which genistein might be acting. Combining treatments is a frequently used method in this field, designed to highlight synergy, interference, or no additional effect between compounds with known channel targets, such as AST, IbTx and TEA, and an uncharacterized molecule, in the manner of the Ouadid-Ahidouch group (Borowiec et al. 2007; Coiret et al. 2007; Coiret et al. 2005; Ouadid-Ahidouch et al. 2004a;

Ouadid-Ahidouch et al. 2004b). In this manner the K^+ channel targets of E2 have been ascertained (section 1.6.6). However, this technique has not previously been used to identify the K^+ channel targets of genistein.

The combination of 4-AP and genistein was intended to confirm that genistein inhibited the VGKCs in MCF7. However, 5 minute treatment resulted in a non-significant increase in whole cell current (Figure 5.23). Upon stepping voltage to +40mV, the current was increased by 21.7%. Three minute treatment had a similar effect (not shown). While it is possible that the two agents interfered with each others activity, what is more likely, due to the rapid degradation of the patch clamp seal following this point, is that the treatment had a toxic effect upon the cells, and resulted in their early death.

Equally, the patched cells were unstable with the combined genistein-AST treatment, and only 3 minutes of recordings were achieved at the n=3 level (Figure 5.24). However, after 3 minutes this combined treatment inhibited a voltage gated current which was apparent upon depolarization to potentials of -40mV or more positive. The current was calculated to be reduced by 15.4% at the 100mV voltage step after treatment. This current was very similar both in characteristics and magnitude to the AST-sensitive current. This suggests that the hEAG channel is potentially a key molecular target of genistein in MCF7 cells. Future experiments looking at the effects of combined genistein and K^+ channel blockers may benefit from the use of lower concentrations of both agents, once dose-responses have been characterized in MCF7.

The role of the hEAG channel in MCF7 has previously been confirmed (Figure 5.10). Furthermore, MCF7 proliferation with genistein concentrations >10µM was sub-maximal and reducing as concentration increased (Figure 3.3). The current data suggests that in addition to the slight increase in the induction of apoptosis seen in MCF7 with 31.6µM genistein, in parallel this treatment inhibits hEAG current in a rapid non-genomic manner, which has a further negative impact on cell proliferation. The mechanism through which genistein inhibits hEAG current is not known.

Others have described genistein mediated inhibition of hERG current also, although not in MCF7 cells to date (section 1.6.7..6). Although this channel had no activity under basal conditions in MCF7, it would be of interest to investigate the activity of

hERG in pro-apoptotic genistein concentrations, due to the known role of this channel in apoptosis (section 1.6.5).

The role of the VGKCs, including hEAG, in volume regulation is not yet known, and unfortunately little can be inferred from the current results with genistein for cell volume and K^+ channel activity. One set of data shows that 31.6µM genistein results in (apoptotic) shrinkage of MCF7 cells, which is frequently mediated by an outward flux of ions including K^+, but in parallel, this concentration of genistein inhibits outward K^+ current, including that mediated by the hEAG channel. This implies that hEAG is not involved in genistein-induced AVD in MCF7. However, it is apparent that many of the K^+ channels are involved in both pro-apoptotic and pro-proliferative responses in some cell lines, depending upon the stimulus, intermediate regulatory mechanisms, and potential for cross-talk between pathways. It is hoped that this pilot data will lead to further research regarding the mechanisms through which soy isoflavones regulate ion channel activity, and hence proliferation and apoptosis in breast cancer cells.

6.5 The discrepancy between the *in vitro* and *in vivo* effects of soy isoflavones

The aims of this investigation were two-fold. Firstly, the intention was to better characterize the proliferative and apoptotic effects of physiologically relevant concentrations of genistein and daidzein on two breast cancer cell lines of differing ER status, and to understand more clearly the impact of pre- and post-menopausal E2 concentrations on these responses. Secondly, this project was designed to begin to elucidate several novel mechanisms through which the soy isoflavones may be mediating these proliferative and apoptotic effects.

In ERα+ MCF7 cells, the increase in proliferation due to the isoflavones was compounded by the presence of physiological postmenopausal E2 levels, and premenopausal to a lesser extent, suggesting that in this particular breast cancer model, physiological levels of isoflavones are associated with an increase in breast cancer risk. However, this contradicts gathering epidemiological evidence which points to a protective effect of even relatively modest intakes of soy isoflavones against breast cancer incidence, recurrence, and mortality. Furthermore, this benefit appears to be greater for ERα+ breast cancer.

In the course of this research, a number of possible reasons behind this discrepancy have been uncovered and investigated, which will be discussed in the following section.

6.5.1 Recommendation to re-classify ER status in breast cancer

This study builds on the evidence suggesting that soy isoflavones could be of benefit for breast cancers expressing greater levels of ERβ than ERα. The current evidence is in the form of the reduction in proliferation, and associated increase in the induction of apoptosis described in the ERα-/ERβ+ breast cancer cell line MDA-MB-231. This supports the hypothesis that ERβ mediates many of the protective effects of soy isoflavones seen, while through ERα they act to enhance proliferation.

There is a case for the actions of ERβ explaining some of the discrepancies between the *in vitro* and epidemiological effects of soy isoflavones on breast cancer. The level of ERβ expression in the breast tumours of the women involved in all the epidemiological studies regarding isoflavones and breast cancer is not known. As described, the epidemiological studies categorized the women according to their ERα expression level as either ER+ or ER-, according to standard medical practice, due to the clinical significance of ERα expression levels indicating the potential for benefit from endocrine therapy. However, to better understand the impact of soy isoflavones on breast cancer in the future, if possible four categories should be used, based on the relative levels of both ERs (Figure 6.4).

This hypothesis may explain the net reduction in risk and recurrence of ERα+ (ER+) breast cancer associated with a high intake of isoflavones. It is possible that, despite the potential for an increase in risk in the minority ERα+/ERβ- subgroup of this population, for the majority of the ERα+ women, their tumours would also express ERβ, potentially at high enough levels to be associated with a reduction in risk with high isoflavone intakes.

Likewise, the ERα-/ERβ+ sub-population could also benefit from high isoflavone intakes, for the reasons described. This was not evident from the epidemiological evidence for the ERα- (ER-) population, possibly due to low numbers or masking by the lack of any effect of physiological levels of isoflavones in the final ERα-/ERβ- group.

However, before clinical practice can be changed, or recommendations can be made, considerable further research is needed in this field. While a great deal is understood regarding the mechanisms through which isoflavones may modulate breast cancer risk, much more research is required.

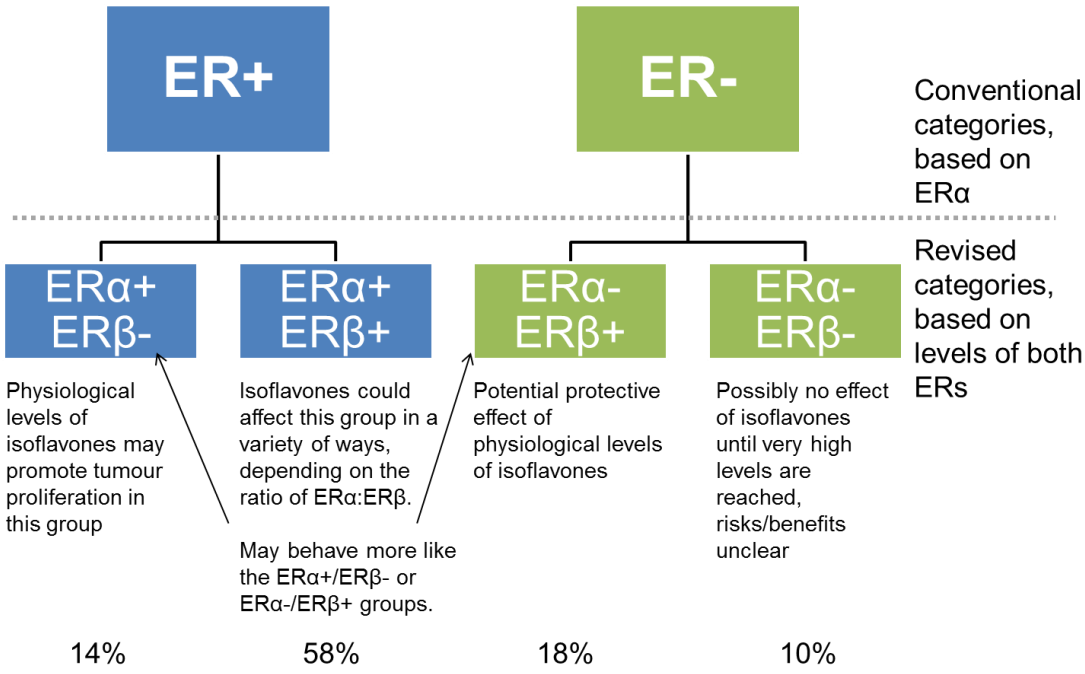

Figure 6.4: Conventional and suggested new categories for breast cancer ER classification

Diagrammatical representation of how the conventional breast cancer ER classifications of ER+ and ER- would subdivide into four new categories, based on the levels of both ERs. The percentages represent the estimated frequency of that ER subtype occurring, as published by Skliris et al. (2008).

As discussed, this must include unequivocal confirmation of the role of ERβ. Initially steps should include knockout or silencing of the ERβ gene in MDA-MB-231, or isoflavone feeding to βERKO mice to confirm that ERβ mediates the protective effects of isoflavones in ERβ-dominant scenarios. If specific ERβ antagonists can be developed than they would aid this field also. Furthermore, the epidemiological evidence for the protective effect of isoflavones should be revisited, with a focus in the expression levels of ERβ.

In the longer term, it must be determined whether the cost of routine testing for ERβ outweighs its potential benefit to women with breast cancer. This would require clinical testing. Furthermore, this would likely highlight the difficulties surrounding testing for ERβ. Due to its many isoforms (Figure 1.2), the various ERβ antibodies

currently in use vary in their isoform specificity depending on their target sequence. To date there are no specific downstream clinical markers of ERβ expression which can be used diagnostically (Clark et al. 2012). Many questions remain which must be addressed, regarding the physiological roles of the individual isoforms, which vary in their ligand binding and transcriptional activating abilities (section 1.4.2; Cappelletti et al. 2006; Maruyama et al. 1998; Ogawa et al. 1998).

6.5.2 Isoflavones and breast cancer survivors: interactions with treatment regimes

It is of key importance to further investigate whether isoflavones interact with any chemotherapeutic treatments that women with breast cancer may undergo. As many of these agents work as oestrogen antagonists, or interfere with oestrogen synthesis or other key signaling pathways, any interaction between them and isoflavones has the potential to be of great benefit or harm to the women.

In one prospective cohort of Chinese breast cancer survivors, among the group with ERα+ cancer (n =3181), a protective effect was associated with high soy intake for mortality (all causes) and breast cancer recurrence and mortality, in both tamoxifen and non-tamoxifen users (Shu et al. 2009). Among non-tamoxifen users the hazard ratio (HR) and 95% CI for breast cancer recurrence and mortality with the highest quartile of total soy intake compared to the lowest (1: reference) was 0.65 (0.36-1.17). For women using tamoxifen these values were 0.93 (0.58-1.51) for women in the lowest quartile of soy intake and 0.66 (0.40-1.09) for the highest soy intake quartile. Interestingly, this suggests that among the women in the highest soy intake quartiles, use of tamoxifen did not appear to provide any additional protection. When the HR was calculated for isoflavone intake (mg/day) instead of total soy, the values were similar.

However, another smaller prospective cohort of Chinese women with breast cancer reported no additional benefit of postmenopausal ERα+ breast cancer recurrence with increasing isoflavone intake (Kang et al. 2009). Importantly, they did not observe any increased risk associated with interference between the isoflavones and tamoxifen. It may be of relevance that numbers in this study were low (438 women received tamoxifen).

Overall, a pooled analysis of breast cancer survivor cohorts (which did not include the above study, reported no significant effect of soy intake on the inverse relationship between tamoxifen use and breast cancer recurrence and mortality (Nechuta et al. 2012). This study pooled the results of four cohorts from both the US and China, and included 9514 breast cancer cases.

On the other hand, high soy intake appeared to have an additional benefit for breast cancer recurrence among postmenopausal women receiving anastrazole, an

aromatase inhibitor which interferes with E2 biosynthesis (Kang et al. 2009). Among anastrazole users (n=86) compared to the lowest quartile of soy intake, women in the highest quartile had significantly reduced risk of recurrence (HR 0.65, 95% CI 0.47-0.85, p for trend = 0.005).

As both tamoxifen and E2 are known to act similarly on the activity of the BK channel (section 1.6.6; Coiret et al. 2007), it would be interesting to characterize the impact of genistein and daidzein on this channel. In each case where they have been tested, daidzein has shown considerably reduced or no effect on K^+ current, compared to genistein. It is possible that this difference between the two molecules may provide a mechanism for their opposing effects on tamoxifen-inhibition of cancer cell proliferation observed in animal models of the disease (section 1.3.3).

Overall, these studies are promising, and argue that dietary isoflavones do not antagonize the effects of tamoxifen and anastrazole treatment. In addition, depending upon the treatment regime, they may be able to reduce the risk of breast cancer recurrence or mortality independently, conferring an additional benefit. Regrettably, animal studies using various rodent models have failed to conclusively back this up (section 1.3.3). However, as discussed, the use of rodent models for breast cancer may be of limited value. There have been no studies in other model systems, including both primary tissue and cultured cells which were specifically designed to investigate this outcome.

6.5.3 The choice of breast cancer model: *in vitro* versus *in vivo*

In an attempt to understand some of the mechanisms behind the effects of isoflavones on breast cancer risk, two *in vitro* models of breast cancer were used: the cell lines MCF7 and MDA-MB-231. MCF7 cells are the most widely used cell line in the world (Burdall et al. 2003), although MDA-MB-231 cells are commonly used also. As described, they differ in their ER status (Table 1.2). Both cell lines were a gift from the Hannah Research Institute (Prof. D. Flint). There are many advantages to using cultured cell lines. In particular, due to their wide use, they allow reproducible results, and aid comparison between studies. However they are prone to contamination, genetic drift over time, and their phenotypes can change when they are continuously cultured (see section 2.1.1, regarding the use of phenol red free experimental medium for MCF7 cells).

An alternative for future study is the use of primary cell culture, directly derived from tumours. Their characteristics more accurately reflect the original tumour. However, they have a finite lifespan, often only surviving several passages, and they are easily contaminated by non-cancerous cells. Both cell lines and primary cells will behave differently to the parent tissue as the cell-cell interactions present in the organ are lost *in vitro* (Burdall et al. 2003). Whichever model is used, it is important to bear in mind its limitations. In addition, comparison between studies *in vitro* is often complicated by the use of a diverse range of growing conditions, cell lines, and tests. In this field, rodent models are not particularly appropriate, for a number of reasons, discussed previously (section 1.3.3). Furthermore, clinical trials in women with breast cancer are complicated by the burden of their disease, and the potential for the increase in ERα+ cancer proliferation, and as discussed, supplementation in this group continues to be contraindicated for this reason (NICE 2009b).

In the current cell culture models a number of potentially protective mechanisms of soy isoflavones were documented, including the induction of apoptosis (MDA-MB-231 and MCF7), shrinkage, which may relate to AVD (MCF7), and inhibition of hEAG current (MCF7). In addition, numerous other protective mechanisms of soy isoflavones have been proposed, including modulation of oestrogen synthesis, cell cycle control, breast tissue development, antioxidant activity, angiogenesis and protein tyrosine kinase inhibition (Steiner et al. 2008). These are too numerous to discuss in any detail.

However, despite the innumerable protective mechanisms frequently associated with physiological isoflavone levels such as those used in this investigation, the inhibition of breast cancer cell growth by isoflavones is outweighed by their ability to induce ERα-mediated cell proliferation, at all but the very highest (non-physiological) concentrations. There is growing evidence to suggest that the balance between the protective and proliferative effects of soy isoflavones may be in greater favour of their growth-inhibitory pro-apoptotic properties in a human *in vivo* model of the disease.

As discussed above, there are the obvious differences between cell culture and women, including the cell-cell interactions, organs, and immune system, which could impact upon the efficacy of isoflavones. Furthermore, genistein and daidzein do not circulate in the serum of soy consumers in isolation, but exist with alongside a number of secondary metabolites with varying activities (discussed in section 1.2.3). The report by Hwang et al. (2006) highlights the fact that the impact of the isoflavone metabolites frequently differed to that of the parent molecule, and thus they had varying abilities to promote ERα-mediated proliferation, and act as E2 agonists or antagonists. Due to the significant inter-species and inter-individual variation in isoflavone metabolism it is difficult to design studies and draw conclusions regarding this. However, Hwang et al. (2006) suggested that many of the key metabolites of soy isoflavones, including dihydrogenistein, O-demethylangolensin and tetrahydrodaidzein induce MCF7 proliferation to a considerably lower extent that the parent isoflavones.

In addition, a study feeding male and female Sprague-Dawley rats with genistein, firstly *via* the lactating dam, then post-weaning with supplemented feed (5 and 500 µg/g genistein) for 140 days from birth compared the serum and tissue levels of total genistein and the free (aglycone) form (Chang et al. 2000). They found that compared to the serum levels, mammary gland tissue levels of genistein had a greater proportion of the free genistein fraction, and less total genistein. This suggests that the non-polar aglycone form accumulates more readily in mammary tissue, due to the high adipose content, than the more polar conjugates.

The impact of the varying levels of certain metabolites on the protective mechanisms observed in MCF7, including the induction of apoptosis and hEAG current identified in this project, requires characterization. It is possible that some

metabolites of genistein and daidzein may retain the protective roles of the parent molecules, whilst having a minimal impact on proliferation at physiological concentrations. In this manner, metabolism of isoflavones may explain some of the discrepancy between the conclusions drawn from *in vitro* and *in vivo* research. However, the impact and degree of isoflavone metabolism varies between individuals.

In addition to the issue of isoflavone metabolism, questions have been raised regarding the impact of long term isoflavone exposure, specifically adolescent soy intake (discussed fully in section 1.3.2). This seems to provide lifelong benefit by altering the development of breast tissue during puberty, rendering it less susceptible to carcinogens. Importantly, this protective effect of soy is independent of, and acts in addition to the cancer reducing properties of adult isoflavone intake. Indeed, where adolescent and current adult soy intakes have been assessed, high levels of each had a cumulative beneficial effect on breast cancer risk (Wu et al. 2002).

Finally, the isoflavone concentrations used in this and many other studies were based upon the serum levels seen in women consuming various quantities of soy. However, as covered in section 1.2.4, the levels of isoflavones in the breast tissue itself may not reflect the serum levels. It is possible that isoflavones accumulate in the breast tissue, to greater levels than are seen in the serum, allowing them to achieve the ≥50μM concentrations associated with the greatest inhibition of breast cancer cell proliferation observed *in vitro*. However, equally, tissue levels could be lower than that measured in the serum. Studies to date, assessing the isoflavone levels in nipple aspirate fluid (Hargreaves et al. 1999; Maskarinec et al. 2008) or in tissue samples from biopsies (Bolca et al. 2010; Maubach et al. 2004) are inconclusive. These studies are limited by the invasiveness of the respective procedures, resulting in very low numbers, high drop out rates, and experimental population selection bias. A larger and more comprehensive study looking at the tissue levels of isoflavones and their metabolites is required, but for these reasons, may be difficult to undertake. Until this is forthcoming, the serum concentrations of isoflavones remain the best available evidence of their *in vivo* levels.

Due to the reasons discussed, there is no ideal model with which to study the interactions between soy isoflavones and breast cancer. Despite the limitations

associated with cell culture models of the disease, such as MCF7 and MDA-MB-231 cells, their use continues to be necessary, as part of a multifaceted, multidisciplined approach, including cell culture, primary tissue, animal studies, epidemiological studies, and clinical trials with greater numbers of women with and without breast cancer.

CHAPTER 7. Summary and conclusions

The aims of this research were to determine the effect of achievable (physiological serum) levels of genistein and daidzein, at pre- and post- menopausal oestrogen concentrations, on breast cancer cell apoptosis and proliferation in two cell lines: MCF7 and MDA-MB-231. Following this, to begin to characterize some of the mechanisms through which genistein and daidzein may be acting, preliminary results were gathered regarding their impact upon MCF7 volume regulation and K^+ channel activity, as both these are known to influence proliferation and apoptosis.

This project makes a significant contribution to the analysis of the proliferative and apoptotic effects of soy isoflavones in competition with E2. Indeed, to date, it is the most comprehensive study undertaken where physiological levels of genistein and daidzein have been investigated at both pre- and postmenopausal E2 levels. No previous study has gathered data regarding such a comprehensive range of conditions. Of particular note amongst the proliferation experiments are the combinations of postmenopausal E2 and daidzein in MCF7, and in MDA-MB-231 cells daidzein alone, all the E2-daidzein combinations, and genistein at postmenopausal E2 levels. The effect of these treatments on cell proliferation has not previously been investigated. In addition, very little was previously known regarding the effects of physiological concentrations of isoflavones on the induction of apoptosis in these cell lines. This study contributes key new information regarding the effect of genistein and daidzein, both alone and in combination with E2, on MDA-MB-231 apoptosis. In addition, with the exception of one very limited study, this was the first occasion where the induction of MCF7 apoptosis by a range of achievable concentrations of genistein and daidzein in a physiologically relevant E2 environment has been described. As many of the effects of the soy isoflavones are thought to relate to their oestrogen agonistic or antagonistic properties, how they compete with or displace endogenous oestrogens was thought to be an important potential mechanism for their protective effects *in vivo,* and so this element of the research was highly relevant.

Investigation of the impact of E2 and genistein on MCF7 volume regulation by the calcein fluorescence method was a novel field of research, based on existing knowledge regarding the roles of shrinkage and swelling in apoptosis and proliferation respectively (i.e. shrinkage is an essential early step in apoptosis, and

swelling is required for S phase progression during proliferation). Volume regulation has been characterized in MCF7 previously in response to non-physiological osmotic stimuli, but never due to a physiologically relevant E2 or isoflavone treatment. Mechanisms such as this may be valuable in understanding the protective effects of isoflavones in breast cancer cells, and provide important information regarding potential pharmacological targets for future chemotherapeutic treatments.

Finally, despite the well established ability of genistein to block current through numerous K^+ channels, and the known role of many of these channels in proliferation and/or apoptosis in non-excitable cell lines such as MCF7 or MDA-MB-231, K^+ channel blockade by the soy isoflavones has never previously been considered in breast cancer cells. In addition to the inhibitory effect of genistein, and to a lesser extent daidzein, on macroscopic MCF7 current, there were a number of other elements to this section of the project which contribute novel and important information to this field. Firstly, there is no documented evidence of the impact of control treatments (vehicle only and no solvent) or DOF on whole cell MCF7 current over time. In addition, the impact of 4-AP and DOF on MCF7 proliferation has never previously been characterized. Overall, this section of the project has provided important pilot information regarding a novel mechanism through which the soy isoflavones, in particular genistein, as a novel mechanism through which they may mediate some of their chemoprotective properties.

In the MCF7 cell line (representative of ERα+ breast cancer) evidence is presented showing that at physiologically relevant concentrations soy isoflavones induce several anti-cancer protective mechanisms: namely the induction of apoptosis, cell shrinkage, and the inhibition of outward macroscopic K^+ current through a number of channels including hEAG. K^+ current through a number of channels, including hEAG, has an established role in the proliferation of a number of cell types and lines, including MCF7. Furthermore, the increase in the induction of apoptosis observed after treatment with the isoflavones in combination with pre- or postmenopausal E2 was comparable to increase recorded after treatment with the isoflavones alone. However, in this model of breast cancer, these protective mechanisms were insufficient to counter the ERα-mediated increase in proliferation observed, although at the highest concentrations used a dramatic downward shift in proliferation was documented. Had higher isoflavone concentrations been tested

then a significant inhibition of cell proliferation would likely have been observed, although this was outwith the remit of the investigation and would have had limited physiological relevance.

In addition, rather than antagonize E2-induced MCF7 proliferation as hypothesized, genistein and daidzein acted in an additive, synergistic manner with postmenopausal E2 levels, and to a lesser extent premenopausally, to further increase the proliferation of this cell line. This data suggests that in a physiologically relevant E2-enviroment, soy isoflavones might increase ERα+ breast cancer cell proliferation. This conclusion is repeatedly echoed in the relevant published *in vitro* literature. However, it contradicts with a growing body of epidemiological evidence, including several meta-analyses of large prospective cohorts. The possible reasons behind this have been discussed in the previous section.

However, in the MDA-MB-231 model of ERα-/ERβ+ breast cancer used, evidence is presented for a protective effect of the soy isoflavones genistein and daidzein in their physiological concentrations, particularly postmenopausally. In this cell line the isoflavones induced apoptosis and inhibited proliferation at concentrations which are achievable in the serum through diet alone. It is hypothesized that this effect may be mediated by ERβ. In accordance with the documented E2-insensitivity of this cell line, the presence of E2 had no impact upon isoflavone-induced apoptosis. In many cases the combined E2/isoflavone treatments had a reduced inhibitory effect on MDA-MB-231 cell proliferation compared to the single isoflavone treatments, but a downward trend in proliferation was still observed with the combinations of postmenopausal E2 and daidzein, and where the highest isoflavone concentrations were used. This argues for a protective role of soy isoflavones against ERα-/ERβ+ breast cancer. As discussed, there is no epidemiological evidence to support or contradict this to date, as ERβ is not routinely assessed upon breast cancer diagnosis. However, this receptor status group is believed to account for around 18% of all breast tumours (Skliris et al. 2008).

As identified in the previous sections, a most pressing continuation of this research will be to confirm or reject the role of ERβ in the isoflavone-induced reduction of proliferation observed in the MDA-MB-231 model. To this end, the use of ER antagonists can be used, although no specific ERβ antagonists exist to date. Alternatively, silencing of the ERβ gene by use of siRNA may be a useful technique.

Furthermore, whether soy isoflavones inhibit the proliferation of other ERα-/ERβ+ models of breast cancer would be of value to determine. In particular, if sufficient numbers are achievable, it would be of great value to determine the impact of dietary isoflavones on survival and recurrence in a clinical trial or prospective manner with women with ERα-/ERβ+ cancer, although understandably this currently would be very difficult to accomplish. Confirmation of the role of ERβ in the inhibition of ERα-/ERβ+ breast cancer by levels of isoflavones achievable in the serum through diet alone would be powerful evidence supporting the case for routine assessment of ERβ expression levels in breast cancer. This would allow this large group of women to benefit from the potential chemotherapeutic properties of soy isoflavones, a cheap, safe, and readily available treatment.

In the MCF7 model, and indeed in MDA-MB-231 cells, it is important to follow up the preliminary findings presented here regarding the ability of the soy isoflavones, and in particular genistein, to inhibit current through numerous K^+ channels. While the link between K^+ current and proliferation and/or apoptosis in breast cancer cell lines is not new, this represents the first of hopefully many investigations looking into K^+ current modulation as a novel mechanism for the chemotherapeutic benefits of isoflavones. In particular, it would be of benefit to characterize the modulation of other K^+ channels by isoflavones, including $K_v1.1$, $K_v1.3$ and the Ca^{2+} activated K^+ channels (BK, IK and SK), as each of these has a suggested role in proliferation.

Furthermore, it still remains to identify hERG channel activity in MCF7. It is possible that in this cell line the hERG channel is only active under apoptotic stimulation. In this vein, it would be interesting to determine whether genistein and daidzein at their pro-apoptotic concentrations can induce hERG current, or whether the hERG blocker DOF can prevent isoflavone-induced apoptosis in MCF7. In each case these experiments can be conducted using specific K^+ channel blockers in the manner of this investigation. However, further characterization of the activities of the various channels can also be attempted by silencing the channel gene (such as with siRNA). To date little is known regarding the expression of K^+ channels in MDA-MB-231 cells. To follow up whether inhibition of K^+ current in this cell line is a mechanism through which isoflavones mediate their proliferation-reducing properties, this would also require clarification.

In summary, there continue to exist two contradictory hypotheses regarding soy and breast cancer which are both supported by aspects of this research. These are:

1. Soy isoflavones are protective against breast cancer, and can reduce its incidence, recurrence and mortality, through numerous mechanisms. The potential for benefit may be greater for some groups (i.e. women with ERα-/ERβ+ tumours) but as yet these populations are not defined on a large scale. As a result soy should be consumed by healthy women and women with breast cancer as part of a healthy diet and lifestyle.

2. Evidence shows that soy isoflavones can increase the proliferation of ERα+ (ER+) breast cancer cells and as such should be avoided by women with, or at high risk of breast cancer.

However, to date there remains no really convincing supporting evidence for either case, with many of the mechanisms for both only occurring *in vitro*. Furthermore, for each hypothesis there exists a great deal of contradictory evidence. Until further research can be conducted, the only conclusion which can be drawn regarding soy isoflavones is that for the general population, and women with breast cancer, normal dietary levels appear safe, do not incur any additional risk for breast cancer or other conditions, and can be a healthy way to reduce saturated fat intake in the Western diet by replacing meat products. On the other hand, the safety of the higher levels of isoflavones achieved by supplement use is not yet established. In conclusion, if healthy women, or breast cancer patients and survivors enjoy soy foods, then there is no reason why they should not continue to consume them, in moderation, and as part of a healthy balanced diet and lifestyle, and they may contribute towards a reduction in breast cancer risk. However, in line with current medical guidance, isoflavone supplementation for the relief of menopausal symptoms should be avoided by certain groups of women, such as breast cancer survivors or those with a strong family history of the disease, as the risks and benefits are not yet established clearly.

CHAPTER 8. References

Abdul, M., Santo, A. and Hoosein, N. 2003. Activity of potassium channel-blockers in breast cancer. *Anticancer Research*, 23 (4), pp.3347-3351.

Adlercreutz, H., Yamada, T., Wahala, K. and Watanabe, S. 1999. Maternal and neonatal phytoestrogens in Japanese women during birth. *American Journal of Obstetrics and Gynecology*, 180, pp.737-743.

Adlercreutz, H. 1995. Phytoestrogens: epidemiology and a possible role in cancer protection. *Environmental Health Perspectives*, 103 Suppl 7 pp.103-112.

Adlercreutz, H., Markkanen, H. and Watanabe, S. 1993. Plasma concentrations of phyto-oestrogens in Japanese men. *Lancet*, 342 (8881), pp.1209-1210.

Akter, R., Hossain, M. Z., Kleve, M. G. and Gealt, M. A. 2012. Wortmannin induces MCF7 breast cancer cell death via the apoptotic pathway, involving chromatin condensation, generation of reactive oxygen species, and membrane blebbing. *Breast Cancer: Targets and Therapy*, 4 pp.103-113.

Albanito, L., Madeo, A., Lappano, R., Vivacqua, A., Rago, V., Carpino, A., Oprea, T. I., Prossnitz, E. R., Musti, A. M., Ando, S. and Maggiolini, M. 2007. G protein-coupled receptor 30 (GPR30) mediates gene expression changes and growth response to 17beta-estradiol and selective GPR30 ligand G-1 in ovarian cancer cells. *Cancer Research*, 67 (4), pp.1859-1866.

Alekel, D. L., Germain, A. S., Peterson, C. T., Hanson, K. B., Stewart, J. W. and Toda, T. 2000. Isoflavone-rich soy protein isolate attenuates bone loss in the lumbar spine of perimenopausal women. *The American Journal Of Clinical Nutrition*, 72 (3), pp.844-852.

Allan, G. J., Tonner, E., Szymanowska, M., Shand, J. H., Kelly, S. M., Phillips, K., Clegg, R. A., Gow, I. F., Beattie, J. and Flint, D. J. 2006. Cumulative mutagenesis of the basic residues in the 201-218 region of insulin-like growth factor (IGF)-binding protein-5 results in progressive loss of both IGF-I binding and inhibition of IGF-I biological action. *Endocrinology*, 147 (1), pp.338-349.

Allred, C. D., Ju, Y. H., Allred, K. F., Chang, J. and Helferich, W. G. 2001. Dietary genistin stimulates growth of estrogen-dependent breast cancer tumors similar to that observed with genistein. *Carcinogenesis*, 22 (10), pp.1667-1673.

Allred, C. D., Allred, K. F., Ju, Y. H., Clausen, L. M., Doerge, D. R., Schantz, S. L., Korol, D. L., Wallig, M. A. and Helferich, W. G. 2004. Dietary genistein results in larger MNU-induced, estrogen-dependent mammary tumors following ovariectomy of Sprague-Dawley rats. *Carcinogenesis*, 25 (2), pp.211-218.

An, J., Tzagarakis-Foster, C., Scharschmidt, T. C., Lomri, N. and Leitman, D. C. 2001. Estrogen receptor beta-selective transcriptional activity and recruitment of coregulators by phytoestrogens. *Journal Of Biological Chemistry*, 276 (21), pp.17808-17814.

Anthony, M. S., Clarkson, T. B. and Williams, J. K. 1998. Effects of soy isoflavones on atherosclerosis: potential mechanisms. *American Journal of Clinical Nutrition*, 68 (6 Suppl), pp.1390S-1393s.

Arai, Y., Uehara, M., Sato, Y., Kimira, M., Eboshida, A., Adlercreutz, H. and Watanabe, S. 2000. Comparison of isoflavones among dietary intake, plasma concentration and urinary excretion for accurate estimation of phytoestrogen intake. *Journal Of Epidemiology*, 10 (2), pp.127-135.

Arbildua, J. J., Brunet, J. E., Jameson, D. M., Lopez, M., Nova, E., Lagos, R. and Monasterio, O. 2006. Fluorescence resonance energy transfer and molecular modeling studies on 4',6-diamidino-2-phenylindole (DAPI) complexes with tubulin. *Protein Science*, 15 (3), pp.410-419.

Arcangeli, A., Bianchi, L., Becchetti, A., Faravelli, L., Coronnello, M., Mini, E., Olivotto, M. and Wanke, E. 1995. A novel inward-rectifying K+ current with a cell-cycle dependence governs the resting potential of mammalian neuroblastoma cells. *Journal of Physiology*, 489 (Pt 2) pp.455-471.

Bacallo, R., Sohrab, S. and Phillips, C. 2006. Guiding principles of specimin preservation for confocal fluorescence microscopy. In: Pawley, J. B. ed. *Handbook of confocal microscopy*. 3 ed. New York: Springer, pp. 368-380.

Badger, T. M., Gilchrist, J. M., Pivik, R. T., Andres, A., Shankar, K., Chen, J. R. and Ronis, M. J. 2009. The health implications of soy infant formula. *American Journal of Clinical Nutrition*, 89 (5), pp.1668S-1672S.

Balfe, P., McCann, A., McGoldrick, A., McAllister, K., Kennedy, M., Dervan, P. and Kerin, M. J. 2004. Estrogen receptor alpha and beta profiling in human breast cancer. *European Journal Of Surgical Oncology*, 30 (5), pp.469-474.

Banerjee, S., Li, Y., Wang, Z. and Sarkar, F. H. 2008. Multi-targeted therapy of cancer by genistein. *Cancer Letters*, 269 (2), pp.226-242.

Baum, M. and Schipper, H. 2000. *Breast Cancer: Fast Facts*. London: Oxford.

Baxter, G. T., Kuo, R. C., Jupp, O. J., Vandenabeele, P. and MacEwan, D. J. 1999. Tumor necrosis factor-alpha mediates both apoptotic cell death and cell proliferation in a human hematopoietic cell line dependent on mitotic activity and receptor subtype expression. *Journal Of Biological Chemistry*, 274 (14), pp.9539-9547.

Beatson, G. T. 1896. On the tretament of inoperable cases of carcimoma of the mamma: suggestions for a new method of treatment, with illustrative cases. *Lancet*, 148 (3803), pp.162-165.

Beral, V. 2003. Breast cancer and hormone-replacement therapy in the Million Women Study. *Lancet*, 362 (9382), pp.419-427.

Bernander, R., Stokke, T. and Boye, E. 1998. Flow cytometry of bacterial cells: comparison between different flow cytometers and different DNA stains. *Cytometry*, 31 (1), pp.29-36.

Bernhard, D., Schwaiger, W., Crazzolara, R., Tinhofer, I., Kofler, R. and Csordas, A. 2003. Enhanced MTT-reducing activity under growth inhibition by resveratrol in CEM-C7H2 lymphocytic leukemia cells. *Cancer Letters*, 195 (2), pp.193-199.

Berridge, M. J., Bootman, M. D. and Lipp, P. 1998. Calcium--a life and death signal. *Nature*, 395 (6703), pp.645-648.

Bhagwat S., Haytowitz D. B., and Holden J. M. (2008). *USDA Database for the Isoflavone Content of Selected Foods*. U.S. Department of Agriculture. Maryland, 2.0.

Bianchi, L., Wible, B., Arcangeli, A., Taglialatela, M., Morra, F., Castaldo, P., Crociani, O., Rosati, B., Faravelli, L., Olivotto, M. and Wanke, E. 1998. herg encodes a K+ current highly conserved in tumors of different histogenesis: a selective advantage for cancer cells? *Cancer Research*, 58 (4), pp.815-822.

Bielawski, K., Wolczynski, S. and Bielawska, A. 2001. DNA-binding activity and cytotoxicity of the extended diphenylfuran bisamidines in breast cancer MCF-7 cells. *Biological & Pharmaceutical Bulletin*, 24 (6), pp.704-706.

Birch, P. J., Dekker, L. V., James, I. F., Southan, A. and Cronk, D. 2004. Strategies to identify ion channel modulators: current and novel approaches to target neuropathic pain. *Drug Discovery Today*, 9 (9), pp.410-418.

Bloedon, L. T., Jeffcoat, A. R., Lopaczynski, W., Schell, M. J., Black, T. M., Dix, K. J., Thomas, B. F., Albright, C., Busby, M. G., Crowell, J. A. and Zeisel, S. H. 2002. Safety and pharmacokinetics of purified soy isoflavones: single-dose administration to postmenopausal women. *American Journal of Clinical Nutrition*, 76 (5), pp.1126-1137.

Blom, A., Ekman, E., Johannisson, A., Norrgren, L. and Pesonen, M. 1998. Effects of xenoestrogenic environmental pollutants on the proliferation of a human breast cancer cell line (MCF-7). *Archives Of Environmental Contamination And Toxicology*, 34 (3), pp.306-310.

Boatright, K. M. and Salvesen, G. S. 2003. Mechanisms of caspase activation. *Current Opinion in Cell Biology*, 15 pp.725-731.

Bock, J., Szabo, I., Jekle, A. and Gulbins, E. 2002. Actinomycin D-induced apoptosis involves the potassium channel Kv1.3. *Biochemical And Biophysical Research Communications*, 295 pp.526-531.

Bolca, S., Urpi-Sarda, M., Blondeel, P., Roche, N., Vanhaecke, L., Possemiers, S., Al-Maharik, N., Botting, N., De Keukeleire, D., Bracke, M., Heyerick, A., Manach, C. and Depypere, H. 2010. Disposition of soy isoflavones in normal human breast tissue. *American Journal of Clinical Nutrition*, 91 (4), pp.976-984.

Borowiec, A. S., Hague, F., Harir, N., Guenin, S., Guerineau, F., Gouilleux, F., Roudbaraki, M., Lassoued, K. and Ouadid-Ahidouch, H. 2007. IGF-1 activates hEAG K(+) channels through an Akt-dependent signaling pathway in breast cancer cells: role in cell proliferation. *Journal Of Cellular Physiology*, 212 (3), pp.690-701.

Bortner, C. D. and Cidlowski, J. A. 1999. Caspase independent/dependent regulation of K(+), cell shrinkage, and mitochondrial membrane potential during lymphocyte apoptosis. *Journal Of Biological Chemistry*, 274 (31), pp.21953-21962.

Bortner, C. D. and Cidlowski, J. A. 2004. The role of apoptotic volume decrease and ionic homeostasis in the activation and repression of apoptosis. *Pflugers Archive: European Journal Of Physiology*, 448 pp.313-318.

Boucher, B.A., Cotterchio, M., Curca, A., Kreiger, N., Harris, S.A., Kirsh, V.A. and Goodwin, P.J. 2012. Intake of phytoestrogen foods and supplements among women recently diagnosed with breast cancer in ontario, Canada. *Nutrition and Cancer*, 64 (5), pp.695-703.

Braunstein, G. D., Johnson, B. D., Stanczyk, F. Z., Bittner, V., Berga, S. L., Shaw, L., Hodgson, T. K., Paul-Labrador, M., Azziz, R. and Merz, C. N. B. 2008. Relations between endogenous androgens and estrogens in postmenopausal women with suspected ischemic heart disease. *Journal Of Clinical Endocrinology And Metabolism*, 93 (11), pp.4268-4275.

Brevet, M., Ahidouch, A., Sevestre, H., Merviel, P., El Hiani, Y., Robbe, M. and Ouadid-Ahidouch, H. 2008. Expression of K+ channels in normal and cancerous human breast. *Histology And Histopathology*, 23 (8), pp.965-972.

Brooks, J. D. and Thompson, L. U. 2005. Mammalian lignans and genistein decrease the activities of aromatase and 17beta-hydroxysteroid dehydrogenase in MCF-7 cells. *Journal Of Steroid Biochemistry And Molecular Biology*, 94 (5), pp.461-467.

Brown, N. M., Belles, C. A., Lindley, S. L., Zimmer-Nechemias, L., Witte, D. P., Kim, M. O. and Setchell, K. D. R. 2010. Mammary gland differentiation by early life exposure to enantiomers of the soy isoflavone metabolite equol. *Food And Chemical Toxicology*, 48 (11), pp.3042-3050.

Brumatti, G., Sheridan, C. and Martin, S. J. 2008. Expression and purification of recombinant annexin V for the detection of membrane alterations on apoptotic cells. *Methods*, 44 (3), pp.235-240.

Burdall, S. E., Hanby, A. M., Lansdown, M. R. J. and Speirs, V. 2003. Breast cancer cell lines: friend or foe? *Breast Cancer Research: BCR*, 5 (2), pp.89-95.

Burgers, A. M., Biermasz, N. R., Schoones, J. W., Pereira, A. M., Renehan, A. G., Zwahlen, M., Egger, M. and Dekkers, O. M. 2011. Meta-analysis and dose-response metaregression: circulating insulin-like growth factor I (IGF-I) and mortality. *Journal Of Clinical Endocrinology And Metabolism*, 96 (9), pp.2912-2920.

Burton, J. D.2005. The MTT assay to evaluate chemosensitivity. In: Blumenthal, R. D. ed. *Methods in Molecular Medicine: Chemosensitivity Volume 1*. Totowa, New Jersey: Humana Press, pp. 69-78.

Busby, M. G., Jeffcoat, A. R., Bloedon, L. T., Koch, M. A., Black, T., Dix, K. J., Heizer, W. D., Thomas, B. F., Hill, J. M., Crowell, J. A. and Zeisel, S. H. 2002. Clinical characteristics and pharmacokinetics of purified soy isoflavones: single-dose administration to healthy men. *The American Journal Of Clinical Nutrition*, 75 (1), pp.126-136.

Cahalan, M. D., Wulff, H. and Chandy, K. G. 2001. Molecular properties and physiological roles of ion channels in the immune system. *Journal Of Clinical Immunology*, 21 (4), pp.235-252.

Cannel, M. B. and Thomas, M. V. 1994. Intracellular ion measurement with fluorescent indicators. In: Ogden, D. ed. *Microelectrode Techniques*. 2 ed. Cambridge: The Company of Biologists Ltd, pp. 317-345.

Caplanusi, A., Kim, K. J., Lariviere, E., Van Driessche, W. and Jans, D. 2006. Swelling-activated K+ efflux and regulatory volume decrease efficiency in human bronchial epithelial cells. *Journal Of Membrane Biology*, 214 (1), pp.33-41.

Cappelletti, V., Miodini, P., Di Fronzo, G. and Daidone, M. G. 2006. Modulation of estrogen receptor-beta isoforms by phytoestrogens in breast cancer cells. *International Journal Of Oncology*, 28 (5), pp.1185-1191.

Cardiff, R. D. 2001. Validity of mouse mammary tumour models for human breast cancer: comparative pathology. *Microscopy Research And Technique*, 52 (2), pp.224-230.

Carmichael, J., DeGraff, W. G., Gazdar, A. F., Minna, J. D. and Mitchell, J. B. 1987. Evaluation of a tetrazolium-based semiautomated colorimetric assay: assessment of chemosensitivity testing. *Cancer Research*, 47 (4), pp.936-942.

Casanova, M., You, L., Gaido, K. W., Archibeque-Engle, S., Janszen, D. B. and Heck, H. d. 2012. Developmental effects of dietary phytoestrogens in Sprague-Dawley rats and interactions of genistein and daidzein with rat estrogen receptors alpha and beta in vitro. *Toxicological Sciences*, 51 pp.236-244.

Castillo-Pichardo, L., Martinez-Montemayor, M. M., Martinez, J. E., Wall, K. M., Cubano, L. A. and Dharmawardhane, S. 2009. Inhibition of mammary tumor growth and metastases to bone and liver by dietary grape polyphenols. *Clinical & Experimental Metastasis*, 26 (6), pp.505-516.

Cayabyab, F. S. and Schlichter, L. C. 2002. Regulation of an ERG K+ current by Src tyrosine kinase. *Journal Of Biological Chemistry*, 277 (16), pp.13673-13681.

Chan, M. M., Lu, X., Merchant, F. M., Iglehart, J. D. and Miron, P. L. 2005. Gene expression profiling of NMU-induced rat mammary tumors: cross species comparison with human breast cancer. *Carcinogenesis*, 26 (8), pp.1343-1353.

Chang, E. C., Frasor, J., Komm, B. and Katzenellenbogen, B. S. 2006. Impact of estrogen receptor beta on gene networks regulated by estrogen receptor alpha in breast cancer cells. *Endocrinology*, 147 (10), pp.4831-4842.

Chang, H. C., Churchwell, M. I., Delclos, K. B., Newbold, R. R. and Doerge, D. R. 2000. Mass spectrometric determination of Genistein tissue distribution in diet-exposed Sprague-Dawley rats. *The Journal Of Nutrition*, 130 (8), pp.1963-1970.

Chang, H. T., Huang, J. K., Wang, J. L., Cheng, J. S., Lee, K. C., Lo, Y. K., Liu, C. P., Chou, K. J., Chen, W. C., Su, W., Law, Y. P. and Jan, C. R. 2002. Tamoxifen-induced increases in cytoplasmic free Ca2+ levels in human breast cancer cells. *Breast Cancer Research And Treatment*, 71 (2), pp.125-131.

Chen, J., Zheng, R., Melman, Y. F. and McDonald, T. V. 2009. Functional interactions between KCNE1 C-terminus and the KCNQ1 channel. *Plos One*, 4 (4), p.e5143.

Chen, J-Q., Contreras, R.G., Wang, R., Fernandez, S.V., Shoshani, L., Russo, I.H., Cereijido, M. and Russo, J. 2006. Sodium/potassium ATPase (Na+, K+-ATPase) and oubain/related cardiac glycosides: a new paradigm for the development of anti-breast cancer drugs? *Breast Cancer Research and Treatment*, 96, pp.1-15.

Chen, L. and Kass, R. S. 2011. A-kinase anchoring protein 9 and Iks channel regulation. *Journal of Cardiovascular Pharmacology*, 58 pp.459-461.

Chen, M. X., Gorman, S. A., Benson, B., Singh, K., Hieble, J. P., Michel, M. C., Tate, S. N. and Trezise, D. J. 2004. Small and intermediate conductance Ca(2+)-activated K+ channels confer distinctive patterns of distribution in human tissues and differential cellular localisation in the colon and corpus cavernosum. *Naunyn-Schmiedeberg's Archives Of Pharmacology*, 369 (6), pp.602-615.

Chen, S. Z., Jiang, M. and Zhen, Y. s. 2005. HERG K+ channel expression-related chemosensitivity in cancer cells and its modulation by erythromycin. *Cancer Chemotherapy And Pharmacology*, 56 (2), pp.212-220.

Chen, W. F., Gao, Q. G. and Wong, M. S. 2007. Mechanism involved in genistein activation of insulin-like growth factor 1 receptor expression in human breast cancer cells. *British Journal Of Nutrition*, 98 (6), pp.1120-1125.

Chen, Z., Zhang, Z., Gu, Y. and Bai, C. 2011. Impaired migration and cell volume regulation in aquaporin 5-deficient SPC-A1 cells. *Respiratory Physiology & Neurobiology*, 176 (3), pp.110-117.

Cheng, G., Wilczek, B., Warner, M., Gustafsson, J. A. and Landgren, B. M. 2007. Isoflavone treatment for acute menopausal symptoms. *Menopause*, 14 (3 Pt 1), pp.468-473.

Cherdshewasart, W. and Sriwatcharakul, S. 2008. Metabolic activation promotes estrogenic activity of the phytoestrogen-rich plant. *Maturitas*, 59 (2), pp.128-136.

Cherubini, A., Taddei, G. L., Crociani, O., Paglierani, M., Buccoliero, A. M., Fontana, L., Noci, I., Borri, P., Borrani, E., Giachi, M., Becchetti, A., Rosati, B., Wanke, E., Olivotto, M. and Arcangeli, A. 2000. HERG potassium channels are more frequently expressed in human endometrial cancer as compared to non-cancerous endometrium. *British Journal Of Cancer*, 83 (12), pp.1722-1729.

Chlebowski, R. T., Hendrix, S. L., Langer, R. D., Stefanick, M. L., Gass, M., Lane, D., Rodabough, R. J., Gilligan, M. A., Cyr, M. G., Thomson, C. A., Khandekar, J., Petrovitch, H. and McTiernan, A. 2003. Influence of estrogen plus progestin on breast cancer and mammography in healthy postmenopausal women: the Women's Health Initiative Randomized Trial. *Journal Of The American Medical Association*, 289 (24), pp.3243-3253.

Chlebowski, R. T., Kuller, L. H., Prentice, R. L., Stefanick, M. L., Manson, J. E., Gass, M., Aragaki, A. K., Ockene, J. K., Lane, D. S., Sarto, G. E., Rajkovic, A., Schenken, R., Hendrix, S. L., Ravdin, P. M., Rohan, T. E., Yasmeen, S. and Anderson, G. 2009. Breast cancer after use of estrogen plus progestin in postmenopausal women. *New England Journal Of Medicine*, 360 (6), pp.573-587.

Choi, E. J. and Kim, G. H. 2008. Daidzein causes cell cycle arrest at the G1 and G2/M phases in human breast cancer MCF-7 and MDA-MB-453 cells. *Phytomedicine*, 15 (9), pp.683-690.

Choi, J. N., Kim, D., Choi, H. K., Yoo, K. M., Kim, J. and Lee, C. H. 2009. 2'-hydroxylation of genistein enhanced antioxidant and antiproliferative activities in mcf-7 human breast cancer cells. *Journal Of Microbiology And Biotechnology*, 19 (11), pp.1348-1354.

Chua, B. T., Guo, K. and Li, P. 2000. Direct cleavage by the calcium-activated protease calpain can lead to inactivation of caspases. *Journal Of Biological Chemistry*, 275 (7), pp.5131-5135.

Clark, J. A., Alves, S., Gundlah, B., Rocha, B., Birzin, E. T., Cai, S.-J., Flick, R., Hayes, E., Ho, K., Warrier, S., Pai, L.-P., Yudkovitz, J., Fleischer, R., Colwell, L., Li, S., Wilkinson, H., Schaeffer, J., Wilkening, R., Mattingly, E., Hammond, M. and Rohrer, S. P. 2012. Selective estrogen receptor beta (SERM-beta) compunds modulate raphe nuclei tryptophan hydroxylase-1 (TPH-1) mRNA expression and cause antidepressent-like effects in the forced swim test. *Neuropharmacology*, 63 (6), pp.1051-1063.

Clarke, R., Leonessa, F., Welch, J. N. and Skaar, T. C. 2001. Cellular and molecular pharmacology of antiestrogen action and resistance. *Pharmacological Reviews*, 53 (1), pp.25-71.

Clavel-Chapelon, F. and the E3N-EPIC group 2002. Differential effects of reproductive factors on the risk of pre- and postmenopausal breast cancer. Results from a large cohort of French women. *British Journal Of Cancer*, 86 (5), pp.723-727.

Cohen, L. A., Zhao, Z., Pittman, B. and Scimeca, J. A. 2000. Effect of intact and isoflavone-depleted soy protein on NMU-induced rat mammary tumorigenesis. *Carcinogenesis*, 21 (5), pp.929-935.

Coiret, G., Borowiec, A. S., Mariot, P., Ouadid-Ahidouch, H. and Matifat, F. 2007. The antiestrogen tamoxifen activates BK channels and stimulates proliferation of MCF-7 breast cancer cells. *Molecular Pharmacology*, 71 (3), pp.843-851.

Coiret, G., Matifat, F., Hague, F. and Ouadid-Ahidouch, H. 2005. 17-beta-estradiol activates maxi-K channels through a non-genomic pathway in human breast cancer cells. *FEBS Letters*, 579 (14), pp.2995-3000.

Collaborative Group on Hormonal Factors in Breast Cancer 1997. Breast cancer and hormone replacement therapy: collaborative reanalysis of data from 51 epidemiological studies of 52,705 women with breast cancer and 108,411 women without breast cancer. *Lancet*, 350 (9084), pp.1047-1059.

Constantinou, A. I., Krygier, A. E. and Mehta, R. R. 1998. Genistein induces maturation of cultured human breast cancer cells and prevents tumor growth in nude mice. *American Journal of Clinical Nutrition*, 68 (6 Suppl), pp.1426S-1430s.

Constantinou, A. I., Lantvit, D., Hawthorne, M., Xu, X., van Breemen, R. B. and Pezzuto, J. M. 2001. Chemopreventive effects of soy protein and purified soy isoflavones on DMBA-induced mammary tumors in female Sprague-Dawley rats. *Nutrition And Cancer*, 41 (1-2), pp.75-81.

Constantinou, A. I., White, B. E. P., Tonetti, D., Yang, Y., Liang, W., Li, W. and van Breemen, R. B. 2005. The soy isoflavone daidzein improves the capacity of tamoxifen to prevent mammary tumours. *European Journal Of Cancer (Oxford, England: 1990)*, 41 (4), pp.647-654.

Coward, L., Smith, M., Kirk, M. and Barnes, S. 1998. Chemical modification of isoflavones in soyfoods during cooking and processing. *The American Journal Of Clinical Nutrition*, 68 (6 Suppl), pp.1486S-1491s.

Crowe, W.E., Altamirano, J., Huerto ,L., Alvarez-Leefmans, F.J. 1995. Volume changes in single N1E-115 neuroblastoma cells measured with a fluorescent probe. *Neuroscience*, 51 (1), pp.283-296.

Cui, Q., Tashiro, S. i., Onodera, S., Minami, M. and Ikejima, T. 2007. Autophagy preceded apoptosis in oridonin-treated human breast cancer MCF-7 cells. *Biological & Pharmaceutical Bulletin*, 30 (5), pp.859-864.

Cummings, S. R., Lee, J. S., Liu, L., Stone, K., Ljung, B. M., Cauleys, J. A. and Study of Ostoeporotic Fractures Research Group 2005. Sex hormones, risk factors, and risk of estrogen receptor-positive breast cancer in older women: a long term prospective study. *Cancer Epidemiology, Biomarkers & Prevention*, 14 (5), pp.1047-1051.

Daniel, B. and DeCoster, M. A. 2004. Quantification of sPLA2-induced early and late apoptosis changes in neuronal cell cultures using combined TUNEL and DAPI staining. *Brain Research Brain Research Protocols*, 13 (3), pp.144-150.

Darzynkiewicz, Z., Galkowski, D. and Zhao, H. 2008. Analysis of apoptosis by cytometry using TUNEL assay. *Methods*, 44 (3), pp.250-254.

Davis, D. D., Diaz-Cruz, E. S., Landini, S., Kim, Y. W. and Brueggemeier, R. W. 2008. Evaluation of synthetic isoflavones on cell proliferation, estrogen receptor binding affinity, and apoptosis in human breast cancer cells. *Journal Of Steroid Biochemistry And Molecular Biology*, 108 (1-2), pp.23-31.

Davis, M. J., Wu, X., Nurkiewicz, T. R., Kawasaki, J., Gui, P., Hill, M. A. and Wilson, E. 2001. Regulation of ion channels by protein tyrosine phosphorylation. *American Journal Of Physiology Heart And Circulatory Physiology*, 281 (5), p.H1835-H1862.

De Saint-Hubert, M., Prinsen, K., Mortelmans, L., Verbruggen, A. and Mottaghy, F. M. 2009. Molecular imaging of cell death. *Methods*, 48 (2), pp.178-187.

Deblois, G. and Giguere, V. 2003. Ligand-independent coactivation of ERalpha AF-1 by steroid receptor RNA activator (SRA) via MAPK activation. *Journal Of Steroid Biochemistry And Molecular Biology*, 85 (2-5), pp.123-131.

DeCoster, M. A. 2007. The Nuclear Area Factor (NAF): a measure for cell apoptosis using microscopy and image analysis. *Modern Research and Education Topics in Microscopy*, 1, pp. 378-384.

Dewick, P. M. 1994. Isoflavonoids. In: Harborne, J. B. ed. *The Flavonoids: Advances in Research Since 1986*. 1 ed. London: Chapman & Hall, pp. 117-238.

Dhar, M. S. and Plummer, H. K., III 2006. Protein expression of G-protein inwardly rectifying potassium channels (GIRK) in breast cancer cells. *BMC Physiology*, 6 p.8.

Dick, G. M., Rossow, C. F., Smirnov, S., Horowitz, B. and Sanders, K. M. 2001. Tamoxifen activates smooth muscle BK channels through the regulatory beta 1 subunit. *Journal Of Biological Chemistry*, 276 (37), pp.34594-34599.

Dick, G. M. 2002. The pure anti-oestrogen ICI 182,780 (Faslodex) activates large conductance Ca(2+)-activated K(+) channels in smooth muscle. *British Journal Of Pharmacology*, 136 (7), pp.961-964.

Dixon, R. A. 2004. Phytoestrogens. *Annual Review Of Plant Biology*, 55 pp.225-261.

Djuric, Z., Chen, G., Doerge, D. R., Heilbrun, L. K. and Kucuk, O. 2001. Effect of soy isoflavone supplementation on markers of oxidative stress in men and women. *Cancer Letters*, 172 (1), pp.1-6.

Dong, J. Y. and Qin, L. Q. 2011. Soy isoflavones consumption and risk of breast cancer incidence or recurrence: a meta-analysis of prospective studies. *Breast Cancer Research And Treatment*, 125 (2), pp.315-323.

Dong, M. Q., Sun, H. Y., Tang, Q., Tse, H. F., Lau, C. P. and Li, G. R. 2010. Regulation of human cardiac KCNQ1/KCNE1 channel by epidermal growth factor receptor kinase. *Biochimica Et Biophysica Acta*, 1798 (5), pp.995-1001.

Doonan, F. and Cotter, T. G. 2008. Morphological assessment of apoptosis. *Methods*, 44 (3), pp.200-204.

Dorgan, J. F., Stanczyk, F. Z., Kahle, L. L. and Brinton, L. A. 2010. Prospective case-control study of premenopausal serum estradiol and testosterone levels and breast cancer risk. *Breast Cancer Research*, 12 (6), p.R98.

dos Santos Silva, I., Mangtani, P., McCormack, V., Bhakta, D., McMichael, A. J. and Sevak, L. 2004. Phyto-oestrogen intake and breast cancer risk in South Asian women in England: findings from a population-based case-control study. *Cancer Causes & Control: CCC*, 15 (8), pp.805-818.

Dos Santos, E., Dieudonne, M. N., Leneveu, M. C., Serazin, V., Rincheval, V., Mignotte, B., Chouillard, E., De Mazancourt, P., Giudicelli, Y. and Pecquery, R. 2010. Effects of 17beta-estradiol on preadipocyte proliferation in human adipose tissue: Involvement of IGF1-R signaling. *Hormone And Metabolic Research*, 42 (7), pp.514-520.

Du, M., Yang, X., Hartman, J. A., Cooke, P. S., Doerge, D. R., Ju, Y. H. and Helferich, W. G. 2012. Low-dose dietary genistein negates the therapeutic effect of tamoxifen in athymic nude mice. *Carcinogenesis*, 33 (4), pp.895-901.

Dubois, J.-M. and Rouzaire-Dubois, B. 2004. The influence of cell volume changes on tumour cell proliferation. *European Biophysics Journal*, 33 pp.227-232.

Dupont, S., Krust, A., Gansmuller, A., Dierich, A., Chambon, P. and Mark, M. 2000. Effect of single and compound knockouts of estrogen receptors alpha (ERalpha) and beta (ERbeta) on mouse reproductive phenotypes. *Development*, 127 (19), pp.4277-4291.

Eliassen, A. H., Missmer, S. A., Tworoger, S. S., Spiegelman, D., Barbieri, R. L., Dowsett, M. and Hankinson, S. E. 2006. Endogenous steroid hormone concentrations and risk of breast cancer among premenopausal women. *Journal Of The National Cancer Institute*, 98 (19), pp.1406-1415.

Elliott, J. I. and Higgins, C. F. 2003. IKCa1 activity is required for cell shrinkage, phosphatidylserine translocation and death in T lymphocyte apoptosis. *EMBO Reports*, 4 pp.189-194.

Enomoto, K., Cossu, M. F. and Oka, T. 1986. Induction of distinct types of spontaneous electrical activities in mammary epithelial cells by epidermal growth factor and insulin. *Proceedings Of The National Academy Of Sciences*, 83 pp.4754-4758.

Enyedi, P. and Czirjak, G. 2010. Molecular background of leak K+ currents: two-pore domain potassium channels. *Physiological Reviews*, 90 (2), pp.559-605.

Fahey, S. M. L., Jordan, C., Fritz, N. F., Robinson, S. P., Waters, D. and Tormey, D. C.1994. Clinical pharmacology and endocrinology of long-term tamoxifen therapy. In: Jordan, V. C. ed. *Long-term tamoxifen treatment for breast cancer*. 1 ed. Madison, Wisconsin: University of Wisconsin Press, pp. 28-50.

Fanger, C. M., Ghanshani, S., Logsdon, N. J., Rauer, H., Kalman, K., Zhou, J., Beckingham, K., Chandy, K. G., Cahalan, M. D. and Aiyar, J. 1999. Calmodulin mediates calcium-dependent activation of the intermediate conductance KCa channel, IKCa1. *Journal Of Biological Chemistry*, 274 (9), pp.5746-5754.

Farinas, J. and Verkman, A. S. 1996. Cell volume and plasma membrane osmotic water permeability in epithelial cell layers measured by inferometry. *Biophysical Journal*, 71 pp.3511-3522.

Feigelson, H. S., Jonas, C. R., Teras, L. R., Thun, M. J. and Calle, E. E. 2004. Weight gain, body mass index, hormone replacement therapy, and postmenopausal breast cancer in a large prospective study. *Cancer Epidemiology, Biomarkers & Prevention: A Publication Of The American Association For Cancer Research, Cosponsored By The American Society Of Preventive Oncology*, 13 (2), pp.220-224.

Felipe, A., Vicente, R., Villalonga, N., Roura-Ferrer, M., Martinez-Marmol, R., Sole, L., Ferreres, J. C. and Condom, E. 2006. Potassium channels: new targets in cancer therapy. *Cancer Detection And Prevention*, 30 (4), pp.375-385.

Feranchak, A. P., Kilic, G., Wojtaszek, P. A., Qadri, I. and Fitz, J. G. 2003. Volume-sensitive tyrosine kinases regulate liver cell volume through effects on vesicular trafficking and membrane Na+ permeability. *Journal Of Biological Chemistry*, 278 (45), pp.44632-44638.

Ferenc, P., Solar, P., Kleban, J., Mikes, J. and Fedorocko, P. 2010. Down-regulation of Bcl-2 and Akt induced by combination of photoactivated hypericin and genistein in human breast cancer cells. *Journal Of Photochemistry And Photobiology*, 98 (1), pp.25-34.

Fletcher, R. J. 2003. Food sources of phyto-oestrogens and their precursors in Europe. *British Journal Of Nutrition*, 89 Suppl 1 p.S39-S43.

Food and Drug Administration (1999). *Food labeling: health claims, soy protein and coronary heart disease; final rule*. Federal Register. 64.

Fortunati, N., Catalano, M. G., Boccuzzi, G. and Frairia, R. 2010. Sex Hormone-Binding Globulin (SHBG), estradiol and breast cancer. *Molecular And Cellular Endocrinology*, 316 (1), pp.86-92.

Franke, A. A., Halm, B. M., Custer, L. J., Tatsumura, Y. and Hebshi, S. 2006. Isoflavones in breastfed infants after mothers consume soy. *American Journal of Clinical Nutrition*, 84 (2), pp.406-413.

Frasor, J., Danes, J. M., Komm, B., Chang, K. C. N., Lyttle, C. R. and Katzenellenbogen, B. S. 2003. Profiling of estrogen up- and down-regulated gene expression in human breast cancer cells: insights into gene networks and pathways underlying estrogenic control of proliferation and cell phenotype. *Endocrinology*, 144 (10), pp.4562-4574.

Gallo, D., Giacomelli, S., Cantelmo, F., Zannoni, G. F., Ferrandina, G., Fruscella, E., Riva, A., Morazzoni, P., Bombardelli, E., Mancuso, S. and Scambia, G. 2001. Chemoprevention of DMBA-induced mammary cancer in rats by dietary soy. *Breast Cancer Research And Treatment*, 69 (2), pp.153-164.

Galluzzi, L., Aaronson, S. A., Abrams, J., Alnemri, E. S., Andrews, D. W., Baehrecke, E. H., Bazan, N. G., Blagosklonny, M. V., Blomgren, K., Borner, C., Bredesen, D. E., Brenner, C., Castedo, M., Cidlowski, J. A., Ciechanover, A., Cohen, G. M., De Laurenzi, V., De Maria, R., Deshmukh, M., Dynlacht, B. D., El-Deiry, W. S., Flavell, R. A., Fulda, S., Garrido, C., Golstein, P., Gougeon, M. L., Green, D. R., Gronemeyer, H., Hajnoczky, G., Hardwick, J. M., Hengartner, M. O., Ichijo, H., Jaattela, M., Kepp, O., Kimchi, A., Klionsky, D. J., Knight, R. A., Kornbluth, S., Kumar, S., Levine, B., Lipton, S. A., Lugli, E., Madeo, F., Malomi, W., Marine, J.-C. W., Martin, S. J., Medema, J. P., Mehlen, P., Melino, G., Moll, U. M., Morselli, E., Nagata, S., Nicholson, D. W., Nicotera, P., Nunez, G., Oren, M., Penninger, J., Pervaiz, S., Peter, M. E., Piacentini, M., Prehn, J. H. M., Puthalakath, H., Rabinovich, G. A., Rizzuto, R., Rodrigues, C. M. P., Rubinsztein, D. C., Rudel, T., Scorrano, L., Simon, H. U., Steller, H., Tschopp, J., Tsujimoto, Y., Vandenabeele, P., Vitale, I., Vousden, K. H., Youle, R. J., Yuan, J., Zhivotovsky, B. and Kroemer, G. 2009. Guidelines for the use and interpretation of assays for monitoring cell death in higher eukaryotes. *Cell Death And Differentiation*, 16 (8), pp.1093-1107.

Galluzzi, L., Vitale, I., Abrams, J., Alnemri, E. S., Baehrecke, E. H., Blagosklonny, M. V., Dawson, T. M., Dawson, V. L., El-Deiry, W. S., Fulda, S., Gottlieb, E., Green, D. R., Hengartner, M., Kepp, O., Knight, R. A., Kumar, S., Lipton, S. A., Lu, X., Madeo, F., Malorni, W., Mehlen, P., Nunez, G., Peter, M. E., Piacentini, M., Rubinsztein, D. C., Shi, Y., Simon, H.-U., Vandenabeele, P., White, E., Yuan, J., Zhivotovsky, B., Melino, G. and Kroemer, G. 2011. Molecular definitions of cell death subroutines: recommendations of the Nomenclature Committee on cell Death 2012. *Cell Death And Differentiation*, pp.1-14.

Garcia-Ferreiro, R. E., Kerschensteiner, D., Major, F., Monje, F., Stuhmer, W. and Pardo, L. A. 2004. Mechanism of block of hEag1 K+ channels by imipramine and astemizole. *Journal Of General Physiology*, 124 (4), pp.301-317.

Garvin, S., Ollinger, K. and Dabrosin, C. 2006. Resveratrol induces apoptosis and inhibits angiogenesis in human breast cancer xenografts in vivo. *Cancer Letters*, 231 (1), pp.113-122.

Gierten, J., Ficker, E., Bloehs, R., Schlomer, K., Kathofer, S., Scholz, E., Zitron, E., Kiesecker, C., Bauer, A., Becker, R., Katus, H. A., Karle, C. A. and Thomas, D. 2008. Regulation of two-pore-domain (K2P) potassium leak channels by the tyrosine kinase inhibitor genistein. *British Journal Of Pharmacology*, 154 (8), pp.1680-1690.

Gil-Parrado, S., Fernandez-Montalvan, A., Assfalg-Machleidt, I., Popp, O., Bestvater, F., Holloschi, A., Knoch, T. A., Auerswald, E. A., Welsh, K., Reed, J. C., Fritz, H., Fuentes-Prior, P., Spiess, E., Salvesen, G. S. and Machleidt, W. 2002. Ionomycin-activated calpain triggers apoptosis. A probable role for Bcl-2 family members. *Journal Of Biological Chemistry*, 277 (30), pp.27217-27226.

Gilchrist, J. M., Moore, M. B., Andres, A., Estroff, J. A. and Badger, T. M. 2010. Ultrasonographic patterns of reproductive organs in infants fed soy formula: comparisons to infants fed breast milk and milk formula. *Journal Of Pediatrics*, 156 (2), pp.215-220.

Goldstein, S. A. N., Bayliss, D. A., Kim, D., Lesage, F., Plant, L. D. and Rajan, S. 2005. International Union of Pharmacology. LV. Nomenclature and molecular relationships of two-P potassium channels. *Pharmacological Reviews*, 57 (4), pp.527-540.

Gow, I. F., Thomson, J., Davidson, J. and Shennan, D. B. 2005. The effect of a hyposmotic shock and purinergic agonists on K+(Rb+) efflux from cultured human breast cancer cells. *Biochimica Et Biophysica Acta*, 1712 (1), pp.52-61.

Grace, P. B., Taylor, J. I., Low, Y. L., Luben, R. N., Mulligan, A. A., Botting, N. P., Dowsett, M., Welch, A. A., Khaw, K. T., Wareham, N. J., Day, N. E. and Bingham, S. A. 2004. Phytoestrogen concentrations in serum and spot urine as biomarkers for dietary phytoestrogen intake and their relation to breast cancer risk in European prospective investigation of cancer and nutrition-norfolk. *Cancer Epidemiology, Biomarkers & Prevention*, 13 (5), pp.698-708.

Grissmer, S., Nguyen, A. N., Aiyar, J., Hanson, D. C., Mather, R. J., Gutman, G. A., Karmilowicz, M. J., Auperin, D. D. and Chandy, K. G. 1994. Pharmacological characterization of five cloned voltage-gated K+ channels, types Kv1.1, 1.2, 1.3, 1.5, and 3.1, stably expressed in mammalian cell lines. *Molecular Pharmacology*, 45 (6), pp.1227-1234.

Gruber, C. J., Tschugguel, W., Schneeberger, C. and Huber, J. C. 2002. Production and actions of estrogens. *New England Journal Of Medicine*, 346 (5), pp.340-352.

Gu, L., House, S. E., Prior, R. L., Fang, N., Ronis, M. J. J., Clarkson, T. B., Wilson, M. E. and Badger, T. M. 2006. Metabolic phenotype of isoflavones differ among female rats, pigs, monkeys, and women. *Journal Of Nutrition*, 136 (5), pp.1215-1221.

Guan, L., Huang, Y. and Chen, Z. Y. 2008. Developmental and reproductive toxicity of soybean isoflavones to immature SD rats. *Biomedical And Environmental Sciences: BES*, 21 (3), pp.197-204.

Guha, N., Kwan, M. L., Quesenberry, C. P., Jr., Weltzien, E. K., Castillo, A. L. and Caan, B. J. 2009. Soy isoflavones and risk of cancer recurrence in a cohort of breast cancer survivors: the Life After Cancer Epidemiology study. *Breast Cancer Research And Treatment*, 118 (2), pp.395-405.

Gutman, G. A., Chandy, K. G., Grissmer, S., Lazdunski, M., McKinnon, D., Pardo, L. A., Robertson, G. A., Rudy, B., Sanguinetti, M. C., Stuhmer, W. and Wang, X. 2005. International Union of Pharmacology. LIII. Nomenclature and molecular relationships of voltage-gated potassium channels. *Pharmacological Reviews*, 57 (4), pp.473-508.

Hacker, G. 2000. The morphology of apoptosis. *Cell And Tissue Research*, 301 (1), pp.5-17.

Hadsell, D. L. 2003. The insulin-like growth factor system in normal mammary gland function. *Breast Disease*, 17 pp.3-14.

Haider, S. and Knofler, M. 2009. Human tumour necrosis factor: physiological and pathological roles in placenta and endometrium. *Placenta*, 30 (2), pp.111-123.

Hamann, S., Kiilgaard, J. F., Litman, T., Alvarez-Leefmans, F. J., Winther, B. R. and Zeuthen, t. 2002. Measurement of cell volume changes by fluorescence self-quenching. *Journal of Fluorescence*, 12 (2), pp.139-145.

Hamilton-Burke, W., Coleman, L., Cummings, M., Green, C. A., Holliday, D. L., Horgan, K., Maraqa, L., Peter, M. B., Pollock, S., Shaaban, A. M., Smith, L. and Speirs, V. 2010. Phosphorylation of estrogen receptor beta at serine 105 is associated with good prognosis in breast cancer. *American Journal Of Pathology*, 177 (3), pp.1079-1086.

Haren, N., Khorsi, H., Faouzi, M., Ahidouch, A., Sevestre, H. and Ouadid-Ahidouch, H. 2010. Intermediate conductance Ca2+ activated K+ channels are expressed and functional in breast adenocarcinomas: correlation with tumour grade and metastasis status. *Histology And Histopathology*, 25 (10), pp.1247-1255.

Hargreaves, D. F., Potten, C. S., Harding, C., Shaw, L. E., Morton, M. S., Roberts, S. A., Howell, A. and Bundred, N. J. 1999. Two-week dietary soy supplementation has an estrogenic effect on normal premenopausal breast. *Journal Of Clinical Endocrinology And Metabolism*, 84 (11), pp.4017-4024.

Harvey, A. L. and Robertson, B. 2004. Dendrotoxins: structure-activity relationships and effects on potassium ion channels. *Current Medicinal Chemistry*, 11 (23), pp.3065-3072.

Health Protection Agency. 2012. *European Collection of Cell Cultures*. [online] Available at: http://www.hpacultures.org.uk/ [Accessed September 11, 2012].

Hedelin, M., Lof, M., Olsson, M., Adlercreutz, H., Sandin, S. and Weiderpass, E. 2008. Dietary phytoestrogens are not associated with risk of overall breast cancer but diets rich in coumestrol are inversely associated with risk of estrogen receptor and progesterone receptor negative breast tumors in Swedish women. *Journal Of Nutrition*, 138 (5), pp.938-945.

Hemmerlein, B., Weseloh, R. M., Mello de Queiroz, F., Knotgen, H., Sanchez, A., Rubio, M. E., Martin, S., Schliephacke, T., Jenke, M., Heinz, J. R., Stuhmer, W. and Pardo, L. A. 2006. Overexpression of Eag1 potassium channels in clinical tumours. *Molecular Cancer*, 5 p.41.

Hendrix, S. L., Wassertheil-Smoller, S., Johnson, K. C., Howard, B. V., Kooperberg, C., Rossouw, J. E., Trevisan, M., Aragaki, A., Baird, A. E., Bray, P. F., Buring, J. E., Criqui, M. H., Herrington, D., Lynch, J. K., Rapp, S. R. and Torner, J. 2006. Effects of conjugated equine estrogen on stroke in the Women's Health Initiative. *Circulation*, 113 (20), pp.2425-2434.

Heneman, K. M., Chang, H. C., Prior, R. L. and Steinberg, F. M. 2007. Soy protein with and without isoflavones fails to substantially increase postprandial antioxidant capacity. *Journal of Nutritional Biochemistry*, 18 (1), pp.46-53.

Hewitt, S.C. and Korach, K.S. 2003. Oestrogen receptor knockout mice: roles for oestrogen receptors alpha and beta in reproductive tissues. *Reproduction*, 125, pp. 143-149.

Hewitt, A. L. and Singletary, K. W. 2003. Soy extract inhibits mammary adenocarcinoma growth in a syngeneic mouse model. *Cancer Letters*, 192 (2), pp.133-143.

Hille, B. 2001. *Ion channels of excitable membranes*. 3 ed. Sunderland, MA: Sinauer Associates Inc.

Hirata, T., Terai, T., Komatsu, T., Hanaoka, K. and Nagano, T. 2011. Development of a potassium ion-selective fluorescent sensor based on 3-styrylated BODIPY. *Bioorganic & Medicinal Chemistry Letters*, 21 (20), pp.6090-6093.

Ho, S. C., Chan, S. G., Yi, Q., Wong, E. and Leung, P. C. 2001. Soy intake and the maintenance of peak bone mass in Hong Kong Chinese women. *Journal Of Bone And Mineral Research*, 16 (7), pp.1363-1369.

Hockenbery, D. M., Oltvai, Z. N., Yin, X. M., Milliman, C. L. and Korsmeyer, S. J. 1993. Bcl-2 functions in an antioxidant pathway to prevent apoptosis. *Cell*, 75 (2), pp.241-251.

Hoffmann, E. K. 2011. Ion channels involved in cell volume regulation: effects on migration, proliferation, and programmed cell death in non adherent EAT cells and adherent ELA cells. *Cellular Physiology And Biochemistry: International Journal Of Experimental Cellular Physiology, Biochemistry, And Pharmacology*, 28 (6), pp.1061-1078.

Hooper, L., Ryder, J. J., Kurzer, M. S., Lampe, J. W., Messina, M. J., Phipps, W. R. and Cassidy, A. 2009. Effects of soy protein and isoflavones on circulating hormone concentrations in pre- and post-menopausal women: a systematic review and meta-analysis. *Human Reproduction Update*, 15 (4), pp.423-440.

Horn-Ross, P. L., Lee, M., John, E. M. and Koo, J. 2000. Sources of phytoestrogen exposure among non-Asian women in California, USA. *Cancer Causes & Control*, 11 (4), pp.299-302.

Horn-Ross, P. L., Hoggatt, K. J., West, D. W., Krone, M. R., Stewart, S. L., Anton, H., Bernstei, C. L., Deapen, D., Peel, D., Pinder, R., Reynolds, P., Ross, R. K., Wright, W. and Ziogas, A. 2002. Recent diet and breast cancer risk: the California Teachers Study (USA). *Cancer Causes & Control: CCC*, 13 (5), pp.407-415.

Hu, V. W., Black, G. E., Torres-Duarte, A. and Abramson, F. P. 2002. 3H-thymidine is a defective tool with which to measure rates of DNA synthesis. *FASEB Journal*, 16 pp.1456-1457.

Huang, C. C., Lim, P. H., Hall, A. C. and Huang, C. N. 2011. A key role for KCl cotransport in cell volume regulation in human erythroleukemia cells. *Life Sciences*, 88 (23-24), pp.1001-1008.

Hughes, F. M., Jr., Bortner, C. D., Purdy, G. D. and Cidlowski, J. A. 1997. Intracellular K+ suppresses the activation of apoptosis in lymphocytes. *The Journal Of Biological Chemistry*, 272 (48), pp.30567-30576.

HUGO Gene Nomenclature Committee. 2012. *HUGO Gene Nomenclature Committee Database*. [online] European Bioinformatics Institute. Available at: http://www.genenames.org. [Accessed September 11, 2012].

Hussain, M., Banerjee, M., Sarkar, F. H., Djuric, Z., Pollak, M. N., Doerge, D., Fontana, J., Chinni, S., Davis, J., Forman, J., Wood, D. P. and Kucuk, O. 2003. Soy isoflavones in the treatment of prostate cancer. *Nutrition And Cancer*, 47 (2), pp.111-117.

Hwang, C. S., Kwak, H. S., Lim, H. J., Lee, S. H., Kang, Y. S., Choe, T. B., Hur, H. G. and Han, K. O. 2006. Isoflavone metabolites and their in vitro dual functions: they can act as an estrogenic agonist or antagonist depending on the estrogen concentration. *Journal Of Steroid Biochemistry And Molecular Biology*, 101 (4-5), pp.246-253.

Indelicato, M., Pucci, B., Schito, L., Reali, V., Aventaggiato, M., Mazzarino, M. C., Stivala, F., Fini, M., Russo, M. A. and Tafani, M. 2010. Role of hypoxia and autophagy in MDA-MB-231 invasiveness. *Journal Of Cellular Physiology*, 223 (2), pp.359-368.

Information Services Division Scotland. 2012. *Cancer Information Program. 2010*. [online] NHS National Services Scotland, Edinburgh. Available at: http://www.isdscotland.org/Health-Topics//Cancer/Publications/index.asp#839. [Accessed September 11, 2012].

International Union of Pharmacology. 2012. *IUPHAR Committee on Receptor Nomenclature and Drug Classification Database*. [online] International Union of Pharmacology. Available from: http://iuphar-db.org. Accessed September 11, 2012.

Ishibashi, K., Kondo, S., Hara, S. and Morishita, Y. 2011. The evolutionary aspects of aquaporin family. *American Journal Of Physiology Regulatory, Integrative And Comparative Physiology*, 300 (3), p.R566-R576.

Iwasaki, M., Inoue, M., Otani, T., Sasazuki, S., Kurahashi, N., Miura, T., Yamamoto, S. and Tsugane, S. 2008. Plasma isoflavone level and subsequent risk of breast cancer among Japanese women: a nested case-control study from the Japan Public Health Center-based prospective study group. *Journal of Clinical Oncology*, 26 (10), pp.1677-1683.

Iwasaki, M. and Tsugane, S. 2011. Risk factors for breast cancer: epidemiological evidence from Japanese studies. *Cancer Science*, 102 (9), pp.1607-1614.

Jacobs, E., Bulpitt, P. C., Coutts, I. G. and Robertson, J. F. 2000. New calmodulin antagonists inhibit in vitro growth of human breast cancer cell lines independent of their estrogen receptor status. *Anti-Cancer Drugs*, 11 (2), pp.63-68.

Jakes, R. W., Duffy, S. W., Ng, F. C., Gao, F., Ng, E. H., Seow, A., Lee, H. P. and Yu, M. C. 2002. Mammographic parenchymal patterns and self-reported soy intake in Singapore Chinese women. *Cancer Epidemiology, Biomarkers & Prevention*, 11 (7), pp.608-613.

Jakob, S., Corazza, N., Diamantis, E., Kappeler, A. and Brunner, T. 2008. Detection of apoptosis in vivo using antibodies against caspase-induced neo-epitopes. *Methods*, 44 pp.255-261.

Jang, S. H., Kang, K. S., Ryu, P. D. and Lee, S. Y. 2009. Kv1.3 voltage-gated K(+) channel subunit as a potential diagnostic marker and therapeutic target for breast cancer. *BMB Reports*, 42 (8), pp.535-539.

Janicke, R. U., Sprengart, M. L., Wati, M. R. and Porter, A. G. 1998. Caspase-3 is required for DNA fragmentation and morphological changes associated with apoptosis. *Journal Of Biological Chemistry*, 273 (16), pp.9357-9360.

Janicke, R. U. 2009. MCF-7 breast carcinoma cells do not express caspase-3. *Breast Cancer Research And Treatment*, 117 (1), pp.219-221.

Jefcoate, C. R., Leihr, J. G., Santen, R. J., Sutter, T. R., Yager, J. D., Yue, W., Santner, S. J., Tekmal, R., Demers, L., Pauley, R., Naftolin, F., Mor, G. and Berstein.L. 2000. Chapter 5: Tissue-specific synthesis and oxidative metabolism of estrogens. *Journal of the National Cancer Institute Monographs*, 27 pp.95-112.

Jemal, A., Bray, F., Center, M. M., Ferlay, J., Ward, E. and Forman, D. 2011. Global cancer statistics. *CA Cancer Journal For Clinicians*, 61 (2), pp.69-90.

Jiang, Y., Lee, A., Chen, J., Ruta, V., Cadene, M., Chait, B. T. and MacKinnon, R. 2003. X-ray structure of a voltage-dependent K+ channel. *Nature*, 423 (6935), pp.33-41.

Jin, Q. and Esteva, F. J. 2008. Cross-talk between the ErbB/HER family and the type I insulin-like growth factor receptor signaling pathway in breast cancer. *Journal Of Mammary Gland Biology And Neoplasia*, 13 (4), pp.485-498.

Jin, S., Zhang, Q. Y., Kang, X. M., Wang, J. X. and Zhao, W. H. 2010. Daidzein induces MCF-7 breast cancer cell apoptosis via the mitochondrial pathway. *Annals Of Oncology*, 21 (2), pp.263-268.

Jin, Z. and MacDonald, R. S. 2002. Soy isoflavones increase latency of spontaneous mammary tumors in mice. *Journal Of Nutrition*, 132 (10), pp.3186-3190.

Ju, Y. H., Allred, C. D., Allred, K. F., Karko, K. L., Doerge, D. R. and Helferich, W. G. 2001. Physiological concentrations of dietary genistein dose-dependently stimulate growth of estrogen-dependent human breast cancer (MCF-7) tumors implanted in athymic nude mice. *Journal Of Nutrition*, 131 (11), pp.2957-2962.

Ju, Y. H., Doerge, D. R., Allred, K. F., Allred, C. D. and Helferich, W. G. 2002. Dietary genistein negates the inhibitory effect of tamoxifen on growth of estrogen-dependent human breast cancer (MCF-7) cells implanted in athymic mice. *Cancer Research*, 62 (9), pp.2474-2477.

Kaaks, R., Rinaldi, S., Key, T. J., Berrino, F., Peeters, P. H. M., Biessy, C., Dossus, L., Lukanova, A., Bingham, S., Khaw, K. T., Allen, N. E., Bueno-de-Mesquita, H. B., van Gils, C. H., Grobbee, D., Boeing, H., Lahmann, P. H., Nagel, G., Chang-Claude, J., Clavel-Chapelon, F., Fournier, A., Thiebaut, A., Gonzalez, C. A., Quiros, J. R., Tormo, M. J., Ardanaz, E., Amiano, P., Krogh, V., Palli, D., Panico, S., Tumino, R., Vineis, P., Trichopoulou, A., Kalapothaki, V., Trichopoulos, D., Ferrari, P., Norat, T., Saracci, R. and Riboli, E. 2005a. Postmenopausal serum androgens, oestrogens and breast cancer risk: the European prospective investigation into cancer and nutrition. *Endocrine-Related Cancer*, 12 (4), pp.1071-1082.

Kaaks, R., Berrino, F., Key, T., Rinaldi, S., Dossus, L., Biessy, C., Secreto, G., Amiano, P., Bingham, S., Boeing, H., Bueno de Mesquita, H. B., Chang-Claude, J., Clavel-Chapelon, F., Fournier, A., van Gils, C. H., Gonzalez, C. A., Gurrea, A. B., Critselis, E., Khaw, K. T., Krogh, V., Lahmann, P. H., Nagel, G., Olsen, A., Onland-Moret, N. C., Overvad, K., Palli, D., Panico, S., Peeters, P., Quiros, J. R., Roddam, A., Thiebaut, A., Tjonneland, A., Chirlaque, M. D., Trichopoulou, A., Trichopoulos, D., Tumino, R., Vineis, P., Norat, T., Ferrari, P., Slimani, N. and Riboli, E. 2005b. Serum sex steroids in premenopausal women and breast cancer risk within the European Prospective Investigation into Cancer and Nutrition (EPIC). *Journal Of The National Cancer Institute*, 97 (10), pp.755-765.

Kang, H. B., Zhang, Y. F., Yang, J. D. and Lu, K. L. 2012. Study on soy isoflavone consumption and risk of breast cancer and survival. *Asian Pacific Journal Of Cancer Prevention*, 13 (3), pp.995-998.

Kang, X., Jin, S. and Zhang, Q. 2009. Antitumor and antiangiogenic activity of soy phytoestrogen on 7,12-dimethylbenz[alpha]anthracene-induced mammary tumors following ovariectomy in Sprague-Dawley rats. *Journal Of Food Science*, 74 (7), p.H237-H242.

Kang, X., Zhang, Q., Wang, S., Huang, X. and Jin, S. 2010. Effect of soy isoflavones on breast cancer recurrence and death for patients receiving adjuvant endocrine therapy. *Canadian Medical Association Journal*, 182 (17), pp.1857-1862.

Kano, M., Takayanagi, T., Harada, K., Sawada, S. and Ishikawa, F. 2006. Bioavailability of isoflavones after ingestion of soy beverages in healthy adults. *The Journal Of Nutrition*, 136 (9), pp.2291-2296.

Kaplan, W. D. and Trout, W. E., III 1969. The behavior of four neurological mutants of Drosophila. *Genetics*, 61 (2), pp.399-409.

Katzenellenbogen, B. S., Kendra, K. L., Norman, M. J. and Berthois, Y. 1987. Proliferation, hormonal responsiveness, and estrogen receptor content of MCF-7 human breast cancer cells grown in the short-term and long-term absence of estrogens. *Cancer Research*, 47 (16), pp.4355-4360.

Kauffmann, S. H., Lee, S.-H., Wei Meng, X., Loegering, D. A., Kottke, T. J., Henzing, A. J., Ruchaud, S., Samejima, K. and Earnshaw, W. C. 2008. Apoptosis-associated caspase activation assays. *Methods*, 44 (3), pp.262-272.

Keeton, E. K. and Brown, M. 2005. Cell cycle progression stimulated by tamoxifen-bound estrogen receptor-alpha and promoter-specific effects in breast cancer cells deficient in N-CoR and SMRT. *Molecular Endocrinology*, 19 (6), pp.1543-1554.

Kerr, J. F., Wyllie, A. H. and Currie, A. R. 1972. Apoptosis: a basic biological phenomenon with wide-ranging implications in tissue kinetics. *British Journal Of Cancer*, 26 (4), pp.239-257.

Khaitan, D., Sankpal, U. T., Weksler, B., Meister, E. A., Romero, I. A., Couraud, P. O. and Ningaraj, N. S. 2009. Role of KCNMA1 gene in breast cancer invasion and metastasis to brain. *BMC Cancer*, 9 p.258.

Kim, H., Chung, H., Kim, H. J., Lee, J. Y., Oh, M. Y., Kim, Y. and Kong, G. 2008. Id-1 regulates Bcl-2 and Bax expression through p53 and NF-kappaB in MCF-7 breast cancer cells. *Breast Cancer Research And Treatment*, 112 (2), pp.287-296.

Kim, N., Gross, C., Curtis, J., Stettin, G., Wogen, S., Choe, N. and Krumholz, H. M. 2005. The impact of clinical trials on the use of hormone replacement therapy. A population-based study. *Journal Of General Internal Medicine*, 20 (11), pp.1026-1031.

Kim, S., Moon, S. and Popkin, B. M. 2000. The nutrition transition in South Korea. *The American Journal Of Clinical Nutrition*, 71 (1), pp.44-53.

Kirkegaard, S. S., Lambert, I. H., Gammeltoft, S. and Hoffmann, E. K. 2010. Activation of the TASK-2 channel after cell swelling is dependent on tyrosine phosphorylation. *American Journal Of Physiology Cell Physiology*, 299 (4), p.C844-C853.

Klapperstuck, T., Glanz, D., Klapperstuck, M. and Wholrab, J. 2009. Methodological aspectes of measuring absolute values of membrane potential in human cells by flow cytometry. *Cytometry Part A*, 75A pp.593-608.

Klimatcheva, E. and Wonderlin, W. F. 1999. An ATP-sensitive K(+) current that regulates progression through early G1 phase of the cell cycle in MCF-7 human breast cancer cells. *Journal Of Membrane Biology*, 171 (1), pp.35-46.

Koch, C. and Stratling, W. H. 2004. DNA binding of methyl-CpG-binding protein MeCP2 in human MCF7 cells. *Biochemistry*, 43 (17), pp.5011-5021.

Koeberle, P. D., Wang, Y. and Schlichter, L. C. 2010. Kv1.1 and Kv1.3 channels contribute to the degeneration of retinal ganglion cells after optic nerve transection in vivo. *Cell Death And Differentiation*, 17 (1), pp.134-144.

Kok, M., Holm-Wigerup, C., Hauptmann, M., Michalides, R., Stal, O., Linn, S. and Landberg, G. 2009. Estrogen receptor-alpha phosphorylation at serine-118 and tamoxifen response in breast cancer. *Journal Of The National Cancer Institute*, 101 (24), pp.1725-1729.

Kossler, S., Nofziger, C., Jakab, M., Dossena, S. and Paulmichl, M. 2012. Curcumin affects cell survival and cell volume regulation in human renal and intestinal cells. *Toxicology*, 292 (2-3), pp.123-135.

Kostelac, D., Rechkemmer, G. and Briviba, K. 2003. Phytoestrogens modulate binding response of estrogen receptors alpha and beta to the estrogen response element. *Journal of Agricultural and Food Chemistry*, 51 (26), pp.7632-7635.

Kroemer, G., El-Deiry, W. S., Golstein, P., Peter, M. E., Vaux, D., Vandenabeele, P., Zhivotovsky, B., Blagosklonny, M. V., Malorni, W., Knight, R. A., Piacentini, M., Nagata, S. and Melino, G. 2005. Classification of cell death: recommendations of the Nomenclature Committee on Cell Death. *Cell Death And Differentiation*, 12 pp.1463-1467.

Kroemer, G., Galluzzi, L., Vandenabeele, P., Abrams, J., Alnemri, E. S., Baehrecke, E. H., Blagosklonny, M. V., El-Deiry, W. S., Golstein, P., Green, D. R., Hengartner, M., Knight, R. A., Kumar, S., Lipton, S. A., Malorni, W., Nunez, G., Peter, M. E., Tschopp, J., Yuan, J., Piacentini, M., Zhivotovsky, B. and Melino, G. 2009. Classification of cell death: recommendations of the Nomenclature Committee on Cell Death 2009. *Cell Death And Differentiation*, 16 (1), pp.3-11.

Krysko, D. V., Vanden Berghe, T., D'Herde, K. and Vandenabeele, P. 2008. Apoptosis and necrosis: detection, discrimination and phagocytosis. *Methods*, 44 (3), pp.205-221.

Kubo, Y., Adelman, J. P., Clapham, D. E., Jan, L. Y., Karschin, A., Kurachi, Y., Lazdunski, M., Nichols, C. G., Seino, S. and Vandenberg, C. A. 2005. International Union of Pharmacology. LIV. Nomenclature and molecular relationships of inwardly rectifying potassium channels. *Pharmacological Reviews*, 57 (4), pp.509-526.

Kudwa, A.E. and Rissman, E.F. 2012. Double receptor alpha and beta knockout mice reveal differences in neural oestrogen-mediated progestin receptor induction and female sex behaviour. Journal of Neuroendocrinology, 15, pp. 978-983.

Kuhnle, G. G. C., Dell'Aquila, C., Aspinall, S. M., Runswick, S. A., Mulligan, A. A. and Bingham, S. A. 2008. Phytoestrogen content of beverages, nuts, seeds, and oils. *Journal Of Agricultural And Food Chemistry*, 56 (16), pp.7311-7315.

Kuiper, G. G., Lemmen, J. G., Carlsson, B., Corton, J. C., Safe, S. H., van der Saag, P. T., van der Burg, B. and Gustafsson, J. A. 1998. Interaction of estrogenic chemicals and phytoestrogens with estrogen receptor beta. *Endocrinology*, 139 (10), pp.4252-4263.

Kumar, A., Klinge, C. M. and Goldstein, R. E. 2010. Estradiol-induced proliferation of papillary and follicular thyroid cancer cells is mediated by estrogen receptors alpha and beta. *International Journal Of Oncology*, 36 (5), pp.1067-1080.

Kumar, N. B., Cantor, A., Allen, K., Riccardi, D. and Cox, C. E. 2002. The specific role of isoflavones on estrogen metabolism in premenopausal women. *Cancer*, 94 (4), pp.1166-1174.

Kunisue, T., Tanabe, S., Isobe, T., Aldous, K. M. and Kannan, K. 2010. Profiles of phytoestrogens in human urine from several Asian countries. *Journal Of Agricultural And Food Chemistry*, 58 (17), pp.9838-9846.

Kurebayashi, J., Otsuki, T., Kunisue, H., Tanaka, K., Yamamoto, S. and Sonoo, H. 2000. Expression levels of estrogen receptor-alpha, estrogen receptor-beta, coactivators, and corepressors in breast cancer. *Clinical Cancer Research*, 6 (2), pp.512-518.

Kurian, A. W., Fish, K., Shema, S. J. and Clarke, C. A. 2010. Lifetime risks of specific breast cancer subtypes among women in four racial/ethnic groups. *Breast Cancer Research*, 12 (6), p.R99.

Lai, J., Chien, J., Staub, J., Avula, R., Greene, E. L., Matthews, T. A., Smith, D. I., Kaufmann, S. H., Roberts, L. R. and Shridhar, V. 2003. Loss of HSulf-1 up-regulates heparin-binding growth factor signaling in cancer. *Journal Of Biological Chemistry*, 278 (25), pp.23107-23117.

Lamartiniere, C. A., Zhang, J. X. and Cotroneo, M. S. 1998. Genistein studies in rats: potential for breast cancer prevention and reproductive and developmental toxicity. *American Journal of Clinical Nutrition*, 68 (6 Suppl), pp.1400S-1405s.

Lamartiniere, C. A., Wang, J., Smith-Johnson, M. and Eltoum, I. E. 2002. Daidzein: bioavailability, potential for reproductive toxicity, and breast cancer chemoprevention in female rats. *Toxicological Sciences*, 65 (2), pp.228-238.

Lammersfeld, C. A., King, J., Walker, S., Vashi, P. G., Grutsch, J. F., Lis, C. G. and Gupta, D. 2009. Prevalence, sources, and predictors of soy consumption in breast cancer. *Nutrition Journal*, 8 p.2.

Lampe, J. W. 2003. Isoflavonoid and lignan phytoestrogens as dietary biomarkers. *Journal Of Nutrition*, 133 Suppl 3 pp.956S-964s.

Lastraioli, E., Guasti, L., Crociani, O., Polvani, S., Hofmann, G., Witchel, H., Bencini, L., Calistri, M., Messerini, L., Scatizzi, M., Moretti, R., Wanke, E., Olivotto, M., Mugnai, G. and Arcangeli, A. 2004. herg1 gene and HERG1 protein are overexpressed in colorectal cancers and regulate cell invasion of tumor cells. *Cancer Research*, 64 (2), pp.606-611.

Lattrich, C., Lubig, J., Springwald, A., Goerse, R., Ortmann, O. and Treeck, O. 2011. Additive effects of trastuzumab and genistein on human breast cancer cells. *Anti-Cancer Drugs*, 22 (3), pp.253-261.

Lau, W. S., Chen, W. F., Chan, R. Y.-K., Guo, D. A. and Wong, M. S. 2009. Mitogen-activated protein kinase (MAPK) pathway mediates the oestrogen-like activities of ginsenoside Rg1 in human breast cancer (MCF-7) cells. *British Journal Of Pharmacology*, 156 (7), pp.1136-1146.

Lavigne, J. A., Takahashi, Y., Chandramouli, G. V. R., Liu, H., Perkins, S. N., Hursting, S. D. and Wang, T. T. Y. 2008. Concentration-dependent effects of genistein on global gene expression in MCF-7 breast cancer cells: an oligo microarray study. *Breast Cancer Research And Treatment*, 110 (1), pp.85-98.

Le Corre, L., Chalabi, N., Delort, L., Bignon, Y. J. and Bernard-Gallon, D. J. 2006. Differential expression of genes induced by resveratrol in human breast cancer cell lines. *Nutrition And Cancer*, 56 (2), pp.193-203.

Le Corre, L., Fustier, P., Chalabi, N. r., Bignon, Y. J. and Bernard-Gallon, D. 2004. Effects of resveratrol on the expression of a panel of genes interacting with the BRCA1 oncosuppressor in human breast cell lines. *Clinica Chimica Acta; International Journal Of Clinical Chemistry*, 344 (1-2), pp.115-121.

Lee, G. W., Park, H. S., Kim, E. J., Cho, Y. W., Kim, G. T., Mun, Y. J., Choi, E. J., Lee, J. S., Han, J. and Kang, D. 2012. Reduction of breast cancer cell migration via up-regulation of TASK-3 two-pore domain K+ channel. *Acta Physiologica*, 204 (4), pp.513-524.

Lee, S. A., Shu, X. O., Li, H., Yang, G., Cai, H., Wen, W., Ji, B. T., Gao, J., Gao, Y. T. and Zheng, W. 2009. Adolescent and adult soy food intake and breast cancer risk: results from the Shanghai Women's Health Study. *American Journal of Clinical Nutrition*, 89 (6), pp.1920-1926.

Legler, J., van den Brink, C. E., Brouwer, A., Murk, A. J., van der Saag, P. T., Vethaak, A. D. and van der Burg, B. 1999. Development of a stably transfected estrogen receptor-mediated luciferase reporter gene assay in the human T47D breast cancer cell line. *Toxicological Sciences*, 48 (1), pp.55-66.

Lennartsson, J., Burovic, F., Witek, B., Jurek, A. and Heldin, C. H. 2010. Erk 5 is necessary for sustained PDGF-induced Akt phosphorylation and inhibition of apoptosis. *Cellular Signalling*, 22 (6), pp.955-960.

LGC-ATCC. 2012. *ATCC Cultures and Products*. [online] LGC-ATCC. Available from: http://www.lgcstandards-atcc.org/. Accessed September 21, 2012.

Li, H. F., Chen, S. A. and Wu, S. N. 2000. Evidence for the stimulatory effect of resveratrol on Ca(2+)-activated K+ current in vascular endothelial cells. *Cardiovascular Research*, 45 (4), pp.1035-1045.

Li, X., Zhang, S. and Safe, S. 2006. Activation of kinase pathways in MCF-7 cells by 17beta-estradiol and structurally diverse estrogenic compounds. *Journal Of Steroid Biochemistry And Molecular Biology*, 98 (2-3), pp.122-132.

Li, Z., Joyal, J. L. and Sacks, D. B. 2001. Calmodulin enhances the stability of the estrogen receptor. *Journal Of Biological Chemistry*, 276 (20), pp.17354-17360.

Li, Z., Li, J., Mo, B., Hu, C., Liu, H., Qi, H., Wang, X. and Xu, J. 2008. Genistein induces cell apoptosis in MDA-MB-231 breast cancer cells via the mitogen-activated protein kinase pathway. *Toxicology In Vitro*, 22 (7), pp.1749-1753.

Liggins, J., Bluck, L. J., Runswick, S., Atkinson, C., Coward, W. A. and Bingham, S. A. 2000. Daidzein and genistein content of fruits and nuts. *Journal of Nutritional Biochemistry*, 11 (6), pp.326-331.

Linseisen, J., Piller, R., Hermann, S. and Chang-Claude, J. 2004. Dietary phytoestrogen intake and premenopausal breast cancer risk in a German case-control study. *International Journal Of Cancer*, 110 (2), pp.284-290.

Liu, B., Edgerton, S., Yang, X., Kim, A., Ordonez-Ercan, D., Mason, T., Alvarez, K., McKimmey, C., Liu, N. and Thor, A. 2005. Low-dose dietary phytoestrogen abrogates tamoxifen-associated mammary tumor prevention. *Cancer Research*, 65 (3), pp.879-886.

Liu, H., Du, J., Hu, C., Qi, H., Wang, X., Wang, S., Liu, Q. and Li, Z. 2010. Delayed activation of extracellular-signal-regulated kinase 1/2 is involved in genistein- and equol-induced cell proliferation and estrogen-receptor-alpha-mediated transcription in MCF-7 breast cancer cells. *Journal of Nutritional Biochemistry*, 21 (5), pp.390-396.

Liu, M. M., Albanese, C., Anderson, C. M., Hilty, K., Webb, P., Uht, R. M., Price, R. H., Jr., Pestell, R. G. and Kushner, P. J. 2002. Opposing action of estrogen receptors alpha and beta on cyclin D1 gene expression. *Journal Of Biological Chemistry*, 277 (27), pp.24353-24360.

Liu, Y. C., Lo, Y. C., Huang, C. W. and Wu, S. N. 2003. Inhibitory action of ICI-182,780, an estrogen receptor antagonist, on BK(Ca) channel activity in cultured endothelial cells of human coronary artery. *Biochemical Pharmacology*, 66 (10), pp.2053-2063.

Lodish, H., Berk, A., Kaiser, C.A., Krieger, M., Scott, M.P., Bretscher, A., Ploegh, H. and Matsudaira, P. 2008. *Molecular Cell Biology*. 6th ed. New York: W.H. Freeman and Company.

Low Dog, T. 2005. Menopause: a review of botanical dietary supplements. *American Journal Of Medicine*, 118 Suppl 12B pp.98-108.

Lucki, N. C. and Sewer, M. B. 2011. Genistein stimulates MCF-7 breast cancer cell growth by inducing acid ceramidase (ASAH1) gene expression. *Journal Of Biological Chemistry*, 286, pp.19399-19409.

Lux, H. D. and Brown, A. M. 1984. Patch and whole cell calcium currents recorded simultaneously in snail neurons. *Journal Of General Physiology*, 83 (5), pp.727-750.

Mady, E. A. 2000. Association between estradiol, estrogen receptors, total lipids, triglycerides, and cholesterol in patients with benign and malignant breast tumors. *Journal Of Steroid Biochemistry And Molecular Biology*, 75 (4-5), pp.323-328.

Maeno, E., Ishizaki, Y., Kanaseki, T., Hazama, A. and Okada, Y. 2000. Normotonic cell shrinkage because of disordered volume regulation is an early prerequisite to apoptosis. *Proceedings Of The National Academy Of Sciences Of The United States Of America*, 97 (17), pp.9487-9492.

Maggiolini, M., Bonofiglio, D., Marsico, S., Panno, M. L., Cenni, B., Picard, D. and Ando, S. 2001. Estrogen receptor alpha mediates the proliferative but not the cytotoxic dose-dependent effects of two major phytoestrogens on human breast cancer cells. *Molecular Pharmacology*, 60 (3), pp.595-602.

Maggiolini, M., Vivacqua, A., Fasanella, G., Recchia, A. G., Sisci, D., Pezzi, V., Montanaro, D., Musti, A. M., Picard, D. and Ando, S. 2004. The G protein-coupled receptor GPR30 mediates c-fos up-regulation by 17beta-estradiol and phytoestrogens in breast cancer cells. *Journal Of Biological Chemistry*, 279 (26), pp.27008-27016.

Mahaut-Smith, M. P., Hussain, J. F. and Mason, M. J. 1999. Depolarization-evoked Ca2+ release in a non-excitable cell, the rat megakaryocyte. *Journal of Physiology*, 515 (Pt 2) pp.385-390.

Marthyn, P., Beuscart, A., Coll, J., Moreau-Gachelin, F. and Righi, M. 1998. DMSO reduces CSF-1 receptor levels and causes apoptosis in v-myc immortalized mouse macrophages. *Experimental Cell Research*, 243 (1), pp.94-100.

Martin, S. J., Reutelingsperger, C. P., McGahon, A. J., Rader, J. A., van Schie, R. C., LaFace, D. M. and Green, D. R. 1995. Early redistribution of plasma membrane phosphatidylserine is a general feature of apoptosis regardless of the initiating stimulus: inhibition by overexpression of Bcl-2 and Abl. *Journal Of Experimental Medicine*, 182 (5), pp.1545-1556.

Martin, S. J. 2008. Getting the measure of apoptosis. *Methods*, 44 (3), pp.197-199.

Martinez-Montemayor, M. M., Otero-Franqui, E., Martinez, J., De La Mota-Peynado, A., Cubano, L. A. and Dharmawardhane, S. 2010. Individual and combined soy isoflavones exert differential effects on metastatic cancer progression. *Clinical & Experimental Metastasis*, 27 (7), pp.465-480.

Maruyama, K., Endoh, H., Sasaki-Iwaoka, H., Kanou, H., Shimaya, E., Hashimoto, S., Kato, S. and Kawashima, H. 1998. A novel isoform of rat estrogen receptor beta with 18 amino acid insertion in the ligand binding domain as a putative dominant negative regular of estrogen action. *Biochemical And Biophysical Research Communications*, 246 (1), pp.142-147.

Maskarinec, G. and Meng, L. 2001. An investigation of soy intake and mammographic characteristics in Hawaii. *Breast Cancer Research*, 3 (2), pp.134-141.

Maskarinec, G., Williams, A. E. and Carlin, L. 2003. Mammographic densities in a one-year isoflavone intervention. *European Journal Of Cancer Prevention*, 12 (2), pp.165-169.

Maskarinec, G., Hebshi, S., Custer, L. and Franke, A. A. 2008. The relation of soy intake and isoflavone levels in nipple aspirate fluid. *European Journal Of Cancer Prevention*, 17 (1), pp.67-70.

Maskarinec, G., Takata, Y., Franke, A. A., Williams, A. E. and Murphy, S. P. 2004. A 2-year soy intervention in premenopausal women does not change mammographic densities. *Journal Of Nutrition*, 134 (11), pp.3089-3094.

Maskarinec, G., Takata, Y., Murphy, S. P., Franke, A. A. and Kaaks, R. 2005. Insulin-like growth factor-1 and binding protein-3 in a 2-year soya intervention among premenopausal women. *British Journal Of Nutrition*, 94 (3), pp.362-367.

Maskarinec, G., Verheus, M., Steinberg, F. M., Amato, P., Cramer, M. K., Lewis, R. D., Murray, M. J., Young, R. L. and Wong, W. W. 2009. Various doses of soy isoflavones do not modify mammographic density in postmenopausal women. *Journal Of Nutrition*, 139 (5), pp.981-986.

Mathiasen, I. S., Sergeev, I. N., Bastholm, L., Elling, F., Norman, A. W. and Jaattela, M. 2002. Calcium and calpain as key mediators of apoptosis-like death induced by vitamin D compounds in breast cancer cells. *Journal Of Biological Chemistry*, 277 (34), pp.30738-30745.

Matsumura, A., Ghosh, A., Pope, G. S. and Darbre, P. D. 2005. Comparative study of oestrogenic properties of eight phytoestrogens in MCF7 human breast cancer cells. *Journal Of Steroid Biochemistry And Molecular Biology*, 94 (5), pp.431-443.

Maubach, J., Depypere, H. T., Goeman, J., Van der Eycken, J., Heyerick, A., Bracke, M. E., Blondeel, P. and De Keukeleire, D. 2004. Distribution of soy-derived phytoestrogens in human breast tissue and biological fluids. *Obstetrics And Gynecology*, 103 (5 Pt 1), pp.892-898.

Mawson, A., Lai, A., Carroll, J. S., Sergio, C. M., Mitchell, C. J. and Sarcevic, B. 2005. Estrogen and insulin/IGF-1 cooperatively stimulate cell cycle progression in MCF-7 breast cancer cells through differential regulation of c-Myc and cyclin D1. *Molecular And Cellular Endocrinology*, 229 (1-2), pp.161-173.

McLaughlin, J. M., Olivo-Marston, S., Vitolins, M. Z., Bittoni, M., Reeves, K. W., Degraffinreid, C. R., Schwartz, S. J., Clinton, S. K. and Paskett, E. D. 2011. Effects of tomato- and soy-rich diets on the IGF-I hormonal network: a crossover study of postmenopausal women at high risk for breast cancer. *Cancer Prevention Research*, 4 (5), pp.702-710.

McMichael-Phillips, D. F., Harding, C., Morton, M., Roberts, S. A., Howell, A., Potten, C. S. and Bundred, N. J. 1998. Effects of soy-protein supplementation on epithelial proliferation in the histologically normal human breast. *American Journal of Clinical Nutrition*, 68 (6 Suppl), pp.1431S-1435s.

McPherson, K., Steel, C. M. and Dixon, J. M. 2000. ABC of breast diseases. Breast cancer-epidemiology, risk factors, and genetics. *BMJ (Clinical Research Ed)*, 321 (7261), pp.624-628.

Medema, J. P., Scaffidi, C., Kischkel, F. C., Shevchenko, A., Mann, M., Krammer, P. H. and Peter, M. E. 1997. FLICE is activated by association with the CD95 death-inducing signaling complex (DISC). *EMBO Journal*, 16 (10), pp.2794-2804.

Mei, J., Yeung, S. S. and Kung, A. W. 2001. High dietary phytoestrogen intake is associated with higher bone mineral density in postmenopausal but not premenopausal women. *Journal Of Clinical Endocrinology And Metabolism*, 86 (11), pp.5217-5221.

Messina, M., Nagata, C. and Wu, A. H. 2006. Estimated Asian adult soy protein and isoflavone intakes. *Nutrition & Cancer*, 55 (1), pp.1-12.

Messina, M. J. and Wood, C. E. 2008. Soy isoflavones, estrogen therapy, and breast cancer risk: analysis and commentary. *Nutrition Journal*, 7 p.17.

Miglietta, A., Bozzo, F., Bocca, C., Gabriel, L., Trombetta, A., Belotti, S. and Canuto, R. A. 2006. Conjugated linoleic acid induces apoptosis in MDA-MB-231 breast cancer cells through ERK/MAPK signalling and mitochondrial pathway. *Cancer Letters*, 234 (2), pp.149-157.

Miki, Y., Suzuki, T., Nagasaki, S., Hata, S., Akahira, J. I. and Sasano, H. 2009. Comparative effects of raloxifene, tamoxifen and estradiol on human osteoblasts in vitro: estrogen receptor dependent or independent pathways of raloxifene. *Journal Of Steroid Biochemistry And Molecular Biology*, 113 (3-5), pp.281-289.

Miller, W.R., Anderson, T.J., Dixon, J.M. and Suanders, P.T.K. 2006. Oestrogen receptor beta and neoadjuvant therapy with tamoxifen: prediction of response and effects of treatment. *British Journal of Cancer*, 94 (9), pp.1333-1388.

Miller, W. R., Bartlett, J. M. S., Canney, P. and Verrill, M. 2007. Hormonal therapy for postmenopausal breast cancer: the science of sequencing. *Breast Cancer Research And Treatment*, 103 (2), pp.149-160.

Miodini, P., Fioravanti, L., Di Fronzo, G. and Cappelletti, V. 1999. The two phytoestrogens genistein and quercetin exert different effects on estrogen receptor function. *British Journal Of Cancer*, 80 (8), pp.1150-1155.

Missan, S., Linsdell, P. and McDonald, T. F. 2006. Tyrosine kinase and phosphatase regulation of slow delayed-rectifier K+ current in guinea-pig ventricular myocytes. *Journal of Physiology*, 573 (Pt 2), pp.469-482.

Mitra, A. K., Faruque, F. S. and Avis, A. L. 2004. Breast cancer and environmental risks: where is the link? *Journal Of Environmental Health*, 66 (7), p.24.

Mohan, N., Karmakar, S., Choudhury, S. R., Banik, N. L. and Ray, S. K. 2009. Bcl-2 inhibitor HA14-1 and genistein together adeptly down regulated survival factors and activated cysteine proteases for apoptosis in human malignant neuroblastoma SK-N-BE2 and SH-SY5Y cells. *Brain Research*, 1283 pp.155-166.

Molleman, A.2002. Basic Theoretical Principles. *Patch Clamping: An Introductory Guide to Patch Clamp Electrophysiology*. Hoboken, NJ: John Wiley & Sons, pp. 5-42.

Moon, Y. J., Shin, B. S., An, G. and Morris, M. E. 2008. Biochanin A inhibits breast cancer tumor growth in a murine xenograft model. *Pharmaceutical Research*, 25 (9), pp.2158-2163.

Moore, J. T., McKee, D. D., Slentz-Kesler, K., Moore, L. B., Jones, S. A., Horne, E. L., Su, J. L., Kliewer, S. A., Lehmann, J. M. and Willson, T. M. 1998. Cloning and characterization of human estrogen receptor beta isoforms. *Biochemical And Biophysical Research Communications*, 247 (1), pp.75-78.

Mosmann, T. 1983. Rapid colorimetric assay for cellular growth and survival: application to proliferation and cytotoxicity assays. *Journal Of Immunological Methods*, 65 (1-2), pp.55-63.

Mu, D., Chen, L., Zhang, X., See, L. H., Koch, C. M., Yen, C., Tong, J. J., Spiegel, L., Nguyen, K. C. Q., Servoss, A., Peng, Y., Pei, L., Marks, J. R., Lowe, S., Hoey, T., Jan, L. Y., McCombie, W. R., Wigler, M. H. and Powers, S. 2003. Genomic amplification and oncogenic properties of the KCNK9 potassium channel gene. *Cancer Cell*, 3 (3), pp.297-302.

Nagata, C., Shimizu, H., Takami, R., Hayashi, M., Takeda, N. and Yasuda, K. 2003. Dietary soy and fats in relation to serum insulin-like growth factor-1 and insulin-like growth factor-binding protein-3 levels in premenopausal Japanese women. *Nutrition And Cancer*, 45 (2), pp.185-189.

Nakagawa, T. and Yuan, J. 2000. Cross-talk between two cysteine protease families. Activation of caspase-12 by calpain in apoptosis. *Journal Of Cell Biology*, 150 (4), pp.887-894.

Nassarre, P., Constantin, B., Rouhaud, L., Harnois, T., Raymond, G., Drabkin, H. A., Bourmeyster, N. and Roche, J. 2003. Semaphorin SEMA3F and VEGF have opposing effects on cell attachment and spreading. *Neoplasia*, 5 (1), pp.83-91.

Nechuta, S. J., Caan, B. J., Chen, W. Y., Lu, W., Chen, Z., Kwan, M. L., Flatt, S. W., Zheng, Y., Zheng, W., Pierce, J. P. and Shu, X. O. 2012. Soy food intake after diagnosis of breast cancer and survival: an in-depth analysis of combined evidence from cohort studies of US and Chinese women. *American Journal of Clinical Nutrition*, 96 (1), pp.123-132.

Neumar, R. W., Xu, Y. A., Guttmann, R. P. and Siman, R. 2003. Cross-talk between calpain and caspase proteolytic systems during neuronal apoptosis. *Journal Of Biological Chemistry*, 278 (16), pp.14162-14167.

NICE. 2006. *Trastuzumab for the adjuvant treatment of early-stage HER2-positive breast cancer: NICE technology appraisal guidance 107.* [online] London: NHS, National Institute for Health and Clinical Excellence (NICE). Available at: http://www.nice.org.uk/nicemedia/live/11586/33458/33458.pdf. [Accessed September 11, 2012].

NICE. 2009a. *Advanved breast cancer: NICE Clinical Guideline 81*. [online] London: NHS, National Institute for Health and Clinical Excellence (NICE). Available from: http://guidance.nice.org.uk/CG81. [Accessed September 11, 2012].

NICE (2009b). *Early and locally advanced breast cancer: NICE Clinical Guideline 80*. [online] London: NHS, National Institute for Health and Clinical Excellence (NICE). Available from: http://guidance.nice.org.uk/CG80. [Accessed September 11, 2012].

O'Lone, R., Knorr, K., Jaffe, I. Z., Schaffer, M. E., Martini, P. G. V., Karas, R. H., Bienkowska, J., Mendelsohn, M. E. and Hansen, U. 2007. Estrogen receptors alpha and beta mediate distinct pathways of vascular gene expression, including genes involved in mitochondrial electron transport and generation of reactive oxygen species. *Molecular Endocrinology*, 21 (6), pp.1281-1296.

Office for National Statistics (2012). *Cancer indicence and mortality in the UK, 2007 - 2009*. Office for National Statistics. London.

Ogawa, S., Inoue, S., Watanabe, T., Orimo, A., Hosoi, T., Ouchi, Y. and Muramatsu, M. 1998. Molecular cloning and characterization of human estrogen receptor betacx: a potential inhibitor ofestrogen action in human. *Nucleic Acids Research*, 26 (15), pp.3505-3512.

Ogden, D. 1994. *Microelectrode Techniques: The Plymouth Workshop Handbook*. 2 ed. Cambridge: The Company of Biologists Ltd.

Ogden, D. and Stanfield, P.1994. Patchclamp techniques for single channel and whole-cell recording. In: Ogden, D. ed. *Microelectrode Techniques: The Plymouth Workshop Handbook* 2 ed. Cambridge: The Company of Biologists Ltd, pp. 53-78.

Okumura, N., Imai, S., Toyoda, F., Isoya, E., Kumagai, K., Matsuura, H. and Matsusue, Y. 2009. Regulatory role of tyrosine phosphorylation in the swelling-activated chloride current in isolated rabbit articular chondrocytes. *Journal of Physiology*, 587 (Pt 15), pp.3761-3776.

Orrenius, S., Zhivotovsky, B. and Nicotera, P. 2003. Regulation of cell death: the calcium-apoptosiis link. *Nature Reviews*, 4 pp.552-565.

Ouadid-Ahidouch, H., Chaussade, F., Roudbaraki, M., Slomianny, C., Dewailly, E., Delcourt, P. and Prevarskaya, N. 2000. KV1.1 K(+) channels identification in human breast carcinoma cells: involvement in cell proliferation. *Biochemical And Biophysical Research Communications*, 278 (2), pp.272-277.

Ouadid-Ahidouch, H. and Ahidouch, A. 2008. K+ channel expression in human breast cancer cells: involvement in cell cycle regulation and carcinogenesis. *Journal Of Membrane Biology*, 221 (1), pp.1-6.

Ouadid-Ahidouch, H., Roudbaraki, M., Ahidouch, A., Delcourt, P. and Prevarskaya, N. 2004a. Cell-cycle-dependent expression of the large Ca2+-activated K+ channels in breast cancer cells. *Biochemical And Biophysical Research Communications*, 316 (1), pp.244-251.

Ouadid-Ahidouch, H., Roudbaraki, M., Delcourt, P., Ahidouch, A., Joury, N. and Prevarskaya, N. 2004b. Functional and molecular identification of intermediate-conductance Ca(2+)-activated K(+) channels in breast cancer cells: association with cell cycle progression. *American Journal Of Physiology: Cell Physiology*, 287 (1), p.C125-C134.

Pagliacci, M. C., Spinozzi, F., Migliorati, G., Fumi, G., Smacchia, M., Grignani, F., Riccardi, C. and Nicoletti, I. 1993. Genistein inhibits tumour cell growth in vitro but enhances mitochondrial reduction of tetrazolium salts: a further pitfall in the use of the MTT assay for evaluating cell growth and survival. *European Journal Of Cancer*, 29A (11), pp.1573-1577.

Palmieri, C., Cheng, G.J., Saji, S., Zelada-Hedman, M., Warri, A., Weihua, Z., Van Noorden, S., Wahlstrom. T., Coombes, R.C., Warner, M. and Gustafsson, J.A. 2002. Estrogen receptor beta in breast cancer. *Endocrine-Related Cancer*, 9, pp.1-13.

Pan, Z., Capo-Aponte, J. E., Zhang, F., Wang, Z., Pokorny, K. S. and Reinach, P. S. 2007. Differential dependence of regulatory volume decrease behavious in rabbit corneal epithelial cells on MAPK superfamily activation. *Experimental Eye Research*, 84 (5), pp.978-990.

Pardo, L. A., Contreras-Jurado, C., Zientkowska, M., Alves, F. and Stuhmer, W. 2005. Role of voltage-gated potassium channels in cancer. *Journal Of Membrane Biology*, 205 (3), pp.115-124.

Pardo, L. A. 2004. Voltage-gated potassium channels in cell proliferation. *Physiology*, 19 pp.285-292.

Park, S. Y., Wilkens, L. R., Franke, A. A., Le Marchand, L., Kakazu, K. K., Goodman, M. T., Murphy, S. P., Henderson, B. E. and Kolonel, L. N. 2009. Urinary phytoestrogen excretion and prostate cancer risk: a nested case-control study in the Multiethnic Cohort. *British Journal Of Cancer*, 101 (1), pp.185-191.

Park, S. Y., Murphy, S. P., Wilkens, L. R., Henderson, B. E. and Kolonel, L. N. 2008. Legume and isoflavone intake and prostate cancer risk: The Multiethnic Cohort Study. *International Journal Of Cancer*, 123 (4), pp.927-932.

Park, W. S., Firth, A. L., Han, J. and Ko, E. A. 2010. Patho-, physiological roles of voltage-dependent K+ channels in pulmonary arterial smooth muscle cells. *Journal Of Smooth Muscle Research*, 46 (2), pp.89-105.

Parkin D. M., Whelan S. L., Ferlay J., Teppo L., and Thomas D. B. (2002). *Cancer Incidence in Five Continents Vol. VIII*. International Agency for Research on Cancer (IARC). Lyon, France.

Parkin, D. M., Bray, F., Ferlay, J. and Pisani, P. 2005. Global cancer statistics, 2002. *CA Cancer Journal For Clinicians*, 55 (2), pp.74-108.

Paruthiyil, S., Parmar, H., Kerekatte, V., Cunha, G. R., Firestone, G. L. and Leitman, D. C. 2004. Estrogen receptor beta inhibits human breast cancer cell proliferation and tumor formation by causing a G2 cell cycle arrest. *Cancer Research*, 64 (1), pp.423-428.

Patel, A. J. and Honore, E. 2001. Properties and modulation of mammalian 2P domain K+ channels. *Trends in Neuroscience*, 24 (6), pp.339-346.

Perez, R., Melero, R., Balboa, M. A. and Balsinde, J. 2004. Role of group VIA calcium-independent phospholipase A2 in arachidonic acid release, phospholipid fatty acid incorporation, and apoptosis in U937 cells responding to hydrogen peroxide. *Journal Of Biological Chemistry*, 279 (39), pp.40385-40391.

Perez-Jimenez, J., Hubert, J., Hooper, L., Cassidy, A., Manach, C., Williamson, G. and Scalbert, A. 2010. Urinary metabolites as biomarkers of polyphenol intake in humans: a systematic review. *American Journal of Clinical Nutrition*, 92 (4), pp.801-809.

Perillo, B., Sasso, A., Abbondanza, C. and Palumbo, G. 2000. 17beta-estradiol inhibits apoptosis in MCF-7 cells, inducing bcl-2 expression via two estrogen-responsive elements present in the coding sequence. *Molecular And Cellular Biology*, 20 (8), pp.2890-2901.

Peterson, G. 1995. Evaluation of the biochemical targets of genistein in tumor cells. *Journal Of Nutrition*, 125 (3 Suppl), pp.784S-789s.

Peterson, G. and Barnes, S. 1996. Genistein inhibits both estrogen and growth factor-stimulated proliferation of human breast cancer cells. *Cell Growth & Differentiation*, 7 (10), pp.1345-1351.

Peterson, T. G., Ji, G. P., Kirk, M., Coward, L., Falany, C. N. and Barnes, S. 1998. Metabolism of the isoflavones genistein and biochanin A in human breast cancer cell lines. *American Journal of Clinical Nutrition*, 68 (6 Suppl), pp.1505S-1511s.

Piller, R., Chang-Claude, J. and Linseisen, J. 2006. Plasma enterolactone and genistein and the risk of premenopausal breast cancer. *European Journal Of Cancer Prevention: The Official Journal Of The European Cancer Prevention Organisation (ECP)*, 15 (3), pp.225-232.

Pillozzi, S., Brizzi, M. F., Balzi, M., Crociani, O., Cherubini, A., Guasti, L., Bartolozzi, B., Becchetti, A., Wanke, E., Bernabei, P. A., Olivotto, M., Pegoraro, L. and Arcangeli, A. 2002. HERG potassium channels are constitutively expressed in primary human acute myeloid leukemias and regulate cell proliferation of normal and leukemic hemopoietic progenitors. *Leukemia*, 16 (9), pp.1791-1798.

Platet, N., Cathiard, A. M., Gleizes, M. and Garcia, M. 2004. Estrogens and their receptors in breast cancer progression: a dual role in cancer proliferation and invasion. *Critical Reviews In Oncology/Hematology*, 51 (1), pp.55-67.

Plumb, J. A., Milroy, R. and Kaye, S. B. 1989. Effects of the pH dependence of 3-(4,5-dimethylthiazol-2-yl)-2,5-diphenyl-tetrazolium bromide-formazan absorption on chemosensitivity determined by a novel tetrazolium-based assay. *Cancer Research*, 49 (16), pp.4435-4440.

Pollak, M. 2001. How do anti-oestrogens work? In: Tobias, J. S., J. Houghton and I. C. Henderson eds. *Breast Cancer: New Horizons in Research and Treatment*. London: Arnold, pp. 72-80.

Popkin, B. M. and Du, S. 2003. Dynamics of the nutrition transition toward the animal foods sector in China and its implications: a worried perspective. *Journal Of Nutrition*, 133 (11 Suppl 2), pp.3898S-3906S.

Pugazhendhi, D., Watson, K. A., Mills, S., Botting, N., Pope, G. S. and Darbre, P. D. 2008. Effect of sulphation on the oestrogen agonist activity of the phytoestrogens genistein and daidzein in MCF-7 human breast cancer cells. *Journal Of Endocrinology*, 197 (3), pp.503-515.

Qu, X., Zou, Z., Sun, Q., Luby-Phelps, K., Cheng, P., Hogan, R. N., Gilpin, C. and Levine, B. 2007. Autophagy gene-dependent clearance of apoptotic cells during embryonic development. *Cell*, 128 (5), pp.931-946.

Rae, J. M., Creighton, C. J., Meck, J. M., Haddad, B. R. and Johnson, M. D. 2007. MDA-MB-435 cells are derived from M14 melanoma cells--a loss for breast cancer, but a boon for melanoma research. *Breast Cancer Research And Treatment*, 104 (1), pp.13-19.

Rajah, T. T., Du, N., Drews, N. and Cohn, R. 2009. Genistein in the presence of 17beta-estradiol inhibits proliferation of ERbeta breast cancer cells. *Pharmacology*, 84 (2), pp.68-73.

Reddy, M. and Given-Wilson, R. 2006. Screening for breast cancer. *Women's Health Medicine*, 3 (1), pp.22-27.

Ren, Z., Zou, C., Ji, H. and Zhang, Y. A. 2010. Oestrogen regulates proliferation and differentiation of human islet-derived precursor cells through oestrogen receptor alpha. *Cell Biology International*, 34 (5), pp.523-530.

Renehan, A. G., Zwahlen, M., Minder, C., O'Dwyer, S. T., Shalet, S. M. and Egger, M. 2004. Insulin-like growth factor (IGF)-I, IGF binding protein-3, and cancer risk: systematic review and meta-regression analysis. *Lancet*, 363 (9418), pp.1346-1353.

Riccardi, C. and Nicoletti, I. 2006. Analysis of apoptosis by propidium iodide staining and flow cytometry. *Nature Protocols*, 1 pp.1458-1461.

Riedle, F. and Scott, F. L. 2009. Caspases: activation, regulation and function. In: Xiao-Ming Yin, Zheng Dong eds. *Essentials of Apoptisis: A Guide for Basic and Clinical Research*. 2 ed. New York: Humana Press, pp. 3-24.

Rock, C. L., Flatt, S. W., Laughlin, G. A., Gold, E. B., Thomson, C. A., Natarajan, L., Jones, L. A., Caan, B. J., Stefanick, M. L., Hajek, R. A., Al-Delaimy, W. K. and Stanczyk, F. Z.. 2008. Reproductive Steroid Hormones and Recurrence-Free Survival in Women with a History of Breast Cancer. *Cancer Epidemiology, Biomarkers & Prevention*, 17 (3), pp.614-620.

Rodriguez-Mora, O. G., LaHair, M. M., McCubrey, J. A. and Franklin, R. A. 2005. Calcium/calmodulin-dependent kinase I and calcium/calmodulin-dependent kinase kinase participate in the control of cell cycle progression in MCF-7 human breast cancer cells. *Cancer Research*, 65 (12), pp.5408-5416.

Rody, A., Holtrich, U., Solbach, C., Kourtis, K., von Minckwitz, G., Engels, K., Kissler, S., Gatje, R., Karn, T. and Kaufmann, M. 2005. Methylation of estrogen receptor beta promoter correlates with loss of ER-beta expression in mammary carcinoma and is an early indication marker in premalignant lesions. *Endocrine-Related Cancer*, 12 (4), pp.903-916.

Roger, S., Potier, M., Vandier, C., Le Guennec, J. Y. and Besson, P. 2004. Description and role in proliferation of iberiotoxin-sensitive currents in different human mammary epithelial normal and cancerous cells. *Biochimica Et Biophysica Acta*, 1667 (2), pp.190-199.

Rowell, C., Carpenter, D. M. and Lamartiniere, C. A. 2005. Chemoprevention of breast cancer, proteomic discovery of genistein action in the rat mammary gland. *Journal Of Nutrition*, 135 (12 Suppl), pp.2953S-2959S.

Roy, J., Vantol, B., Cowley, E. A., Blay, J. and Linsdell, P. 2008. Pharmacological separation of hEAG and hERG K+ channel function in the human mammary carcinoma cell line MCF-7. *Oncology Reports*, 19 (6), pp.1511-1516.

Roy, S. S. and Hajnoczky, G. 2008. Calcium, mitochondria and apoptosis studied by fluorescence measurements. *Methods*, 46 (3), pp.213-223.

Rubin, M. R., Schussheim, D. H., Kulak, C. A. M., Kurland, E. S., Rosen, C. J., Bilezikian, J. P. and Shane, E. 2005. Idiopathic osteoporosis in premenopausal women. *Osteoporosis International*, 16 (5), pp.526-533.

Rybarczyk, B.J. and Simpson-Haidaris, P.J. 2000 Fibrinogen assembly, secretion and deposition into extracellular matric by MCF-7 human breast carcinoma cells. *Cancer Research*, 60, pp.2033-2039.

Sakamoto, T., Horiguchi, H., Oguma, E. and Kayama, F. 2010. Effects of diverse dietary phytoestrogens on cell growth, cell cycle and apoptosis in estrogen-receptor-positive breast cancer cells. *Journal of Nutritional Biochemistry*, 21 pp.856-864.

Salata, J. J., Jurkiewicz, N. K., Wallace, A. A., Stupienski, R. F., III, Guinosso, P. J., Jr. and Lynch, J. J., Jr. 1995. Cardiac electrophysiological actions of the histamine H1-receptor antagonists astemizole and terfenadine compared with chlorpheniramine and pyrilamine. *Circulation Research*, 76 (1), pp.110-119.

Salvi, M., Brunati, A. M., Clari, G. and Toninello, A. 2002. Interaction of genistein with the mitochondrial electron transport chain results in opening of the membrane transition pore. *Biochimica Et Biophysica Acta*, 1556 (2-3), pp.187-196.

Sanguinetti, M. C. and Tristani-Firouzi, M. 2006. hERG potassium channels and cardiac arrhythmia. *Nature*, 440 (7083), pp.463-469.

Sartippour, M. R., Rao, J. Y., Apple, S., Wu, D., Henning, S., Wang, H., Elashoff, R., Rubio, R., Heber, D. and Brooks, M. N. 2004. A pilot clinical study of short-term isoflavone supplements in breast cancer patients. *Nutrition & Cancer*, 49 (1), pp.59-65.

Sarwar, N., Kim, J. S., Jiang, J., Peston, D., Sinnett, H. D., Madden, P., Gee, J. M., Nicholson, R. I., Lykkesfeldt, A. E., Shousha, S., Coombes, R. C. and Ali, S. 2006. Phosphorylation of ERalpha at serine 118 in primary breast cancer and in tamoxifen-resistant tumours is indicative of a complex role for ERalpha phosphorylation in breast cancer progression. *Endocrine-Related Cancer*, 13 (3), pp.851-861.

Saunders, P.T.K., Millar, M.R., Williams, K., Macpherson, S., Bayne, C., O'Sullivan, C., Anderson, T.J., Groome, N.P. and Miller, W.R. 2002. Expression of oestrogen receptor beta (ERbeta1) protein in human breast cancer biopsies. *British Journal of Cancer*, 86 (2), pp.250-256.

Schmidt, S., Michna, H. and Diel, P. 2005. Combinatory effects of phytoestrogens and 17beta-estradiol on proliferation and apoptosis in MCF-7 breast cancer cells. *Journal Of Steroid Biochemistry And Molecular Biology*, 94 (5), pp.445-449.

Schwarz, J. R. and Bauer, C. K. 2004. Functions of erg K+ channels in excitable cells. *Journal Of Cellular And Molecular Medicine*, 8 (1), pp.22-30.

Schyver, T. and Smith, C. 2005. Reported Attitudes and Beliefs toward Soy Food Consumption of Soy Consumers versus Nonconsumers in Natural Foods or Mainstream Grocery Stores. *Journal of Nutrition Education & Behavior*, 37 (6), pp.292-299.

Seino, S. and Miki, T. 2003. Physiological and pathophysiological roles of ATP-sensitive K+ channels. *Progress In Biophysics And Molecular Biology*, 81 (2), pp.133-176.

Seo, H. S., DeNardo, D. G., Jacquot, Y., Lanos, I., Vidal, D. S., Zambrana, C. R., Leclercq, G. and Brown, P. H. 2006. Stimulatory effect of genistein and apigenin on the growth of breast cancer cells correlates with their ability to activate ER alpha. *Breast Cancer Research And Treatment*, 99 (2), pp.121-134.

Seo, H. S., Ju, J. H., Jang, K. and Shin, I. 2011. Induction of apoptotic cell death by phytoestrogens by up-regulating the levels of phospho-p53 and p21 in normal and malignant estrogen receptor α-negative breast cells. *Nutrition Research*, 31 (2), pp.139-146.

Sergeev, I. N. 2004. Genistein induces Ca2+ -mediated, calpain/caspase-12-dependent apoptosis in breast cancer cells. *Biochemical And Biophysical Research Communications*, 321 (2), pp.462-467.

Setchell, K. D. 1998. Phytoestrogens: the biochemistry, physiology, and implications for human health of soy isoflavones. *American Journal of Clinical Nutrition*, 68 (6 Suppl), pp.1333S-1346s.

Setchell, K. D., Zimmer-Nechemias, L., Cai, J. and Heubi, J. E. 1997. Exposure of infants to phyto-oestrogens from soy-based infant formula. *Lancet*, 350 (9070), pp.23-27.

Setchell, K. D. R., Brown, N. M. and Lydeking-Olsen, E. 2002. The clinical importance of the metabolite equol-a clue to the effectiveness of soy and its isoflavones. *Journal Of Nutrition*, 132 (12), pp.3577-3584.

Setchell, K. D. R., Brown, N. M., Zhao, X., Lindley, S. L., Heubi, J. E., King, E. C. and Messina, M. J. 2011. Soy isoflavone phase II metabolism differs between rodents and humans: implications for the effect on breast cancer risk. *The American Journal Of Clinical Nutrition*, 94 (5), pp.1284-1294.

Setchell, K. D. R. and Cole, S. J. 2003. Variations in isoflavone levels in soy foods and soy protein isolates and issues related to isoflavone databases and food labeling. *Journal Of Agricultural And Food Chemistry*, 51 (14), pp.4146-4155.

Shim, H. Y., Park, J. H., Paik, H. D., Nah, S. Y., Kim, D. S. H. L. and Han, Y. S. 2007. Genistein-induced apoptosis of human breast cancer MCF-7 cells involves calpain-caspase and apoptosis signaling kinase 1-p38 mitogen-activated protein kinase activation cascades. *Anti-Cancer Drugs*, 18 (6), pp.649-657.

Shon, Y. H., Park, S. D. and Nam, K. S. 2006. Effective chemopreventive activity of genistein against human breast cancer cells. *Journal Of Biochemistry And Molecular Biology*, 39 (4), pp.448-451.

Shu, X. O., Jin, F., Dai, Q., Wen, W., Potter, J. D., Kushi, L. H., Ruan, Z., Gao, Y. T. and Zheng, W. 2001. Soyfood intake during adolescence and subsequent risk of breast cancer among Chinese women. *Cancer Epidemiology, Biomarkers & Prevention*, 10 (5), pp.483-488.

Shu, X. O., Zheng, Y., Cai, H., Gu, K., Chen, Z., Zheng, W. and Lu, W. 2009. Soy food intake and breast cancer survival. *Journal Of The American Medical Association*, 302 (22), pp.2437-2443.

Simoes-Wust, A. P., Schurpf, T., Hall, J., Stahel, R. A. and Zangemeister-Wittke, U. 2002. Bcl-2/bcl-xL bispecific antisense treatment sensitizes breast carcinoma cells to doxorubicin, paclitaxel and cyclophosphamide. *Breast Cancer Research And Treatment*, 76 (2), pp.157-166.

Singh, B., Mense, S. M., Bhat, N. K., Putty, S., Guthiel, W. A., Remotti, F. and Bhat, H. K. 2010. Dietary quercetin exacerbates the development of estrogen-induced breast tumors in female ACI rats. *Toxicology And Applied Pharmacology*, 247 (2), pp.83-90.

Singletary, K. W., Frey, R. S. and Yan, W. 2001. Effect of ethanol on proliferation and estrogen receptor-alpha expression in human breast cancer cells. *Cancer Letters*, 165 (2), pp.131-137.

Skliris, G. P., Leygue, E., Watson, P. H. and Murphy, L. C. 2008. Estrogen receptor alpha negative breast cancer patients: estrogen receptor beta as a therapeutic target. *Journal Of Steroid Biochemistry And Molecular Biology*, 109 (1-2), pp.1-10.

Smith, I. and Chua, S. 2006a. Medical treatment of early breast cancer. I: adjuvant treatment. *BMJ (Clinical Research Ed)*, 332 (7532), pp.34-37.

Smith, I. and Chua, S. 2006b. Medical treatment of early breast cancer. IV: neoadjuvant treatment. *BMJ (Clinical Research Ed)*, 332 (7535), pp.223-224.

So, F. V., Guthrie, N., Chambers, A. F. and Carroll, K. K. 1997. Inhibition of proliferation of estrogen receptor-positive MCF-7 human breast cancer cells by flavonoids in the presence and absence of excess estrogen. *Cancer Letters*, 112 pp.127-133.

Sohn, S. J., Lewis, G. M. and Winoto, A. 2008. Non-redundant function of the MEK5-ERK5 pathway in thymocyte apoptosis. *EMBO Journal*, 27 (13), pp.1896-1906.

Song, R. X. D., Zhang, Z., Chen, Y., Bao, Y. and Santen, R. J. 2007. Estrogen signaling via a linear pathway involving insulin-like growth factor I receptor, matrix metalloproteinases, and epidermal growth factor receptor to activate mitogen-activated protein kinase in MCF-7 breast cancer cells. *Endocrinology*, 148 (8), pp.4091-4101.

Sontheimer, H. and Olsen, M. L. 2007. Whole Cell Patch Clamp Recordings. In: Walz, W. ed. *Patch Clamp Analysis*. 2 ed. New York: Humana Press, pp. 35-68.

Sotoca, A. M., Ratman, D., van der Saag, P., Strom, A., Gustafsson, J. A., Vervoort, J., Rietjens, I. M. C. M. and Murk, A. J. 2008. Phytoestrogen-mediated inhibition of proliferation of the human T47D breast cancer cells depends on the ERalpha/ERbeta ratio. *Journal Of Steroid Biochemistry And Molecular Biology*, 112 (4-5), pp.171-178.

Speirs, V., Parkes, A. T., Kerin, M. J., Walton, D. S., Carleton, P. J., Fox, J. N. and Atkin, S. L. 1999. Coexpression of estrogen receptor alpha and beta: poor prognostic factors in human breast cancer? *Cancer Research*, 59 (3), pp.525-528.

Speirs, V. 2008. The evolving role of oestrogen receptor beta in clinical breast cancer. *Breast Cancer Research*, 10 (5), p.111.

Standen, N. B., Davies, N. W. and Langton, P. D.1994. Separation and analysis of macroscopic currents. In: Ogden, D. ed. *Microelectrode Techniques*. 2 ed. Cambridge: The Company of Biologists Ltd, pp. 37-52.

Steiner, C., Arnould, S., Scalbert, A. and Manach, C. 2008. Isoflavones and the prevention of breast and prostate cancer: new perspectives opened by nutrigenomics. *British Journal Of Nutrition*, 99 E Suppl 1 p.ES78-ES108.

Stephan, D., Winkler, M., Kuhner, P., Russ, U. and Quast, U. 2006. Selectivity of repaglinide and glibenclamide for the pancreatic over the cardiovascular K(ATP) channels. *Diabetologia*, 49 (9), pp.2039-2048.

Storey, N. M., Gomez-Angelats, M., Bortner, C. D., Armstrong, D. L. and Cidlowski, J. A. 2003. Stimulation of Kv1.3 potassium channels by death receptors during apoptosis in Jurkat T lymphocytes. *Journal Of Biological Chemistry*, 278 (35), pp.33319-33326.

Stringer, B. K., Cooper, A. G. and Shepard, S. B. 2001. Overexpression of the G-protein inwardly rectifying potassium channel 1 (GIRK1) in primary breast carcinomas correlates with axillary lymph node metastasis. *Cancer Research*, 61 (2), pp.582-588.

Strobl, J. S., Wonderlin, W. F. and Flynn, D. C. 1995. Mitogenic signal transduction in human breast cancer cells. *General Pharmacology*, 26 (8), pp.1643-1649.

Strom, A., Hartman, J., Foster, J. S., Kietz, S., Wimalasena, J. and Gustafsson, J. A. 2004. Estrogen receptor beta inhibits 17beta-estradiol-stimulated proliferation of the breast cancer cell line T47D. *Proceedings Of The National Academy Of Sciences Of The United States Of America*, 101 (6), pp.1566-1571.

Sun, X. H., Ding, J. P., Li, H., Pan, N., Gan, L., Yang, X. L. and Xu, H. B. 2007. Activation of large-conductance calcium-activated potassium channels by puerarin: the underlying mechanism of puerarin-mediated vasodilation. *Journal Of Pharmacology And Experimental Therapeutics*, 323 (1), pp.391-397.

Sundelacruz, S., Levin, M. and Kaplan, D.L. 2009. Role of membrane potential in the regulation of cell proliefration and differentiation. *Stem cell Reviews and Reports*, 5, pp.231-246.

Suzuki, K., Koike, H., Matsui, H., Ono, Y., Hasumi, M., Nakazato, H., Okugi, H., Sekine, Y., Oki, K., Ito, K., Yamamoto, T., Fukabori, Y., Kurokawa, K. and Yamanaka, H. 2002. Genistein, a soy isoflavone, induces glutathione peroxidase in the human prostate cancer cell lines LNCaP and PC-3. *International Journal Of Cancer*, 99 (6), pp.846-852.

Suzuki, T., Matsuo, K., Tsunoda, N., Hirose, K., Hiraki, A., Kawase, T., Yamashita, T., Iwata, H., Tanaka, H. and Tajima, K. 2008. Effect of soybean on breast cancer according to receptor status: a case-control study in Japan. *International Journal Of Cancer*, 123 (7), pp.1674-1680.

Szabo, I., Bock, J., Grassme, H., Soddemann, M., Wilker, B., Lang, F., Zoratti, M. and Gulbins, E. 2008. Mitochondrial potassium channel Kv1.3 mediates Bax-induced apoptosis in lymphocytes. *Proceedings Of The National Academy Of Sciences Of The United States Of America*, 105 (39), pp.14861-14866.

Taku, K., Umegaki, K., Sato, Y., Taki, Y., Endoh, K. and Watanabe, S. 2007. Soy isoflavones lower serum total and LDL cholesterol in humans: a meta-analysis of 11 randomized controlled trials. *American Journal of Clinical Nutrition*, 85 (4), pp.1148-1156.

Taku, K., Melby, M. K., Kurzer, M. S., Mizuno, S., Watanabe, S. and Ishimi, Y. 2010. Effects of soy isoflavone supplements on bone turnover markers in menopausal women: systematic review and meta-analysis of randomized controlled trials. *Bone*, 47 (2), pp.413-423.

Tanos, V., Brzezinski, A., Drize, O., Strauss, N. and Peretz, T. 2002. Synergistic inhibitory effects of genistein and tamoxifen on human dysplastic and malignant epithelial breast cells in vitro. *European Journal Of Obstetrics, Gynecology, And Reproductive Biology*, 102 (2), pp.188-194.

Taylor, A. H. and Al-Azzawi, F. 2000. Immunolocalisation of oestrogen receptor beta in human tissues. *Journal Of Molecular Endocrinology*, 24 (1), pp.145-155.

Teisseyre, A. and Michalak, K. 2005. Genistein inhibits the activity of kv1.3 potassium channels in human T lymphocytes. *Journal Of Membrane Biology*, 205 (2), pp.71-79.

Teisseyre, A. and Michalak, K. 2006. Inhibition of the activity of human lymphocyte Kv1.3 potassium channels by resveratrol. *Journal Of Membrane Biology*, 214 (3), pp.123-129.

Thanos, J., Cotterchio, M., Boucher, B. A., Kreiger, N. and Thompson, L. U. 2006. Adolescent dietary phytoestrogen intake and breast cancer risk (Canada). *Cancer Causes & Control*, 17 (10), pp.1253-1261.

Theil, C., Briese, V., Gerber, B. and Richter, D. U. 2011. The effects of different lignans and isoflavones, tested as aglycones and glycosides, on hormone receptor-positive and -negative breast carcinoma cells in vitro. *Archives Of Gynecology And Obstetrics*, 284 (2), pp.459-465.

Tice, J. A., Ettinger, B., Ensrud, K., Wallace, R., Blackwell, T. and Cummings, S. R. 2003. Phytoestrogen supplements for the treatment of hot flashes: the Isoflavone Clover Extract (ICE) Study: a randomized controlled trial. *Journal Of The American Medical Association*, 290 (2), pp.207-214.

Tong, D., Schuster, E., Seifert, M., Czerwenka, K., Leodolte, S. and Zeillinger, R. 2002. Expression of estrogen receptor beta isoforms in human breast cancer tissues and cell lines. *Breast Cancer Research And Treatment*, 71 (3), pp.249-255.

Travis, R. C., Allen, N. E., Appleby, P. N., Spencer, E. A., Roddam, A. W. and Key, T. J. 2008. A prospective study of vegetarianism and isoflavone intake in relation to breast cancer risk in British women. *International Journal Of Cancer*, 122 (3), pp.705-710.

Trock, B. J., Hilakivi-Clarke, L. and Clarke, R. 2006. Meta-analysis of soy intake and breast cancer risk. *Journal Of The National Cancer Institute*, 98 (7), pp.459-471.

Twentyman, P. R. and Luscombe, M. 1987. A study of some variables in a tetrazolium dye (MTT) based assay for cell growth and chemosensitivity. *British Journal Of Cancer*, 56 pp.279-285.

Ueda, M., Niho, N., Imai, T., Shibutani, M., Mitsumori, K., Matsui, T. and Hirose, M. 2003. Lack of significant effects of genistein on the progression of 7,12-dimethylbenz(a)anthracene-induced mammary tumors in ovariectomized Sprague-Dawley rats. *Nutrition And Cancer*, 47 (2), pp.141-147.

Ulukaya, E., Ozdikicioglu, F., Oral, A. Y. and Demirci, M. 2008. The MTT assay yields a relatively lower result of growth inhibition than the ATP assay depending on the chemotherapeutic drugs tested. *Toxicology In Vitro*, 22 (1), pp.232-239.

Umehara, K., Nemoto, K., Matsushita, A., Terada, E., Monthakantirat, O., De-Eknamkul, W., Miyase, T., Warashina, T., Degawa, M. and Noguchi, H. 2009. Flavonoids from the heartwood of the Thai medicinal plant Dalbergia parviflora and their effects on estrogenic-responsive human breast cancer cells. *Journal Of Natural Products*, 72 (12), pp.2163-2168.

Van Coppenolle, F., Skryma, R., Ouadid-Ahidouch, H., Slomianny, C., Roudbaraki, M., Delcourt, P., Dewailly, E., Humez, S., Crepin, A., Gourdou, I., Djaine, J., Bonnal, J.-L., Mauroy, B. and Prevarskaya, N. 2004. Prolactin stimulates cell proliferation through a long form of prolactin receptor and K+ channel activation. *Biochemical Journal*, 337 pp.569-578.

Van Patten, C. L., Olivotto, I. A., Chambers, G. K., Gelmon, K. A., Hislop, T. G., Templeton, E., Wattie, A. and Prior, J. C. 2002. Effect of soy phytoestrogens on hot flashes in postmenopausal women with breast cancer: a randomized, controlled clinical trial. *Journal of Clinical Oncology*, 20 (6), pp.1449-1455.

Vandhana, S., Deepa, P. R., Aparna, G., Jayanthi, U. and Krishnakumar, S. 2010. Evaluation of suitable solvents for testing the anti-proliferative activity of triclosan - a hydrophobic drug in cell culture. *Indian Journal Of Biochemistry & Biophysics*, 47 (3), pp.166-171.

Vanoye, C. G., Welch, R. C., Tian, C., Sanders, C. R. and George, A. L., Jr. 2010. KCNQ1/KCNE1 assembly, co-translation not required. *Channels*, 4 (2), pp.108-114.

vanTol, B. L., Missan, S., Crack, J., Moser, S., Baldridge, W. H., Linsdell, P. and Cowley, E. A. 2007. Contribution of KCNQ1 to the regulatory volume decrease in the human mammary epithelial cell line MCF-7. *American Journal Of Physiology Cell Physiology*, 293 (3), p.C1010-C1019.

Vega-Lopez, S., Yeum, K. J., Lecker, J. L., Ausman, L. M., Johnson, E. J., Devaraj, S., Jialal, I. and Lichtenstein, A. H. 2005. Plasma antioxidant capacity in response to diets high in soy or animal protein with or without isoflavones. *American Journal of Clinical Nutrition*, 81 (1), pp.43-49.

Vellonen, K. S., Honkakoski, P. and Urtti, A. 2004. Substrates and inhibitors of efflux proteins interfere with the MTT assay in cells and may lead to underestimation of drug toxicity. *European Journal Of Pharmaceutical Sciences*, 23 (2), pp.181-188.

Verheus, M., van Gils, C. H., Keinan-Boker, L., Grace, P. B., Bingham, S. A. and Peeters, P. H. M. 2007. Plasma phytoestrogens and subsequent breast cancer risk. *Journal of Clinical Oncology*, 25 (6), pp.648-655.

Verkasalo, P. K., Appleby, P. N., Allen, N. E., Davey, G., Adlercreutz, H. and Key, T. J. 2001. Soya intake and plasma concentrations of daidzein and genistein: validity of dietary assessment among eighty British women (Oxford arm of the European Prospective Investigation into Cancer and Nutrition). *British Journal Of Nutrition*, 86 (3), pp.415-421.

Verkman, A.S. 2000. Water permeability measurement in living cells and complex tissues. *Journal of Membrane Biology*, 173, pp.73-87.

Vu, C. C., Bortner, C. D. and Cidlowski, J. A. 2001. Differential involvement of initiator caspases in apoptotic volume decrease and potassium efflux during Fas- and UV-induced cell death. *Journal Of Biological Chemistry*, 276 (40), pp.37602-37611.

Wagner, B. A., Britigan, B. E., Reszka, K. J., McCormick, M. L. and Burns, C. P. 2002. Hydrogen peroxide-induced apoptosis of HL-60 human leukemia cells is mediated by the oxidants hypochlorous acid and chloramines. *Archives Of Biochemistry And Biophysics*, 401 (2), pp.223-234.

Wang, C. and Kurzer, M. S. 1998. Effects of phytoestrogens on DNA synthesis in MCF-7 cells in the presence of estradiol or growth factors. *Nutrition And Cancer*, 31 (2), pp.90-100.

Wang, H., Zhang, Y., Cao, L., Han, H., Wang, J., Yang, B., Nattel, S. and Wang, Z. 2002. HERG K+ channel, a regulator of tumor cell apoptosis and proliferation. *Cancer Research*, 62 (17), pp.4843-4848.

Wang, J., Betancourt, A. M., Mobley, J. A. and Lamartiniere, C. A. 2011. Proteomic discovery of genistein action in the rat mammary gland. *Journal Of Proteome Research*, 10 (4), pp.1621-1631.

Wang, L., Yin, F., Du, Y., Chen, B., Liang, S., Zhang, Y., Du, W., Wu, K., Ding, J. and Fan, D. 2010. Depression of MAD2 inhibits apoptosis and increases proliferation and multidrug resistance in gastric cancer cells by regulating the activation of phosphorylated survivin. *Tumour Biology*, 31 (3), pp.225-232.

Wang, Z. 2004. Roles of K+ channels in regulating tumour cell proliferation and apoptosis. *European Journal Of Physiology*, 448 (3), pp.274-286.

Ward, H. A., Kuhnle, G. G. C., Mulligan, A. A., Lentjes, M. A. H., Luben, R. N. and Khaw, K. T. 2010. Breast, colorectal, and prostate cancer risk in the European Prospective Investigation into Cancer and Nutrition-Norfolk in relation to phytoestrogen intake derived from an improved database. *American Journal of Clinical Nutrition*, 91 (2), pp.440-448.

Weber, C., Mello de Queiroz, F., Downie, B. R., Suckow, A., Stuhmer, W. and Pardo, L. A. 2006. Silencing the activity and proliferative properties of the human EagI Potassium Channel by RNA Interference. *Journal Of Biological Chemistry*, 281 (19), pp.13030-13037.

Wei, A. D., Gutman, G. A., Aldrich, R., Chandy, K. G., Grissmer, S. and Wulff, H. 2005. International Union of Pharmacology. LII. Nomenclature and molecular relationships of calcium-activated potassium channels. *Pharmacological Reviews*, 57 (4), pp.463-472.

Weinstein, D., Simon, M., Yehezkel, E., Laron, Z. and Werner, H. 2009. Insulin analogues display IGF-I-like mitogenic and anti-apoptotic activities in cultured cancer cells. *Diabetes/Metabolism Research And Reviews*, 25 (1), pp.41-49.

Wen-Xing, D. and Xiao-Ming, Y.2009. The Bcl-2 family proteins. In: Xiao-Ming Yin, Zheng Dong eds. *Essentials of Apoptisis: A Guide for Basic and Clinical Research*. 2 ed. New York: Humana Press, pp. 25-62.

Westlake S. and Cooper N. (2008). *Cancer Incidence and Mortality: Trends in the United Kingdom and Constituent Countries, 1993-2004. (In: Office for National Statistics. Health Statistics Quarterly: no. 38.)*. Palgrave Macmillan. Basingstoke.

WHO. 2012. *ICD-10: Version 2010*. [online] World Health Organisation (WHO). Available from: http://www.who.int/classifications/icd/en/. [Accessed September 11, 2012].

Wiebe, J. P., Beausoleil, M., Zhang, G. and Cialacu, V. 2010. Opposing actions of the progesterone metabolites, 5alpha-dihydroprogesterone (5alphaP) and 3alpha-dihydroprogesterone (3alphaHP) on mitosis, apoptosis, and expression of Bcl-2, Bax and p21 in human breast cell lines. *Journal Of Steroid Biochemistry And Molecular Biology*, 118 (1-2), pp.125-132.

Wiseman, H., O'Reilly, J. D., Adlercreutz, H., Mallet, A. I., Bowey, E. A., Rowland, I. R. and Sanders, T. A. 2000. Isoflavone phytoestrogens consumed in soy decrease F(2)-isoprostane concentrations and increase resistance of low-density lipoprotein to oxidation in humans. *American Journal of Clinical Nutrition*, 72 (2), pp.395-400.

Wolff, C., Fuks, B. and Chatelain, P. 2003. Comparative study of membrane potential-sensitive fluorescent probes and their use in ion channel screening assays. *Journal Of Biomolecular Screening*, 8 (5), pp.533-543.

Wonderlin, W. F. and Strobl, J. S. 1996. Potassium channels, proliferation and G1 progression. *Journal Of Membrane Biology*, 154 (2), pp.91-107.

Wong, N. A. C. S., Malcomson, R. D. G., Jodrell, D. I., Groome, N. P., Harrison, D. J. and Saunders, P. T. K. 2005. ERbeta isoform expression in colorectal carcinoma: an in vivo and in vitro study of clinicopathological and molecular correlates. *Journal Of Pathology*, 207 (1), pp.53-60.

Woo, H. D., Park, K. S., Ro, J. and Kim, J. 2012. Differential influence of dietary soy intake on the risk of breast cancer recurrence related to HER2 status. *Nutrition And Cancer*, 64 (2), pp.198-205.

World Cancer Research Fund / American Institute for Cancer (2007). *Food, nutrition, physical activity, and the prevention of cancer: a global perspective*. AICR. Washington DC.

Wu, A. H., Yu, M. C., Tseng, C. C. and Pike, M. C. 2008. Epidemiology of soy exposures and breast cancer risk. *British Journal Of Cancer*, 98 (1), pp.9-14.

Wu, A. H., Wan, P., Hankin, J., Tseng, C. C., Yu, M. C. and Pike, M. C. 2002. Adolescent and adult soy intake and risk of breast cancer in Asian-Americans. *Carcinogenesis*, 23 (9), pp.1491-1496.

Wu, A. H., Yu, M. C., Tseng, C. C., Twaddle, N. C. and Doerge, D. R. 2004. Plasma isoflavone levels versus self-reported soy isoflavone levels in Asian-American women in Los Angeles County. *Carcinogenesis*, 25 (1), pp.77-81.

Wu, W. K. K., Li, G. R., Wong, H. P. S., Hui, M. K. C., Tai, E. K. K., Lam, E. K. Y., Shin, V. Y., Ye, Y. N., Li, P., Yang, Y. H., Luo, J. C. and Cho, C. H. 2006. Involvement of Kv1.1 and Nav1.5 in proliferation of gastric epithelial cells. *Journal Of Cellular Physiology*, 207 (2), pp.437-444.

Xu, X., Duncan, A. M., Wangen, K. E. and Kurzer, M. S. 2000. Soy consumption alters endogenous estrogen metabolism in postmenopausal women. *Cancer Epidemiology, Biomarkers & Prevention*, 9 (8), pp.781-786.

Xu, X., Harris, K. S., Wang, H. J., Murphy, P. A. and Hendrich, S. 1995. Bioavailability of soybean isoflavones depends upon gut microflora in women. *Journal Of Nutrition*, 125 (9), pp.2307-2315.

Xu, X., Wang, H. J., Murphy, P. A., Cook, L. and Hendrich, S. 1994. Daidzein is a more bioavailable soymilk isoflavone than is genistein in adult women. *Human & Clinical Nutrition*, 24 pp.825-832.

Yager, J. D. 2000. Chapter 3: Endogenous estrogens as carcinogens through metabolic activation. *Journal of the National Cancer Institute Monographs*, 27 pp.67-73.

Yamashita, H., Nishio, M., Toyama, T., Sugiura, H., Kondo, N., Kobayashi, S., Fujii, Y. and Iwase, H. 2008. Low phosphorylation of estrogen receptor alpha (ERalpha) serine 118 and high phosphorylation of ERalpha serine 167 improve survival in ER-positive breast cancer. *Endocrine-Related Cancer*, 15 (3), pp.755-763.

Yang, X., Yang, S., McKimmey, C., Liu, B., Edgerton, S. M., Bales, W., Archer, L. T. and Thor, A. D. 2010. Genistein induces enhanced growth promotion in ER-positive/erbB-2-overexpressing breast cancers by ER-erbB-2 cross talk and p27/kip1 downregulation. *Carcinogenesis*, 31 (4), pp.695-702.

Yao, X. and Kwan, H. Y. 1999. Activity of voltage-gated K+ channels is associated with cell proliferation and Ca2+ influx in carcinoma cells of colon cancer. *Life Sciences*, 65 (1), pp.55-62.

Ye, Y. B., Tang, X. Y., Verbruggen, M. A. and Su, Y. X. 2006. Soy isoflavones attenuate bone loss in early postmenopausal Chinese women : a single-blind randomized, placebo-controlled trial. *European Journal Of Nutrition*, 45 (6), pp.327-334.

Yellen, G. 2002. The voltage-gated potassium channels and their relatives. *Nature*, 419 (6902), pp.35-42.

Yigong, S. 2009. Structural biology of programmed cell death. In: Xiao-Ming Yin, Zheng Dong eds. *Essentials of Apoptisis: A Guide for Basic and Clinical Research*. 2 ed. New York: Humana Press, pp. 95-118.

Ying, C., Hsu, J. T., Hung, H. C., Lin, D. H., Chen, L. F. O. and Wang, L. K. 2002. Growth and cell cycle regulation by isoflavones in human breast carcinoma cells. *Reproduction, Nutrition, Development*, 42 (1), pp.55-64.

Yu, X., Zhu, J., Mi, M., Chen, W., Pan, Q. and Wei, M. 2012. Anti-angiogenic genistein inhibits VEGF-induced endothelial cell activation by decreasing PTK activity and MAPK activation. *Medical Oncology*, 29 (1), pp.349-357.

Yuan, B., Wang, L., Jin, Y., Zhen, H., Xu, P., Xu, H., Li, C. and Xu, H. 2012. Role of metabolism in the effects of genistein and its phase II conjugates on the growth of human breast cell lines. *Americal Association of Pharmaceutical Scientists Journal*, 14 (2), pp.329-344.

Zava, D. T. and Duwe, G. 1997. Estrogenic and antiproliferative properties of genistein and other flavonoids in human breast cancer cells in vitro. *Nutrition And Cancer*, 27 (1), pp.31-40.

Zeleniuch-Jacquotte, A., Adlercreutz, H., Akhmedkhanov, A. and Toniolo, P. 1998. Reliability of serum measurements of lignans and isoflavonoid phytoestrogens over a two-year period. *Cancer Epidemiology, Biomarkers & Prevention*, 7 (10), pp.885-889.

Zhan, S. and Ho, S. C. 2005. Meta-analysis of the effects of soy protein containing isoflavones on the lipid profile. *American Journal of Clinical Nutrition*, 81 (2), pp.397-408.

Zhang, D. Y., Wang, Y., Lau, C. P., Tse, H. F. and Li, G. R. 2008. Both EGFR kinase and Src-related tyrosine kinases regulate human ether-á-go-go-related gene potassium channels. *Cellular Signalling*, 20 (10), pp.1815-1821.

Zhang, Y., Song, T. T., Cunnick, J. E., Murphy, P. A. and Hendrich, S. 1999. Daidzein and genistein glucuronides in vitro are weakly estrogenic and activate human natural killer cells at nutritionally relevant concentrations. *Journal Of Nutrition*, 129 (2), pp.399-405.

Zhang, Y. F., Kang, H. B., Li, B. L. and Zhang, R. M. 2012. Positive effects of soy isoflavone food on survival of breast cancer patients in China. *Asian Pacific Journal Of Cancer Prevention*, 13 (2), pp.479-482.

Zhang, Z. H. and Wang, Q. 2000. Modulation of a cloned human A-type voltage-gated potassium channel (hKv1.4) by the protein tyrosine kinase inhibitor genistein. *Pflugers Archive*, 440 (5), pp.784-792.

Zhao, C., Dahlman-Wright, K. and Gustafsson, J. A. 2008. Estrogen receptor beta: an overview and update. *Nuclear Receptor Signaling*, 6 p.e003.

Zhao, C., Lam, E. W. F., Sunters, A., Enmark, E., De Bella, M. T., Coombes, R. C., Gustafsson, J. A. and Dahlman-Wright, K. 2003. Expression of estrogen receptor beta isoforms in normal breast epithelial cells and breast cancer: regulation by methylation. *Oncogene*, 22 (48), pp.7600-7606.

Zhao, C., Matthews, J., Tujague, M., Wan, J., Strom, A., Toresson, G., Lam, E. W. F., Cheng, G., Gustafsson, J. A. and Dahlman-Wright, K. 2007. Estrogen receptor beta2 negatively regulates the transactivation of estrogen receptor alpha in human breast cancer cells. *Cancer Research*, 67 (8), pp.3955-3962.

Zheng, X., Baker, H., Hancock, W. S., Fawaz, F., McCaman, M. and Pungor, E., Jr. 2006. Proteomic analysis for the assessment of different lots of fetal bovine serum as a raw material for cell culture. Part IV. Application of proteomics to the manufacture of biological drugs. *Biotechnology Progress*, 22 (5), pp.1294-1300.

Zhou, J. R., Yu, L., Mai, Z. and Blackburn, G. L. 2004. Combined inhibition of estrogen-dependent human breast carcinoma by soy and tea bioactive components in mice. *International Journal Of Cancer*, 108 (1), pp.8-14.

Zhou, Z., Gong, Q., Ye, B., Fan, Z., Makielski, J. C., Robertson, G. A. and January, C. T. 1998. Properties of HERG channels stably expressed in HEK 293 cells studied at physiological temperature. *Biophysical Journal*, 74 (1), pp.230-241.

Zhou, Z., Vorperian, V. R., Gong, Q., Zhang, S. and January, C. T. 1999. Block of HERG potassium channels by the antihistamine astemizole and its metabolites desmethylastemizole and norastemizole. *Journal Of Cardiovascular Electrophysiology*, 10 (6), pp.836-843.

Ziechner, U., Schonherr, R., Born, A. K., Gavrilova-Ruch, O., Glaser, R. W., Malesevic, M., Kullertz, G. and Heinemann, S. H. 2006. Inhibition of human ether a go-go potassium channels by Ca2+/calmodulin binding to the cytosolic N- and C-termini. *FEBS Journal*, 273 (5), pp.1074-1086.

Ziegler, R. G., Hoover, R. N., Pike, M. C., Hildesheim, A., Nomura, A. M., West, D. W., Wu-Williams, A. H., Kolonel, L. N., Horn-Ross, P. L., Rosenthal, J. F. and Hyer, M. B. 1993. Migration patterns and breast cancer risk in Asian-American women. *Journal Of The National Cancer Institute*, 85 (22), pp.1819-1827.

Ziv, E., Tice, J., Smith-Bindman, R., Shepherd, J., Cummings, S. and Kerlikowske, K. 2004. Mammographic density and estrogen receptor status of breast cancer. *Cancer Epidemiology, Biomarkers & Prevention*, 13 (12), pp.2090-2095.

Zubik, L. and Meydani, M. 2003. Bioavailability of soybean isoflavones from aglycone and glucoside forms in American women. *American Journal of Clinical Nutrition*, 77 (6), pp.1459-1465.